The Potentiating Effects of Cell Stress upon Osteoclast Differentiation

A. Gabrielle Josephine van der Kraan

A thesis submitted in total fulfilment of the requirements for the degree of Doctor of Philosophy
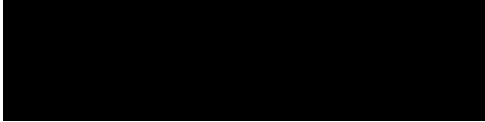
Department of Biochemistry and Molecular Biology, Faculty of Medicine, Nursing and Health Sciences, Monash University

September 2015

Copyright Notice

Abstract

Osteoclast formation is a highly regulated multi-step process, which involves the differentiation of haemopoietic progenitor cells into mature, active osteoclasts. This involves complex interactions between the progenitor haematopoietic cells and osteoblast lineage cells that produce RANKL, the key osteoclast differentiation factor. RANKL binding to its receptor RANK on progenitor cells activates signalling cascades, causing activation of key transcription factors and signalling molecules including NFκB, NFATc1, c-FOS, MITF and p38, which are required for osteoclast differentiation. Dysregulation of these molecules can cause an increase in osteoclast formation, a symptom present in many pathological bone conditions. Stressed cells i.e. under pathological conditions, increase the transcription of molecular chaperone, HSP90. Previous studies by our group found the anti-cancer N-terminal HSP90 inhibitor, 17-AAG, increased osteoclast numbers and tumour growth in bone *in vivo* of MDA-MB-231 cancer cells. The 17-AAG-mediated increase in osteoclast numbers was also reproduced in the absence of tumour load. The increase in osteoclast numbers was not attributed to osteoblast activity i.e., the production of RANKL, but rather a direct increase of osteoclast differentiation in response to the HSP90 inhibitor. However, why 17-AAG affects osteoclasts in this way and whether other anti-cancer agents act similarly was unknown.

In this thesis, 17-AAG and the more recently developed N-terminal HSP90 inhibitors CCT018159 and NVP-AUY922 were shown to increase osteoclast formation. This study identified that 17-AAG did not affect the transcriptional activity nor protein levels of transcription factors NFκB, NFATc1, and c-FOS. However, both 17-AAG and NVP-AUY922 increased levels of the transcription factor MITF, not often studied since its activation is downstream of the other factors. These N-terminal HSP90 inhibitors not only inhibit HSP90 but also indirectly cause HSF-1 mediated cell stress response, suggesting cell stress may affect osteoclast differentiation. The 17-AAG- and NVP-AUY922-mediated increase in osteoclast formation was found to be dependent on HSF1-mediated cell stress. These N-terminal inhibitors also activated another stress-associated factor, p38, which is essential for osteoclast differentiation and phosphorylates MITF.

These findings suggested other cell stressors might increase MITF levels and osteoclastogenesis. Chemotherapeutics, doxorubicin, MG132, cisplatin and bortezomib do

not inhibit HSP90 but act to cause cancer cell death through various cytotoxic actions including proteasome inhibition and DNA damage. These compounds induced an HSF1-mediated cell stress response, and increased NFATc1 and MITF protein expression. These therapeutics also increased osteoclast formation in a HSF-1 dependent manner with pharmacological inhibition of HSF-1 abolishing the increase. These data indicate that cell stress inducing chemotherapeutic drugs act on osteoclast formation at least partly in a HSF-1 dependent manner and show parallels with HSP90 inhibitors although NFATc1 was also activated by these compounds. Likewise ethanol, which induces a classic oxidative stress also acted in the same manner.

The novel findings in this thesis suggest stress-inducing compounds including clinically used cancer therapeutics may have bone-damaging effects by increasing osteoclastogenesis in a HSF-1 dependent manner. Furthermore, this work suggests a more general effect of cell stress in regulating osteoclast differentiation and indicates that any therapeutic that induces cell stress in bone may increase osteoclastogenesis and bone loss.

Declaration

This is to certify that: (i) this thesis contains no material that has been accepted for the award of any other degree or diploma in any University, (ii) to the best of my knowledge and understanding, this thesis contains no material previously published or written by another person, except were due reference has been made, and (iii) this thesis is less than 100,000 words in length, excluding tables, figures and bibliographies.
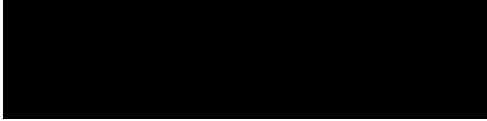
A. Gabrielle Josephine van der Kraan

Publications arising from this work

VAN DER KRAAN, A. G., CHAI, R. C., SINGH, P. P., LANG, B. J., XU, J., GILLESPIE, M. T., PRICE, J. T. & QUINN, J. M. 2013. HSP90 inhibitors enhance differentiation and MITF (microphthalmia transcription factor) activity in osteoclast progenitors. *Biochem J,* 451**,** 235-44.

SINGH, P. P., VAN DER KRAAN, A. G. J., XU, J., GILLESPIE, M. T. & QUINN, J. M. W. 2012. Membrane-bound receptor activator of NFκB ligand (RANKL) activity displayed by osteoblasts is differentially regulated by osteolytic factors. *Biochemical and Biophysical Research Communications,* 422**,** 48-53.

CHAI, R. C., KOUSPOU, M. M., LANG, B. J., NGUYEN, C. H., VAN DER KRAAN, A. G. J., VIEUSSEUX, J. L., LIM, R. C., GILLESPIE, M. T., BENJAMIN, I. J., QUINN, J. M. W. & PRICE, J. T. 2014. Molecular Stress Inducing Compounds Increase Osteoclast Formation in a Heat Shock Factor 1 Dependent Manner. *Journal of Biological Chemistry*.

Acknowledgments

My (my' My), your friendship since honours has meant so much to me. I am so glad we could do honours together. Since then you have always supported me, with our Max Brenner hot chocolate catch ups, giving me presents along the way just because and talking. Those beautiful Oroton hair ties you gave me were worn pretty much every day in the lab and reminded me of our friendship and you. Thank you for your encouragement, belief, time, constancy and love that you have given to me since I have known you. Thank you to Jess, for your friendship, which started when we and Michel were the new recruits at the Red Cross. Thank you for your support at that time and ever since. I still cherish the going away book you made for me when I finished up with the temporary job- "The escapades of Waffle, Capeman and Special Effects Girl". Your friendship throughout the years has meant a lot to me. Thank you for the catch ups with me even though sometimes I was half asleep and for the talking and laughter. Thank you for your excitement, innovations with your productions and writing that you bring to my life but most of all your love. Heidi and Daniella, you have been wonderful friends and have always supported and encouraged me since I have known you. Thank you for your warmth, care, hospitality and adventures that we have together. I am looking forward to many more adventures and wonderful years of friendship. Thank you for your help with the formatting of my thesis. To Upi, thank you for being such a considerate, supportive and great friend. Thank you for helping with my abbreviations. To Dale (or Gaby) thank you for your support and care that you gave to me along the years and your continuing friendship now. I used to look forward so much to our chats every day. Thank you for the laughter, your warmth, and the light and sometimes heavy/topical conversations. You always made me smile. Thank you for the large and small presents including the strawberries and macaroons and money put towards the hiking boots so I could survive NZ hiking! Thank you for your encouragement and belief in me, amongst all your support that helped the most. To my cousins, Tim, Amy and Libby thank you for our friendship over the years. It has been really good to share growing up with you all and our friendship is only getting better.

Nadia, I am so glad we met at uni. You have been the best friend that I could ask for. You have supported me all along the way, and have given me constant affection and love. Thank you for being there always, for your genuine care, encouragement and help. Thank you for the time we have spent together. I have cherished our friendship so much and am looking forward to the many more years. Having you in my life as a friend has been wonderful and life is better for having you in it. Your support throughout the PhD made it easier for me. Thank you for your parents, Nancy and Frank also for supporting me by letting me stay with you and for the constant warmth, belief and oversupply of food for the next day in the laboratory.

To my family, thank you for being a continual support and for all the love that you have given me throughout the years. To Panda Bear, thank you for being the best dog! You are such an obedient dog but so full of love, joy and cheekiness. Thank you for the love you always gave, especially on the hard days.

To my Nana and Grandpa, thank you for your unconditional love. I was well loved by you and loved you both so much. You always gave me so much love, warmth, support, and genuine love. You always believed in me 100% wherever I was in life. Thank you for your belief and continual affirmation. You both taught me the love of science and the love of people, which culminated in doing my PhD. Grandpa, Oswald Charles Gordon, thank for your constant interest in me and what I liked. Your love of science and inventiveness/novelty grew on me and we shared that love. We used to talk about it from when I was 5 and it never stopped. There was always something new and interesting to talk about every time I saw you. Your room full of radio machines, which came out of you learning of radar during War II, was always the most exciting room of the house to be in. During my PhD you always asked about my project and wanted to know what I was doing and how. Thank you for the many memories and input of when I was growing up- the constant love, affection, care, belief, time, giving, love of learning, warmth and humour. You always gave although you did not have much. You knew what was important in life. You meant so much to me. Nana, Josephine 'Susan', thank you for your love and affection, it will always be cherished. You were so supportive and then some more. You were always full of life and joy. Whenever there was a party, you were the life of it. People a third of your age could not keep up with you. You were constantly talking, laughing, dancing and singing even though you grew up during the war in Malta, which was bombed to oblivion. Your courage and not giving up despite severe hardships was so admirable even though you did not ever talk of it. When we were little, we used to love going to be looked after by you and Grandpa. We used to go down to the shops where all your friends were and get jellybeans, liquorice and donuts, Then Grandpa would make us potato chips. Mum and dad must have blinked with all the sugar overdoses. More than the sugar loading though was being around you and Grandpa. You were people orientated, always. You gave care and were always beyond generous. You did not have much but you would have given your last dollar away to help someone. The last five years were I helped mum look after you were a blessing and a joy. I am so glad that I got to spend so much time with you and know you as an adult and be your friend. You were the joy of not only of me but the family. You loved me very much and I loved you so much.

To my sister, Laura, thank you so much for your love and friendship that has been constant. We were almost like twins being so close in age and that is what it was like when we grew up, always together. I think the only time we were not together was when you were doing tennis and I was at art school. I am so grateful that we could do life together. You have been a wonderful best friend to have by my side. Your kindness, warmth, love, care and affection have provided so much happiness and we have had a lot of fun together. During my PhD, you have supported me all the way through. Your affection and checking to see how I was going was really appreciated. You have always been generous but you were generous to a fault during my studies even though you a mortgage to pay off. Thank you for being the best sister.

To my dear younger brother and best friend, James, thank you for keeping it real and helping provide balance. You are the best brother in the world and I am so grateful that you are my

brother. The family was whole when you were born. During my PhD, I remember getting home really late to have plastic darts from your Nerf gun flying down the hall and sticking to my head. Then there were all the times you put me over your shoulder and carried me to my bedroom to go to sleep. This is not to mention all the fun that we have had since you were born including soccer games, climbing trees, Lego building, trampoline jumping, water fights, swimming and snorkelling in the ocean to mention a few. You have provided so much happiness and fun to me. Thank you for your constant encouragement and belief. You are wonderful.

To dear mum and dad, thank you so much for your continual support and love. To my Dad, Thank you for all your support and love over the years. Thank you for all your help which has ranged from the little things to big things which includes fixing my tyres on my bike when I was little as I skidded around so much- to fixing my car that breaks down a lot now. Thank you for your support with finances, to logic, to your skillset including precision, help with drawings and technical understanding Thank you for your hard working work ethic and for your example of being willing to help others out. Thank you for the stability that you have always provided and for working hard to provide the many opportunities provided to me whilst growing up like piano lessons, horse riding and my art lessons, which went for 7 years. I remember when we enrolled into the astronomy course when I was about 10. We used to travel to the other side of town to Box Hill Tafe to learn theory and look through telescopes. Then we would use what we had learned and found the moon, Venus, Jupiter and Saturn through my telescope. Those are memories I treasure.

To dear Mum, thank you for your constant love and affection. You have helped me beyond words and I am so grateful to you for all your love and care throughout my life. Thank you for your encouragement and for your belief. Both your encouragement and belief have bolstered me to where I am today. You always took such good care of me since I was little and have constantly affirmed me. Thank you for your warmth, sincerity, positivity and faithfulness. You are the best mum and I love you. Thank you so much for your sacrifice to provide a good education for me. You taught me so much. I appreciate it so much. One of the aspects I am grateful for the most is the time that you have always invested in me. In a busy world, time is sparse and I treasure that time. Thank you for giving me and my siblings so many opportunities and always giving us the wings through belief in us. Thank you for the example you give in effort, giving, genuine care and doing a job well done. The care that you place upon all people and with whatever task is at hand has taught me so much. Thank you for the fun and the adventures that we have had together as a family and together. You always are so positive, and ready and willing to help and do. Thank you for your love.

"Praise the Lord. Give thanks to the Lord, for he is good; his love endures forever."
Psalm 106.1

TABLE OF CONTENTS

CHAPTER 1 LITERATURE REVIEW

CHAPTER 3 The Influence of HSP90 Inhibitors upon Osteoclast Formation and RANKL/RANK Dependent Transcription Factors

CHAPTER 5 The Effect of Chemotherapeutics Agents and Ethanol Upon HSF1 Mediated Cell Stress, Osteoclast Transcription Factors and Osteoclast Formation

CHAPTER 6 The Effect of 17-AAG Treatment on RAW264.7 Transcriptome

CHAPTER 7 Summary and Conclusions

List of Figures

List of Tables

Abbreviations

(PI) 3-OH	Lipid kinase phosphatidylinositol
$1,25(OH)_2D_3$ (Vit D_3)	$1\alpha 25$ dihydroxy vitamin D_3
1205Lu	Human Metastatic Melanoma Cells
17AG	Amino, 17-demethoxygeldanamcyin
17-AAG	17-allylamino-17 demethoxygeldanamycin
17-DMAG	17-(dimethylaminoethylamino)-17-demethoxygeldanamycin
19S	19 Svedberg units pre-ribosomal subunit of the proteasome
20S	20 Svedberg units pre-ribosomal subunit of the proteasome
26S	26 Svedberg units pre-ribosomal subunit of the proteasome
4T1	4T1 mammary carcinoma
9L	gliosarcoma cell line
$\alpha_2\beta_1$	Integrin $\alpha_2\beta_1$
$\alpha_v\beta_3$	Integrin $\alpha v\beta_3$
aGB	a Glioblastoma multiforme cell line
A2780	Human ovarian carcinoma cell line
A549	Adenocarcinomic human alveolar basal epithelial cells
ACP5 (TRAP)	Acid phosphatase 5, tartrate resistant
ADAM8	A Disintegrin and Metalloproteinase Domain 8
ADP	Adenosine diphosphate
AHA1	Activator of heat shock protein ATPase 1
AKT	Protein kinase B or serine /threonine protein kinase AKT
ALK	Anaplastic Lymphoma Receptor Tyrosine Kinase
ALP	Alkaline phosphatase
α-MEM	α- Minimum Essential Medium
AML	Acute Myeloid Leukaemia
ANOVA	Analysis of variance
AP-1	Activator protein-1
AR	Androgen receptor
AS4.1	Renin-expressing cell line
ASK1	Apoptosis signal-regulating kinase 1
ATF2	Activating transcription factor 2
ATF6	Activating transcription factor 6
ATG5	Autophagy related gene 5
ATG7	Autophagy related gene 7
ATM	Ataxia-telangiectasia mutated
ATP	Adenosine triphosphate
ATPase	Class of enzymes which converts ATP to ADP and P_i
Atp6v0d2	ATPase, H+ transporting, lysosomal 38kDa, V0 subunit d2
BA	Benzoquinone ansamycins
Balb/c	Albino, laboratory-bred strain of the house mouse

BAM	Binary version of a SAM file, which is a tab-delimited text file that contains sequence alignment data.
Bcl-2	B-cell lymphoma 2 protein
Bcr-Abl	Fusion gene of BCR and ABL, coding protein is a tyrosine kinase
BiP	Heat shock 70kDa protein 5 (glucose-regulated protein, 78kDa)
BLAST	Basic Local Alignment Search Tool
BMK1	Mitogen-activated protein kinase 7
BMM	Bone marrow macrophage
BMP	Bone Morphogenic Protein
BMU	Basic multicellular unit
BRACA1	Breast cancer 1, early onset
BRAF	Protoncogene B-raf
BSA	Bovine serum albium
BT472	Breast cancer cell line
BT-474	Breast cancer cell line
C57BL6/J	Common inbred strain of laboratory mouse
C57BL/6N	NIH subline of C57BL/6 contains 5 SNP
C83-2C	Melanoma cell line
Ca^{2+}	Calcium ion
CaMKs	Calcium/calmodulin-activated kinases
CAR2	Carbonic anhydrase II
CCl7	Chloride channel, voltage-sensitive 7
CCL9	Chemokine (C-C motif) ligand 9
CCT018159	4-[4-(2,3-dihydo-1,4-benzodioxin-6-yl)-5-methyl-1H-pyrazol-3-yl]-6-ethyl-1,3-benzenediol, HSP90 inhibitor
CD40	CD40 molecule, TNF receptor superfamily member 5
CD74	Major histocompatibility complex, class II invariant chain
CDK4	Cyclin-dependent kinase 4
cDNA	Complementary-deoxyribonucleic acid
c-FMS	Colony stimulating factor 1 receptor
c-FOS	FBJ murine osteosarcoma viral oncogene homolog
CFU-GM-derived	Colony forming unit granulocyte-macrophage progenitor derived
CFU-M	Colony forming unit macrophage
CGF	Connective tissue growth factor
CHIP	Carboxyl terminus of Hsc70-interacting protein
ChK1	Checkpoint kinase 1
ChK2	Checkpoint kinase 1
CHOP	CCAAT-enhancer-binding protein homologous protein
c-JUN	c-jun proto-oncogene
Cl^-	Chloride iron
CICN7	Chloride channel-7 voltage-sensitive 7

CNF2024(BIIB021)	[6-Chloro-9-(4-methoxy-3,5-dimethylpyridin-2-ylmethyl)-9H-purin-2-yl]amine
Colo205	Colon cancer cell line
COX-2	Cyclooxygenase 2
c-RAF	c-Raf proto-oncogene,
c-REL	C-reticuloendotheliosis oncogene
CRYGF	Crystallin, gamma F
CSF1	Colony stimulating factor 1 (macrophage)
c-SRC	Proto-oncogene tyrosine-protein kinase Src
CTGF	Connective tissue-derived growth factor
CTR	Calcitonin Receptor
CTSK	Cathepsin K
CXCR4	Bone homing chemokine receptor
CYLD	Cylindromatosis
CYP450	Cytochromes P450
DAB	3,3'-Diaminobenzidine
D_3	Vitamin D_3
DAAX	Death-associated protein
DAG	diacyl-glycerol
DAP12	DNAX activating protein 12
DBD	DNA-binding domain (DBD)
DC-STAMP	Dendritic cell-specific transmembrane protein
DDR	DNA damage response
DHN2	3'-descarbamoyl-4-deshydroxynovobiocin
dKO	double-knockout
DMEM	Dulbecco's Modified Eagle Medium
DMSO	Dimethyl sulfoxide
DNA	Deoxyribonucleic acid
DNase	Deoxyribonuclease
DNAX	DNA polymerase III/DNA elongation factor III, tau and gamma subunits
dNTP	Deoxynucleotide
DPX	Distrene, Plasticiser, Xylene
DXA	Dual-energy X-ray absorptiometry
ECM	Extracellular Matrix
EDTA	Ethylenediaminetetraacetic acid
EGCG	Epigallocatechin-3-gallate
EGF	Epidermal Growth Factor
EGFP	Enhanced Green Fluorescent Protein
EGFR	Epidermal Growth Factor Receptor
ER	Endoplasmic reticulum
ERBB2 (HER2)	Erb-b2 receptor tyrosine kinase 2/ human epidermal growth factor

ERK	Extracellular signal- related kinase
ERK1/2	Extracellular signal- related kinases
ERK6	p38 γ
ES cells	Embryonic stem cells
ETS-1	E26 avian leukemia oncogene 1, 5' domain
FACS	Fluorescence-activated cell sorting
FBS	Foetal Bovine Serum
Fc	Fragment crystallizable region of an antibody
FcRγ	Fc fragment of IgE, high affinity I, receptor for; gamma polypeptide
F4/80	EGF-like module-containing mucin-like hormone receptor-like1
FGF23	Fibroblast growth factor 23
FGF	Fibroblast growth factor
FGF7	Fibroblast growth factor 7
FK506	FK506 (Tacrolimus) Calcineurin Inhibitor
G418	Geneticin/ aminoglycoside antibiotic
GA	Geldanamycin
GAB22	GRB2-associated-binding protein 2
GABRA4	Gamma-Aminobutyric Acid (GABA) A Receptor, Alpha 4
GBM	Glioblastomas (GBM) multiforme
GC content	Guanine-cytosine content
gDNA	Genomic DNA
GMCSF	Granulocyte-macrophage colony stimulating factor 2
gp130	Glycoprotein 130
GRB2	Growth factor receptor-bound protein 2
GRP94	Heat shock protein 90kDa beta member 1 found in ER
GSH	Reduced Glutathione
GSK3β	Glycogen synthase kinase 3β
GSSH	Oxidized Glutathione
GTP	Guanosine triphosphate
GTPases	Guanosine triphosphate enzyme, which hydrolyzes GTP
H^+	Hydrogen ions
H-2b	Histone protein 2b
HBSS	Hank's Balanced Salt Solution
HCT116	Human colon cancer cells
HDAC6	Histone Deacetylase 6
HEK293T	Human Embryonic Kidney 293 cells transformed by expression of the large T antigen from SV40 virus that inactivates pRb
HEK-HSE	HEK293T cells stably transfected with pHSE-luc construct, which has the HSP70B promoter upstream of mCherry
HEMEC	Human Endometrial Microvascular Endothelial Cells

HEPES	4-(2-hydroxyethyl)-1-piperazineethanesulfonic acid) is a zwitterionic organic chemical buffering agent
HER2	Human epidermal growth factor receptor 2
HER2/NEU	Erb-b2 receptor tyrosine kinase 2
HET	Heterozygote
HIF1α	Hypoxia inducible-factor 1-α
HIP	Hsc70-interacting protein
HOP	Hsc70-Hsp90-organizing protein (also known as p60 or Sti1)
HRPT	Hypoxanthine phosphoribosyl transferase 1
Hs578T	breast cancer cell line
HSC70	Heat shock cognate 70 (also called Heat shock protein 70)
HSE	Heat Shock Element
HSF1	Heat Shock transcription Factor 1
HSF-1-Het	Heterozygous to heat shock transcription factor 1
HSF-1-KO	Knock out heat shock transcription factor 1
HSF-1-WT	Wild type to heat shock transcription factor 1
HSF2	Heat Shock Factor 2
HSF2A	Heat Shock Factor isoform 2A
HSF3	Heat Shock Factor 3
HSF4	Heat Shock Factor 4
HSP	Heat Shock Protein
HSC70/HSP73(HSPA8)	Heat shock 70kDa protein 8
HSP27 (HSPB1))	Heat shock protein27
HSP33	Heat shock protein 33
HSP40	Heat shock protein 40
HSP70 (HSPA2)	Heat Shock protein 70
HSP72 (HSPAIA)	Heat shock protein 72, stress inducible
HSP90 (HSP90A/N)	Heat Shock Protein 90
HSP70B	Heat Shock Protein 70 B strictly inducible isoform
HSP60	Heat shock protein 60
HSP70	Heat Shock Protein 70
HSP105	Heat shock protein 105
HSP90α	Heat shock protein 90 α isoform
HSP90β1	Heat shock protein 90 β1 isoform
HSR	Heat shock response
HUVEC	Human Umbilical Vein Endothelial Cells
IFNγ	Interferon-γ
IFNβ	Interferon beta
IFN-γ	Interferon gamma
IGF	Insulin growth factor
IGF-1	Insulin growth factor-1
IgG1	Immunoglobulin G1
IgG$_2$	Immunolgobin G2

Igp110	Lysosomal membranes 110
IκB	Inhibitor of nuclear factor kappa-B
IκK	Inhibitor of nuclear factor kappa-B kinase
IκKβ	IκB kinase β
IL-1	Interleukin-1
IL-1β	Interleukin-1β
IL-11	Interleukin-11
IL-1R	Interleukin-receptor
IL-6	Interleukin-6
IL-8	Interleukin-8
IL-34	Interleukin-34
IP3	Inositol 1,4,5-triphosphate
IPI-504	Retaspimycin hydrochloride, HSP90 inhibitor
IRE1	Inositol-requiring transmembrane kinase/endonuclease 1
IRF8	Interferon regulatory factor 8
ITAM	Immunoreceptor tyrosine-based activation motif
JAK	Janus protein kinase
JNK	c-JUN N terminal kinase
JNK2	c-JUN N terminal kinase-2
kDa	Kilodalton
KF5833	Radicicol analogue, HSP90 inhibitor
KNK437	N-formyl-3,4-methylenedioxy-benzylidene- γ-butyrolactam, HSF1 inhibitor
KO	Knockout
KW2478	Non-ansamycin type HSP90 inhibitor
LCM	L cell media
lGP110 proteins	Lysosomal type I integral membrane proteins
LIF	Leukaemia inhibitory factor
LPS	Lipopolysaccharide
LTBP3	Latent transforming growth factor beta binding protein 3
E-box motif	CACTGTG Enhancer Box motif cytosine-adenine-cytosine-thyamine-guanine-thyamine-guanine
MAP kinase family	Mitogen Activated Protein Kinase Family
MAPK	Mitogen Activated Protein Kinase
MAPKKK	Mitogen-activated protein kinase kinase kinase
MAPKKKK	Mitogen-activated protein kinase kinase kinase kinase
MC3T3-G2/PA6	Bone marrow-derived stromal cell line
MCF-7	Breast cancer cell line (Michigan Cancer Foundation-7)
MCP-1	Monocyte chemoattractant protein-1
M-CSF	Macrophage-colony stimulating factor
MDA-MB-231	Breast cancer cell line (M. D. Anderson Cancer Center)
MEF2	myocyte enhancer factor-2
MEK	Methyl ethyl ketone

MEK inhibitors	Methyl ethyl ketone inhibitors
Met	Hepatocyte growth factor receptor
MEXF 276	Melanoma xenograft model
MEXF 462	Melanoma xenograft model
MEXF 514	Melanoma xenograft model
MEXF 989	Melanoma xenograft model
MG132	N-(benzyloxycarbonyl)leucinylleucinylleucinal, proteasomal inhibitor
$MGCl_2$	Magnesium chloride
MIF	Macrophage Migration Inhibitory Factor
MIP-1	Macrophage inflammatory protein 1
MiT family	Members of the microphthalmia family
MITF	Microphthalmia-associated transcription factor
MITF A	Microphthalmia-associated transcription factor isoform A
MITF-E	Microphthalmia-associated transcription factor isoform E
MITF-M	Microphthalmia-associated transcription factor isoform M
MK2	Mitogen-activated protein kinase-activated protein kinase 2
MK3	Mitogen-activated protein kinase-activated protein kinase 3
MKK	MAPK (Mitogen Activated Protein Kinase)kinase kinase
MKK3	MAPK (Mitogen Activated Protein Kinase)kinase kinase3
MKK4	MAPK (Mitogen Activated Protein Kinase)kinase kinase4
MKK6	MAPK (Mitogen Activated Protein Kinase)kinase kinase6
M(M1-3) vATPase-d2	Mutated ATP6v0d2 construct
MMP-1	Matrix metalloproteinase-1
MMP-2	Matrix metalloproteinase-2
MMP-3	Matrix metalloproteinase-3
MMP-9	Matrix metalloproteinase-9
MMP-12	Matrix metalloproteinase-12
MMP-13	Matrix metalloproteinase-13
mRNA	messenger Riboneucleic acid
MSC	Mesenchymal stem cell
Mtor	Mammalian target of rapamycin
NaCl	Sodium Chloride
NCIH2052	human malignant pleural mesothelioma cell line
NCIH2452	human malignant pleural mesothelioma cell line
NFAT	Nuclear Factor of activated T cells
NFATc1	Nuclear factor of activated T cells-1
NFATc2	Nuclear factor of activated T cells-2
NFATc4	Nuclear factor of activated T cells-4
NFAT RAW	RAW264.7 cells stably transfected with a NFAT driven luciferase construct
NFκB	Nuclear Factor kappa-B
NFκBp100	NFκBp100 inhibitor

NFκB-RAW	RAW264.7 cells stably transfected with a NFκB driven luciferase construct
NIH3T3 R	R-Ras transformed NIH3T3 mouse embryonic fibroblast cell line
NIH3T3	mouse embryonic fibroblast cell line
NVP-AUY922	5-(2,4-Dihydroxy-5-isopropylphenyl)-N-ethyl-4-(4-(morpholinomethyl)phenyl)isoxazole-3-carboxamide, HSP90 inhibitor
OB	Osteoblast
OC	Osteoclast
OC-STAMP	Osteoclast Stimulatory Transmembrane Protein
OPG	Osteoprotegerin
OPN	Osteopontin
OSCAR	Osteoclast-associated receptor
OSM	Oncostatin M
OSTM1	Osteopetrosis associated transmembrane protein
P13K	Phosphatidylinositol-4,5-bisphosphate 3-kinase
P23	HSP90 co-chaperone
p300/CBP	p300/CREB-binding protein coactivator family
p38	p38 Mitogen-activated protein Kinase
p38α	p38 MAP kinases alpha
p38β	p38 MAP kinases beta
p38γ	p38 MAP kinases gamma
p38δ	p38 MAP kinases delta
p50	Rel protein (Rel/NF-kB proteins) p50
p50/p52	Rel protein (Rel/kB proteins) p50 (NF-kB1) and p65 (RelA) complex
p52/RelB	Heterodimeric complex composed of NF-kB mature subunits p50 and Transcription factor RelB
p53	Tumor suppressor protein p53
p65	Rel protein (Rel/NF-kB proteins) p65 (RelA)
PBS	Phosphate Buffered Saline
PCA	Principle component analysis
PC3	Prostate cancer cell line
PC-3M	Prostate cancer cell line
PCR	Polymerase chain reaction
PD98059	MEK1 inhibitor
PDGF	Platelet-derived growth factor
PERK	Pancreatic ER kinase
pGB	Glioblastoma tumour cell lines
PGE	Prostaglandin
PGE_2	Prostaglandin E_2
pHSE-mCherry	Construct Reporter with Red fluorescent protein

PhosSTOP	Phosphatase Inhibitors
PI3K	Phosphoinositide 3 kinase
PIP2	Phosphatidylinositol 4,5-bisphosphate
PIR-A	Paired immunolgobin-like receptor A
PKC	Protein Kinase C
PLAU (uPA)	Plasminogen Activator, Urokinase
PLCγ	Phospholipase Cγ
PR	Progesterone Receptor
pTEFb	Positive transcription elongation factor
PTH	Parathyroid hormone
PTHrP	Parathyroid hormone-related protein
PU.1	Transcription factor encoded by Spi-1 proto-oncogene
PVDF	Polyvinylidene difluoride
Quercetin	Quercetin 3, 3′, 4′, 5, 7-pentahydroxylflavone
RAB7	RAB7A, member RAS oncogene family
RAC1	Ras-related C3 botulinum toxin substrate 1
RAF-1	Raf-1 proto-oncogene, serine/threonine kinase
RANK	Receptor activator of NFκB
RANK.Fc	Soluble recombinant RANKL decoy receptor and functional blocker
RANKL	Receptor activator of NFκB ligand
RAW264.7	Mouse macrophage cell line
RBP-J	RANKL inhibitor
RGD	Arginine-glycine-aspartic acid
RIPA	Radioimmunoprecipitation assay buffer
RNA	Ribonucleic acid
RNAPII	RNA polymerase II
RNase	Ribonuclease
ROS	Reactive oxygen species
RTK	Receptor tyrosine kinases
RT-qPCR	Real time-quantitative PCR
Runx2/cbfa1	Runt related transcription factor 2/core-binding factor 1
SAPK/JNK	Stress-activated protein kinases/Jun amino-terminal kinases
SAPK 3	Stress-activated protein kinase 3
SAPK 4	Stress-activated protein kinase 4
SB203580	4-(4-Fluorophenyl)-2-(4-methylsulfinylphenyl)-5-(4-pyridyl)-1H-imidazole, p38 inhibitor
SCID	Severe combined immunodeficiency
SCP2 cells	Mouse mammary epithelial cell line
SD	Standard deviation
SDF-1:CXCL12	Stromal-derived factor-1, or Chemokine receptor ligand 12
SDS-PAGE	Sodium dodecyl sulfate polyacrylamide gel electrophoresis
SEM	Standard error of mean

SHIP	SH2-containing inositol phosphatase
ShRNA	Short hairpin RNA
shRNAi	Short hairpin ribonucleic acid interference
shRNAmir	MicroRNA-embedded shRNA
siRNA	Small interfering RNA
SIRPβ1	Signal regulatory protein β1
SKMEL 2	Melanoma cell line
SMAD2	SMAD family member 2
SMAD4	SMAD family member 4
SMAD7	SMAD family member 7
SOC	Super optimal broth with catabolic repression medium
SNX-5422	HSP90 inhibitor
SRE	Skeletal related events
STE20	Yeast 'Sterile 20' gene, functions upstream of MAPK cascade
SYK	Syk protein-tyrosine kinase
T cells	T lymphocytes
TAB1/2	TGF-beta activated kinase 1/MAP3K7 binding protein 1
TAK1	Transforming growth factor beta-activated kinase 1
TANK	TRAF Family Member-Associated NFκB Activator
TBRII	Serine and threonine kinase receptors, the type II
TBST	Tris buffered Saline with Tween
TE buffer	Tris EDTA buffer
TFE3	Transcription factor binding to IGHM enhancer 3
TFEB	Transcription factor EB
TFEC	Transcription factor EC
TGFβ	Transforming Growth Factor β
TLR	Toll-like receptor
TNF	Tumour Necrosis Factor
TNF-α	Tumour Necrosis Factor α
TNFR	Tumour Necrosis Factor Receptor
TNFR11B	TNF nomenclature for OPG
TNFRSF11A	TNF nomenclature for RANKL
TOV112D	Human ovarian cancer cell line
TPR	Tetratricopeptide repeat-binding
TRAF6	TNF receptor-associated factor 6
TRAFs	Tumour necrosis factor receptor-associated factors
TRANCE	TNF-related activation-induced cytokine (RANKL)
TRAP (Apc5)	Tartrate Resistant Acid Phosphatase
TREM-2	Triggering Receptor Expressed on Myeloid cells-2
tRNA	Transfer ribonucleic acid
TβRII (DNTβII)	TGFβ receptor II
U0126	1,4-diamino-2,3-dicyano-1,4-bis(2-aminophenylthio)butadiene
U87MG	glioma cell line

uPA(PLAU)	Urokinase Plasminogen activator
uPAR	uPA receptor
UPP	Ubiquitin Proteasome Pathway
UPR	Unfolded protein response
UV	Ultraviolet
v-ATPase	Vacuolar-type H^+-ATPase proton pump
v-ATPase a3	Vacuolar-type H^+-ATPase proton pump, a3 subunit
v-ATPase-d2	Vacuolar-type H^+-ATPase proton pump, d2 subunit
-ve	Negative untreated control
VEGF	Vascular epidermal growth factor
VER-49009	3-(5-chloro-2,4-dihydroxyphenyl)-N-ethyl-4-(4-methoxyphenyl)-1H-pyrazole-5-carboxamide, HSP90 Inhibitor
VER52296	5-[2,4-dihydroxy-5-(1-methylethyl)phenyl]-N-ethyl-4-[4-(4-morpholinylmethyl)phenyl]-3-isoxazolecarboxamide, HSP90 inhibitor
VNR	Vitronectin receptor
v-SRC	Rous sarcoma virus oncogene that encodes a tyrosine kinase
wHTH	winged helix turn-helix
WM266.4	Human melanoma cell line
WT	wild type
XBP1	X-box binding protein 1
XL888	XL888, HSP90 inhibitor
XL1-Blue	XL1-Blue Supercompetent Cells *E. coli* cells used for plasmid cloning

Chapter 1
Literature Review

Chapter 1 Literature Review

1.1 Introduction

Bone is a dynamic tissue, which has numerous functions including maintaining the integrity and function of the skeletal system (Clarke, 2008; Boyce, 2002). Bone cells, osteoblasts and osteoclasts lay down new bone matrix, and resorb damaged or old bone, respectively (Takayanagi, 2008a; Schett and Redlich, 2009). The actions of these cells are coupled such that the formation of bone and resorption of bone is matched under physiological conditions (Soysa *et al.*, 2012; Iqbal *et al.*, 2009; Ikeda and Takeshita, 2014). Pathophysiological conditions where osteoblast or osteoclast differentiation and function are altered can cause a loss of balance in this coupled effect (Feng and McDonald, 2011; Rucci, 2008; Boyle *et al.*, 2003). This can have a major negative impact upon skeletal health and consequently the wellbeing of the individual. Many pathological diseases including rheumatoid arthritis and some metastatic bone diseases exhibit increased numbers and hence activity of osteoclasts (Mundy, 2002; Yin *et al.*, 2005; Kingsley *et al.*, 2007; Goldring, 2003). Due to the damaging effects of osteoclast overactivity the differentiation of osteoclasts from progenitor bone marrow cells is a highly regulated process (Boyce, 2013; Aeschlimann and Evans, 2004; Boyle *et al.*, 2003). Many transcription factors including NFκB, NFATc1, c-FOS, MITF and signalling proteins, such as p38, positively regulate osteoclast differention through signalling pathways activated by RANKL binding to its receptor, RANK (Boyle *et al.*, 2003; Takayanagi, 2008b; Asagiri and Takayanagi, 2007). Therefore if the function of these transcription factors or signalling molecules is increased by molecules such as chemotherapeutics, osteoclast differentiation could be increased. HSP90, a widely expressed molecular chaperone whose transcription is increased in response to cell stress, has an important role in cancer (Li and Buchner, 2013a; Cheng *et al.*, 2012; Drysdale *et al.*, 2006). Resultingly, HSP90 inhibition in cancer has been a much studied area of research (Drysdale and Brough, 2008; Workman, 2004b; Neckers and Workman, 2012). In 2005, Price *et al.,* found the anti-cancer N-terminal HSP90 inhibitor, 17-AAG, increased bone tumour growth in a MDA-MB231 inoculation mouse model, and increased osteoclast numbers in mice and *in vitro*. The increase in osteoclast numbers was attributed to a direct increase of osteoclast differentiation in response to the anti-cancer HSP90 inhibitor, 17-AAG (Price *et al.*, 2005). 17-AAG, not only mechanistically inhibits HSP90, but also indirectly causes a HSF1 cell stress response suggesting cell stress may affect osteoclast differentiation under certain conditions (Travers *et al.*, 2012; Taldone *et al.*, 2008; Jego *et al.*, 2013; Doubrovin *et al.*,

2012). This thesis addresses if experimental and clinically used chemotherapeutics cause HSF-1 cell stress upon osteoclast progenitors and determines whether this cellular stress impacts the regulation osteoclast differentiation.

1.2 The Structure of Bone

Bone is a rigid connective tissue, which provides structural support for the body and protection of vital internal organs (Marieb, 2004). Bone also participates in the regulation of calcium and phosphate levels (and therefore serum mineral homeostasis), and is the primary site of haematopoiesis in adults (Harada and Rodan, 2003; Iqbal *et al.*, 2009; Boyle *et al.*, 2003; Downey and Siegel, 2006; Marieb, 2004; Asagiri and Takayanagi, 2007). The adult human skeleton consists of 206 bones that are broadly classified in four general types: long, short, flat and irregular bones (Marieb, 2004; Kingsley *et al.*, 2007; Chen *et al.*, 2010a). Although displaying many features in common, bones vary in their structure, material composition and in their development in ways that reflect their functions (Marieb, 2004; Boskey and Coleman, 2010).

1.2.1 Bone Composition

In bone, cartilage and teeth, the extracellular matrices have the unique ability to become calcified, i.e., mineralized (Tortora, 2000; Clarke, 2008). The extracellular matrix of mature bone is a very dense specialized form of connective tissue, which is composed of both organic and inorganic phases (35% and 65%, respectively, by mass) (Marieb, 2004; Downey and Siegel, 2006; Clarke, 2008). The inorganic phase of bone is composed mainly of solid particles of calcium phosphate in the form of crystals of hydroxyapatite, $Ca_{10}(PO_4)_6(OH)_2$ (Marieb, 2004; Clarke, 2008). This inorganic phase gives the bone rigidity and its ability to resist structural compression (Downey and Siegel, 2006; Marieb, 2004). The organic bone matrix is comprised mainly of type I collagen-rich fibrils, which resist mechanical tension (Alberts *et al.*, 2002; Marieb, 2004; Downey and Siegel, 2006). In addition to type I collagen (and a smaller quantity of type III collagen), the organic bone matrix is abundant in many other protein components such as osteocalcin (bone Gla protein), bone sialoprotein and a ground substance that consists principally of proteoglycans, acid mucopolysaccharides and lipids (Marieb, 2004; Martin *et al.*, 1988; Clarke, 2008). The combination of the collagenous, non-collagenous proteins and ground substance components of bone provides a composite material that is mechanically strong yet has a degree of elasticity, and the ability to bind

inorganic phase components and cells (Bandyopadhyay-Ghos, 2008). Collectively, the components of the organic matrix are produced by osteoblasts initially in an immature form, termed 'osteoid' (Marieb, 2004). Over time osteoid matures and calcium phosphate crystals are deposited to form the hard, mineralised bone matrix (Alberts *et al.*, 2002).

The main cellular components of bone include osteoclasts and osteoblasts, which together through their actions determine bone mass (Bandyopadhyay-Ghos, 2008). Osteoclasts are multinucleated macrophage–like cells with the unique capability to actively form bone resorption pits, i.e., break down bone matrix and release the mineral phase from the bone surface (Raggatt and Partridge, 2010; Katagiri and Takahashi, 2002; Boyle *et al.*, 2003). Bone also contains cells with regulatory functions such as osteocytes and osteal macrophages, together with other local stromal cells (Marieb, 2004; Tortora, 2000; Clarke, 2008). Mesenchymally-derived osteoblasts lay down bone matrix, which gradually becomes mineralised as noted above, but with time become quiescent to form bone lining cells that secrete little if any bone matrix (Katagiri and Takahashi, 2002; Iqbal *et al.*, 2009). Osteoblasts also form osteocytes (Clarke, 2008). Osteocytes are cells which are embedded within the bone itself and through their interconnections provide a communication network between the bone tissue locations, while also secreting important hormonal and regulatory factors (Clarke, 2008). Osteocytes also have a limited ability to release mineral from around the lacunae where they reside, so (like osteoclasts) may participate in mineral homeostasis (Atkins and Findlay, 2012; Bélanger, 1969; Teti and Zallone, 2008). Most bones also contain significant quantities of haematopoietic bone marrow in a central cavity, which contains a rich mixture of cells (Tortora, 2000; Morrison and Scadden, 2014). Osteoblasts, osteoclasts and osteocytes are discussed in more detail in Chapter 1.3.

1.2.2 Bone Anatomy

Mature bone consists of two principle forms: cortical (or compact) bone and trabecular (or cancellous) bone, which differ both structurally and functionally (Marieb, 2004; Tortora, 2000; Bandyopadhyay-Ghos, 2008). Cortical bone forms the solid framework of the bone being located on the external surfaces, such as on the shafts of long bones, e.g., the tibia, femur and humerus (Tortora, 2000; Brandi, 2009; Clarke, 2008). As such cortical bone is dense, with a high composition of collagen type I and III-rich fibres that are closely bound to hydroxyapatite mineral (Marieb, 2004; Downey and Siegel, 2006). The mineralised matrix of cortical bone often occurs in most species as osteonal structures, which are bony columns or

cylinders that can be seen by histology or x-ray based scanning methods to consist of concentric layers around a central or Haversian canal (Clarke, 2008; Tortora, 2000; Marieb, 2004). The central Haversian canal contains nerve filaments and blood vessels, which supply the bone (Marieb, 2004; Tortora, 2000; Bandyopadhyay-Ghos, 2008). Trabecular bone, which makes up the remaining 20% or so of bone volume consists of plates or struts (trabeculae) present within chambers formed by the cortical bone (Clarke, 2008; Marieb, 2004; Tortora, 2000). In long bones trabecular bone is typically found in its greatest quantity at the metaphysis and epiphysis regions, and also at the inner parts of flat and irregular bones such as the calvarial bone, scapula, mandible and ileum (Brandi, 2009; Downey and Siegel, 2006; Clarke, 2008). Individual trabeculae (literally 'little beams') appear in tissue sections as irregularly shaped spicules of bone, but are, in fact, arranged in 3-dimensions as interconnected plate-like structures that mechanically reinforce the cortical bone structures such that trabecular bone forms a loosely organized porous complex of bone (Tortora, 2000; Marieb, 2004). In regions of thicker trabeculae and in cortical bone, long processes of inter-connected osteocytes embedded within the bone form a network of thin canaliculi (Clarke, 2008).These osteocyte networks thus permeate the entire bone matrix (Kerschnitzki *et al.*, 2013). Bone without osteocytes (i.e., with empty osteocyte lacunae) is by most definitions dead bone, being unable to function and requiring replacement (Tortora, 2000). Relative to cortical bone, trabecular bone is more metabolically active since it has a larger surface area with many resident osteoclasts and osteoblasts that remodel the bone (Clarke, 2008; Brandi, 2009). For this reason, when bone cells are stimulated to break down or to form new bone, it is usually most clearly and rapidly evident in trabecular bone (Brandi, 2009). Thus, trabecular bone is relatively more important in the regulation of serum calcium levels since it is rapidly broken down and reformed compared to cortical bone (Clarke, 2008).

1.2.3 Bone Development

The skeleton is formed during embryogenesis, followed by bone growth during the period of childhood-early adulthood (Marieb, 2004). In adulthood, bones do not grow but the processes of bone modelling and remodelling (described below) maintain bone structure as required to resist forces placed upon it (Marieb, 2004).

The process by which bone forms is called ossification or osteogenesis (Tortora, 2000; Marieb, 2004). Before this, the embryonic skeleton initially consists of condensed embryonic connective tissue and hyaline cartilage, which resemble miniature bones (Marieb, 2004;

Tortora, 2000; Gilbert, 2000). Mature bone can form through two distinct processes: intramembranous and endochondral ossification (Gilbert, 2000; Marieb, 2004). Intramembranous ossification is the formation of bone directly on or within fibrous connective tissue membranes that are rich in collagen type I (Marieb, 2004; Tortora, 2000). Only flat bones, including the cranial bones of the skull and the clavicle, form through this process (Gilbert, 2000; Marieb, 2004). These form directly from pre-existing fibrous tissues without going through a cartilaginous stage (Tortora, 2000). Intramembranous ossification involves four main processes (Tortora, 2000; Marieb, 2004). Firstly, an ossification centre appears in the fibrous connective tissue membrane (Tortora, 2000; Marieb, 2004). Secondly, bone matrix is secreted within the fibrous membrane and calcification occurs, followed by trabeculae bone formation (Gilbert, 2000; Tortora, 2000; Marieb, 2004). Lastly, the development of compact, spongy (trabecular) and bone marrow bone occurs (Tortora, 2000). Endochondral ossification is the replacement of cartilage (collagen type II-rich tissue) with bone (Gilbert, 2000; Tortora, 2000). Endochondral ossification in humans begins during the second month of life, and uses hyaline cartilage as a pattern for subsequent bone development, which occurs through five stages (Marieb, 2004). Firstly, mesenchymal cells form chondrocytes and produce an original anlage or template that approximates to the shape of future bones (Tortora, 2000). In this stage the perichondrial membrane also develops around the hyaline cartilage (Tortora, 2000; Gilbert, 2000). Secondly, growth of the cartilage anlage occurs lengthwise (interstitial growth) through chondrocytes division and in thickness (appositional growth), which occurs through matrix deposition by the chondrocytes (Tortora, 2000). Calcification of the cartilage also starts to occur during this stage (Tortora, 2000). The third step is the development of the primary ossification centre, which is the region where bony tissue replaces most of the cartilage (Tortora, 2000; Marieb, 2004). Arterial penetration of the perichondrium occurs followed by the differentiation of mesenchymally derived osteogenic cells into osteoblasts (Marieb, 2004; Tortora, 2000). The osteoblasts then deposit bone matrix over the remaining cartilage to form low density or woven bone (Gilbert, 2000). The low density bone is gradually resorbed by bone-resorbing osteoclasts, which in turn causes the formation of denser trabecular bone by osteoblasts in a process similar to bone remodelling, described below (Robson, 1999). As the primary ossification centre enlarges towards the ends of the bone, the bone marrow cavity emerges by excavation of the bone by osteoclasts (Tortora, 2000; Robson, 1999). Fourthly, the majority of hyaline cartilage is replaced with the outer compact bone (Tortora, 2000; Marieb, 2004). Hyaline cartilage only remains on the epiphyseal surfaces as the articular cartilage and also at the junctions between

the epiphysis and the diaphysis, which are known as growth plates (discussed below) (Marieb, 2004; Tortora, 2000). The final step in endochondral ossification is ossification of the epiphysis (Marieb, 2004). This process involves the centre of the epiphysis deteriorating and a periosteal bud entering followed by the formation of trabecular bone (Marieb, 2004).

1.2.4 Bone Modelling and Remodelling

After the development of bone through ossification, bone undergoes longitudinal (interstitial growth) and appositional growth (radial) growth, modelling, and remodelling during life (Marieb, 2004; Tortora, 2000; Clarke, 2008). Interstitial growth occurs at the growth plates, which are present until the onset of adulthood and allow for the growth by elongation of the long bones during childhood and adolescence (Tortora, 2000; Marieb, 2004; Clarke, 2008). To achieve this, the growth plate cartilage lengthens and undergoes ossification at its two ends, the latter process eventually predominating until the whole growth plate has become bone (Robson, 1999). After this growth plate 'closure', longitudinal bone growth (height gain) stops. Appositional growth at the periosteal membrane causes the thickening of bones (Marieb, 2004; Tortora, 2000; Clarke, 2008). These two processes occur during childhood and adolescent years; however, some facial bones including those of the jaw keep growing throughout life (Marieb, 2004).

The processes of bone modelling and remodelling underlie the skeletal system's development and maintenance (Raggatt and Partridge, 2010). Bone modelling is the process of bone apposition by osteoblasts such as that occurring at periosteal sites noted above (Clarke, 2008). This plays an important role in bone shape change in response to physiological stimuli or mechanical loading, and is reflected by Wolff's Law, which states that long bones change shape to meet the stresses placed upon them (Clarke, 2008; Marieb, 2004). Thus in response to stimuli, bones may widen or move axis (Clarke, 2008). During bone modelling, bone formation, whilst being regulated as a whole, occurs only in distinct regions of the bone and osteoclasts are not involved in this process (Raggatt and Partridge, 2010). Bone modelling in adults is not as common as bone remodelling (discussed below) but is increased in some instances including hypoparathyroidism and treatment with certain bone anabolic agents (Clarke, 2008).

Adult bone is subject to continual remodelling and repairs through life to maintain skeletal integrity (Raggatt and Partridge, 2010; Boyle et al., 2003). As reviewed by Iqbal and others,

bone remodelling is responsible for removal and repair of damaged bone, and is the main metabolic process regulating bone structure and function during adult life (Boyle *et al.*, 2003; Iqbal *et al.*, 2009; Tang *et al.*, 2009; Raggatt and Partridge, 2010; Tortora, 2000). Unlike in bone modelling where bone is formed and shaped by osteoblasts alone, the bone resorbing osteoclast has an active role in bone remodelling (Marieb, 2004; Boyle *et al.*, 2003). Whilst osteoclasts remove old or damaged bone, osteoblasts present nearby lay down new bone matrix that becomes mineralized (Figure 1.1) (Raggatt and Partridge, 2010; Katagiri and Takahashi, 2002; Harada and Rodan, 2003; Iqbal *et al.*, 2009). The coordinated process of bone resorption followed by bone formation is called 'coupling' and it is proposed to underlie the long term preservation of bone mass (Iqbal *et al.*, 2009; Boyle *et al.*, 2003; Raggatt and Partridge, 2010; Tang *et al.*, 2009). In bone pathologies, the coupling becomes weaker or uncoupling occurs, resulting in excessive bone formation or bone loss (Tang *et al.*, 2009; Boyle *et al.*, 2003; Ikeda and Takeshita, 2014). Increased bone formation can impede joint mobility or other complications that depend on its site (Office of the Surgeon General (US), 2004). Excessive bone loss can severely degrade the structure and strength of bone with resulting complications to an individual's life due to an increased propensity to fracture (Boyle *et al.*, 2003; Iqbal *et al.*, 2009; Tang *et al.*, 2009).

Adult skeletal diseases can be associated with excessive bone formation such as ankylosing spondylitis, osteopetrosis and at some prostate cancer-affected sites, but the majority of common bone diseases are caused by excessive osteolytic activity, which leads to an imbalance in bone remodelling favouring bone loss (Iqbal *et al.*, 2009; Boyle *et al.*, 2003; Sharma *et al.*, 2007; Andersen *et al.*, 2009). These skeletal disorders include postmenopausal osteoporosis, inflammatory periodontal disease, autoimmune and inflammatory rheumatoid arthritis, multiple myeloma and many other types of metastatic cancers, which invade bone (Mori *et al.*, 2015a; Office of the Surgeon General (US), 2004). In the latter, cancer cells cause local recruitment of osteoclasts, which destroy the bone and cause clinical symptoms such as pain and hypercalcaemia (Iqbal *et al.*, 2009; Boyle *et al.*, 2003; Sharma *et al.*, 2007; Ikeda and Takeshita, 2014). The recruited osteoclasts can also stimulate further cancer growth and progression (Chapter 1.6.2) (Mundy, 1997; Guise *et al.*, 2006; Kingsley *et al.*, 2007).
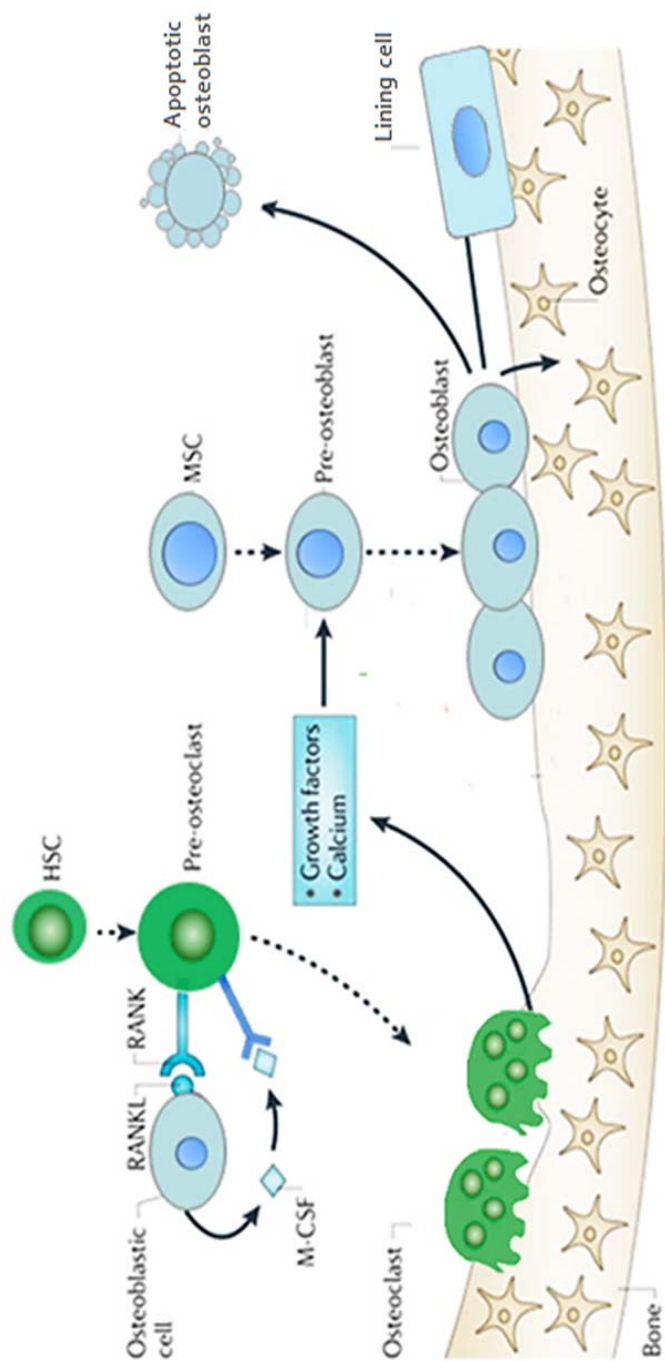
Figure 1.1 Bone Remodelling

Bone is a dynamic hard tissue that undergoes a continual remodelling process to maintain the body's skeletal integrity. Bone remodelling is a finely balanced, coupled and sequential process (represented by the dashed arrows). Osteoclasts, which derive from hematopoietic stem cell (HSC) resorb bone and release growth factors and calcium. In a synchronized manner mesenchymal stem cell (MSC)-derived osteoblasts lay down new osteoid. The newly laid osteoid is subsequently mineralized to form the calcified bone matrix. After the osteoblasts lay down new osteoid osteoblasts have one of three fates: undergo apoptosis, become a bone lining cell or become embedded in the bone matrix to become osteocytes. Osteocytes sense mechanical strain through canciculi networks, and bone lining cells on the bone surface communicate with these osteocytes to transmit the signal to osteoblasts and osteoclasts. Image adapted from (Weilbaecher *et al.*, 2011).

1.3 Cells of the Bone

The three major types of bone cells are osteoclasts, osteoblasts and osteocytes. These cells regulate bone mass and are discussed in more detail below.

1.3.1 Osteoblasts and Osteoblast-related Cells

Osteoblasts are large and highly secretory mesenchymal-derived cells, which make new bone at sites of bone modelling (where bone forms *de novo*) and bone remodelling (Raggatt and Partridge, 2010; Marieb, 2004; Tortora, 2000; Katagiri and Takahashi, 2002). Mature osteoblasts are characteristically large, cuboidal cells being typically 20-30μm in size, and are also polarized, secreting matrix onto the existing bone surface (Neve *et al.*, 2011; Mackie, 2003; Katagiri and Takahashi, 2002; Rosenberg and Roth, 2012). They are generally found in clusters on the bone surface where they are connected to one another through gap junctions (Katagiri and Takahashi, 2002; Mackie, 2003). Mature osteoblasts express parathyroid hormone (PTH) receptors (PTH1R), have high enzyme activity of alkaline phosphatase (ALP) and secrete a number of bone-related proteins including osteocalcin, which is both a bone matrix component and a hormone influencing energy metabolism (Raggatt and Partridge, 2010; Katagiri and Takahashi, 2002; Neve *et al.*, 2011). Importantly, osteoblasts also produce osteoclastogenic factors including macrophage colony-stimulating factor (M-CSF) and receptor activator of Nuclear Factor κB Ligand (RANKL) (Chapter 1.5.1 and 1.5.2) (Raggatt and Partridge, 2010; Katagiri and Takahashi, 2002).

Upon ceasing bone matrix production, osteoblasts have several possible fates: they may become osteocytes buried in lacunae below the bone surface, become bone lining cells (flat cells occupying endosteal and trabecular bone surfaces) or they may undergo apoptosis (Figure 1.1) (Manolagas, 2000; Raggatt and Partridge, 2010; Franz-Odendaal *et al.*, 2006; Boyce *et al.*, 2002). Bone lining cells can be considered inactive osteoblastic cells in that they secrete little or no bone matrix; however, they do express hormone receptors i.e., PTH1R and produce cytokines and growth factors (Manolagas, 2000; Downey and Siegel, 2006). Bone lining cells may become active osteoblasts again when intermittently stimulated with PTH, as indicated in recent *in vivo* rat studies, but this is highly controversial (Kim *et al.*, 2012).

1.3.2 Osteocytes

The stellate-shaped osteocytes are the most abundant bone cell accounting for 95% of bone cells (Noble, 2008; Dallas *et al.*, 2013; Bonewald and Johnson, 2008). As mentioned above, an osteoblast can become embedded into the bone matrix to form an osteocyte (Franz-Odendaal *et al.*, 2006; Boyce *et al.*, 2002). They are highly singular cells that exist for very long periods of time within their lacunae (decades in the case of humans) buried inside the cortical and trabecular bone (Dallas *et al.*, 2013; Noble, 2008). As previously mentioned, channels termed canaliculi penetrate the solid bone to allow interconnection of the osteocytes to one another by means of highly extended neuronal-like cellular processes running through the canaliculi (Bonewald and Johnson, 2008; Noble, 2008; Dallas *et al.*, 2013). These extended processes also connect the osteocytes to Haversian canals and to cells at the bone surface (Bonewald and Johnson, 2008; Noble, 2008; Dallas *et al.*, 2013). As such, these connections between osteocytes provide a broader communication network between the different areas of bone and allow penetration of nutrients to osteocytes, helping maintain them (Bonewald and Johnson, 2008). Osteocytes are major regulators of bone metabolism, having a major influence on osteoclast and osteoblast activity through their production of sclerostin (Bonewald and Johnson, 2008). Osteocytes also act as mechano-sensors to regulate local bone metabolism by detecting mechanical movement through the movement of fluid through canaliculi, which exerts shear stress on their cell processes (Dallas *et al.*, 2013; Bonewald and Johnson, 2008). Osteocytes also affect calcium and phosphate metabolism in other organs such as the kidney through their hormonal secretions such as FGF23 (Noble, 2008; Dallas *et al.*, 2013). It is interesting to note that osteocytes themselves have been reported to resorb minor amounts of bone in their lacunae, termed osteocyte osteolysis (Nakashima *et al.*, 2011; Bélanger, 1969; Pajevic, 2009). As a result osteocytes have a role in the mineral metabolism of bone by mobilizing calcium from their lacunae (Nakashima *et al.*, 2011; Bélanger, 1969; Pajevic, 2009).

1.3.3 Osteoclasts

In 1873, the early Swiss micro-anatomist Albert von Kölliker suggested that the multinucleated cells observed on bone surfaces were responsible for bone resorption and named these cells 'osteoklasts' (which remains the spelling in German) from the Greek for 'bone" and "destroy/break" (Grob, 2011; Vaananen *et al.*, 2000; Zaidi *et al.*, 1993). Osteoclasts are the only cells capable of excavating resorption pits in bone (they also resorb dentine and other calcified tissues), hence a cell that can perform this task is by definition an

osteoclast (Stenbeck and Horton, 2004; Wu *et al.*, 2008; Boyce, 2003; Raggatt and Partridge, 2010; Katagiri and Takahashi, 2002). Other cells in bone including osteoblasts, osteocytes, and inflammatory macrophages and tumour cells modulate the formation and activity of the osteoclasts; however, these cells do not resorb bone (with the exception of minor resorptive capability of osteocytes in their lacunae) (Sims and Martin, 2014; Kansara *et al.*, 2014; Katagiri and Takahashi, 2002; Roodman, 2004; Al-Dujaili *et al.*, 2011; Bonewald and Johnson, 2008). For example, invading metastatic tumours destroy bone, but this is performed by recruited osteoclasts not the tumour cells themselves (Chapter 1.6.2) (Mundy, 1997; Mundy, 1991; Roodman, 2004; Sterling *et al.*, 2011). This is an important observation clinically, as it has emerged that osteoclast inhibitory treatments can block tumour osteolysis (Chapter 1.6.3) (Sturge *et al.*, 2011; Steger and Bartsch, 2011; Guise, 2009). Osteoclasts are found on most bone surfaces, including the endosteal, trabecular and periosteal surfaces in primary spongiosa (Boyle *et al.*, 2003; Hakeda and Kumegawa, 1991). They can be arranged with osteoblasts into micro-anatomical structures called bone multicellular units (BMUs), which allows for effective coupling (Raggatt and Partridge, 2010; Jilka, 2003; Iqbal *et al.*, 2009). Osteoclasts in the BMUs excavate channels through bone to allow vascular and nerve penetration, which is followed by osteoblasts laying down osteoid (Raggatt and Partridge, 2010; Jilka, 2003). Aside from some pathological lesions such as giant cell tumours of bone and of tendon sheath, osteoclasts are not seen in the absence of bone (Darling *et al.*, 1997; Seethala *et al.*, 2004).

1.3.3.1 The Osteoclast Lineage

Osteoclasts form from hematopoietic progenitor cells of the monocyte-macrophage lineage, thus forming part of the mononuclear phagocyte system (Boyle *et al.*, 2003; Loutit and Nisbet, 1982; Ash *et al.*, 1980; Scheven *et al.*, 1986). A number of studies using lethally irradiated rodents showed that osteoclasts could be generated from transplanted bone marrow, and osteoclast-forming cells were present in the circulation (Walker, 1975b; Walker, 1975a). In the 1970s and 1980s studies of osteoclasts and mononuclear phagocytes of various types showed both phenotypic and histochemical similarities, which suggested that these cells shared the same lineage (Baron and Kneissel, 2013; Baron *et al.*, 1986). Comparison with cells of the mononuclear phagocyte system showed that they and mature osteoclasts and their mononuclear precursors all shared many cellular characteristics (Gordon and Taylor, 2005; Matsuo and Ray, 2004; Baron *et al.*, 1986). Furthermore, *in vitro* culture of peripheral blood

monocytes with M-CSF and RANKL resulted in the formation of mature and functional osteoclasts (Quinn *et al.*, 1998).

Another line of evidence, which indicates a close relationship between osteoclast progenitors and those of macrophages is the importance of M-CSF to both osteoclast and macrophage differentiation (Grasset *et al.*, 2010). The role of M-CSF in osteoclast formation is discussed in Chapter 1.5.1 but, briefly, bone marrow cells from M-CSF deficient (op^-/op^-) mice are deficient in macrophage lineage populations and are also incapable of differentiating into osteoclasts (Yoshida *et al.*, 1990; Ross, 2006; Suda *et al.*, 1999). These mice are osteopetrotic, meaning they have greatly increased bone mass due to the defects in osteoclast formation and function (Sobacchi *et al.*, 2013; Stark and Savarirayan, 2009). The mice also have very small bone marrow cavities for the same reason (Sobacchi *et al.*, 2013; Stark and Savarirayan, 2009). If the mice survive they can partially recover over time, possibly through the effects of IL-34, which is discussed more in Chapter 1.5.1 (Lin *et al.*, 2008). Osteopetrosis also occurs as a result of mutations in other important osteoclastic genes (Del Fattore *et al.*, 2008).

Phenotypic similarities between osteoclasts and macrophages include similar prominence of lysosomal organelles, their immunohistochemical profiles and structural processes including filopodia and lamepodia, which allow for motility (Athanasou and Quinn, 1990). More similarities include that both osteoclasts and macrophages are capable of phagocytosing particular material and have the ability to undergo fusion (Baron *et al.*, 1986; Pierce *et al.*, 1991; Alberts *et al.*, 2002; Marks, 1983; Sutton and Weiss, 1966; James *et al.*, 2010). Activated macrophages can undergo fusion *in vitro* and *in vivo*, for example to form foreign body giant cells, which are a type of macrophage polykaryon (Vignery, 2005; MacLauchlan *et al.*, 2009). In spite of the similarities between osteoclasts, macrophages and macrophage polykaryons, differences are very much evident including: macrophage inability to resorb bone, lack of formation of the ruffled border, lack of actin ring formation, the lack of calcitonin receptor (CTR) expression and peroxidise activity (Teitelbaum *et al.*, 1997; Vignery, 2005; Athanasou and Quinn, 1990; Steinman and Cohn, 1972). Other qualitative differences exist, for example osteoclasts express cathepsin K (Ctsk) and Dendritic cell-specific transmembrane protein (DC-STAMP) molecules, but do not usually express the F4/80 antigen (Figure 1.2) (Yagi *et al.*, 2005; Clover *et al.*, 1992; Hume *et al.*, 2002). The major specific differences noted above are generally associated with osteoclast function.

The current position is that hematopoietic stem cells in response to M-CSF undergo differentiation into macrophage- colony- forming units CFU-M, which are common precursor cells of macrophages and osteoclasts (Figure 1.2) (Asagiri and Takayanagi, 2007; Katagiri and Takahashi, 2002; Boyle *et al.*, 2003). Stimulation with RANKL causes these cells to express osteoclastogenic genes including those involved in fusion such as DC-STAMP (Boyle *et al.*, 2003; Katagiri and Takahashi, 2002; Asagiri and Takayanagi, 2007). The fusion of these CFU-M-derived cells in the presence of RANKL results in osteoclasts (Figure 1.2) (Boyle *et al.*, 2003; Katagiri and Takahashi, 2002; Asagiri and Takayanagi, 2007). RANKL driven expression of genes required for the osteoclast's resorptive ability including chloride channel 7 (ClCN7), tartrate resistant phosphatase (TRAP), β_3 integrins, acid pump subunit v-Atpv06d2, carbonic anhydrase II (CAR2) amongst others results in a fully mature and functional osteoclast (Figure 1.2) (Asagiri and Takayanagi, 2007; Katagiri and Takahashi, 2002; Boyle *et al.*, 2003; McHugh *et al.*, 2000).

1.3.3.2 Characteristics of Osteoclast Progenitors and Mature Osteoclasts

The earliest expressed osteoclast-associated markers in *in vitro* RANKL-exposed immature bone marrow-derived macrophages are matrix metalloproteinase-2 and -9 (MMP-2, -9) followed by the expression of TRAP and then CTR expression (Boyle *et al.*, 2003; Asagiri and Takayanagi, 2007; Katagiri and Takahashi, 2002). The sequential expression of TRAP followed by CTR has been shown in a 1,25-dihydroxyvitamin D_3 treated co-culture system of murine bone marrow cultures and osteoblasts (Lee *et al.*, 1995; Wada *et al.*, 1995). 1,25-dihydroxyvitamin D_3 induction of RANKL causes osteoclast differentiation with TRAP expression being followed chronologically by calcitonin receptor expression (Lee *et al.*, 1995; Wada *et al.*, 1995) (Figure 1.2). Consistent with their lineage of origin, osteoclast progenitor cells are present wherever monocytes or haemopoietic cells are present, including near bone surfaces as well as calcified cartilage at the growth plate, but they are also present at extra-skeletal sites (Katagiri and Takahashi, 2002; Boyle *et al.*, 2003). Osteoclast progenitors have also been directly demonstrated to be present within the circulating monocyte population and haematopoietic tissue and capable of forming bone resorbing osteoclasts when appropriately stimulated by co-culture with osteoblastic cells *in vitro* (Athanasou, 1996; Walker, 1975b; Walker, 1975a).
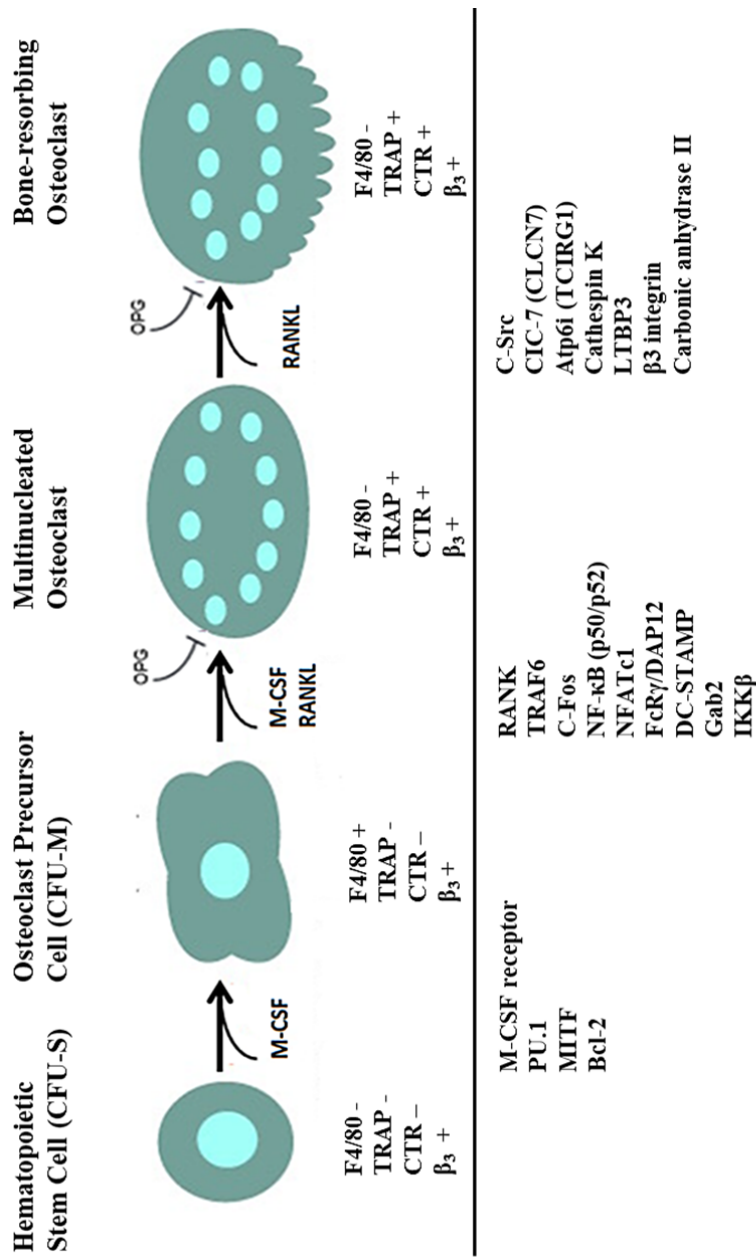
Figure 1.2 Osteoclast Progenitor Differentiation

In response to M-CSF stimulation, hematopoietic stem cells undergo differentiation into macrophage colony-forming units (CFU-M), which are the common precursor cells of macrophages and osteoclasts. Cell differentiation from CFU-M cells into multinucleated cells by cell-cell fusion is induced by RANKL inducing expression of molecules including DC-STAMP. M-CSF and RANKL induced expression of genes required for bone resorption occurs in the activation/ maturation stage. Molecules above the line are cell markers which are expressed at different stages of osteoclast differentiation. Molecules depicted under the line are stage specific molecules which are required for the differentiation and function of osteoclasts. Figure adapted from (Boyle *et al.*, 2003; Downey and Siegel, 2006).

Mature osteoclasts are characterized by their morphology, size and multinucleated phenotype (Roodman, 1991). Osteoclasts are large cells typically being between 10µm and 50µm across, although their size is variable and differs between species (Teitelbaum, 2007; Alberts *et al.*, 2002; Pierce *et al.*, 1991). The osteoclast has a high ratio of cytoplasm to nucleus (Lucht, 1972; Stenbeck, 2002). Human osteoclasts normally contain 10 to 20 nuclei while in comparison rodent and avian species have fewer (Athanasou and Sabokbar, 1999; Pierce *et al.*, 1991). Osteoclasts generally have a large cell body reflecting the fusion with a number of osteoclast precursors during the process of active osteoclast formation (Miyamoto, 2011). The purpose of osteoclast fusion is not fully clear, but it is believed to increase resorptive activity and permit deeper excavations of the bone matrix (Miyamoto, 2011; Yagi *et al.*, 2005; Lee *et al.*, 2006). vATP6V0d2, DC-STAMP and probably OC-STAMP are essential for osteoclast fusion (Xing *et al.*, 2012; Yagi *et al.*, 2005; Lee *et al.*, 2006). Mice deficient in DC-STAMP do not form multinucleated osteoclasts, and their bone resorption markers are low; however, functional mononuclear osteoclasts are present (Yagi *et al.*, 2005). These active mononuclear osteoclasts do exist *in vivo* and have been observed *in vitro* but are not considered common (Hattersley and Chambers, 1989). Osteoclasts also show distinctive long lamellipodia and filopodial processes that reflect their often high levels of motility (Alberts *et al.*, 2002; Jansen *et al.*, 2012). Chambers and colleagues have previously shown that osteoclast activity can be very rapid with overnight cultures of osteoclasts being able to resorb bone pits several micrometres deep and tens of micrometres long (Chambers *et al.*, 1984).

1.4 Bone Resorption

Osteoclasts have been estimated to resorb approximately 10% of the total adult bone mass each year (Asagiri and Takayanagi, 2007). As mentioned previously, the most common skeletal diseases in adults arise from excessive osteolytic activity that decreases bone mass impairing its structure and mechanical functions (Boyle *et al.*, 2003). Osteoclasts are highly specialised to break down bone and bone matrix at periosteal, trabecular and endosteal sites; however, they can also tunnel into compact bone (Hakeda and Kumegawa, 1991; Alberts *et al.*, 2002) . Bone tissue can be invaded by other cell types such as cancer cells, which have metastasized to the bone although this requires recruitment of osteoclasts to break down the bone (Tumber *et al.*, 2001; Mundy, 1997; Mundy, 1991; Weilbaecher *et al.*, 2011). For bone resorption to occur, a sequence of cellular events is needed (Vaananen *et al.*, 2000; Raggatt and Partridge, 2010). This sequence of events is collectively termed the resorption cycle and includes: migration of the osteoclast to the resorption site, its attachment to bone, polarization and formation of new membrane domains, dissolution of hydroxyapatite, degradation of organic matrix, removal of degradation products and lastly either apoptosis of the osteoclasts or their return to the non-resorbing state (Vaananen *et al.*, 2000; Raggatt and Partridge, 2010; Teitelbaum, 2000). Note that the term 'bone resorption' refers only to the activity of a mature functional osteoclast (Vaananen *et al.*, 2000). After resorption *in vivo*, under physiological circumstances, osteoblasts fill in the resorption pits with new bone matrix, which gradually becomes mineralised (Raggatt and Partridge, 2010; Clarke, 2008; Alberts *et al.*, 2002).

Once an osteoclast has migrated to a site of bone damage and adhered to the bone surface, it reorganises its membrane into four distinct domains: a sealing zone, a basolateral domain, apical or secretory domain and the ruffled border membrane (Vaananen *et al.*, 2000; Itzstein *et al.*, 2011; Takahashi *et al.*, 2007; Vaananen and Laitala-Leinonen, 2008). Osteoclasts rearrange their membranes through polarization of the osteoclast plasma membrane (Vaananen *et al.*, 2000; Itzstein *et al.*, 2011). Whilst ultrastructural studies have shown that osteoclasts engaged in resorbing bone are highly polarized cells, non-resorbing osteoclasts are not polarized (Vaananen and Horton, 1995; Zhao *et al.*, 2001). These membranes or domains are associated with different vesicle pathways and the resorptive cycle (Vaananen *et al.*, 2000). At a remodelling site, osteoclasts attach strongly to the bone surface through the sealing zone (Vaananen *et al.*, 2000; Raggatt and Partridge, 2010; Teitelbaum, 2000; Stenbeck, 2002). This occurs through the formation of a specific membrane domain between

the plasma membrane of the osteoclast and the bone surface (sealing zone) (Vaananen *et al.*, 2000; Suda *et al.*, 1997; Raggatt and Partridge, 2010). The sealing zone creates a quartered off resorption site, which does not allow escape of osteoclast secretions (acid and proteolytic enzymes) to affect the surrounding bone matrix (Vaananen *et al.*, 2000; Suda *et al.*, 1997; Raggatt and Partridge, 2010). The sealing zone is rich in filamentous actin (F-actin), which arranges into plasma membrane extensions called podosomes, and forms an actin ring around the ruffled border membrane (discussed below) (Suda *et al.*, 1997; Schlesinger *et al.*, 1997; Kanehisa *et al.*, 1990; Teitelbaum, 2000).The actin rings lying above the sealing zone are directly related to the osteoclast's resorptive activity, i.e., they indicate that an osteoclast is engaged in excavating a pit (Suda *et al.*, 1997). The molecular interactions which occur between the osteoclast and bone matrix to enable such sealing is not fully clear but involves integrin $\alpha_v\beta_3$ receptor (vitronectin receptor [VNR]) mediated adhesion to exposed arginine-glycine-aspartic acid (RGD) sites on the bone matrix (Figure 1.3) (Raggatt and Partridge, 2010; Li *et al.*, 2006). These RGD motives are cell adhesions sites to which adhesive proteins including integrins bind (Ruoslahti, 1996). The sealing zone also contains cytoskeletal molecules vinculin, talin, and α-actin, which connect the β-tails of integrins to the osteoclast's cytoskeleton (Teitelbaum, 2000). McHugh *et al*. (2000) showed that integrin β_3 null mice have osteoclasts but the osteoclasts do not spread or form actin rings resulting in decreased resorption. Morphological studies suggest the basal membrane is the homogenous membrane region (Vaananen *et al.*, 2000). In contrast, the apical domain is a functional secretory domain in osteoclasts (Vaananen *et al.*, 2000; Itzstein *et al.*, 2011). Nesbitt and Horton (1997) and Salo *et al*. (1997) both showed that the apical membrane is where the exocytosis of resorbed and transcytosed matrix degradation products occurred (Nesbitt and Horton, 1997; Salo *et al.*, 1997). The ruffled border is present within the sealing zone interfacing the bone undergoing resorption, and is one of the key characteristics of active mature osteoclasts on a bone or calcified surface (Figure 1.3) (Teitelbaum, 2000; Schlesinger *et al.*, 1997; Stenbeck, 2002; Ross and Teitelbaum, 2003). The ruffled border is a critical resorbing organelle (Schlesinger *et al.*, 1997; Yang *et al.*, 2012) It is similar to late endosomal membranes having high concentrations of the GTPase Rab7 proteins, v-type-H-ATPase proton pumps and glycosylated intrinsic protein of lysosomal membranes 110 (Igp110) (Palokangas *et al.*, 1997; Bucci *et al.*, 2000; Granger *et al.*, 1990). Structurally, it consists of deeply folded projections of an osteoclast's plasma membrane, which are fused

A.
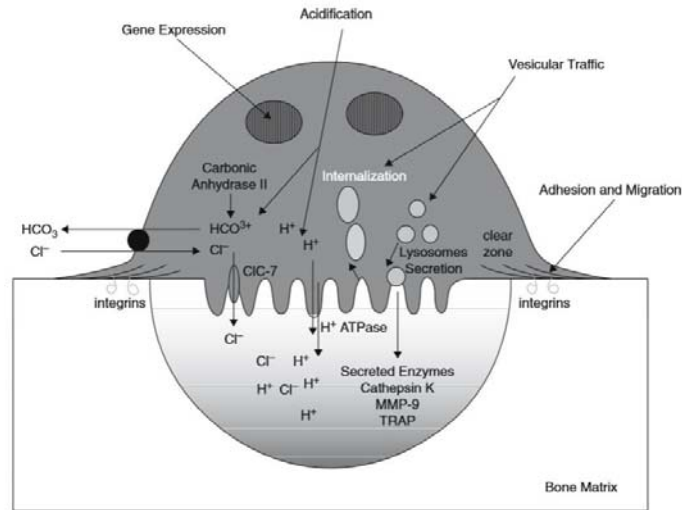
B.
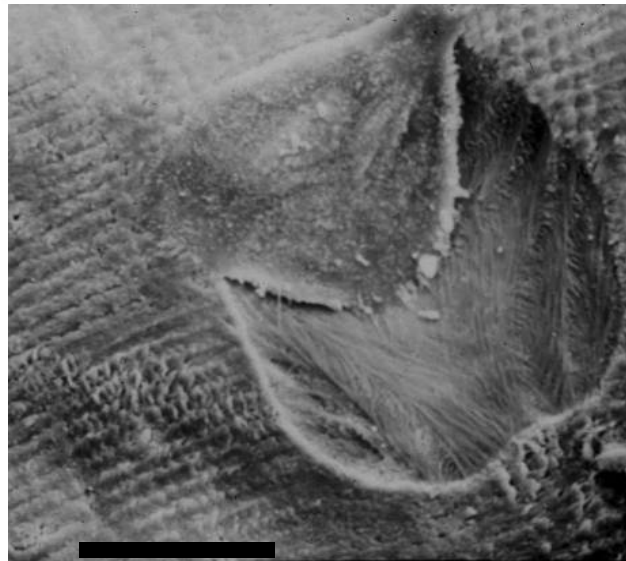
Figure 1.3 Osteoclast Mediated Bone Resorption
(A.) Schematic of a polarized osteoclast resorbing bone. Once an osteoclast has
migrated to a site of bone damage, it starts the process of resorption. First it seals off a
sealing zone area, which is called Howship's Lacuna. This region is acidified by the
pumping of protons and chloride ions through the v-ATPase proton pump and the chloride
channel 7 (ClC7), respectively, which are present in the osteoclast's ruffled border. The
protons and Cl⁻ ions mobilize the inorganic phase of the bone and cause the activation of
Ctsk and TRAP, which break down the collagen fibres. Figure sourced from (Baron and
Horne, 2005). **(B.)** Transmission electron micrograph of an actively resorbing osteoclast
derived from human giant cell tumour of bone. Scale bar - 100µm. Image courtesy of Dr.
Julian Quinn.

with intracellular acidic vesicles (Figure 1.3) (Schlesinger *et al.*, 1997; Stenbeck, 2002; Yang *et al.*, 2012). Therefore, the ruffled border is associated with the secretion of acid (H$^+$ ions) and proteolytic enzymes, which breaks down the hydroxyapatite material (Schlesinger *et al.*, 1997; Stenbeck, 2002). Hydrogen ions are secreted into the sealed zone through the acidifying proton pump v-ATPase, which is expressed on the surface of ruffled membrane (Figure 1.3) (Vaananen *et al.*, 2000; Schlesinger *et al.*, 1997; Stenbeck, 2002; Yang *et al.*, 2012).

The proton pump is divided into two functional domains, V$_1$ and V$_0$ (Qin *et al.*, 2012). The V$_1$ and V$_0$ subunits isoforms expressed by osteoclasts vary but are commonly a3 and d2, respectively (Matsumoto *et al.*, 2014). Inhibition of the v-ATPase pump suppresses the acidification of the sealing zone resulting in decreased bone resorption (Visentin *et al.*, 2000; Laitala and Väänänen, 1994). Interestingly, deletion of the v-ATPase V0d2 (Atp6v0d2) subunit in mice results in poor osteoclast activity and, similar to mice lacking DC-STAMP, osteoclast, fusion is perturbed (Lee *et al.*, 2006; Walsh and Choi, 2014). This suggests that the Atp6v0d2 isoform is involved in the fusion of mononuclear osteoclasts as noted before (Lee *et al.*, 2006; Wu *et al.*, 2009). The ruffled border also contains chloride channel ClC7 proteins that pump chloride (Cl$^-$) into the resorption cavity (Figure 1.3) (Stenbeck, 2002). After the osteoclast has formed its sealing zone, its plasma membrane polarized and the formation of the ruffled border, the next stage of resorption is the degradation of bone matrix (Figure 1.3) (Raggatt and Partridge, 2010; Teitelbaum, 2000). The area of bone, which the osteoclast breaks down under the sealing zone is the resorption pit or, more formally, the Howship's lacuna (Figure 1.3) (Raggatt and Partridge, 2010). Secretion of H$^+$ and Cl$^-$ ions acidifies and mobilizes the inorganic phase of bone (Figure 1.3) (Stenbeck, 2002; Clarke, 2008; Czupalla *et al.*, 2006). Thirdly, the organic matrix is broken down by the actions of lysosomal enzyme, cathepsin K (and probably other cathepsins) that retains activity at low pH (Figure 1.3) (Teitelbaum, 2000; Vaananen and Laitala-Leinonen, 2008; Clarke, 2008). In addition, MMP-9 and MMP-2 that are produced in abundance by osteoclasts may also play a role in removing some matrix; however, studies to date have shown that they are not essential to degrade organic matrix (Teitelbaum, 2000; Vaananen and Laitala-Leinonen, 2008). Another cellular factor involved in bone resorption is TRAP, which is active at acidic pH 5 (Stenbeck, 2002). The function of TRAP in osteoclast actions is unclear as its deletion does not greatly affect bone resorption; however, a role for TRAP has been suggested in transcytosis and breakdown of collagen fragments (Halleen *et al.*, 1999). After the osteoclasts

have finished resorbing the bone matrix, the remaining debris present in the resorption lacuna is removed through a transcytotic vesicular pathway (Nesbitt and Horton, 1997; Vaananen *et al.*, 2000; Salo *et al.*, 1997).

The debris is removed from the ruffled border to the functional secretory domain, the apical domain, which is where the breakdown products are released into the extracellular space (Vaananen *et al.*, 2000; Nesbitt and Horton, 1997; Salo *et al.*, 1997; Pavlos *et al.*, 2005). Halleen *et al.* reported that TRAP was localized to transcytotic vesicles in the apical membrane and through its generation of reactive oxygen species is able to break down collagen (Halleen *et al.*, 1999). The Rab3 protein, which has a role in exocytosis in a number of cells has been shown to important for osteoclast activity (Pavlos *et al.*, 2005). Pavlos *et al.* (2005) suggested that the Rab3 protein regulates a trafficking step in osteoclasts that comes after the trans-golgi network. After transcytosis occurs, the osteoclast can either move on to a new area of bone to resorb or undergo apoptosis (Nesbitt and Horton, 1997).

1.5 Osteoclastogenesis: Osteoclast Differentiation Pathways

As mentioned earlier osteoclasts are tissue-specific macrophage polykarons, which differentiate from haemopoietic cells that have themselves differentiated into bone marrow monocyte/macrophage precursor cells (Alberts *et al.*, 2002; Boyle *et al.*, 2003; Nakamura, 2007; Asagiri and Takayanagi, 2007). Bone marrow macrophages present on or near the surface of bone differentiate into pre-osteoclasts, called CFU-GM followed by further differentiation into a mature and active osteoclast (Figure 1.2) (Boyle *et al.*, 2003). This differentiation process, osteoclastogenesis, depends upon the received signals from local cells in the bone microenvironment (Boyle *et al.*, 2003). Osteoclast formation *in vitro* was originally modelled by co-culture systems employing either stromal cells or osteoblasts with haemopoietic cells from the spleen (Boyle *et al.*, 2003; O'Brien, 2010; Takahashi *et al.*, 1988a). Multinucleated and TRAP positive cells capable of resorbing pits were formed from mouse marrow cells cultures in the presence of osteotropic factors including 1,25-dihydroxyvitamin D_3 [$1\alpha,25$-$(OH)_2D_3$] and human PTH and prostaglandin E_2 (PGE_2) (Takahashi *et al.*, 1988b). It was noted that TRAP positive multinucleated cells were only found near cells expressing ALP, which were proposed to be osteoblast cells (Takahashi *et al.*, 1988b). Takahashi *et al.* 1988 went on to show that the interaction between stromal osteoblasts and bone marrow cell types was required for osteoclast differentiation (Takahashi

et al., 1988a; Takahashi *et al.*, 1988b; Boyle *et al.*, 2003; Udagawa *et al.*, 1990). This suggested that stromal-derived factors stimulate osteoclastogenesis (Takahashi *et al.*, 1988a; Boyle *et al.*, 2003; Asagiri and Takayanagi, 2007). Subsequently, it was determined that the stromal cells produce RANKL, which acts in concert with M-CSF to specifically drive osteoclast differentiation (Boyle *et al.*, 2003; Asagiri and Takayanagi, 2007; Katagiri and Takahashi, 2002). These factors bind to their respective receptors present on the membrane of osteoclast precursor cells (Katagiri and Takahashi, 2002; Teitelbaum, 2000; Boyle *et al.*, 2003). Both M-CSF and RANKL are required for osteoclast differentiation and for functional, mature osteoclasts *in vivo*, although IL-34 can substitute for M-CSF (Cappellen *et al.*, 2002; Raggatt and Partridge, 2010; Lin *et al.*, 2008; Asagiri and Takayanagi, 2007). These factors act to differentiate bone marrow precursor cells into active osteoclasts by the induction of osteoclastic gene expression (Boyle *et al.*, 2003; Cappellen *et al.*, 2002; Ross and Teitelbaum, 2003). Although these two factors are essential for osteoclast differentiation, there are many other factors which regulate the process of osteoclastogenesis and osteoclast activation (Boyle *et al.*, 2003). In addition, direct interaction of osteoclast precursors with damaged bone sites has been shown to regulate osteoclast differentiation(McHugh *et al.*, 2010). M-CSF and RANKL are discussed in detail below. The identification of these molecules has enabled the osteoclast differentiation process to be studied in detail using many of the cell culture techniques employed in the projects described in this thesis.

1.5.1 M-CSF

M-CSF, which is also called colony-stimulating factor-1 (CSF-1), stimulates the survival, proliferation and differentiation of early osteoclast precursors that are immature members of the monocytes/macrophage lineage (Ross, 2006; Datta *et al.*, 1992). As noted above, *op⁻/op⁻* mice lacking M-CSF form no or only very small numbers of osteoclasts, but injecting M-CSF into these mice restores osteoclast formation (Felix *et al.*, 1990; Kodama *et al.*, 1991b; Yoshida *et al.*, 1990; Hattersley *et al.*, 1991). Similar results were obtained *in vitro* with *op⁻/op⁻* bone marrow (Takahashi *et al.*, 1991; Kodama *et al.*, 1991a). Together this evidence demonstrates M-CSF is a necessary factor required for osteoclast differentiation (Katagiri and Takahashi, 2002; Kodama *et al.*, 1991a).

M-CSF, secreted by bone marrow stromal cells in the bone microenvironment, binds to its receptor c-FMS (Ross, 2006; Suda *et al.*, 1999). C-Fms, is a receptor tyrosine kinase (Ross, 2006). The c-FMS alternative ligand IL-34 also exerts the same influence as M-CSF on *c-*

Fms^{+} cells, although IL-34 is expressed little if at all in bone (Datta *et al.*, 1992; Ross, 2006; Lin *et al.*, 2008). Mice that lack the *c-Fms* gene also show a similar phenotype as the *op⁻/op⁻* mice but more severe (Ross, 2006). M-CSF binding to c-Fms causes its dimerization, activation and autophosphorylation upon specific tyrosine residues (Ross, 2006; Datta *et al.*, 1992). These phosphorylated tyrosine residues are binding sites for SH2 or PTB domain containing proteins, which transduce the signal downstream resulting in osteoclast precursor proliferation and survival (Ross, 2006).

1.5.2 Tumour Necrosis Factor Family Members RANKL, RANK and OPG

The discovery and characterization of Tumour Necrosis Factor (TNF) receptor ligand family members: osteoprotegerin (OPG), receptor activator of Nuclear Factor κ B Ligand (RANKL), and receptor activator of Nuclear Factor κ B (RANK) in the late 1990s showed how osteoblast lineage cells are able to regulate and drive the formation of osteoclasts from monocytic/macrophage progenitors (Simonet *et al.*, 1997; Yasuda *et al.*, 1998b; Odgren *et al.*, 2003; Lacey *et al.*, 1998; Wong *et al.*, 1997; Dougall *et al.*, 1999).

1.5.2.1 Osteoprotegerin

Osteoprotegerin (OPG) was first discovered by Simonet *et al.* (1997) by screening transgenic mice over-expressing cDNA of different TNF receptor molecules in an attempt to identify TNF-related molecules with therapeutic potential (Katagiri and Takahashi, 2002; Simonet *et al.*, 1997). Due to the bone phenotype of mice overexpressing this factor it was named osteoprotegerin, a Greek/French portmanteau meaning 'bone protector'; in the TNFR nomenclature it is TNFR11B, which is also the coding gene name (Simonet *et al.*, 1997). Human OPG protein is 60kDa protein that exists as a 120kDa dimer (Hofbauer *et al.*, 2000). Each monomer has an N-terminal TNFR domain, a putative death-domain like region and a C-terminal terminal dimerization motif (Hofbauer *et al.*, 2000). OPG is expressed by various stromal cell lines including primary human marrow stromal cells, osteosarcoma cell lines and primary murine osteoblasts (Hofbauer *et al.*, 2000). OPG has also been implicated in the coupling process with the murine promoter of OPG having a response element for the osteoblast differentiation transcription factor Runx2 (Hofbauer *et al.*, 2000). OPG production is regulated by osteolytic factors including calcitropic hormones and cytokines including dexamethasone, $1,25(OH)_2D_3$, Interleukin-1β, (IL-1β), IL-11, Tumour Necrosis Factor-α (TNF-α), PTH, PGE_2 and Transforming Growth Factor-β (TGF-β) (Hofbauer *et al.*, 2000).

Mice lacking OPG (*Tnfr11b*) have very high osteoclast numbers with correspondingly high bone resorption and low bone mass, while transgenic mice overexpressing OPG *(Tnfr11b)* have very high bone density and volume due to low numbers of osteoclasts (Yasuda *et al.*, 1998a; Simonet *et al.*, 1997). In osteoblast and bone marrow co-cultures, recombinant OPG inhibits osteoclastogenesis induced by $1,25(OH)_2D_3$, PTH, PGE_2 and IL-11 (Yasuda *et al.*, 1998b). Concomitantly, injected recombinant OPG increases bone density and reduces osteoclast numbers in mice (Yasuda *et al.*, 1998b).

1.5.2.2 RANKL

RANKL is a type II transmembrane protein expressed on the membrane surface of osteoblasts and osteocytes; however, RANKL is also present in soluble form (Boyle *et al.*, 2003; O'Brien, 2010; Walsh and Choi, 2014). Soluble RANKL is achieved by either proteolytic cleavage of its transmembrane domain or alternative gene splicing (Boyle *et al.*, 2003; O'Brien, 2010). RANKL (TNF family nomenclature: TNFSF11) was first discovered for its role in T cell immunity (Wong *et al.*, 1997). Wong and colleagues were the first to describe RANKL (calling it TRANCE) in an attempt to identify dendritic cell apoptosis-regulatory factors using a somatic cell genetic approach in T cell hybridomas (Wong *et al.*, 1997). The isolated protein was characterized to be a type II membrane protein of 316 amino acids (35 kDa estimated molecular mass) expressed in the thymus, lymph nodes (not in non-lymphoid tissues) and in T cells (Wong *et al.*, 1997). The human form of RANKL was found by cross-hybridisation experiments of mouse cDNA against a human thymus library (Wong *et al.*, 1997). Subsequently, RANKL was confirmed to be the binding partner of RANK (its membrane bound receptor) and of OPG, which acts as a decoy receptor for RANKL (Boyle *et al.*, 2003; Walsh and Choi, 2014).

RANKL expression and production on bone stromal cells and osteoblasts *in vitro* and *in vivo* is induced by osteotropic factors and hormones that induce bone resorption consistent with observations with the co-culture models (Katagiri and Takahashi, 2002; Boyle *et al.*, 2003). Osteotropic factors and hormones including $1,25(OH)_2D_3$, PTH, and PGE_2 increase RANKL expression in osteoblasts, which is again consistent with the actions of these factors to indirectly induce osteoclast formation through the mediation of osteoblasts and related cells (Yasuda *et al.*, 1998b; Suda *et al.*, 1999; Takahashi *et al.*, 1999; Lacey *et al.*, 1998). Recombinant RANKL has also been shown to drive osteoclast formation *in vitro* and *in vivo* in the presence of M-CSF, confirming its role in osteoclastogenesis (Lacey *et al.*, 1998;

Yasuda *et al.*, 1998b; Kikuta *et al.*, 2013). Furthermore, human osteoclasts were formed from RANKL and M-CSF stimulated peripheral blood mononuclear cells (Matsuzaki *et al.*, 1998; Quinn *et al.*, 1998). Mice that lack RANKL are severely osteopetrotic with no tooth eruption, markedly reduced skeletal growth and growth plate chondrodystrophy (Odgren *et al.*, 2003). Transgenic rescue of these RANKL null mice induced osteoclastogenesis with TRAP positive cells being identified (Odgren *et al.*, 2003). In addition, the transgenic rescue led to lamellar bone production in the diaphyses of long bones, restored marrow space and the identification of osteoclasts on many endosteal sites; however, the rescue was not complete i.e., no tooth eruption was seen and highly sclerotic bone epiphyses remained (Odgren *et al.*, 2003). Bone tissue samples from 6 human patients with autosomal recessive osteopetrosis, due to mutations in the *RANKL* gene, lacked osteoclasts (Sobacchi *et al.*, 2007). Treating peripheral blood monocytes obtained from these individuals with recombinant RANKL induced osteoclast differentiation *in vitro* (Sobacchi *et al.*, 2007). Moreover, in a serum transfer model of arthritis, RANKL null mice exhibited osteopetrosis and were protected from bone erosion (Pettit *et al.*, 2001).

RANKL expression in bone is also regulated by a number of key hormones/cytokines including the IL-6/glycoprotein130-mediated family members (notably IL-11 and oncostatin M [OSM]) and inflammatory cytokines such as IL-1 and TNFα (Boyle *et al.*, 2003; Kim *et al.*, 2009; Jules *et al.*, 2012; Bezerra *et al.*, 2005). These factors, thereby, indirectly promote osteoclast formation where osteoclast progenitors and osteoblasts are present together (Katagiri and Takahashi, 2002; O'Brien, 2010). In addition, treatment of bone marrow cell and primary osteoblast co-cultures with compounds, which increase intracellular calcium or calcium levels in the culture media increases the RANKL mRNA expression in osteoblasts *in vitro*. Many other factors have also been found to modulate RANKL stimulatory effects (Quinn *et al.*, 2001; Katagiri and Takahashi, 2002). A small number of hormones, including TNF-α and TGFβ family members can enhance RANKL actions (Quinn *et al.*, 2001; Mundy, 2007; Pacifici *et al.*, 1991). TNF-α in particular has been shown to induce osteoclastogenesis in a RANKL independent manner in both RANKL$^{-/-}$ and RANK$^{-/-}$ cells *in vitro* although this does not happen *in vivo* without other gene deletions (Kim *et al.*, 2005b). TGF-β can increase RANKL actions on osteoclast precursors but negatively affects RANKL expression by osteoblasts, making its actions complex (Quinn *et al.*, 2001). Interestingly, activated TGF-β is released during osteoclast mediated bone resorption; however, the full implications of this is not known (Dallas *et al.*, 2002; Quinn *et al.*, 2001; Kim *et al.*, 2005b). Another molecule that

has complex actions on RANKL and osteoclastogenesis is interferon -γ (IFNγ) (Katagiri and Takahashi, 2002; Gao *et al.*, 2007). In the absence of osteoblasts, IFNγ directly inhibits osteoclast progenitor differentiation but through indirect actions upon osteoblasts causes the secretion of RANKL and TNFα from activated T cells (Kohara *et al.*, 2011; Gao *et al.*, 2007).

Pathological conditions such as inflammation and bone metastasis invasion of bone are associated with increased RANKL expression and osteoclastogenesis through the upregulation of inflammatory cytokines such as IL-1, IL-11, TNFα and osteotropic factors such as Parathyroid hormone-related protein (PTHrP) (Gupta and Massagué, 2006; Mundy, 2002; Thomas *et al.*, 1999; Bezerra *et al.*, 2005; Weitzmann, 2013). A number of factors produced by osteoclasts themselves act in an autocrine action to affect the outcome of RANKL induction (Layh-Schmitt *et al.*, 2013; Boyle *et al.*, 2003). One example is interferon-β, which is induced by RANKL treatment itself and has been suggested to form a negative feedback signal limiting osteoclast formation (Layh-Schmitt *et al.*, 2013).

OPG moderates the stimulatory effects of RANKL by acting as a decoy receptor by blocking its interactions with the RANK receptor (Boyle *et al.*, 2003; Yasuda *et al.*, 1998b; Takahashi *et al.*, 1999). Factors, which stimulate osteoclast formation including PTH, $1,25(OH)_2$-D_3 and glucocorticoids increase RANKL expression whilst decreasing OPG production (Khosla, 2001). Likewise factors, which influence osteoclast differentiation such as TGF-β and estrogen increase OPG levels in bone cells (Khosla, 2001). The generally inverse relationship between RANKL and OPG regulation is highlighted in pathological bone diseases (Grimaud *et al.*, 2003). This is supported by observations of RANKL and OPG mRNA expression in clinical specimens of giant cell tumours (Atkins *et al.*, 2000). Giant cell tumours of bone (osteoclastomas) are rare cancers, which arise in the bone and cause severe bone loss (Atkins *et al.*, 2000). Within these tumours are large multinucleated cells that are morphologically and functionally osteoclasts, but they are not the neoplastic component of the tumour (Atkins *et al.*, 2000). Patient mRNA samples of giant cell tumours have shown that they have greatly increased RANKL compared to OPG (Atkins *et al.*, 2000). The ratio of RANKL:OPG in human tissues from patients presenting with osteolysis from various bone aetiologies was severely skewed in favour of RANKL (Grimaud *et al.*, 2003). The inverse relationship of RANKL:OPG may break down in some diseases such as rheumatoid arthritis due to the effects of other factors that modulate osteoclast formation (Collin-Osdoby, 2004). This

inverse relationship is also seen in periprosthetic osteolysis where RANKL levels are increased and OPG levels are decreased (Haynes *et al.*, 2001). It should be noted that RANKL and OPG mRNA expression has to date been found to correlate with their respective protein expression, at least in bone cells (Singh *et al.*, 2012).

1.5.2.3 RANK

RANK (TNFRSF11A) is a type I transmembrane receptor of the TNF receptor family, which binds to RANKL (Anderson *et al.*, 1997; Boyce, 2003; Mellis *et al.*, 2011). RANK is encoded by 616 and 625 amino acids in humans and mice, respectively, and when activated forms a trimer complex (Kuroda and Matsuo, 2012; Mellis *et al.*, 2011). RANK is expressed on the surface membrane of osteoclasts, their progenitor and precursor cells, dendritic cells and macrophages, as well as a number of extraosseous cells such as breast epithelium (Dougall *et al.*, 1999; Palafox *et al.*, 2012; Mellis *et al.*, 2011). Additionally, RANK is expressed on the surface of a number of breast and prostate cancer cell lines and may have a role in targeting cancer cells to metastasize to bone (Casimiro *et al.*, 2013). In 1999, RANK was confirmed to be the sole receptor by which RANKL mediates its osteoclastogenic effects (Dougall *et al.*, 1999; Li *et al.*, 2000). Mice, which lacked RANK were shown to completely lack osteoclasts and display severe osteopetrosis (Dougall *et al.*, 1999). Consistent with this, transfecting a RANKL expressing DNA construct into RANK null haemopoietic progenitors restored osteoclastogenesis in the presence of RANKL and M-CSF (Dougall *et al.*, 1999). These RANK null mice therefore resemble the osteopetrotic RANKL null mice (Dougall *et al.*, 1999). Interestingly, the co-crystal structure of the RANK-RANKL complex has indicated a tight binding between the ligand and its receptor (Mellis *et al.*, 2011). This tight binding suggests that amino acid substitutions, even a gene point mutation, may have dramatic effects in biological function (Mellis *et al.*, 2011). These studies show that RANKL and RANK expression in the relevant cell types are both necessary and sufficient for osteoclast formation, aside from the requirement of osteoclast progenitors for M-CSF stimulation.

Like all TNF receptors, RANK intracellular cytoplasmic domains lack intrinsic kinase activity and require the recruitment of adaptor proteins to mediate downstream signalling (Boyce and Xing, 2007; Walsh and Choi, 2014). RANKL binding to RANK recruits intracellular adaptor proteins of the TNF receptor-associated factors (TRAFs) family (1-7 members) (Boyce and Xing, 2007; Boyle *et al.*, 2003; Asagiri and Takayanagi, 2007). TRAFs

1, 2, 3, 5 and, in particular, TRAF6 have a role in RANK signalling (Boyle *et al.*, 2003; Walsh and Choi, 2014; Boyce and Xing, 2007; Katagiri and Takahashi, 2002; Feng, 2005). TRAF6 recruitment to the C-terminal domain of RANK cytoplasmic tails initiates the signalling cascades associated with osteoclast formation (Figure 1.4) (Kuroda and Matsuo, 2012; Walsh and Choi, 2014; Boyce and Xing, 2007). Other intracellular adaptors, which have been shown to modulate RANK signalling include: TGF-β activating kinase 1 (TAK1), TAK1 binding protein 1 (TAB1), TAK1 binding protein 2 (TAB2), Grb2-associated binding protein 2 (GAB2), epidermal growth factor receptor (EGFR), four-and-a-half LIM domain 2 (FHL2), Lyn, cylindromatosis (CYLD) deubiquitinase and TRAF family member-associated NFκB activator (TANK) (Walsh and Choi, 2014). In addition, RANK regulates calcium fluxes, which are important to osteoclast formation (Walsh and Choi, 2014). Regulation of RANK mRNA or protein has not convincingly been shown to play a major role in regulating osteoclast formation. Rather, most influences on osteoclast formation appear to be exerted on signal pathways, such as that involving nuclear factor of activated T cells 1 (NFATc1), which are downstream of RANK.

1.5.3 RANK Signalling Pathways Influencing Osteoclast Formation

Both in osteoclast lineage cells and in other RANK-expressing cell types, pathways involved in RANK signalling include: nuclear factor kappa B (NFκB) c-jun N-terminal kinase (JNK), p38, extracellular signal- related kinases (ERK1/2) and Src-dependent pathways, although there are likely to be other significant pathways involved that are also involved (Figure 1.4) (Boyle *et al.*, 2003; Katagiri and Takahashi, 2002; Asagiri and Takayanagi, 2007). Some of these pathways are not critical to osteoclast formation but do influence osteoclast activity and survival such as Extracellular Signal-Related Kinase-1 and -2 (ERK1/2) and Proto-oncogene protein tyrosine kinase SRC (C-SRC) (Boyce and Xing, 2007). RANK-mediated activation of these intracellular signalling pathways leads to the increased expression and or activation of transcription factors, which are important for the control of osteoclast maturation, survival and activity (Boyle *et al.*, 2003; Feng, 2005). As reviewed by Boyle *et al.*, transcription factors and signalling molecules particularly important in regulating osteoclastogenesis include NFκB, Activator-Protein 1 (AP-1), NFATc1, p38, PU.1 and Microphthalmia-Associated Transcription Factor (MITF) (Boyle *et al.*, 2003; Feng *et al.*, 2009; Asagiri and Takayanagi, 2007). These transcription factors form complexes, which bind gene promoter motifs driving expression of many proteins essential for osteoclast function (Asagiri and Takayanagi, 2007; Boyle *et al.*, 2003; Sharma *et al.*, 2007). In this thesis the effect of cell

stressors, mainly cancer therapeutics, upon the activation, transcriptional activation and protein levels of osteoclast transcription factors and signalling proteins NFκB, NFATc1, p38 and MITF are studied.

As mentioned above, RANK activation, by RANKL binding, causes the recruitment of adaptor proteins TRAFs and, in particular, TRAF6 to the cytoplasmic tail of RANK (Figure 1.4) (Boyle *et al.*, 2003; Katagiri and Takahashi, 2002; Asagiri and Takayanagi, 2007). TRAF6 mediates signals from only one other TNFR family member, CD40, but it is also involved in signals emanating from IL-1R and TLR family members (Lomaga *et al.*, 1999). TRAF6 has three binding sites on RANKs cytoplasmic tail including a membrane-proximal Pro-X-Glu-X-X- binding motif. Knockout studies in mice suggest that TRAF6 is critical for osteoclast formation with TRAF6 knockout mice having severe osteopetrosis (Asagiri and Takayanagi, 2007; Walsh and Choi, 2014; Mellis *et al.*, 2011). Initially, it was thought that TRAF6 knockout mice were osteopetrotic due to a lack of osteoclast activity; however, many further studies have provided evidence for the osteoclast differentiation role of TRAF6 in TRAF6$^{-/-}$ osteopetrotic mice (Asagiri and Takayanagi, 2007; Boyce and Xing, 2007). TRAF-2, -3 and -5 also bind to the cytoplasmic tail of RANK at membrane distal sites; however, site directed mutagenesis of their binding sites has shown that these TRAFs do not affect osteoclast formation to a large degree (Asagiri and Takayanagi, 2007; Mellis *et al.*, 2011). Upon binding to RANK, TRAF6 trimerizes and recruits transcription factors and proteins in signalling complexes from which RANK downstream signalling occurs (Asagiri and Takayanagi, 2007; Boyle *et al.*, 2003). Transcription factors and signalling proteins involved in osteoclastogenesis including NFκB and the c-FOS subunit of AP-1 are recruited into this protein scaffold with RANK and TRAF6 (Boyle *et al.*, 2003; Takayanagi, 2008b). Other members of this signalling scaffold include atypical protein kinase C (aPKC), TAK1/2 binding proteins and TGFβ-activating kinase (TAK1) (Feng, 2005; Asagiri and Takayanagi, 2007; Mellis *et al.*, 2011).

1.5.3.1 NFκB Signalling

Formation of the RANK, TRAF6 and TAK1 signalling complex results in the activation of NFκB, which is one of the earliest events of RANK signalling (Takayanagi, 2008a; Kuroda and Matsuo, 2012; Armstrong *et al.*, 2008). NFκB is a transcription factor, which has an important role in regulating osteoclast formation, function, and survival (Soysa and Alles, 2009). NFκB1 (p100) and NFκB2 (p105) are synthesized as long precursor molecules, which

are shortened to p52 and p50, respectively, by post-translational modifications (Soysa and Alles, 2009; Boyce *et al.*, 2010). Typically, these molecules do not activate the transcription of genes unless they associate with subfamily of REL proteins, REL A (p65), REL B and c-REL, which contain transcriptional activation domains (Soysa and Alles, 2009; Asagiri and Takayanagi, 2007). Normally, NFκB is present as a dimer of p65/p52 within the cytoplasm, and this is complexed to IκB, which inhibits its activity (Soysa and Alles, 2009; Boyce *et al.*, 2010). The role of the p65/p50 dimer NF-κB in osteoclast formation was discovered through knockout studies in mice (Soysa and Alles, 2009; Boyce *et al.*, 2010). The double-knockout (dKO) of p50 and p52 in mice causes them to have severe osteopetrosis, and the mice are unable to form osteoclasts (Franzoso *et al.*, 1997; Iotsova *et al.*, 1997). In contrast, single knockouts of either p50 or p52 do not cause osteopetrosis, and osteoclasts can still form (Franzoso *et al.*, 1997). NFκB can be activated by two pathways, the canonical and non-canonical pathways (NFκB1 and NFκB2, respectively) (Soysa and Alles, 2009; Asagiri and Takayanagi, 2007) The canonical pathway depends upon IκB phosphorylation (Asagiri and Takayanagi, 2007; Soysa and Alles, 2009). Phosphorylation of IκB targets it for ubiquitin-tagged degradation, resulting in its displacement from the p50/p52 NFκB complex (Soysa and Alles, 2009). This allows for the p50 and p52 containing NFκB to bind to any of the REL proteins such as p65 and become a functionally active trimer (Asagiri and Takayanagi, 2007; Soysa and Alles, 2009). TRAF6 has a role in activating NFκB through its canonical pathway (Figure 1.4) (Asagiri and Takayanagi, 2007; Mellis *et al.*, 2011). The formation of the signalling complex containing RANK, TRAF6, TAB1/2 and TAK1 causes the activation of TAK1 (Feng, 2005; Asagiri and Takayanagi, 2007). TRAF6 mediates the activation of TAK1, which results in the phosphorylation of NFκB inducing kinase (NIK) (Figure 1.4) (Feng, 2005; Mellis *et al.*, 2011). NIK then activates IκB kinase (IKK) complexes (Figure 1.4) (Asagiri and Takayanagi, 2007; Mellis *et al.*, 2011). Degradation of these IκB molecules releases NFκB, allowing it to -translocate to the nucleus where it mediates the transcription of osteoclast effector genes (Asagiri and Takayanagi, 2007; Mellis *et al.*, 2011). Dominant negative studies of TAK1 and TAB2 have shown that they are essential for NFκB activation (Takayanagi, 2008a; Boyle *et al.*, 2003). A second NFκB pathway, the non-canonical pathway, involves p52/p65 dimer activation (Sun, 2012). RANKL has been shown to activate this pathway and there has been some evidence that suggests that inhibition of p52/p65 has a negative effect on osteoclast formation (Asagiri and Takayanagi, 2007; Franzoso *et al.*, 1997; Jimi *et al.*, 2004; Takayanagi, 2008a; Soysa and Alles, 2009). Novack *et al.*2003 have

suggested that there is crosstalk between the two pathways therefore their functions may not be mutually exclusive (Novack *et al.*, 2003).

1.5.3.2 MAP Kinase Signalling in Osteoclast Differentiation

RANK signalling causes the activation and the downstream signalling of MAP kinases. The MAP kinase family is comprised of the JNK, ERK1/2, p38 and ERK/ big MAPK kinase 1 (BMK1) family subgroups (Boyle *et al.*, 2003; Asagiri and Takayanagi, 2007; Zarubin and Han, 2005). These signalling molecules, which regulate many cellular activities have an important role in osteoclastogenesis (Boyle *et al.*, 2003; Asagiri and Takayanagi, 2007). As mentioned above, the recruitment of TRAF6 to RANK and the subsequent formation of the signalling complex containing RANK, TRAF6, TAK1, and TAB1/2 leads to the activation of TAK1 (Asagiri and Takayanagi, 2007). In addition, to activating NFκB, TAK1 also activates c-Jun N-terminal Kinase (JNK) (Figure 1.4) (Mizukami *et al.*, 2002; Asagiri and Takayanagi, 2007; Feng, 2005). This is essential for the activation of transcription factor AP-1 (Figure 1.4) (Eriksson, 2005). Structurally, AP-1 is a dimer composed of the subunits c-FOS and c-Jun and is activated through JNK phosphorylation of its c-FOS component (Boyle *et al.*, 2003; Asagiri and Takayanagi, 2007; Eriksson, 2005). Mice that lack c-FOS develop severe osteopetrosis resulting from the block in early osteoclast differentiation (Wang *et al.*, 1992; Grigoriadis *et al.*, 1994).

MAP kinase family member ERK1/2 and its downstream signalling pathway have also been shown to influence osteoclast formation, although its function may be more important in RANK-mediated stimulation of osteoclast activity and survival (Figure 1.4) (Asagiri and Takayanagi, 2007; Boyle *et al.*, 2003). RANKL stimulation induces ERK1/2 activation by phosphorylation (Hotokezaka *et al.*, 2002). Interestingly, ERK1/2 activation has been shown to have an inhibitory effect upon osteoclast formation from RAW264.7 cells (Hotokezaka *et al.*, 2002). Inhibiting ERK1/2 through the highly specific upstream MEK inhibitors including PD98059 increased osteoclast formation in RAW264.7 cells (Hotokezaka *et al.*, 2002). In contrast however, PD98059 inhibited osteoclast formation in both a co-culture system of primary osteoblasts and osteoclast progenitor cells and in RANKL stimulated bone marrow cultures, but only at extremely high concentrations (Lee *et al.*, 2002a). In addition, PD98059 also caused the loss of the ruffled border and osteoclast apoptosis in another study where primary cultures were used (Nakamura *et al.*, 2003). This data raises two possibilities, either the inhibitory effect of ERK1/2 activation upon osteoclast formation is specific to the

RAW264.7 cell line or the concentration of PD98059 has adverse effects upon the cells. More osteoclast formation cultures using murine progenitor cells need to be studied to determine what is occurring.

The most important of the MAP kinase pathways in osteoclast progenitors appears to be the stress activated protein kinase p38, which is activated by cellular stresses including UV irradiation, heat shock, osmotic stress, inflammatory cytokines and reactive oxygen species (ROS) (Zarubin and Han, 2005; Matsumoto *et al.*, 2000). The p38 stress pathway in relation to cell stress is discussed in Chapter 1.8.2. RANKL is thought to activate p38α through TAB1-dependent autophosphorylation of p38α, which occurs when TAB1 recruits p38 to the RANK-TRAF6-TAK1 complex (Ge *et al.*, 2006; Feng, 2005). P38 has multiple non-degenerate critical actions on many aspects of osteoclast differentiation pathways including the regulation of multiple osteogenic transcription factors including NFATc1, MITF and c-FOS (Figure 1.4) (Huang *et al.*, 2006). P38 regulation of NFATc1 occurs through the c-FOS subunit in the AP-1 complex (Figure 1.4) (Huang *et al.*, 2006). Inhibiting p38 with compound SB203580 in bone marrow macrophages inhibits RANKL-induced c-FOS mRNA expression (Huang *et al.*, 2006). In addition, using dominant negative forms of MKK3 and MKK6, which are upstream activators of p38 reduced both RANKL-stimulated c-FOS and NFATc1 mRNA expression and protein levels (Huang *et al.*, 2006). Overexpression of c-FOS was able to restore NFATc1 expression, and osteoclastogenesis in cells where p38 was inhibited with SB203580 (Huang *et al.*, 2006). This suggests that upon RANKL stimulation of p38 results in activation of C-FOS, which then participates in NFATc1 activation (Huang *et al.*, 2006). P38 also directly regulates transcription factor MITF and downstream (i.e., MITF and NFATc1-dependent) expression of TRAP during osteoclastogenesis (Figure 1.4) (Mansky *et al.*, 2002a). RANKL-induced p38 phosphorylation causes MITF to be phosphorylated on Ser^{307} (Figures 1.2 and 1.4) (Mansky *et al.*, 2002a; Boyle *et al.*, 2003). The necessity of p38 activity in osteoclast formation has been shown through inhibition studies with its inhibition by SB203580 abolishing all osteoclast formation (Matsumoto *et al.*, 2000). These findings of p38 actions on so many RANKL-induced factors may explain why its inhibition has particularly potent effects upon osteoclast differentiation (Mansky *et al.*, 2002a; Lu *et al.*, 2010a).

1.5.3.3 SRC-PI3K-AKT Signalling

The SRC-phosphatidylinositol 3'-OH kinase (PI(3)K)-AKT signalling axis also has a significant influence on the outcome of RANKL-RANK signalling in osteoclasts (Boyle *et al.*, 2003) (Figure 1.4). The c-terminal of RANK recruits c-SRC, which is able to bind to TRAF6 increasing its kinase activity (Mellis *et al.*, 2011). It is notable that c-SRC is not necessary for osteoclast differention but rather survival and osteoclast activity (Figure 1.4) (Mellis *et al.*, 2011). *C-src*$^{-/-}$ mice have differentiated osteoclasts, but these osteoclasts lack ruffled borders and are almost without bone resorption activity (Asagiri and Takayanagi, 2007; Zou *et al.*, 2007). Despite c-SRC not having a clear role in osteoclast differentiation, downstream of c-SRC is phosphoinositide-3-OH kinase (PI3- kinase) and AKT, which are both important in osteoclast differentiation (Moon *et al.*, 2012b; Feng, 2005). TRAF6 increases the kinase activity of c-SRC to activate PI3-kinase, which then recruits and activates AKT (also known Protein kinase B (PKB)) (Feng, 2005). Both the PI3-kinase and AKT molecules have been found to be important in osteoclast differentiation by inhibiting the kinase activity of AKT substrate, glycogen synthase kinase-3β (GSK3β) (Moon *et al.*, 2012b). GSK3β has shown to be involved in osteoclast differentiation by modulating NFAT family transcription factors and inhibiting its activity allows for NFATc1 (discussed below) translocation (Moon *et al.*, 2012b). However, osteoclast formation in mice lacking c-*Src* would suggest that C-SRC is not essential for PI3K/AKT activation in differentiation.

1.5.3.4 NFATc1 Signalling

RANK-dependent signalling through NFκB, p38 and AP-1 results in downstream NFATc1 transcription, translation, stabilisation, nuclear translocation, transcription factor formation and transactivation (Figures 1.2 and 1.4) (Boyle *et al.*, 2003). NFATc1 belongs to the nuclear factor of activated T-cells cytoplasmic family of transcription factors, which has 5 members, NFATc1, -2, -3, -4 and -5 (Zhao *et al.*, 2010; Hogan *et al.*, 2003; Serfling *et al.*, 2012; Sharma *et al.*, 2007). Expression of NFATc1, -2, -3 and -4 are regulated by Ca^{2+} and the Ca^{2+} dependent serine phosphatase calcineurin (Chapter 1.5.3.5) (Mancini and Toker, 2009; Hogan *et al.*, 2003).

NFATc1 activation occurs over a number of steps. Initial induction of NFATc1 occurs by NFκB and NFATc2 recruitment to the NFATc1 promoter after RANKL stimulation (discussed below) (Asagiri and Takayanagi, 2007; Zhao *et al.*, 2010). Full induction is achieved when through calcium signalling NFATc1 is activated and binds to its own

promoter in a process called autoamplification (Asagiri *et al.*, 2005; Hogan *et al.*, 2003; Kim *et al.*, 2005c; Takayanagi, 2007b). This process also requires the binding of c-FOS to the NFATc1 promoter (Asagiri and Takayanagi, 2007; Zhao *et al.*, 2010).TRAF6 plays an important role in NAFTc1 activation (Figure 1.4)(Takayanagi *et al.*, 2002). In RANKL stimulated osteoclast progenitor cells from TRAF6$^{-/-}$ mice, NFATc1 mRNA induction was significantly reduced and protein levels were barely detectable (Takayanagi *et al.*, 2002). TRAF6 role in NFATc1 activation is thought to occur through its interaction with NFκB, c-FOS and calcium mobilization (Boyce and Xing, 2007; Feng, 2005). TRAF6 ability to mobilize intracellular calcium is dependent upon the Ca^{2+}/Calcineurin pathway, which is discussed in Chapter 1.5.3.5 (Figure 1.4) (Feng, 2005; Asagiri and Takayanagi, 2007). Initial NFATc1 transcription activation occurs through the cooperation of NFATc2 with NFκB, which are recruited to the NFATc1 promoter post RANKL stimulation (Zhao *et al.*, 2010; Asagiri and Takayanagi, 2007). NFκB is important to NFATc1 activation as NFATc1 induction has been shown to be reduced when NFκB is pharmacologically inhibited and in NFκB$^{-/-}$ cells (Figure 1.4) (Asagiri and Takayanagi, 2007). Moreover, chromosome immunoprecipitation (ChIP) studies have shown that NFκB binds to the NFATc1 promoter within minutes of RANKL stimulation (Asagiri and Takayanagi, 2007). These data show that NFκB is involved in the activation of immediate-early RANKL target genes one of which includes NFATc1; however, NFATc1 expression extends to the mid and later stages of osteoclastogenesis through autoamplification. This extended expression of NFATc1 throughout osteoclastogenesis is discussed in the next paragraph (Asagiri and Takayanagi, 2007).
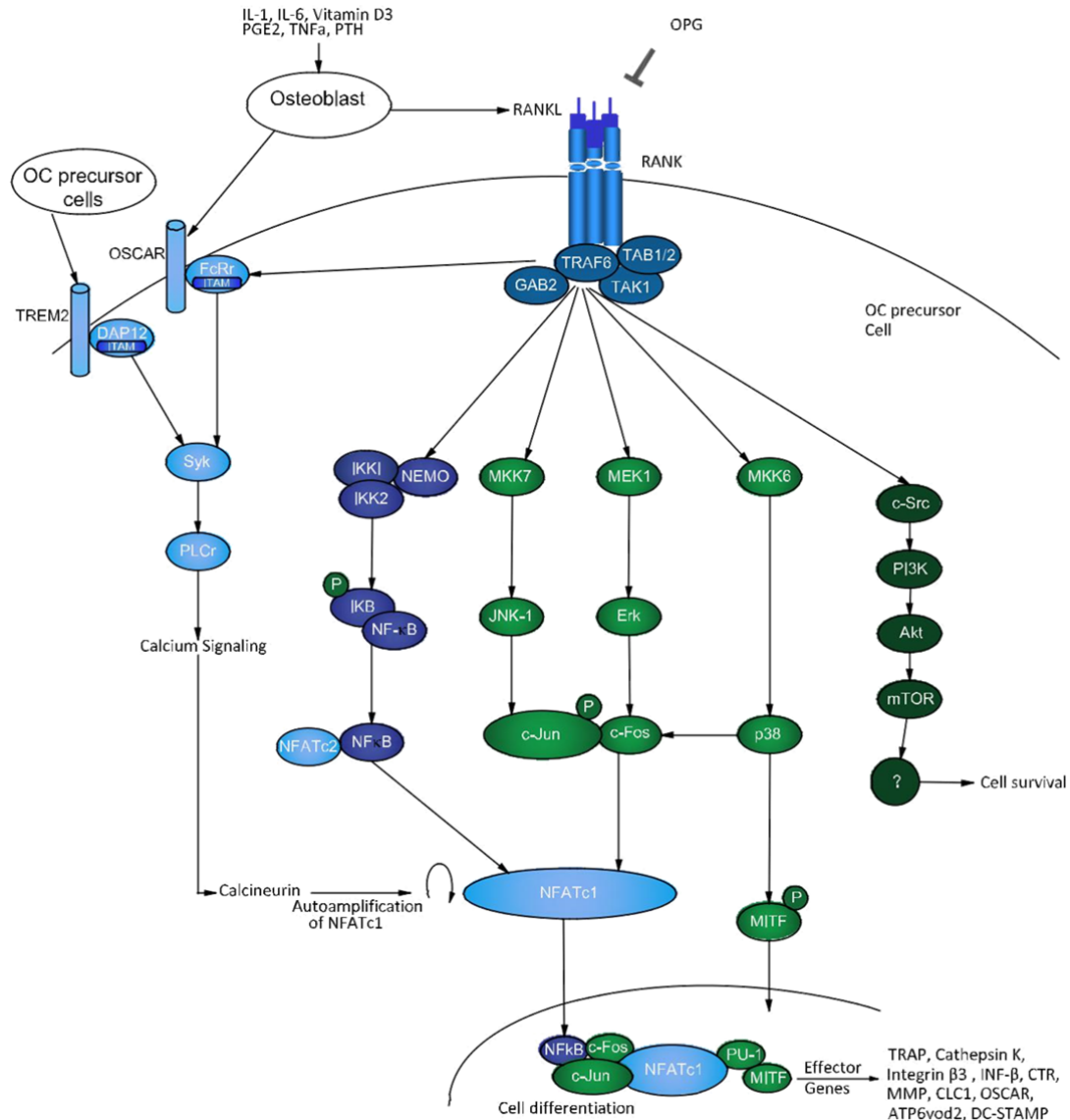
Figure 1.4 Schematic of RANK Signalling Network in Osteoclasts

RANKL binding to RANK causes the recruitment of TRAF6 to RANKs cytoplasmic tails. Through TRAF6, RANK transmits its downstream signals. TRAF6 first recruits TAK1, GAB2 and TAB1 the latter of which activates TAK1. TAK1 activation leads to NFκB activation, nuclear translocation and binding to target osteoclastogenic genes promoters i.e., c-FOS. Cooperation of NFκB2 and NFATc2 activate the initial induction of NFATc1. Full NFATc1 activation occurs through the actions of c-FOS, which is activated by MAP kinase p38. MAP kinases are also activated by TRAF6 and p38 phosphorylates the transcription factor MITF. RANK signalling also associates with ITAMs to activate calcium signals and downstream calcineurin, which activates and causes NFATc1 autoamplification. Transcription factors NFATc1, MITF, PU.1 and AP-1 (c-FOS and c-JUN) form transcription complexes in the nucleus, which bind to the promoters and drive the transcription of osteoclastogenic genes including *Apc5*. Image adapted from (Boyle *et al.*, 2003; Takayanagi, 2008b; Wada *et al.*, 2006; Aeschlimann and Evans, 2004; Lee and Kim, 2003; Katagiri and Takahashi, 2002).

In addition to NFκB, both subunits of the AP-1 complex: c-JUN and c-FOS are integral components in NFATc1 activation (Zhao *et al.*, 2010). It has been shown that the osteoclast activities of NFATc1 are inhibited by dominant negative c-jun, but overexpression of NFATc1 rescues the dominant negative phenotype (Zhao *et al.*, 2010). As mentioned above, Huang *et al.* 2006 showed that RANKL mediated c-FOS and NFATc1 protein expression induction is dependent upon the p38 pathway and that p38 first induces c-FOS expression, which causes the subsequent activation of NFATc1 (Zhao *et al.*, 2010; Huang *et al.*, 2006). In cells lacking c-FOS, RANKL is unable to stimulate NFATc1 mRNA induction and protein expression (Takayanagi *et al.*, 2002). NFATc1 also regulates its own gene expression through a process of auto-amplification. After initial activation through NFκB and NFATc2, NFATc1 in combination with c-FOS also binds to its own promoter within 24 hours of RANKL stimulation (Asagiri *et al.*, 2005; Kuroda and Matsuo, 2012; Zhao *et al.*, 2010). The increased expression of NFATc1 coincides with oscillating calcium levels, which through calcineurin dephosphorylates NFATc1 (Figure 1.4) (Kuroda and Matsuo, 2012; Asagiri *et al.*, 2005). Interestingly, calcium levels have been shown increased 24 hours post RANKL stimulation (Feng, 2005). The dephosphorylated NFATc1 subsequently translocates to the nucleus where it persists until the late stages of osteoclastogenesis. The activation and auto-amplification of NFATc1 has been termed the 'amplification phase' of osteoclast differentiation (Figure 1.4) (Kuroda and Matsuo, 2012; Asagiri *et al.*, 2005). Therefore, both the c-FOS subunit of AP-1 and calcium are necessary for NFATc1 auto-amplification (Zhao *et al.*, 2010; Takayanagi, 2007a). The ternary NFAT: Fos: Jun complex integrates calcium, MAPK family members (JNK, ERK1/2 and p38) and other RANKL-dependent signalling cascades in osteoclast progenitor cells regulating a large number of osteoclast specific genes (Boyle *et al.*, 2003).

1.5.3.5 NFATc1, ITAM motifs and Calcium Signalling Cascades in Osteoclast Formation

As noted above, full activation of NFATc1 transcription is regulated by calcium signals (Asagiri and Takayanagi, 2007). Osteoclast-associated receptor (OSCAR), triggering receptor expression in myeloid cells-2 (TREM-2), signal regulatory protein β1 (SIRPβ1) and paired immunolgobin-like receptor A (PIR-A) are the immunoglobulin like receptors, which are associated with adaptor proteins, FcRγ and DNAX activating protein 12 (DAP12) (Figure 1.4) (Takayanagi, 2007a; Zhao *et al.*, 2010; Kuroda and Matsuo, 2012). These receptors and the associated FcRγ and DAP12 proteins are essential for osteoclastogenesis (Zhao *et al.*, 2010). In the presence of RANKL, activation of SIRPβ1, OSCAR and PIR-A increases the

rate of osteoclast formation; however, activation of these receptors without RANKL stimulation does not cause osteoclast formation (Zhao *et al.*, 2010; Takayanagi, 2007a). It is proposed that putative ligands for OSCAR and TREM-2 are present upon osteoblasts, thus further showing the importance of the interaction between progenitor osteoclast cells and osteoblasts (Kim *et al.*, 2005c). The associated FcRγ and DAP12 adaptor proteins have an immunoreceptor tyrosine-based activation motif (ITAM), which is needed for the activation of calcium signalling (Figure 1.4) (Zhao *et al.*, 2010; Takayanagi, 2007a). Mice that lack DAP12 and FcRγ exhibit severe osteopetrosis (Zhao *et al.*, 2010). Therefore, ITAM signalling is referred to as co-stimulatory signals for RANK (Asagiri and Takayanagi, 2007; Takayanagi, 2007a). Calcium-induced phosphorylation of ITAM motifs allows for the recruitment of Syk, which is then phosphorylated (Figure 1.4) (Zhao *et al.*, 2010; Kuroda and Matsuo, 2012). This recruitment and phosphorylation of Syk to ITAM motifs is essential for osteoclastogenesis (Zhao *et al.*, 2010; Negishi-Koga and Takayanagi, 2009). Syk tyrosine kinase phosphorylates phospholipase Cγ (PLCγ), which then cleaves Phosphatidylinositol 4, 5-bisphosphate (PIP_2) into inositol 1,4,5-trisphosphate (IP_3) and diacyl glycerol (DAG). IP3 then releases calcium from the endoplasmic reticulum calcium stores (Figure 1.4) (Zhao *et al.*, 2010; Negishi-Koga and Takayanagi, 2009). This increase in intracellular calcium ions causes the calcium bound calmodulin to undergo a conformational change to the active form, which then results in the activation of phosphatase calcineurin and effector proteins calcium/calmodulin-activated kinases (CaMKs**).** Calcineurin activation causes NFATc1 to translocate to the nucleus with resulting in subsequent expression of osteoclast specific genes (Figure 1.4) (Zhao *et al.*, 2010; Negishi-Koga and Takayanagi, 2009). Inhibiting calcineurin with FK506 and cyclosporin A inhibits NFATc1 induction and reduces osteoclast formation (Takayanagi, 2007a; Hogan *et al.*, 2003). In addition, inhibiting calcineurin-NFATc1 with 11R-VIVIT and FK506 reduces ITAM factor expression in human osteoclasts (Zawawi *et al.*, 2012).

As noted above, TRAF6-dependent signals mobilize intracellular calcium 24 hours post RANKL stimulation, which activates calcineurin. This causes NFATc1 activation and translocation to the nucleus for the autoamplification phase of NFATc1 induction (Figure 1.4) (Zhao *et al.*, 2010; Negishi-Koga and Takayanagi, 2009; Feng, 2005). This ability of TRAF6 signals to mobilize calcium may be through its association with the adaptor protein Gab2, which binds to PLC-γ, thereby linking the two pathways together (Figure 1.4) (Kuroda

and Matsuo, 2012; Feng, 2005). Therefore, the full activation of NFATc1 requires cross-talk between both the RANKL and ITAM-dependent pathways (Feng, 2005).

1.5.3.6 NFATc1 is the Master Regulator of Osteoclastogenesis

NFATc1 is often referred to as a 'master regulator' of osteoclast formation due not only to its central importance in osteoclast formation but also as a result of to the many osteoclast-influencing factors that regulate its expression or activity (Sharma *et al.*, 2007). In a DNA array-based search for RANKL dependent factors, NFATc1 was found to be the transcription factor which is most strongly regulated by RANKL (Takayanagi, 2007a). Embryonic stem (ES) cells that lack NFATc1 do not differentiate into osteoclasts upon RANKL and M-CSF stimulation whereas wild type ES cells do have this ability (Takayanagi, 2007a; Zhao *et al.*, 2010). Mice that congenitally lack NFATc1 die by embryonic age of E14.5 due to defective cardiac valve formation; however, using chimeric mouse approaches and also a transgenic mouse model the role of NFATc1 in osteoclast formation *in vivo* was demonstrated (Zhao *et al.*, 2010; Takayanagi, 2007a). In a transgenic mouse model where NFATc1 was expressed only in the heart (thus enabling the mice to survive) the mice were found to be osteopetrotic (Zhao *et al.*, 2010; Winslow *et al.*, 2006).

NFATc1 positively regulates the expression of a number of osteoclast genes essential for osteoclast functions including *Atp6v0d2, Dc-stamp, Acp5* (TRAP)*, Calcr (CTR), Cstk, MMP9, c-Src, ClCN7, latent TGF-β binding protein 3 (Ltbp3) and Integrin β3* (Song *et al.*, 2009; Takayanagi, 2007a; Takayanagi, 2008a; Mellis *et al.*, 2011; Kuroda and Matsuo, 2012). Differential patterns of NFATc1 and binding transcriptional factors regulate the expression of different osteoclast specific genes (Kuroda and Matsuo, 2012; Takayanagi, 2008a). For example, the NFATc1:AP-1 complex have been shown to be important in inducing both TRAP and CTR expression whilst NFATc1: PU.1: MITF complex is required to induce CSTK and OSCAR gene expression (Asagiri *et al.*, 2005; Takayanagi, 2008a). NFATc1: PU.1 induces Integrin β3 (Crotti *et al.*, 2008). This may explain the spatiotemporal expression of osteoclast specific genes during the period of osteoclast formation (Asagiri and Takayanagi, 2007). NFATc1 expression has also been shown to regulate RANKL-mediated osteoclast fusion, which increases the resorptive activity of osteoclasts (Asagiri and Takayanagi, 2007; Kuroda and Matsuo, 2012). NFATc1 was shown by use of a luciferase-driven reporter construct to directly increase the transcriptional activity of fusion genes: vAtp6v0d2 and DC-STAMP (Kim *et al.*, 2008b).

NFATc1 activity has been shown to be increased in the bone pathology, Rheumatoid arthritis (Yarilina *et al.*, 2011; Crotti *et al.*, 2012). TNF, which is a major mediator of Rheumatoid arthritis, has been shown to increase the activity of NFATc1 in human macrophages (Pan *et al.*, 2013; Yarilina *et al.*, 2011). In a human study of of rheumatoid arthritis, inhibiting calcineurin and NFAT through cyclosporin A stops the disease activity (van Rijthoven *et al.*, 1986).

1.5.3.7 RANKL Signalling Effects upon Microphthalmia Transcription Factor, MITF

M-CSF and RANKL-dependent signalling also leads to activation of MITF, which is a basic helix-loop-helix-leucine zipper transcription factor and the archetype of the MiT family of transcription factors (Sharma *et al.*, 2007; Kuiper *et al.*, 2004). Other MiT family members include Tfeb, Tfec and Tfe3 (Lu *et al.*, 2010a; Kuiper *et al.*, 2004). MITF can form homodimers as well as heterodimers with other MiT family members and is expressed in a range of different cell types including melanocytes, splenocytes, mast cells and osteoclasts (Lu *et al.*, 2010a; Pogenberg *et al.*, 2012). The role of MITF varies depending upon the cell type in which it is expressed (Lu *et al.*, 2010a). For example, MITF is considered the master regulator of melanocyte development, function and survival (Levy *et al.*, 2006). In osteoclast progenitor cells, its key role is to drive the terminal differentiation of osteoclasts (Bronisz *et al.*, 2006; Hershey and Fisher, 2004).

TAK1 a member of the signalling complex, which forms after RANK binding to RANKL is important to MITF expression (Qi *et al.*, 2014). TAK1 deficiency results in lack of RANK: TRAF6:TAB1/2 complex formation and decreased MITF expression (Qi *et al.*, 2014). MITF is chiefly a cytoplasmic protein; however, upon activation it translocates to the nucleus (Lu *et al.*, 2010b; Bronisz *et al.*, 2006). MITF is sequestered in the cytoplasm through its phosphorylation dependent interaction with adaptor protein 14-3-3 and also through its association with TAK1, which promotes the 14-3-3 interaction (Bronisz *et al.*, 2006). M-CSF and RANKL signals result in dephosphorylation of MITF at serine 173 allowing MITF dissociation from 14-3-3 and its translocation to the nucleus (Bronisz *et al.*, 2006; Lu *et al.*, 2010b). *In vitro* studies have also shown that M-CSF stimulation causes Erk1/2 mediated phosphorylation of MITF at serine 73 (Hershey and Fisher, 2004; Weilbaecher *et al.*, 2001). This phosphorylation causes the recruitment of p300/CBP transcriptional co-activator in

RAW264.7 cells, which may increase osteoclast maturation and fusion (Weilbaecher *et al.*, 2001; Hershey and Fisher, 2004) .

As discussed above, RANKL-elicited MITF levels are induced relatively slowly in osteoclast progenitors after NFATc1 induction. Thus, MITF probably drives the latter stages of osteoclast formation rather than earlier stages of progenitor commitment, and it is essential for transcription of many osteoclast associated genes (Bronisz *et al.*, 2006; Hershey and Fisher, 2004). Over twenty spontaneous or induced mutations have been identified on the mouse *Mitf* locus (Steingrímsson *et al.*, 2004; Arnheiter, 2010). These mutations result in many significant phenotypic effects on skin pigmentation, eye development, bone and other tissues, effects, which also range in severity with the type of mutation (Arnheiter, 2010; Steingrimsson *et al.*, 2002). These mutations are classified as semi-dominant or as recessive based on their effect on the melanocyte lineage (Hershey and Fisher, 2004). All *Mitf* mutations result in melanocyte defects, which are seen by a reduction or total loss of pigmentation of the coat and inner ear (Hershey and Fisher, 2004; Nakayama *et al.*, 1998). The original semi-dominant *mitf* allele (Mitf^{mi}) has a three nucleotide deletion that causes the protein to act in a dominant negative manner (Hershey and Fisher, 2004). As a result Mitf$^{mi/mi}$ mice are osteopetrotic and have non-erupted teeth (Hershey and Fisher, 2004). Mitf$^{mi/mi}$ mice are osteopetrotic due to reduced bone resorption with experiments showing that resorption in these mice is reduced by more than 90%, which is consistent with poor or absent osteoclast formation (Hershey and Fisher, 2004). Ultrastructural studies have shown the reduced bone resorption occurs because osteoclasts derived from Mitf$^{mi/mi}$ mice are small, are either mononuclear or have significantly reduced nuclei numbers, their ruffled border is less well formed and they express low levels of TRAP and Ctsk (Hershey and Fisher, 2004; Steingrimsson *et al.*, 2002; Motyckova *et al.*, 2001; Luchin *et al.*, 2000). Studies *in vitro* have shown similar findings (Hershey and Fisher, 2004). The differences in osteoclast morphology and downstream resorptive activity are thought to arise due to problems arising late in the process of osteoclast differentiation (Steingrimsson *et al.*, 2002; Luchin *et al.*, 2000). In humans loss of function and dominant negative mutations result in the related albinism and deafness syndromes: Waardenburg syndrome type 2a, and Teitz syndrome, respectively (Tachibana, 2001; Pogenberg *et al.*, 2012).

MITF is a large and complex gene (Figure 1.5) (Hershey and Fisher, 2005). The human *MITF* gene locus spans 229kb while the mouse *Mitf* locus is 214 kb (Figure 1.5) (Hershey and

Fisher, 2005). The *MITF/Mitf* genes have a split promoter feature and is alternatively spliced resulting in expression of as a series of isoforms that are structurally and biologically different (Hershey and Fisher, 2005; Lu *et al.*, 2010b; Wan *et al.*, 2011; Lu *et al.*, 2010a). Currently 9 isoforms of MITF/Mitf have been identified and these are designated MITF/Mitf-A, -B, -C, -D, -E, -H, -J, -M, and –Mc (Figure 1.5 excluding isoform J) (Hershey and Fisher, 2005). These isoforms vary at the exon 1b- 5′ (prime) end of the mRNA transcript, which differs in the 5′ untranslated region and, although not in all cases, the N-terminus of the translated protein (Figure 1.5) (Hershey and Fisher, 2004) Exon 1b is then spliced onto common exons 2-9 (Figure 1.5) (Hershey and Fisher, 2004). The isoforms are expressed in varied tissues (Hershey and Fisher, 2005; Cheli *et al.*, 2010). Human osteoclasts express, A-, E-, H- and B- and J and mouse osteoclasts express: A, C-, E-, H- and J- (Hershey and Fisher, 2004; Hershey and Fisher, 2005). Mitf mouse isoforms A and E have been recently shown to be important in osteoclast formation (Lu *et al.*, 2010a). Lu *et al.* found RANKL stimulation increased MITF E protein levels and also identified MITF isoform E to be a more potent osteoclastogenic factor than isoform A (Lu *et al.*, 2010a). Lu and colleagues also suggested that MITF E has a close association with chromatin and therefore is able to mediate strong effects upon target genes (Lu *et al.*, 2010a).

MITF binds to the DNA of its target promoters through its alpha helical basic domain, which is located near the N terminal region (Figure 1.5) (Krylov *et al.*, 1997; Arnheiter, 2010). MITF binds to an E-box motif CACTGTG and also an M box motif TCATGTG in the promoters of target genes causing their transcription (Pogenberg *et al.*, 2012; Levy *et al.*, 2006). There are a few additional sequences that MITF has also been shown to bind to including the non-palindromic sequence CACATG (Levy *et al.*, 2006). In osteoclastogenesis target genes include those encoding Ctsk, TRAP, E-cadherin, OSCAR, osteopetrosis-associated transmembrane protein 1 (OSTM), and ClC-*7* (Lu *et al.*, 2010a). It is proposed that post-translational modifications may have a role in MITF binding to different promoter sequences and therefore regulate differential gene transcription (Cheli *et al.*, 2010).

As previously discussed transcription factors NFATc1, PU.1, AP-1 and MITF form an osteoclast specific transcriptional complex in which they regulate target genes although the molecules within the complex are not always the same (Figure 1.4). RANKL phosphorylation of p38 causes the downstream phosphorylation of MITF on serine 307 (Mansky *et al.*, 2002a). This phosphorylation is required for MITF cooperation with the small GTPases,

MAP kinase kinase 6 (MKK6) and or Rac1, to bind to the TRAP promoter (Kim *et al.*, 2005c; Sharma *et al.*, 2007; Asagiri and Takayanagi, 2007; Takayanagi, 2008a). MITF and PU.1 are involved in the regulation of a large number of osteoclast genes (Sharma *et al.*, 2007). PU.1 and phosphorylated MITF were identified at TRAP and Ctsk promoters maximally from day 3-5 (Sharma *et al.*, 2007). RANKL-activated p38 was proposed to mediate this phosphorylation of MITF (Ser^{307}) and phosphorylated p38 was found to be present on the Ctsk promoter (Sharma *et al.*, 2007). Furthermore, ChIP experiments showed the phosphorylated forms of MITF and p38 correlated with the recruitment of SWI/SNF chromatin-remodelling complex and presence activated RNA pol II at the TRAP and Ctsk promoters (Sharma *et al.*, 2007). In addition, Sharma *et al.* 2007 showed by sequential ChIP experiments that NFATc1, PU.1 and MITF are present on Ctsk and TRAP promoters but only after 5 days of M-CSF and RANKL co-treatment upon haemopoietic precursors (Sharma *et al.*, 2007).
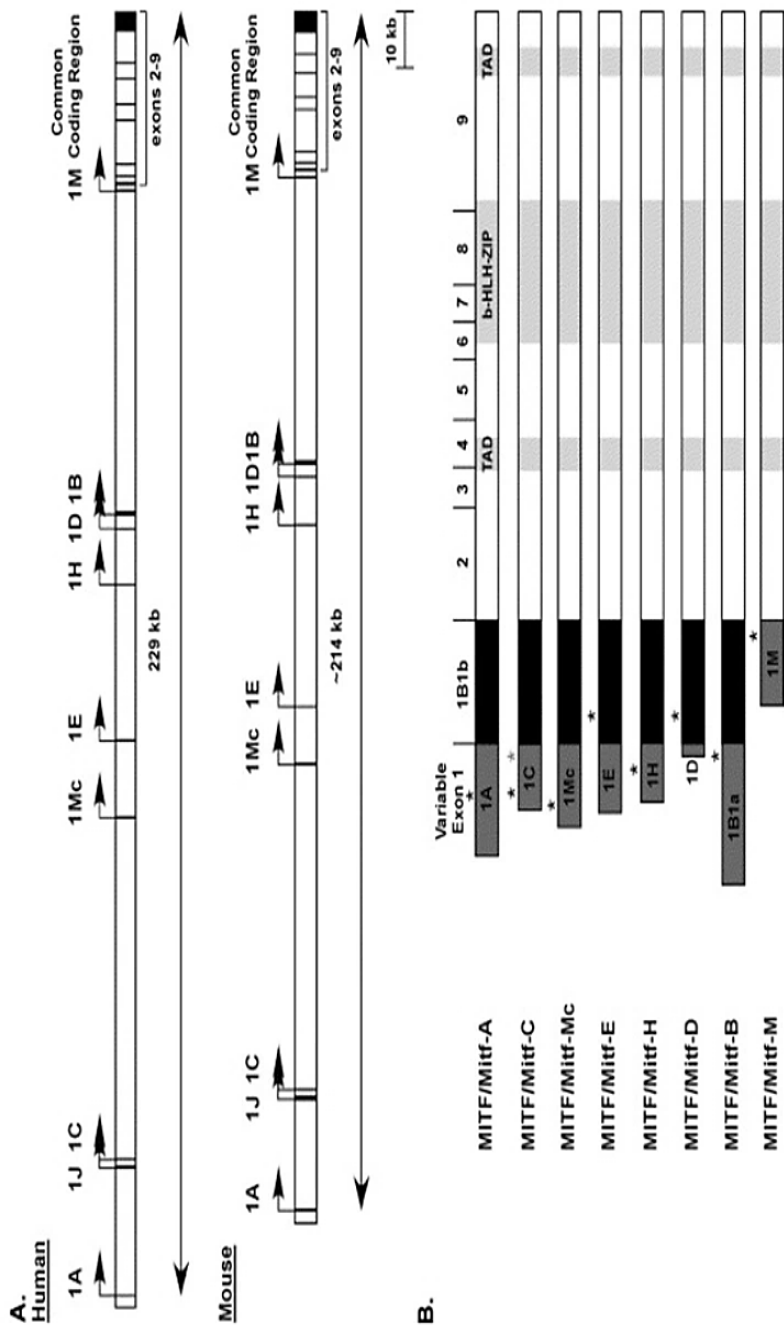
Figure 1.5 MITF Gene Structure and MITF gene isoforms

(**A.**) MITF is a 229kb gene in humans and Mitf is ~214kb in mice. (**B.**) Both the MITF and the Mitf gene locus contain nine currently identified isoform-specific promoters. Each Mitf isoform transcript contains an isoform-specific first exon that is spliced to exon 1B1b and then to common exons 2–9, which encode the known functional motifs of MITF. The only exception is Mitf-M, which is only expressed in melanocytes and mast cells. Isoforms A and E have been reported to have a role in osteoclast formation. Figure sourced from (Hershey and Fisher, 2005).

1.6 Bone Metastasis

Bone is one of the most common sites of cancer metastasis and most cancer patients die from metastasis rather than primary tumour growth (Mundy, 2002; Coleman, 2006). Tumour cells that have metastasized to bone stimulate either osteoclasts or osteoblasts to achieve bone invasion and tumour growth (Mundy, 2002). The incidence of bone metastasis is unknown but it is estimated that 350,000 people die with bone metastases per year in the United States, and unfortunately once the tumours have metastasized to bone they are usually incurable, being refractory to treatment (Mundy, 2002).

Many cancers commonly metastasize to bone including breast, prostate, thyroid, kidney, lung, colon, stomach, bladder, uterus and rectum cancers (Roodman, 2004; Mundy, 2002). As reviewed by Mundy and others, breast and prostate cancer are the two most common cancers that metastasize to bone, which is important due to the incidence rates of these diseases (Mundy, 2002; Roodman, 2004; Lipton *et al.*, 2009a). Post-mortem examinations have shown that 70% of prostate cancer patients have some degree of metastatic bone disease (Mundy, 2002; Roodman, 2004). Breast cancer is the most common invasive cancer diagnosed in females both in Australia and in the world, and the majority (80-85%) of breast cancer patients, which develop advanced disease also develop osteolytic metastasis (Sterling *et al.*, 2011; Lipton *et al.*, 2009a; AIHW, 2006). Renal, lung and thyroid cancer also metastasize to the bone (Jimenez-Andrade *et al.*, 2010). Lung cancer is the third most common form of cancer to spread to bone after breast cancer and prostate cancer and is present in 30-40% of lung cancer patients (D'Antonio *et al.*, 2014). Kidney and thyroid cancer bone metastasis is present in approximately 20-30% of patients (Muresan *et al.*, 2008; Sahi *et al.*, 2010). Bone metastases often occur in the load-bearing bones of the axial skeleton (Mundy, 2002; Sahi *et al.*, 2010; Pittas *et al.*, 2000; Coleman, 2006). Studies have shown that breast, thyroid, and kidney patients commonly have metastasis in the proximal ends of long bones, the shaft of long bones, ribs, spine, sacrum, illeum and skull (Sahi *et al.*, 2010; Pittas *et al.*, 2000).

Bone metastases reduce the structural integrity of the skeleton and can cause many skeletal complications, which present as clinical symptoms in bone metastases patients (Simos *et al.*, 2013; Weilbaecher *et al.*, 2011). These skeletal complications are collectively called skeletal-related events (SREs) and severely impact the patient's wellbeing as they are associated with morbidity and mortality (Weilbaecher *et al.*, 2011; Simos *et al.*, 2013; Li *et al.*, 2014). SRE's

of osteolytic metastases include: severe bone pain, increased bone fragility thereby markedly increasing fracture rates, deformity of bones, hypercalcaemia, nerve-compression syndromes and leukoerythroblastic anaemia (Mundy, 2002; Coleman, 2006; Jimenez-Andrade *et al.*, 2010; Weilbaecher *et al.*, 2011; Simos *et al.*, 2013).

1.6.1 Osteolytic Metastases

Cancer metastases to bone can be classified as either osteolytic or osteoblastic depending upon the effect the cancer invasion has upon the bone environment (Baltasar Sanchez and Gonzalez Sistal, 2014; Roodman, 2004; Mundy, 2002). Osteolytic lesions are characterized by bone destruction caused by the actions of osteoclast stimulating factors upon osteoclasts (Mundy, 2002; Guise *et al.*, 2006; Ortiz and Lin, 2012). In comparison, osteoblastic metastases are caused by cancer cells producing factors that stimulate osteoblast proliferation, differentiation and bone formation resulting in poor quality bone formation often leading to fractures. Osteoblastic metastases are observed in prostate cancer invasion (Mundy, 2002; Guise *et al.*, 2006; Ortiz and Lin, 2012). However, despite lesions being predominantly osteolytic or osteoblastic a smaller resorptive or bone laying counterpart is most often present and can be due to the complex interactions between the bone and tumour cells and is referred to as a "mixed lesion" (Mundy, 2002; Mundy and Guise, 1997; Roodman, 2004; Ortiz and Lin, 2012). The reasons for tumour associated bone loss or formation are typically unclear or controversial but are clinically of great importance.

1.6.2 The Vicious Cycle Model of Tumour Invasion of Bone

It has been proposed by a number of scientists in the metastatic bone disease field including George Mundy and Theresa Guise that there is a 'vicious cycle' of actions between tumour cells, osteoclasts, osteoblasts and the bone matrix microenvironment, which promotes bone resorption and encourages tumour cell growth and survival (Figure 1.6) (Mundy, 2002; Roodman, 2004; Weilbaecher *et al.*, 2011; Sterling *et al.*, 2011). As described in Chapter 1.3.3.1 osteoclasts derive from the monocytic line of haematopoiesis through signals from M-CSF and RANKL (Gupta and Massagué, 2006; Boyle *et al.*, 2003; Kopesky *et al.*, 2014). Cancer cells, which have invaded the bone use the physiological processes of osteoclast and osteoblast differentiation to their own ends of growth and proliferation (Gupta and Massagué, 2006). In osteolytic metastases, the cancer cells typically inhibit osteoblast differentiation through the secretion of soluble factors including bone morphogenic proteins (BMPs), Wnt-family ligands, endothelin-1 and Platelet derived growth factor (PDGF), which are

osteoblastic potentiators (Figure 1.6) (Gupta and Massagué, 2006; Rahim *et al.*, 2014; Weilbaecher *et al.*, 2011). In contrast, tumour cells stimulate osteoclast formation by secreting factors such as PTHrP, Leukaemia inhibitory factor (LIF), IL-6, IL-11, (TNF-α, Epidermal growth factor (EGF) and PGE$_2$, which have been shown to act upon osteoblasts to stimulate RANKL production (Figure 1.6) (Mundy, 2002; Thomas *et al.*, 1999; Park *et al.*, 2003; Boyle *et al.*, 2003; Gupta and Massagué, 2006; Yin *et al.*, 2005; Chen *et al.*, 2010a; Palmqvist *et al.*, 2002; Weilbaecher *et al.*, 2011). This increased RANKL expression results in a concomitant increase in osteoclast formation and enhanced osteolysis (Figure 1.6) (Chen *et al.*, 2010b; Guise, 2013; Roodman, 2004). The breaking down of the bone matrix releases calcium as well as factors that are favourable to tumour growth such as TGF-β, connective tissue growth factor (CTGF), insulin-like growth factor 1 (IGF-1), fibroblast growth factor (FGF), PDGF, and BMPs (Figure 1.6) (Chen and Dou, 2010; Yin *et al.*, 2005; Mundy, 2002; Guise, 2013). Such factors encourage tumour growth and positively feedback into tumour cell cytokine production (Figure 1.6) (Mundy, 2002; Yin *et al.*, 2005; Guise, 2013; Chen *et al.*, 2010b).

The vicious cycle described above has been described in bone metastases derived from a number of xenografts mouse models including: breast cancer, prostate cancer, multiple myeloma, B cell lymphoma, Adult T-cell Leukaemia, and melanoma and oral squamous cell carcinoma (Krishnan *et al.*, 2014; Abe *et al.*, 2002; Abe *et al.*, 2004; Chen *et al.*, 2010b; Quan *et al.*, 2012; Shu *et al.*, 2010; Mundy, 2002; Shibata *et al.*, 2005; Javelaud *et al.*, 2007). In addition, molecules that are involved in the vicious cycle have been implicated in human disease although the extent to which the vicious cycle occurs in humans is not known. It is likely that this model of tumour invasion of bone whilst providing a physiological model of what occurs in metastatic bone disease would not encompass all the signalling networks and interactions that occur. Within this model one of the most well-studied molecules is PTHrP. PTHrP is described as being one of the most important molecules in promoting the vicious cycle of tumour cell growth (Mundy, 2002; Guise, 1997; Yin *et al.*, 2005; Roodman, 2004). In MDA-MB-231 human breast cancer cell-inoculated nude mice with bone cancer metastasis, the serum levels of PTHrP are increased and osteolysis is observed (Guise *et al.*, 1996). Neutralizing PTHrP actions by a specific antibody decreased the osteolytic bone destruction development and also decreased the tumour load in bone (Guise, 1997; Mundy, 1997; Guise *et al.*, 1996). In addition, numerous mouse cancer model studies have shown that tumour-secreted PTHrP stimulate osteoblasts to express RANKL although this has yet to be

demonstrated *in vivo* (Mundy, 2002; Thomas *et al.*, 1999; Gupta and Massagué, 2006; Weitzmann, 2013). Immunohistochemistry and *in situ* hybridization studies of human bone metastasis tissue samples have shown that PTHrP expression is greater in metastatic bone lesions than in the primary tumour site or in metastases that are growing in a soft tissue site (Mundy, 2002). This is consistent with PTHrP conferring a bone-invasive and osteolytic profile (Mundy, 2002). In addition to PTHrP, IL-11 has been proposed to participate in tumour invasion of bone as it increases RANKL expression on osteoblasts, and often Overexpression of these molecules is implicated in pathological states including metastasis and metastatic bone disease (Kang *et al.*, 2003). MDA-MB-231 cell inoculation into mice that overexpressed both IL-11 with osteopontin (OPN), a secretory protein, which stimulates osteoclast adhesion to the bone matrix, increased the incidence and rate of metastasis (Kang *et al.*, 2003). Over-expression of these molecules increased osteoclast (TRAP positive cells) numbers present at sites of bone metastases suggesting their role in osteolysis and tumour progression (Kang *et al.*, 2003). Other interleukins including IL-1 and IL-6 may be released by tumour cells and act indirectly by increasing RANKL expression or directly upon osteoclast progenitors to increase osteoclast differentiation (Chen *et al.*, 2010b; Mundy, 2002). Another molecule that has been studied for its role in the vicious cycle is TGF-β, which is released from the bone matrix whenever osteoclasts resorb bone (Filvaroff *et al.*, 1999). Although TGF-β seems to have a negative impact upon early tumours, in late stages it acts to promote the cancer phenotype (Lebrun, 2012). Yin *et al.* first demonstrated the role of TGF-β in the vicious cycle (Yin *et al.*, 1999). Blocking TGF-β signalling using a dominant negative mutant form of the TGF-β receptor, TβRII (DNTβII), in an intracardiac MDA-MB-231 inoculation model caused a decrease in bone resorption; smaller tumour burden, lower number of osteoclasts and an increase in mice survival times (Yin *et al.*, 1999). Reversing the TGF-β dominant-negative phenotype increased PTHrP expression with a subsequent increase in downstream osteolysis (Yin *et al.*, 1999). In addition to supporting tumour growth and their subsequent secretion of PTHrP, TGF-β also increases the expression of other mediators of the vicious cycle including of other mediators of the vicious cycle including IL-1, IL-6, IL-11, and cyclooxygenase 2 (COX-2) (Javelaud *et al.*, 2007; Lebrun, 2012; Kingsley *et al.*, 2007). Inhibition of TGF-β by the inhibitory SMAD7 decreases PTHrP, CTGF and IL-1 mRNA expression in melanoma bone metastases (Javelaud *et al.*, 2007). Interestingly in 75% of patients with biopsied bone metastases, the tumour cells stained positive for phosphorylated and nuclear localized, SMAD 2, which is recruited by the TGF-β receptor (Kang *et al.*, 2005). The role of TGF-β signalling has been shown to be common in bone

metastasis with TGF-β signalling occurring in bone metastases but not adrenal metastasis both derived from inoculation with MDA-MB-231 cells (Kang *et al.*, 2005). Another molecule, COX-2, is expressed in 87% of the bone metastases from patient samples suggesting it also has an important role in metastatic bone disease (Kingsley *et al.*, 2007). Inhibiting COX-2 decreases osteoclast numbers at the tumour- bone interface and decreases the tumour load in mice inoculated with MDA-MB-231 cells (Kingsley *et al.*, 2007).

In addition, calcium and growth factors (e.g., IGFs, CTGF, and FGF), which are released from the bone matrix by osteoclast bone resorption may increase the production of tumour associated factors thereby directly promoting tumour cell growth and progression by stimulating such processes as angiogenesis (Kingsley *et al.*, 2007). Other molecules implicated in the vicious cycle, which are currently being studied include: MMPs, A Disintegrin And Metalloproteinase Domain 8 (ADAM8), Monocyte chemoattractant protein-1 (MCP-1) and Ctsk (Chen *et al.*, 2010b). Thus, in summary, a large body of work indicates that tumour invasion of bone is potentiated by osteoclastic bone resorption and suggests osteoclast inhibition may help reduce tumour invasion.

1.6.3 Inhibition of Osteoclast Activity and RANKL Targeted Therapy in Bone Metastasis

Because osteolysis encourages tumour growth, inhibition of osteoclast activity, and RANKL actions in particular, have become important therapeutic targets (Roodman and Dougall, 2008; Casimiro *et al.*, 2009; Hofbauer *et al.*, 2008; Simos *et al.*, 2013). Bisphosphonates are pyrophosphate analogues that inhibit osteoclasts (Mundy, 2002; Ramaswamy and Shapiro, 2003; Simos *et al.*, 2013). Bisphosphonates bind with high affinity to hydroxyapatite crystals on the mineralized bone surfaces and during osteolysis are taken up by osteoclasts inhibiting resorption (Baron *et al.*, 2011; Casimiro *et al.*, 2009; Drake *et al.*, 2008). There are many bisphosphonates: pamidronate, aldreonate, clodronate and probably the most commonly administered, zoledronate (Mundy, 2002; Baron *et al.*, 2011; Ramaswamy and Shapiro, 2003; Simos *et al.*, 2013). In addition to treating patients with osteolytic metastases, bisphosphonates are used to treat patients with bone loss diseases including osteoporosis, arthritis and Paget's disease (Casimiro *et al.*, 2009; Feng *et al.*, 2013; Drake *et al.*, 2008). Bisphosphonates inhibit osteoclast resorption by a number of mechanisms including
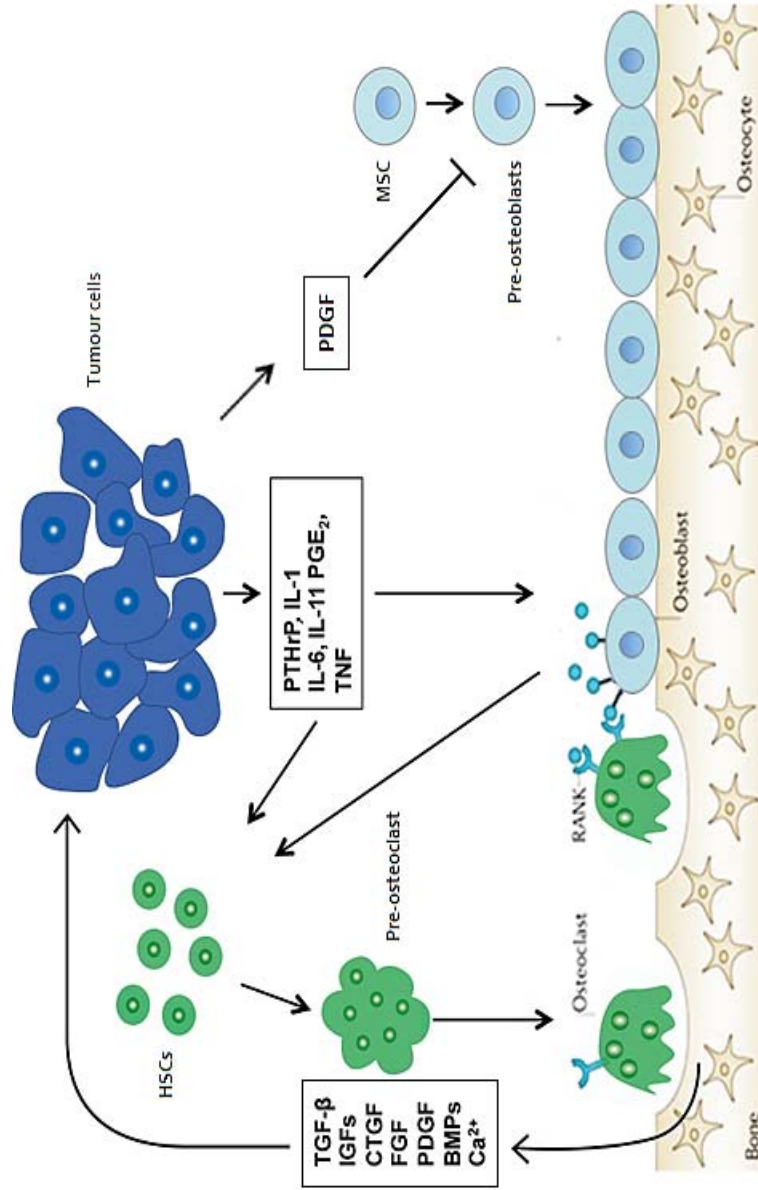
Figure 1.6 Schematic of the proposed vicious cycle of bone loss and tumour growth, which occurs in osteolytic metastasis
Tumour cells recruit osteoclasts to destroy the bone causing the release of bone matrix factors including TGF-β, IGFs, BMPs and Ca^{2+}. These factors stimulate the metastatic tumour cells grow and proliferate. The tumour cells release osteolytic factors including PTHrP, Il-11, PGE_2 and TNFα amongst others, which act upon osteoblasts to stimulate the expression of RANKL increasing the formation of osteoclasts from osteoclast precursor cells. In addition some of these osteolytic factors can act directly upon osteoclast precursors to stimulate their differentiation. In addition the tumour cells also secrete factors such as PDGF, which acts to impede osteoblast differentiation. Figure adapted from (Weilbaecher *et al.*, 2011; Mundy, 2002; Chen *et al.*, 2010b; Guise, 2013).

osteoclast apoptosis, alteration of osteoclast cytoskeleton assembly and inactivation of the adenosine triphosphate-dependent proton pump, the latter resulting in inhibition of the acid secretion, which is required to dissolve the bone mineral matrix (Ramaswamy and Shapiro, 2003; Baron *et al.*, 2011; Hofbauer *et al.*, 2008). In addition, bisphosphonates have been reported to directly affect tumour cells themselves although the reasons for this are unclear (Ramaswamy and Shapiro, 2003; Weilbaecher *et al.*, 2011). Treatment with bisphosphonates has been shown to decrease the incidence of SRE, bone lesions and tumour burden (Mundy, 2002; Simos *et al.*, 2013). The bisphosphonate, zoledronic acid, is the standard of care for patients, which have advanced cancer and bone metastases (Polascik and Mouraviev, 2008; Israeli, 2008; Berenson, 2005; Lipton, 2004). In many human clinical trials zoledronate has been shown to decrease bone lesions and the incidence of SRE that arise from metastatic bone disease (Berenson, 2005; Polascik and Mouraviev, 2008; Simos *et al.*, 2013; Holen and Coleman, 2010).

RANKL-targeted therapy has emerged as significant target for bone loss diseases including osteolytic metastases (Hofbauer *et al.*, 2008; Simos *et al.*, 2013). The effect of RANKL inhibition was first evaluated in preclinical and clinical studies using chimeric proteins consisting of the RANKL-binding domains of OPG or of RANK fused with the Fc portion of human IgG$_1$ (Baron *et al.*, 2011) Originally trialed clinically as anti-osteolytic agents, they have been superseded by denosumab, which is a fully humanized RANKL-binding monoclonal antibody (Roodman and Dougall, 2008; Baron *et al.*, 2011). Denosumab inhibits RANKL binding to RANK and persists in the circulation for up to 3 months (Baron *et al.*, 2011; Dubois *et al.*, 2011; Rizzoli *et al.*, 2010). Denosumab thus inhibits the differentiation of osteoclast progenitors into mature osteoclasts, unlike bisphosphonates that kill or disable osteoclasts when they are ingested during the process of bone resorption (Baron *et al.*, 2011; Casimiro *et al.*, 2009). Another important clinical difference between bisphosphonates and denosumab as anti-resorptive drugs is that bisphosphonates have high affinity for bone and persist for many years (Bock and Felsenberg, 2008). In contrast, denosumab binds to soluble RANKL in the extracellular milieu and is cleared from the body over months (Miyazaki *et al.*, 2014; Rizzoli *et al.*, 2010). Comparative studies between the potent bisphosphonate, zoledronate, and denosumab treatment showed denosumab treatment to be the more effective, increasing the time to the first SRE and also decreasing bone turnover markers (Henry *et al.*, 2011; Lipton *et al.;* Stopeck *et al.*, 2010; Dougall, 2010; Dougall *et al.*, 2014). In prostate

cancer patients free from metastasis, denosumab prolonged bone metastasis-free survival and delayed the time to first bone metastasis (Dougall *et al.*, 2014). In addition, a comparative study assessing the anti-cancer effects of denosumab upon lung cancer patients with bone metastasis in comparison to zoledronate treated patients with bone metastasis from solid tumours or multiple myeloma, showed denosumab increased survival (Smith *et al.;* Dougall *et al.*, 2014). A Phase I clinical trial with denosumab was trialled on patients with Multiple Myeloma or breast cancer with bone metastasis. Twenty-four hours after denosumab treatment, bone turnover markers were reduced greater than 50% and 75%, respectively and these reductions were maintained throughout the 84 day trial period (Body *et al.*, 2006; Roodman and Dougall, 2008). Denosumab treatment has also been shown to decrease the severe pain, which is the most common SRE in patients with metastatic bone disease (Weilbaecher *et al.*, 2011).

1.7 Cancer Cell Stress

Cancer cells have a phenotype that displays greatly increased dependence upon cell stress response pathways, which is termed 'stress phenotype' (Solimini *et al.*, 2007; Wondrak, 2015). This stress phenotype allows them to grow despite the internal and external environmental insults (Solimini *et al.*, 2007; Wondrak, 2015). Malignant mutations, which either confer gain of function (e.g., amplification or overexpression of key oncogenes) or loss of function mutations (e.g., deletions and epigenetic silencing of major tumour suppressor genes) result in cell deregulation that is associated with enhanced cell stress (Hahn and Weinberg, 2002). The multiple mutations, often arising in a multistep manner, confer a common set of properties or hallmarks that achieve the malignant cancer cell phenotype (Vogelstein and Kinzler, 1993; Bernards and Weinberg, 2002; Luo *et al.*, 2009). Cancer cell hallmarks include unchecked proliferation, self-sufficiency in growth signals, resistance to anti-proliferative and apoptotic cues, angiogenesis (that feeds oxygen and nutrients to the tumour cells allowing the tumour to grow), evade immune detection and metastasis to distant organs (Hanahan and Weinberg, 2011; Luo *et al.*, 2009; Neckers and Workman, 2012; Kroemer and Pouyssegur, 2008). As reviewed by Solimini *et al*., many of the aforementioned mutations give rise to 'oncogenic addiction'; however, 'non-oncogene addiction' also occurs where the cancer cells rely heavily on factors, which are not classified as oncogenes to promote their cancerous state (Solimini *et al.*, 2007). Such molecules include heat shock factor 1 (HSF1) and heat shock protein 90 (HSP90) the latter of which is regulated by HSF1

(Solimini *et al.*, 2007). In addition to the stresses generated from within the cell, tumour microenvironment stresses are present including pH imbalance, hypoxia and nutrient deprivation (Figure 1.9) (Travers *et al.*, 2012; Trepel *et al.*, 2010; Workman *et al.*, 2007). In order to survive these oncogenesis-associated cellular stresses, a number of stress responses or stress support pathways are activated, which allow the cancer cells not only to survive but proliferate allowing for tumour progression (Luo *et al.*, 2009; Solimini *et al.*, 2007). These stress responses are additional phenotypic hallmarks of cancer cells and include proteasome stress (unfolded protein response [UPR]), ER stress (UPR), oxidative stress, metabolic stress, HSF1 mediated cell stress (heat shock response [HSR]), genotoxic stress (DNA damage), and membrane stress (Chapter 1.8) (Luo *et al.*, 2009; Solimini *et al.*, 2007). The cancer stress phenotypes are not responsible for initiating tumorigenesis, but they are common characteristics of many tumour types and allow for the cancer cell to survive (Luo *et al.*, 2009). Interestingly, interplay between the stress response pathways often occurs in tumour cells (Luo *et al.*, 2009). These stress phenotypes are also seen in other pathological conditions including chronic inflammation (Luo *et al.*, 2009). Because these stress response pathways are typically activated in cancer cells, targeting the molecules or organelles that mediate the stress responses provides a way to selectively target processes, which are increased in cancer cells (Luo *et al.*, 2009). As such many cancer therapeutics have been developed to inhibit the pro-tumour responses that the stress support pathways garner (Chapter 1.9) (Solimini *et al.*, 2007). These stress pathways are activated not only in cancer cells, but are common pathways that can be activated an many cell types in response to stress and are discussed in this context below (Fulda *et al.*, 2010).

1.8 Cell Stress Pathways

As described above, cancer cells have many stress response pathways highly activated; however, these pathways are also activated in noncancerous cells and maintain cell viability when the cell is exposed to stress (Fulda *et al.*, 2010). Stressors which activate the heat shock response, oxidative stress, ER stress and genotoxic stress are varied and include: UV irradiation, pH imbalance, inflammatory cytokines, therapeutic compounds, and heat (Fulda *et al.*, 2010; Richter *et al.*, 2010; Zarubin and Han, 2005; Birben *et al.*, 2012; Chaudhari *et al.*, 2014; Peng *et al.*, 2010).

1.8.1 Heat Shock Response

Heat is a major cell stressor, with temperatures varying only a couple of degrees higher posing a significant threat to cell survival and, therefore, organism survival in many species (Verghese *et al.*, 2012; Richter *et al.*, 2010). A classic heat shock response (HSR) is triggered by a temperature increase of only a couple of degrees relative to the optimum temperature of that species in both prokaryotes and eukaryotes alike (Richter *et al.*, 2010; Wu, 1995). The effect of heat was first identified in *Drosophila* cells in the 1930s but was not well characterised until in the 1960s (Wu, 1995; Richter *et al.*, 2010; Åkerfelt *et al.*, 2010). It was from this work that the HSR was found to be regulated by heat shock factor 1 (HSF1) (Lindquist, 1986; Neidhardt *et al.*, 1984). Heat shock stress to the cell causes proteins to incorrectly fold and also denature thus become unfolded and allowing for protein aggregation (Figure 1.7). The high concentration of misfolded, unfolded, or aggregated proteins signals to the cell for the activation of the HSR, which increases the transcription and translation of Heat Shock Proteins (HSPs) to protect against stress-induced death (ÅKerfelt *et al.*, 2007; Morimoto, 2008).

Heat shock proteins are conventionally divided into 5 main families based on molecular weight: HSP60, HSP70, HSP90, HSP100 and the small heat shock proteins, such as HSP25/27 and HSP33 (Goetz *et al.*, 2003; Nover and Scharf, 1997). The main characterised function of HSPs is as molecular chaperones, facilitating correct protein folding and targeting misfolded proteins to ubiquitin tagged degradation to maintain protein homeostasis and therefore cell viability (Gabai and Sherman, 2002; Lila *et al.*, 2001; Richter *et al.*, 2010; Whitesell and Lindquist, 2005). As mentioned above, when a cell experiences stress unfolded proteins or incorrectly folded proteins aggregate and cause proteotoxic stress driving the rapid transcription and translation of HSPs (Figure 1.7) (Calderwood, 2013; Morimoto, 2008; Stephanou and Latchman, 2011; Richter *et al.*, 2010). Increasing the stoichiometric ratio of HSPs pushes the reaction toward maintaining and correcting protein folding within the cell (Calderwood, 2010; Calderwood, 2013; Stephanou and Latchman, 2011; Morimoto, 2008; Richter *et al.*, 2010). Thus, HSPs act to protect the cell against proteotoxic stress by maintaining correct protein folding, refolding misfolded proteins and targeting aggregated proteins to the proteasome for degradation (Figure 1.7) (Morimoto, 2008; Verghese *et al.*, 2012; Vabulas *et al.*, 2010). In addition to heat, a wide range of other stressors including: UV and X-ray irradiation, acidosis, inflammatory cytokines, viruses and cytotoxic compounds all result in protein misfolding similarly activate the HSR and often through similar mechanisms

(Dai *et al.*, 2007; Åkerfelt *et al.*, 2010; Fulda *et al.*, 2010; Richter *et al.*, 2010). The increased expression of HSPs avoids the cellular cytoplasmic microenvironment becoming crowded with unstable proteins, which risk causing the cell proteotoxic stress and death (Vabulas *et al.*, 2010; Taipale *et al.*, 2010).

When a cell undergoes an HSR, it not only results in misfolded and aggregated proteins, but it also affects the cell as a whole including: transport and nuclear activities, organelle localizations and their correct functions, the cell's structural integrity and cell growth and proliferation (Richter *et al.*, 2010). The deregulation of protein folding is most likely to account for the wider cellular effects of heat shock (Richter *et al.*, 2010; Taipale *et al.*, 2010). Heat shock causes vimentin, a major cytoskeleton protein filament component to aggregate with subsequent breakdown of the actin and tubulin cytoskeleton causing the cell morphology to be distorted, which occurs during apoptosis (Richter *et al.*, 2010; Welch and Suhan, 1985; Toivola *et al.*, 2010; Szalay *et al.*, 2007). Membrane permeability is also increased by a changed protein:lipid membrane ratio, resulting in a change in both pH and ion homeostasis (Kruuv *et al.*, 1983; Richter *et al.*, 2010; Nakamoto and Vígh, 2007). Organelles affected by heat shock include the mitochondria, Golgi and ER of which the latter two may undergo fragmentation (Welch and Suhan, 1985; Richter *et al.*, 2010). Relating to the nucleus, RNA is incorrectly processed in the ribosomes and aggregates similar to protein in response to heat shock (Welch and Suhan, 1985; Boulon *et al.*, 2010). In addition, heat shock causes the formation of stress granules (Nover and Scharf, 1997; Buchan *et al.*, 2011). These are structures that hold non-translational mRNA and RNA-protein composites as well as regulators of translation (Nover and Scharf, 1997; Buchan *et al.*, 2011). Overall in response to the HSR there is a decrease in transcription (Buchan *et al.*, 2011; Boulon *et al.*, 2010). Additionally, studies have shown that the cell cycle is arrested the G1/S and G2/M phases stopping growth and proliferation (Kuhl and Rensing, 2000; Richter *et al.*, 2010). Thus, the result of heat shock and related responses to other stressors upon the cell is usually either cellular death or survival depending upon the extent of the stress insult (Richter *et al.*, 2010). Sometimes, however, resistance to the stressor may also develop, for example some cancer cells may acquire resistance to chemotherapeutics through HSF1 and non-oncogene addiction (Richter *et al.*, 2010). Mice that lack HSF1 are protected against tumorigenesis to a large extent with reduced tumour load and extended survival times, indicating that cancer cells are more reliant upon HSF1 for their survival than non-cancerous cells (Dai *et al.*, 2007). The protective role of HSF1 against tumorigenesis is thought to occur through the increased

expression of HSPs (Solimini *et al.*, 2007). The increased HSP levels decreases the stress incurred through the increased load of unstable and mutated proteins, increased protein turnover and proteasome stress (Solimini *et al.*, 2007).

1.8.1.1 Heat Shock Factor 1

HSF1 is described as the major regulator of cellular responses to stress (Gandhapudi *et al.*, 2013). As described earlier, HSF1 activation causes the downstream transcription of target genes i.e., HSPs, which act to stabilize proteins by refolding them or cause their degradation (Neueder *et al.*, 2014; Morimoto, 1993; Dai *et al.*, 2007). These actions act to maintain protein homeostasis within the cell (Dai *et al.*, 2007). HSF1 is a member of the heat shock family of proteins, which also includes HSF2 and HSF4 in mammals and HSF3 in avian species (Åkerfelt *et al.*, 2010; Pirkkala *et al.*, 2001; Powers and Workman, 2007; Diller, 2006). Between the family members there is a degree of redundancy in their response to stress but also specialized responses (Åkerfelt *et al.*, 2010; Diller, 2006). HSF1 is the principle regulator of the HSR; however, HSF2 can cooperate with HSF1 during the HSR (Stephanou and Latchman, 2011; Åkerfelt *et al.*, 2010). For example, HSF-2 can form heterotrimers with HSF1 and bind to DNA binding motifs in *Hsp* genes (Åkerfelt *et al.*, 2010). In addition, HSF1 and HSF2 co-localize in nuclear stress bodies (Åkerfelt *et al.*, 2010). HSF1 is expressed in most cell types and its expression is required for not only increased expression of HSPs but also their basal levels, which are very low activity at around 5% compared to stressed cells (Åkerfelt *et al.*, 2010; Diller, 2006).

HSF1 Function

In response to heat, HSF1 activates the HSR and causes the rapid increase in the transcription of particular HSPs especially HSP90, HSP27 and HSP70 family members (Åkerfelt *et al.*, 2010; Morimoto, 1993; Morimoto, 2008; Fulda *et al.*, 2010; Dai *et al.*, 2014). As described earlier these HSPs act to maintain correct protein folding the protein homeostasis with the cell (Fulda *et al.*, 2010; Morimoto, 1993). This process occurs after the classical heat shock response to heat but also applies to various environmental and pathophysiological stressors including: UPR, heavy metals, UV, viral infections, acidosis, nutritional deprivation and treatments with chemotherapeutics (Åkerfelt *et al.*, 2010; Morimoto, 1993; Morimoto, 2008; Fulda *et al.*, 2010; Dai *et al.*, 2014). The activation of HSF1 and its induction of the HSR confer a tolerance to stress making cells more resistant to various toxic insults and therefore maintains cell viability during stress conditions (Craig and Schlesinger, 1985; Lindquist,

1986; Fulda *et al.*, 2010). HSF1 knockout mice and cell line models have demonstrated that HSF1 is essential for the transcription of many HSPs (Åkerfelt *et al.*, 2010; Diller, 2006). HSF1$^{-/-}$ cells do not develop thermotolerance whilst undergoing heat shock and therefore go through heat-induced apoptosis (McMillan *et al.*, 1998; Zhang *et al.*, 2002b). In addition, these HSF1$^{-/-}$ cells have much lower levels of HSP70 and HSP25, which are no longer inducible (McMillan *et al.*, 1998). This consequently results in the lack of HSP mediated inhibition of apoptosis through both the caspase and caspase independent pathways (McMillan *et al.*, 1998).

HSF1 Structure, Localization and Activation

HSF1 belongs to the winged helix turn-helix (wHTH) family of DNA binding proteins (Åkerfelt *et al.*, 2010; Ahn *et al.*, 2001). HSF1 has an N terminal DNA-binding domain (DBD), an adjacent coiled coil trimerization domain and a transcriptional activation domain at the carboxyl terminal region (Pirkkala *et al.*, 2001; Åkerfelt *et al.*, 2010). Under normal physiological conditions, HSF1 is mostly localized to the cytoplasm of the cell and is present in a latent monomeric form bound to HSP90 and other components of the multichaperone complex (Chapter 1.9.2, Figure 1.7) (Neef *et al.*, 2013; Whitesell and Lindquist, 2009; Diller, 2006; Zou *et al.*, 1998). During cell stress, unfolded and aggregated proteins start to accumulate and compete with HSF1 for HSP90 binding (Whitesell and Lindquist, 2009). The recruitment of HSP90 and HSP70 to proteins that are misfolded, titrates these molecules away from their association with HSF1 (Figure 1.7) (Pirkkala *et al.*, 2001; Whitesell and Lindquist, 2009). Once dissociated from the HSP90 multichaperone complex, the HSF1 monomers are activated by a multi-step process which includes: trimerization that gives HSF1 its DNA binding affinity; nuclear translocation; nuclear accumulation and broad posttranslational modifications including phosphorylation, acetylation and sumoylation, which regulate HSF1 activity (Figure 1.7) (Stephanou and Latchman, 2011; Åkerfelt *et al.*, 2010; Whitesell and Lindquist, 2009; Diller, 2006; Anckar and Sistonen, 2011).

HSF1 mediates HSP transcription by binding to consensus sequences called heat shock response elements (HSEs), which are found in HSP gene promoters but also many other genes including *RANKL* (Jaeger *et al.*, 2014; Åkerfelt *et al.*, 2010; Stephanou and Latchman, 2011; Roccisana *et al.*, 2004). HSEs are comprised of extended repeats of the sequence nGGAn (Jaeger *et al.*, 2014; Trinklein *et al.*, 2004). It has been found that HSF1 prefers to bind to HSE with at least three contiguous inverted nGAAn repeats (nTTCnnGAAnnTTCn)

with the DBD of each HSF1 monomer in the trimer recognizes the sequence nGGAn in the major groove of the DNA helix (Trinklein *et al.*, 2004; Jaeger *et al.*, 2014; Anckar and Sistonen, 2011). The trimerization of HSF1 that occurs under stress events increases HSF1 affinity for HSEs by several orders of magnitude (Anckar and Sistonen, 2011; Liu and Thiele, 1999).

1.8.1.2 HSF1 and the Stress Inducible HSP72

One of the key targets of HSF1 is the stress inducible HSP72 (HSPA1A). HSP72 belongs to the HSP70 family of HSPs, which has served as a model system for inducible transcription in eukaryotes (Åkerfelt *et al.*, 2010; Lindquist, 1986). HSP72 is considered to be a protective molecule against stress stimuli, and its expression is often used as a biomarker of cell stress. In this thesis, HSP72 expression is used as an indicator of HSF1 activation and HSR induction. HSP72 expression has been shown to be increased in the nucleolus by a myriad of stressors including hypothermia, heat shock, osmotic stress, ROS and chemotherapeutics (Kregel, 2002; Wang *et al.*, 2012; Morimoto, 2002; Melling *et al.*, 2009; Latchman, 2001; Gupta *et al.*, 2010; Beck *et al.*, 2000; Richter *et al.*, 2010; Hendrick and Hartl, 1993; Mayer and Bukau, 2005). HSP72 mediates its protective effect by participating in the refolding of misfolded proteins, maintenance of proteins in their native folded state and minimizing protein aggregation (Agashe and Hartl, 2000; Richter *et al.*, 2010; Hendrick and Hartl, 1993; Mayer and Bukau, 2005). Like most HSPs, HSP72 expression is regulated by HSF1 (Melling *et al.*, 2009; Morimoto, 1998). The HSP70 gene has two HSE within its 5′ prime region and HSF1 binds to the proximal HSE to induce HSP72 expression (Melling *et al.*, 2009; Morimoto, 1998; Kregel, 2002).
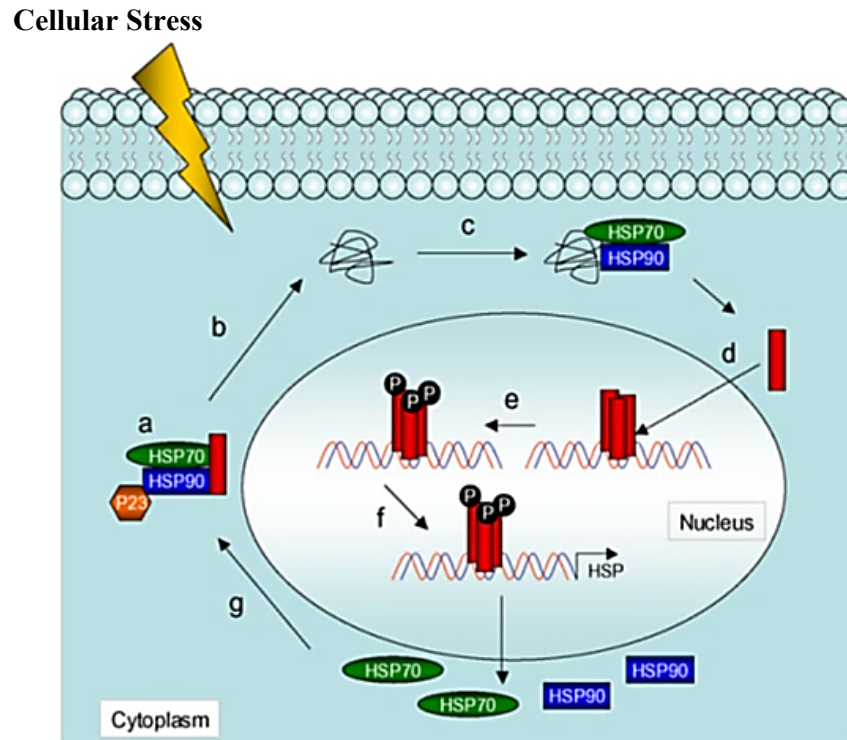
Figure 1.7 HSF1 Activation
(a.) Under physiological conditions, HSF1 is present as monomer that is bound to the N-terminal of HSP90, which exists as a HSP90/HSP70 (and HDAC6 and p23) chaperone complex. This interaction with HSP90 inhibits HSF1 transcriptional activity. (b.) Upon stress misfolded proteins accumulates (c.), which causes the HSP90/HSP70 chaperone to dissociate from HSF1. HSP90/HSP70 binds to misfolded proteins to refold them (d.). The monomeric HSF1 then trimerizes and translocates to the nucleus where (e.) it undergoes a series of post-translational phosphorylation events. (f.) HSF1 then binds to HSE in the promoters of *Hsp* genes including *Hsp90* and *Hsp70* and other target genes. (g.) The increased cellular concentration HSP negatively feedbacks upon HSF1 by binding to and repressing its activity. Imaged sourced from (Powers and Workman, 2007).

1.8.2 The p38 Stress MAP Kinase Signalling Pathway

Although HSF1 is a major mediator of many forms of cellular stress within cells, another important stress pathway in the cell is the p38-signalling cascade (Robinson and Cobb, 1997; Zarubin and Han, 2005). P38 is a stress-associated MAPK and is one of the four MAPK subfamilies, which include: extracellular signal-regulated kinases (ERKs), c-jun N-terminal or stress-activated protein kinases (JNK/SAPK), and ERK/big MAPK kinase 1 (BMK1) (Zarubin and Han, 2005; Obata *et al.*, 2000; Sudo *et al.*, 2005). P38 was first isolated as a 38kDa protein that was quickly phosphorylated on tyrosine residues when treated with Lipopolysaccharides (LPS) (Zarubin and Han, 2005; Nahas *et al.*, 1996). There are four splice variants of the p38 family described: p38α, p38β, p38γ (ERK6, SAPK3) and p38δ (SAPK4) (Wagner and Nebreda, 2009). All of these can be recognized by a Thr-Gly-Tyr (TGY) dual phosphorylation motif (Zarubin and Han, 2005; Waskiewicz and Cooper, 1995). Both p38α and p38β are expressed ubiquitously in cells; however, p38γ and p38δ are differentially expressed in different tissue-types (Lawson *et al.*, 2013; Zarubin and Han, 2005; Koul *et al.*, 2013).

P38 is activated through phosphorylation by a range of stressors including pro-inflammatory cytokines, UV, heat shock, osmotic stress, bacterial endotoxins i.e., LPS, DNA damage and oxidative stress (Zarubin and Han, 2005; Junttila *et al.*, 2008; Wagner and Nebreda, 2009). Phosphorylation of p38 causes a wide range of downstream effects including apoptosis, cytokine production, transcriptional regulation and cytoskeletal organization (Wagner and Nebreda, 2009; Junttila *et al.*, 2008; Obata *et al.*, 2000). In the pathophysiology of cancer, the p38 MAP kinase signalling pathway has been shown to both negatively and positively affect tumorigenesis, suggesting its actions may be cell context-specific (Wagner and Nebreda, 2009). For example, p38 activation has been shown to be significantly less in 20 human hepatocellular carcinoma cell lines in comparison to non-cancerous cells (Bradham and McClay, 2006). However, a gene expression profiling study of cancer cell in response to TNF-α showed that p38 had a strong prosurvival role by downregulation of pro-apoptotic genes and the upregulation of *Bcl2* genes (Phong *et al.*, 2010). p38 activation is regulated by the dual kinases MAP kinase kinases (MKK): MKK3 and MKK6 (Zarubin and Han, 2005; Jiang *et al.*, 1996; Wagner and Nebreda, 2009; Brancho *et al.*, 2003). It has also been reported that the upstream kinase of JNK, MKK4, can aid in p38α and p38δ activation in certain cell types, which would explain the redundancy seen between these pathways

(Wagner and Nebreda, 2009; Brancho *et al.*, 2003; Zarubin and Han, 2005). Further upstream of MKK are MAP kinase kinase kinases (MAPKKK) and STE20 kinases or small GTP-binding proteins (MAPKKKK), which regulate p38 activity (Axmann *et al.*, 2009; Garrington and Johnson, 1999; Turjanski *et al.*, 2007). In addition, a MAPKK independent p38 activation pathway that involves the adaptor protein TAB1 has been identified (Zarubin and Han, 2005; Cuenda and Rousseau, 2007; Ge *et al.*, 2002). Ge *et al.* showed a complex containing TAB1, p38α and TRAF6 after RANKL binding to the RANK receptor (Ge *et al.*, 2002). In this activation mechanism, TAB1 interaction with p38 causes its autophosphorylation (Cuenda and Rousseau, 2007; Zarubin and Han, 2005; Ge *et al.*, 2002). The p38 Stress MAP kinase pathway is essential for osteoclastogenesis (Li *et al.*, 2002). As described earlier, p38 activation is required for osteoclastogenesis and mice which lack p38 do not have osteoclasts (Li *et al.*, 2002). Upon onset of cell stress and p38 phosphorylation, p38 translocates to the nucleus where it phosphorylates target proteins among its nuclear substrates, which are transcription factors already bound to the DNA (Chang and Karin, 2001; Gong *et al.*, 2012; Cargnello and Roux, 2011). P38 has many substrates including MAP kinase-activated protein kinase 2 and 3 (MK2 and MK3), and the p38 regulated/activated kinase (Zarubin and Han, 2005; Wagner and Nebreda, 2009). These p38 substrates activate many downstream targets including heat shock protein 27 (HSP27), which is involved in regulating cell apoptosis (Zarubin and Han, 2005; Xu *et al.*, 2006). It is interesting to note that p38 has been shown to be involved in the HSR (Patel, 2009). P38 has been reported to regulate HSP70 protein levels and HSF1 activation in osmotically stressed murine cortical and medullary cells (Patel, 2009). Moreover, HSF1 inhibition decreases p38 phosphorylation in these cells (Patel, 2009). Further suggesting a regulatory role between these two proteins is that p38 and JNK have been shown to phosphorylate HSF1 in a ras-dependent manner in heat shocked or osmotically stressed NIH3T3 cells that constitutively express active Ras (Kim *et al.*, 1997). Rafiee *et al.* identified that p38 MAPK inhibition through SB-203580 and p38 knockdown inhibited Hsp27 and Hsp70 mRNA induction in human esophageal microvascular endothelial cells (HEMEC) (Rafiee *et al.*, 2006). This data suggests a role for MAPKs in the HEMEC HSR (Rafiee *et al.*, 2006). In addition in 9L rat brain tumour cells, cadmium (100µM) treatment phosphorylates p38, which is followed by HSP70 induction (Hung *et al.*, 1998). The necessity of p38 activation in cadmium mediated HSP70 expression was shown by pharmacological inhibition of p38 (SB203580), which inhibited the induced HSP70 expression (Hung *et al.*, 1998).

1.8.3 Oxidative Stress

Organisms that live in an aerobic environment are constantly exposed to reactive ROS. Reactive oxygen species are a number of reactive molecules and free radicals, which are derived from molecular oxygen. Some examples of ROS include superoxide anions, hydrogen peroxide, peroxide hydroxyl radicals, and hydroxyl ions (Martindale and Holbrook, 2002; Stadtman, 2004; Held, 2015). These molecules have a higher reactivity than molecular oxygen and if produced in too high a level cause oxidative stress resulting in serious cell damage (Sharma *et al.*, 2012; Poljsak *et al.*, 2013; Noori, 2012; Held, 2015). Thus, oxidative stress occurs when the redox equilibrium in the cell is disturbed, and there are more oxidants than antioxidants (Birben *et al.*, 2012; Poljsak *et al.*, 2013).

ROS are generated in response to either intracellular or exogenous sources (Martindale and Holbrook, 2002; Noori, 2012). Intracellularly, most ROS are produced in the mitochondria, which is where redox potential is maintained (Martindale and Holbrook, 2002; Gutterman, 2005). ROS are generally generated as a result of electron leakage from the oxidative phosphorylation pathway (Gutterman, 2005; Martindale and Holbrook, 2002). However, ROS are also formed by metal catalysed oxidation and oxidoreductase enzymes (Martindale and Holbrook, 2002; Held, 2015). Cells can also take up exogenous ROS or generate them in response to environmental insults such as ethanol exposure (Held, 2015; Martindale and Holbrook, 2002; Birben *et al.*, 2012; Noori, 2012). Normally within the cell, ROS levels fluctuate whilst still maintaining redox equilibrium (Poljsak *et al.*, 2013; Trachootham *et al.*, 2008). Low levels of ROS are present normally within cells and are mitogenic promoting cell proliferation (Martindale and Holbrook, 2002; Trachootham *et al.*, 2008). However, as mentioned above, high levels or sustained levels of ROS can cause severe DNA, protein and lipid damage through oxidative stress (Stadtman, 2004; Sharma *et al.*, 2012; Martindale and Holbrook, 2002; Birben *et al.*, 2012). This damage can affect cell proliferation, cause growth arrest, senescence and cell death (Martindale and Holbrook, 2002; Trachootham *et al.*, 2008; Guo *et al.*, 2010). To counteract ROS, a large number of cellular defence systems are in place including antioxidants such as vitamins C, E and A, and ROS scavengers including superoxide dismutases (SOD), catalase, and glutathione peroxide (Poljsak *et al.*, 2013; Sharma *et al.*, 2012; Martindale and Holbrook, 2002; Birben *et al.*, 2012). Oxidative stress is involved in the pathogenesis of many diseases including diabetes, atherosclerosis, pulmonary fibrosis, cancer and bone loss diseases including arthritis (Martindale and Holbrook, 2002; Birben *et al.*, 2012). In cancer, oxidative stress is increased and has been associated with

cancer formation and progression including: cell proliferation, invasiveness, angiogenesis and chemoresistance (Kumar *et al.*, 2008; Mates *et al.*, 2013; Reuter *et al.*, 2010). Consistent with this, oxidative stress has been shown to be increased in the prostate cancer cell line PC3 and its expression was correlated with a more aggressive phenotype (Kumar *et al.*, 2008).

ROS also has a role as an intra- and inter-cellular messenger, relaying redox signalling messages from the mitochondria to the rest of the cell, which are thought to activate a number of genes important in cancer cell growth (Reuter *et al.*, 2010; Klaunig *et al.*, 2010; Murphy, 2009; Valko *et al.*, 2006). In addition to having a prominent role in cancer, oxidative stress is a well-known mediator of pathological bone loss; however, the mechanism by which this occurs is not fully known (Kajarabille *et al.*, 2013; Shen *et al.*, 2009; Engdahl *et al.*, 2013; Kajiya *et al.*, 2006). More recently, ROS have been shown to prolong the survival of osteoclast progenitors, affect osteoclast differentiation and osteoclast resorptive activity (Wang *et al.*, 2011c; Yamasaki *et al.*, 2009; Yeon *et al.*, 2012; Basu and Krishnamurthy, 2010). Inhibiting ROS with redox regulatory proteins and antioxidants has been shown to decrease ROS- enhanced osteoclast formation (Xu *et al.*, 2010; Moon *et al.*, 2012a). It may be that ROS imbalance and the subsequent oxidative stress act to increase osteoclast differentiation through their actions as both intra- and inter-cellular messengers (Murphy, 2009; Held, 2015). Pathways involved in ROS generation include calcium dependent pathways, protein tyrosine kinases, protein tyrosine phosphatases, serine threonine kinases, phospholipase, MAPK, NFκB, cytokine, growth and G-coupled receptors and ion channel receptors (Martindale and Holbrook, 2002; Noori, 2012; Touyz, 2004). Molecules affected by ROS include ataxia-telangectasia mutated (ATM); ERK, HSF1, Janus protein kinase (JAK), JNK, NFκB, PI3K, protein kinase C (PKC), phospholipase C-γ1 (PLC-γ1) and signal transducers and activators of transcription (STAT) (Martindale and Holbrook, 2002; Gutterman, 2005). Many of these signalling networks and molecules are known to play essential major role in osteoclast differentiation. This suggests that this stress pathway may affect the regulation of osteoclastogenesis.

Interestingly, oxidative stress has been linked to a number of stress pathways including the HSR (Pignataro *et al.*, 2007). For example, ROS generated by ethanol ingestion have been shown to cause HSF1 translocation to the nucleus and the transcription of HSPs (Pignataro *et al.*, 2007). ROS have also been shown to activate endoplasmic reticulum stress (UPR) with

studies suggesting that these pathways are closely linked (Bhandary *et al.*, 2013; Liu *et al.*, 2011; Nakka *et al.*, 2014).

1.8.4 Endoplasmic Stress and the Unfolded Protein Response

The endoplasmic reticulum (ER) is the main organelle within the cell where transmembrane, secretory and ER-resident proteins are synthesized, folded and modified (Liu and Kaufman, 2003; Oslowski and Urano, 2011). Many environmental stressors including heat shock, glucose deprivation, chemotherapeutic stress and changes in intracellular Ca^{2+} pools lead to the accumulation of incorrectly folded proteins (Chaudhari *et al.*, 2014; Kim *et al.*, 2008a; Marcu *et al.*, 2002). In addition, the pathobiology of some diseases leads to misfolded proteins (Doyle *et al.*, 2011; Marcu *et al.*, 2002). In response to stress and the accumulation of incorrectly folded proteins in the ER lumen, cells activate a number of signalling pathways that are collectively termed the unfolded protein response (UPR) (Liu and Kaufman, 2003; Oslowski and Urano, 2011; Ron and Walter, 2007). The UPR acts to decrease ER stress and restore homeostasis (Oslowski and Urano, 2011; Chaudhari *et al.*, 2014). The UPR signalling pathway has three distinct actions (Liu *et al.*, 2003; Ron and Walter, 2007; Levonen *et al.*, 2014; Marcu *et al.*, 2002). These actions include the global attenuation of protein translation that reduces the load of newly synthesized proteins and increased transcription of ER chaperones as well as other related stress proteins including immunoglobulin binding protein (BiP) and the ER HSP90 analogue Glucose regulated protein 94 (GRP94, or HSP90B1) (Liu *et al.*, 2003; Ron and Walter, 2007; Levonen *et al.*, 2014; Marcu *et al.*, 2002). In addition, ER-associated degradation pathways are activated to clear the ER of misfolded proteins through retrograde transport targeting them for proteasome degradation (Levonen *et al.*, 2014; Marcu *et al.*, 2002; Ron and Walter, 2007; Liu and Kaufman, 2003). These three actions are mediated through the stress induced expression and activation of pancreatic ER kinase (PERK) an ER transmembrane kinase, inositol-requiring transmembrane kinase/endonuclease 1 (IRE1) an ER transmembrane glycoprotein and activating transcription factor 6 (ATF6), which is an ER transmembrane-activating transcription factor (Kaufman *et al.*, 2002; Oslowski and Urano, 2011; Todd *et al.*, 2008; Liu and Kaufman, 2003). These factors are the main transducers of the UPR (Kaufman *et al.*, 2002; Born *et al.*, 2013; Oslowski and Urano, 2011; Davenport *et al.*, 2007; Liu and Kaufman, 2003). The latter two factors act to increase ER molecular chaperones, folding enzymes and proteins, which are involved in ER associated protein degradation (Born *et al.*, 2013). The induction of these molecules during the UPR serves as a protective mechanism increasing protein folding

capacity (Born *et al.*, 2013). Under physiological conditions PERK, IRE1 and ATF6 are negatively regulated by BiP; however, upon stress BiP dissociates from these proteins' luminal domains (Kaufman *et al.*, 2002; Oslowski and Urano, 2011; Davenport *et al.*, 2007). If ER stress persists, then JNK is activated and the mitochondria/ Apaf1 dependent capases are cleaved resulting in cell apoptosis (Kaufman *et al.*, 2002; Oslowski and Urano, 2011). It is interesting to note that during tumorigenesis the high proliferation rate of cancer cells requires increased ER actions including increased protein folding, assembly and transport, which can cause ER stress and UPR activation (Li *et al.*, 2011; Yadav *et al.*, 2014). The UPR has also been implicated in bone metabolism (Yamada *et al.*, 2015). ER stress, which activates the UPR has been shown to cause bone loss in experimental periodontitis in mice independent of inflammatory cytokines (Yamada *et al.*, 2015).

1.8.5 Genotoxic Stress

Genotoxic stress occurs when DNA is damaged (Christmann and Kaina, 2013). This can occur: with exposure to many types of chemical agents ingested from smoking tobacco or from food; from UV irradiation; from ROS produced by oxidative stress or generated by reactions catalysed by heavy metals and from treatments with therapeutics (Jackson and Bartek, 2009; Shackelford *et al.*, 1999; Yang *et al.*, 2003; Pontano *et al.*, 2008). In addition, DNA mismatches, which occasionally occur during DNA replication and DNA strand breaks, which result from abortive topoisomerase I and topoisomerase II activity also cause genotoxic stress (Jackson and Bartek, 2009; Yang *et al.*, 2003). When DNA damage occurs the 'DNA damage response' (DDR) is activated (Jackson and Bartek, 2009; Christmann and Kaina, 2013; Cargnello and Roux, 2011). DDR involves activation of a number of DNA repair genes including checkpoint kinase 2 (Chk2), and ataxia telangiectasia mutated (ATM), and affects a number of transcription factors and kinases, which are involved in the regulation of DNA repair genes including PI3K, NFκB, BRAC1, p53 and AP-1 (Christmann and Kaina, 2013; Jackson and Bartek, 2009; Bartkova *et al.*, 2005; Yang *et al.*, 2003). The activation of these factors stabilises the cell genome and promotes cell survival (Solimini *et al.*, 2007; Ciccia and Elledge, 2010). Excessive genotoxic stress however, causes the suppression of transcription, which occurs when RNA polymerase II (RNAPII) is degraded (Busa *et al.*, 2010). When DNA damage caused by genotoxic stress is too great, the DDR signals for the cells to undergo apoptosis (Ghosal and Chen, 2013). Genotoxic stress is another hallmark of human cancers and the resulting genomic instability is involved in the initiation and promotion of tumourigenesis (Pontano *et al.*, 2008; Nakayama *et al.*, 1998; Pikor *et al.*,

2013). Precursor lesions present in clinical specimens from different stages of progression of human tumour of the urinary bladder, breast, lung and colon express the markers of an activated DNA damage response (Bartkova *et al.*, 2005). Interestingly, genotoxic stress has been shown to mediate the phosphorylation and proteasomal degradation of IκB through IKK α, β or γ allowing nuclear translocation of NFκB (Weber, 2007). As discussed in Chapter 1.5.1 NFκB is an essential transcription factor for osteoclast differentiation from progenitor cells and mice (Asagiri and Takayanagi, 2007).

1.9 Cancer Therapeutics

Many cancer therapeutics have been designed to target proteins, organelle or processes in the aforementioned stress pathways to cause cell death. These therapeutics include HSP90 inhibitors and proteasome inhibitors, which affect both the HSR and ER stress pathways. Other anti-cancer agents include alkylating, intercalating and cross-linking compounds. These compounds cause genotoxic stress to cells and the activation of the DDR. Although cancer agents typically have one mode of action, many have been reported to cause a myriad of stress responses in the cell (Luo *et al.*, 2009). Due to the cytotoxic nature of chemotherapeutics, many of these compounds including targeted chemotherapeutics decrease bone density although the exact processes are not known (Hu *et al.*, 2010; Lipton *et al.*, 2009b; Guise, 2006). The long term negative effects, which can arise from anti-cancer agent treatments include pronounced bone loss, osteomalacia, and avascular necrosis (Hu *et al.*, 2010). Due to the processes of chemotherapeutic-induced bone loss being unclear, the effect of experimental and clinically used chemotherapeutics upon progenitor osteoclast differentiation through a stress mechanism is studied in this thesis. HSP90 inhibitors, which are being tested as anti-cancer compounds in many clinical trials are an example of targeted therapy, and their effect upon osteoclastogenesis is studied in detail in this thesis. HSP90 and HSP90 inhibitors are discussed in Chapters 1.9.2 and 1.9.4.

1.9.1 Targeted Therapies

Targeted therapeutics are cancer therapeutics that target specific mutant and oncogenic proteins or biochemical pathways, which are required for cancer cell growth and tumour progression (Sawyers, 2004). One highly successful example of a target therapy is the BCR-ABL kinase inhibitor, imatinib, which is effective against Chronic Myelogenous Leukemia (CML) in more than 75% of the cases (Vanneman and Dranoff, 2012). More examples of

targeted therapy include bortezomib, which is a proteasome inhibitor and thus inhibits protein degradation (Chapter 1.9.6) and HSP90 inhibitors (Chapter 1.9.4) (Chen *et al.*, 2011; Adams, 2004; Neckers and Workman, 2012; Drysdale *et al.*, 2006). From the research of imatinib many oncogenic proteins including EGFR, BRAF, HER2 and PRG have been identified to be key in driving oncogenic processes in cancers (Vanneman and Dranoff, 2012; Bauer *et al.*, 2007; Sanderson *et al.*, 2006). Many of these proteins maintain their correct tertiary structure and thus function by their interaction with HSP90.

As previously described, when a cell experiences stress unfolded proteins or incorrectly folded proteins aggregate and cause proteotoxic stress (Calderwood, 2013; Morimoto, 2008; Stephanou and Latchman, 2011; Richter *et al.*, 2010). In response HSF1 activates the HSR, which increases the expression of a group of proteins called HSPs (Pirkkala *et al.*, 2001; Voellmy, 2004; Stephanou and Latchman, 2011). Because cancer cells have a stress phenotype they require high levels of HSPs to maintain cell viability (Whitesell and Lindquist, 2005; Ciocca and Calderwood, 2005; Mosser and Morimoto, 2004). In a large number of malignancies, both solid and haematological, HSP expression is increased (Calderwood *et al.*, 2006; Jego *et al.;* Whitesell and Lindquist, 2005; Ciocca and Calderwood, 2005). Of the HSPs, HSP70, HSP27 and HSP90 have been reported to be overexpressed in cancer and their expression is correlated with a poor prognosis (Whitesell and Lindquist, 2005; Mosser and Morimoto, 2004). HSP90, in particular, is enhanced ten-fold in a number of tumour cell types in comparison to non-cancerous cells (Zuehlke and Johnson, 2010). The very high expression of HSPs in cancer cells supports oncogenesis on both the physiological and molecular levels (Workman, 2004b; Whitesell and Lindquist, 2005). The increased expression of HSPs in advanced cancer is believed to be a cyto-protective stress response to the genotypic and phenotypic characteristics of tumour cells and the toxic nature of the tumour microenvironment, which is hypoxic, acidotic and lacking in nutrients (Ciocca and Calderwood, 2005; Mosser and Morimoto, 2004; Workman, 2004a; Whitesell and Lindquist, 2005). For this reason, inhibition of HSPs or HSP-inducing pathways has been a significant focus of new anti-cancer drug development (Powers and Workman, 2007; de Billy *et al.*, 2009; Travers *et al.*, 2012; Workman *et al.*, 2007; Drysdale and Brough, 2008). The effect of HSP90 inhibitors upon osteoclastogenesis is studied in this thesis extensively.

1.9.2 Heat Shock Protein 90

HSP90 is ubiquitously and abundantly expressed and can account for up to 2-5% of the total protein of a cell (Bagatell *et al.*, 2000; Taipale *et al.*, 2010). Under conditions of cell stress HSP90 expression is greatly increased beyond this amount (Workman, 2004b; Richter *et al.*, 2010; Zuehlke and Johnson, 2010). The main role of HSP90 is protein quality control either through promoting protein folding, refolding and the stabilization of client proteins, targeting misfolded proteins for proteasomal degradation (Theodoraki and Caplan, 2012; Li and Buchner, 2013a; Koga *et al.*, 2009). By doing this HSP90 maintains protein homeostasis within the cell under physiological and stressful periods. HSP90 is expressed in a number of isoforms that may be localized differently in different cell types (Subbarao Sreedhar *et al.*, 2004; Hendrick and Hartl, 1993). HSP90α, a stress inducible isoform and HSP90β, which is a constitutively expressed isoform, are found principally in the cytosol (Subbarao Sreedhar *et al.*, 2004; Li *et al.*, 2012). Cytosolic HSP90α and HSP90β, which are expressed from different genes constitute the great bulk of HSP90 activity and are essential for the viability of the organism (Zuehlke and Johnson, 2010; Richter *et al.*, 2010; Hendrick and Hartl, 1993; Li *et al.*, 2012). HSP90 analogues include the previously mentioned GRP94 that is localized to the endoplasmic reticulum and tumour necrosis factor receptor-associated protein 1 (TRAP1, found mainly in mitochondria (Subbarao Sreedhar *et al.*, 2004; Li *et al.*, 2012).

In the cytoplasm, HSP90 is present as latent homodimers (α/α) or (β/β) that are bound to a number of proteins in a multichaperone complex and HSF1 at its N-terminal Domain (Figure 1.9) (Taylor *et al.*, 2007; Zou *et al.*, 1998; Whitesell and Lindquist, 2009). As described earlier, interaction of HSP90 with HSF1 acts to repress HSF1 activity (Bagatell *et al.*, 2000). However, when cells undergo stress, HSP90 binds misfolded client proteins and undergoes a conformational change causing the dissociation of HSF1 (Zou *et al.*, 1998; Cheung *et al.*, 2005; Cervantes-Gomez *et al.*, 2009). After a series of activation steps, HSF1 binds to HSE present within the HSP90 promoter (Figure 1.9) (Kamal *et al.*, 2004; Morimoto, 2008). Thus under stress conditions, HSP90 expression is upregulated by HSF1 and this upregulation acts to maintain cellular proteostasis and homeostasis (Chen *et al.*, 2013).

HSP90 has three currently defined domains: an N-terminal ATP-binding domain, a middle domain and a C-terminal domain (Figure 1.9) (Fukuyo *et al.*, 2010; Whitesell and Lindquist, 2005; Zuehlke and Johnson, 2010). The N-terminal domain has the adenine binding domain,

which contains ATPase activity, essential for the function of HSP90 (Whitesell and Lindquist, 2005; Minami *et al.*, 2001; Young *et al.*, 2001). The middle domain is a charged linker region that contains the binding sites for client proteins and co-chaperones including p50^{CDC37}, p23 and Activator of *Hsp90* ATPase protein 1 (Aha1) (Zuehlke and Johnson, 2010; Richter *et al.*, 2010; Jego *et al.*, 2013). The carboxyl dimerization terminal has a ATP binding site and a tetratricopeptide repeat-binding (TPR) motif EEVD, which binds to a number of co-chaperones that recognize this motif and including Hsp70/Hsp90 organizing protein (HOP) and Carboxyl terminus of Hsc70 interacting protein (CHIP) (Whitesell and Lindquist, 2005; Jego *et al.*, 2013; Pratt *et al.*, 2010).

1.9.2.1 HSP90 Function

Unlike other HSPs including cognate HSP70 (HSC70), which can fold nascent proteins and also refold damaged proteins back to their native state, HSP90 does not participate in most nascent protein folding (Koga *et al.*, 2009; Minami *et al.*, 2001; Whitesell and Lindquist, 2005; Zuehlke and Johnson, 2010). Rather, HSP90 binds to client proteins which are in a near native state and are at a late stage of folding (Young *et al.*, 2001; Jakob *et al.*, 1995). HSP90, therefore, has an activity similar to that of a holding chaperone with most HSP90 molecules being engaged in the stabilisation of the functional status of their client proteins (Workman, 2004b; Theodoraki and Caplan, 2012; Hendrick and Hartl, 1993; Whitesell and Lindquist, 2005). Thus, HSP90 regulates function of many cell proteins (Marcu *et al.*, 2002). In this role HSP90 works with a large number of co-chaperones to: promote protein folding; client protein re-folding; stabilization of protein structure; participate in protein transport to appropriate cellular compartments and, like other chaperones, in the assembly of large multi-protein complexes (Figure 1.8) (Kamal *et al.*, 2004; Mayer and Bukau, 2005; Richter *et al.*, 2010; Zuehlke and Johnson, 2010; Muller *et al.*, 2013). The client protein association with HSP90 and co-chaperones thus stabilize them and holds them in a metastable state in which they are able to bind to ligands or respond to stimuli (Figure 1.8) (Isaacs *et al.*, 2003; Koga *et al.*, 2009). HSP90 client proteins include many important protein kinases, transcription factors including nuclear receptors and telomeric proteins (Richter *et al.*, 2010; Zuehlke and Johnson, 2010; Muller *et al.*, 2013). These client proteins are important in regulating cell viability, differentiation, proliferation and homeostasis and their activities and regulation are often perturbed in the context of disease, most notably in the case of cancer cells (Workman, 2004b; Kamal *et al.*, 2004; Richter *et al.*, 2010; Zuehlke and Johnson, 2010; Muller *et al.*, 2013).

1.9.2.2 HSP90 Function is Dependent upon ATP Hydrolysis

HSP90 maintains protein homeostasis within the cell under both physiological conditions as well as during periods of acute and chronic stress (Theodoraki and Caplan, 2012; Koga *et al.*, 2009). HSP90 functionality depends upon ATP hydrolysis and its association with other chaperones, co-chaperones and adaptors that are bound to the HSP90 multi-chaperone complex (Figure 1.8) (Koga *et al.*, 2009; Workman, 2004b; Neckers, 2002). Members of the HSP90 multi-chaperone complex include HSP70 (often) and a range of co-chaperones, which are often client specific (Figure 1.8) (Zuehlke and Johnson, 2010; Calderwood, 2013; Koga *et al.*, 2009). HSP90 is able to bind to 20 co-chaperones some of which include p23, p50^{cdc37}, HIP, HOP, and AHA1 (Figure 1.8) (Neckers, 2002; Calderwood, 2013; Whitesell and Lindquist, 2005). Co-chaperones have a number of different actions including regulating the interaction between HSP70 and HSP90, as well as the regulation of HSP90 ATPase activity (Figure 1.8, B.) (Calderwood, 2013; Whitesell and Lindquist, 2005).

Cycling between ADP and ATP hydrolysis regulates whether a protein is folded and stabilized or targeted for proteasomal degradation (Figure 1.8) (Neckers, 2002; Isaacs *et al.*, 2003; Whitesell and Lindquist, 2005). Therefore, ATP hydrolysis is essential to HSP90 function (Koga *et al.*, 2009). HSP90 promotes correct protein folding and stabilization of misfolded and synthesized client proteins when ATP is bound to its N-terminal (Figure 1.8) (Whitesell and Lindquist, 2005; Trepel *et al.*, 2010). In addition to HSP90 binding ATP, the co-chaperones p23 and p50^{cdc37} must also be complexed to HSP90 for promotion of correct folding and protein stabilization to occur (Figure 1.8) (Neckers, 2002; Whitesell and Lindquist, 2005). In this confirmation, HSP90 is 'closed' and clamps around its client protein (Figure 1.8) (Koga *et al.*, 2009). Conversely, HSP90 plays an important role in protein degradation (Taipale *et al.*, 2010; Isaacs *et al.*, 2003). Misfolded or unstable proteins tend to aggregate through their hydrophobic regions and may cause proteotoxic stress if the concentration of these proteins is too high (Pogenberg *et al.*, 2012). HSP90's role in targeting these protein aggregates thereby reduces the risk of prototoxic stress (Figure 1.8) (Koga *et al.*, 2009; Theodoraki and Caplan, 2012). Targeting proteins for proteasomal degradation occurs when HSP90 is bound to ADP and is complexed to HSP70/HSP40 and co-chaperones: HSP90 cochaperone STI1 (p60) and Carboxyl terminus of Hsc70 interacting protein (CHIP) (Figure 1.8) (Koga *et al.*, 2009; Taipale *et al.*, 2010). Some co-chaperones including CHIP have been shown to have binding regions for the E3 ubiquitin ligase (Isaacs *et al.*, 2003; McDonough and Patterson, 2003; Murata *et al.*, 2003). Protein degradation may occur for a

number of reasons including mutations, proteolytic cleavage, post-synthetic changes such as oxygen radicals and intracellular degradation (Lecker *et al.*, 2006; Goldberg, 2003). All of these processes denature proteins causing them to be misfolded (Goldberg, 2003). During stress events such as heat shock or during oxidative stress or inflammation where reactive oxygen species are generated, the ratio of misfolded to folded proteins increases and HSP90 directs proteins for ubiquitin mediated degradation by the proteasome (Takalo *et al.*, 2013; Taipale *et al.*, 2010; Morimoto, 2008; Goldberg, 2003). HSP90 is also involved in the UPR , which results from ER stress (Chapter 1.8.4) (Born *et al.*, 2013; Davenport *et al.*, 2007).

It is interesting to note the HSR has been shown to be involved in modulating the UPR (Marcu *et al.*, 2002). Not only does the UPR cause the HSP90 ER isoform GRP94 to be increased but cystolic HSP90 has also been involved in modulating the UPR (Marcu *et al.*, 2002). Both IRE1α and PERK are client protein of HSP90 and HSP90 has been shown to regulate the UPR by stabilizing IRE1α (Marcu *et al.*, 2002). In COS cells, HSP90 inhibition with geldanamycin decreases the half-life of IRE1α (Marcu *et al.*, 2002). Similar results were also shown for PERK (Marcu *et al.*, 2002). It has also been shown that a short inhibition of HSP90 induces ER stress and the UPR, consistent with upregulation of BiP expression (Marcu *et al.*, 2002). In addition, inhibiting HSP90 with 17-AAG and radicicol (see Chapter 1.9.4) alongside ER inhibitors thapsigargin and tunicamycin have been shown to activate all three signalling branches of the UPR: PERK, IRE1 and ATF6 (Chapter 1.8.4) (Davenport *et al.*, 2007). These HSP90 and ER inhibitors mediate early IRE1 mediated splicing of X-box binding protein 1 (XBP1) and increased expression of CCAAT-enhancer-binding protein homologous protein (CHOP) through PERK activation and ATF6 splicing (Davenport *et al.*, 2007). ER molecular chaperones BiP, which belongs to the HSP70 family and the ER HSP90 analogue GRP94 expression was also increased after treatment with these drugs (Davenport *et al.*, 2007). Bortezomib, a proteasome inhibitor (Chapter 1.14.3) also activates PERK and ATF6; however, it does not affect XBP1 to any large extent (Davenport *et al.*, 2007). These drugs also caused the activation of JNK caspase cleavage leading to cellular apoptosis (Davenport *et al.*, 2007). HSP90 inhibition therefore results in the accumulation of misfolded proteins, which causes cell death through both non-ER and ER-dependent stress pathways (Davenport *et al.*, 2007). Interestingly the ER inhibitors thapsigargin and tunicamycin have been shown to increase levels of osteoclast-associated proteins TRAP and cathepsin K, (Wang *et al.*, 2011b).

A.
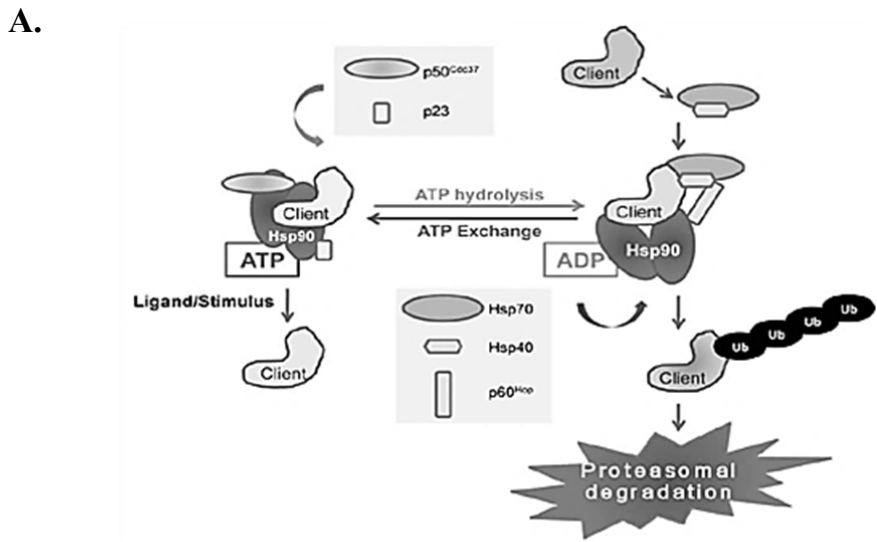
B

Important components of the HSP90 chaperone machinery

Protein family	Classification	Function
HSP90	Chaperone	Supports meta-stable protein conformations, especially in signal transducers
HSP70	Chaperone	Helps fold nascent polypeptide chains; participates in assembly of multiprotein complexes
HSP40	Co-chaperone	Stimulates HSP70 ATPase activity
HIP,HOP	Adapters	Mediate interaction of HSP90 and HSP70
CDC37/p50	Co-chaperone	Modulates interaction with kinases
AHA1	Co-chaperone	Stimulates HSP90 ATPase activity
p23	Co-chaperone	Stabilizes HSP90 association with clients
Immunophilin	Prolylisomerase	Modulates interactions with hormone receptors

Figure 1.8 Nucleotide-dependent Cycling of the HSP90 Chaperone Machinery
(A.) Nascent HSP90 client protein associate with an HSP70/40 chaperone complex first to undergo protein folding. This client/HSP70/40 complex then is linked to ADP bound HSP90 through co-chaperone p60Hop, which is a HSP70/HSP90 interacting protein. In this state HSP90 is bound to ADP and has an open confirmation. Exchange of ADP for ATP changes the confirmation of HSP90 to a closed state, which causes the dissociation of the HSP70/40 complex and p60Hop. In this closed state HSP90 clamps around its client protein and recruits another set of co-chaperones including p50Cdc37 and p23, which assist in the final stages of protein folding and also in client protein stabilization. In this state the HSP90 client protein can bind to receptors or can receive a stimulus. In the ADP open state, the HSP90/ HSP40/70/ p60Hop /CHIP complex mediates protein degradation. **(B.)** Table 1.1 Describes members of the HSP90 chaperone machinery. Images sourced from **(A.)** (Koga *et al.*, 2009) and **(B.)** (Whitesell and Lindquist, 2005; Urban *et al.*, 2012; Workman and Collins, 2010).

1.9.3. HSP90 in Cancer

As mentioned earlier, HSP90 expression is expressed at very high levels in tumour cells (Maloney and Workman, 2002; Richardson *et al.*, 2011; Zuehlke and Johnson, 2010). The high HSP90 levels are associated with increased cancer progression, and this is correlated with poor prognosis (Wang *et al.*, 2013; Cheng *et al.*, 2012; Bagatell *et al.*, 2000; Whitesell and Lindquist, 2005). The increased levels of HSP90 acts to protect cancer cells against tumour microenvironmental stresses including low or high pH and nutrient deprivation, and the buffering of HSP90 client oncogenes through a process called 'oncogene addiction' (Figure 1.9) (Travers *et al.*, 2012; Trepel *et al.*, 2010; Workman *et al.*, 2007).

HSP90 under normal physiological conditions binds over 200 client proteins to facilitate their given functions; however, in the context of malignancy many of the client proteins of HSP90 function as *bona fide* oncogenes (Ipenberg *et al.*, 2013; Karkoulis *et al.*, 2013; Li *et al.*, 2012; Whitesell and Lindquist, 2005; Travers *et al.*, 2012). HSP90 client proteins include: kinases (Protein kinase B [Akt] and Met), transcription factors (Hypoxia-induced factor α [HIF-α] and p53), growth factors (Her2 and PDGF) and many other proteins (Chiosis, 2006b; Goetz *et al.*, 2003; Workman, 2004a). These proteins have important roles in signalling pathways that drive tumour cell survival and proliferation therefore facilitating cancer progression (Neckers and Workman, 2012). HSP90 acts to provide functional and structural stabilization of these client oncogenes allowing them to participate in the cancer process while preserving enough of their normal functions to allow cell survival (Taldone *et al.*, 2011; Travers *et al.*, 2012; Whitesell and Lindquist, 2005; Workman, 2004b). Thus, the increased HSP90 expression in tumour cells allows for the cell to cope with the genetically mutated or overexpressed proteins (increased protein load) and the irregular signalling cascades in cancer cells (Workman, 2004a; Zuehlke and Johnson, 2010). It is proposed that HSP90 acts as buffer in the cell enabling it to survive genotypic and phenotypic variations (Travers *et al.*, 2012; Zuehlke and Johnson, 2010; Karkoulis *et al.*, 2013). Without the increased expression of HSP90, the genetic mutations would increase protein concentrations of both stable and unstable proteins resulting in proteostatic imbalance, subsequent proteotoxic stress and eventually cell apoptosis (Travers, Sharp et al. 2012). HSP90 in cancer has been shown to be present in an altered multi-chaperone state (Workman, 2004a; Kamal *et al.*, 2003; Li *et al.*, 2012). HSP90 in cultured cancer cells, mouse tumours and human tumour specimens is present mostly in a superchaperone complex state, which is bound to p23 and HOP (Kamal *et al.*, 2003). In comparison, HSP90 is mostly present in its latent homodimer conformation in

non-cancerous cells (Kamal *et al.*, 2003). In addition, the ATPase activity of HSP90 is increased about 10 fold relative to normal cells; therefore in cancer cells HSP90 is more biochemically active (Kamal *et al.*, 2003). The increased activity of HSP90 in cancer cells to stabilize oncogenic client proteins makes HSP90 an exciting anti-cancer target (Workman *et al.*, 2007; Travers *et al.*, 2012; Neckers, 2002).

1.9.4 HSP90 as a Therapeutic Target

HSP90 was chosen to be a target for an anti-cancer compound development for a number of reasons including: stabilization of its oncogenic client proteins, its protective role against the microenvironment and its actions as a hub (central) protein interconnecting multiple oncogenic signalling pathways, which are involved in cancer cell hallmarks (Figure 1.8) (Whitesell and Lindquist, 2005; Isaacs *et al.*, 2003; Xu and Neckers, 2007). HSP90 inhibition causes oncogenic proteins to incorrectly fold and be destabilized, thus targeting them for proteasomal degradation (Isaacs *et al.*, 2003; Neckers, 2002). Inhibition of HSP90 is twofold in that oncogenic proteins are targeted for proteasomal degradation and secondly that proteotoxic stress will occur due to the proteasome not being able to degrade all the proteins (limited rate of action)(Neckers, 2002). Both these actions cause cancer cell death (Isaacs *et al.*, 2003; Neckers, 2002). A large number of HSP90 inhibitors have been discovered from naturally occurring sources or through drug design (Drysdale and Brough, 2008; Eccles *et al.*, 2008; Taldone *et al.*, 2008; Workman, 2004b). These drugs either bind to the C-terminal or the N-terminal regions of HSP90, the latter being a focus of study in this thesis (Workman, 2004b; Donnelly and Blagg, 2008; Wang and McAlpine, 2015).

1.9.4.1 HSP90 N-terminal Inhibitors

A large number of HSP90 inhibitors bind to the N-terminal ATP-binding domain of HSP90 including: geldanamycin and its derivatives 17-AAG and 17-DMAG, radicicol, herbamycin A, CNF2024(BIIB021), SNX-5422, KW2478, XL888 and the pyrazole compounds CCT018159 and NVP-AUY922 (Table 1.1) (Neckers, 2002; Taldone *et al.*, 2008; Richardson *et al.*, 2011; Drysdale and Brough, 2008). Until recently, N-terminal HSP90 inhibitors, whilst having distinct characteristics, could be classified into three categories based on their scaffold

© 2012 American Association for Cancer Research
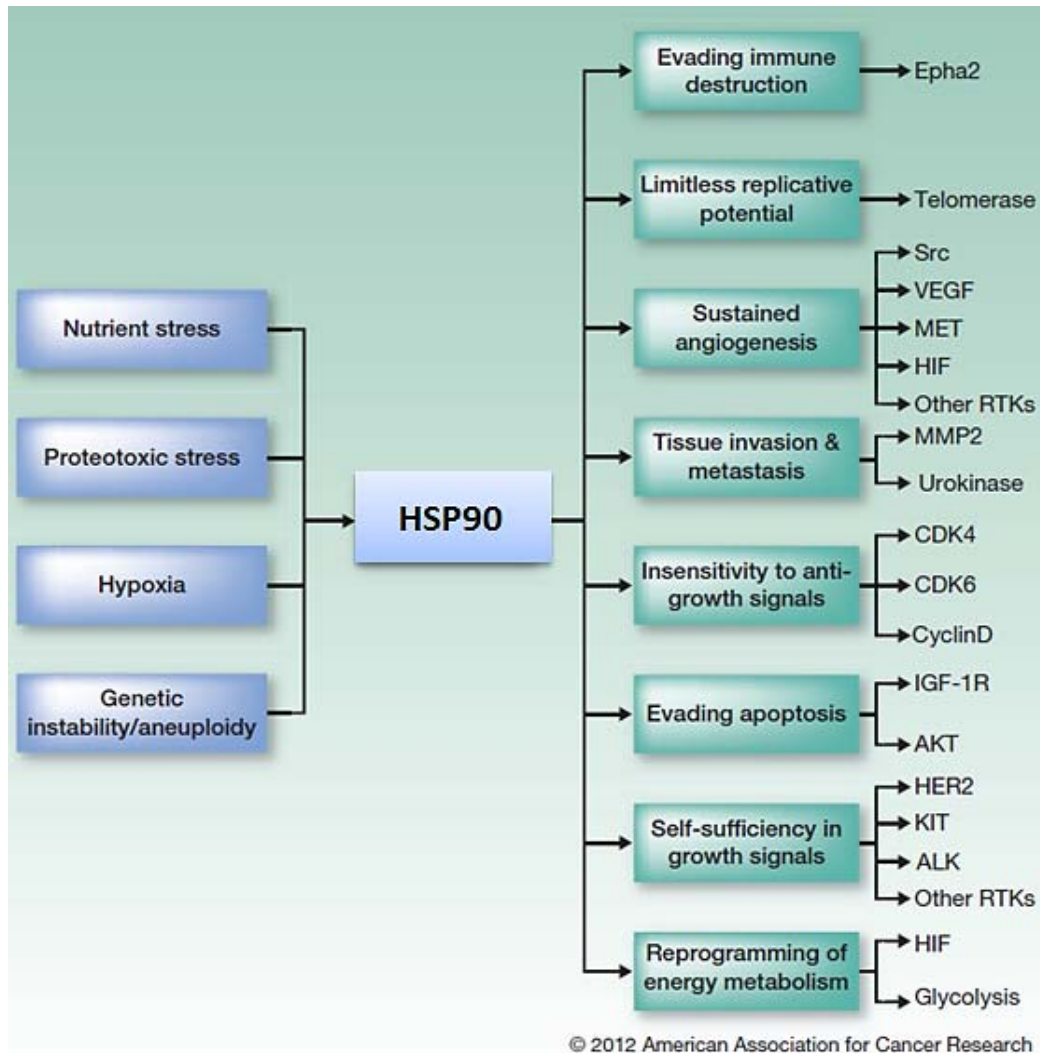
Figure 1.9 HSP90 Roles in Cancer

HSP90 has a dual role in supporting cancer. HSP90 protects the cell from extracellular stresses (hypoxic and nutrient deprived tumour microenvironment) and also from the intracellular stresses (genetic instability through mutations and proteotoxic stress). Secondly, HSP90 supports all of the hallmarks of cancer cells through the stabilization of oncogenic client proteins, which are involved in aberrant signalling pathways, which promote cancer cell growth and progression. These proteins include HIF-1α, AKT, MET and other RTK, VEGF, Cyclin D, and telomerase, which potentiates cancer cells to escape replicate control, evade apoptosis, potentiates invasion and metastasis, self-sufficiency in growth signals and angiogenesis, evade immune destruction and reprogram energy metabolism. Image sourced from (Neckers and Workman, 2012).

similarities: benzoquinone ansamysins, macrolide and purine (Jhaveri *et al.*, 2012). More recently HSP90 inhibitors based upon other scaffolds including pyrazole and 6,7-dihydro-indazol-4-one have been developed (Jhaveri *et al.*, 2012). In 2012, seventeen HSP90 inhibitors entered the clinic and more than eighty Phase I or II trials had been completed or were ongoing (Neckers and Workman, 2012). Some of these inhibitors have had promising effects but are limited by adverse side effects such as hepatic-, cardio-, ocular-toxicity, and peripheral neuropathy (Jhaveri *et al.*, 2012; Neckers and Workman, 2012). Another general concern for HSP90 inhibitors is the effect that inhibiting a large number of HSP90 clients has upon tissue health (Whitesell and Lindquist, 2005). Geldanamycin and radicicol were the first HSP90 inhibitors, which were initially identified by screening *Streptomyces* and fungi extracts for antiprotozoal and antifungal properties, respectively (Whitesell *et al.*, 1994; Uehara, 2003; Workman, 2004b). Although they display high levels of toxicity in mammals, their chemical structures have subsequently been used as a basis for the design of new generations of HSP90 inhibitors for clinical use (Jego *et al.*, 2013; Workman *et al.*, 2007). Their identification and use helped characterise HSP90 biology, in particular identifying the importance of the N-terminal domain of HSP90 (the ATPase domain) (Travers *et al.*, 2012; Workman *et al.*, 2007).

Benzoquinone Ansamycins: Geldanamycin

A class of compounds that show specific binding to HSP90 are the antibiotic benzoquinone ansamycins (BA), which includes geldanamycin and its derivatives (Table 1.1) (Schulte and Neckers, 1998; Tsutsumi and Neckers, 2007). These antibiotic benzoquinone ansamycins are characterised by their macrocyclic lactam amide (Uehara, 2003; Tsutsumi and Neckers, 2007). Geldanamycin was first identified and isolated from the geldanus variant of the soil bacterium *Streptomyces hygroscopius* and early studies showed it had inhibitory growth effects upon Hela derived KB cells although its mechanisms were not known (Travers *et al.*, 2012). In 1994, Whitesell and Neckers showed that Src-HSP90 interaction in both intact cells and reticulocyte lysates was inhibited by geldanamycin (Whitesell *et al.*, 1994; Porter *et al.*, 2010). Interestingly before this observation, it was thought that geldanamycin was a Src inhibitor rather than a HSP90 inhibitor (Whitesell *et al.*, 1994). This publication was a landmark in HSP90 inhibition studies providing the framework for subsequent HSP90 rationale drug development (Porter *et al.*, 2010). X-ray crystallography later determined the co-crystal structure and found that geldanamycin bound to the N-terminal region of HSP90 in

the ATP/ADP binding pocket (Porter *et al.*, 2010). Geldanamycin was shown to have strong anti-cancer properties; however, it was too hepatotoxic to be developed clinically (Kamal *et al.*, 2003; Porter *et al.*, 2010; Travers *et al.*, 2012) As a result, a large number of geldanamycin derivatives were developed (Travers *et al.*, 2012; Workman, 2004b). These derivatives include 17-AAG, which is used extensively in this thesis projects and second generation GA derivatives such as 17DMAG and IPI-504 (Table 1.1) (Travers *et al.*, 2012; Workman, 2004b; Taldone *et al.*, 2008).

Benzoquinone Ansamycins: 17-AAG

17-allylamino-17-demethoxygeldanamycin (tanespimycin or 17-AAG as referred to in this thesis; Table 1.1) has a greater therapeutic index than geldanamycin whilst exhibiting better pharmacokinetic properties i.e., increased solubility and less toxicity in human tumour xenograft mouse studies (Workman *et al.*, 2007; Jego *et al.*, 2013; Travers *et al.*, 2012). As a result, 17-AAG was tested in preclinical investigations and mouse tumour growth models before entering patient clinical trials in 1999 as a first-in-class HSP90 inhibitor (Taldone *et al.*, 2008; Jhaveri *et al.*, 2012; Jego *et al.*, 2013). The early trials were to show proof of concept i.e., HSP90 client protein degradation and HSP70 induction and also to determine its pharmacokinetics for dosing regimens (Travers *et al.*, 2012). 17-AAG has since been studied extensively in over 30 clinical trials and entered phase II trials in 2006 (Workman *et al.*, 2007; Jego *et al.*, 2013; Den and Lu, 2012). Within these clinical trials 17-AAG was shown to have anti-cancer properties in soft tissue despite a number of clinical issues presenting (Jego *et al.*, 2013; Goetz *et al.*, 2003; Fukuyo *et al.*, 2010).

17-AAG was been found to reduce tumour growth in a number of cancer models including breast and prostate cancer, melanoma and glioblastoma multiforme through the degradation of its client proteins: protoncogene b-RAF (b-RAF), protoncogene c-RAF (c-RAF), Anaplastic Lymphoma Receptor Tyrosine Kinase (ALK) and cyclin dependent kinase 4 (CDK4), human epidermal growth factor receptor 2 (HER2), AR (androgen receptor), Protein kinase B (AKT), Checkpoint kinase 1 (CHK1) and fusion protein BCR-ABL (Rodrigues *et al.*, 2012; Solit *et al.*, 2002; Arlander *et al.*, 2003; George *et al.*, 2005). HER2 is a HSP90 client, which when expressed in breast cancer increases the aggressiveness and metastatic potential (Jego *et al.*, 2013; Modi *et al.*, 2011; Baselga, 2001). 17-AAG depletes HER2 and causes a dose-dependent regression in tumour growth in mammary HER2 positive tumours (Jego *et al.*, 2013; Rodrigues *et al.*, 2012). Like HER2, the progesterone receptor (PR) is

another HSP90 client protein , which is often expressed in breast cancer and confers a poor prognosis (Bagatell *et al.*, 2000). 17-AAG treatment of severe combined immunodeficiency (SCID) mice with breast tumour xenograft models decreases PR tissue levels and also significantly inhibited tumour growth (Bagatell *et al.*, 2000). 17-AAG treatment also inhibits prostate tumour growth in mice by decreasing the expression of HSP90 oncogenic client proteins: HER2, AR, and AKT (Solit *et al.*, 2002). In melanoma studies, 17-AAG treatment has variable results on tumour growth (Burger *et al.*, 2004; Taldone *et al.*, 2008). In human melanoma xenograft models, 17-AAG markedly decreased tumour growth in the MEXF 276, MEXF 989 xenografts in athymic mice; however, two other xenograft models MEXF 462 and MEXF 514 were only weakly impacted by 17-AAG (Burger *et al.*, 2004). 17-AAG has also been shown to have activity against glioblastoma multiforme (GBM), which is the most common and malignant of the brain gliomas (Sauvageot *et al.*, 2009). 17-AAG treatment is able to inhibit human glioma cell line and glioma stem cell growth *in vitro* (Sauvageot *et al.*, 2009). Additionally, 17-AAG can act alone or in concert (synergistically) with radiation to inhibit intracranial tumour growth (Sauvageot *et al.*, 2009).

17-AAG does not have the same anti-cancer response in soft tumour cancers that it does to cancer that has metastasized to bone, an observation central to the studies in this thesis (Price *et al.*, 2005). Price *et al.* found, in accordance to previous observations, 17-AAG treatment dramatically shrunk the size of mammary tumours and inhibited IGF-1-dependent chemotactic migration (Price *et al.*, 2005). However, in contrast, 17-AAG treatment significantly increased cancer cell invasion and growth in bone in an intracardiac MDA-MB-231 inoculation model (Price *et al.*, 2005). The ability of 17-AAG treatment to increase tumour growth in bone was suggested to be due to the drug having pro-osteolytic activity rather than any effect on the tumour cells since its treatment stimulated osteoclast formation *in vivo* and *in vitro* (Price *et al.*, 2005). Notably, 17-AAG treatment caused decreased total trabecular bone mass in tumour naïve mice with a concomitant increase in osteoclast numbers although no effects upon osteoblast numbers were observed (Price *et al.*, 2005). Such an osteolytic action may augment tumour growth through the vicious cycle despite the anti-tumour effects of the drug (Price *et al.*, 2005). Similarly Yano *et al*. found that 17-AAG increased the growth of PC-3M cancer cells, which had been injected into the bone (Yano *et al.*, 2008). The increased growth of PC-3M was found to associated with increased osteoclast numbers (Yano *et al.*, 2008). Administration of the bisphosphonate alendronate to tumour bearing mice markedly decreased the 17-AAG mediated increase in tumour growth (Yano *et*

al., 2008). As earlier described, the contribution of vicious cycle-based tumour invasion in mouse xenograft models has much experimental support although its contribution to human disease needs to be further studied. Whilst 17-AAG has provided some positive results in the clinic as a single agent anti-cancer drug, and more so in combination therapies, all the trials were cancelled in early 2008 and further clinical trials stopped (National Institute of Health, 2014). 17-AAG, like geldanamycin, proved to be too toxic for the therapeutic window and patients being treated with 17-AAG exhibited nausea, gastrointestinal discomfort, and eyesight problems (Workman, 2004b; Jhaveri *et al.*, 2012). These side effects of 17-AAG are thought to be due in part to its quinone moiety, which is converted to hydroquinone that is readily oxidized (Workman, 2004b; Powers and Workman, 2007; Porter *et al.*, 2010). In addition, cytochrome P450 (CYP450) converts 17-AAG into the more toxic amino, 17-demethoxygeldanamcyin (17AG), which contributes to the hepatic toxicity observed in 17-AAG treated patients (Powers and Workman, 2007; Whitesell and Lindquist, 2005).

Due to solubility issues of 17-AAG, the 17-AAG derivative 17a-(2-dimethylaminoethyl) amino-17-demethoxygeldanamycin (17DMAG or alvespimycin hydrochloride) was developed (Workman, 2004b; Xiong *et al.*, 2009). 17-DMAG is more soluble than its 17-AAG counterpart due to the salt of the basic amine addition (Workman, 2004b; Porter *et al.*, 2010). 17-DMAG, however, was discontinued from the clinic due to severe clinical side effects including hepta, gastrointestinal and bone marrow toxicities (Ramsey *et al.*, 2014). Another 17-AAG derivative is IPI-504 (retaspimycin hydrochloride) that was developed in response to 17-AAG conversion of its quinone moiety to a hydroquinone, which corresponded with poor pharmaceutical properties (Taldone *et al.*, 2008; Porter *et al.*, 2010). This compound has advanced to clinical trials and has been shown to have anti-cancer effects against multiple myeloma and some solid cancers (Ramsey *et al.*, 2014).

Radicicol

Radicicol (Table 1.1) is a macrocyclic anti-fungal antibiotic, which is a naturally occurring HSP90 inhibitor (Jego *et al.*, 2013; Travers *et al.*, 2012; Zubrienė *et al.*, 2010). Radicicol, originally isolated from the fungus *Monocillium nordinii*, binds to the HSP90 N-terminal ATPase binding domain with nanomolar activity having a dissociation constant (K_d) of 19nM (Table 1.1) (Jego *et al.*, 2013; Zubrienė *et al.*, 2010). Radicicol has potent anti-cancer effects *in vitro;* however, due to its toxicity profile *in vivo* studies were not permissible (Jego *et al.*, 2013; Li *et al.*, 2012). Despite the inactivity *in vivo*, radicicol has been used as a scaffold for

rationale synthetic drug development of resorcinol based pyrazole and isoxazole HSP90 inhibitors including NVP-AUY922 (VER-52296) and the oxime derivatives including KF5833 (Workman *et al.*, 2007; Jego *et al.*, 2013). X- ray crystallography studies showed that radicicol and all subsequent resorcinol based HSP90 inhibitors bind to the ATP site of HSP90 through its resorcinol moiety (Xiao *et al.*, 2006; Drysdale and Brough, 2008; Travers *et al.*, 2012). In addition to their highly specific nature, one particularly desirable aspect of the resorcinol group of HSP90 inhibitors is their lack of liver hepatoxicity seen in ansamycin benzoquinone antibiotics (Xiao *et al.*, 1999).

Synthetic Drug Development

With the stereochemical, biochemical and structural knowledge of the natural inhibitors, geldanamycin and radicicol, synthetic HSP90 inhibitors were developed. These synthetic inhibitors were developed using a range of techniques including: ATP substrate-based mimicry, structure based design using x-ray crystallography, biophysical approaches, virtual screening and high-throughput biochemical screening of compound libraries (Workman, 2004b; Jego *et al.*, 2013; Whitesell and Lindquist, 2005). In 2005 resorcinylic pyrazole derivatives were identified to have activity against HSP90 (Sharp *et al.*, 2007a; Cheung *et al.*, 2005). CCT08159 (Table 1.1) was identified at the Cancer Research UK Centre for Cancer Therapeutics from a high throughput screen of 50,000 compounds against the yeast HSP90 ATPase using a malachite green assay (Sharp *et al.*, 2007b; Cheung *et al.*, 2005). CCT018159 was shown to have anti-cancer activity by inhibiting the proliferation of HCT116 human colon cancer cells (a sulforhodamine B SRB *in vitro* assay) (Sharp *et al.*, 2007b).

Further structure-based design of the CCT018159 prototype resulted in the development of VER-49009 by targeting the Gly97 human residue of the human ATP binding site (Drysdale and Brough, 2008). This inhibitor showed high potency and increased anti-cancer activity in HCT116 cells (Drysdale and Brough, 2008). Using VER-49009 as a scaffold, analogous isoxazole HSP90 inhibitors have been developed including VER52296/NVP-AUY922, which is used in this thesis projects (Brough *et al.*, 2007). NVP-AUY922 (Table 1.1) depletes HSP90 client proteins ERB, c-RAF and BRAF in HCT116 colon carcinoma cells, A2780 ovarian, SKMEL2 and WM266.4 melanoma and BT474 breast carcinoma cells (Eccles *et al.*, 2008). This resorcinylic isoxazole analog has been described as having much greater cellular activity than its pyrazole counterpart as a result of increased uptake and increased half-life

(Sharp *et al.*, 2007b). Biochemically the NVP-AUY922 analog is more soluble and its resorcinol 5-substitutent moiety has been optimized (Sharp *et al.*, 2007b). It is also extremely potent having a GI_{50} of 9nM when screened against a range of human cancer cells lines (Drysdale and Brough, 2008). NVP-AUY922 anti-proliferative effects have been seen against a panel of breast cancer cell lines, multiple myeloma, prostate, colon, melanoma, glioma and HUVEC cell lines (Eccles *et al.*, 2008). NVP-AUY922 also has been shown to have anti-tumour properties as a single agent *in vivo* in BT-474 breast, HCT116 colorectal, and U87MG glioblastoma xenografts in mice (Eccles *et al.*, 2008). In HCT116 human xenograft tumour bearing mice, NVP-AUY922 inhibited tumour growth by 50% when dosed at 50 mg/kg i.p. daily (Drysdale and Brough, 2008; Taldone *et al.*, 2008). Additionally, in athymic mice that had established U87MG glioblastoma xenografts, NVP-AUY922 had anti-proliferative pro-apoptotic and anti-angiogenic effects by decreasing micro-vessel density and HIF1α levels (Gaspar *et al.*, 2010).

NVP-AUY922 entered the clinic in 2007 and is currently in a number of Phase I-II trials. Initially Phase I trials were limited to HER2 positive or ER positive locally advanced or metastatic breast cancer (National Institute of Health, 2014). Since August of 2012, NVP-AUY922 Phase II clinical trials in patients with lymphoma, myeloproliferative neoplasms, advanced non-small lung cancer are active (National Institute of Health, 2014). A Phase I clinical trial on stomach neoplasms, esophageal neoplasms and metastatic gastric cancer has also been completed (National Institute of Health, 2014). More recently, patients with non-small cell lung cancer and also patients with advanced and recurrent non-small cell lung cancer, squamous cell lung cancer, anaplastic lymphoma kinase (ALK) are being recruited for phase I and II clinical trials (National Institute of Health, 2014).

1.9.4.2 HSP90 N -terminal Inhibitor Mode of Action

Despite being structurally unrelated, all N-terminal HSP90 inhibitors bind to a 24kDa moiety in the ATP binding region of the HSP90 N terminal domain (Figure 1.10) (Koga *et al.*, 2009; Patel *et al.*, 2011; Goetz *et al.*, 2003). These N-terminal inhibitors bind with much greater affinity than ATP and their binding inhibits the intrinsic ATPase activity of HSP90 (Koga *et al.*, 2009; Workman, 2004b; Goetz *et al.*, 2003). As a result the ATP hydrolysis cycle, which is essential for HSP90 client protein function, is stopped (Patel *et al.*, 2011; Workman, 2004b; Goetz *et al.*, 2003). When the HSP90 inhibitors are bound to its N-terminal, the multi-chaperone complex has a similar conformation to when ADP is bound (Koga *et al.*, 2009;

Patel *et al.*, 2011). In this conformation HSP90 binds to HSP70/40 and co-chaperones p60 and CHIP and targets proteins for degradation (Koga *et al.*, 2009; Zuehlke and Johnson, 2010; Li *et al.*, 2012). Therefore N-terminal inhibitors inhibit HSP90 from clamping around its client protein and mediating its folding and stabilization (Patel *et al.*, 2011). This causes the release of client proteins, which then undergo ubiquitin tagged proteasome degradation (Maloney and Workman, 2002; Goetz *et al.*, 2003; Jego *et al.*, 2013). Therefore, HSP90 oncogenic client protein de-stabilization and degradation causes cancer cell apoptosis (Ozgur and Tutar, 2014; Zhang *et al.*, 2014b; Workman, 2004b).

N-terminal inhibitors bind to the same region of HSP90 where HSF1 is complexed thus causing the dissociation of HSF1 and its subsequent activation (Figure 1.7) (Taylor *et al.*, 2007; Kamal *et al.*, 2004; Zou *et al.*, 1998). As described earlier, these steps collectively lead to HSF1 transcriptional activity and increased HSP expression, which make up the HSR (Kamal *et al.*, 2004; Morimoto, 2008). Several structurally unrelated N-terminal HSP90 inhibitors all similarly cause HSF1 displacement and a downstream HSR (Goetz *et al.*, 2003; Kamal *et al.*, 2004). Geldanamycin has been shown to activate HSF1 both *in vitro* and *in vivo* and increase HSP72 expression (Kim *et al.*, 1999; Zou *et al.*, 1998). 17-AAG treatment has been shown to increase HSP70 mRNA and protein levels in a number of cancer cells and has also been shown to increase HSP70 expression in human xenografts mouse models (Powers and Workman, 2007; Guo *et al.*, 2005b; Doubrovin *et al.*, 2012). 17-AAG treatment has also been shown to induce HSP70 expression in transformed fibroblasts derived from mice with wild type HSF1; however, in fibroblasts from HSF1$^{-/-}$ mice 17-AAG treatment did not increase HSP70 expression (Bagatell *et al.*, 2000). Moreover, 17-AAG treatment has been shown to induce HSP70 expression in patient tissue samples (Banerji *et al.*, 2005a). The 17-AAG derivative, 17 DMAG, and the naturally occurring radicicol and herbamycin A also cause a HSR as seen by increased protein levels of HSP70 (Chai *et al.*, 2014). In addition, the more recently developed N-terminal inhibitors NVP-AUY922 and CCT108159 have also been shown to induce the HSR (Eccles *et al.*, 2008; Cheung *et al.*, 2005; Gaspar *et al.*, 2010). Treating HCT116 colon cancer cells with CCT018159 increased HSP70 protein expression (Cheung *et al.*, 2005). Similarly, NVP-AUY922 treatment causes a HSF1 stress response in a number of tumour cell lines including HCT116 colon cells, A2780 ovarian, SKMEL2 and WM266.4 melanoma, BT472 breast cancer cells and in the aGB and pGB glioblastoma tumour cell lines (Gaspar *et al.*, 2010; Eccles *et al.*, 2008).
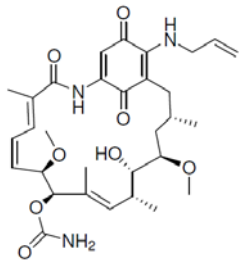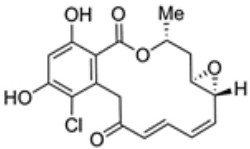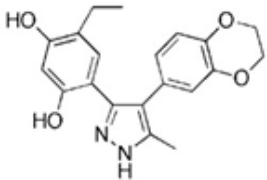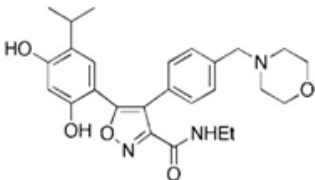
HSP90 Inhibitor	Chemical Structure	Binding site	Chemical Class
17-AAG		N-terminal ATP-binding Pocket	Benzoquinone ansamycin
Radicicol		N-terminal ATP-binding Pocket	Macrolide
CCT018159		N-terminal ATP-binding Pocket	Pyrazole
NVP-AUY922		N-terminal ATP-binding Pocket	Pyrazole

Table 1.1 N-Terminal HSP90 Inhibitors

N-terminal HSP90 inhibitors bind to the ATPase site of the N-terminal molecule to inhibit HSP90 chaperone activity. There are a number of N-terminal HSP90 inhibitors classes including the macrolide, benzoquinone ansamycin and pyrazole classes. To these classes belong naturally occurring and synthetically developed compounds including 17-AAG, Radicicol, CCT018159 and NVP-AUY922. Information sourced from (Neckers, 2002; Eccles *et al.*, 2008).

1.9.5 C–Terminal HSP90 Inhibitors

The C-terminal of HSP90 has also been targeted as a region for anti-cancer therapeutics to bind (Figure 1.10). The HSP90 C-terminal mediates HSP90 dimerization; therefore its inhibition can regulate some HSP90 functions but unlike the N-terminal ATPase domain it does not form a complex with HSF1 (Zhang *et al.*, 2011; Yamada *et al.*, 2003). Examples of C-terminal inhibitors include Novobiocin, epigallocatechin-3-gallate (EGCG), cisplatin, molybdate and taxol (Zhang *et al.*, 2011; Donnelly and Blagg, 2008). Novobiocin, the most studied of the C terminal inhibitors, is a member of the coumermycin antibiotic family (Figure 1.10) (Donnelly and Blagg, 2008). It binds weakly to the C-terminal; however, at high concentrations its' binding alters the structural conformation of HSP90 (Figure 1.10) (Donnelly and Blagg, 2008; Fukuyo *et al.*, 2010; Zhang *et al.*, 2011). The conformational change of HSP90 results in the destabilization of some HSP90 client proteins including Raf-1, mutant p53, Src and ERBB2 that act as oncogenic proteins in cancer (Fukuyo *et al.*, 2010; Donnelly and Blagg, 2008; Whitesell and Lindquist, 2005). Structural modification of Novobiocin generated the 3'-descarbamoyl-4-deshydroxynovobiocin (DHN2) molecule (Zhang, 2011). Further optimization of DHN2 resulted in the production of the indole derivate 46, which is the most potent analogue of Novobiocin (Zhang, 2011). By binding to the C-terminal ATP site, these inhibitors block HSP90 chaperone activity and client interaction by preventing its formation as a dimer (Sgobba *et al.*, 2010). Unlike N-terminal domain HSP90 inhibitors, C-terminal HSP90 inhibitors do not cause the displacement and subsequent activation of HSF1 (Wang and McAlpine, 2015). Consistent with this, they do not induce an HSR (Wang and McAlpine, 2015; Chai *et al.*, 2014).

1.9.6 Proteasomal Inhibitors

The proteasome is the organelle where many (but not all) ubiquitin-tagged proteins are degraded (Alberts *et al.*, 2002; Adams, 2003). The ubiquitin-proteasome pathway (UPP) degrades more than 80% of a cell's proteins (Adams, 2002). Proteasomes are 2,000 kDa cylindrical multi-subunit complexes, which have a 20S core catalytic component and have a 19S subunit either at both ends or only one (Adams, 2003; Genin *et al.*, 2010; Alberts *et al.*, 2002). Proteasome inhibitors inhibit the proteasome by binding to the 26S proteasome thereby inhibiting its proteolytic activity (Adams, 2004; Adams, 2003; Genin *et al.*, 2010). The proteolytic activity is required for protein degradation (Adams, 2003; Genin *et al.*, 2010). There are a number of proteasome inhibitors, which are categorized into different classes: peptide aldehydes, peptide vinyl sulfones, peptide boronates, peptide epoxyketones and β-

lactones (Adams, 2004; Genin *et al.*, 2010). Some examples of proteasome inhibitors include MG132, lactacystin and bortezomib (Genin *et al.*, 2010; Holmberg *et al.*, 2000; Piperdi *et al.*, 2011). Bortezomib is a widely used compound and in combination with a number of other chemotherapeutics is the standard of care for Multiple Myeloma patients (Roussel *et al.*, 2011). A number of proteasomal inhibitors have been shown to activate HSF1 and increase HSP70 transcription (Holmberg *et al.*, 2000; Du *et al.*, 2009; Kim *et al.*, 1999). In addition, some may activate ER stress and the stress signalling molecule p38 (Selimovic *et al.*, 2013; Kim *et al.*, 1999).

1.9.7 Alkylating Agents

Alkylating cancer agents directly damage DNA to prevent the cancer cell from undergoing mitosis (Mkele, 2010; Siddik, 2005). Alkylating drugs can act at any stage of the cell cycle and alkylate DNA bases in either the minor or major grooves (Ralhan and Kaur, 2007; Mkele, 2010). They are used to treat many different cancers including leukaemia, lymphoma, Hodgkin's disease, multiple myeloma, and sarcoma, as well as cancers of the lung, breast and ovary (Mkele, 2010). These drugs can cause long-term damage to the bone marrow (Kemp *et al.*, 2011). There are different classes of alkylating agents, including: nitrogen mustards, nitrosoureas, alkyl sulfonates, triazines and ethylenimines (Siddik, 2005; Mkele, 2010). Because alkylating agents damage DNA, they cause genotoxic stress (Busa *et al.*, 2010). Alkylating agents have also been shown to cause a HSR by decreasing cellular levels of glutathione (GSH), which induces oxidative stress (Chen *et al.*, 1990; Chen and Stevens, 1991; Freeman *et al.*, 1995; Lee and Hahn, 1988; Donati *et al.*, 1990; Beckmann *et al.*, 1992).

1.9.8 Cross-linking Agents

Another group of cancer therapeutics, which mediate their toxicity through genotoxic stress are the cross-linking agents (Basu and Krishnamurthy, 2010; Nussbaumer *et al.*, 2011). These cancer therapeutics are sometimes classified as alkylating agents because they kill cells in a similar way (Nussbaumer *et al.*, 2011). Cross-linking agents include nitrogen mustards and nitrosurea platinum complexes, which include cisplatin, carboplatin and oxaliplatin (Nussbaumer *et al.*, 2011; Basu and Krishnamurthy, 2010). These drugs are used to treat ovarian, testicular, lung cancer and metastatic colorectal cancer (Nussbaumer *et al.*, 2011; Basu and Krishnamurthy, 2010; Mkele, 2010). The platinum complex, cisplatin, is the most commonly used cancer therapeutics (Rafique, 2010). Cisplatin and the second generation

platinum complex, carboplatin, have been reported to affect HSF1 activity and HSP70 expression (Huber, 1992; Desai *et al.*, 2013; Ohtsuboa *et al.*, 2000).

1.9.9 Intercalating Agents

Intercalating agents are a class of therapeutics, which reversibly interact with the DNA double helix (Brana *et al.*, 2001a). Intercalating agents, like alkylating agents, are not cell cycle phase specific and can disrupt at any phase of the cell cycle phase (Perez *et al.*, 1994). Intercalating agents are mainly classified into the anthracycline class but mitoxantrone and actinomycin are also intercalating agents, which do not fall into this subclasss (Nussbaumer *et al.*, 2011). All intercalating agents retain structural features, which include a polyaromatic system that bind by insertion between DNA base pairs with a marked preference for 5-pyrimidine-purine-3 step (Nussbaumer *et al.*, 2011; Brana *et al.*, 2001b). The anti-tumour antibiotics, anthracyclines include doxorubicin, daunorubicin and aclarubicin, epirubicin and idarubicin (Nussbaumer *et al.*, 2011). The first three of these are naturally-occurring products derived from *Streptomyces peucetiusor* or *S. galilaeus* (Nussbaumer *et al.*, 2011; Conti, 2007). These anthracyclines are used to treat a large number of tumours including acute leukaemia, lymphomas, myelocytic leukaemia, and solid tumours including sarcoma, breast cancer and ovarian cancer (Nussbaumer *et al.*, 2011; Smith *et al.*, 2010). These agents are also used as second line treatments and also in the cases of advanced cancer (Nussbaumer *et al.*, 2011). Many of these cancers affect the bone marrow due to their site of origin or nature i.e. metastatic to bone.

Due to their interaction with DNA and inhibition of transcription, these agents cause genotoxic stress (Ohno *et al.*, 2008). Despite these agents primarily causing cell death through the inhibition of DNA synthesis, transcription and replication, they have also been shown to activate stress pathways within the cells (Smith *et al.*, 2010). Anthracyclines have been shown to increase ROS and also causes mitochondrial dysfunction resulting in oxidative stress (Ewer and Lippman, 2005; Kelland, 2007). There also has been a report that anthracyclines increase the expression of HSPs in a number of tumour cell lines (Fucikova *et al.*, 2011).

A.
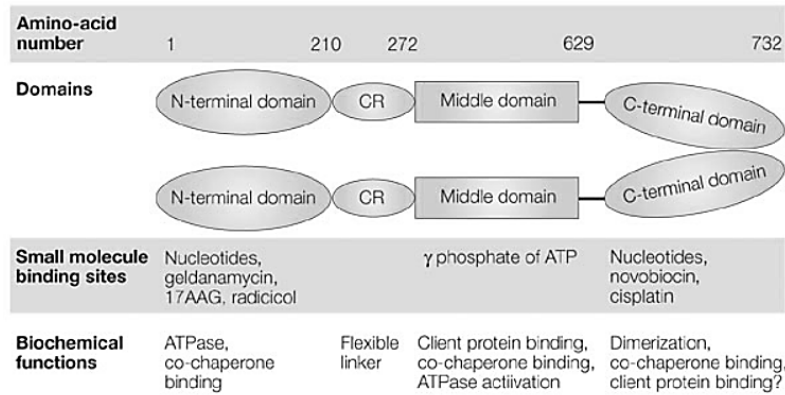
B.
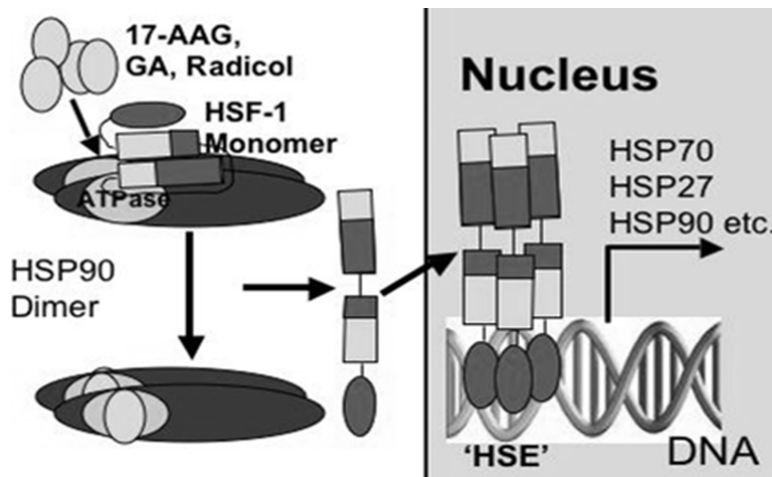
Figure 1.10 The Structure of HSP90 and Binding Regions of HSP90 Inhibitors
(A.) HSP90 is present in the cytoplasm as a dimer. Each HSP90 monomer has three domains: an N-terminal ATP-binding domain, a middle domain and a C- terminal domain. The N-terminal domain contains the adenine-binding pocket, which is responsible for HSP90 ATPase activity that is essential for its function. This ATP binding site is where N terminal HSP90 inhibitors including: 17-AAG, 17-DMAG, radicicol, CCT108159 and NVP-AUY922 bind as shown in **(B.)**. This region is also where the latent HSF1 binds to HSP90 but is displaced by N-terminal HSP90 inhibitors **(B.)**. The middle domain is a charged linker region, which contains the binding sites for client proteins and co-chaperones including p50^{CDC37} and p23. The carboxyl dimerization terminal has a tetratricopeptide repeat-binding (TPR) motif (EEVD) to which co-chaperones bind such as HOP and CHIP. C-terminal HSP90 inhibitors including novobiocin also bind to this region to inhibit HSP90 chaperone activity. Image sourced from (Whitesell and Lindquist, 2005). **(B.)** The displaced HSF1 translocates to the nucleus and is activated as shown in Figure 1.7 Image from Dr John Price.

1.9.10 Antimetabolites

Antimetabolites interfere with DNA and RNA growth by substituting the normal pyrimidine compounds and purine bases with pyrimidine or purine analogues (Mkele, 2010). Substitution with these analogues inhibits DNA synthesis by exerting their influences during the S phase of the cell cycle (Parker, 2009). These drugs are classified into folate, purine and pyrimidine compouonds (Nussbaumer *et al.*, 2011; Mkele, 2010). Examples of antimetabolites include 5-flurouracil (5-FU), floxuridine, gemcitabine (Gemzar[®]) and methotrexate (Mkele, 2010). These drugs are used to treat leukaemias, non-Hodgkin's lymphomas and many solid tumours including breast, ovarian, and intestinal cancer (Mkele, 2010; Nussbaumer *et al.*, 2011). Since antimetabolites inhibit DNA and RNA replication, these cancer therapeutics also cause genotoxic stress (Mkele, 2010). Recently evidence has emerged that the antimetabolite methotrexate activates HSF1 as shown to by increased HSP70 protein expression (Chai *et al.*, 2014).

1.10 Scope of this Thesis

The work presented in this thesis focusses on the osteoclast differentiation process and the effect of a number of anticancer therapeutics upon this process as well as the mechanisms that underlie these observed effects. Many chemotherapeutic drugs show cytotoxic effects on bone marrow and therefore indirectly affect bone metabolism. It is generally believed that such drugs damage bone cells in a non-specific way and this causes the associated bone loss. While this does often occur, bone loss involves the active resorption of bone by a single type of cell, the osteoclast. This suggests increased osteoclast numbers and osteoclast actions, not loss of osteoclasts. This idea follows thematically from an earlier publication by Price *et al.* (2005), which demonstrated that 17-AAG increased osteoclast formation *in vitro* and *in vivo* and this was associated with bone loss (Price *et al.*, 2005). The increased numbers of osteoclasts is associated with in an even more harmful effect: that this anti-cancer drug, effective in reducing tumour growth in soft tissue, caused *increased* breast cancer growth and invasion in bone (Price *et al.*, 2005). This suggests that a therapy, which affects osteoclasts in this way would have very undesirable effects, both on bone integrity and cancer growth. With this in mind the aims of this thesis are to answer the following questions:

1) What is the mechanism that underlies the 17-AAG-induced increase in osteoclast numbers and does it involve 17-AAG activation of HSF1 and a cell stress response?

2) Do other structually-unrelated HSP90 inhibitors act to increase osteoclast formation?

3) Do other chemotherapeutics, which act through quite different anti-cancer mechanisms also stimulate osteoclast formation like 17-AAG and, if so, do they act in the same manner?

Chapter 2
Experimental
Methods

2.1 Materials

2.1.1 Mouse Strains

Mice of the C57Black/6 background, male and between 8-14 weeks of age, were used as a source of fresh tissue for *in vitro* experiments unless otherwise indicated. C57Black/6 mice were obtained from Monash Animal Research Platform, Monash University, Clayton, Vic, and used with the approval of the Monash Medical Centre (MMC) Animal Ethics Committee B, approval number MMCB-2011/19. The mice were maintained at the MMC Animal Facility (Clayton, Vic) according to procedures approved by Animal Ethics Committee B (Clayton, Australia). HSF1 knockout mutant mice mouse strain HSF1$^{tm1Ijb/tm1Ijb}$ (here designated HSF1$^{-/-}$), were obtained from Prof. Ivor Benjamin of the University of Utah, USA. They were previously confirmed by our group and by Prof Benjamin's laboratory to completely lack HSF1. These mice were bred on a mixed Balb/c x 129 genetic background since HSF1 knockout mice are not viable on pure C57Black/6 pure genetic backgrounds since they die *in utero* due to failure of implantation (Xiao *et al.*, 1999). Female HSF1$^{-/-}$ are infertile so HSF1 knockout mice were generated using male knockouts crossed with heterozygote females, or male heterozygotes with female heterozygotes. This resulted in greatly sub-Mendelian ratios of knockout mice born, likely due to implantation or development failure. For experiments, either littermates or age-matched mice that were closely related from the same colony were employed. Mice were kept under high barrier conditions at the Monash University Animal Facilities. Monash University Ethics approval number: SOBSB/B/2010/28BC.

2.1.2 Tissue Culture Materials and Consumables

Medium supplements and fetal bovine serum (FBS) were all purchased from Life Technologies (Grand Island, NY, USA). These included Alpha modification of Minimal Essential Medium (α-MEM) (cat no. 12561-072), RPMI Medium 1640 (cat no. 21870-092), Dulbecco's Modified Eagle Medium (DMEM) (cat no. 21063-029), Penicillin (10000 U/ml)/Streptomycin (10000 U/ml) (cat no. 15140-122), L-Glutamine (29.95 mg/ml) (cat no. 25040-081), Trypsin-EDTA (10x) (cat no. 15400-054) HEPES buffer solution (1M) (cat no. 15630-080), Phosphate buffered saline (PBS) (1x) without calcium or magnesium (cat no. 14190-250). Foetal bovine serum (FBS) batches 029, batch no. 8164473 and batch no. 044 (cat no. 16000044) were employed. Minocycline (cat no. M-9511), Geneticin **(**G418) (50mg/ml) (cat no. G8186), Cell dissociation solution, Non-enzymatic, in Hank's buffered

salt solution (HBSS) (1x) (cat no. C1419) and thapsigargin (0.5mg) (cat no. T9033) were all purchased from Sigma (Castle Hill, NSW, AUS). Ampicillin (sodium salt, USP Grade) (cat no.AM0339) was purchased from Astral Scientific (Gymea, NSW, AUS). Mouse RANK-Fc (692-RK-100) and TGF-β1 (cat no. 240-b-002) were purchased from R&D systems/Bioscientific Pty. Ltd. (Sydney, NSW, AUS). RANKL (cat no. 47197900) was purchased from the Oriental Yeast Co. Ltd. (Tokyo, Japan). M-CSF (100μg) (cat no. 11795-H08H) was purchased from Sino Biologicals (Beijing, P.R. China). KNK437 HSF1 inhibitor (5mg) (cat no. 373260) and KRIBB11, Heat Shock Protein Inhibitor II (cat no. 385570) were purchased from Calbiochem through Merck Millapore (Billerica, MA, USA.). Dimethyl sulfoxide (DMSO) (cat no. 276855) was purchased from Ajax Chemicals (NSW, AUS). L Cells were purchased from ATCC (Manassus, VA, USA). 17-AAG and cisplatin were kind gifts from Dr John Price (Monash University, AUS). CCT018159 was obtained from Cayman Chemical Company (Ann Arbor, Michigan, USA). NVP-AUY922 was purchased from Biovision (Milpitas, CA, USA). MG132 (cat no. S2619) and doxorubicin (cat no. S1208) were purchased from Selleck chemicals (Houston, TX, USA). Bortezomib (free base) (cat no. B-1408) was purchased from LC labs Scientific (Woburn, MA, USA) through Scientifix Pty Ltd (Cheltenham, Vic. AUS). SB203580 (cat no. 5633) was purchased from Cell Signalling (Danvers, MA. USA). Hoescht (cat no. H3570) from Life Technologies was a kind gift from Trevor Wilson. Corning 96 well flat clear bottom black polystrene cell culture treated microplates (cat no. COR3603), Corning costar sterile serological pipette 5 ml (cat no.4487) 10ml (cat no.4488) and 25ml (cat no.4489) Corning 15ml (cat no.4307666) and 50ml (cat no.4308291) centrifuge tubes were all purchased from In Vitro Technologies (Noble Park, VIC, AUS). Nunclon white plate 96 well (cat no. 236105), Starstedt 96 well plates sterile (cat no. 83.1835), Nunc tissue culture flasks T25 (cat no 156367), T75 (cat no.156499) and T175 (cat no. 159910), Nunc delta surface 6 well (cat no. 140675), 24 well (cat no. 142475), 48 well (cat no.150687) and Starstedt 96 well sterile plastic tissue culture plates (cat no. 83.1835) and 6mm diameter glass coverslips were all purchased from Thermo Fischer Scientific (Taren Point, NSW, AUS). 96 well white plates for luciferase assays (cat no. 136101) and Corning® tissue-culture treated culture dishes 10mm (cat no. CLS430167) were purchased from Sigma (Castle Hill, NSW, AUS). Qualitive Filter paper size 55mm was purchased from Micro Analytix (Taren Point, NSW, AUS). Microscope slides twin frost 45° ground edge (cat no. S41104A), and 15mm diameter coverslips (cat no. CS15100) were purchased from Grale Scientific (Ringwood, Vic, AUS). Syringes and needles were purchased from Terumo Corporation (Elkton, MD, USA).

2.1.3 Molecular Biology Materials

Acetic acid (Analar, cat no. 1-2.5L GL), glycerol (cat no. 242-2.5 GL), calcium chloride (CaCl$_2$) dihydrate (cat no. 127-500G), magnesium chloride (MgCl$_2$) (cat no. 296-500G), sodium deoxcholate (cat no. D6750-25G), IGEPAL (Nonidet) (cat no. I3021-50ML), ethanol (analytical grade, Ajax Finechem, cat no. 214-2.5L) and acetone (cat no.A35010-2.5L), Ethanol absolute UNIVAR ACS (cat no.AJA214-2.5LPL), propan-2-ol UNIVAR PL (cat no. AJA425-2.5PL), formaldehyde (36.5-38% solution) UNIVAR) (cat no. AJA809-2.5LPL), Pierce Halt Proteinase Inhibitor Cocktail (cat no. 78410), Whatman filter circle, Grade 1, 125 mm (cat no. 1001-125) and Pierce goat anti-mouse secondary antibody (cat no. PIE 31444) were purchased from Thermo Fischer Scientific (Taren Point, NSW, AUS). Fast red violet (cat no. F3381), Naphthol ASMX Phosphate (N4875) and Betaine (>98%) (cat no. B2629)) were purchased from Sigma (Castle Hill, NSW, AUS). Tris (cat no. 0497) was purchased from Astral (Amresco). Tryptone (cat no. LP0042), Yeast Extract (cat no. LP0021) Agar, LB (cat no. LP0011) were all purchased from OXOID (Unipath Ltd., Hampshire UK). Nupage 4-12% Bis-Tris gels 10 well (cat no. NP0321BOX), 12 well (cat no. NP0322BOX), 15 well (cat no. NP0323BOX), 17 well (cat no. NP0329BOX), 20 well (cat no. WG1402BOX) and 26 well (cat no. WG1403BOX), NuPage MES SDS Running Buffer (20x) (cat no. NP0002), NuPage Antioxidant (cat no. NP0005) and Sample Reducing Agent (cat no. NP0004), Seeblue2 plus2 prestained standard (1x) (cat no. LC5925), Superscript III First strand Synthesis System for RT-PCR (cat no. 18080-051), Sybr safe (cat no. S33102) and Lipofectamine® LTX Reagent with PLUS™ Reagent (cat no. 15338100) were all purchased from Life Technologies (Mulgrave, VIC, AUS). Anti-MITF C5 antibody (cat no. Ab12039) was purchased from Sapphire Bioscience (Waterloo, NSW, AUS). Mouse anti-NFATc1 antibody (cat no. 556602) was purchased from Becton Dickinson (North Ryde, NSW, AUS). p38 MAPK antibody (cat no. 9212) and Phospho-p38 MAPK (Thr180/Tyr182) (3D7) antibody (cat no.9215) were purchased from Cell Signalling (Danvers, MA, USA). HSP70/HSP72 antibody (cat no. ADI-SPA-812F) was purchased from Enzo Life Sciences/ Sapphire Bioscience (Waterloo, NSW, AUS). Immobilon-P Transfer membrane PVDF 0.45µM Roll 26.5cm x3.75m (cat no. IPVH00010) and Re-blot Strong Solution (10x)(cat no. 2504) were purchased from Merck Millipore (Bayswater, VIC, AUS) Amersham Hyperfilm ECL (18 x 24cm) 100 sheets (cat no. 28-906837) from GE Healthcare (Silverwater NSW, AUS). Fuji Medical X-ray film super RX, size 18cm x 24 cm (cat no. 100NIF) was purchased from Fujifilm (Minato-ku, Tokyo, Japan). Skim milk used for Western blotting was Carnation brand (Sydney, NSW, AUS). Complete EDTA free protease inhibitor cocktail (cat

no. 04693132991), PhosSTOP phosphatase inhibitor cocktail (cat no. 04906845001), Lumilight Western Blotting Substrate (cat no 12015200001) and Fugene HD transfection reagent (cat no. 4709705001) were purchased from Roche (Dee Why, NSW, AUS). Luciferase kit (cat no. E1501) and Luciferase passive lysis buffer x5 (cat no. E194a) were bought from Promega (Alexandria, NSW, AUS). DAB liquid chromagen system (cat no 346811), goat anti-rabbit IgG-HRP (cat no. P044801), rabbit anti-goat IgG-HRP (cat no. P044901) were purchased from DAKO (North Sydney, NSW, AUS). Qiagen RNeasy kit (50 samples) (cat no. 74104) was purchased from Qiagen (Doncaster, VIC, AUS) XL1-Blue Subcloning - Grade Competent Cells (cat no. 200130) were purchased from Stratagene (La Jolla, CA, USA). Primers were purchased from Sigma (Castle Hill, NSW, AUS) or Bioneer (Daejeon, Republic of Korea).

2.1.4 Cell Lines

2.1.4.1 RAW264.7

RAW264.7 cells are a M-CSF-independent clonal murine macrophage-like leukemic cell line, which was derived from Abelson murine leukemia virus-induced ascites from a male mouse: Ig^- $H-2d^+$, $H-2b^-$, Thy-$1-2^-$, Ia^- (Ralph and Nakoinz, 1977; Raschke et al., 1978). The RAW264.7 cell line is a well characterized and accepted model of osteoclast formation with RANKL stimulated RAW264.7 cells forming TRAP and CTR expressing multinucleated cells, which are capable of bone resorption (Collin-Osdoby et al., 2003; Battaglino et al., 2004; Matsumoto et al., 2004; Matsuo et al., 2004; Liu et al., 2003; Collin-Osdoby and Osdoby, 2012; Cuetara et al., 2006). The genotype of RAW264.7 cells closely resembles that of the osteoclast precursors and also of fully differentiated and active osteoclast. Furthermore, RAW264.7 cells also have a similar signalling pathway profile to that of osteoclasts and are therefore an appropriate model to use to study osteoclastogenesis (Collin-Osdoby et al., 2003).

2.1.4.2 L-Cells and L-Cell Conditioned Medium

L-cells are a mouse fibroblast-like cell line, which constitutively secretes M-CSF. In this thesis L-cells are used as a source of growth medium containing M-CSF for bone marrow macrophage preparation (Stanley and Guilbert, 1981). For this, L-cell conditioned medium (LCM) was prepared. L-cells (5×10^6 cells) were cultured $75cm^2$ flask in 20 ml RPMI with 10% heat-inactivated FBS (HI-FBS). The cells were allowed to grow for 7 days and the

supernatant collected at day 7. The supernatant was collected into 50 ml sterile polypropylene tubes, followed by centrifugations for 5 mins at 2,000 rpm to remove cells and cell debris. The supernatant was transferred to a fresh tube and centrifuged again. The resulting LCM supernatant was then passed through a sterile 0.45µm filter and stored at -20°C until use. Typically, 30% LCM was added to cultures containing bone marrow cells to prepare bone marrow macrophages.

2.1.4.3 HEK-HSE Cells

The HEK-HSE cells were generated by Dr Chau Nguyen. Briefly HEK293t cells were transduced with the bicistronic retroviral vector, pBABE_HSF1wt_IRES_EGFP to overexpress HSF1 wt, which was co-expressed at the gene level with an EGFP separated by an internal ribosomal entry site (IRES) (Nguyen *et al.*, 2013). The HEK294t cells with stable expression of HSF1 wt and EGFP were selected by puromycin (1µg/ml) treatment for 2 weeks (Nguyen *et al.*, 2013). These cells were further transfected with a pHSE-mCherry vector in which mCherry expression is under the control of an inducible HSP70 (HSP70B) promoter (HSE removed and the HSP70B promoter, which contains HSE, inserted upstream of mCherry) (Nguyen *et al.*, 2013; Winklhofer *et al.*, 2001). The HSP70B promoter is 'strictly' inducible having no to very little basal expression in most cells (Noonan *et al.*, 2007). This differs from the major inducible HSP72, which has basal expression levels in cells (Noonan *et al.*, 2007) Comparative heat shock studies between the major inducible HSP72 gene and HSP70B show a transient increase in HSP70B levels whereas HSP72 levels persist for days (Noonan *et al.*, 2007). Cells stably containing the HSE-mCherry construct were selected by G418 treatment (1µg/ml) for 2 weeks (Nguyen *et al.*, 2013). Subsequently, cells with high levels of EGFP and mCherry were sorted by FACS (Nguyen *et al.*, 2013).

2.1.4.4 NFAT-response Element Dependent Luciferase Expressing RAW264.7 Cells (NFAT-RAW Cells)

NFAT RAW cells, which were made previously by Dr Julian Quinn were generated by stable transfection of RAW264.7 cells with pGL4.30 [luc2P/NFAT-RE/Hygro] construct (Promega Corp., NSW, AUS) (Singh *et al.*, 2012). This construct is a plasmid containing luciferase-2P expressed under the control of an NFAT response element, i.e., luciferase is produced in response to activated NFAT transcription factors. Cells were transfected using purified plasmid and Fugene 6 reagent (Promega) according to manufacturer's instructions. Transfected cells were selected using hygromycin (200µg/ml) and became stable within three

passages. These cells were used to test NFAT transcriptional activity in response to RANKL and other compounds (Singh *et al.*, 2012; van der Kraan *et al.*, 2013).

2.1.4.5 NFκB Response Element Dependent Luciferase Expressing RAW264.7 Cells

NFκB-RAW cells, RAW264.7 cells containing a NFκB reporter were generated (and generously supplied) by Prof. Jiake Xu, University of Western Australia, as previously described by Wang *et al.* (Wang *et al.*, 2003a). Briefly, RAW264.7 cells were transfected with a luciferase reporter gene*3kB-Luc-SV40* reporter (Wang *et al.*, 2003b). This reporter contains three NFκB sites from the interferon gene upstream of the luciferase coding region, previously described (Steer *et al.*, 2000; Akama *et al.*, 1998; Wang *et al.*, 2003a). The *3kB-Luc-SV40* reporter construct (20 μg) and pcDNA3.1 (2 μg) vectors were transfected into RAW264.7 cells using electroporation with the following conditions (280 V and 960 μF) (Wang *et al.*, 2003a). The transfected cells were then selected with G418 (400 μg/ml) (Gibco BRL, Life Technologies, Melbourne Australia) (Wang *et al.*, 2003a). The resulting stable cell line was used to investigate NFκB activation by RANKL and other compounds (Wang *et al.*, 2003a; Singh *et al.*, 2012; van der Kraan *et al.*, 2013).

2.2 Equipment

Quantitative real-time RT-PCR (qRT-PCR) was performed using the Stratagene MX3000P machine, and PCR analysis was performed using the MX PRO software version mx3000P (Stratagene, Cedar Creek, TX, USA). The spectrophotometer, used to measure RNA concentrations, was the NanoDrop ND-1000 (Thermo Fisher Scientific, MA, USA). Tissue culture microscopes included the Olympus IMT (Olympus Optical Company Limited, Tokyo, Japan), Wilovert (Helmut Hund GmbH, Wetzlar, Germany), Leica Diavert Microscope, Olympus Ck2 microscope. Centrifuges included: tissue culture centrifuges, Beckman Coulter Allegra X-22, X-30R, X-ISR; eppendorf centrifuges, 5417C and 5424. Sorvall T6000D centrifuge (DuPont, OH, USA) and Beckman Avanti-J-301 centrifuges (Beckman) were used to pellet bacterial cultures. Membranes and bacterial cultures were shaken using the orbital mixer and orbital mixer incubator Ratek instruments. In addition, Ratek dry heat blocks were used to boil cell lysates and for cDNA synthesis. mCherry levels from the HSE-HEK cells were collected by the Arrayscan VTI (Thermo Fischer Scientific). To read the absorbance levels and luciferase levels the EnVision Multilabel Plate Reader (Perkin Elmer) and Sunrise

Tecan Magellan (6.3 version) plate reader were used. Waterbaths included Grant Water Bath (42°C) and a 37°C temperature maintained Waterbath (Julabo P) scientific equipment manufacturing Co. Ltd. Cells lysates were sonicated using the Bandelin Sonorex digitec (Sonicator). Film was developed using the AGFA CP1000 developer (AGFA).

2.3 Tissue Culture

All cell cultures were incubated at 37°C in a humidified atmosphere with 5% CO_2.

2.3.1 Preparation of Bone Marrow (BM) Cells

Adult C57Bl/6J male mice (8-12 weeks) were humanely killed by carbon dioxide inhalation followed by cervical dislocation. After rinsing the mouse with 70% ethanol the hind limbs were dissected out, skin and muscle were removed and femora and tibiae were isolated free of extraneous tissues. These long bones were cut just below the growth plate (removing the epiphyseal region) and then bone marrow flushed from the shaft of the bone using PBS in a syringe fitted with a 25 gauge needle. Cells were collected in a sterile 30ml falcon tube. This bone marrow was agitated and vortexed to break up cell aggregates. The suspension was then passed through a fine strainer to remove remaining aggregates and particles. The supernatant was centrifuged at 2,000 rpm for 5 min and the pelleted cells resuspended in 10 ml MEM/FBS and counted. Generally 5 x 10^7 bone marrow cells were obtained from the four hind limb bones of one 6 to 12 week old C57Black 6 mouse.

2.3.2 Preparation of Bone Marrow-derived Macrophages

Isolated bone marrow cells were resuspended in endotoxin free RPMI media containing heat-inactivated FBS (10%) plus LCM (30%); or alternatively recombinant M-CSF (30ng/ml) was used in place of LCM. The cells were seeded at the density of 2.5x10^7 cells/ml media in a 10 cm^2 petri dish and incubated at 37°C in a humidified atmosphere with 5% CO_2 for 3 days. On day 3, the non-adherent bone marrow-derived macrophages (BMM) were collected from supernatant into a sterile 50 ml falcon tube and centrifuged for 5 min at 2000 rpm. To obtain adherent bone marrow-derived macrophages, the cells remaining in the petri dish were washed three times with PBS (1x) and incubated with 5 ml of a non-enzymatic cell dissociation solution (cat. No C5789, Sigma-Aldrich, MO, USA) for 20 min in a humidified incubator (37°C with 5 % CO_2). The cells were then scraped with a sterile cell scraper, transferred to a sterile falcon tube containing 5ml media and centrifuged for 5 min at 2000

rpm. The cells were then resuspended in media and counted. For osteoclast cultures, both adherent BMM and BMM were seeded at 10^5 cells in 6mm diameter wells. This method to generate BMM follows previously described protocols (Quinn *et al.*, 1998).

2.4 Kill Curves: Finding the Cell Tolerance Levels for Pharmaceutical Compounds

RAW264.7 cells were seeded at 2 x10^3 and 10^4 in 6mm diameter wells to determine seeding density. The RAW264.7 cell density 10^4 was determined to be best seeding density for a 6 day culture in 6mm diameter wells. Thus this seeding density was used for experiments with these parameters throughout the course of the thesis. RAW264.7 cells were treated with the compounds of interest over an appropriate concentration range. The cells were incubated at 37°C and 5%CO_2 for 1, 3, and 6 days or 1 and 2 days as noted. The media and non-adherent cells were removed through aspiration and the cells were rinsed in PBS (1x). The cells were then fixed in buffered formaldehyde (4%) for 5 minutes at room temperature. The formaldehyde was discarded and the cells washed again in PBS. After washing out the formaldehyde the cells were stained with crystal violet solution (3-4 drops) (Appendix A) and were incubated at room temperature for 10 minutes. The stain was removed by washing the cells in cold water until the water ran clear. The cells were air dried overnight. The crystal violet stain was extracted from the cells by eluting with of 10% acetic acid (200μl). The eluted cells were shaken for 15 minutes on a rocker at room temperature to facilitate the extraction process. The absorbance (560nM) was read on an EnVision Plate reader.

HEK-HSE cells were seeded at 2.5 x10^4 cells, were left to settle for three hours and were treated with compounds to be tested. The procedure followed was similar to RAW264.7 cells above; however, due to the HEK-HSE cells being semi-adherent cells, the washing steps were limited and instead of aspiration solutions were removed through individual pipetting.

2.5 *In Vitro* RANKL Stimulated Osteoclast Formation Assays

2.5.1 RAW264.7 Cells

RAW264.7 cells were seeded at 10^4 cells in 6mm diameter wells. Cells were then treated with recombinant RANKL. Concentrations of RANKL depended on the experiment details but were typically 20ng/ml and 100ng/ml, which are the minimum threshold concentration and

the maximal concentration required for osteoclast formation, respectively. Cells were treated with cytokines, compounds or DMSO vehicles appropriate to the experiment. All experiments included negative control cultures without RANKL treatment to demonstrate the necessity of RANKL to drive osteoclast formation. Cells were incubated at 37°C in a humidified atmosphere containing 5% CO_2 for 3 days and then media and treatments were replenished. The cells were then incubated for a further 3 days. On day 6 the cells were stained for TRAP, a marker produced by fully differentiated osteoclast cells (see Chapter 2.6.1). Cells, which were TRAP positive and multi-nucleated (nuclei ≥2), were counted as osteoclasts.

2.5.2 Bone Marrow Cells

Bone marrow cells were seeded at 10^5 cells in 6mm diameter wells in the presence of RANKL (20ng/ml) and M-CSF (30ng/ml). Bone marrow cells were found to be generally more sensitive to the drug treatments than RAW264.7 cells and concentrations employed were generally lower than employed with RAW264.7 cells. The bone marrow cell cultures were otherwise treated in the same manner described for RAW264.7 cells above.

2.6 Identification of Osteoclast-like Cells in Culture

2.6.1 TRAP Histochemical Staining

Cells were washed in PBS (1x) and then fixed in PBS-buffered formaldehyde (4%) for 10 minutes. The formaldehyde was removed, and the cells permeabilized with an ethanol: acetone mixture (1:1 ratio) for approximately 1 minute. The ethanol: acetone mixture was discarded, and the cells were left until almost dry. The cells were then stained with TRAP histochemical staining solution which consists of Naphthol AS-MX Phosphate (Sigma) (0.01%) and Fast Red Violet LB Salt (Sigma) (0.03 %) (Appendix A). Briefly, Naphthol AS-MX Phosphate (0.5-10 mg) was dissolved in dimethylformamide (BDH) (0.5 ml) and TRAP Buffer (50 ml) (Appendix A) was added. Fast Red Violet LB Salt (20-30 mg) was then dissolved in the buffer and the solution thoroughly mixed. The solution could be stored for up to 7 days at 4°C. The cells were stained with the TRAP stain solution. During the 10 minute incubation the stain was monitored as there is variability in the time taken for the cells to stain. Upon staining, the histochemical stain substrate was then washed out with tap water and the cells allowed to dry. Stained plates were examined by light microscopy and photography.

2.6.2 CTR Staining

2.6.2.1 Preparation of Cell Cultures Glass Coverslip Substrate

Glass coverslips, 6mm in diameter (Thermo Fischer Scientific), were first cleaned of oily residues by boiling in non-ionic detergent (5 % Extran 3, Crown Scientific, VIC). Using a microwave, coverslips were gently boiled in detergent solution (250ml) within a conical flask for 5 min. The coverslips were then cooled, rinsed at least ten times in distilled H_2O, and washed overnight in distilled H_2O. They were rinsed a further 4 times in dH_2O prior to being sterilized in 70 % ethanol for 15 min and air-drying in a laminar flow sterile cabinet. The coverslips were further sterilized by UV exposure overnight.

Mouse bone marrow cells were seeded at 10^5 cells per well in 10mm diameter wells containing the cleaned 6 mm diameter coverslips. This allowed for the cells on coverslips to be removed for immunostaining while the remaining cells on the tissue culture plastic wells were histochemically stained for TRAP to confirm the presence of osteoclasts. Cells were typically incubated with M-CSF (30ng/ml) and RANKL (20ng/ml), unless otherwise stated and other compounds of interest as indicated in the relevant sections. Cells were grown at 37°C in a humidified atmosphere containing 5% CO_2. After 6 days of incubation the coverslips were removed from the wells, air dried, fixed with acetone at -20°C for 10 min, dried again and then affixed cell side facing upwards to glass slides for ease of handling. These slides were left at 4°C overnight allowing for the DPX to solidify.

2.6.2.2 CTR Immunohistochemistry

Cells affixed to a glass slide were incubated in purified rabbit anti-mouse CTR (IgG fraction purified in house from rabbit antiserum (5µg/ml) in PBS (1x)/BSA (0.5%) overnight at 4°C. Controls included PBS (1x)/BSA (0.5%) alone and antibody pre-incubated with CTR (1mg/ml) antigen. After incubation, the cells were washed three times in PBS (1x), and peroxidase blocked by immersion in H_2O_2 (3%) / methanol for 30 min followed by 10 min of washing in PBS (1x). Cells were incubated in goat anti-rabbit IgG-HRP (1/100)/BSA (0.5%)/PBS (1x) for 1 hr at room temperature and washed in PBS (1x) for an additional three times. Cells were immune-stained with the DAB substrate (Dako liquid substrate chromogen system) and washed in dH_2O. Cells were counter-stained with haematoxylin for 2 min and rinsed in running H_2O.

2.7 Osteoclast Survival Assay

Osteoclasts were generated *in vitro* from bone marrow in 10 cm diameter petri dishes in α-MEM/FBS media supplemented with RANKL (100 ng/ml), M-CSF (30 ng/ml). On day 3, the media, RANKL and M-CSF were changed. Generally from day 4, the presence of many large osteoclasts was observed. Osteoclast numbers were estimated by field counting before they were harvested. The cultures were washed three times in PBS (1x) and proprietary Sigma Dissociation Buffer (5ml) (Sigma) was added to the cultures. The cells were incubated in the Dissociation Buffer for 30 minutes at 37°C. Cells were then very gently scrapped with a tissue culture cell scraper (Falcon) and centrifuged at 1,000 rpm for 2 mins. The cells were then seeded at various densities (e.g., usually 100 estimated osteoclast numbers per well) in 6 mm diameter wells in α-MEM/FBS with or without RANKL and test reagents. RANKL (100 ng/ml) is maximal for osteoclast survival and was used as positive control. The cultures were incubated at 37°C in 5 % CO_2 for 24hr and were then fixed with formaldehyde (4%). The osteoclasts were histochemically stained for TRAP. The number of osteoclasts survived per treatment group was counted under the microscope, with survival expressed as a proportion (%) relative to positive control.

2.8 Transient Transfection vATPase-d2 promoter-dependent Luciferase Constructs in RAW264.7 Cells

RAW264.7 cells were transiently transfected with the 'WT' vATPase-d2 promoter construct, which contains NFATc1, MEF2- and MITF-binding sites or a mutated M(M1− 3)vATPase-d2 promoter-driven firefly luciferase expression construct. The mutated construct contains mutations in the three MITF-binding sites rendering them non-functional (Figure 2.1). The NFATc1-, MEF2- and MITF- promoters were inserted at a 5′ prime site relative to a firefly luciferase coding region (Figure 2.1). Both constructs were kindly supplied by Prof. Jiake Xu (University of Western Australia, WA). After bacterial transformation, growth and midiprep purification of the two plasmids, transient transfection of RAW264.7 cells with the wt and mutant v-ATPase-d2 promoter were carried out using Lipofectamine LTX Plus Reagent (Life Technologies) according to manufacturer's instructions. RAW264.7 cells were seeded at 6 x10^4 the day prior to transfection to achieve 70-90% confluence at the time of transfection. The following day the Lipofectamine LTX Reagent was diluted in Opti-MEM media. In the presence of pRL *Renilla* luciferase construct (0.1μg/well) (Promega), the DNA, 'WT'

vATPase-d2 promoter driven firefly luciferase construct (0.2 μg/well) or the 'mutated' M (M1– 3)vATPase-d2 promoter-driven firefly luciferase expression construct (0.2 μg/well) was diluted in Opti-MEM media and PLUS reagent added. The diluted DNA was added to the diluted Lipofectamine LTX reagent in a 1:1 ratio and the solution incubated at room temperature for 5 minutes. The vATPase-d2 promoter construct and pRL *Renilla* luciferase construct/ Lipofectamine LTX lipid complexes were then added to the cells. The cells were incubated at 37°C and 5% CO_2 for 24 hours and viewed under the microscope before being treated with RANKL and/ or17-AAG (Chapter 2.9.2).

2.9 Luciferase Reporter Assays

2.9.1 NFAT and NFκB Luciferase Reporter Assays

Two reporter cell lines for luciferase assays were developed from RAW264.7 cells as described in Chapter 2.1.4.4 and 2.1.4.5. NFκB-RAW and NFAT-RAW cells (see section 2.1.4) were used to study the effect of 17-AAG treatment upon NFAT or NFκB transcriptional activity. NFκB-RAW and NFAT-RAW cells were seeded at in 6mm diameter culture wells at 4 x 10^4 cells and incubated overnight at 37°C before use. The following day the cells were treated with both a sub-maximal dose of RANKL (20ng/ml) and a higher concentration of RANKL (50ng/ml or 100ng/ml) for NFAT cells and NFκB cells, respectively. These cultures were treated with or without the addition of 17-AAG (200nM). To confirm the signalling is RANKL dependent and specific, the cells were treated with recombinant RANK-Fc (300ng/ml), which is a decoy receptor that specifically binds to RANKL. As negative controls, untreated cultures and a DMSO vehicle control treatments (1/1000 dilution) were included. TGF-β (5ng/ml), a known enhancer of NFATc1, was used as a positive control in NFAT-RAW reporter cells. Treatments were performed in triplicate cultures for all individual experiments. The cultures were, unless stated, treated for 24 hours. After washing in cold PBS (1x), the cells were lysed in passive lysis buffer (1x) (Promega) overnight at 4°C. Lysates were then transferred to a white flat bottomed 6mm diameter microplate wells (Corning, Lowell, MA, USA). Luciferase activity per well was read using an Envision Plate reader (Perkin Elmer) and proprietary Promega luciferase substrate

A.
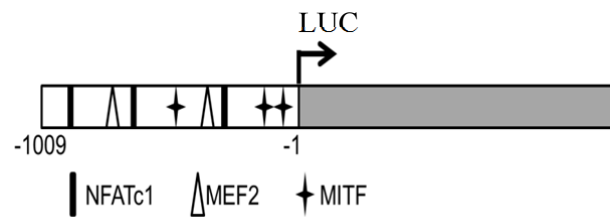
B.
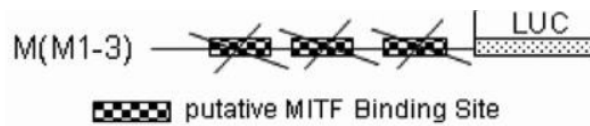
Figure 2.1 Diagram of the vATPase-d2 Construct
(A.) Diagram of the 1kb-vATPase-d2 construct showing the structure of the 'WT' vATPase-d2 promoter construct with its transcription factor binding domains for NFATc1-, MEF2- and MITF-binding sites. In addition the luciferase coding region (grey) is also depicted. **(B.)** The mutated M(M1– 3)vATPase-d2 promoter-driven firefly luciferase expression construct is shown. This construct contains mutations in the three MITF-binding sites rendering them non-functional. Image was sourced from (Feng *et al.*, 2009).

(Luciferin; 50 µl/well). The Luciferase substrate (Promega) was injected automatically by the Envision machine and after 2 sec delay the signal was accumulated for a further 2 sec. Background was virtually zero, typical readings were above 50,000 light units for a strong stimulus such as RANKL. Data was presented as normalised to untreated control cultures within the experiment.

2.9.2 vATPase-d2 Luciferase Reporter Assays

To test the effects of 17-AAG upon MITF target gene, v-ATPase-d2, RAW264.7 cells that were transiently co-transfected with a vATPase-d2 promoter driven firefly luciferase construct, and a transfection control pRL *Renilla* luciferase construct were used. The cells were treated 24 hours post transfection. First the cells were washed with PBS (1x) and fresh α-MEM/FBS (200µl) added. Cells were then treated with RANKL and or 17-AAG. Both untreated and DMSO vehicle control treatments (1/10,000 DMSO) were included as negative controls, as specified. After 24hr or 48 hr, as indicated, the cells were lysed in passive lysis buffer (1x) (Promega) and levels of luciferase and Renilla luciferase determined using Luciferase substrate and Stop and Glo® reagent (Promega), respectively (according to the manufacturers' instructions). The luciferase light emissions were measured using the EnVision plate reader (Perkin Elmer), which was described in the previous section. To confirm that the increased vATPase-d2 transcriptional activity was a result of MITF activation, the 'mutant' M(M1– 3)vATPase-d2 promoter-driven firefly luciferase expression construct was used. This construct, which is the same as the 'WT' construct except for engineered mutations in the three MITF binding sites that renders them non-functional was transiently transfected as described in Chapter 2.8 into RAW264.7 cells. RAW264.7 cells were transfected with the WT or mutant vATPase-d2 promoter driven firefly luciferase construct (in addition to pRL) alongside each other. Twenty-four hours after transfection, these cells were treated with 17-AAG (0.5 or 1µM) for 24 hours. As a negative control, untreated cultures were used. The cells were then lysed and luciferase quantified according to the method in Chapter 2.9.1.

2.10 HEK-HSE Based Cell Stress Assays

HEK-HSE cells generated by Dr Chau Nguyen as described earlier (Chapter 2.1.4) were seeded at 2.5 x 10^4 cells/well in DMEM phenol-free media. The cells were allowed to settle for $\geq$ 3 hours then treated with chemotherapeutics (17-AAG, NVP-AUY922, cisplatin,

doxorubicin, bortezomib and MG132) or appropriate DMSO vehicle control (1/2000 DMSO). After treatment, the cells were incubated for 24 hours at 37°C and 5% CO_2. At 24 hours, a nuclear fluorescent stain Hoechst dye (10μg/ml) was added to the wells and the cells incubated at 37°C and 5% CO_2 for 15 minutes. The levels of mCherry were collected using the Arrayscan VTI High Content Screening instrument (Thermo Fischer Scientific), which is designed for high-capacity automated fluorescence imaging and quantitative analysis that can measure both fixed and live cells. Individual cells were identified by Hoechst nuclear staining (green filter), and cells were selected based on size and average intensity. Hoecsht "bright" cells > 600 arbitrary units (a measurement output from the machine), and cells that were smaller than 20μM were gated out. The DMSO vehicle control wells were selected as the reference wells for the mCherry levels (red filter) and mCherry levels were read (2μM radius around nucleus measured). Cells that had mCherry levels 2 standard deviations from the average were counted as positive. The percentage threshold of mCherry levels for each treatment group was measured against the reference wells. Eight images were taken per well and the intensities averaged.

2.11 Cell Lysate Preparation for Western Blotting

RAW264.7 cell lysates were prepared in modified radioimmunoprecipitation assay (RIPA) buffer (Appendix A). EDTA free Complete Protease Inhibitors (Halt; Thermo Fisher Scientific, Rockford, IL, USA) and Phosphatase inhibitors (Roche) were added prior to lysing cells. Culture media was aspirated off the cells and the plates were placed directly onto ice. The cells were rinsed with ice cold PBS (1x), which was removed by aspiration. Ice-cold RIPA buffer (up to 150μl) was added to the cells and the adherent cells were scraped off. The cells were transferred to a fresh eppendorf tube on ice. The cell lysates were left on ice for 10 min and were sonicated in a water bath sonicator, containing ice, for 15 minutes. The cell lysates were then centrifuged at 4° C for 15 min at 10,000 x g.

For detection of protein phosphorylation, cell lysates were prepared in a slightly altered manner After the cells were lysed in RIPA buffer, supplemented with protease and phosphatase inhibitors, on ice for 10 minutes, the lysates were passed through a 19 gauge needle five times to homogenize the lysates. After homogenization, the lysates were then centrifuged at 4° C for 15 min at 10,000 x g.

Protein concentrations were determined the by BCA protein assay (Pierce) as per the manufacturer's instructions (Pierce, Rockford, IL, USA). BSA standards (125, 250, 500, 750, 1000, 1500, and 2000μg/ml) and a blank (i.e., RIPA buffer alone) used as a negative control, were prepared according to manufacturer's instructions. For the assay, BSA standards (10μl) and the blank (10μl) were pipetted into 6mm diameter wells in 96 well plates. For the unknown protein samples, protein (2μl) was diluted into RIPA buffer (8μl) for a 1/5 dilution. The working protein detection reagent (200μl) was prepared according to manufacturer's instructions and added to each of the wells. The plates were mixed gently on a plate shaker followed by incubation at 37°C and 5% CO_2 for 30 minutes. The plates were then let to cool to room temperature as per manufacturer's instructions. The optical density of the samples were measured at 560nM using a Tecan Mallagen plate reader using Mallagen version 6.3 software. A standard curve was plotted by graphing the average blank corrected 560nm measurement for each BSA standard vs. its concentration on the x axis. As per the Pierce kit recommendation a Polynomial curve (over 2 orders of magnitude) was used rather than a linear fit due to the curve-fitting algorithms associated with a microplate reader. The standard curve was used to determine the protein concentration of each unknown sample.

2.12 Protein Preparation for Western Blotting

Protein (30μg) was pipetted into a new eppendorf, and a final concentration of 1x reducing agent and 1x sample buffer was added. The contents were collected by brief centrifugation and afterwards were boiled at 95° C for 5 minutes. The eppendorf tubes containing the reduced and boiled protein were then placed on ice for at least one minute, and the contents were collected again by brief centrifugation. The samples were then ready for loading onto the SDS-PAGE gel.

2.13 Western Blot Analysis of Lysed Cell Samples

For immunoblotting, each reduced protein sample (30μg) was loaded onto the 4-12% Bis-Tris gradient SDS-page gels. SDS-PAGE gels were run under reducing conditions at 150V (constant) and typically 400mA current for 60 minutes. Proteins were transferred to polyvinylidene difluoride (PVDF) membranes using a wet transfer system with Novex buffer (25x) (Appendix A). Protein was transferred at 90V (constant), 300mA for 2 hours at 4°C. After the transfer the membranes were blocked with skim milk (3%) in TBST (1x, pH7.4) (Appendix A) for 1 hr at room temperature to prevent non-specific binding. The membranes

were incubated with the appropriate primary antibodies at 4°C overnight in TBST (1 x)/ skim milk (3%). The membrane was then rinsed three times in TBST (1x) for 10 minutes each before being incubated with the appropriate secondary antibody, usually anti-goat or anti-mouse IgG horseradish peroxidase (HRP)–conjugated antibodies for 1 hr at room temperature. The membranes were again washed three times for ten minutes each in TBST (1x). To detect the HRP signal, the Roche Lumilight detection system (Roche) was used according to manufacturer's instructions. Film (Amersham or Fuji) was used to capture the signal.

2.14 Isolation of Total RNA

Cells (10^4 in 35mm diameter wells) were incubated overnight (37°C and 5 CO_2) followed by treatment with experimental reagents. At designated time points, the media and the treatments were aspirated off the cells, and the cells washed once in PBS (1x). RNA extraction was achieved by use of the Quigen RNeasy Mini Kit (cat no.74104) according to manufactures instructions

Briefly, the cells were lysed by adding RLT lysis buffer (300μl) to each well. The cells were then scraped with a sterile cell scraper, and the cells from the duplicate wells were collected into a sterile autoclaved eppendorf. The lysed cells were homogenized and one volume of 70% ethanol (600μl) was added to the homogenized lysate. Each sample (700μl) including precipitate was added to an RNeasy spin column. Cells were then centrifuged at 8,000x g for 15 seconds followed by RW1 washing buffer (700μl) being added to the spin column to wash the membrane-bound RNA. After re-centrifugation the membrane was washed using RPE Buffer (500μl), which removes the remaining traces of salts and the spin column and was re-centriguged. To elute the RNA, RNase-free water (30μl) was added directly onto the spin column's membrane and the tube centrifuged. The concentrations of the samples were measured using NanoDrop™ spectrophotometer (Thermo Fischer Scientific). The RNA was stored at -80°C until use. When isolating RNA for RNA-seq, an additional DNase treatment step was used (described below), as the technique is sensitive to very small amounts of genomic DNA.

2.14.1 DNase Treatment of RNA

On-column DNase digestion was done using the RNase-free DNase Set (Qiagen) as per manufacturer's instructions. Follow the RNA extraction procedure as above up to the step where the cell lysate:ethanol solution (700μl) was transferred to a RNeasy spin column. Then add RW1 wash buffer (350μl). Centrifuge the RNeasy spin column at 8,000 x g for 15 seconds before preparing the DNase treatment. To prepare the DNase treatment, DNase I stock solution (10μl) and Buffer RDD (70μl) were combined and mixed by inverting the tubes For each sample, the DNase I incubation mix (80μl) was added directly to the RNeasy spin column membrane and was incubated at room temperature (20-30°C) for 15 minutes. The remaining RW1 buffer (350 μl) was added to the RNeasy spin column, which was then centrifuged for 15 seconds at 8,000 x g. The RNA extraction process was then completed following the manufacturer's instructions as described above.

2.15 Quantitative Reverse Transcription Polymerase Chain Reaction (qRT-PCR)

2.15.1 Oligonucleotide Primer Preparation

Oligonucleotide primer sequences were designed or obtained that spanned exon-intron boundaries to avoid amplification of genomic DNA (gDNA). In addition, the primers were checked for GC ratios, melting temperatures and length (18-20-mers). The chosen primers were also analyzed for: self-dimer, heterodimer, hairpins GC content and mismatched melting temperature through nucleotide BLAST software and oligo analyzer (Integrated DNA Technologies). Oligonucleotides were synthesized by either Sigma (Castle Hill, NSW, AUS) or Bioneer (Daejeon, Republic of Korea). The dried oligonucleotide pellet was resuspended in RNase free water to a stock concentration of 100μM. The sequences and accession numbers for the oligonucleotides used in these studies are listed in Table 2.1.

Table 2.1 qRT-PCR Oligonucleotides

Gene (Mouse)	Accession Number	Sequence 5′ to 3′prime
Cd74	NM_010545.3	F-CGCATGAAGCTTCCGAAATC R-GCCCAAGGAGCATGTTATCC
Oc-Stamp	NM_029021.1	F-TGGGCCTCCATATGACCTCGAGTAG R-TCAAAGGCTTGTAAATTGGAGGAGT
Atp6v0d2	NM_175406.3	F-AAGCCTTTGTTTGACGCTGT R-TTCGATGCCTCTGTGAGATG
Car2	NM_009801.4	F-GATAAAGCTGCGTCCAAGAGC R-GCATTGTCCTGAGAGTCATCAAA
Ccl9	NM_011338	F-CAACAGAGACAAAAGAAGTCCAGAG R-CTTGCTGATAAAGATGATGCCC
Il-1	NM_010554.4	F-AGTATCAGCAACGTCAAGCAA R-TCCAGATCATGGGTTATGGACTG
uPA (Plau)	NM_008873.3	F-GGTTCGCAGCCATCTACCAG R-TTCCTTCTTTGGGAGTTGAATGAA
Hrpt	<u>NM_013556.2</u>	F-TGATTAGCGATGATGAACCAG R-AGAGGGCCACAATGTGATG

2.15.2 Reverse Transcriptase (RT)

CDNA was prepared with the Superscript III Reverse Transcriptase Synthesis System for RT-PCR kit (Invitrogen), according to the company's protocol. Firstly, RNA was converted to first- strand cDNA by the following procedure. Components of the RNA/primer mix (Table 2.2) were centrifuged before use and combined in an autoclaved eppendorf tube. After these components were combined and gently mixed, the RNA/primer mix was incubated at 65°C for 5 min. The reaction was then cooled on ice. The cDNA synthesis mix was then prepared, see Table 2.3.

Table 2.2 RNA/Primer Mix

Component	Concentration
Total RNA	up to 5μg
Random hexamer primers	50ng
dNTP mix	10mM
DPEC H_2O	up to 10μl

2.15.3 First Strand cDNA Synthesis

The cDNA synthesis mix was prepared by adding each of these components in the indicated order.

Table 2.3 cDNA synthesis Mix

Component	Volume (μl)
10x RT buffer	2
25mM $MgCl_2$	4
0.1 M DTT	2
RNaseOUT^{TM} (40 U/μl)	1
Superscript^{TM} III RT (200U/μl)	1

cDNA synthesis mix (10 μl) was added to the RNA/primer mix and was pipetted gently to combine the reactants followed by brief centrifugation. The combined cDNA synthesis mixture was then incubated at 25°C for 10 minutes that was followed by a second incubation at 50°C for 50 minutes. The reaction was heat inactivated at 85°C for 5 minutes followed incubation on ice. The reactions were collected by centrifugation and RNase H (1μl as indicated by the kit) was added to the mixture to remove any remaining traces of RNA. Lastly the reactions were incubated at 37°C for 20 minutes. The cDNA was then diluted in DEPC water from the kit to a final cDNA concentration of 25ng/μl and stored at -20°C.

2.15.4 Quantitative RT-PCR

For qRT-PCR analysis, the components in Table 2.4 were added to make the PCR reaction mix. The mRNA expression levels were analysed from synthesized cDNA using the Mx3000P^{TM} Multiplex Quantitative PCR system (Stratagene, USA).

Table 2.4 qRT- PCR Reaction mix

Component	Volume (μl)
cDNA (25ng/μl)	3μl
SYBR Green Master Mix	10μl
Forward Primer (10μM)	0.8μl
Reverse Primer (10μM)	0.8μl
Betaine (10M)	2μl
dH$_2$O	3.5μl

Each reaction was subject to the following PCR conditions for 40 PCR cycles following an initial denaturing cycle at 95°C for 10 minutes.

Segment	Temperature (°C)	Time (sec)
1. Denaturing	95	10
2. Annealing	60	45
3. Polymerisation	72	45

The quantity of the gene was normalized to the quantity of HRPT, and the data were expressed as fold-induction relative to the calibrator (DMSO vehicle control unless noted "no treatment negative control' "ve"). Within each experiment, the samples were run in triplicate and 3 independent experiments (unless noted) using separate sets of samples were used. A 'no RT' (i.e., no cDNA) and H$_2$O control was run for each sample.

2.16 RNA Sequencing

RNA extracted from three independent replicate experiments of cultured RAW264.7 cells treated with or without 17-AAG (500nM) for 24 hours. The samples were then tested for RNA integrity before tRNA depletion. The libraries were then prepared and RNA sequencing (RNA-seq) performed (17 million reads per sample) using a Applied Biosystems SOLiD 5500/EZ Bead System at the Gandel Trust Sequencing Laboratory, Hudson Institute of Medical Research, Clayton, Vic. Initial analysis (first approach)(Figure 6.1) was performed using Cufflinks, Cuffdiff and Cubmerge software on BAM files. A second approach called the tuxedo protocol was used to decrease data noise and used Tophat software and cufflinks software (as above) to provide a transcriptional annotation list (Figure 6.1) (Trapnell *et al.*, 2012). Bam files were generated by Dr Ross Chapman (Centre for Innate Immunity and Infectious Diseases, Hudson Institute of Medical Research). Subsequent informatics analysis

on the data files was kindly performed by Dr Gholamreza Haffari and Milena Mitic (Dept of Information Technology, Monash University). See Chapter 6.2 and Figure 6.1 for a more detailed description of the analysis and a schematic.

2.17 Cloning of Plasmid Constructs

2.17.1 Cell Transformation

XL1-Blue subcloning-grade competent cells were thawed on ice and WT' vATPase-d2 promoter-driven expression luciferase construct or the mutated M(M1– 3)vATPase-d2 promoter-driven luciferase expression construct, DNA (40 ng) added. The tube was gently swirled to mix. The cells were incubated on ice for 20 min followed by a heat pulse in a 42°C water bath for 45 seconds to maximise the efficiency of transformation. The cells were then incubated on ice for 2 minutes and pre-heated super optimal broth with catabolic repression medium (SOC) (900 µl) (Appendix A) was added. The cells were incubated at 37°C for 30 min with shaking at 225-250 rotations per minute (rpm). The transformation mix (200µl) was plated onto L-broth (LB) agar plates containing ampillicin (100 µg/ml), which were then incubated at 37°C overnight.

2.17.2. DNA Plasmid Purification and Extraction

To generate a starter culture, single colonies from DNA glycerol stock streaked plates or from a transformed bacteria-DNA plate were picked and used to inoculate 5 ml of LB-broth (Appendix A) with ampicillin (100 µg/ml). These cultures were left for a maximum of 8 hr at 37°C with vigorous shaking, approximately 250rpm. A region without evident colonies was picked and treated the same as the sample as a negative control for the bacterial growth.

To purify DNA for transfection a plasmid preparation Midi-prep kit (Qiagen) was used. Medium colonies were prepared prior to the commencement of the Midi-prep. The starter culture was diluted by 1/50 in LB medium (Appendix A) with ampicillin (100 ug/ml) and grown at 37°C overnight with shaking at 250 rpm. The DNA was purified according to the manufacturer's instructions (midi-prep kit). Briefly, the bacterial cells were centrifuged at 4°C at 6000 x g for 15 min and the pellet resuspend in the kit P1 Buffer. Kit buffer P2 was added and the cells lysed at room temperature for 5 min. The lysates was precipitated with cold P3 kit buffer. The nucleic acids were then purified by centrifugation by putting the

supernatant through a calibrated resin filter. The extracted DNA was eluted and precipitated by the addition of isopropanol. The DNA was centrifuged at 15,000 x g for 30 min at 4°C, washed with 70% ethanol and re-centrifuged for an additional minute. The DNA was dissolved in TE buffer (Appendix A), and the DNA concentration measured in ng/μl using a Nanodrop spectrophotometer (Thermo Fischer Scientific) and associated Nanodrop software.

2.18 Statistical Analysis

All data are presented as mean ± SEM of three independent experiments unless otherwise noted. Statistical analysis was performed on experiments by Student's t test t (pairwise comparison) or ANOVA (for multiple comparison, with Dunnett's *post hoc* test) which were done n=3. For all analyses, p value ≤ 0.05 was considered significant. All statistical analyses were performed using GraphPad Prism 6 software (La Jolla, CA, USA).

Chapter 3
The Influence of HSP90 Inhibitors upon Osteoclast Formation and RANKL/RANK-Dependent Transcription Factors

Chapter 3 The Influence of HSP90 Inhibitors upon Osteoclast Formation and RANKL/RANK-Dependent Transcription Factors

3.1 Introduction

Bone remodelling is a dynamic process involving bone resorption followed by the formation of new bone and is regulated by osteoblast and osteoclast differentiation (Crockett *et al.*, 2011; Raggatt and Partridge, 2010; Boyle *et al.*, 2003; Katagiri and Takahashi, 2002). Osteoclastogenesis depends on the stimulation of osteoclast precursor cells to survive by M-CSF and to differentiate by RANKL stimulation (Boyle *et al.*, 2003; Feng, 2005). Both RANKL and M-CSF are generated *in vivo* by local stromal cells, osteoblasts and osteocytes (Boyle *et al.*, 2003). Genetically-modified mouse strains deficient in either RANKL or M-CSF lack osteoclasts, confirming their central role in osteoclast biology (Lacey *et al.*, 1998; Li *et al.*, 2000; Marks, 1982; Wiktor-Jedrzejczak *et al.*, 1982). Furthermore, RANKL inhibition, through the administration of recombinant OPG or soluble recombinant RANK, reduces or eliminates osteoclasts in models of osteolysis, and reduces human pathological bone loss (Boyce and Xing, 2007; Chambers, 2000; Bezerra *et al.*, 2005; Zhang *et al.*, 2001; Roodman and Dougall, 2008).

RANKL binding to its receptor, RANK, causes the activation of downstream signalling pathways that induces the expression of osteoclast transcription genes, and the activation of signalling molecules, which are necessary for the differentiation and activation of osteoclasts (Feng, 2005; Boyle *et al.*, 2003). Amongst these transcription factors and signalling molecules are NFκB, NFATc1, c-FOS, MITF and p38 (Asagiri and Takayanagi, 2007; Mansky *et al.*, 2002a; Gohda *et al.*, 2005; Yamashita *et al.*, 2007; Boyle *et al.*, 2003; Raggatt and Partridge, 2010). Mice that lack these molecules are osteopetrotic and have increased bone mass (Del Fattore *et al.*, 2008; Asagiri and Takayanagi, 2007; Mansky *et al.*, 2002a; Gohda *et al.*, 2005; Yamashita *et al.*, 2007). In contrast, over-expression of these molecules generally increases osteoclast differentiation and resorptive activity (Matsumoto *et al.*, 2004; Yamashita *et al.*, 2007; Meadows *et al.*, 2007; Yu *et al.*, 2011). Therefore, the regulation of these important molecules is critical to determining the balance between osteoclast activity and osteoblast production of new bone (Boyle *et al.*, 2003). Increased bone resorption can result from increased osteoclastogenesis, and therefore this is a major point of control in bone metabolism. For example, inflammatory cytokines, IL-1, IL-11 and TNFα, affect

osteoclastogenesis through their direct actions upon osteoclast progenitors to potentiate RANKL signals or by their regulation of RANKL expression by osteoblasts (Gupta and Massagué, 2006; Mundy, 2002; Weitzmann, 2013; Kim *et al.*, 2005a; Bezerra *et al.*, 2005). Many other pathological conditions including cancers, which metastasize to bone utilize the bone microenvironment and affect the differentiation pathway of the bone cells (Gupta and Massagué, 2006).

The HSP90 molecule is a molecular chaperone that acts to stabilize cells, including bone cells, undergoing stress thereby allowing cell viability (Subbarao Sreedhar *et al.*, 2004; Lindquist, 1986; Li and Buchner, 2013b). The expression of this molecule is increased in many cancers and its over-expression is directly correlated to poor prognosis (Cheng *et al.*, 2012; Koga *et al.*, 2009; Kamal *et al.*, 2004). As a result the HSP90 molecule has been targeted to inhibit for cancer treatment (Drysdale and Brough, 2008; Neckers, 2002; Chiosis, 2006a; Powers and Workman, 2007). Price *et al.* previously described the effects of HSP90 inhibitor, 17-AAG, upon bone loss and osteoclast formation (Price *et al.*, 2005). When studying the effects of 17-AAG, upon metastasis bone disease, Price *et al.* discovered 17-AAG significantly increased cancer growth in bone in an intracardiac MDA-MB-231 inoculation model though its pro-osteolytic activity (Price *et al.*, 2005). 17-AAG treatment stimulated osteoclast formation *in vivo* and *in vitro*, causing a concomitant increase in osteoclast numbers, and decreased total trabecular bone mass in tumour naïve mice (Price *et al.*, 2005). In contrast, 17-AAG did not affect osteoblast differentiation (Price *et al.*, 2005). Similarly Yano *et al*. found that 17-AAG also increased osteoclast numbers (Yano *et al.*, 2008). 17-AAG's ability to increase osteoclast formation through HSP90 inhibition raised many questions as to the mechanism by which it acts. The work in this chapter addresses how 17-AAG affects osteoclasts. Firstly by characterising 17-AAG effects upon osteoclast differentiation, and secondly by investigating the influence of HSP90 inhibition on RANKL-dependent signalling pathways. In addition, other N-terminal HSP90 inhibitors have been more recently developed including CCT018159 and NVP-AUY922, and their effects upon osteoclastogenesis were studied. NVP-AUY922 is currently undergoing phase I and II clinical trials in non-small lung cancer, lymphoma, stomach and esophageal neoplasms, making it of importance to study (Cheung *et al.*, 2005; Eccles *et al.*, 2008; Sharp *et al.*, 2007a; National Institute of Health, 2014). The results point to a novel mechanism of control of osteoclast formation that may underlie the higher bone loss and indirectly the increased tumour growth in bone seen in 17-AAG treated mice (Price *et al.*, 2005).

3.2 Results

3.2.1 RANKL Drives Osteoclast Formation from Bone Marrow Cells and RAW264.7 Cells

As discussed above, osteoclast differentiation is a multi-step process that involves recruitment, proliferation and differentiation of haematopoietic myeloid progenitor cells into mature and active osteoclasts (Boyle *et al.*, 2003). Committed or specific precursors of osteoclasts have yet to be identified, but osteoclasts can be readily generated from proliferating progenitors that also form macrophages or dendritic cells i.e., monocyte and macrophage lineage (Scheven *et al.*, 1986; Ash *et al.*, 1980; Akagawa *et al.*, 1996). These progenitor cells reside in the bone marrow (BM), spleen, peripheral blood and any tissue containing immature macrophage populations (Quinn *et al.*, 1998; Quinn *et al.*, 1997). Two models, bone marrow cells and the RAW264.7 cell line, are used throughout this thesis to study the effects of compounds upon osteoclastogenesis. These two models and their responses to RANKL and M-CSF to differentiate into mature and active osteoclasts are described below.

3.2.1.1 RAW264.7 Cells

The RAW264.7 cells were used to study osteoclast differentiation as they are a well characterized and accepted model of osteoclast formation (Collin-Osdoby *et al.*, 2003; Battaglino *et al.*, 2004; Matsumoto *et al.*, 2004; Matsuo *et al.*, 2004; Liu *et al.*, 2003). Furthermore, RAW264.7 cells have a similar signalling pathway profile to that of osteoclasts, making them an appropriate model to use to study osteoclastogenesis. (Collin-Osdoby *et al.*, 2003).

To test the responses of this laboratory's RAW264.7 cells for RANKL-elicited osteoclast formation, the cells (between passages 3 and 15) were treated with RANKL (2, 5, 10, 20, 50 and 100ng/ml) in 6mm diameter wells for 6 days at an initial cell density of 10^4 cells. The RAW264.7 cells were not treated with M-CSF as they do not require M-CSF or any other growth factor to proliferate and survive in standard medium containing FBS. To quantify osteoclast formation, two markers were used: cells staining positive for TRAP and multinuclarity. In the absence of RANKL no TRAP staining was noted, although some cell fusion was evident. This appears to be a common occurrence in undifferentiated RAW264.7

RANKL Stimulates Osteoclast Formation in Cultured RAW264.7 Cells
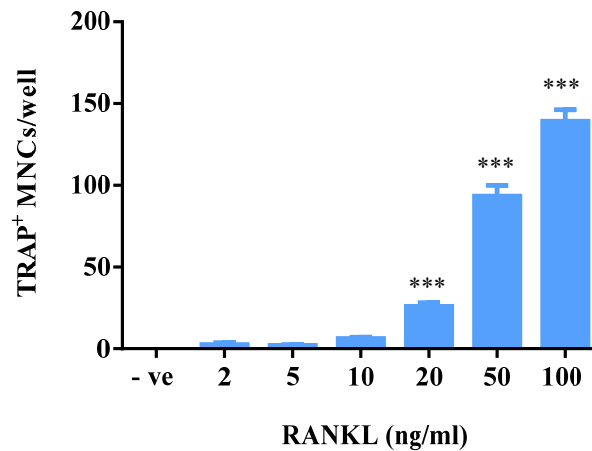
Figure 3.1

RAW264.7 cells were seeded at 10^4 cells in 6mm diameter wells. For all cultures, media and treatments were replaced on day 3. The cells were treated with a range of RANKL (2, 5, 10, 20, 50 and 100ng/ml) concentrations. Cultures untreated with RANKL were included as a negative control, which is denoted by "-ve". The cultures were performed in quadruplicate in each experiment. On day 6, the cells were fixed, permeabilized and histochemically stained for TRAP. Multinucleated and TRAP positive cells were counted as osteoclasts. RANKL 20, 50 and 100ng/ml all significantly drive osteoclast formation relative to the negative control. Data is expressed as mean ± SEM of four independent experiments. Statistical analysis was performed by ANOVA, Dunetts *post hoc* test ***p $\leq$ 0.001.

cells; however, without RANKL stimulation these multinucleated cells always lack TRAP expression (Figure 3.1). RANKL increased osteoclast formation in a dose dependent manner (Figure 3.1). Increased fusion was observed as the RANKL concentration increased. RANKL (20ng/ml), which is considered the submaximal dose for osteoclast differentiation generated relatively small numbers of TRAP positive multinucleated cells. While RANKL (100ng/ml), the maximal concentration resulted in the formation of many large multinucleated osteoclasts (Figure 3.1).

3.2.1.2 Bone Marrow Cells

As a source of osteoclast progenitors, bone marrow cells were isolated from the tibiae and femora of 8 to 14 week old, male C57Black/6 strain mice. These bone marrow cells were used as a source of fresh tissue for *in vitro* experiments unless otherwise indicated. The bone marrow cells differentiate into mature osteoclasts in the presence of M-CSF (30ng/ml), which allows for survival and immature macrophage (or macrophage progenitor) proliferation and maturation as previously described in Chapter 1.1.5. In the presence of M-CSF, RANKL stimulates the differentiation and the expression of osteoclast genes in these cells.

Bone marrow cells were seeded at a density of 10^5 cells per 6mm diameter culture well, which has previously been determined in our laboratory to be sufficient to yield good osteoclast formation within 6 days. The cells were cultured in the presence of M-CSF and RANKL (2, 5, 10, 20, 50 and 100ng/ml) for 6 days. No TRAP histochemical staining or and multinuclarity was observed in cultured cells with M-CSF treatment alone, indicating a complete lack of osteoclast commitment (Figure 3.2B). RANKL treatment caused osteoclast formation in a dose-dependent manner, as evident in TRAP positive multinucleated cells formed after 6 days of culture (Figure 3.2A-B). At concentrations below RANKL 5 ng/ml, few if any osteoclasts were seen; however, at RANKL 10ng/ml significant but highly variable numbers of mononuclear cells were seen with typically 4 or 5 bi- or tri-nucleate TRAP positive cells. As with the RAW264.7 cells, RANKL 20ng/ml caused formation of many osteoclasts but was a submaximal dose for their formation (Figure 3.2A-B.). RANKL (50 and 100ng/ml) treatment was maximal and resulted in large numbers of osteoclasts (Figure 3.2 A-B). In addition, the latter osteoclasts were morphologically large with many nuclei (Figure 3.2 B). Unless otherwise specified, RANKL doses 20ng/ml and 100ng/ml are throughout the thesis to show submaximal and maximal responses to compounds.

RANKL Stimulates Osteoclast Formation in Cultured Bone Marrow Cells

A.
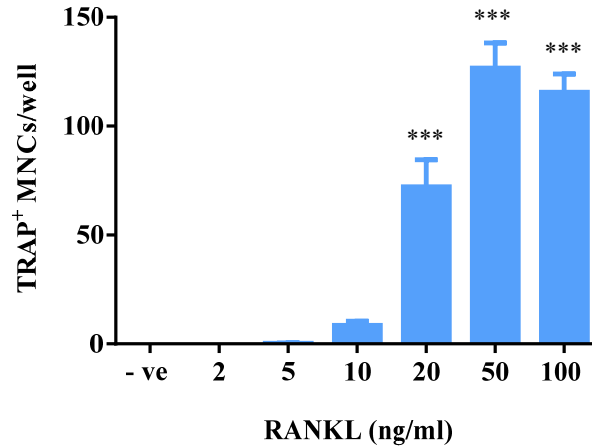
B.
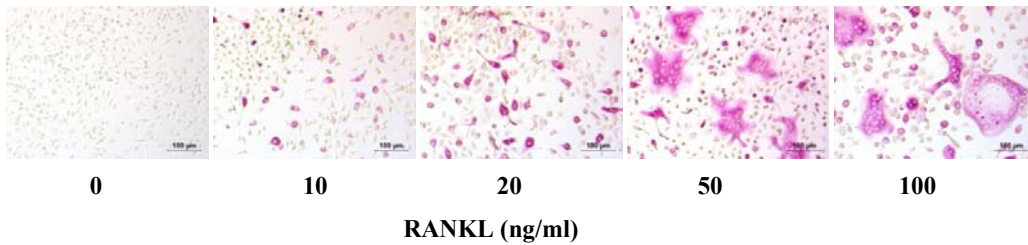
Figure 3.2

(A-B.) Bone marrow cells were seeded at 10^5 cells in 6mm diameter wells. The cells were treated with a range of RANKL (2, 5, 10, 20, 50 and 100ng/ml) concentrations. As a negative control, the cells were also left untreated, denoted "– ve". Treatments were performed in quadruplicates. For all cultures, media and treatments were replaced on day 3. On day 6, the cells were fixed in formaldehyde (4%), permeabilized and histochemically stained for TRAP. Multinucleated and TRAP positive cells were counted as osteoclasts. **(A.)** RANKL (20, 50 and 100ng/ml) all significantly drive osteoclast formation relative to the untreated negative control. **(B.)** Photomicrograph images of untreated and RANKL treated cells Scale bar- 100μM. The data is expressed as the mean ± SEM of three independent experiments. Statistical analysis was performed by ANOVA, Dunnett's *post hoc* test ***p ≤ 0.001.

3.2.2 The N-terminal HSP90 Inhibitor 17-AAG Increases Osteoclast Formation

17-AAG has previously been found to increase osteoclast formation both *in vitro* and *in vivo,* an action that can enhance cancer invasion and growth in the bone microenvironment (Price *et al.*, 2005; Yano *et al.*, 2006). To investigate HSP90 inhibition in osteoclast formation, first the effects of 17-AAG treatment upon osteoclastogenesis were confirmed. Secondly, 17-AAG effects were compared to those of the next generation HSP90 inhibitors CCT018159 and NVP-AUY922 (Eccles *et al.*, 2008; Sharp *et al.*, 2007b; Cheung *et al.*, 2005).

To determine the concentrations of 17-AAG that should be used to treat the RAW264.7 cells, firstly a range of 17-AAG concentrations were used to treat the cells (Appendix Figure B1). After days 1, 3 and 6, the cells were: stained with crystal violet, unbound crystal violet washed away, cell-bound stain eluted and the absorbance read at 560nM (Appendix Figure B1). Following 6 days of incubation, 17-AAG concentrations greater than 500nM were evidently toxic to the cells although the cell tolerated this concentration for shorter periods. Bone marrow macrophages were not tested as extensively, but they typically tolerated 17-AAG concentrations at about half that of RAW264.7 cells. Thus for most studies 17-AAG 200nM was the highest concentration employed.

To determine whether 17-AAG increases the formation of osteoclasts in RAW264.7 cells, RAW264.7 cells (10^4) were seeded in 6 mm diameter tissue culture wells and treated with RANKL (20ng/ml) and 17-AAG (50, 100, 200 and 500nM) and were allowed to differentiate. At day 6, the cells were fixed and histochemically stained for osteoclast marker TRAP, which is the most useful phenotypic marker due to the simplicity of its detection by histochemical stain in fixed and permeabilized cells. 17-AAG treatment significantly increased osteoclast formation in a dose dependent manner (Figure 3.3). Osteoclast numbers were greatest and morphologically the largest following treatment with 17-AAG 200nM (Figure 3.3). 17-AAG (500nM) caused significant cell death (data not shown). In order to confirm 17-AAG actions upon osteoclast formation, primary mouse bone marrow progenitor cells were isolated from the hind limbs of C57Black/6 mice. Bone marrow cells (10^5) were seeded in 6mm diameter tissue culture wells and stimulated with M-CSF (30ng/ml) and the sub-maximal concentration of RANKL (20ng/ml). The cells were then treated with 17-AAG (25, 50, and 100nM). 17-AAG treatment increased osteoclast formation over a 6 day period in a dose dependent manner (Figure 3.4 A.). The maximal response was observed at 17-AAG

17-AAG Increases RANKL Stimulated RAW264.7 Cell Osteoclast Formation

A.

B.
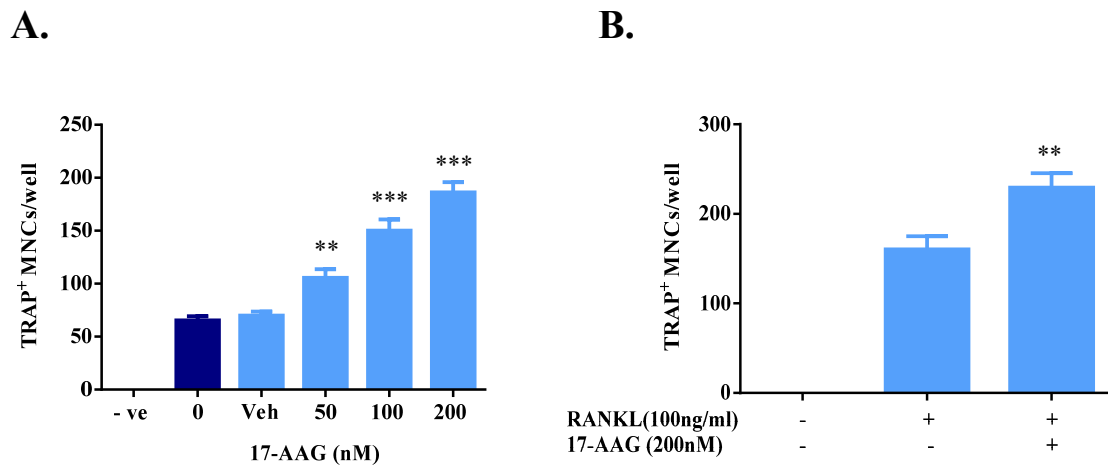
Figure 3.3

RAW264.7 cells were seeded at 10^4 cells onto 6mm diameter wells. **(A.)** The cells were treated with RANKL (20ng/ml) and 17-AAG (50, 100, 200 and 500nM) for 6 days. As a negative control the cells were also left untreated as signified by "-ve". The cells were also treated with RANKL (20ng/ml) alone ('0') or in the presence of vehicle DMSO (1/10,000) ('Veh'). **(B.)** The cells were treated with RANKL (100ng/ml) in the presence or absence of 17-AAG (200nM) for 6 days. **(A-B.)** On day 3 the media and treatments were replenished. On day 6, the cells were fixed and histochemically stained for TRAP. The multinucleated cells and TRAP stained cells were counted as osteoclasts. All treatments were performed in quadruplicate. **(A.)** 17-AAG significantly increased osteoclast formation in a dose dependent manner relative to the DMSO vehicle control. **(B.)** Co-treatment of RANKL and 17-AAG increased osteoclast formation above that of RANKL treatment alone. The data is shown as mean ± SEM of **(A.)** five and **(B.)** three independent experiments. Statistical analysis was performed by ANOVA, Dunnett's *post hoc* test. ** $p < 0.01$, *** $p < 0.001$.

(100nM) (Figure 3.4A). Bone marrow cells treated with 17-AAG 100nM also formed morphologically large osteoclasts, which indicate high rates of fusion (Figure 3.4B). Concentrations of 17-AAG 200nM and higher were toxic to the cells, with treatment causing much cell death (data not shown).

Although TRAP expression is an invariable feature of osteoclasts, activated macrophages can also express TRAP and are capable of fusion in long-term cultures. While TRAP expression was absent in all cultures where RANKL was not added (indicating that TRAP positive macrophages were not arising) it nevertheless cannot be ruled out that HSP90 inhibitors cause an increase in TRAP$^+$ macrophages. To rule out this possibility, use of another osteoclast marker is required. The calcitonin receptor (CTR) is regarded as a gold standard and highly specific marker for osteoclasts among the myelomonocytic lineage as it is not expressed by macrophages (Nicholson *et al.*, 1986). It is not widely used since it usually requires radiolabelled ligand binding methods that are specialised and cumbersome; however, our laboratory has developed and validated antibody based methods of CTR detection (Quinn *et al.*, 1999). Therefore to confirm that the 17-AAG mediated increase in TRAP positive multinucleated cells arising in the cultures described here are indeed *bona fide* osteoclasts, their CTR protein expression was examined. Multinucleated cells formed from bone marrow cells treated with 17-AAG (100nM), in the presence of RANKL (20ng/ml) and M-CSF (30ng/ml), all expressed CTR. In contrast, cells treated with the DMSO vehicle control did not (Figure 3.5). This confirms that the TRAP positive multinucleated cells thus formed were indeed osteoclasts. An antibody-antigen pre-absorption control confirmed that the stain was CTR specific (Figure. 3.5).

RANKL has several effects on osteoclast and macrophages aside from differentiation, including effects on survival and activity (pit formation). Thus to test if 17-AAG affected RANKL pro-survival effects, osteoclasts were generated *in vitro* from BMM in 10 cm diameter petri dishes in MEM/FBS supplemented with RANKL (100 ng/ml) and M-CSF (30 ng/ml). On day 3, the media, RANKL and M-CSF were changed. Osteoclast numbers were estimated by field counting before they were harvested with proprietary Sigma Dissociation Buffer (Sigma) in order to provide an approximate estimate of their number in suspension (their numbers and viability in suspension is not easy to measure). The cells were incubated in the Sigma Dissociation Buffer (Sigma) for 30 minutes at 37°C then gently scraped from

17-AAG Increases Bone Marrow Cell Osteoclastogenesis

A.

B.

Veh + RANKL 20ng/ml + M-CSF

17-AAG 100nM + RANKL 20ng/ml + M-CSF

Figure 3.4

(A-B.) Bone marrow cells were seeded at 10^5 cells in 6mm wells and stimulated with RANKL (20ng/ml) and M-CSF (30ng/ml). The cells were treated with 17-AAG (25, 50 and 100nM) for 6 days. As a negative control, the cells were not treated with RANKL, which is denoted by "-ve". The cells were also treated with RANKL and M-CSF treatment alone ('0') and a DMSO vehicle control ("Veh") in the presence of RANKL. On day 3 the media and treatments were replenished, and on day 6, the cells were fixed and histochemically stained for TRAP. Multinucleated cells and TRAP stained cells were counted as osteoclasts. **(A.)** 17-AAG treatment significantly increased RANKL/M-CSF stimulated bone marrow osteoclastogenesis in a dose dependent manner. **(B.)** Photomicrograph of "Veh" and RANKL+17-AAG treated cultures, showing the increased size and number of osteoclasts formed with 17-AAG treatment. Scale bar - 50μm. The data is shown as the mean ± SEM of 5 independent experiments. Statistical analysis was performed by ANOVA, Dunnett's post *hoc* test. *** $p \leq 0.001$.

17-AAG Treatment Increases Osteoclast Formation: Confirmation of CTR Expression

Veh + RANKL (20ng/ml) + M-CSF

17-AAG (100nM) + RANKL (20ng/ml) + M-CSF

Antibody Control: 17-AAG (100nM) + RANKL (20ng/ml) + M-CSF
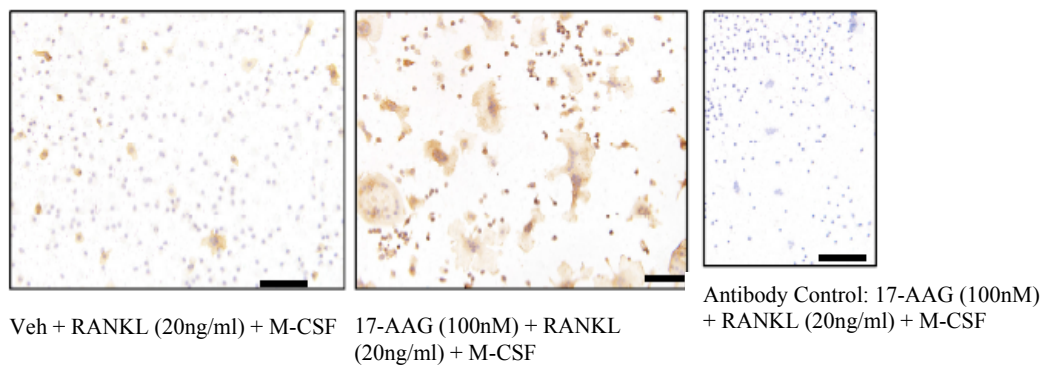
Figure 3.5

Bone marrow cells were seeded 10^5 onto 6mm diameter glass coverslips and stimulated with RANKL (20ng/ml) and M-CSF (30ng/ml). After 6 days incubation the cultures were dried, acetone fixed and then immunoperoxidase stained with purified anti-CTR antibody (5 µg/ml; left and centre panel). The cells were then counterstained with haematoxylin. As an immunostaining control the anti-CTR antibody was neutralized by antigen (CTR peptide 100 µg/ml; right panel) before incubation. 17-AAG treatment increased CTR positive cell numbers and size, which is consistent with the TRAP histochemical stain results. Scale bar-100µM.

the petri dish surface. The cells were then seeded at 100 'estimated' osteoclasts per well in 6 mm diameter wells in MEM/FBS with or without RANKL (20ng/ml and 100ng/ml) and 17-AAG (100nM). After 24 hours incubation, the cells were fixed with formaldehyde (4%) and the osteoclasts histochemically stained for TRAP. The number of osteoclasts that survived this period were counted under the microscope, with survival expressed as a proportion (%) relative to positive control, i.e., cultures treated with RANKL (100ng/ml). No osteoclast survival was observed in the absence of RANKL treatment after 24hrs of incubation while RANKL (100ng/ml) stimulus (in the absence of M-CSF) resulted in large numbers of TRAP$^+$ multinucleated cells surviving 24hrs (Figure 3.6). RANKL (20ng/ml) resulted in lower survival levels than RANKL (100ng/ml). Co-treatment of the cells with 17-AAG (100nM) was found to have no effect on the osteoclast survival effects of RANKL at any of these concentrations (Figure 3.6).

17-AAG does not Affect RANKL Pro-survival Effects upon Osteoclasts
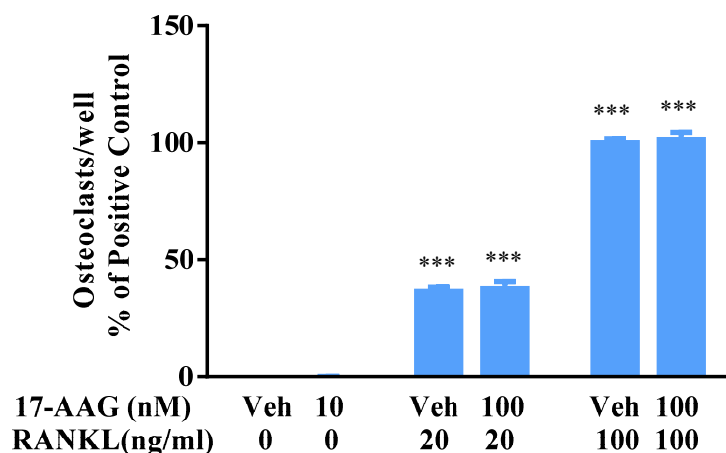
Figure 3.6

Osteoclasts were generated *in vitro* from bone marrow macrophages in 10 cm diameter petri dishes in MEM/FBS supplemented with RANKL (100 ng/ml) and M-CSF (30 ng/ml). Osteoclast numbers were estimated and then harvested with proprietary Sigma Dissociation Buffer (Sigma). The cells were then seeded at an estimated 100 osteoclast per 6 mm diameter well with or without RANKL (20ng/ml or 100ng/ml) and 17-AAG (100nM). After 24 hours incubation the cells were fixed, histochemically stained for TRAP and the surviving osteoclasts counted. The number of osteoclasts present (i.e., survived) was expressed as a proportion (%) relative to positive control RANKL (100ng/ml) treated cultures. No osteoclast survival was observed in the absence of RANKL treatment. RANKL (100ng/ml) stimulus in the absence of M-CSF resulted in large numbers of TRAP^{+} multinucleated cells surviving 24hrs. RANKL (20ng/ml) treatment resulted in lower survival levels than RANKL (100ng/ml) treatment. Co-treatment of the cells with 17-AAG had no effect on the osteoclast survival effects of RANKL. Experiments were performed with the help of Dr. Julian Quinn. All data is expressed as mean ± SEM of five independent experiments. Statistical analysis was performed by ANOVA, Dunnett's *post hoc* test; *** $p \leq 0.001$.

3.2.3 Next Generation HSP90 Inhibitors: CCT018159 and NVP-AUY922 Enhance Osteoclast Formation

The HSP90 inhibitor 17-AAG has a number of limitations as a cancer therapeutic including limited aqueous solubility, low oral bioavailability, metabolism by polymorphic enzymes and hepatoxicity (Egorin *et al.*, 2001; Kelland *et al.*, 1999; Pacey *et al.*, 2006; Egorin *et al.*, 1998; Guo *et al.*, 2005b; Goetz *et al.*, 2003; Goetz *et al.*, 2005). These limitations caused 17-AAG to be dropped from the clinic in 2008(National Institute of Health, 2014). However, due to the potential for inhibiting HSP90 in cancer cells, numerous other less toxic HSP90 inhibitors have been developed by rational drug design methods (National Institute of Health, 2014). Two N-terminal HSP90 inhibitors, CCT018159 and NVP-AUY922, have significantly better pharmokinetics than 17-AAG (Chiosis, 2006a; Eccles *et al.*, 2008; Sharp *et al.*, 2007b). These resorcylic pyrazole derivatives are structurally distinct from 17-AAG and are based on a purine scaffold; however, they bind to the same N-terminal ATP domain of HSP90 as 17-AAG. As they are binding the same molecular target as 17-AAG, the ability of these compounds to affect osteoclast formation was studied.

3.2.3.1 CCT018159

CCT08159, which was discovered by high throughput screening is a resorcinylic pyrazole derivative that has activity against HSP90 (Sharp *et al.*, 2007a; Cheung *et al.*, 2005). This compound has been shown to have anti-cancer activity inhibiting the proliferation of HCT116 human colon cancer cells (Sharp *et al.*, 2007b). To determine the concentrations of CCT018159 that could be tolerated by RAW264.7 cells over the 6 day culture period, kill curves were performed. RAW264.7 cells were treated with CCT018159 (0.2, 0.5, 1, 2, 5, 10, 20 and 50μM) for 1, 3 and 6 days. This demonstrated that concentrations of CCT018159 (5μM) and higher were toxic to the RAW264.7 cells over 6 days (Appendix Figure B1). RANKL (20ng/ml) stimulated RAW264.7 osteoclast differentiation assays were then performed and RAW264.7 cells treated with CCT018159 (0.2, 0.5, 1 and 2μM). CCT018159 treatment significantly increased osteoclast formation (Figure 3.7 A.). CCT018159 2μM caused the most significant increase in osteoclast formation and the derived osteoclasts were morphologically large due to cell fusion (Figure 3.8 B.). CCT018159 5μM caused extensive cell death after 6 days of culture, although this was not necessarily the case with shorter culture times. RAW264.7 cells that were treated with the maximal dose of RANKL (100ng/ml) and CCT018159 (2μM) increased osteoclast formation significantly compared with RANKL treatment alone (Figure 3.7 B.). To determine the effects of CCT018159 upon

osteoclast formation from primary mouse bone marrow cells were treated with CCT018159 (0.2, 0.5, 1, 2µM) in the presence of RANKL (20ng/ml) and M-CSF (30ng/ml). At day 6, the numbers of TRAP positive and multinucleated cells were counted. CCT018159 treatment significantly increased osteoclast numbers above DMSO vehicle control cultures in a dose-dependent manner (Figure 3.8 A.). Osteoclast numbers were significantly increased at all the CCT018159 concentrations tested (Fig. 3.8 A.).

3.2.3.2 NVP-AUY922

Due to low potency of CCT018159 HSP90 inhibition, further compounds were developed based on its chemical structure, including NVP-AUY922 (Sharp *et al.*, 2007b). NVP-AUY922 is a potent inhibitor being able to block HSP90 at nanomolar concentrations (Sharp *et al.*, 2007b) This resorcinylic isoxazole analog has been described as having much greater cellular activity than its pyrazole counterpart as a result of increased uptake and decreased half-life (Drysdale and Brough, 2008). Whilst not being structurally related to 17-AAG, NVP-AUY922 binds to same ATP binding pocket in the N- terminal to inhibit the binding of ATP and causes HSP90 to be in an ADP bound closed confirmation (Koga *et al.*, 2007; Goetz *et al.*, 2003). NVP-AUY922 (Table 1.1) NVP-AUY922 depletes HSP90 client proteins, has anti-tumour properties as single agent in vivo in a number of cell lines and has entered Phase I-II clinical trials for a number of cancers (Eccles *et al.*, 2008; National Institute of Health, 2014). Firstly, NVP-AUY922 concentration ranges were determined by kill curves (Appendix Figure B1). RAW264.7 cells were then stimulated with RANKL (20ng/ml) and treated with NVP-AUY922 (1, 2, 5 and 10nM) for 6 days. This compound also significantly increased osteoclast numbers in a dose-dependent manner in these cultures (Figure. 3.9). NVP-AUY922 (2, 5, 10nM) also significantly increased osteoclast formation in primary bone marrow cells stimulated with M-CSF (30ng/ml) and the submaximal concentration of RANKL (20ng/ml) relative to the DMSO vehicle control. Like treatment with 17-AAG and CCT918159, NVP-AUY922 treatment caused the formation of larger osteoclasts suggesting that these HSP90 inhibitors increase osteoclast fusion (Figure 3. 10 B). NVP-AUY922 treatment did not drive the formation of osteoclasts in the absence of RANKL.

CCT018159 Treatment Increases Osteoclast Formation in RAW264.7 Cells

A.

B.
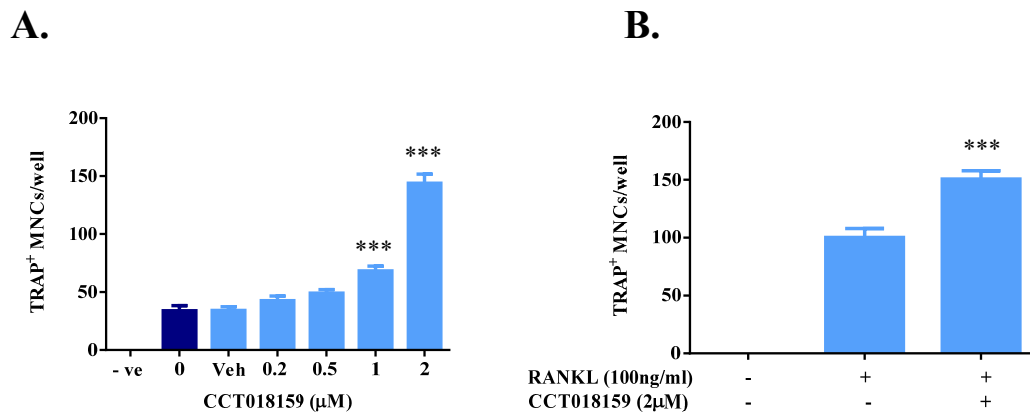
Figure 3.7

RAW264.7 cells were seeded at 10^4 cells in 6mm diameter wells. The cells were stimulated with **(A.)** RANKL (20ng/ml) and CCT018159 (0.2, 0.5, 1 and 2μM). according to the osteoclast assay protocol. Controls included, negative control ("-ve"), RANKL alone ("0") and DMSO vehicle ("Veh"), were also included **(B.)** The cells were treated with RANKL (100ng/ml) and CCT108159 (2μM). **(A-B.)** On day 6, cells were fixed and histochemically stained for TRAP. Cells that were TRAP positive and multinucleated were counted as osteoclasts **(A.)** CCT018159 treatment significantly increased osteoclast formation in a dose dependent manner relative to the DMSO vehicle control. **(B.)** The addition of CCT018159 to RANKL (100ng/ml) also significantly increased osteoclast formation. All data is expressed as mean ± SEM of **(A.)** three and **(B.)** five independent experiments. Statistical analysis was performed using **(A.)** ANOVA, Dunnett's *post hoc* test; ***$p \geq 0.001$ **(B.)** unpaired two tailed t test; ***$p < 0.001$.

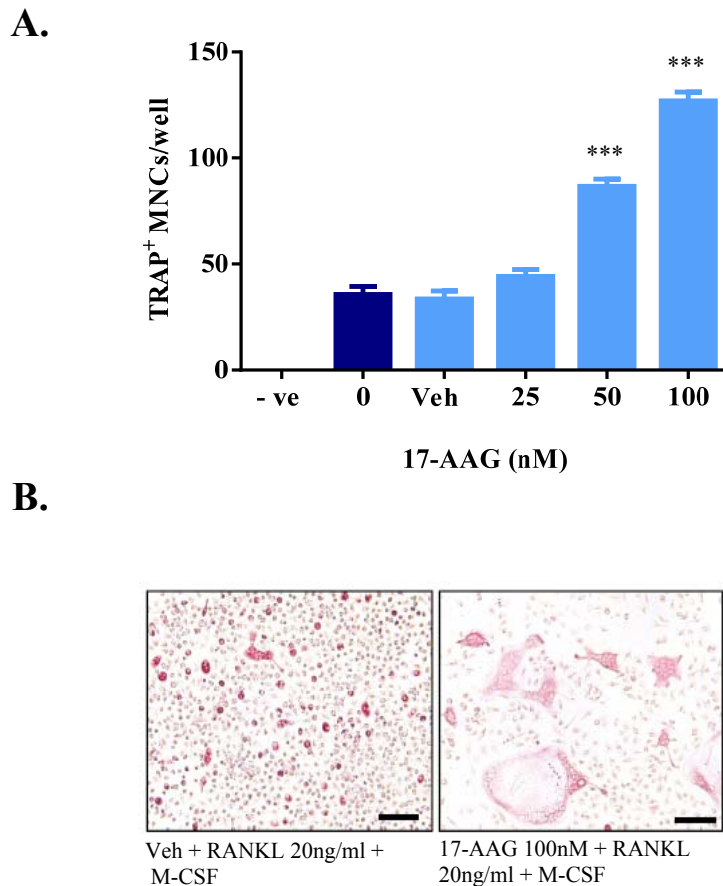# CCT018159 Treatment Increases Osteoclastogenesis in Bone Marrow Cells

A.

B.
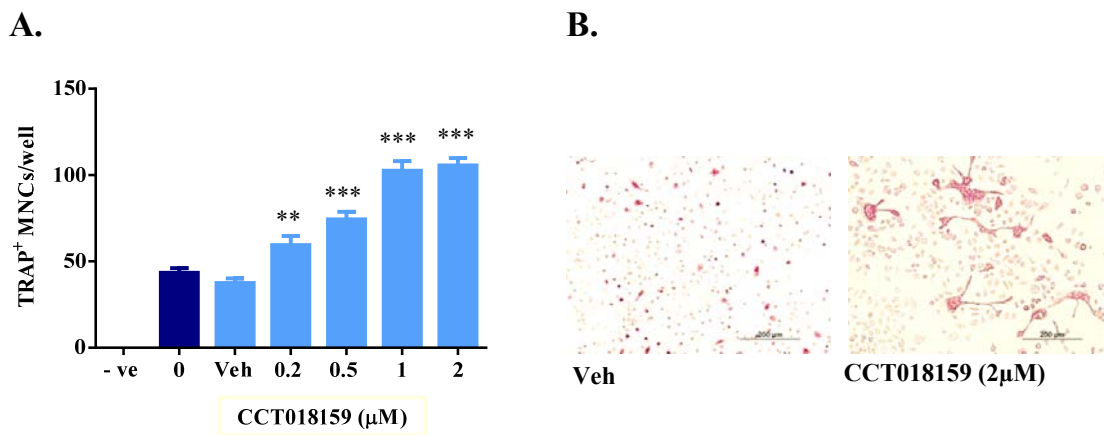
Figure 3.8

(A-B.) Bone marrow cells were seeded at 10^5 cells in 6mm wells and stimulated with RANKL (20ng/ml) and M-CSF (30ng/ml) to induce osteoclast differentiation. **(A-B.)** The cells were stimulated with RANKL (20ng/ml) and treated with CCT018159 (0.2, 0.5, 1 and 2μM) for 6 days according the osteoclast assay protocol. Controls include negative control ("-ve"), RANKL alone ("0") and DMSO vehicle ("Veh"), were included. All treatments were performed in quadruplicate. The cells were histochemically stained for TRAP on day 6 and multinucleated and TRAP positive cells were counted as osteoclasts. **(A.)** CCT018159 treatment significantly increased osteoclast formation in a dose dependent manner relative to the DMSO vehicle control. **(B.)** Photomicrographs of DMSO vehicle control and CCT018159 (2μM) treated cultures, the latter showing its mediated increase in osteoclast numbers. Scale bar - 200μM. The data is expressed as the mean ± SEM of five independent experiments. Statistical analysis was performed by ANOVA Dunnett's *post hoc* test; **p ≤0 .01, ***p ≤ 0.001.

NVP-AUY922 Enhances RANKL-mediated Osteoclast Formation in RAW264.7 Cells
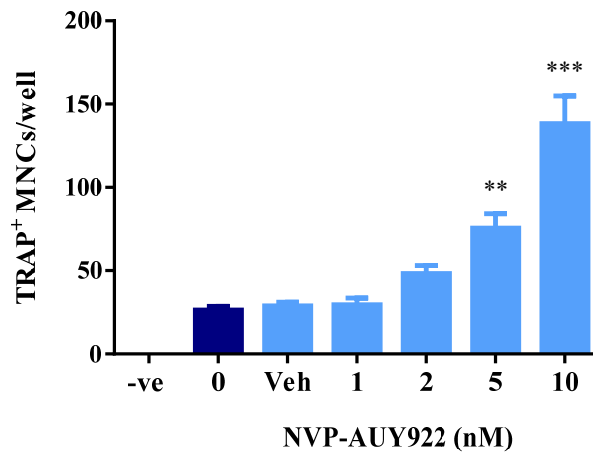
Figure 3.9

RAW264.7 cells were seeded at 10^4 cells in 6mm diameter wells in the presence of RANKL (20ng/ml). The cells were treated with NVP-AUY922 (1, 2, 5 and 10 nM) for 6 days and then fixed and histochemically stained for TRAP. Controls included negative control ("-ve"), RANKL alone ("0") and DMSO vehicle ("Veh"), were included. All treatments were performed in quadruplicate. NVP-AUY922 treatment significantly increased osteoclast formation relative to the DMSO vehicle control. The data is expressed as the mean ± SEM of three independent experiments. Statistical analysis was performed by ANOVA, Dunnett's *post hoc* test ** p ≤ 0.01, *** p ≤ 0.001.

NVP-AUY922 Enhances RANKL-mediated Osteoclast Formation in Bone Marrow Cells

A.

B.
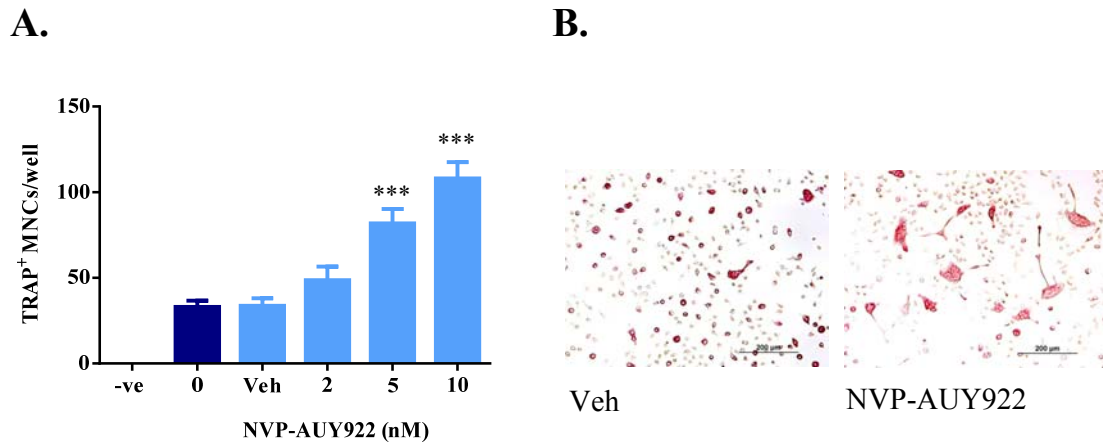
Figure 3.10

RAW264.7 cells were seeded at 10^5 cells in 6mm diameter wells in the presence of RANKL (20ng/ml) and M-CSF (30ng/ml). **(A.)** The cells were treated with NVP-AUY922 (1, 2, 5 and 10 nM). Controls included negative control ("-ve"), RANKL alone ("0") and DMSO vehicle ("Veh"), were included. On day 6, the cells were histochemically stained for TRAP. NVP-AUY922 significantly increased osteoclast formation relative to the DMSO vehicle control. **(B.)** Photomicrographs of DMSO vehicle control and NVP-AUY922 (10nM) treated cultures. NVP-AUY922 increases the number and the size of osteoclasts, which have many nuclei. Scale bar-100μm. The data is shown as mean ± SEM of five independent experiments. Statistical analysis was performed by ANOVA, Dunnett's *post hoc* test. ******* $p \leq 0.001$.

This data shows that the tested N-terminal HSP90 inhibitors, which inhibit the ATPase region of the molecule, all significantly increased RANKL-mediated osteoclast formation in both primary bone marrow and RAW264.7 cell cultures. This data suggests that HSP90 inhibitors may increase osteoclast formation by enhancing RANKL differentiation signals, thereby increasing osteoclast precursor commitment to the osteoclast differentiation pathway. Stimulating osteoclast progenitors to differentiate thus increases osteoclast numbers. However, the mechanism of action of these HSP90 inhibitors is unclear, and is examined in the next section.

3.2.4 17-AAG and TGF-β Act through Different Mechanisms to Increase Osteoclast Differentiation

The cytokine TGF-β is a powerful enhancer of osteoclast formation (Figure 3.11) (Quinn *et al.*, 2001). Previous evidence suggests that TGF-β can enhance the effects of osteoclastogenic stimuli like RANKL and does so through actions early in the culture period (Quinn *et al.*, 2001). This early phase is characterised by cell proliferation commitment to the osteoclast lineage, whereas later phase (typically after day 3) is characterised by strong expression of osteoclast-associated genes at the protein level. Thus the previous data suggests that TGF-β influences the early stage commitment of progenitor cells (Quinn *et al.*, 2001). Since 17-AAG also enhances osteoclast formation, its actions were compared with those of TGF-β by the same approach. Therefore, the actions of these factors in the early and late phases of osteoclast formation were examined and compared.

Bone marrow cells, stimulated with RANKL (20ng/ml) and M-CSF (30ng/ml), were treated with **(A.)** TGF-β (5ng/ml) or 17-AAG (100nM) for: 0-3, 3-6 or 0-6 days. Both TGF-β and 17-AAG treatment for the whole period (day 0 to 6) had the expected strong effects since this is the same culture stimulation protocol as employed in previous studies (Figure 3.12). A significant increase in osteoclast formation was observed in cultures treated with TGF-β from day 0 to 3 but not in cultures treated with 17-AAG for this period (Figure 3.12). In contrast, TGF-β addition during days 3 to 6 had no effect on osteoclastogenesis; however, 17-AAG treatment during this period had a strong effect (Figure. 3.12). Thus, all of the effects of TGF-β on osteoclast differentiation were exerted early within the osteoclastogenesis process. While in contrast, 17-AAG actions are probably exerted later in the osteoclast differentiation process. This data suggests that the two factors have different mechanisms by which they increase osteoclastogenesis.

TGF-β Increases Osteoclast Formation in RANKL Treated RAW264.7 Cells
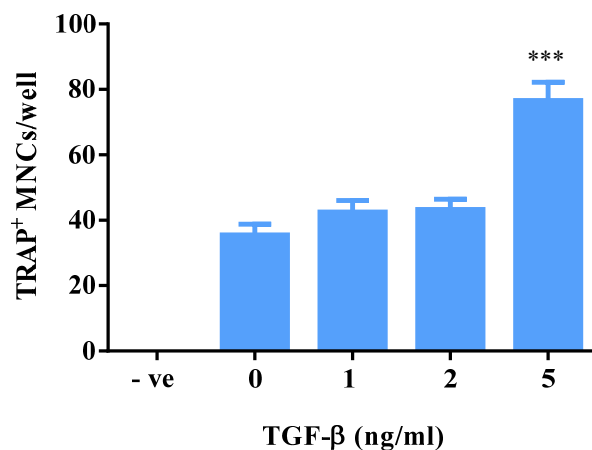
Figure 3.11

RAW264.7 cells were seeded at 10^4 cells in 6mm diameter wells. The cells were stimulated with RANKL (20ng/ml) and TGF-β (1, 2 or 5ng/ml) for 6 days and then stained for TRAP, according to the osteoclast and TRAP staining protocols, respectively. TGF-β (5ng/ml) treatment significantly increased osteoclast formation relative to the positive control. The data is shown as mean ± SEM of three independent experiments. Statistical analysis was performed by ANOVA, Dunnett's *post hoc* test ***$p \geq 0.001$.

TGF-β Acts Early whilst 17-AAG Acts Late During Osteoclastogenesis to Increase Osteoclast Formation

A.
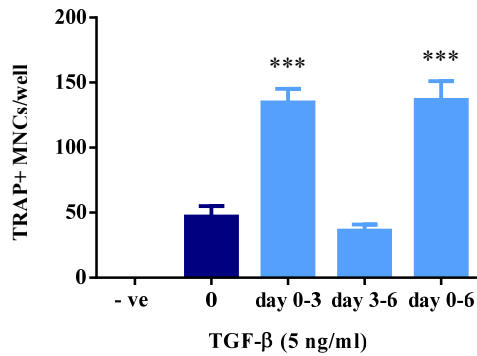
B.
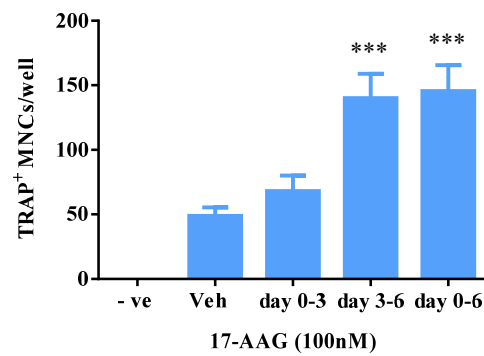
Figure 3.12

Bone marrow cells were seeded at 10^5 cells in 6mm diameter wells and were stimulated with RANKL (20ng/ml) and M-CSF (30ng/ml). Cells were also treated with **(A.)** TGF-β (5ng/ml) or **(B.)** 17-AAG (100nM), which were added for the indicated time periods: first half of the culture period ("day 0-3"), the second half of the culture period ("day 3-6") or for the whole culture period ("day 0-6"). As a negative control, the cells were left untreated as denoted by "-ve" or were treated with DMSO vehicle ("Veh"). TGF-β treatment significantly increased osteoclast formation when added in the first half of the culture period ("day 0-3") (or all the way through "day 0-6"), but its actions to increase osteoclastogenesis were not observed if it was added in the second half of the period ("day 3-6"). In contrast, **(B.)** 17-AAG treatment significantly increased osteoclast formation when added in the second half of the culture ("day 3-6") but not the first ("day 0-3"). The data is expressed as mean ± SEM of **(A.)** four and **(B.)** three independent experiments. Statistical analysis was performed using ANOVA, Dunnett's *post hoc* test ***$p \leq 0.001$.

3.2.5 The Effect of 17-AAG upon the Osteogenic Transcription Factors

When RANKL binds to the RANK receptor on the surface of the progenitor cells it sets into motion a cascade of signalling pathways, which activate transcription factors important within the osteoclast formation pathway (Chapter 1.5.3). These transcription factors including NFκB, NFATc1, AP-1 and MITF collectively and in cooperation with other unregulated transcription i.e. PU.1 drives the transcription of osteoclast-associated genes (Boyle *et al.*, 2003; Sharma *et al.*, 2007; Asagiri and Takayanagi, 2007). The transcribed osteoclast associated genes included: *Atp6v0d2, Apc5* (TRAP), Ctsk, *Oscar, integrin αvβ₃* (Boyle *et al.*, 2003; Asagiri and Takayanagi, 2007; Sharma *et al.*, 2007). These factors are also influenced by other signalling molecules elicited by RANKL stimulation such as p38 and JNK (Mansky *et al.*, 2002a; Matsumoto *et al.*, 2000). The strong enhancement of 17-AAG upon RANKL-dependent osteoclast formation suggests 17-AAG affects these RANKL-dependent signalling and transcription factors. Therefore, the effects of 17-AAG upon these transcription factors in the presence and absence of RANKL was examined in order to try to clarify how 17-AAG acts to increase osteoclast formation.

As described in Chapter 1.5.3.1, the transcription factor NFκB has an important role in regulating osteoclast formation, function, and survival (Soysa and Alles, 2009). The role of the p52/p50 dimer NF-κB in OC formation was discovered through knockout studies, which showed the double-knockout (dKO) of p50 and p52 in mice causes them to have severe osteopetrosis and no osteoclasts (Soysa and Alles, 2009; Boyce *et al.*, 2010). NFκB activation is one of the earliest events of RANK signalling (Takayanagi, 2008a; Kuroda and Matsuo, 2012). To determine whether 17-AAG affects NFκB transcriptional activity in RAW264.7 cells, RAW264.7 cells stably transfected with an NFκB-dependent luciferase reporter construct (a kind gift of Dr Jiake Xu, University of Western Australia) were employed. Note that this assay detects increased nuclear transcriptional activity of NFκB, not simply levels of activated NFκB. These transfected cells are termed RAW-NFκB cells for the remainder of this thesis. The assay is described in detail in Chapter 2.9.1, but briefly RAW-NFκB cells were treated with RANKL submaximal (20ng/ml) or maximal (100ng/ml) concentration in the presence or absence of 17-AAG (200nM) for 6 and 24 hours. In addition, these cells were also treated with 17-AAG (200nM) in the absence of RANKL. At 6 hours, RANKL (20ng/ml) treatment significantly increased NFκB dependent luciferase signals compared to the untreated control (Figure 3.13 A.). RANKL 20ng/ml and 17-AAG (200nM) combination treatment also increased NFκB luciferase levels to a similar degree showing the combination

treatment did not further increase NFκB transcriptional levels above that of RANKL treatment alone (Figure 3.13 A.). Treatment with 17-AAG (200nM) in the absence of RANKL did not affect the NFκB signal. The maximal RANKL concentration (100ng/ml) also increased NFκB activity relative to the untreated control at 6 hours. RANKL (100ng/ml) and 17-AAG (200nM) combination treatment also significantly increased NFκB transcriptional levels above that of the negative control but again did not enhance the RANKL-dependent signal (Figure 3.13 B.). Similar experiments were performed with RAW-NFκB cells for 24 hour treatment; however, only the maximal concentration of RANKL (100ng/ml) was used. The results were very similar. RANKL (100ng/ml) treatment alone and RANKL (100ng/ml) plus 17-AAG (200nM) combination treatment increased NFκB activity levels to a similar degree (Figure 3.14). 17-AAG 200nM treatment alone had no effect on NFκB (Figure 3.14). This data indicates that 17-AAG is unlikely to affect the activity of NFκB induced by RANKL. To show the specificity of the experiment, RANKL (100ng/ml) signalling was blocked by treating the cells with RANK-Fc (300ng/ml), a decoy receptor that binds only to RANKL. RANK-Fc (300ng/ml) treatment reduced NFκB levels to untreated control levels, showing that the increase in NFκB transcriptional activity is RANKL mediated (Figure 3.14).

A transcription factor essential to osteoclastogenesis and the commitment of cells to the osteoclast lineage is NFATc1. RANK signalling activates NFκB, p38 and AP-1, which along with oscillating levels of Ca^{2+} results in NFATc1 activation, nuclear translocation and transcription (Takayanagi *et al.*, 2002). Once activated, NFATc1 binds to its own promoter recruiting AP-1 (Hogan *et al.*, 2003; Zhao *et al.*, 2010). Together NFATc1 and AP-1 increases NFATc1 and NFATc2 mRNA expression as previously described (Chapter 1.5.3.4) (Zhao *et al.*, 2010; Hogan *et al.*, 2003). NFATc1 is often considered a master regulator of osteoclast formation as it is influenced by most of the different signalling networks involved in osteoclast formation including calcium and MAP Kinase dependent signals (Boyle *et al.*, 2003; Sharma *et al.*, 2007; Takayanagi, 2007a). Note that the NFAT family of transcription factors are constitutively phosphorylated leading to their degradation; however, RANKL signals increase their dephosphorylation thereby increasing their protein levels (as detected by immunoblotting). To study 17-AAG effects on NFATc1, the transcriptional activity and protein expression of NFATc1 was examined. RAW-NFAT cell, RAW264.7 cells stably transfected with a NFAT-dependent luciferase reporter construct that were previously

17-AAG does not Increase the Transcriptional Activity of NFκB at 6 hours in RAW264.7 Cells

A.

B.

RANKL (20ng/ml)	-ve	-	-	+	+
17-AAG (200nM)	-	Veh	+	-	+

RANKL (100ng/ml)	-ve	-	-	+	+
17-AAG (200nM)	-	Veh	+	-	+
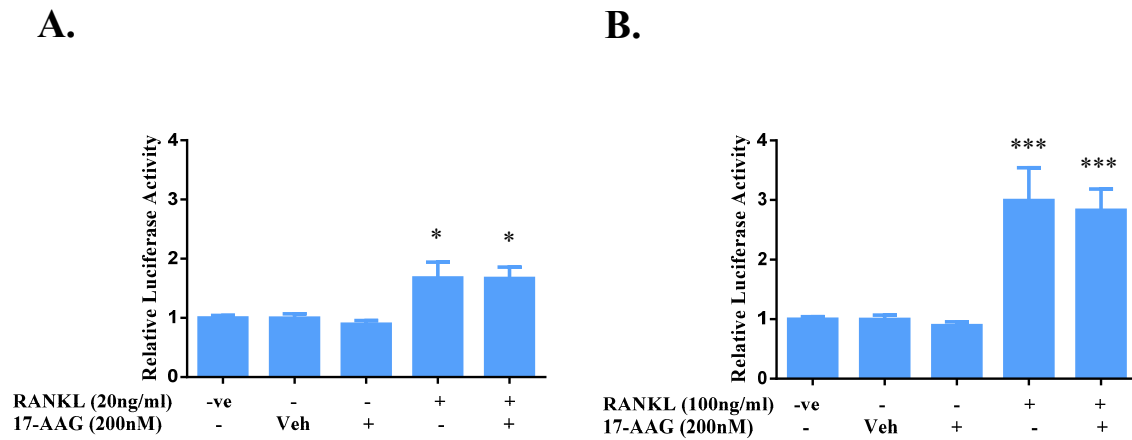
Figure 3.13

(A-B.) NFκB-RAW cells were seeded at 4 x 10^4 cells in 6mm diameter wells and were left to settle overnight. The following day, the cells were treated with **(A.)** RANKL (20ng/ml) or **(B.)**, RANKL (100ng/ml). **(A-B.)** The cultures were treated with or without 17-AAG (200nM) as indicated. Treatments were performed in triplicates. Cultures were treated for 6 hours before being lysed overnight in passive lysis buffer (1x) (Promega). The following day luciferase activity was determined by a luminometer. Both concentrations of RANKL significantly increased NFκB activity relative to the negative controls. Addition of 17-AAAG (200nM) to RANKL (20ng/ml and 100ng/ml) did not further increase NFκB activity, nor did 17-AAG treatment alone. Data was normalised against negative controls, "-ve" to which data from treated cultures was compared. Data is expressed as mean ± SEM of three independent experiments. Statistical analysis was performed using ANOVA, Dunnett's *post hoc* test * p ≤ 0.05, *** p ≤ 0.001.

17-AAG does not Increase the Transcriptional Activity of NFκB at 24 hours

Relative Luciferase Activity

17-AAG (nM)	0	Veh	200	0	200	200
RANKL (ng/ml)	-ve	0	0	100	100	100
RANKFc (ng/ml)	0	0	0	0	0	300
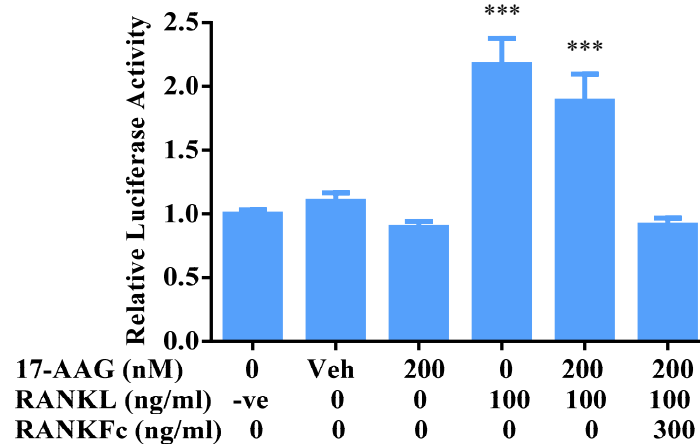
Figure 3.14

NFκB-RAW were seeded at 4 x 10^4 in 6mm diameter wells. The following day the cells were treated with RANKL (100ng/ml), 17-AAG (200nM) or combination treatment of RANKL (100ng/ml) + 17-AAG (200nM). Cells were also treated with RANK.Fc (300ng/ml) to show the NFκB induction is RANKL specific. Treatments were performed in triplicates. Cultures were treated for 24 hours before being lysed in passive lysis buffer (1x) (Promega) overnight and luciferase activity determined by luminometer. 17-AAG (200nM) treatment did not affect NFκB dependent transcriptional activity. RANKL (100ng/ml) significantly increased NFκB dependent transcriptional activity. Co-treatment of 17-AAG (200nM) and RANKL (20ng/ml) did not further increase the RANKL-induced activity. 17-AAG treatment alone did not affect NFκB activity. Data was normalised against the negative, "-ve", control to which the data was compared. Data is expressed as mean ± SEM of five independent experiments. Statistical analysis was performed by using ANOVA, Dunnett's *post hoc* test *** $p \leq 0.001$.

established in our laboratory by Dr Julian Quinn, were used (Singh *et al.*, 2012; van der Kraan *et al.*, 2013). Treating RAW-NFAT cells with RANKL (20ng/ml and 50ng/ml) significantly increased NFAT-dependent transcriptional activity at 24 hours in comparison to the untreated negative control (Figure 3.15). However, 17-AAG (200nM) treatment alone did not affect NFAT transcription at the 24 hour time point (Figure 3.15). Co-stimulation of RANKL (20ng/ml) and 17-AAG (200nM) did not enhance the RANKL-induced activity in this assay. Rather the NFAT activity levels were markedly reduced (Figure 3.15). RANKL (50ng/ml) and 17-AAG (200nM) co-stimulation treatment increased NFAT transcriptional activity above that of the untreated negative control, but the NFAT levels was reduced compared to RANKL (50ng/ml) treatment alone (Figure 3.15). To further characterize the fundamental differences between 17-AAG and TGF-β enhanced osteoclast formation, the RAW-NFAT cells were treated with TGF-β, which is a known stimulator of NFATc1. TGF-β (5ng/ml) significantly increased the transcriptional activity of NFAT compared to the untreated negative control cultures (Figure 3.16). This data further suggests that the mechanism whereby 17-AAG acts to increase osteoclastogenesis is different to TGF-β.

To further study the apparent lack of effects of 17-AAG upon NFATc1 activity, NFATc1 immunoblotting was performed on non-transfected RAW264.7 cells. NFATc1 levels were detected as three bands (the top two often merging into a single thick band) in the range 90 to 110kDa. A time course experiment (this was kindly performed by Dr Ryan Chai, Monash University) showed RANKL (50ng/ml) to increase NFATc1 protein expression in a time dependent manner from 8 to 24 hours (Figure 3.17). At 48 hours, NFATc1 protein levels were starting to drop in the RANKL treated samples but were still clearly higher than in the control (Figure 3.17). Co-treatment of 17-AAG (500nM) with RANKL (50ng/ml) increased NFATc1 protein levels at 8 to 24 hours, but protein levels were dampened compared to the RANKL (50ng/ml) stimulation alone (Figure 3.17). Treatment with 17-AAG (500nM) alone dose-dependently decreased NFATc1 protein levels (Figure 3.17). At 24 hrs there was only a small amount of NFATc1 protein detectable in the lysates and 48 hours of treatment further diminished NFATc1 protein levels (Figure 3.17). In summary, 17-AAG treatment has a negative effect on both NFAT transcriptional activity and protein levels of NFATc1. This would suggest 17-AAG might reduce osteoclast formation, rather than increases it from what is known in the literature regarding the importance of NFATc1 in osteoclastogenesis. This data shows that 17-AAG effects osteoclastogenesis are not exerted through NFATc1. In contrast, this data shows 17-AAG decreases NFATc1 levels. Another transcription factor that

17-AAG does not Increase NFAT-dependent Transcriptional Activity of the at 24 Hours
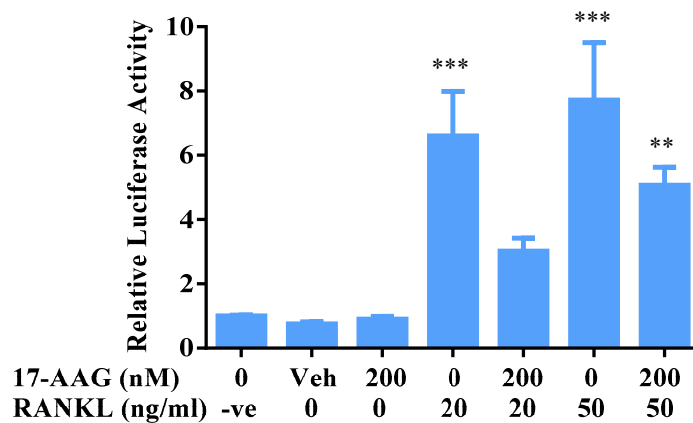
Figure 3.15

NFAT-RAW cells were seeded at 4×10^4 cells in 6mm diameter wells and left to settle overnight. The following day the cells were treated with RANKL (20ng/ml or 50ng/ml) in the presence or absence of 17-AAG (200nM) as indicated. The cells were treated for 24 hours before being lysed in passive lysis buffer (1x) (Promega) overnight at 4°C. The luciferase activity in the lysates was then determined by luminometer. At 24 hours both RANKL (20ng/ml) and RANKL (50ng/ml) significantly increased NFAT-dependent transcriptional activity. 17-AAG alone also did not induce activity. RANKL and 17-AAG co-treatment did not increase NFAT transcriptional activity above that of RANKL treatment alone but rather decreased it. Data was normalised against the negative control, "-ve" to which the data was compared. Data is expressed as mean ± SEM of five independent experiments. Statistical analysis was performed using ANOVA, Dunnett's *post hoc* test ** $p \leq 0.01$, *** $p \leq 0.001$.

TGF-β Increases NFAT Transcriptional Activity at 24 Hours in RAW264.7 Cells
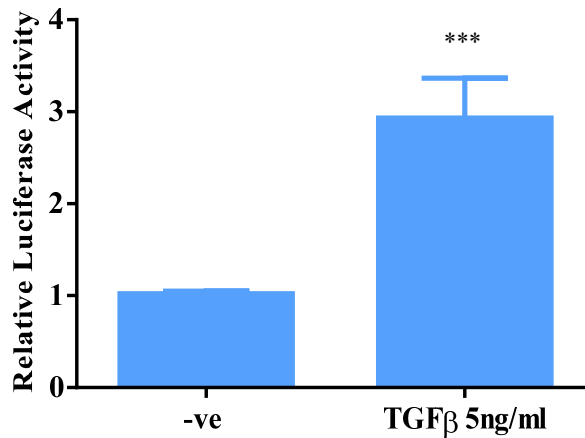
Figure 3.16

RAW-NFAT cells were seeded at 4 x 10^4 cells in 6mm diameter wells and were left to settle overnight. The following day the cells were treated for 24 hours with TGF-β (5ng/ml), a concentration that greatly enhances osteoclast formation. An untreated negative control, "-ve" was included. The cells were treated for 24 hours before being lysed overnight 4°C in passive lysis buffer (1x) (Promega). The luciferase activity in the RAW-NFAT cell lysates was determined using a luminometer. TGF-β (5ng/ml) treatment significantly increased NFAT-dependent transcriptional activity relative to the negative control. Data was normalised to the negative controls. All data is expressed as mean ± SEM of four independent experiments. Statistical analysis was performed using Student's t test, *** $p \leq 0.001$.

17-AAG Treatment does not Increase NFATc1 nor c-FOS Protein Levels in RAW264.7 Cells
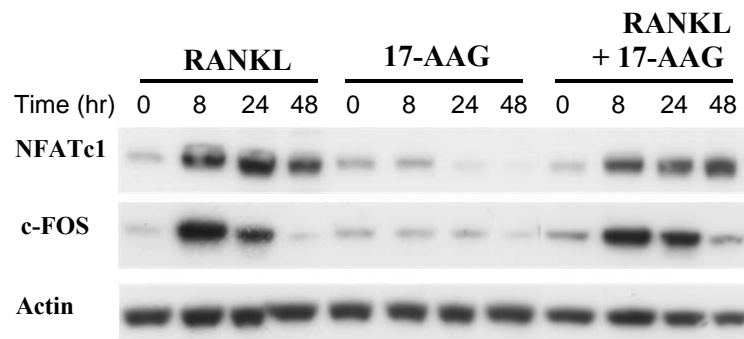
Figure 3.17

RAW264.7 cells, seeded at 2.5 x 10^4 in 35mm diameter culture wells, were treated with RANKL (50ng/ml), 17-AAG (500nM) or RANKL (50ng/ml) + 17-AAG (500nM) co-treatment for 8, 24 and 48 hours as indicated. The cells were lysed and NFATc1 and C-FOS protein levels determined by immunoblot analysis. RANKL treatment increased NFATc1 protein expression. In contrast, 17-AAG treatment decreased NFATc1 protein expression in a time-dependent manner. RANKL and 17-AAG combination treatment did not further increase NFATc1 protein levels than that of RANKL treatment. Similarly, RANKL treatment increased c-FOS protein levels but 17-AAG treatment did not. RANKL and 17-AAG co-treatment did not increase c-FOS levels above that of RANKL treatment alone. Western blot data courtesy of Dr Ryan Chai, Monash University.

is critical to osteoclastogenesis is c-FOS (Wang *et al.*, 1992). Mice that lack c-FOS exhibit severe osteopetrosis and lack osteoclasts (Wang *et al.*, 1992). As previously published, RANKL increases c-FOS protein levels in a time dependent manner. However, 17-AAG treatment did not affect c-FOS protein levels (Figure 3.17). This data shows that 17-AAG treatment does not act to increase osteoclast formation through NFATc1 or c-FOS transcription factors, which point to some pathway mediator downstream of these factors.

Most of the well-characterised RANKL-dependent cell signalling pathways are thought to be upstream of NFATc1 activation, i.e., they lead to NFATc1 activation and their blockade reduces NFATc1 levels. However, NFATc1 activity also represses the transcription of anti-osteoclastogenic genes downstream of its activation. NFATc1 activation induces B lymphocyte-induced maturation protein-1 (BLIMP1), which transcriptionally represses anti-osteoclastogenic genes i.e., Interferon regulatory factor 8 (IRFf8) and MAFB (Nishikawa *et al.*, 2010). Investigations of the mRNA expression levels of these factors were examined by our group but were not affected by 17-AAG treatment (data not shown) consistent with the NFATc1 data above. This further implicates factors that are downstream of NFATc1 in 17-AAG actions to increase osteoclast formation. The transcription factor, MITF, is enhanced relatively slowly in osteoclast progenitors compared to NFATc1 and has recently been shown to depend on NFATc1(Lu *et al.*, 2014) . MITF is critical for the transcription of osteoclast specific genes such as *Apc5* (TRAP), proton pump components i.e *v-Atp6v0d2* and *Cstk* (Bronisz *et al.*, 2006; Hershey and Fisher, 2004). *Mitf$^{mi/mi}$* mice are osteopetrotic with few osteoclasts and have non-erupted teeth due to reduced bone resorption (Hershey and Fisher, 2004). Ultrastructural studies have shown the reduced bone resorption occurs because osteoclasts derived from *Mitf^{mi}/Mitf^{mi}* mice are small, either mononuclear or have significantly reduced nuclei numbers, have defective ruffled borders and express low levels of TRAP and Cstk (Hershey and Fisher, 2004; Steingrimsson *et al.*, 2002; Motyckova *et al.*, 2001; Luchin *et al.*, 2000). MITF A isoform and, in particular, E isoform have been shown to be critical in osteoclastogenesis (Lu *et al.*, 2010a). Very recently MITF-E and -A protein levels have been shown to be NFATc1 dependent (Lu *et al.*, 2014).

To determine the effect of 17-AAG upon MITF, RAW264.7 cells were seeded in 35mm diameter culture wells and treated with 17-AAG (50,100, 200 and 500nM) for 48 hours. The cells were lysed and MITF protein levels analysed by Western blotting. Treatment of the cells with 17-AAG resulted in increased MITF protein levels in a dose-dependent manner under

these conditions. This data was surprising given the role NFATc1 has upon osteoclast formation, being considered the master regulator of osteoclastogenesis (Figure 3.18 A). MITF levels were observed to be the greatest at 17-AAG (500nM) (Figure 3.18 A.). RANKL treatment also caused an increase in MITF levels (Figure 3.18 A.). Effects of 17-AAG upon MITF protein levels over a time course was also examined. RAW264.7 cells were treated with RANKL (100ng/ml), 17-AAG (500nM) or in combination treatment at 6, 24 and 48 hours. RANKL treatment increased MITF expression as previously described (Figure 3.18 B.) (Lu *et al.*, 2010a). 17-AAG (500nM) treatment also increased MITF protein expression in a time-dependent manner (Figure 3.18 B.). MITF protein expression was greatest at 48 hours (Figure 3.18 B.). This is consistent with the observation showing 17-AAG acts late in the osteoclastogenic processes (Figure 3.12). Combination treatment of RANKL (100ng/ml) with 17-AAG (500nM) increased the expression of MITF protein, but their actions were not additive or synergistic. This requires further study to clarify this as the MITF levels may peak (and start degrading) at different times with the different stimuli. Note also that MITF has a number of described isoforms and in the MITF immunoblots throughout this thesis; a thick doublet band was always observed. Both bands (upper and lower) had increased expression with RANKL treatment.

3.2.6 HSP90 Inhibitor NVP-AUY922 Increases MITF Protein Expression

NVP-AUY922 was shown to increase osteoclast formation in both RAW264.7 and bone marrow cells. To determine the effect NVP-AUY922 has upon MITF protein levels, RAW264.7 cells were treated with NVP-AUY22 for 48 hours. At 48 hours the cells were lysed and MITF protein expression examined immunoblot. NVP-AUY922 increased MITF protein expression (Figure 3.19). This suggests that NVP-AUY922 may in part mediate its enhancing effects upon osteoclast numbers through MITF action.

17-AAG Increases MITF Protein Levels in RAW264.7 Cells

A.

B.
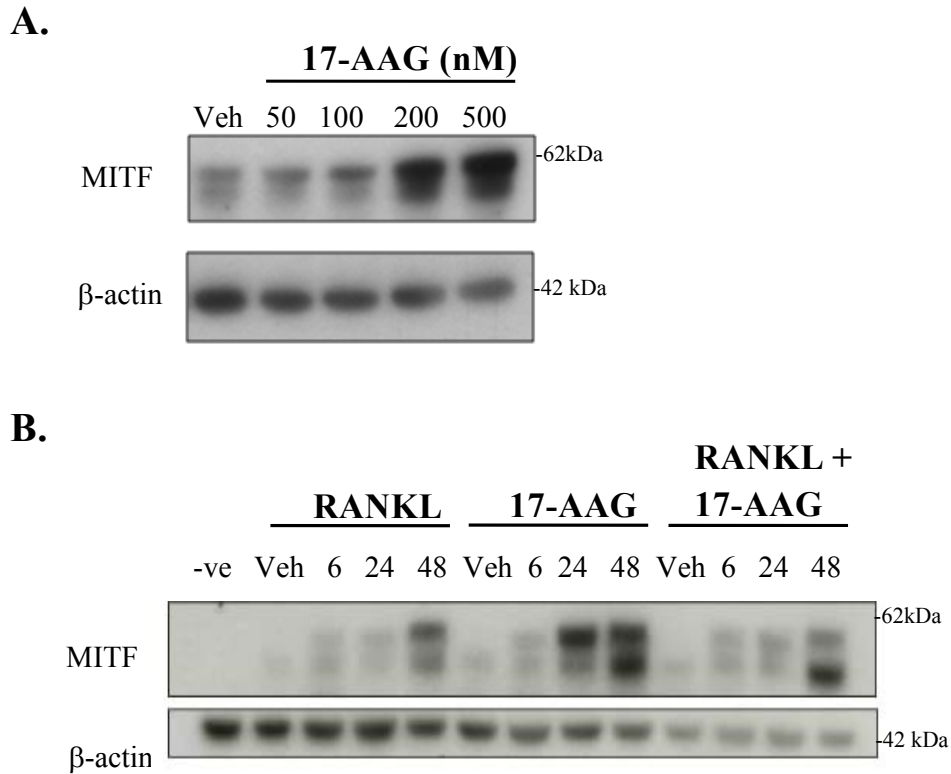
Figure 3.18

RAW264.7 cells were seeded at 2 x10^5 in 35mm diameter culture wells and were left to settle overnight. The cells were treated with **(A.)** 17-AAG (50, 100, 200 and 500nM) for 48 hours and **(B.)** with RANKL (100ng/ml), 17-AAG (500nM) and combination treatment of RANKL (100ng/ml) + 17-AAG (500nM) for 6, 24 or 48 hours**.** At the designated time points, the cells were lysed and MITF levels determined by immunoblotting with β-actin detection to indicate loading. **(A.)** 17-AAG treatment increased MITF protein levels in a dose-dependent manner. **(B.)** 17-AAG treatment also increased MITF protein expression in a time-dependent manner. Co-treatment of RANKL and 17-AAG also increased MITF protein expression. Western blots were performed three times with lysate samples from independent RAW264.7 isolates.

NVP-AUY922 Treatment Increases MITF Protein Levels in RAW264.7 Cells

NVP-AUY922 (nM)

| -ve | Veh | 2 | 5 | 10 | 20 |

MITF — 62kDa

β-actin — 42 kDa
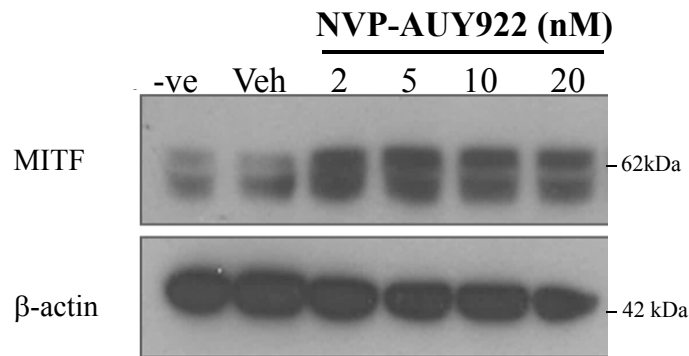
Figure 3.19

RAW264.7 cells were seeded at 2 x10^5 cells in 35 mm diameter well and were allowed to settle overnight. The cells were treated with NVP-AUY922 (2, 5, 10 and 20nM) for 48 hours. Cells were then lysed and MITF protein levels determined by immunoblotting, with β-actin detection to indicate loading. NVP-AUY922 increases MITF protein expression at 48 hours. Western blots were performed three times with lysate samples from independent RAW264.7 isolates.

3.2.7 17-AAG Enhances the Promoter Activity of the MITF Target Gene, v-Atp6v0d2

The vacuolar H^+-adenosinetriphosphatase (vATPase) proton pump is essential for osteoclast activity. In particular, the d2 subunit, which is one of the 14 subunits of the vATPase proton pump has been shown to have an important role in maintaining bone homeostasis (Lee *et al.*, 2006). The Atp6v0d2gene has been shown to be transcriptionally regulated by MITF as well as NFATc1 (Feng *et al.*, 2009; Kim *et al.*, 2008b). ChIP analysis revealed that the promoter of v-Atp6v0d2 contains NFATc1, MEF and MITF binding sites (Feng *et al.*, 2009). Furthermore, retroviral overexpression of MITF in RAW264.7 cells increased Atp6v0d2 expression and potentiated osteoclast formation (MITF and MEF2 enhanced NFATc1 mediated activation of vATPase-d2) (Feng *et al.*, 2009). A collaborator, Prof. Jiake Xu from the University of Western Australia (UWA), kindly provided the v-Atp6v0d2 promoter dependent luciferase construct as well as a similar construct with the MITF binding sites mutated. The mutated construct was employed as a control to confirm the involvement of MITF.

The constructs were isolated and purified from transformed bacterial cells (Chapter 2.17). RAW264.7 cells were transiently transfected with the Atp6v0d2reporter constructs, and a constitutively active *Renilla* luciferase expressing construct (Chapter 2.8). Transfected cells were subsequently treated with RANKL (100ng/ml) for 24 hours, which significantly increased the relative activity of v-ATPase-d2 transcriptional activity (Figure 3.20). Treatment with 17-AAG (1μM) also significantly increased the transcriptional activation relative to the DMSO vehicle control (Figure 3.21). A combination treatment of RANKL (20ng/ml) with 17-AAG (0.5 μM or 1μM) resulted in a significantly higher transcriptional activity compared to the RANKL (20ng/ml) treatment alone (Figure 3.21). The effect of 17-AAG treatment alone as well as in combination with RANKL treatment upon v-ATPase-d2 transcriptional activity was also observed at 48 hours. The cells were treated with 17-AAG (0.25, 0.5 and 1μM). 17-AAG (1μM) significantly increased v-Atp6v0d2 transcriptional activity at 48 hours (Figure 3.22 A.). In addition, RANKL (20ng/ml) and 17-AAG (1μM) co-treatment significantly increased v-Atp6v0d2 transcriptional activity at 48 hours (Figure 3.22 B.). This data indicates that 17-AAG treatment activates MITF target gene v-Atp6v0d2 in the absence or presence of RANKL at both 24 and 48 hours.

The M(M1-3)Atp6v0d2 construct, which contains inactivation mutations in all three MITF binding sites in the promoter was used as a method control to confirm the requirement for MITF binding in the actions of 17-AAG. The RAW264.7 cells were transiently transfected with the M(M1-3) Atp6v0d2 construct or wt construct in the presence of a constitutively active *Renilla* luciferase-expressing construct in the same manner as described above. The following day the cells were treated with 17-AAG (0.5μM and 1μM). RAW264.7 cells containing the M(M1-3) Atp6v0d2 mutated construct did not respond to 17-AAG treatment (Figure 3.23 B.). In contrast, cells that had been transfected with the wt construct alongside showed increased Atp6v0d2 transcriptional activity when treated with 17-AAG as seen prior (Figure 3.23 A.). This data indicates that 17-AAG acts in a MITF-dependent manner to increase the transcriptional activity of v-Atp6v0d2. This data is consistent with an enhancing action of 17-AAG in osteoclastogenesis occurring through its ability regulate MITF protein activity.

RANKL Treatment Increases the Activity of MITF Target Gene V-ATPase6d2

A.
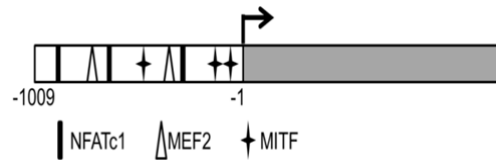
B.
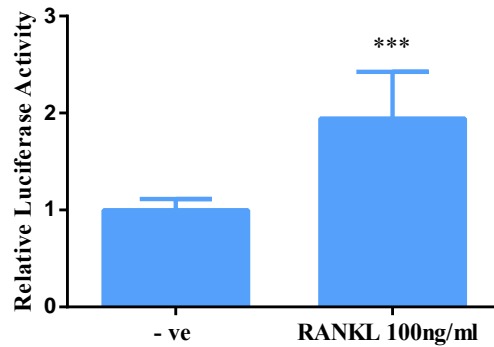
Figure 3.20

(A.) Structure of Atp6v0d2 promoter construct showing the NFATc1-, MEF2- and MITF-binding sites. The promoter was inserted at a 5′ site relative to a firefly luciferase coding region (gray). The construct was made and kindly supplied by Prof Jiake Xu. (UWA) **(B.)** RAW264.7 cells (6 $\times 10^4$ cells/well) were transiently co-transfected with Atp6v0d2promoter-driven firefly luciferase construct (0.2 µg/well) and a control pRL *Renilla* luciferase construct (0.1µg/well) using Lipofectamine TM LTX Plus reagent. After 24 hours, the cells were treated with RANKL (100ng/ml) for 24 hours, lysed in passive lysis buffer (1x) (Promega) overnight at 4ºC and luciferase levels read on a luminometer. RANKL (100ng/ml) increases vATPased2 transcriptional activity. Luciferase levels were calculated as a ratio of firefly luciferase to *Renilla* luciferase activity and shown as normalised relative to the untreated negative control, "-ve". RANKL (100ng/ml) increases vATPased2 transcriptional activity. These experiments were performed with the help of Dr John Price and Dr Julian Quinn. Data is presented as mean ± SEM of five independent experiments. Statistical analysis was performed using an unpaired two-tailed t test, *** p $\leq$ 0.001.

17-AAG and RANKL+17-AAG Co-treatment Increases vATPase6d2 Transcriptional Activity
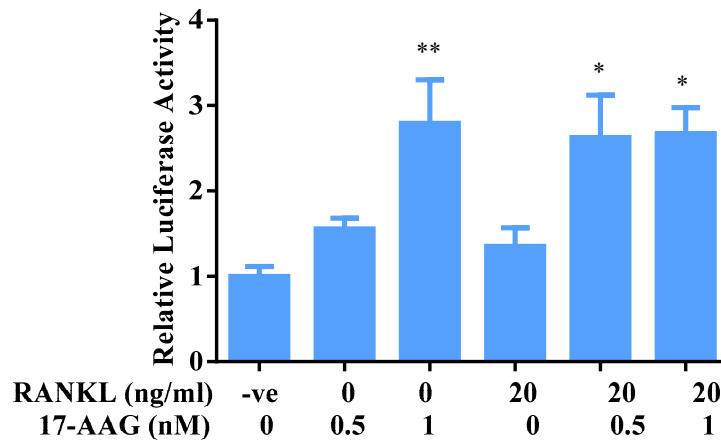
Figure 3.21

RAW264.7 cells (6 $\times 10^4$ cells/well) were transiently co-transfected with Atp6v0d2promoter driven firefly luciferase construct (0.2 μg/well) and a control pRL *Renilla* luciferase construct (0.1μg/well) using Lipofectamine TM LTX Plus reagent. The cells were allowed to settle for 24 hours and were then treated with17-AAG (0.5 or 1μM). Cells were also co-treatment of RANKL (20ng/ml) and 17-AAG (0.5 and 1μM). At 24 hours the cells were lysed in passive lysis buffer (1x) (Promega) and the luciferase levels read using a luminometer.17-AAG treatment increased vATPased2 transcriptional activity in the presence of absence of RANKL. Luciferase levels were calculated as a ratio of firefly luciferase to *Renilla* luciferase activity and shown as normalised relative to the untreated negative control, "-ve". **(A-B.)** 17-AAG treatment increases Atp6v0d2 transcriptional activity in the presence and absence of RANKL treatment. These experiments were performed with the help of Dr John Price and Dr Julian Quinn. Data is expressed as mean ± SEM of five independent experiments. Statistical analysis was by ANOVA, Bonferroni's *post hoc* test, *p $\leq$ 0.05 **p $\leq$ 0.01.

17-AAG and 17-AAG+RANKL Co-treatment Increases vATPase6d2 Transcriptional Activity at 48 hours

A.

B.
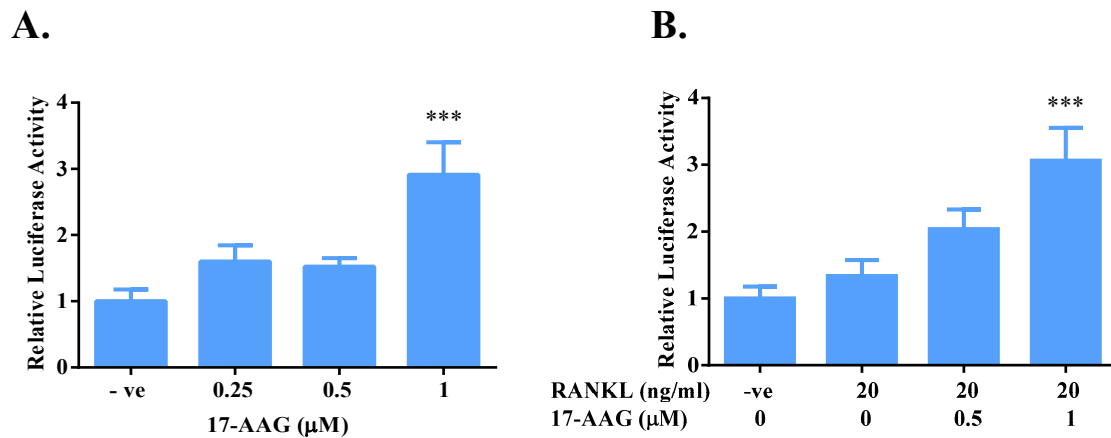
Figure 3.22

RAW264.7 cells (6×10^4 cells/well) were transiently co-transfected with Atp6v0d2promoter-drive firefly luciferase construct (0.2 μg/well) and a control pRL *Renilla* luciferase construct (0.1μg/well) using Lipofectamine TM LTX Plus reagent. After 24 hours the cells were treated with **(A.)** 17-AAG (0.25, 0.5 and 1 μM) and **(B.)** co-treatment of RANKL (20ng/ml) and 17-AAG (0.5 and 1 μM). The cells were lysed after 48 hours in passive lysis buffer (1x) (Promega) overnight (4°C), and luciferases levels read using a luminometer. **(A.)** 17-AAG significantly increased Atp6v0d2 transcriptional activity relative to the untreated negative control at 48 hours. **(B.)** 17-AAG dose-dependently increased vATPased2 transcriptional activity in the presence of RANKL (20ng/ml). These experiments were performed with the help of Dr John Price and Dr Julian Quinn. Luciferase levels were calculated as a ratio of firefly luciferase to *Renilla* luciferase activity and shown as normalised relative to untreated control. Data is expressed as the mean ± SEM of three independent experiments. Statistical analysis was performed by ANOVA, Dunnett's *post hoc* test, *** $p \leq 0.001$.

Mutating the MITF Binding Sites Abolishes the 17-AAG Induced v-ATPase6d2 Activity

A. **WT Atp6v0d2**   **B.**   **Mutated Atp6v0d2**
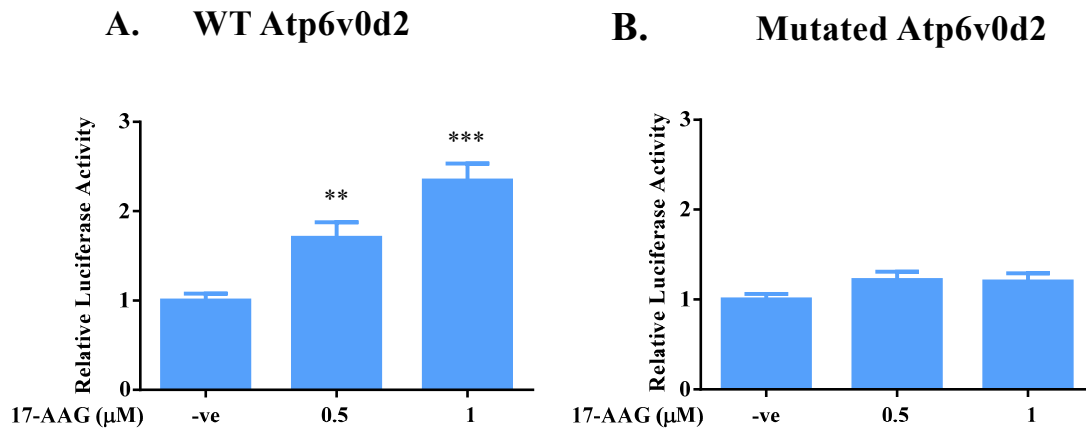
Figure 3.23

RAW264.7 cells were transiently transfected with **(A.)** M(M1– 3)Atp6v0d2promoter-driven firefly luciferase expression construct (0.2 μg/well), which contains mutations in the three MITF-binding sites rendering them non-functional or **(B.)** the wt Atp6v0d2promoter (0.2 μg/well). The cells were also simultaneously transiently transfected with pRL *Renilla* luciferase construct (0.1μg/well) as transfection controls. The co-transfection was carried out using the Lipofectamine TM LTX Plus reagent. At 24 hours both the cells containing the **(A.)** mutated Atp6v0d2 promoter and **(B.)** the wt Atp6v0d2 promoter were treated with 17-AAG (0.5 and 1 μM) for 24 hours before being lysed in passive lysis buffer (1x) (Promega) and Luciferase levels read. **(A.)** 17-AAG treatment increased Atp6v0d2 transcriptional activity. **(B.)** 17-AAG treatment did not affect vATPased2 transcriptional activity in the Mutated M(M1-3) Atp6v0d2 promoter. These experiments were performed with the help of Dr John Price and Dr Julian Quinn. Luciferase levels were calculated as a ratio of firefly luciferase to *Renilla* luciferase activity and shown as normalised relative to the untreated negative control "-ve". The data is expressed as the mean ± SEM of five independent experiments. Statistical analysis was performed by ANOVA, Dunnett's *post hoc* test, ** $p \leq 0.01$, *** $p \leq 0.001$.

3.3 Discussion

We and others have previously identified that benzoquinone ansamycin HSP90 inhibitors such as 17-AAG and herbamycin A enhance osteoclast formation *in vitro* and *in vivo* (Price *et al.*, 2005; Yano *et al.*, 2008). These were surprising observations given that HSP90 is an important molecular chaperone, which maintains the activity and stability of many important cell signalling proteins that are important in the osteoclastogenesis pathways including NFκB (Travers *et al.*, 2012; Eccles *et al.*, 2008; Bohonowych *et al.*, 2010). Because HSP90 inhibitors 17-AAG and herbamycin A increased osteoclast formation, it was hypothesized that HSP90 inhibitors from other classes of compounds may similarly act to increase osteoclastogenesis. The alternative hypothesis is that increased osteoclast differentiation is a unique feature of this particular benzoquinone ansamycin class of HSP90 inhibitors.

NVP-AUY922 has shown to have promising anti-cancer effects with anti-proliferative effects seen against a panel of breast cancer cell lines and primary cultures, multiple myeloma, prostate, colon, melanoma, glioma and HUVEC cell lines (Eccles *et al.*, 2008). NVP-AUY922 also has been shown to have anti-tumour properties as a single agent *in vivo* in BT-474 breast, HCT116 colorectal, and U87MG glioblastoma xenografts in mice and is currently in Phase I-II clinical trials (National Institute of Health, 2014). Both CCT08159 and NVP-AUY922 have better pharmacokinetic profiles than 17-AAG, which has been discontinued from clinical trials (Sharp *et al.*, 2007b). First, 17-AAG actions upon RAW264.7 and bone marrow cells progenitors were confirmed. 17-AAG treatment very significantly increased osteoclast formation in a dose-dependent manner, which was confirmed using both TRAP and CTR markers of the osteoclast phenotype. Similarly to 17-AAG, both CCT018159 and NVP-AUY922 significantly increased osteoclastogenesis in both RAW264.7 and bone marrow cells *in vitro*. NVP-AUY922 increased osteoclast formation potently at low concentrations (10nM), which may be due to the fact that NVP-AUY922 has an increased half-life and, in addition, enters the cell more easily (Sharp *et al.*, 2007b). The results in this chapter demonstrate that both CCT018159 and NVP-AUY922, which are compounds that are quite structurally distinct from 17-AAG, significantly increase osteoclast formation *in vitro*. This data suggests that the pro-osteoclastic properties of HSP90 inhibitors is not found only in benzoquinone ansamycin-based HSP90 inhibitors but is likely to be a more generalised property of N-terminal HSP90 inhibitors. Based on our characterization of these compounds, it is plausible to hypothesize that these compounds may act to cause bone loss *in vivo*, like 17-AAG, but further studies would be required to determine this. In cancers that metastasize

to bone, such as breast neoplasms, bone metastasis establishment results in focal bone damage and skeletal related events (SRE) (Simos *et al.*, 2013; Weilbaecher *et al.*, 2011). As previously described by Price and co-workers, 17-AAG treatment increased tumour growth in metastatic bone disease through its pro-osteolytic actions (Price *et al.*, 2005). Any osteolysis caused by CCT018159 and NVP-AUY922 would have the potential to increase tumour growth in bone potentially through the vicious cycle model. Therefore these compounds need to be screened for their effects on bone metabolism *in vivo* in tumour laden and naïve mice.

Osteoclastogenesis occurs through the stimulation of osteoclast precursor cells to survive by M-CSF signals and to differentiate by RANKL stimulation (Boyle *et al.*, 2003; Feng, 2005). RANKL binding to its receptor RANK and its downstream signalling pathways induces the expression of osteoclast transcription genes and the activation of signalling molecules, which are necessary for the differentiation and activation of osteoclasts (Feng, 2005; Boyle *et al.*, 2003). Amongst these transcription factors and signalling molecules are: NFκB, NFATc1, C-FOS, MITF, and p38 (Asagiri and Takayanagi, 2007; Mansky *et al.*, 2002a; Gohda *et al.*, 2005; Yamashita *et al.*, 2007; Boyle *et al.*, 2003; Raggatt and Partridge, 2010). These molecules are essential for RANKL action and therefore regulate osteoclast numbers and activity. Actions of RANKL to increase survival of osteoclasts were not affected by 17-AAG treatment. This data provides strong evidence that RANK and immediate downstream signals are probably not affected by 17-AAG, i.e., general sensitivity to RANKL was not increased. Regarding RANKL actions on osteoclast activity, previous work in our laboratory has found no effects of 17-AAG treatment. However, bone resorption assays are notoriously insensitive and can realistically detect only very large (>30%) effects, so this was not investigated here. The role of p38 in osteoclast formation and 17-AAG actions are included in Chapter 4.

The transcription factors c-FOS and NFκB are considered to be early transcription factors since they are very rapidly enhanced upon RANKL stimulus and they are crucial for the early commitment phases of osteoclast differentiation (Matsuo *et al.*, 2004; Yamashita *et al.*, 2007). Using a luciferase induction construct 17-AAG treatment was shown not to affect the transcriptional activity of NFκB at both 6 and 24 hours. Likewise, 17-AAG treatment did not affect c-FOS protein levels. Downstream of (i.e., dependent on) these osteoclastogenic transcription factors is the 'early to mid-stage' transcription factor NFATc1. NFATc1 is commonly referred to in the osteoclast literature as a "master regulator" of osteoclast formation due to the very large number of both intrinsic and extrinsic factors that act on

osteoclast formation by affecting NFATc1 levels (Takayanagi, 2007b; Kim and Kim, 2014). It was therefore particularly interesting to note that 17-AAG did not increase NFAT transcriptional activity and NFATc1 protein levels but rather decreased it. These findings are consistent with the observation that NFATc1 is a HSP90 client protein (Ruffenach *et al.*, 2015). In addition, 17-AAG mechanism to increase osteoclast differentiation was shown to be distinct from TGF-β mediated enhancement of osteoclast formation. TGF-β acts early in the osteoclast differentiation course to increase osteoclast formation (Quinn *et al.*, 2001). TGF-β increases NFATc1 levels, although it probably acts through a number of mechanisms to increase osteoclast commitment of progenitors (Fox *et al.*, 2008). In comparison, 17-AAG acts relatively late in the differentiation process and as mentioned above does not affect NFATc1. This data suggests that NFATc1 is not the rate-limiting step in osteoclastogenesis.

In contrast to the lack of effects on NFATc1, 17-AAG increased MITF protein expression in a dose-dependent manner. MITF is a basic helix loop-leucine zipper transcription factor that is considered to act late in osteoclastogenesis (Bronisz *et al.*, 2006; Hershey and Fisher, 2004). MITF forms part of a complex with NFAT, PU.1, NFκB and AP-1 during the late stages of osteoclastogenesis to drive the expression of osteoclast-specific genes (Asagiri and Takayanagi, 2007; Boyle *et al.*, 2003; Sharma *et al.*, 2007). 17-AAG time-dependently increased MITF protein expression and its expression was the greatest at 48 hours. This data is consistent with the notion that MITF is a relatively late-acting osteoclast transcription factor. Moreover as earlier described, 17-AAG actions upon osteoclast formation occur in the latter half of osteoclastogenesis. This data therefore supports the idea that 17-AAG actions upon osteoclast formation occur through the late acting MITF although this is difficult to prove since silencing or deletion of MITF blocks all osteoclast formation (Lu *et al.*, 2010a; Boyle *et al.*, 2003). The *mi* gene coding for MITF is a complex gene having different splice sites with the resultant expression of 9 proteins isoforms (Hershey and Fisher, 2005; Steingrimsson *et al.*, 1994). Isoforms A and in particular E have been shown to be important in osteoclast formation with forced over-expression of these isoforms increasing osteoclastogenesis (Lu *et al.*, 2010a). In particular, isoform E was able to most potently induce osteoclast formation and also increased the expression of osteoclast specific genes (Lu *et al.*, 2014). MITF binds to a 7 base-pair motif TCANGTG in the promoter regions of target genes some of which include the v-Atp6v0d2, TRAP, Ctsk and E-cadherin (Levy *et al.*, 2006; Pogenberg *et al.*, 2012; Lu *et al.*, 2010a). More recently, Lu *et al*. also found MITF

expression to be regulated by NFATc1 although no NFAT-binding site has been reported in the *mi* gene promoter regions (Lu *et al.*, 2014).

The data presented herein shows an ability of 17-AAG to increase the transcriptional activity of the MITF target gene v-ATPase-d2. This further supports the notion that 17-AAG actions upon MITF cause the subsequent increase in osteoclast formation. In summary, this data shows that 17-AAG exerts its pro-osteoclastogenic actions through its regulation of MITF (and its downstream targets). This suggests the regulation of MITF is a rate-limiting step in osteoclastogenesis, and implies a novel role of MITF in osteoclastogenesis. MITF is essential for osteoclasts formation (Lu *et al.*, 2010a). Mice, which express mutant alleles of the MITF gene *mi* have a small number of defective osteoclasts, and mice with mutations that result in a lack of MITF Zip domains exhibit osteopetrosis and have no osteoclasts (Luchin *et al.*, 2000; Lipton, 2004; Hershey and Fisher, 2004; Motyckova *et al.*, 2001; Steingrimsson *et al.*, 2002). Despite its essential role in osteoclast formation, it is generally not identified as a major regulatory mechanism in osteoclastogenesis. Although Kim *et al.* have suggested that IL-1 increases RANKL-driven osteoclast formation through its regulation of MITF activity (when added late in the osteoclast differentiation course in the maturation phase) (Kim *et al.*, 2009). This latter data is consistent with our laboratories findings of 17-AAG actions upon MITF and MITF's role in osteoclastogenesis. Therefore, this data provides new and interesting evidence for a novel role of MITF regulation in osteoclastogenesis.

This data suggests several possible ways in which 17-AAG might increase osteoclast formation. One of these ways may involve proteasomal inhibition. Inhibition of HSP90 causes proteasomal degradation of HSP90 client proteins, which are often oncogenes or other proteins that have a role in non-oncogene addiction therefore reducing their concentration within the cell (Neckers and Workman, 2012; Jhaveri *et al.*, 2012). This raises the possibility that an endogenous inhibitor or inhibitors of osteoclast formation (perhaps one that reduces MITF levels) are degraded resulting in an increase in osteoclast formation. In line with this, the removal of a RANKL inhibitor, RBP-J and NFκB inhibitor, NFκBp100 have been used to explain increases in osteoclast formation (Zhao *et al.*, 2012; Yao *et al.*, 2009). Removal of these factors however, resulted in greatly enhanced NFATc1 levels, which 17-AAG did not affect (Zhao *et al.*, 2012; Yao *et al.*, 2009). Another more likely possibility is that N-terminal HSP90 inhibitors cause HSF1 to dissociate from HSP90, which it is complexed to and causes a downstream cellular stress response (Powers and Workman, 2007; Neckers and Workman,

2012; Whitesell and Lindquist, 2005). The dissociated HSF1 is activated, translocates to the nucleus and causes the initiation of a HSF1 stress response characterized by increased levels of HSPs i.e.HSP72 (Powers and Workman, 2007). Interestingly, C-terminal inhibitors including Novobiocin, which do not displace HSF1 and therefore do not cause a downstream stress response, do not affect osteoclast formation (Chai *et al.*, 2014). This raises the possibility 17-AAG's ability to cause a HSF1-mediated stress response, is affecting MITF and subsequent osteoclast formation. This hypothesis examined in the next chapter.

Chapter 4
The Effects of 17-AAG and NVP-AUY922 upon Cell Stress Molecules HSF1 and p38, and HSF1 Influences on Osteoclast Formation

Chapter 4 The Effects of 17-AAG and NVP-AUY922 upon Cell Stress Molecules HSF1 and p38, and HSF1 Influences on Osteoclast Formation

4.1 Introduction

Cells are frequently exposed to environmental insults that cause acute or chronic cell stress (Morimoto, 1998). Examples of such stressors include: heat shock, anoxia, ethanol, chemotherapeutics and inflammatory cytokines (David *et al.*, 1999; Åkerfelt *et al.*, 2010). The need for a cell to be able to tolerate a particular stress is cell-type dependent; however, some sort of stress response mechanism exists in all cells. In response to stress, cells can activate a number of different mechanisms including the increased expression of heat shock proteins, which are typically central to cell survival (Chapter 1.7) (Fulda *et al.*, 2010; Whitesell and Lindquist, 2005). Amongst the regulatory proteins that are rapidly activated upon cell exposure to stress are two proteins, which play particularly important roles in maintaining cellular survival: HSF1, an inducer of HSP expression, and p38, a MAP kinase (Wagner and Nebreda, 2009; Junttila *et al.*, 2008; Morimoto, 1993). These proteins are the focus of the work described in this chapter.

HSF1, a transcription factor that becomes activated upon cell stress (Chapter 1.8.1.1), is considered the primary mediator of classical cellular stress responses (Dai *et al.*, 2007; Morimoto, 1993). HSF1 is usually found as a latent molecule complexed to HSP90 multi-chaperone protein complexes in the cytoplasm (Zou *et al.*, 1998; Whitesell and Lindquist, 2009). In unstressed cells, a low basal level of transcriptionally-active HSF1 is present (Whitesell and Lindquist, 2009). Its stress-induced activation results in disassociation from the HSP90 complex, trimerization, translocation to the nucleus and binding to Heat Shock Elements in the gene promoters of target genes, which include many HSPs. HSF1 binding to HSE increases the transcription of HSPs and a range of other stress-sensitive factors (Diller, 2006; Anckar and Sistonen, 2011; Åkerfelt *et al.*, 2010). As previously described (Chapter 1.8.1), increased HSP expression maintains cellular pathway integrity and homeostasis through their molecular chaperone functions (Richter *et al.*, 2010; Gabai and Sherman, 2002). HSF1 is likely to be essential for most stress responses although it should be noted that HSF1 null mice are viable on some genetic backgrounds, despite being somewhat runted and having low fertility (Jin *et al.*, 2011).

HSPs, and in particular HSP90, is overexpressed in cancer cells (Jego *et al.*, 2013; Calderwood, 2010; Zuehlke and Johnson, 2010). In a cancer cell, HSP90 protects the cell from environmental stress and also from the genetic and proteotoxic stress within the cell by stabilizing many oncogenic client proteins (Workman, 2004b; Whitesell and Lindquist, 2005). The HSP90 inhibitor, 17-AAG, has been shown to have anti-cancer properties in a number of mouse xenograft models and was going through clinical trials up to 2008 (Sauvageot *et al.*, 2009; Solit *et al.*, 2002; Burger *et al.*, 2004; Price *et al.*, 2005; National Institute of Health, 2014). However, as described by Price *et al.*, 17-AAG treatment significantly increased invasion and growth in bone in an intracardiac MDA-MB-231 inoculation model (Price *et al.*, 2005). The ability of 17-AAG to increase tumour growth in the bone was postulated to occur through its ability to increase osteoclast formation and bone destruction (Price *et al.*, 2005). Price and co-workers showed 17-AAG stimulated osteoclast formation *in vitro* and *in vivo*, causing decreased total trabecular bone in mice even in the absence of tumour challenge (Price *et al.*, 2005). 17-AAG pro-osteoclastic effects were confirmed by using RAW264.7 and bone marrow primary cells (Figures 3.3-3.5). In addition, the more recently developed N-terminal HSP90 inhibitors CCT018159 and NVP-AUY922 were also shown to increase osteoclast formation from RANKL stimulated RAW264.7 and bone marrow progenitors (Figures 3.9-3.12). In the previous chapter, 17-AAG and NVP-AUY922 were also shown to act upon the late acting transcription factor MITF (Figures 3.18-3.19).

The osteolytic and pro-osteoclastic effects of 17-AAG cannot easily be explained by its inhibition of HSP90 as many of HSP90 client proteins, including NFATc1, play an important role in osteoclast formation (Price *et al.*, 2005; Ruffenach *et al.*, 2015). A second line of enquiry followed here is to investigate the known ability of HSP90 inhibitors to induce a HSF1-mediated cell stress response, which may affect osteoclast formation. As described in Chapter 1.9.4.2, N-terminal HSP90 inhibitors, including 17-AAG and NVP-AUY922, cause a HSF1 mediated heat shock response (HSR) by binding to the same region of HSP90 as HSF1 causing its subsequent dissociation (Zou *et al.*, 1998; Taylor *et al.*, 2007; Kamal *et al.*, 2004). HSF1 dissociation from HSP90 normally occurs when high levels of HSP90-binding misfolded proteins are present in cytoplasm due to heat or other toxic cellular insults (Chapter 1.8.1.1) (Åkerfelt *et al.*, 2010; Anckar and Sistonen, 2011). 17-AAG and NVP-AUY922 have thus been shown to induce a HSR in a number of cell types (Gaspar *et al.*, 2010; Eccles *et al.*,

2008; Cheung *et al.*, 2005; Powers and Workman, 2007; Guo *et al.*, 2005b; Doubrovin *et al.*, 2012).

In this chapter several approaches to blocking HSF1 activity, including pharmacological, genetic knockout and knockdown, have been used and the effects of these on 17-AAG and NVP-AUY922 actions upon osteoclast formation examined. In addition to testing the hypothesis of HSF1 mediated cell stress involvement in osteoclast formation, a second hypothesis is tested. This hypothesis examines whether p38 MAP kinase is involved in the cellular responses of HSP90 inhibitors that increase osteoclast formation. The MAP kinase, p38, is an essential signalling molecule in RANKL responses but is also a stress-activated protein kinase. This molecule is thus a good candidate to be another mediator for the observed effects of HSP90 inhibitors either in cooperation with or independently of HSF1.

4.2 Results

4.2.1 17-AAG and NVP-AUY922 Enhance HSF1 Transcriptional Activity and Increase HSP72 Protein Levels

The first step was to confirm the effects of 17-AAG and NVP-AUY922 effects upon HSE transcriptional activity as a proof of principle. This was studied using a reporter cell line generated by Dr Chau Nguyen (Chapter 2.1.4.3), which consisted of the HEK293 cell line that ectopically expressed EGFP, wild-type HSF1 at high levels and also contained a pHSE-mCherry vector. These cells as previously described are designated as HEK-HSE cells (Nguyen *et al.*, 2013). The mCherry expression was under the control of the stress inducible 'HSP70B' promoter containing multiple HSE sites (Nguyen *et al.*, 2013; Winklhofer *et al.*, 2001). The HSP70B promoter is strictly inducible unlike the major inducible form HSP72, which has low basal levels present in the cell (Watanabe *et al.*, 2001; Volloch and Sherman, 1999; Noonan *et al.*, 2007). The high levels of wild type HSF1 expressed in these cells increases the sensitivity to cellular stresses (Nguyen *et al.*, 2013).

HEK-HSE cells were seeded at 2.5 x 10^4 cells in 6mm diameter wells in phenol red free DMEM media and were left to settle for 3 hours. Cells were then treated with 17-AAG (5μM) for 24 hours then nuclear dye Hoechst (10μg/ml), and the cells incubated for 15 minutes at 37°C. The Hoescht dye and mCherry levels were then determined using the

Arrayscan VTI High Content Screening instrument (Thermo Fisher Scientific). At 24 hours, 17-AAG (5μM) treatment significantly increased the activity of HSF1 relative to the DMSO vehicle control (Figure 4.1) in HEK-HSE cells as shown by expression of mCherry. This response needed to be confirmed in the RAW264.7 cells, the cell line of interest that displays a pro-osteoclastogenic response to RANKL (and 17-AAG). Repeated attempts to produce a stable HSF1-dependent (pHSE-mCherry) reporter transfected RAW264.7 cell line were not successful, so instead a classic immunoblot based approach was used to detect stress responses. As noted above, when HSF1 is activated increased expression of HSPs such as HSP70 family members i.e., HSP72 (HSPA1A) and HSP70B, HSP90 (HSP90AA1) and HSP27 (HSPB1) are observed. Stress induced HSP72 (HSPA1A) is a commonly accepted marker of HSF1 activation (Chapter 1.8.1.2), and was used in this thesis to detect HSF1 activation. Treating RAW264.7 cells with 17-AAG for 24 hours increased HSP72 protein expression in a dose-dependent manner (Figure. 4.2 A). The greatest effect was seen at the highest concentration used, 17-AAG (1μM). This was similar to previous observations by our group that 17-AAG treatment increases HSP70 expression in RAW264.7 cells in a dose-dependent manner after 24 hours treatment (Chai *et al.*, 2014). This data is also broadly consistent with kinetic studies of HSP70 gene expression, which show HSP70 expression to be eight times greater than basal levels 24 hours post heat shock (Wang and Diller, 2003). Similar to the RAW264.7 cells, treating mouse BMM with 17-AAG (100nM or 200nM) for 24 hours resulted in increased HSP72 expression relative to the DMSO vehicle control (Figure 4.2 B). With repeated immunoblot analysis of BMM cultures (data not shown), it appeared that the concentration that maximally increased HSP72 levels was variable. This may be due to bone marrow populations from different mouse sources being more or less sensitive to HSP90 inhibition through 17-AAG.

The hypothesis that 17-AAG enhances osteoclast formation by binding to HSP90 to activate HSF1 would infer that another HSP90 inhibitor that has the same ATPase domain-binding profile would have similar actions. As previously described NVP-AUY922 is currently going through Phase I-II trials and has been shown to cause a HSR in a number of cancer cell lines (Eccles *et al.*, 2008; Gaspar *et al.*, 2010; National Institute of Health, 2014). To establish if NVP-AUY922 also causes a stress response in cells, three cell models and two different experimental approaches were used. The effect of NVP-AUY922 upon HSF1 transcriptional activity was studied using HEK-HSE reporter cells, and HSP72 immunoblot analysis was studied in BMM and in RAW264.7 cells. As with 17-AAG, HSE-HEK cells were treated

17-AAG Treatment Increases HSF1 Transcriptional Activity in HEK-HSE Cells

A.

B.
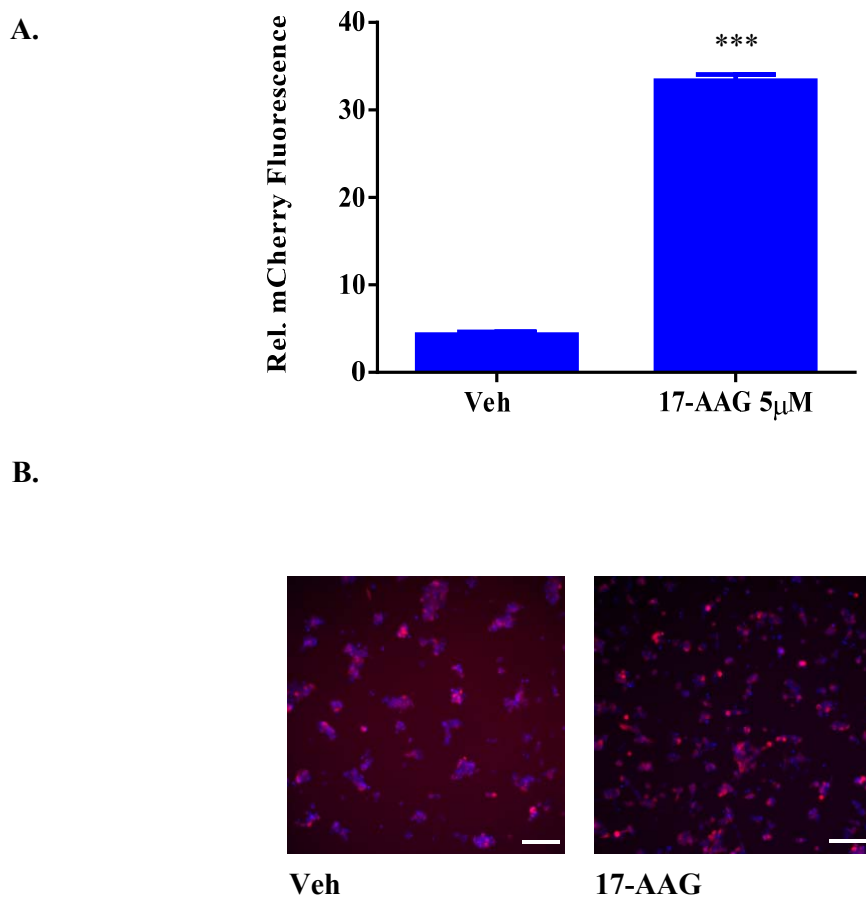
Veh   17-AAG

Figure 4.1

(A-B.) HEK-HSE cells, stably transfected with a mCherry HSE reporter, were seeded at 2.5 x 10^4 cells/well in DMEM phenol-free media. The cells were allowed to adhere for $\geq$ 3 hours then treated with 17-AAG (5μM) or DMSO vehicle control (1/2000). At 24 hours, Hoechst dye (10μg/ml) was added to the wells and the cells incubated at 37°C for 15 minutes. The levels of mCherry were collected using the Arrayscan VTI High Content Screening instrument (Thermo Fischer Scientific). Individual cells were identified by Hoescht nuclear staining. The percentage threshold of mCherry was measured against a DMSO vehicle control. **(A.)** 17-AAG significantly increased HSF1 activity in HEK-HSE cells in comparison to the DMSO vehicle control (1/000). **(B.)** Depiction of mCherry levels in DMSO vehicle control (1/2000) and 17-AAG (5 μM**)** treated cells from the Arrayscan VTI High Content Screening instrument. Scale bar- 100μM. The data is shown as mean ± SEM of four independent experiments. Statistical analysis by unpaired t-test (2 tailed). *** $p \leq 0.001$.

17-AAG Treatment Increases HSP72 Protein Expression

A. RAW264.7 Cells
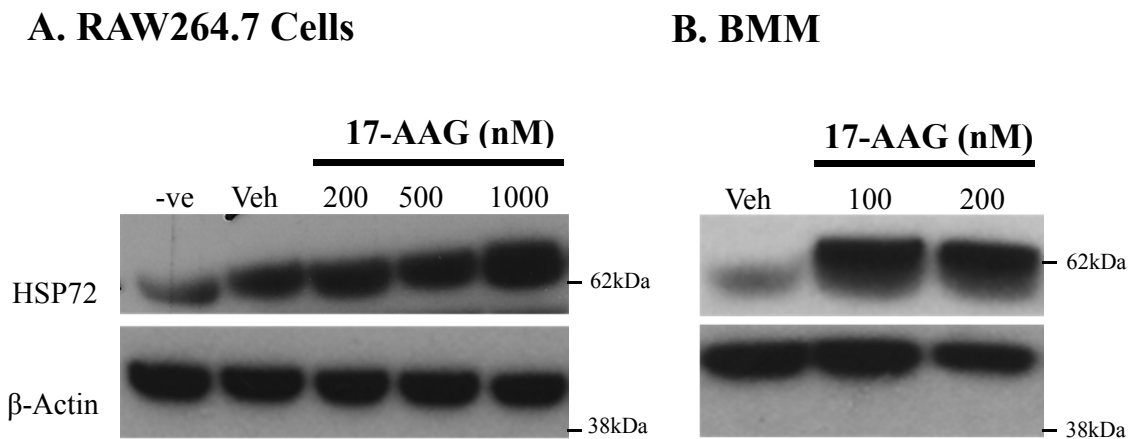
B. BMM

Figure 4.2

(A.) RAW264.7 cells were seeded at 2 x 10^5 cells in 35mm diameter culture wells and were allowed to settle overnight. The cells were then treated with 17-AAG (200, 500 or 100nM) and DMSO (1/10,000) as a DMSO vehicle control. **(B.)** BMM were prepared by incubating bone marrow in LCM media for 3 days prior to treatment. The BMM were then treated with treated with 17-AAG (100 and 200nM) or DMSO vehicle control (1/10,000). **(A-B.)** The cells were lysed and protein expression levels of the stress inducible isoform of HSP70, HSP72 was examined by immunoblot. Briefly, after the lysates were resolved on SDS-page gels and protein transferred the membrane was incubated in primary HSP72 ab (1:2000 at 4°C overnight) followed by a HRP secondary antibody (1:5000 for 1 hr at room temperature). The film was developed using Roche Chemiluminescent reagent. 17-AAG increased HSP72 protein levels at 24 hours in both RAW264.7 cells and in BMM relative to the DMSO vehicle control. Western blots were performed at least 2 times with different RAW264.7 cell isolates.

with NVP-AUY922 (5, 10 and 20nM) for 24 hours. Cells were stained with nuclear dye Hoechst (10μg/ml) and mCherry levels were quantified as previously described. NVP-AUY922 treatment significantly increased mCherry reporter activity in a dose-dependent manner in comparison to the DMSO vehicle control, showing increased HSF1 activity (Figure. 4.3 A-B.).

To confirm that NVP-AUY922 causes a cell stress response in RAW264.7 cells and BMM, these cells were treated with NVP-AUY922 and HSP72 protein levels were investigated by immunoblotting. RAW264.7 cells were treated with NVP-AUY922 (10, 20 or 50nM) for 24 hours. In addition, primary BMM were treated with NVP-AUY922 (2 and 5nM). Consistent with the HEK-HSE cells, NVP-AUY922 treatment increased HSP72 protein expression in RAW264.7 in a dose-dependent manner. NVP-AUY922 (10nM) maximally increased HSP72 protein expression (Figure 4.4 A.). A decrease in HSP72 levels in response to NVP-AUY922 at the higher concentrations, of 20 and 50nM, was noted. This may be due to the fact that at these concentrations, the stress response had peaked and was either being resolved or the cells were entering apoptosis. If so, one might expect that at a 12 hour time point NVP-AUY922 (20nM and 50nM) would increase HSP72 protein levels higher than that of 10nM. In BMM, NVP-AUY922 also increased HSP72 expression at 24 hours relative to the DMSO vehicle control (Figure 4.4 B.). Note that different sensitivities of the two cell types may reflect different tolerances or the degree to which the cells take up the drug. Thus, NVP-AUY922 increased HSP72 expression in both RAW264.7 and mouse primary BMM.

4.2.2 Pharmacological Inhibition of HSF1 Blocked the 17-AAG and NVP-AUY922 Mediated Increase in Osteoclast Formation

As described in Chapter 3 (Figures 3.3-3.5, 3.11 and 3.12), 17-AAG and NVP-AUY922 both increase RANKL-driven osteoclast differentiation in the RAW264.7 cell line model as well as from bone marrow progenitors. To establish a role for HSF1 in the stimulation of osteoclast formation by 17-AAG three approaches were employed: pharmacological inhibition of HSF1, HSF1 knockdown by shRNA, and HSF1 null mice. Heat Shock Protein Inhibitor I (KNK437), a benzylidene lactam compound, is a HSF1 pharmacological inhibitor that decreases the heat shock response in cells (Yokota *et al.*, 2000). KNK437 inhibition of HSF1 decreases the heat shock response by suppressing the induction of multiple HSPs including: HSP105, HSP40 and the stress inducible form of HSP70, HSP72

NVP-AUY922 Treatment Increases HSF1 Transcriptional Activity in HEK-HSE Cells

A.

B.

Veh   **NVP-AUY922**
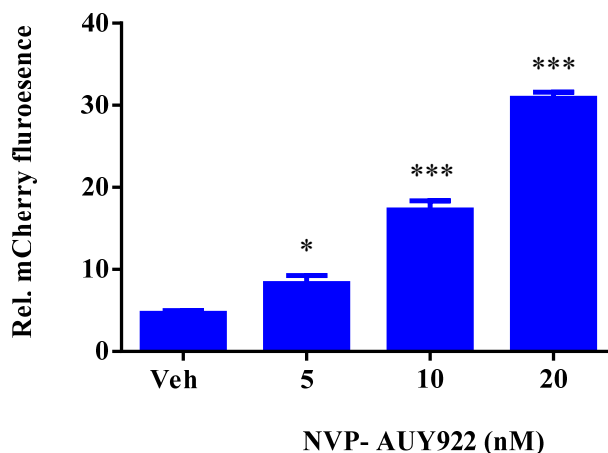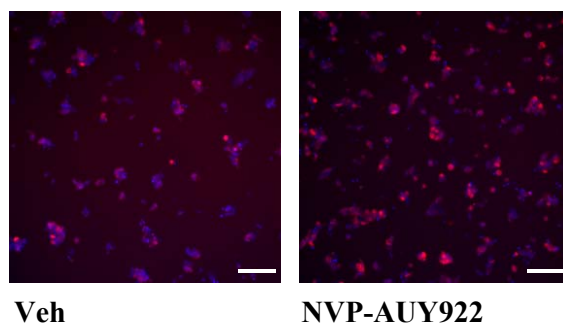
Figure 4.3

(A-B.) HEK-HSE cells, stably transfected with a mCherry HSE reporter driven by a HSP70B promoter, were seeded at 2.5x 10^4 cells in 6mm diameter wells in DMEM phenol red-free media. The cells were allowed to settle for $\geq$ 3 hours and then were treated with NVP-AUY922 (5, 10 and 20 nM) or vehicle DMSO (1/2000) as a control. At 24 hours, Hoechst dye (10μg/ml) was added to the wells and the cells incubated at 37°C for 15 minutes. The levels of mCherry were collected using an Arrayscan VTI High Content Screening instrument (Thermo Fischer Scientific). Individual cells were identified by Hoescht nuclear staining. The percentage threshold of mCherry was measured against the DMSO vehicle control, which was used as a reference. **(A.)** NVP-AUY922 treatment dose-dependently increased HSF1 activity in the HEK-HSE reporter cells.**(B.)** Images of mCherry levels in DMSO vehicle control (1/2000) and NVP-AUY922 (10nM) treated cells from the Arrayscan VTI High Content Screening instrument. Scale bar - 100μM. The data is shown as mean ± SEM of three independent experiments. Statistical analysis was performed by using ANOVA, Dunetts post *hoc* test. * p $\leq$ 0.05, *** p $\leq$ 0.001.

NVP-AUY922 Treatment Increases HSP72 Protein Expression in RAW264.7 Cells and BMM

A. RAW264.7 Cells

B. BMM
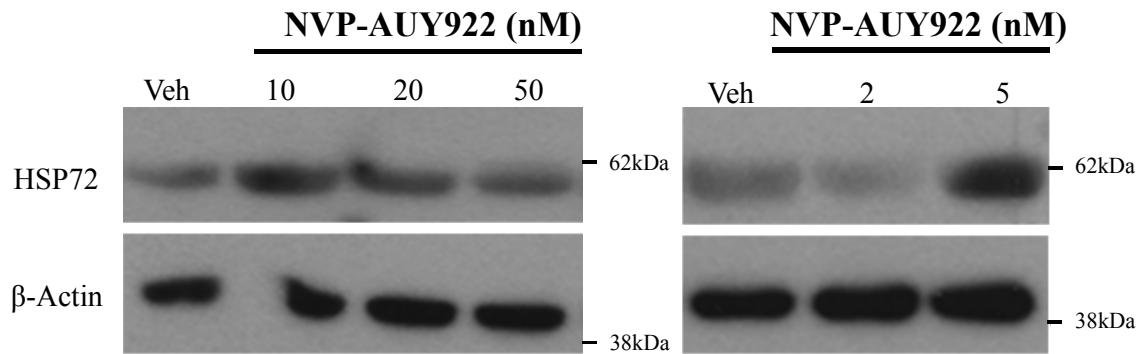
Figure 4.4

(A.) RAW264.7 cells were seeded at 2 x 10^5 cells in 35mm diameter culture wells and were allowed to settle overnight. The cells were then treated with NVP-AUY922 (5, 10 and 20nM) or DMSO vehicle control (1/10,000). **(B.)** BMM were prepared by incubating bone marrow in LCM media for 3 days prior to treatment. The bone marrow macrophages were then treated with NVP-AUY922 (2 or 5nM) or DMSO vehicle control (1/10,000) for 24 hours **(A-B.)** Protein (30µg) from the cell lysate was run on a reducing SDS-PAGE gel and transferred to PVDF membrane. The membrane was immunoblotted for HSP72 (1:2000 at 4 °C overnight). **(A.)** NVP-AUY922 increased HSP72 protein expression relative to the DMSO vehicle control **(B.)** Likewise NVP-AUY922 increased HSP72 protein levels in BMM in comparison to the DMSO vehicle control. Western blots were performed at least 2 times with different RAW264.7 cell isolates.

(Yokota *et al.*, 2000). Ohnishi *et al*, showed that KNK437 inhibits HSF1 actions by interrupting binding of HSF1 to HSE elements present in the promoters of target genes i.e., HSPs (Manwell and Heikkila, 2007; Ohnishi *et al.*, 2004). KNK437 is thought to be more specific than the HSF1 inhibitor, quercertin, which acts to decrease HSF1 but can affect other factors in the cell such as protein kinases (Yokota *et al.*, 2000; Koishi *et al.*, 2001; Manwell and Heikkila, 2007).

To investigate the hypothesis that 17-AAG enhances osteoclast formation in a HSF1 dependent manner, osteoclast assays were performed using RAW264.7 and bone marrow cells. Firstly, the concentrations of KNK437 that are non-toxic to RAW264.7 cells were determined by kill curves (Appendix Figure B2). RAW264.7 cells tolerated concentrations up to KNK437 (20μM) over a 6 day period. Based on the results KNK437 (10μM) was used as the standard KNK437 concentration to inhibit HSF1. Secondly, the effect of KNK437 upon RAW264.7 and bone marrow osteoclast formation were observed. RAW264.7 cells (10^4 cells in 6mm diameter wells) and bone marrow (10^5 cells in 6mm diameter wells) were treated with KNK437 (2, 5, 10, 20μM and 2, 4, 6, 8 and 10μM, respectively) over a 6 day period. Osteoclast quantitation by counting multinucleated TRAP positive cells showed that KNK437 did not affect osteoclastogenesis relative to the DMSO vehicle control in both RAW264.7 and in bone marrow cells (Appendix Figure B5).

To determine whether 17-AAG increases osteoclast formation in a HSF1 dependent manner, Bone marrow cells isolated from the tibia of mice (Chapter 2.3.1) were cultured 10^5 cells in 6mm diameter wells and stimulated with treated with RANKL (20ng/ml) and M-CSF (30ng/ml). BMM were treated with 17-AAG (100nM) in the presence or absence of KNK437 (10μM). As method negative controls, some bone marrow cells did not receive RANKL stimulation and were classed as untreated (-ve control). As further controls, cultures treated with RANKL plus appropriate levels of vehicle (1/4000 DMSO) and with RANKL plus KNK437 (10μM) were included. 17-AAG treatment increased bone marrow cell osteoclast formation relative to the DMSO vehicle control, as previously described. However, the addition of KNK437 (10μM) ablated the increased osteoclast numbers caused by 17-AAG (Figure 4.5). KNK437 (10μM) treatment alone in the presence of RANKL (20ng/ml) did not affect osteoclast formation (Figure 4.5). In a similar manner, the effect of pharmacologically inhibiting HSF1 was studied upon 17-AAG treated RAW264.7 cells. RAW264.7 cells (10^4 cells in 6mm diameter wells) were cultured in the presence of RANKL (20ng/ml) and were

treated with 17-AAG (200nM). These cultures where then treated in the presence or absence of the HSF1 inhibitor, KNK437 (10μM). On day 6, osteoclast formation was examined. Initial experiments showed, as previously described, 17-AAG concentrations increased osteoclast formation relative to the DMSO vehicle control (Appendix Figure B6). However, addition of KNK437 (10μM) ablated the 17-AAG mediated increase in osteoclast formation (Appendix Figure B6). Osteoclast numbers in cultures treated with KNK437 and 17-AAG was comparable to those in DMSO vehicle control cultures. KNK437 (10μM) treatment alone did not affect osteoclast formation in the absence of 17-AAG treatment (Appendix Figure B6).

In the previous chapter NVP-AUY922 like 17-AAG was shown to increase osteoclast formation in both RAW264.7 and bone marrow cell cultures stimulated with RANKL (20ng/ml). Figures (4.3-4.4) demonstrate NVP-AUY922 treatment causes an HSF1 mediated cell stress response through both increased HSE activity and the increased production of HSP72 protein levels. To determine whether inhibiting HSF1 would affect the NVP-AUY922-mediated increase in osteoclast formation, RAW264.7 and bone marrow cells were treated with NVP-AUY922 in the presence or absence of HSF1 inhibitor KNK437. RANKL (20ng/ml) stimulated RAW264.7 and mouse bone marrow cell cultures were treated with NVP-AUY922 (5nM), which significantly increased osteoclast formation compared to the DMSO vehicle control (Figure 4.6). In the presence of KNK437 (10μM), the NVP-AUY922-driven increase in osteoclast numbers was ablated to osteoclast numbers similar to that in the DMSO vehicle control (Figure 4.6). This occurred in both RAW264.7 and bone marrow cells. KNK437 (10μM) treatment alone, in the absence of HSP90 inhibitors, did not affect osteoclast formation, as previously noted.

KNK437 Abolishes the 17-AAG Mediated Increases in Osteoclast Formation
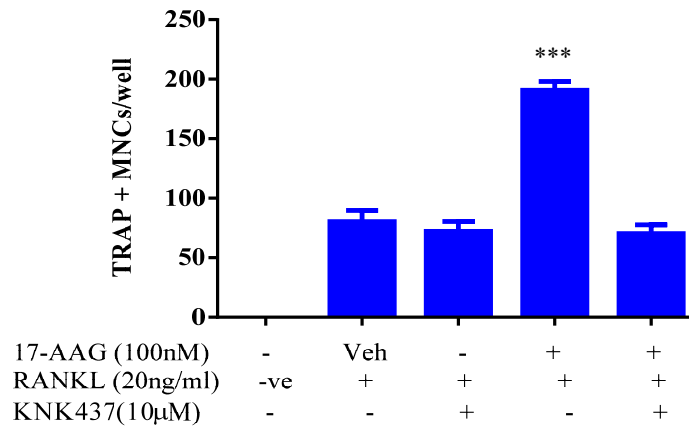
Figure 4.5

Bone marrow cells, seeded at 10^5 cells in 6 mm diameter wells, were stimulated with RANKL (20ng/ml) and M-CSF (30ng/ml). The cells were then treated with 17-AAG (200nM) in the presence or absence of KNK437 (10µM). 17-AAG (200nM) treatment increases osteoclast formation as previously observed. Adding KNK437 (10µM) to inhibit HSF1 abolished the 17-AAG mediated increase in osteoclast numbers to DMSO vehicle control levels (1/4000). The data is expressed as mean ± SEM of four independent experiments. Statistical analysis was performed by ANOVA, Dunnett's *post hoc* test. *** $p \leq 0.001$ relative to DMSO vehicle control.

Inhibiting HSF1 Abolishes the NVP-AUY922 Mediated Increase in Osteoclast Formation

A.

B.

NVP-AUY922 (5nM)	-	Veh	-	+	+
RANKL (20ng/ml)	-ve	+	+	+	+
KNK437(10μM)	-	-	+	-	+

NVP-AUY922 (5nM)	-	Veh	-	+	+
RANKL (20ng/ml)	-ve	+	+	+	+
KNK437(10μM)	-	-	+	-	+
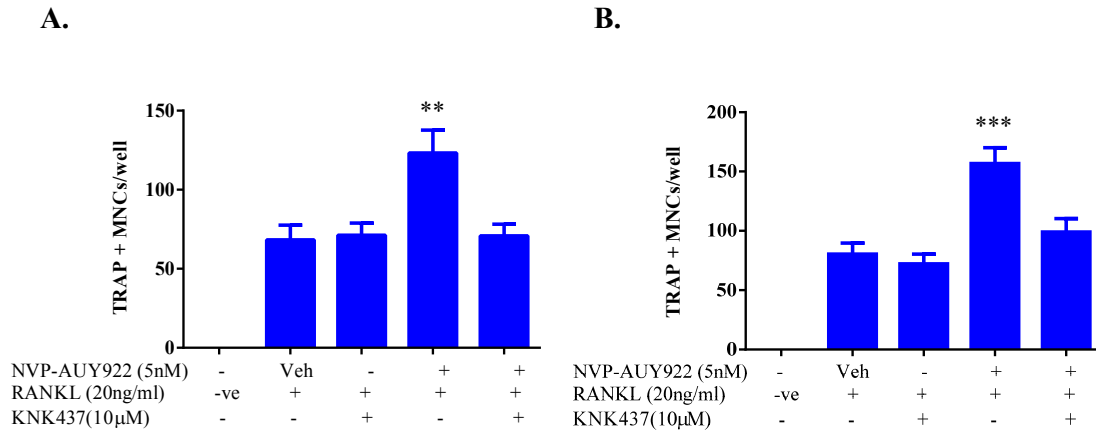
Figure 4.6

(A-B.) (A.) RAW264.7 cells were seeded at 10^4 cells and **(B.)** bone marrow cells at 10^5 cells in 6 mm diameter wells in the presence of RANKL (20ng/ml) and RANKL (20ng/ml) and M-CSF (30ng/ml) respectively. The cells were treated with NVP-AUY922 (5nM) in the presence or absence of KNK437 (10μM). NVP-AUY922 5nM treatment significantly increases osteoclast formation in both RAW264.7 cells and bone marrow cells as previously observed. Adding KNK437 (10μM) to inhibit HSF1 abolished the NVP-AUY922 mediated increase in osteoclast numbers to DMSO vehicle control levels (1/4000). The data is shown as mean ± SEM of **(A.)** three and **(B.)** four independent experiments. Statistical analysis was performed by ANOVA, Dunnett's post *hoc* test. ** $p \le 0.01$, *** $p \le 0.001$.

4.2.3 TGF-β Increases Osteoclast Formation Independent of HSF1 Activity

A well-accepted enhancer of RANKL actions on osteoclast formation is TGF-β (Quinn *et al.*, 2001). As previously discussed, TGF-β acts early in the osteoclast differentiation process and has no effects if added after 3 days of culture, which is approximately the time at which the first TRAP^{+} mononuclear cells appear (Figure 3.7) (Quinn *et al.*, 2001). This is in contrast to 17-AAG actions upon osteoclast formation, which are principally exerted at or after day 3 (Figure 3.7). 17-AAG treatment increases osteoclast numbers by acting in the day 3 to day 6 period of osteoclast differentiation (Figure 3.7). This data suggested that the 17-AAG mechanism of increasing osteoclast numbers is different to that of TGF-β. To further compare TGF-β actions to that of the HSP90 inhibitors, RAW264.7 cells were treated with TGF-β (5ng/ml) in the presence or absence of KNK437 (10μM). TGF-β (5ng/ml) treatment increased osteoclast formation as previously observed (Figure 4.7). KNK437 (10μM) treatment did not affect TGF-β enhanced osteoclast numbers (Figure 4.7). These results suggest that HSF1 is not involved in TGF-β actions on osteoclasts and provides further evidence that the mechanism of action HSP90 in osteoclast formation is different to that of TGF-β.

4.2.4 HSF1 Knockdown Eradicates 17-AAG Enhancement of Osteoclast Formation

Since KNK437 is a pharmaceutical compound that may, by definition, have off target effects that affect osteoclasts, the specific effects of HSF1 upon 17-AAG actions in osteoclast formation was studied by a more highly specific targeting of HSF1, by RNA interference (Chai *et al.*, 2014). HSF1 levels were decreased in RAW264.7 cells using a short hairpin microRNA shMir approach (Chai *et al.*, 2014; Nguyen *et al.*, 2013; Lang *et al.*, 2012). RAW264.7 cells were transduced using lentiviral constructs that expressed either a non-silencing shRNAmir (NS) or shRNAmirs 1 to 5, all of the latter having sequence specificity for mouse HSF1 (Lang *et al.*, 2012; Chai *et al.*, 2014; Nguyen *et al.*, 2013). Immunoblot analysis confirmed HSF1 expression was decreased and shRNAmir5 confirmed to be the most effective at decreasing HSF1 proteins levels (Chai *et al.*, 2014; Lang *et al.*, 2012; Nguyen *et al.*, 2013). To test the effect of 17-AAG upon osteoclast formation in cells that had reduced HSF1, further osteoclast assays were performed. Parental RAW264.7 cells, NS and Mir5 cells (seeded at 10^5 in 6mm diameter wells) were treated with RANKL (100ng/ml) in the presence or absence of 17-AAG (200nM). After 6 days, osteoclast numbers were quantified. Both the parental and NS transfected cells exhibited significantly increased osteoclast formation in response to 17-AAG treatment relative to RANKL (100ng/ml)

KNK437 Treatment does not Affect the TGF-β Stimulated Increase in Osteoclastogenesis

RANKL (20ng/ml)	-ve	+	+	+
TGF-β (5ng/ml)	-	-	+	+
KNK437 (10μM)	-	-	-	+
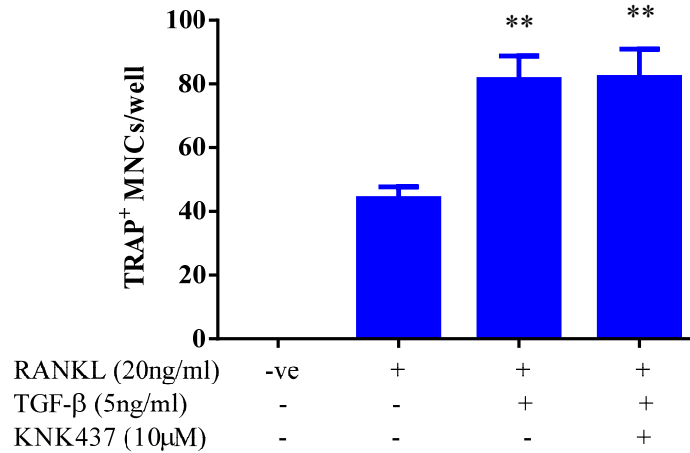
Figure 4.7

RAW264.7 cells were seeded at 10^5 cells in 6mm diameter wells in the presence of RANKL (20ng/ml). The cells were treated with TGF-β (5ng/ml) in the presence or absence of KNK437 (10μM). As a control there was a no treatment negative control i.e. no RANKL treatment, "-ve". As previously described TGF-β treatment enhances osteoclast formation. Inhibiting HSF1 by KNK437 (10μM) treatment does not affect TGF-β stimulated osteoclast differentiation. All data is expressed as mean ± SEM of three independent experiments. Statistical analysis was performed by ANOVA, Dunnett's post hoc test ** p ≤ 0.001.

treatment (Figure 4.8). In contrast, Mir5 cells that have reduced HSF1 levels did not have increased osteoclast numbers in response to 17-AAG treatment (Figure 4.8). This data shows HSF1 is required for 17-AAG ability to increase osteoclast differentiation. Chai *et al.* showed a similar result using the submaximal RANKL (20ng/ml) dose (Chai *et al.*, 2014).

4.2.5 17-AAG Does Not Increase Osteoclastogenesis in Bone Marrow HSF1$^{-/-}$ Cells

In order to study the influence of HSF1 on 17-AAG actions in primary cells, bone marrow cells from HSF1 null mice were employed. This HSF1 knockout mouse line was originally generated and obtained from the Benjamin Laboratory (University of Utah, USA) (McMillan *et al.*, 1998). These mice were maintained at Monash University high barrier animal facility. This mouse strain was maintained on a mixed Balb/c x 129 genetic background. HSF1 mice on other pure strains (such as C57BL6/J) do not produce viable HSF1 knockout mice (Jin *et al.*, 2011). Since HSF1 is required for embryo implantation to proceed, the female knockout mice are infertile. Therefore, female knockouts were used for the experiments described below, and male mice were reserved for breeding (Jin *et al.*, 2011). Mice were crossed HSF1 heterozygote x heterozygote to obtain HSF1-WT, HSF1-Het (heterozygote) and HSF1-KO (HSF1 null) mice. These mice were maintained according to standard husbandry procedures; All procedures were approved by the Monash Animal Research Platform (MARP) 2 Animal Ethics Committee (Clayton, VIC Australia), authorization no. SOBSB/B/2010/28BC.

Bone marrow cells were isolated from female HSF1-WT (HSF$^{+/+}$), HSF1 heterozygotes (HSF$^{+/-}$) and HSF1 null (HSF$^{-/-}$) mice and osteoclast assay performed as previously described. Mouse genotypes were confirmed prior by standard PCR based genotyping assays, which were performed by members of the Price Laboratory. As expected the HSF1-WT cells showed increased osteoclast formation when treated with 17-AAG (25, 50 or 100nM) in comparison to the DMSO vehicle control (Figure 4.9). In contrast, cells from the HSF1 null mice when treated with 17-AAG did not show a significant increase in osteoclast formation significantly above controls (Figure 4.9). These results indicate that osteoclasts were still able to form in the absence of HSF1 but 17-AAG treatment was not able to enhance osteoclast formation. HSF1 heterozygote cells showed minimal response to 17-AAG treatment. Importantly Dr Ryan Chai showed 17-AAG induced MITF is dependent upon HSF1 induction (Chai *et al.*, 2014). Inhibiting HSF1 with KNK437 decreased the 17-AAG

Silencing HSF1 Ablates the 17-AAG Mediated Increase in Osteoclast Formation
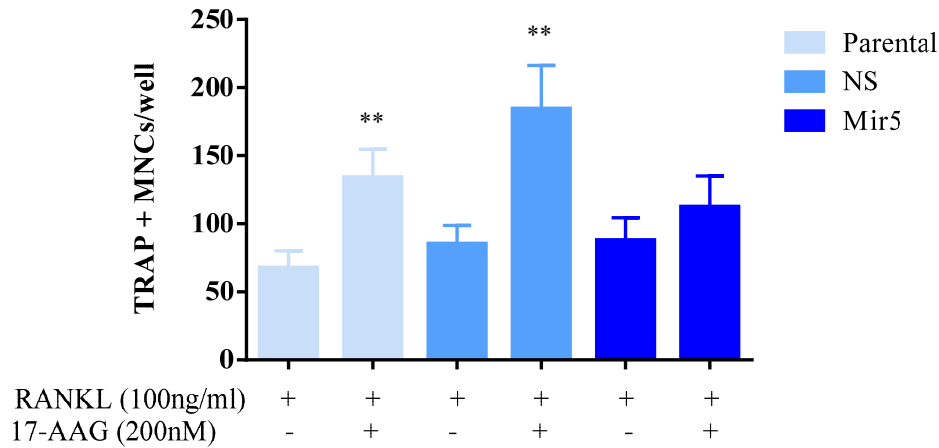
Figure 4.8

RAW264.7 cells were transduced with lentiviral vectors' containing non-silencing (NS mir) or HSF1 targeting shRNAmir (Mir5) constructs (performed by Price laboratory members). These cells and parental cells, seeded at 10^4 in 6mm diameter wells, were treated with RANKL (100ng/m)l in the presence or absence of 17-AAG (200nM) for 6 days. On day 6, osteoclast numbers were quantified. 17-AAG treatment significantly increased osteoclast differentiation in both the Parental and NS cells. In contrast, osteoclast differentiation was not increased in Mir 5 cells in response to 17-AAG treatment. Statistical analysis was performed using t tests between RANKL and RANKL+17-AAG. All data is expressed as mean ± SEM of four independent experiments, ** $p \leq 0.001$.

17-AAG Treatment does not Increase Osteoclast Formation in HSF1$^{-/-}$ Bone Marrow Progenitor Cells
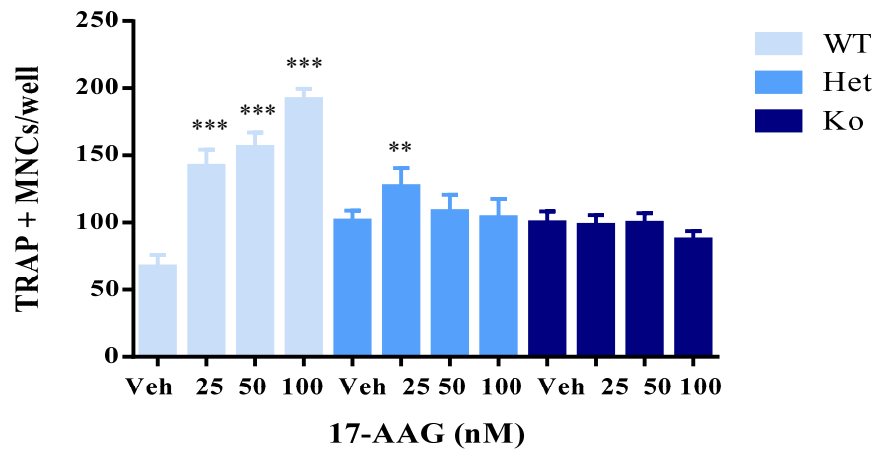
Figure 4.9

Bone marrow cells were isolated from mouse tibia of HSF1 WT, HET and KO and were seeded at 10^5 cells in 6mm diameter culture wells in media containing RANKL (20ng/ml) and M-CSF (30ng/ml). The cells were then treated with 17-AAG (25, 50 and 100nM) for 6 days and then were immuno-histochemically stained with TRAP stain 17-AAG increases osteoclast formation in WT mice; however, heterozygote HSF1$^{+/-}$ mice bone marrow cells responded to 17-AAG treatment minimally. 17-AAG treatment did not increase osteoclast formation from KO HSF1$^{-/-}$ mice bone marrow progenitor cells. The data is expressed as the mean ± SEM of three independent experiments. Statistical analysis was performed using ANOVA, Tukey's post hoc test. ** $p \leq 0.01$ *** $p \leq 0.001$ relative to DMSO vehicle control.

HSF-1 Regulates 17-AAG Induced MITF Protein Expression

A.
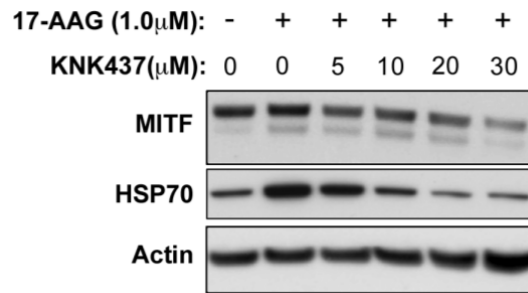
B.
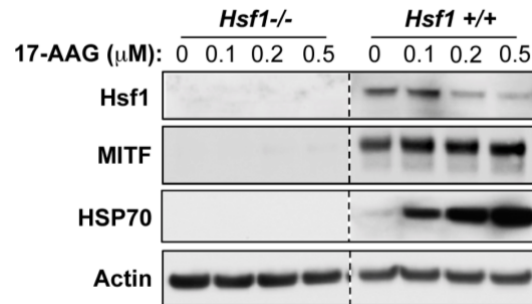
Figure 4.10

(A.) RAW264.7 cells were treated with a range of KNK-437 concentrations (0, 5, 10, 20 and 30μM) in the presence of 17-AAG (1μM) for 24 hours. Protein was extracted and immunoblot analysis of MITF and HSP70 performed. HSF1 inhibition by KNK437 ablated 17-AAG-induced MITF and Hsp70 protein levels after 24hrs. **(B.)** BMM derived from HSF1$^{-/-}$ and HSF1$^{+/+}$ mice were treated with M-CSF (30ng/ml) and indicated concentrations of 17-AAG for 24 hrs. Protein was extracted and immunoblot analysis performed. HSF1$^{-/-}$ BMM showed lower MITF protein expression both with and without 17-AAG. Data used with permission from Dr Ryan Chai (Chai *et al.*, 2014).

mediated induction of MITF in in a dose dependent manner (Figure 4.10) (Chai *et al.*, 2014). Moreover, 17-AAG treatment had lower MITF protein expression in BMM from HSF1^{-/-} mice (Figure 4.10) (Chai *et al.*, 2014). This data suggests that 17-AAG induction of the HSR leads to increased MITF expression with subsequently increased osteoclastogenesis (Chai *et al.*, 2014). Data (Figure 4.10) used with permission from Dr Ryan Chai, see (Chai *et al.*, 2014).

4.2.6 17-AAG and NVP-AUY922 Phosphorylate MAP Kinase p38

Since N-terminal HSP90 inhibitors, 17-AAG and NVP-AUY922 induced HSP72 levels, i.e., cause a HSR, it is possible that these compounds may also affect other cell stress-induced molecules within the cell. One significant stress-responsive pathway in the cell is the p38 signalling cascade. This pathway is activated by phosphorylation in response to stimuli such as UV irradiation, heat shock, osmotic stress, inflammatory cytokines and chemotherapeutics (Chapter 1.8.2) (Zarubin and Han, 2005; Wagner and Nebreda, 2009; Junttila *et al.*, 2008). p38 is an essential mediator in osteoclast formation as its blockade ablates all effects of RANKL on osteoclast progenitor differentiation (Matsumoto *et al.*, 2000). p38 is activated by phosphorylation from "upstream" kinases such as MKK3, MKK6 and sometimes MMK4 (Brancho *et al.*, 2003; Wagner and Nebreda, 2009). In addition, p38 can be activated through TAB1 recruitment to RANK cytoplasmic tails (Chapter 1.5.3.2) (Cuenda and Rousseau, 2007; Ge *et al.*, 2002). This activated p38 then phosphorylates a number of substrates, which includes MITF and HSP27 (Mansky *et al.*, 2002a; Xu *et al.*, 2006). For these reasons, effects of 17-AAG and NVP-AUY922 upon p38 phosphorylation, and of p38 inhibition, were investigated.

RAW264.7 cells were treated with the following stimuli: RANKL (100ng/ml) + DMSO vehicle (DMSO, 1/10,000), 17-AAG (1µM) and co-treatment with RANKL (100ng/ml) + 17-AAG (1µM). As negative controls, cells were untreated or treated only with DMSO vehicle control. After cell stimulation, cells were lysed at 2, 5, 10, 20, 30, and 60 minutes. As previously established, RANKL strongly phosphorylated p38. This was observed very rapidly by 2 minutes with maximal phosphorylation occurring between 2 to 10 minutes (Figure 4.11). At and beyond 20 minutes, the phosphorylation signal reduced dramatically, and after 60 minutes the phosphorylation levels were back to baseline. 17-AAG treatment of RAW264.7 cells also increased p38 phosphorylation relative to the DMSO vehicle control (Figure 4.11). Like RANKL, the kinetics of 17-AAG actions on p38 was rapid like that of RANKL, with

p38 being phosphorylated at 2 minutes and maximal phosphorylation between 2 to 10 minutes (Figure 4.11). After 10 minutes the phosphorylation signal started to wane and at 60 minutes p38 phosphorylation was at or close to DMSO vehicle control levels. In the co-treatment of RANKL (100ng/ml) + 17-AAG (1μM) samples, p38 was activated; however, variation of p38 phosphorylation levels was seen in the additive effect (Figure 4.11). It is possible the combination treatment changes the kinetics, having a mainly additive effect in the initial stages of p38 activation.

To determine whether NVP-AUY922 has similar effects upon p38 phosphorylation, RAW264.7 cells were treated with NVP-AUY922 (100nM), RANKL (100ng/ml) + DMSO (1/10,000) or co-treatment of RANKL (100ng/ml) + NVP-AUY922 (100nM) for 2, 5, 10, 20, 30 and 60 minutes, as for 17-AAG treatment experiments above. As in the 17-AAG experiments, both RANKL and NVP-AUY922 treatments, singularly and in combination, increased p38 phosphorylation (Figure 4.12). Activation of p38 was evident at 2 minutes, and maximal phosphorylation was observed between 2 to 10 minutes with NVP-AUY922 treatment, which is similar to that described above for 17-AAG treatments. Combination treatment of NVP-AUY922 and RANKL phosphorylated p38 also increased phosphorylation levels above that of the DMSO vehicle control; however, the kinetics of p38 activation in the combination treatment is not fully clear (Figure 4.12).

4.2.7 KNK437 Treatment Does Not Decrease N-terminal HSP90 Inhibitor-mediated Phosphorylation of MAP Kinase p38

To determine whether HSF1 inhibition influences the actions of RANKL, NVP-AUY922-, and 17-AAG-induced p38 phosphorylation, RAW264.7 cells were examined in the presence or absence of KNK437 treatment. RAW264.7 cells were pre-treated for 24 hours with KNK437 (10μM) or DMSO vehicle control (1/4000). The RAW264.7 cells were maintained in medium containing 10% FBS plus or minus KNK437 (10μM) for 12 hours. The following 12 hours, the cells were treated in serum-free media. After 24 hours of KNK437 treatment, the cells were treated with NVP-AUY922 (100nM), 17-AAG (1μM) or RANKL (100ng/ml) in the presence or absence of KNK437 (10μM) for 5, 10, 20, 30 and 60 minutes. As a control, a DMSO vehicle control (1/1000) matched to KNK437 concentration was used. In addition an untreated negative control ("–ve") was also included. NVP-AUY922, 17-AAG and RANKL treatment all increased phosphorylation of p38 as previously observed and described above. The kinetics of p38 phosphorylation was similar regardless of KNK437 treatments

17-AAG Treatment Induces p38 Phosphorylation in RAW264.7 Cells
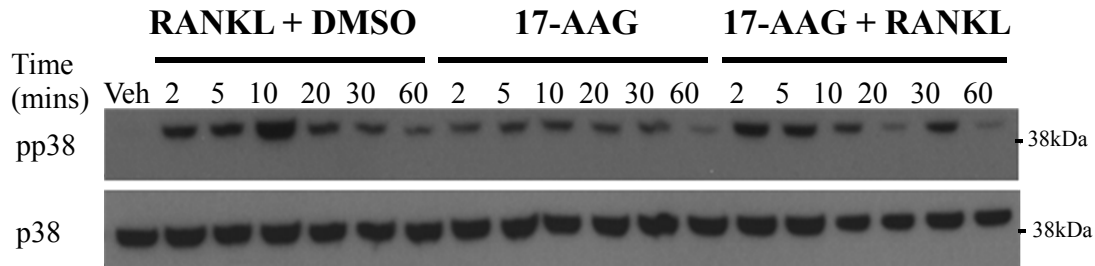
Figure 4.11

RAW264.7 cells were seeded at 10^6 cells in 35mm diameter culture wells and were allowed to adhere until they were serum starved the following night. The cells were treated with 17-AAG (1µM), RANKL (100ng/ml) and DMSO (1/1000), or 17-AAG (1µM) and RANKL (100ng/ml) combination treatment for 2, 5, 10, 20, 30, and 60 minutes. Cells were lysed according to the phosphorylation lysates protocol. Phosphorylated p38 protein levels were examined by immunoblot using the Tyr and Thre phospho p38 Rabbit Ab primary antibody (Cell Signalling) (1:1000 overnight at 4°C). As previously described RANKL treatment causes phosphorylation of p38. Likewise, 17-AAG treatment induces p38 phosphorylation relative to the DMSO vehicle control. Total p38 levels were not affected by treatments with 17-AAG, RANKL and DMSO or RANKL + 17-AAG combination treatments. Immunoblots were performed 2 times with independent lysates from different RAW264.7 cell isolates.

NVP-AUY922 Induces p38 Phosphorylation in RAW264.7 Cells
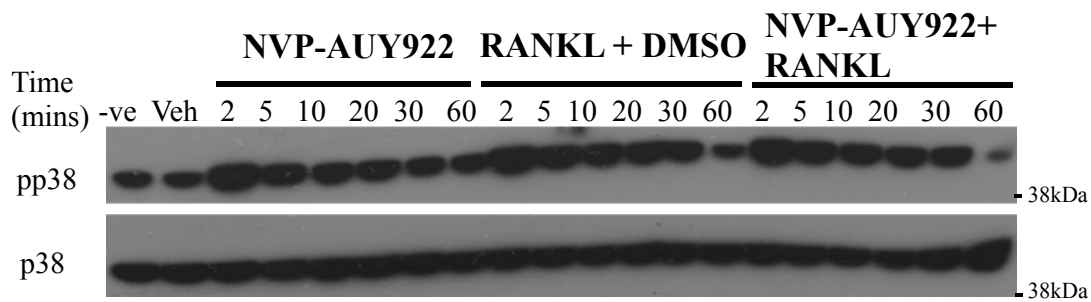
Figure 4.12

RAW264.7 cells were seeded at 10^6 cells in 35mm diameter culture wells and were allowed to adhere until they were serum starved the following night. The cells were treated with NVP-AUY922 (100nM), RANKL (100ng/ml) and DMSO (1/10,000) or combination treatment of NVP-AUY922 (100nM) and RANKL (100ng/ml) for 2, 5, 10, 20, 30, and 60 minutes. Cells were lysed according to the phosphorylation lysates protocol. The lysates were resolved on SDS-gels and immunoblotted for phospho p38 by using anti- phosphor-Tyr/Thre antibody (Cell Signalling) (1:1000 overnight at 4°C). NVP-AUY922 treatment induces the phosphorylation of p38. Total p38 levels were not affected by treatments with: NVP-AUY922, RANKL or RANKL+ NVP-AUY922 co-treatment. Immunoblots were performed with three different independent sets of lysates from RAW264.7 cell isolates.

(Figures 4.13 and 4.14). KNK437 treatment did not decrease the 17-AAG or NVP-AUY922 induced p38 phosphorylation (Figures 4.13 and 4.14). The role of HSF1 in p38 phosphorylation was also examined using a slightly different protocol, where KNK437 was added 1 hour before NVP-AUY922 and 17-AAG treatment. RAW264.7 cells were serum-starved for 12 hours followed by 1 hour pre-treatment of KNK437 (10μM). This approach would only cause the inhibition of HSF1 activity and not downstream transcriptional targets, which might be affected by a longer KNK437 exposure. However, pre-treatment with KNK437 for only 1 hour still did not affect 17-AAG nor NVP-AUY922-elicited phosphorylation of p38 (data not shown).

4.2.8 Inhibiting HSF1 Does Not Decrease RANKL-mediated Phosphorylation of p38

As the *Rankl* gene has a HSE, the effect of HSF1 inhibition upon RANKL mediated p38 phosphorylation was also examined (Roccisana *et al.*, 2004). RAW264.7 cells were pre-treated with KNK437 (10μM) for 24 hours as previously outlined for both 17-AAG (1μM) and NVP-AUY922 (100nM). The cells were then treated with RANKL (100ng/ml) in the absence or presence of KNK437 (10μM) for 60 minutes. Inhibiting of HSF1 and its downstream effectors through KNK437 did not decrease RANKL mediated p38 phosphorylation (Figure 4.15).

The Effect of KNK437 Treatment 17-AAG Mediated p38 Phosphorylation
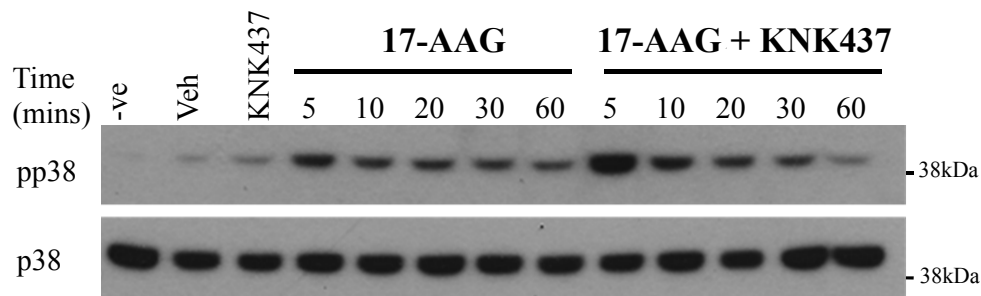
Figure 4.13

RAW264.7 cells were seeded at 10^6 cells in 35mm diameter culture wells and were left to adhere overnight. The cells were treated with plus or minus KNK437 (10µM) for 12 hours in full serum containing media followed by a further 12 hours of treatment whilst being serum starved. After 24 hours of KNK437 (10µM) treatment, the cells were then treated with 17-AAG (1µM) for 5, 10, 20, 30 and 60 minutes. Cells were lysed according to the phosphorylation lysate protocol. The lysates were resolved on SDS- gels and immunoblotted for phospho p38 using the anti-phospho-Tyr/Thre p38 Ab primary antibody (1:1000 overnight at 4°C) (Cell Signalling). 17-AAG treatment induced p38 phosphorylation on Tyr and Thre residues relative to the DMSO vehicle control (1/4000). The addition of KNK437 treatment did not decrease 17-AAG ability to induce p38 phosphorylation. Total p38 levels were not affected by 17-AAG or KNK437 treatment. Western blots were performed three times with independent lysates samples from different RAW264.7 cell lysates.

The Effect of KNK437 upon NVP-AUY922 Mediated p38 Phosphorylation
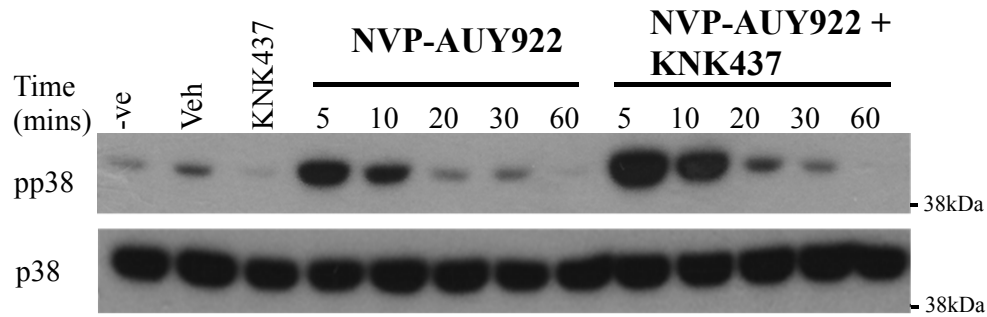
Figure 4.14

RAW264.7 cells were seeded at 10^6 cells in 35mm diameter culture wells and were left to settle overnight. The cells were treated with plus or minus KNK437 (10μM) for 12 hours in full serum media followed by a further 12 hours of treatment whilst being serum starved. After 24 hours of KNK437 (10μM) treatment, the cells were then treated with NVP-AUY922 (100nM) for 5, 10, 20, 30 and 60 minutes. Cells were lysed according to the phosphorylation lysates protocol. The lysates were resolved on SDS- gels and immunoblotted for phospho p38 using the phosphor-Tyr and -Thre p38 Ab primary antibody (1:1000 overnight at 4°C) (Cell Signalling). NVP-AUY922 treatment induces p38 phosphorylation relative to the DSMO vehicle control as shown previously. The addition of KNK437, to NVP-AUY922 treatment did not decrease NVP-AUY922 mediated induction of p38 phosphorylation. Total p38 protein expression was not affected by NVP-AUY922 or KNK437 treatment. Immunoblots were performed 3 times with independent RAW264.7 lysate samples.

The Effect of KNK437 upon RANKL Mediated p38 Phosphorylation
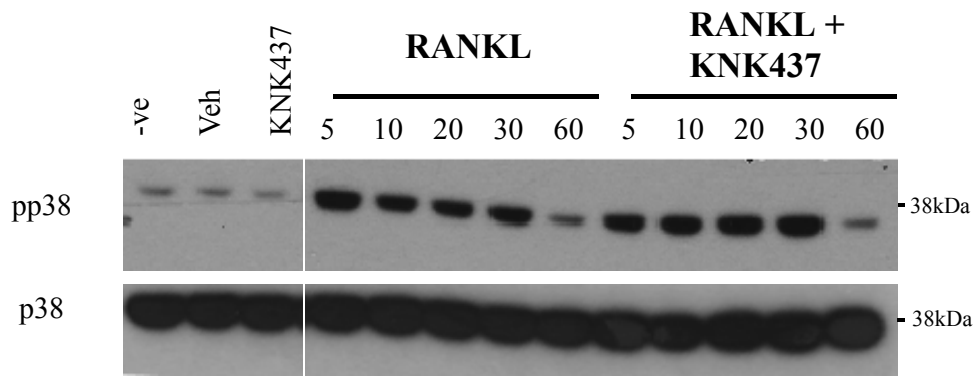
Figure 4.15

RAW264.7 cells, seeded at 10^6 cells in 35mm diameter culture wells, were left to settle overnight. The cells were treated with plus or minus KNK437 (10µM) for 12 hours in full serum media followed by a further 12 hours of treatment whilst being serum starved. After 24 hours of KNK437 (10µM) treatment, the cells were then treated with RANKL (100ng/ml) for 5, 10, 20, 30 and 60 minutes. Cells were lysed according to the phosphorylation lysates protocol and the lysates were immunoblotted for phospho p38 (Tyr and Thre phospho Rabbit Ab primary antibody (Cell Signalling) (1:1000 overnight at 4°C). Addition of KNK437 to RANKL treatment did not decrease the RANKL mediated activation of p38. Immunoblots were performed four times with independent samples from RAW264.7 cell isolates.

4.2.9 P38 Inhibition Decreases MITF Protein Levels

Mansky *et al.* have previously observed RANKL-mediated MITF protein expression is dependent upon p38 phosphorylation (Mansky *et al.*, 2002a). This raises the possibility that p38 activation similarly plays a role upon HSP90 inhibitor induced MITF and HSP72 protein expression. To investigate this possibility, the well-characterised and highly specific p38 inhibitor SB203580 was used (Barančík *et al.*, 2001; Birkenkamp *et al.*, 2000). RAW264.7 cells were either untreated or treated with SB203580 (10μM) for 1 hr, followed by 17-AAG (500nM) and NVP-AUY922 (5nM) treatment. Both untreated controls and a DMSO vehicle control were included as well as cultures treated with SB203580 alone. Cells were treated for 48 hours after which the cells were lysed. As previously found 17-AAG (500nM) increased MITF protein expression at 48 hours (Figure 4.16 A.). SB203580 treatment greatly reduced the 17-AAG mediated increase in MITF protein expression levels (Figure 4.16 A). However, inhibition of p38 by SB203580 treatment alone also decreased MITF protein expression below control levels, which suggested that p38 activity may be required for 'basal' (or unstimulated cell) MITF protein levels in these the cells (Figure 4.16). Treating RAW264.7 cells with NVP-AUY922 (5nM) increased MITF protein expression, as previously shown Inhibition of p38 decreased this elevated MITF protein expression at 48 hours (Figure 4.16 B.). Likewise SB203580 treatment decreased MITF basal levels.

Inhibiting p38 Abolishes the 17-AAG- and NVP-AUY922-Mediated Increase in MITF Protein Levels

A.

B.
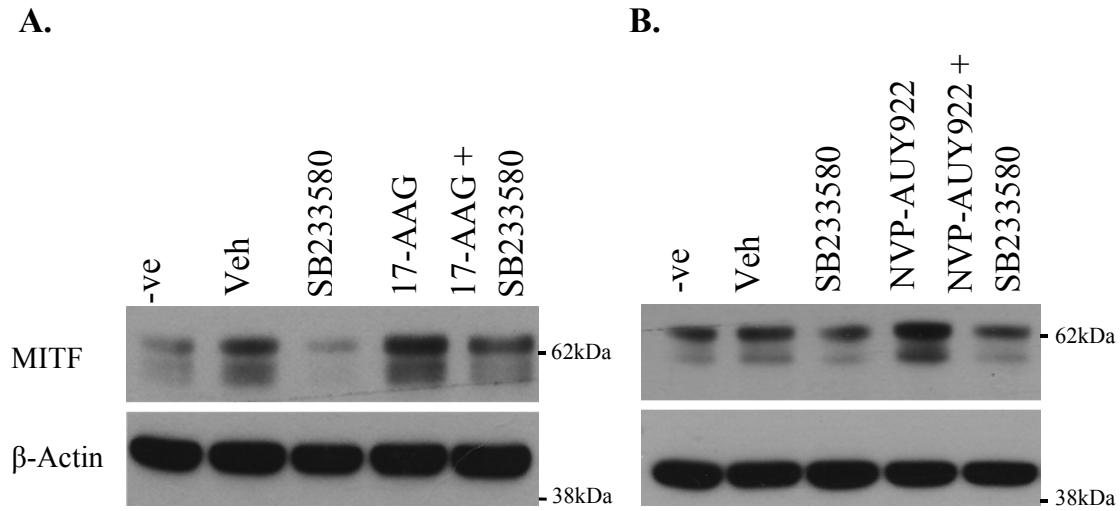
Figure 4.16

(A.) 17-AAG **(B.)** NVP-AUY922 **(A-B.)** RAW264.7 were seeded at 2 x 10^6 cells in 35 mm diameter culture well and were left to adhere overnight. The cells were treated plus or minus SB203580 (10 µM) for 1 hr before being treated with **(A.)** 17-AAG (500nM) or **(B.)** NVP-AUY922 (5nM) (in the presence or absence of SB203580) for 48 hours. The cells were lysed and resolved on SDS-page gels before being immunoblotted for MITF (1:5000, 4°C overnight). **(A-B.)** 17-AAG and NVP-AUY922 induces MITF protein expression; however, addition of SB233580 decreases the HSP90 inhibitors mediated increase in MITF protein levels. SB203580 treatment alone also decreases MITF protein levels. Western blots were performed at least 2, to 4 times with independent lysates samples.

4.3 Discussion

In Chapter 3 HSP90 ATPase domain N-terminal inhibitors, 17-AAG and NVP-AUY922 effects to increase osteoclast formation *in vitro,* was described. The HSP90 inhibitor effects on osteoclast formation *in vitro* are strong and robust and are observed in many different types of osteoclast formation assays (Chai *et al.*, 2014; Price *et al.*, 2005). However, the mechanism underlying their action is unclear from the known actions of HSP90.

In the work described here the mechanisms of this induction were explored As previously discussed in Chapter 1.9.2.1, HSP90 assists in the folding and function of its client proteins many of which are *bona fide* oncogenes, and allows the cancer cell to evade apoptosis and continue growing (Neckers and Workman, 2012). In addition to many of HSP90 client proteins being oncogenes, many transcription factors and signalling proteins, which are important in osteoclast differentiation are also HSP90 client proteins whose levels are reduced by HSP90 inhibition (Ruffenach *et al.*, 2015; Walsby *et al.*, 2012). Thus the inhibition of HSP90 and consequent downstream increase in osteoclastogenesis raised many questions. HSP90 client proteins that are important in osteoclastogenesis and whose expression is reduced by HSP90 inhibition include NFκB, NFATc1 and MAP kinases (Walsby *et al.*, 2012; Ruffenach *et al.*, 2015; Millson *et al.*, 2005). This was evident, for example, in Chapter 3 (Figure 3.15 and 3.17), which showed 17-AAG treatment decreased NFAT transcriptional activity and protein levels. Whilst there are HSP90 client proteins which positively affect osteoclastogenesis there may also be HSP90 client proteins that are endogenous or autocrine inhibitors of osteoclast differentiation such as IRF8 and MAFB (Kim and Kim, 2014). Their release from HSP90 binding and their subsequent mis-folding and/or degradation may result in increased osteoclast formation. Initial studies by members of the laboratory did not find 17-AAG treatment to affect regulation of endogenous inhibitors. Thus, studied in this chapter is an alternative hypothesis that the HSP90 inhibitors, 17-AAG and NVP-AUY922, increase osteoclast formation through their induction of an HSF1-mediated cell stress. This action of N-terminal HSP90 inhibitors, including 17-AAG and NVP-AUY922, to cause a HSR when HSF1 is released from HSP90 is well documented in other cell types and also in patient tissue samples (Gaspar *et al.*, 2010; Eccles *et al.*, 2008; Powers and Workman, 2007; Guo *et al.*, 2005b; Doubrovin *et al.*, 2012; Bagatell *et al.*, 2000; Banerji *et al.*, 2005b). For example, 17-AAG treatment results in elevated HSP70 protein levels, which is a marker of cell stress in both cancer and surrogate tissues (Cervantes-Gomez

et al., 2009). Consistent with the hypothesis that the HSF1 mediated stress is responsible for the increase in osteoclast formation, is data showing C-terminal binding HSP90 inhibitors that, reduce HSP90 chaperone actions without affecting HSF1 activation do not affect osteoclast differentiation (Chai *et al.*, 2014). It is noteworthy that the cell stress induction by N-terminal binding HSP90 inhibitors is recognised as a problem in cancer therapeutics. This is due to these inhibitors helping cancer cells escape from the consequences of lack of HSP90, thus opposing the very approach that is being employed to kill them (Whitesell and Lindquist, 2005). HSF1 inhibition has now been recognised as a promising future avenue in anti-cancer research, and one of the compounds developed for this, KNK437 was employed in the work in this chapter (Whitesell and Lindquist, 2009). The HSR is not the only stress response in the cells as discussed in Chapter 1.8. Another important stress pathway in cells is the p38 signalling cascade of which the p38 member is essential for osteoclastogenesis(Li *et al.*, 2002). Thus, the p38 MAP kinase was also studied and found to have a possible involvement in 17-AAG and NVP-AUY922 actions upon osteoclast formation.

In this chapter 17-AAG and NVP-AUY effects upon HSF1 mediated cell stress, was studied with regard to its influence on osteoclast formation. One approach used to determine whether HSP90 inhibitors 17-AAG and NVP-AUY922 cause a stress response in other cells was to use HEK-HSE cells. These cells overexpress wild type HSF1 and contain a pHSE-mCherry vector in which mCherry expression is under the control of an inducible HSP72 (HSP70B) promoter containing HSE sites to which HSF1 binds. At 24 hours, 17-AAG significantly increased mCherry levels. Similar HSE-reporter responses to 17-AAG have been seen in in transfectable osteoblastic cells (Price laboratory, data not shown). Such observations are consistent with other reports of HSF1 activity being increased in cancer and other cell types in response to 17-AAG and NVP-AUY922. The effect of 17-AAG upon HSF1 activation was studied indirectly through immunoblotting for the HSF1 dependent HSPs, in this case the stress inducible HSP72 isoform in RAW264.7 cells as well as in BMM. These results confirm Ryan Chai's first reports of 17-AAG effects upon HSP70 and HSF1 protein levels in RAW264.7 cells and BMM (Chai *et al.*, 2014). The more recently developed NVP-AUY922 has previously been shown to increase the expression of the HSP70 upon HSF1 activation and transcriptional activity (Gupta *et al.*, 2010; Volloch *et al.*, 2000). Consistent with this, NVP-AUY922 increased HSF1 transcriptional activity, and, in addition, was shown to increase the protein expression of the HSP72 isoform in RAW264.7 cells specifically. As mentioned earlier, HSP72 belongs to the HSP70 family of HSPs, which includes many other

isoforms including HSP8A (HSC70). The HSP8A isoform was identified by RNA-seq analysis to be increased by 17-AAG treatment (Chapter 6.2). This HSP8A isoform has a known role in chaperone-mediated autophagy, and its levels increase when autophagy increases (Benbrook and Long, 2012). It is interesting to note that autophagy processes are known to be affected by cell stress and by HSP90 inhibitors (Riedel *et al.*, 2010; Hocking *et al.*, 2012). Geldanamycin, 17-AAG and NVP-AUY922 have all been shown to induce or enhance autophagic processes including the upregulation of autophagy marker, Autophagy related gene 5 (ATG5)(Qing *et al.*, 2006; Mori *et al.*, 2015b; Rusmini *et al.*, 2011; Hsueh *et al.*, 2013).

The HSF1 inhibitor KNK437, which reduces HSP70 induction and HSF1 binding to HSE in gene promoter targets was shown to block the osteoclast enhancing effects of 17-AAG and NVP-AUY922 (Yokota *et al.*, 2000). This data is consistent with the effects of these HSP90 inhibitors being dependent upon HSF1 and thus perhaps upon the HSR. It was notable however, that RANKL action upon osteoclastogenesis was not affected by HSF1 inhibition. This indicates that osteoclast formation is not HSF1 dependent, but HSF1 activity is nevertheless able to regulate osteoclastogenesis when it is elevated and in the case of 17-AAG and NVP-AUY922. This data shows that both 17-AAG and NVP-AUY922 ability to increase osteoclast formation is at least partially HSF1 dependent. However, since KNK437 may have off target effects, HSF1 dependency in the 17-AAG-mediated increase in osteoclastogenesis was examined using another approach, i.e., knockdown of HSF1 in RAW264.7 cells. RAW264.7 cells transduced with lentiviral vectors containing non-silencing (NS mir) or HSF1 targeting shRNAmir (Mir5) constructs were treated with RANKL (100ng/ml) in the presence or absence of 17-AAG (200nm). Silencing HSF1 decreases the 17-AAG mediated increase in osteoclastogenesis. This data was consistent with Ryan Chai's data, which showed the same effect when treating with the submaximal RANKL (20ng/ml) dose in independent experiments (Chai *et al.*, 2014). Thus, knocking down HSF1 significantly decreased osteoclastogenic responses to 17-AAG treatment, but this knockdown (like KNK437) did not affect their ability to form osteoclasts in response to RANKL This data provided corroborating evidence of a role for HSF1 in osteoclast formation in response to 17-AAG treatment. This approach can be used to further study the role of HSF1 in NVP-AUY922 pro-osteoclastogenic effects.

A third approach was also used to further confirm this HSF1 role in the 17-AAG mediated increase in osteoclastogenesis. This was done by using cells from HSF1 null mice. 17-AAG treatment did not increase osteoclastogenesis in bone marrow cell populations from HSF1 null mice but did so as expected in wild type littermate control mice. Bone marrow cell populations from HSF1 heterozygote mice only responded minimally to 17-AAG treatment i.e., at the lowest concentration. This data was first shown by Dr Ryan Chai and has since been published (Chai *et al.*, 2014). These mice breed poorly due to lack of embryo implantation in female knockouts and general poor fertility in male knockouts. The mice are only fertile at all on a mixed genetic background (Balb/c x 129 strains were employed here) but not on pure C57Black6 or Balb/c backgrounds. This strongly suggests that there may be alternative factors or pathways that are able to partly compensate for the lack of HSF1 (Jin *et al.*, 2011). The animals themselves are generally runted, which may result from bone defects; however, not enough of these mice were generated to make a proper systematic study feasible. It is also not necessarily true that any skeletal abnormalities were osteoclast dependent since numerous pathologies can affect bone. It was also clear that lack of HSF1 did not prevent osteoclast formation from proceeding at reasonably normal levels in response to RANKL and M-CSF stimulation in the performed experiments although there was some variation noted. Thus, HSF1 is required for the 17-AAG mediated enhancement of osteoclast formation but not for osteoclast formation itself (Chai *et al.*, 2014). However, this work was not able to determine whether HSF1 alone mediates 17-AAG effects on osteoclast, or whether 17-AAG treatment also induces some other factors critical in osteoclast formation, i.e., whether HSF1 is sufficient for enhancing osteoclast formation. Some support for this hypothesis can be found in the next chapter in which stressors that do not act through HSP90 inhibition were studied.

Another possible means for cell stress to affect osteoclasts is through a p38-dependent pathway. The p38 MAP kinase pathway is activated by a range of stressors and is a critical part of the actions of RANKL during osteoclastogenesis (Wagner and Nebreda, 2009; Matsumoto *et al.*, 2000). Immunoblot studies showed 17-AAG and NVP-AUY922 treatment both increase p38 phosphorylation and they both had similar kinetics in their activation of p38. This data shows the complexity of the systems and that stress pathways are not mutually exclusive. P38 is a necessary component of the osteoclast differentiation pathway (Li *et al.*, 2002). Thus, to investigate the effect of p38 upon osteoclast differentiation under HSP90 inhibition by inhibiting p38 is not possible as this would abolish osteoclast formation.

However, the possibility of a link between HSF1 and p38 was investigated by studying their possible interactions in osteoclast progenitor cells. Interestingly HSF1, which is a highly phosphorylated protein activity has been suggested to be regulated by the MAP kinase, ERK1 (Kim *et al.*, 1997). The other MAP kinases, p38 and JNK, have also been shown to bind to the same HSF1 region and cause HSF1 phosphorylation in a ras-dependent manner in NIH3T3 cells (Kim *et al.*, 1997). Furthermore, JNK2 has been shown to cause HSF1 hyperphosphorylation, and downstream HSP70 protein expression under heat shock conditions (Park and Liu, 2001). This indicates that HSF1 is modulated by MAP kinases but not whether HSF1 activity influences phosphorylation of p38. To study this question, HSF1 was inhibited with KNK437 in the RAW264.7 cells, but no decreased 17-AAG elicited p38 phosphorylation was seen in RAW264.7 cells. Likewise, NVP-AUY922 ability to phosphorylate p38 was not reduced by HSF1 blockade in RAW264.7 cells. These data indicate that HSF1 elevation is a separate phenomenon to the p38 activation.

In Chapter 3 it was shown that 17-AAG had no effect or a negative effect upon most RANKL-dependent pathway factors such as NFATc1, while in contrast 17-AAG strikingly increased MITF protein expression in both a dose-dependent and time-dependent manner. Consistent with this, 17-AAG increased the transcriptional activity of MITF target gene v-Atp6v0d2 in RAW264.7 cells (Figure 3.21-3.23). In this chapter both 17-AAG and NVP-AUY922 mediated induction of MITF and has been shown to be reduced upon p38 inhibition. Although this interpretation is complicated by the reduction of basal MITF levels with p38 inhibition. This suggests that p38 activation is required for a certain basal level of MITF protein expression and secondly p38 is partly required for the enhanced MITF protein expression in 17-AAG and NVP-AUY922 treated cells. This indicates that p38 might have a role in the 17-AAG-mediated increases in MITF protein expression but this is difficult to explore directly. This finding was also confirmed using the second HSP90 inhibitor NVP-AUY922. Together this data suggests that HSP90 inhibitors that induce a HSF1 stress response increase MITF protein expression partly through p38 phosphorylation/activation. Further work on this aspect of MITF biology found that 17-AAG treatment increased MITF protein levels in RAW264.7 cells, and this was significantly reduced when HSF1 was inhibited with KNK437 treatment (Chai *et al.*, 2014). In addition, HSF1 knockdown by shRNAmir also abolished the effect of 17-AAG upon MITF protein expression (Chai *et al.*, 2014). BMM from HSF1$^{-/-}$ have decreased levels of MITF both without and upon 17-AAG treatment (Chai *et al.*, 2014). This data shows that MITF is regulated by 17-AAG induced

HSF1 activation (Chai *et al.*, 2014). As previously described in bone marrow cultures isolated from HSF1$^{-/-}$ mice, 17-AAG treatment failed to increase osteoclast differentiation (Chai *et al.*, 2014). This data thus further consolidates the conclusions of this Chapter and Chapter 3 and indicate that 17-AAG treatment increases RANKL stimulated osteoclastogenesis by increased MITF protein expression, which is dependent upon the actions of HSF1. It should be noted however, that it is not possible to test this directly by blocking MITF since this would abolish all, or nearly all osteoclast formation as seen in dominant negative *mi/mi* mice. It should also be noted that overexpression of MITF (specifically the MITF-E isoform) in RAW264.7 cells increases osteoclast formation, although this can also be seen with forced overexpression of other RANKL signals such as NFATc1 (Lu *et al.*, 2010a; Takayanagi *et al.*, 2002; Asai *et al.*, 2014). Further work is thus needed to clarify the role of MITF and other members of the MITF/TFE gene family of proteins, and perhaps also the MITF binding partner PU.1, although to date our laboratory has not found any regulation of PU.1 by 17-AAG.

From the first two experimental Chapters of thesis, it has been shown that N-terminal HSP90 inhibitors 17-AAG and NVP-AUY922 cause a HSF1 mediated cell stress response (Figure 4.17). 17-AAG does not affect early-induced osteoclastogenic transcription factors NFκB or NFATc1 at activity or protein levels. However, 17-AAG and NVP-AUY922 do increase the late acting MITF transcription factor (Figure 4.17). This data, as well as the report that MITF contains HSE sites, suggests that the 17-AAG mediated HSF1 cell stress acts upon MITF to increase osteoclast formation (Figure 4.17) (Laramie *et al.*, 2008). This data discussed above implicate the cell stress response and other related pathways in HSP90 inhibitor actions to the extent that inhibition of HSF1 activation reduces these actions. This raises several further questions. For example, do HSF1 dependent stress responses drive increased osteoclast formation in the absence of HSP90 blockade? If so, is it HSF1 levels alone that can increase osteoclastogenesis or are accessory factors important? What other stress responses can drive osteoclast formation? This is examined in the next chapter.

Molecular Mechanism of the HSP90 Mediated Increase in Osteoclastogenesis
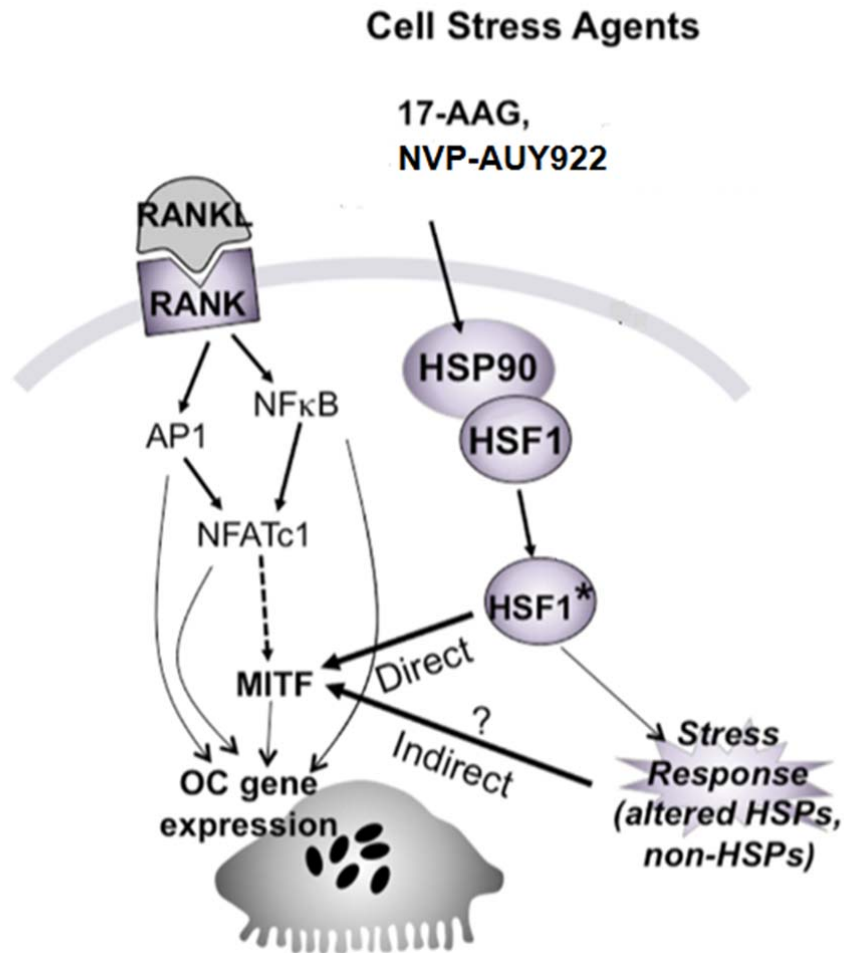
Figure 4.17

RANKL binding of RANK induces the activation of essential transcription factors NFκB, AP1 (c-FOS/jun dimer) and NFATc1. Expression of the late acting transcription factor MITF is increased. These factors induce the activation of osteoclast specific genes causing the progenitor cell to differentiate into a mature osteoclast. 17-AAG and NVP-AUY22 bind to HSP90 causing HSF1 dissociation, its activation and the induction of a HSR. HSF1 activation in turn increases MITF levels either by directly stimulating the *MITF* promoter or indirectly by altering the expression of HSP and/or non-HSP target genes. Increased MITF expression would lead to enhanced differentiation of osteoclast progenitors to RANKL, thus increasing osteoclastogenesis. 17-AAG and NVP-AUY922 also activate the stress MAP kinase p38, which is known to phosphorylate MITF. HSP90 inhibitors may also increase MITF expression in this manner. HSF1*=activated HSF1. Figure adapted from (Chai *et al.*, 2014).

Chapter 5
The Effect of Chemotherapeutic Agents and Ethanol upon HSF1 Mediated Cell Stress, Osteoclast Transcription Factors and Osteoclast Formation

Chapter 5 The Effect of Chemotherapeutic Agents and Ethanol upon HSF1 Mediated Cell Stress, Osteoclast Transcription Factors and Osteoclast Formation

5.1 Introduction

Cytotoxic chemotherapeutics are widely used as cancer treatments since they particularly target proliferating cancer cells causing them to undergo apoptosis (Wondrak, 2015; Cepeda *et al.*, 2007; Adams, 2004). However, their cytotoxicity means that these compounds commonly cause significant levels of cellular stress. The HSP90 inhibitors studied in the previous chapter have been reported to strongly induce HSF1-mediated cell stress responses by causing a dissociation of HSF1 from HSP90 multichaperone complexes in a number of cells lines (Gupta and Massagué, 2006; Gaspar *et al.*, 2010; Jensen *et al.*, 2008; Guo *et al.*, 2005a; Doubrovin *et al.*, 2012) (Chapter 1.9.4.2). In Chapters 3 and 4, 17-AAG and NVP-AUY922 were confirmed to induce such cell stress responses in RAW264.7 cells and bone marrow macrophages, and to increase RANKL-dependent osteoclast formation relative to the DMSO vehicle control. It was also confirmed through HSF1 pharmacological inhibition, HSF1 silencing, and HSF1$^{-/-}$ mice that the latter pro-osteoclastic actions of 17-AAG are dependent upon HSF1 actions. NVP-AUY922 pro-osteoclastic actions were also inhibited by pharmacological inhibition of HSF1. Interestingly, 17-AAG and NVP-AUY922 dependency upon HSF1 for their osteolytic effects may involve increased level of cellular MITF, a transcription factor critical for osteoclast gene expression (Chai *et al.*, 2014). These cell stress-dependent actions of HSP90 inhibitor compounds may explain the earlier observations of 17-AAG-elicited bone loss and tumour growth *in vivo* (Price *et al.*, 2005). This raises the hypothesis that similar effects on osteoclasts (and on bone loss *in vivo*) might also occur with cell exposure to cell stressors acting through other mechanisms, such as cytotoxic compounds. Clinical use of chemotherapeutics such as doxorubicin and cisplatin are often associated with bone loss, although the damage they inflict on bone marrow cell populations, and on bone formation means that it is unclear whether any pro-osteolytic actions may be involved (Hu *et al.*, 2010; Lipton *et al.*, 2009a; Guise, 2006). Nevertheless, these and other cytotoxic compounds are likely to drive cell stress responses in osteoclast progenitors. This raised the hypothesis that assuming the concentrations needed to affect osteoclast progenitors are not lethal to the cells themselves, they may increase osteoclast formation as the HSP90 inhibitors do. This chapter describes studies of a number of potential stressors, including doxorubicin, bortezomib, cisplatin and MG132 (Chapter 1.9) with regards to their ability to

increase osteoclast differentiation *in vitro* and if so, whether any observed effects are due to a HSF1 mediated responses. Ethanol, as a cell stressor, although not cytotoxic but having known detrimental effects on bone was similarly investigated for its actions on osteoclasts (Iitsuka *et al.*, 2012). In addition to investigating the HSF1 dependent effects of these agents, the influence of other stressors on critical osteoclast transcription factors, NFATc1 and MITF were also examined since HSP90 inhibitors induced MITF levels whilst failing to induce NFATc1.

As previously described, HSF1 acts to increase the transcription of HSPs through its interaction with HSE regulatory upstream promoter elements found in HSF1 target genes i.e., HSPs. Based on this, two approaches were used to assess the effect that cancer therapeutics have upon HSF1 activity. HSF1 activity was measured using the HEK-HSE cell line, which was generated by Dr. Chau Nguyen (Nguyen *et al.*, 2013). As previously described, these cells contain a mCherry reporter which is driven by the strictly stress inducible HSP70B. In addition, the effect of chemotherapeutic treatments upon HSF1 and the HSR were assessed by the induction of stress sensitive HSP72 protein levels.

5.2 Results

5.2.1 The Effect of Doxorubicin upon HSF1-mediated Cell Stress

Doxorubicin is one of the most commonly used cancer therapeutics (American Cancer Society, 2007). Doxorubcin treatment is used for haematological cancers, such as multiple myeloma and acute leukaemias as well as solid cancers, for example, lung, endometrium and breast cancers (Banerji *et al.*, 2005a; American Cancer Society, 2007). Doxorubicin is a non-specific DNA-intercalating group of anti-cancer agents, (Chapter 1.9.9), which cause cell death principally by causing genotoxic stress (Kelland, 2007). The cancers that doxorubicin is used to treat often affect the bone marrow because of where they originate i.e. leukaemia and sarcoma or in their metastatic state i.e. breast cancer (Mkele, 2010; Kemp *et al.*, 2011). Many studies have also shown that doxorubicin has a negative effect on the bone marrow (Bhinge *et al.*, 2012; Rana *et al.*, 2013). Interestingly, anthracycline intercalating agents including doxorubicin agents have been described to cause a HSF1 cell stress response suggesting a parallel with HSP90 inhibitors (Zanini *et al.*, 2007). Therefore, the effect of doxorubicin to cause a HSR and also specifically in RAW264.7 cells was examined. This was tested first in

HSE-HEK cells seeded at 2.5×10^4 cells in 6 mm diameter wells in phenol-free DMEM media. The cells were allowed to settle for ≥ 3 hours and then were treated with doxorubicin (10, 20, 50 and 100nM) or DMSO vehicle control for 24 hours. Cells were incubated with nuclear dye Hoechst (10ug/ml) for 15 minutes at 37°C and levels of Hoescht dye and mCherry levels were then determined (Chapter 2.10). Twenty-four hour treatment with doxorubicin significantly increased HSP70B-dependent mCherry signals, showing HSF1 activation (Figure 5.1). Concentrations of doxorubicin greater than 200nM caused cell death. To confirm HSF1 dependency of the observed doxorubicin-mediated mCherry expression, the HSE-HEK based assays were repeated with doxorubicin (50nM) in the presence of HSF1 inhibitor KNK437 (10µM) for 24 hours. Pooled results from two independent experiments showed that inhibiting HSF1 with KNK437 decreases the doxorubicin-mediated increase in mCherry expression (Appendix Figure B7). KNK437 treatment alone reduced HSF1 activity levels below that of the DMSO vehicle control (Appendix Figure B7). This may be a result of the cells experiencing a baseline stress level due to EGFP expression needing to be stabilised. Adding KNK437 may decrease this HSF1 mediated stress.

The actions of doxorubicin on HSF1 mediated cell stress response in the RAW264.7 cell line were therefore investigated, since RAW264.7 cells are an important model of osteoclast biochemical pathways during osteoclast formation and are employed as such in this thesis. Thus, RAW264.7 cells were treated with doxorubicin (20 and 50 nM) for 24 and 48 hours and HSP72 protein expression analysed. At 24 and 48 hours, doxorubicin treatment increased HSP72 protein expression (Figure 5.2). Some variation was observed in the concentration of doxorubicin giving maximal HSP72 response between RAW264.7 cell isolate, however, doxorubicin caused a clear cell HSP72 induction in RAW264.7 cells.

5.2.2 The Effect of Doxorubicin upon Osteoclastic Transcription Factors NFATc1 and MITF

Since doxorubicin caused a HSF1 mediated cell stress response in HSE-HEK cells and in RAW264.7 cells like HSP90 inhibitors, the effects of this compound on osteoclast formation and osteoclastic transcription factors was investigated. As shown in Chapter 3, HSP90 inhibitors increase both osteoclast formation and MITF protein levels but not NFATc1 levels or activity. Expression of NFATc1 and MITF after doxorubicin treatment was thus assessed in RAW264.7 cells. In contrast to 17-AAG, doxorubicin treatment increased NFATc1 treatment increases osteoclastogenesis *in vitro* and MITF expression, in an HSF1- dependent

Doxorubicin Treatment Increases Hsf1 Transcriptional Activity in HEK-HSE Cells

A.

B.
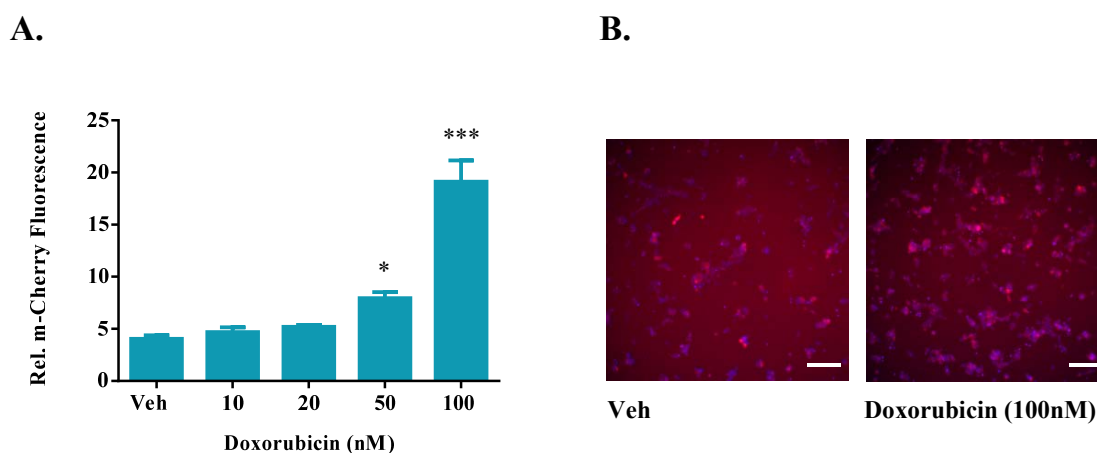
Figure: 5.1

(A-B.) HEK-HSE cells were seeded at 2.5 x 10^4 cells in 6mm diameter well in DMEM phenol-free medium. After settling for a few hours, the cells were treated with doxorubicin (10, 20, 50 and 100nM) or DMSO ("Veh"). At 24 hours, Hoechst dye (10μg/ml) was added to the wells and the cells incubated at 37°C for 15 minutes. The levels of mCherry were collected using the Arrayscan VTI High Content Screening instrument. The percentage threshold of mCherry signal was compared against DMSO vehicle control. **(A.)** At 24 hours, doxorubicin increased HSF1 activity relative to the DMSO vehicle control. **(B.)** Depiction of mCherry levels in the DMSO vehicle control and doxorubicin treated cells from the Arrayscan VTI High Content Screening instrument. Scale bar - 100μm. All data is represented as mean ± SEM of three independent experiments. Statistical analysis used ANOVA, Dunnett's *post hoc* test * $p \leq 0.05$, *** $p \leq 0.001$.

Doxorubicin Increases HSP72, NFATc1 and MITF Protein Levels in RAW264.7 Cells

A.

B.

24 hr

48hr
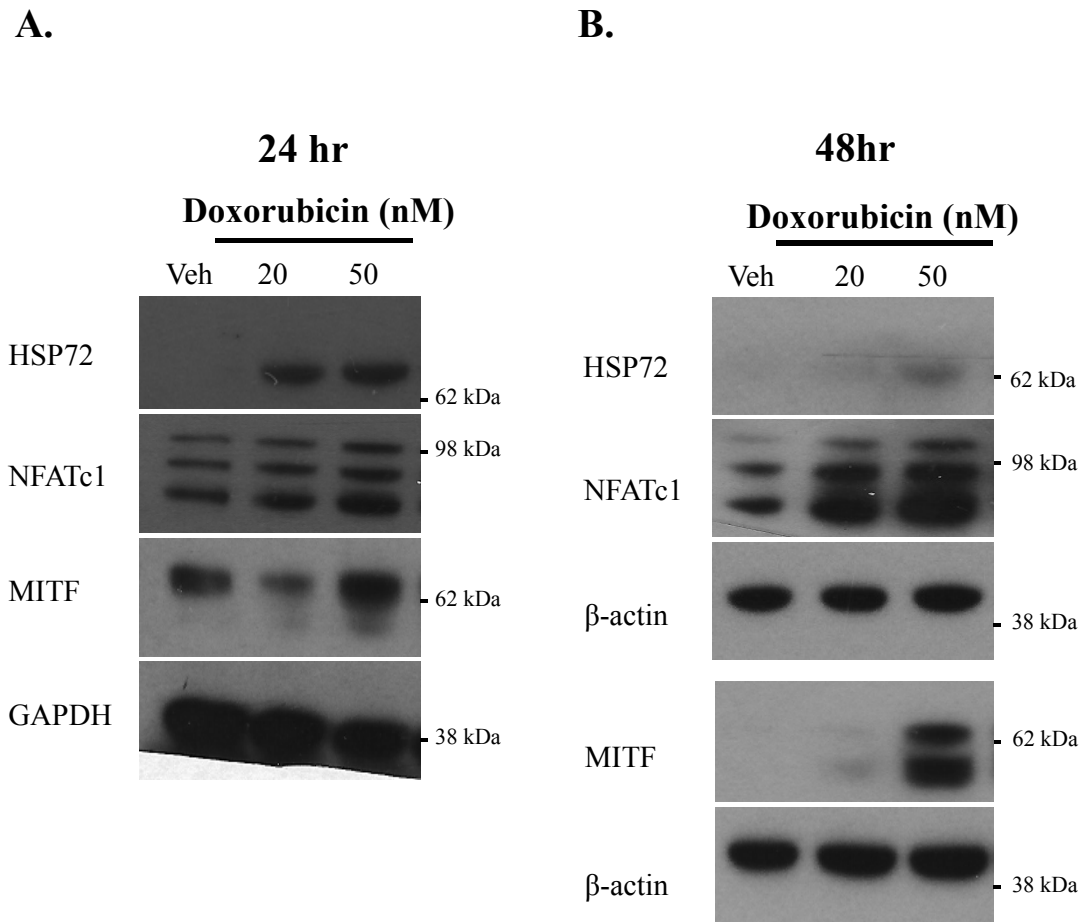
Figure 5.2

RAW264.7 cells were seeded at 2×10^5 cells in 35mm diameter culture wells and were treated the following day with doxorubicin (20 and50nM) for **(A.)** 24 and **(B.)** 48 hours. The cells were lysed and HSP72, NFATc1 and MITF protein levels determined by immunoblot analysis. Doxorubicin treatment increased the protein levels of HSP72 and osteoclast transcription factors NFATc1 at 24 and 48 hours. MITF protein levels were also increased by doxorubicin at both 24 and 48 hours. Western blots were performed at least 2, to 5 times with independent lysates.

manner (Figure 5.2) (Chai *et al.*, 2014). Doxorubicin treatment also increased MITF protein levels after 24 hours of treatment (Figure 5.2). Likewise at 48 hours, doxorubicin treatment markedly increased MITF protein expression relative to the DMSO vehicle control (Figure 5.2).

5.2.3 The Effect of Doxorubicin upon Osteoclast Formation

RAW264.7 cells, seeded at 10^4 cells in 6mm diameter culture wells in the presence of RANKL (20ng/ml), were treated with doxorubicin (10, 20, 50, 100 and 200nM). After 6 days of culture doxorubicin treatment significantly increased RANKL-dependent RAW264.7 cell osteoclast formation in a dose-dependent manner (Figure 5.3). To further confirm this effect of doxorubicin on osteoclast formation, M-CSF and RANKL-stimulated primary bone marrow cells were similarly employed. Cells were seeded at 10^5 cells in 6mm diameter wells with RANKL (20ng/ml) and M-CSF (30ng/ml) and were treated with doxorubicin (5, 10 and 20nM). Doxorubicin treatment significantly increased osteoclast formation in a dose dependent manner in comparison to the DMSO vehicle control (Figure 5.4). Concentrations of doxorubicin greater than 50 nM were determined to be toxic to these cells.

5.2.4 Inhibiting HSF1 Abolishes the Doxorubicin-mediated Increase in Osteoclast Differentiation

To determine whether the above pro-osteoclastic effects of doxorubicin were HSF1-dependent, HSF1 was inhibited using KNK437. Bone marrow cells were seeded at 10^5 cells in 6mm diameter wells in the presence of RANKL (20ng/ml) and M-CSF (30ng/ml). The cells were treated with doxorubicin (5nM) in the presence or absence of KNK437 (10μM). As previously observed, doxorubicin (5nM) treatment significantly increased osteoclast formation (Figure 5.5). However, addition of KNK437 abolished the pro-osteoclastic actions of doxorubicin (Figure 5.5). Initial experiments have also been performed in RAW264.7 cells and a similar pattern has been observed (Appendix Figure B11). These data show that the doxorubicin-mediated enhancement of osteoclast formation is at least partly dependent upon HSF1-mediated cell stress.

Doxorubicin Increases RANKL Mediated RAW264.7 Cell Osteoclast Formation

A.

B.

Figure 5.3

(A-B.) RAW264.7 cells were seeded at 10^4 cells in 6mm diameter wells in the presence of RANKL (20ng/ml). RAW264.7 cells were treated with doxorubicin (5, 10 and 20nM) or DMSO ("Veh") for 6 days. As a negative control, the cells were not treated with RANKL as denoted by "-ve". As per every osteoclast assay, all treatments were performed in quadruplicate. On day 6 the cells were fixed and stained for TRAP. Multinucleated TRAP positive cells were counted as osteoclasts. Doxorubicin treatment increased osteoclast formation relative to the DMSO vehicle control ("Veh"). **(B.)** Image of RAW264.7 cells treated with Veh or doxorubicin (20nM). All data is expressed as mean ± SEM of three independent experiments. Scale bar - 50μm.Statistical analysis was performed by ANOVA, Dunnett's post *hoc* test ** $p \leq 0.01$, *** $p \leq 0.001$.

Doxorubicin Increases Osteoclast Formation from Bone Marrow Cells
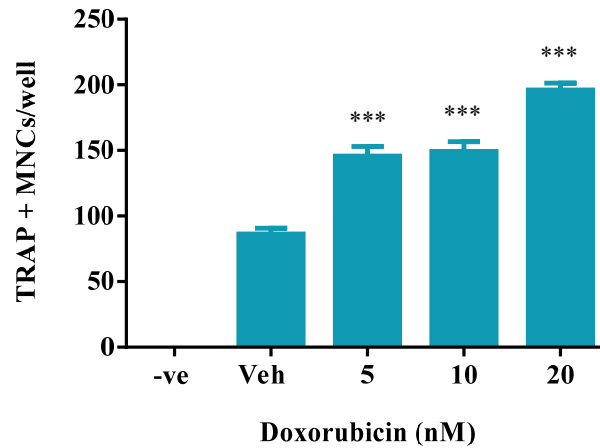
Figure 5.4

Bone marrow cells were seeded at 10^5 cells in 6mm wells and were treated with RANKL (20ng/ml) and M-CSF (30ng/ml) to stimulate low levels of osteoclast formation. The cells were also treated with doxorubicin (5, 10 and 20nM), and DMSO ("Veh") for 6 days and were histochemically stained for TRAP. The negative control, "-ve", shows results from cultures treated with M-CSF only. Multinucleated and TRAP positive cells were counted as osteoclasts. Doxorubicin treatment significantly increased osteoclast formation relative to the DMSO vehicle control. All data is expressed as mean $\pm$ SEM of six independent experiments. Statistical analysis was performed by ANOVA, Dunnett's post hoc test *** $p \leq 0.001$.

KNK437 Treatment Abolishes the Effects of Doxorubicin on Osteoclast Formation
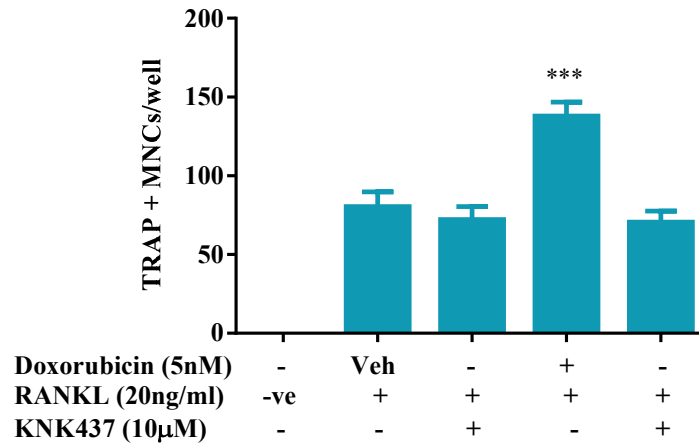
Figure 5.5

Bone marrow cells were seeded at 10^5 cells in 6mm diameter wells in the presence of RANKL (20ng/ml) and M-CSF (30ng/ml), respectively. The cultures were treated with doxorubicin (5nM) in the presence or absence of KNK437 (10μM) treatment for 6 days. The cultures were also treated with DMSO ("Veh") or KNK437 (10μM) alone. As an additional negative control, cells were left untreated "-ve". On day 6 TRAP positive and multinucleated counted as osteoclasts. Doxorubicin (5nM) treatment significantly increased osteoclast formation relative to DMSO vehicle control; however, the addition of KNK437 reduces osteoclast numbers similar to numbers present in the DMSO vehicle control. Data is expressed as mean ± SEM of four independent experiments. Statistical analysis was performed using ANOVA, Dunnett's *post hoc* test *** $p \leq 0.001$.

5.2.5 The Effect of MG132 upon HSF1-mediated Cell Stress

MG132 is a triterpene, peptide-aldehyde proteasome inhibitor derived from a Chinese medicinal plant, which blocks the proteolytic activity of the 26S proteasome complex (Guo and Peng, 2013; Kim *et al.*, 1999). The deregulation of the ubiquitin-proteasomal system by MG132 can result in different cell cycle phase arrests and inhibition of ubiquitin-tagged protein degradation (Han *et al.*, 2010; Yong Hwan Han and Woo Hyun Park, 2010; Oslowski and Urano, 2011). This causes the activation of the UPR (Chapter 1.8.4) (Oslowski and Urano, 2011; Nakajima *et al.*, 2011). In addition other types of cell stress have also been reported to be activated, including oxidative stress and the HSR (Kim *et al.*, 1999; Selimovic *et al.*, 2013). MG132 is not used clinically but there have been numerous studies of MG132 effects on cancer cell apoptosis (Yuan *et al.*, 2008; Guo and Peng, 2013; Wente *et al.*, 2005).

The effect of MG132 upon HSE-dependent activity was first examined. HSE-HEK cells were seeded at 2.5×10^4 cells in 6mm diameter culture wells and were left to settle for a few hours. The cells were treated with MG132 (20, 50, 100, 200, 500, and 1000nM) or DMSO vehicle control for 24 hours and then examined. Treatment with MG132 significantly increased HSF1 activity, as seen by increased mCherry expression in the HSE-HEK-cells relative to the DMSO vehicle control (Figure 5.6 A-B). MG132 (500nM) was the highest concentration before cell toxicity was evident (Appendix B4). To confirm the increased mCherry expression was HSF1 dependent, the cells were treated with MG132 (500nM) in the presence or absence of KNK437 (10μM) for 24 hours. As previously shown, MG132 (500nM) increases mCherry expression activity; however, the addition of KNK437 (10μM) decreased mCherry levels showing the response is dependent upon HSF1 activity (Figure 5.7). MG132 was then studied for its effect to cause a HSR in the RAW264.7 cell line. RAW264.7 cells were treated with MG132 (100 and 200nM) for 24 and 48 hours and HSP72 protein expression analysed by immunoblotting. At both 24 and 48 hours, MG132 treatment increased HSP72 protein expression (Figure 5.8 A-B).

5.2.6 The Influence of MG132 upon Osteoclastic Transcription Factors

The effects of MG132 on the osteoclast transcription factor NFATc1 and MITF were also studied in RAW264.7 cells. MG132 treatment increased NFATc1 protein levels at 24 hours although variability at which concentration increased NFATc1 most potently was different

MG132 Treatment Increases HSF1 Transcriptional Activity in HEK-HSE Cells at 24hr

A.

B.

Veh   **MG132 (500nM)**
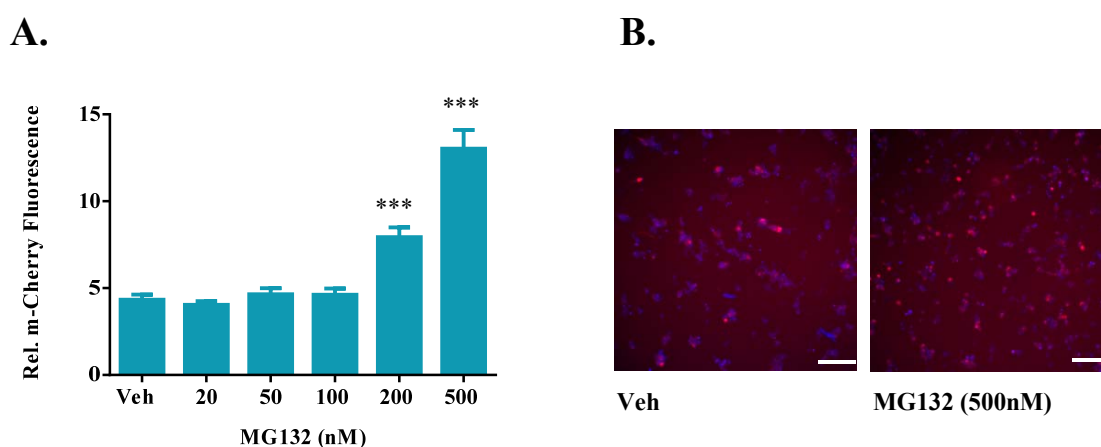
Figure: 5. 6

HEK-HSE cells were seeded at 2.5×10^4 cells in 6mm diameter well in DMEM phenol-free media. The cells were allowed to settle for ≥ 3 hours then treated with MG132 (20, 50, 100, 200 or 500nM) or DMSO ("Veh"). At 24 hours, Hoechst dye (10µg/ml) was added to the wells and the cells incubated (37°C for 15 minutes). The levels of mCherry were collected using an Arrayscan VTI High Content Screening instrument. Individual cells were identified by Hoechst nuclear staining. The percentage threshold of mCherry was measured against the DMSO vehicle control. **(A.)** At 24 hours MG132 (200 and 500nM) significantly increased HSF1 transcriptional activity relative to the DMSO vehicle control. **(B.)** Depiction of mCherry levels in DMSO vehicle control and MG132 treated cells from the Arrayscan VTI High Content Screening instrument. Scale bar - 100µm. All data is expressed as mean ± SEM of four independent experiments. Statistical analysis was performed by ANOVA, Dunnett's post *hoc* test *** $p \leq 0.001$.

KNK437 Treatment Ablates MG132 Mediated Increase in HSE Activity in HSE-HEK Cells
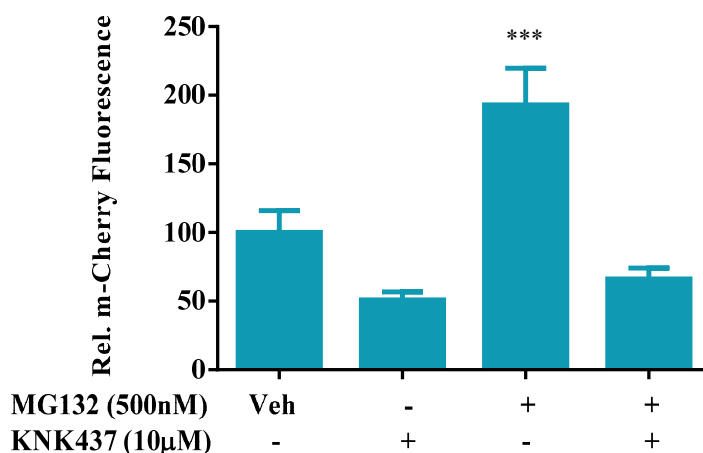
Figure: 5. 7

HEK-HSE cells stably transfected with a mCherry HSE reporter were seeded at 2.5 x 10^4 cells in 6mm diameter well in DMEM phenol-free media. The cells were allowed to settle for ≥3 hours and then were treated with MG132 (500nM) in the presence or absence of KNK437 (10μM). The cultures were also treated with DMSO ("Veh") or KNK437 (10μM) alone. At 24 hours, Hoechst dye (10μg/ml) was added to the wells and the cells incubated (37°C for 15 minutes). The levels of mCherry were collected using an Arrayscan VTI High Content Screening instrument. The percentage threshold of mCherry was measured against the DMSO vehicle control. MG132 treatment significantly increased HSF1 transcriptional activity. However, addition of KNK437 reduced HSF1 activity levels to that similar of the DMSO vehicle control. KNK437 treatment alone also decreased mCherry levels. All data is expressed as mean ± SEM of three independent experiments. Statistical analysis was performed by ANOVA, Dunnett's *post hoc* test *** p ≤ 0.001.

between cell isolates (Figure 5.8 A-B.) Initial studies have shown that MG132 also increase NFATc1 protein levels at 48 hours (data not shown). The effect of MG132 upon MITF protein levels in RAW264.7 cells was also investigated. MG132 treatment increased osteogenic transcription factor MITF protein levels at 24 hour and also at 48 hours (Figure 5.8 A-B.). A clear dose response was not always seen; however, MG132 did increase MITF protein levels.

5.2.7 The Effect of MG132 upon Osteoclast Formation

As described above, MG132 causes HSF1-mediated cell stress response in HSE-HEK cells and in RAW264.7 cells and additionally increases the protein levels of pro-osteoclast transcription factors NFATc1 and MITF. The effect of MG132 upon osteoclastogenesis was then studied in RAW264.7 and bone marrow cells. RAW264.7 cells seeded at 10^4 cells in 6mm diameter culture wells in the presence of RANKL (20ng/ml) and were treated with MG132 (10, 20, 500, 100 and 200nM). After 6 days of culture MG132 significantly increased RANKL-dependent RAW264.7 cell osteoclast formation in a dose-dependent manner (Figure 5.10). To further confirm this effect of MG132 on osteoclast formation, M-CSF and RANKL-stimulated primary bone marrow cells were similarly employed. Cells were seeded at 10^5 cells in 6mm diameter well in the presence of RANKL (20ng/ml) and M-CSF (30ng/ml) and were treated with MG132 (100 and 200nM). Similar to RAW264.7 cells, MG132 treatment significantly increased osteoclast formation compared to DMSO vehicle control from bone marrow progenitor cells (Figure 5.10).

5.2.8 Inhibiting HSF1 Abrogates the MG132-mediated Increase in Osteoclastogenesis

As with the previous studies of cytotoxic compounds, the influence of HSF1 in MG132-elicited increase in osteoclast formation was examined using KNK437 in osteoclast assays. Primary bone marrow cell cultures were treated with MG132 (50nM) in the presence or absence of KNK437 (10μM) for 6 days. As prior, MG132 treatment significantly increased osteoclast formation in bone marrow cells, but the addition of KNK437 abolished this increase in osteoclast numbers (Figure 5.11). KNK437 treatment alone did not affect osteoclast formation (Figure 5.11). Preliminary experiments using RAW264.7 cells also indicated that MG132 mediated enhancement of osteoclast formation was eradicated in the presence of KNK437 treatment (Appendix Figure B12).

MG132 Treatment Increases HSP72, NFATc1 and MITF Protein Levels in RAW264.7 Cells

A.

24hr

MG132 (nM)

Veh   100   200

HSP72 — 62 kDa

β-actin — 38 kDa

MITF — 62 kDa

β-actin — 38 kDa

NFATc1 — 98 kDa

β-actin — 38 kDa

B.

48hr

MG132 (nM)

Veh   100   200

HSP72 — 62 kDa

β-actin — 38 kDa

MITF — 62 kDa

GAPDH — 38 kDa
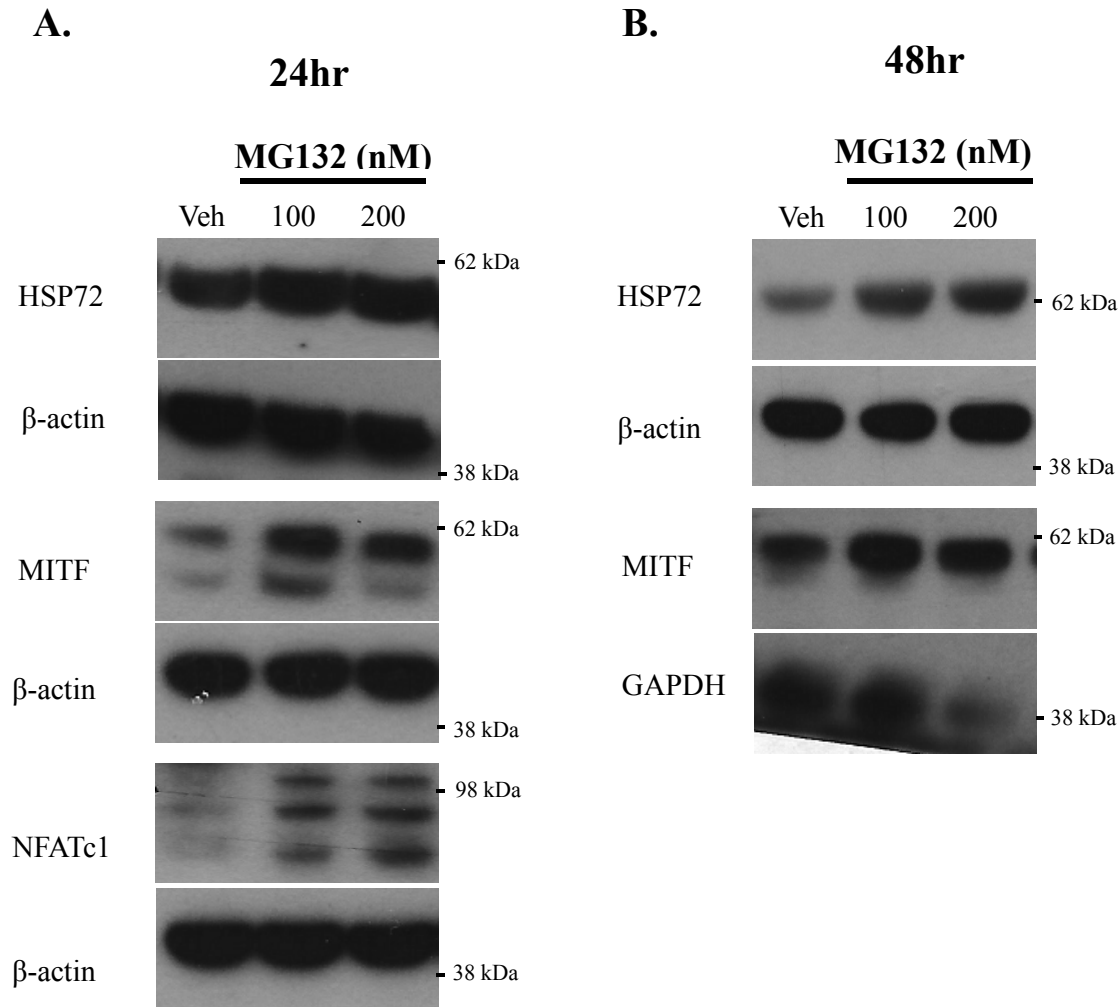
Figure 5.8

RAW264.7 cells were seeded in 35mm diameter culture wells and were treated the following day with MG132 (100 and 200nMd 48 hours **(B.)**. The cells were lysed and HSP72, NFATc1 and MITF protein levels determined by immunoblot analysis. MG132 treatment increases the protein levels of HSP72 at both 24 and 48 hours. In addition MG132 treatment increased the protein levels of osteoclast transcription factors: NFATc1 at 24 hours, and MITF at both 24 and 48 hours. Western blots were performed at least 2, to 4 times with independent lysates.

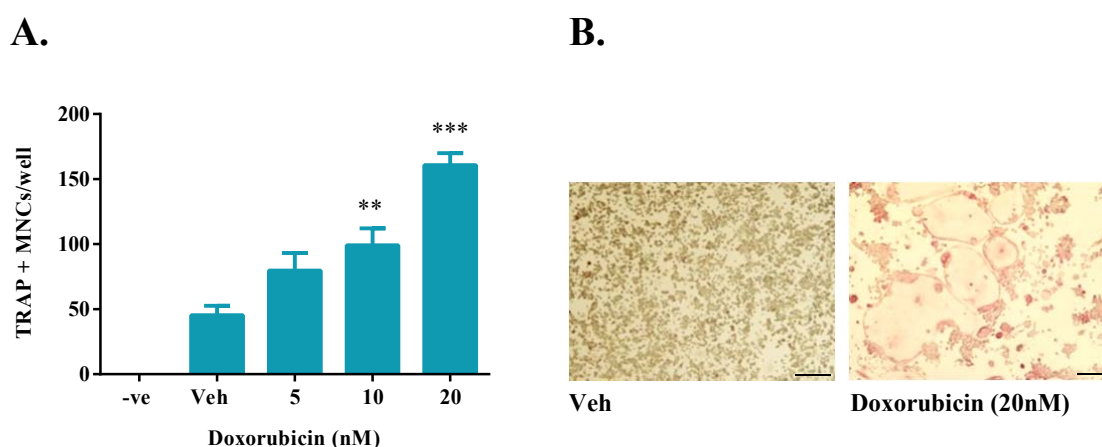# MG132 Enhances RANKL Mediated RAW264.7 Cell Osteoclast Formation
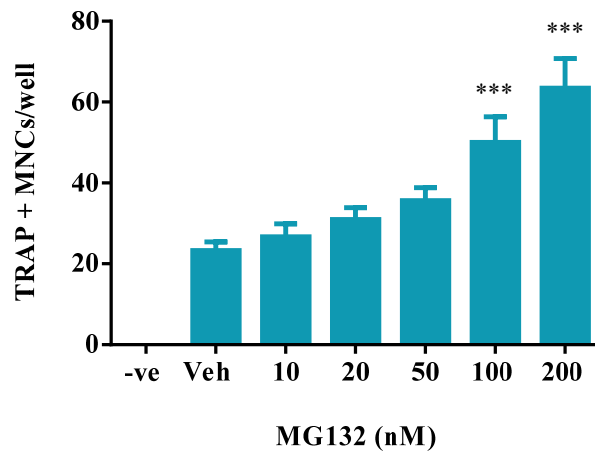
Figure 5 .9

RAW264.7 cells were seeded at 10^4 cells in 6mm diameter culture wells in the presence of RANKL (20ng/ml). RAW264.7 cells were treated with MG132 (10, 20, 50, 100 and 200nM) or DMSO ("Veh") for 6 days. As a negative control the cells were not treated with RANKL as denoted by "-ve". On day 6, TRAP positive and multinucleated cells were counted as osteoclast. MG132 treatment significantly increased osteoclast formation in comparison to the DMSO vehicle control. All data is expressed as mean ± SEM of four independent experiments. Statistical analysis was performed by ANOVA, Dunetts post *hoc* test *** p ≤ 0.001.

MG132 Increases RANKL and M-CSF Mediated-Bone Marrow Osteoclast Formation
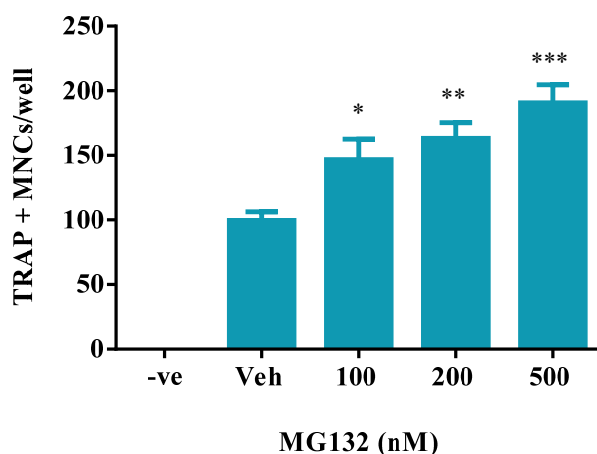
Figure 5.10

Bone marrow cells were seeded at 10^5 cells in 6mm diameter wells. Cells were treated with RANKL (20ng/ml) and M-CSF (30ng/ml) to stimulate osteoclast formation. The cells were then treated with MG132 (100, 200 and 500nM) or DMSO ("Veh") for 6 days. The cells were also treated with DMSO ("Veh") or were treated only with M-CSF ("-ve"). On day 6, TRAP positive and multinucleated cells were counted as osteoclasts. MG132 treatment significantly increased osteoclast formation in a dose-dependent manner relative to the DMSO vehicle control. All data is expressed as mean ± SEM of five independent experiments. Statistical analysis performed using ANOVA, Dunnett's *post hoc* test * $p \leq 0.05$, ** $p \leq 0.01$, *** $p \leq 0.001$.

KNK437 Abolishes the MG132 Mediated Increase in Osteoclast Formation
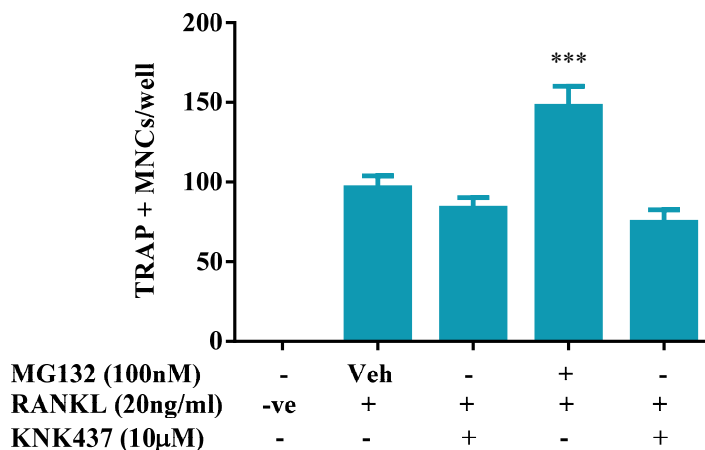
Figure 5.11

Bone Marrow Cells were seeded at 10^5 cells in 6mm diameter wells in the presence of RANKL (20ng/ml). The cultures were treated with MG132 (100nM) in the presence or absence of KNK437 (10μM) for 6 days. The cultures were also treated with DMSO ("Veh") or KNK437 (10μM) alone. As a negative control the cells were not treated with RANKL ("ve"). On day 6, multinucleated and TRAP positive cells were counted as osteoclasts. MG132 (100nM) treatment significantly increased osteoclast formation relative to the DMSO vehicle control as previously described. The addition of KNK437 decreased the enhancement of osteoclast formation. Data is expressed mean ± SEM of four independent experiments. Statistical analysis performed using ANOVA, Dunnett's *post hoc* test *** $p \leq 0.001$.

5.2.9 The Effect of Bortezomib upon HSF1 Mediated Cell Stress

Another commonly used chemotherapeutic is bortezomib, which like MG132 is an example of a targeted therapeutic (Chapter 1.9.2). Bortezomib (Velcade®) is a dipeptide boronate proteasome inhibitor, which causes cell death by reversibly inhibiting the 26 subunit of the proteasome (Piperdi *et al.*, 2011; Mattern *et al.*, 2012). Bortezomib is currently used to treat haematological cancers including multiple myeloma (Piperdi *et al.*, 2011; Chen *et al.*, 2011). Interestingly bortezomib has been reported to activate a number of stress pathways within the cell including the ER stress response, HSF1 mediated cell stress, and the p38 stress MAP kinase cascade (Selimovic *et al.*, 2013). Thus, bortezomib may affect osteoclast formation in the same manner as the other proteasome inhibitor, MG132.

To determine whether bortezomib activates HSF1 causing a subsequent increase in HSF1 transcriptional activity in HSE-HEK cells, the cells were treated with bortezomib (1, 10, 20, 50, and 100nM). At 24 hours, bortezomib, like doxorubicin, increased HSF1 activity, as seen by an increase in mCherry levels, in a dose dependant manner relative to the DMSO vehicle control (Figure 5.12). This data establishes that bortezomib treatment causes HSF1transciprtional activity in HSE-HEK cells. Pooled results from two independent experiments showed HSF1 inhibition by KNK437 (10μM) treatment reduced the bortezomib mediated increase in HSF1 transcriptional activity (Appendix Figure B8). To study if bortezomib causes a HSF1 cell stress response specifically in RAW264.7 cells, RAW264.7 cells were treated with bortezomib (200, 500 and 1000 pM) and HSF1 downstream target protein HSP72 protein levels were analysed by Western blotting. Bortezomib treatment increased the expression of HSP72 at 24 hours in a dose dependent manner (Figure 5.13 A-B.). Bortezomib treatment also increased HSP72 protein expression at 48 hours although at this time point the dose, which caused maximal HSP72 levels varied between 0.5 and 1nM.

5.2.10 The Effects of Bortezomib upon Osteoclast Transcription Factors NFATc1 and MITF

The effects of bortezomib on the osteoclast transcription factors NFATc1 and MITF were studied in RAW264.7 cells. Bortezomib treatment increased NFATc1 protein levels at 24 hours in a dose-dependent manner. NFATc1 expression was most potently induced by the highest concentrations of bortezomib (Figure 5.13 A-B.). The effect of bortezomib upon MITF protein levels was also studied. Bortezomib treatment increased osteoclastogenic

Bortezomib Treatment Increases HSF1 Transcriptional Activity in HEK-HSE Cells

A.

B.
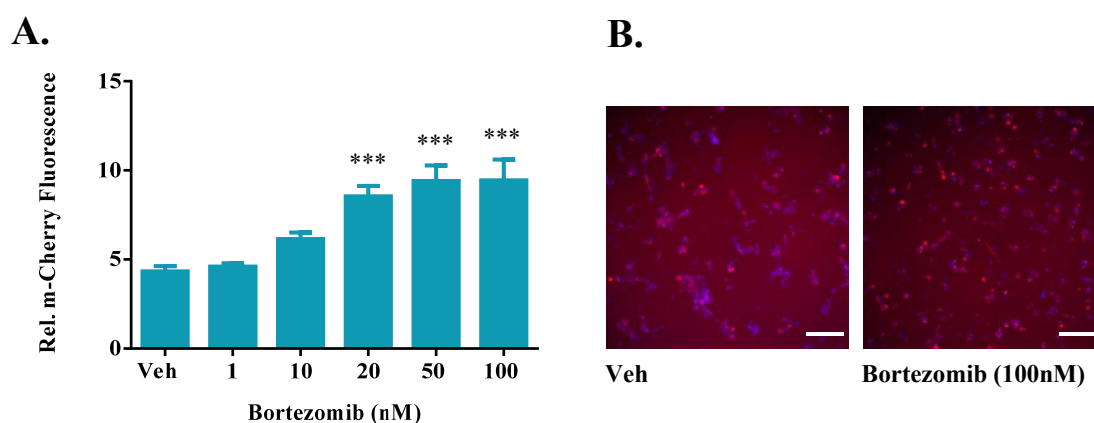
Figure 5.12

HEK-HSE cells stably transfected with a mCherry HSE reporter were seeded at 2.5 x 10^4 cells in 6mm diameter wells in DMEM phenol-free media. The cells were allowed to settle for $\geq$ 3 hours then treated with bortezomib (1, 10, 20, 50 and 100nM) or DMSO ("Veh"). At 24 hours, Hoechst dye (10µg/ml) was added to the wells and the cells incubated (37°C for 15 minutes). The levels of mCherry were collected using an Arrayscan VTI High Content Screening instrument. The percentage threshold of mCherry was measured against the DMSO vehicle control**. (A.)** After 24 hours of treatment, bortezomib treatment significantly increased HSF1 transcriptional activity relative to the DMSO vehicle control. **(B.)** Depiction of mCherry levels in DMSO vehicle control and bortezomib treated cells from the Arrayscan VTI High Content Screening instrument. Scale bar -100µm. All data is expressed as mean ± SEM of four independent experiments. Statistical analysis was performed by ANOVA, Dunnett's post *hoc* test, *** $p \leq 0.001$.

transcription factor MITF protein levels at 24 hours although maximal MITF protein expression varied between cell isolates (Figure 5.13 A-B.).

5.2.11 The Effect of Bortezomib Treatment on Osteoclastogenesis

RAW264.7 cells were seeded at 10^4 cells in 6mm diameter culture wells in the presence of RANKL (20ng/ml) and were treated with bortezomib (100, 200, 500 and 1000 pM). After 6 days of culture bortezomib treatment increased RANKL-dependent RAW264.7 cell osteoclast formation (Appendix Figure B9). To confirm this effect of bortezomib on osteoclast formation the experiment was repeated with primary bone marrow cells. Cells were seeded at 10^5 cells with RANKL (20ng/ml) and M-CSF (30ng/ml) and were treated with bortezomib (100, 200 and 500 pM) for 6 days. Bortezomib treatment significantly increased RANKL (20ng/ml) and MCSF (30ng/ml) stimulated bone marrow osteoclast formation over 6 days (Figure 5.14).

5.2.12 Inhibiting HSF1 Abolishes the Bortezomib-mediated Increase in Osteoclast Formation

As described above, bortezomib treatment causes a stress response in RAW264.7 cells. To determine whether this action and bortezomib enhanced osteoclast formation is dependent upon HSF1, osteoclast formation assays were performed in the presence of KNK437. RAW264.7 cells and primary bone marrow cells were treated with bortezomib (1nM) in the presence or absence of KNK437 (10µM). In RAW264.7 cells, bortezomib treatment significantly increased osteoclast formation as previously described, but the addition of KNK437 abolished the bortezomib-enhanced osteoclast formation back to DMSO vehicle control levels (Figure 5.15 A.). Likewise in primary bone marrow cells, KNK437 (10µM) treatment abolished the pro-osteoclastic actions of bortezomib (Figure 5.15 B.). KNK437 treatment reduced osteoclast numbers to levels similar to that of the DMSO vehicle control (Figure 5.15 A-B.). These data indicate that bortezomib increases osteoclast formation in a manner at least partially dependent upon the actions of HSF1 activity.

5.2.13 Cisplatin Increases HSP72 Protein Levels in RAW264.7 Cells

Cisplatin is one of the most common clinically used anti-cancer compounds and is used to treat cancers including testicular, ovarian, bladder, cervical, head and neck, oesophageal and small cell lung cancer (Cepeda *et al.*, 2007; Rafique, 2010). This compound is a platinum

Bortezomib Treatment Increases the Protein Levels of HSP72, NFATc1 and MITF

A.

24hr

Bortezomib (nM)

B.

48hr
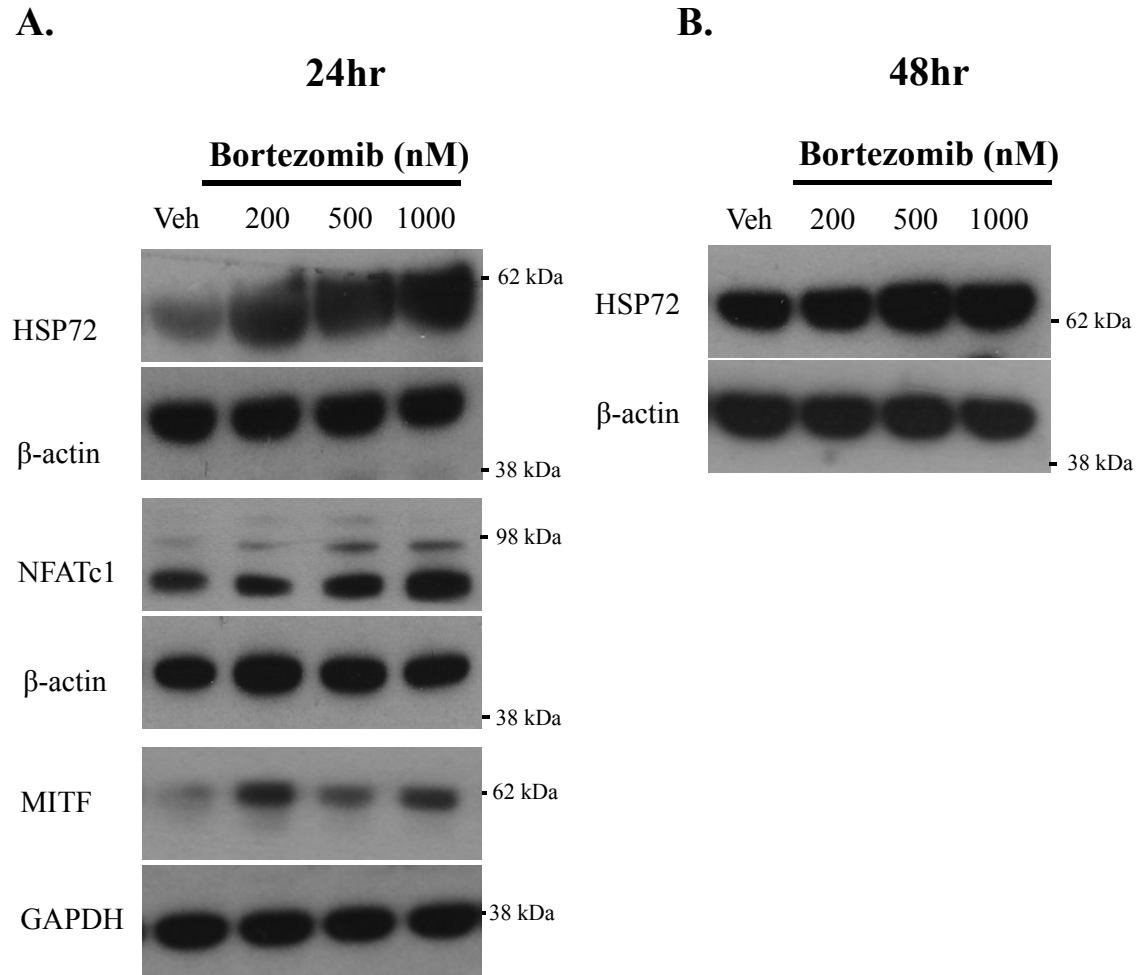
Bortezomib (nM)

Figure 5.13

RAW264.7 cells were seeded in 35mm diameter culture wells and were treated the following day with bortezomib (200, 500 and 1000 pM) or DMSO ("Veh") for **(A.) 24** and **(B.)** 48 hours. The cells were lysed and HSP72, NFATc1 and MITF protein levels determined by immunoblot analysis. Bortezomib treatment increased the protein levels of HSP72 at both 24 and 48 hours. Bortezomib treatment also increased osteoclast transcription factors: NFATc1 and MITF protein levels at 24 hours. Western blots were performed at least 2 to 3 times with independent protein samples.

Bortezomib Increases RANKL and M-CSF Mediated-Bone Marrow Osteoclast Formation
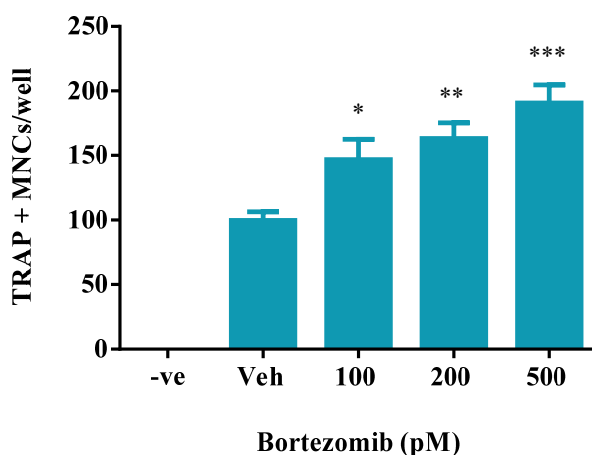
Figure 5 .14

Bone marrow cells were seeded at 10^5 cells in 6mm diameter culture wells. The cells were treated with RANKL (20ng/ml) and M-CSF (30ng/ml to stimulate osteoclast formation. The cells were treated with bortezomib (100, 200 and 500pM) or DMSO ("Veh") for 6 days. As a negative control the cells were only treated with M-CSF as denoted by "-ve". On day 6, TRAP positive multinucleated cells were counted as osteoclasts. Bortezomib treatment dose-dependently increased RANKL mediated osteoclast formation relative to the DMSO vehicle control. All data is expressed as mean ± SEM of five independent experiments. Statistical analysis was performed by ANOVA, Dunnett's *post hoc* test, * $p \leq 0.05$, ** $p \leq 0.01$, *** $p \leq 0.001$.

KNK437 Ablates the Bortezomib Mediated Increase in Osteoclast Formation

A.

B.

Figure 5.15

A. RAW264.7 cells. **B.** Bone Marrow Cells. **(A-B.)** RAW264.7 cells were seeded at 10^4 cells and bone marrow cells at 10^5 cells in 6mm diameter wells in the presence of RANKL (20ng/ml) and RANKL (20ng/ml) and M-CSF (30ng/ml), respectively. The cultures were treated with bortezomib (1nM) in the presence or absence of KNK437 (10μM) for 6 days. The cultures were also treated with KNK437 (10μM) alone, DMSO ("Veh") or had no treatment, "-ve". On day 6, multinucleated and TRAP positive cells were counted as osteoclasts. Bortezomib treatment significantly increases osteoclast formation in both cultures; however, the addition of KNK437 reduces osteoclast numbers similar to that in the DMSO vehicle control ("Veh"). All data is expressed as mean ± SEM of **A.** three and **B**. four independent experiments. Statistical analysis was performed using ANOVA, Dunnett's *post hoc* test, *** $p \le 0.001$.

coordination complex that belongs to the cross linking group of chemotherapeutics (Kostova, 2006). Cisplatin causes cellular apoptosis by genotoxic stress through cross-linking DNA and causing DNA damage (Nussbaumer *et al.*, 2011; Basu and Krishnamurthy, 2010). The work described in this chapter has determined the chemotherapeutics doxorubicin, MG132 and bortezomib, whilst having different modes of cytotoxic action all nevertheless increase HSF1 transcriptional activity in HEK-HSE cells. This approach was thus applied to cisplatin, with HEK-HSE cells treated with cisplatin (0.1, 0.2, 0.5, 1, 5 and 10µM) for a period of 24 hours. However, in contrast to the other chemotherapeutics, cisplatin treatment did not increase HSF1 transcriptional activity above that of the DMSO vehicle control despite concentrations of up to 5µM being used (Figure 5.16 A-B.). Despite cisplatin treatment not affecting HSF1 transcriptional activity in HEK-HSE cells, the effects of cisplatin treatment upon HSF1 activation was examined in RAW264.7 cells. RAW264.7 cells were seed at 2×10^5 cells in 35mm diameter cultures wells and the following day were treated with cisplatin (0.5, 1 and 3µM) for periods of 24 and 48 hours. After these timepoints the protein was extracted, and analysed by immunoblotting. Cisplatin treatment in increased HSP72 protein levels at both 24 and 48 hours in RAW264.7 cells (Figure 5.17 A-B.). The induction of HSP72 protein in the cisplatin treated cells indicates that this chemotherapeutic drug may activate HSF1 in RAW264.7 cells although no such effect was indicated in HSE-HEK cells.

5.2.14 The Effect of Cisplatin upon Protein Expression of NFATc1 and MITF

The effect of cisplatin upon the protein levels of transcription factors NFATc1 and MITF were also studied in RAW264.7 cells. Cisplatin treatment increased the cellular protein levels of NFATc1 at 24 hours and 48 hours treatment although a full dose dependent response was not always seen, suggesting some complexity in the cellular responses to this drug (Figure 5.17 A-B). Cisplatin treatment also increased MITF protein expression at 24 hours (Figure 5.17 A.). Cisplatin also increased MITF protein expression at 48 hours (Appendix Figure B10).

5.2.15 The Influence of Cisplatin upon Osteoclast Formation

As for the other chemotherapeutic agents the effects of cisplatin upon osteoclast formation was studied in both RAW264.7 and bone marrow cells. RAW264.7 cells were seeded in the presence of RANKL and were treated with cisplatin (0.1, 0.2, 0.5, and 1µM) (Figure 5.18 A.). Cisplatin treatment significantly increased osteoclastogenesis in the RANKL stimulated RAW264.7 cell line. RANKL (20ng/ml) and M-CSF (30ng/ml) stimulated primary bone

Cisplatin Does Not Increase HSF1 Transcriptional Activity in HEK-HSE Cells

A.

B.
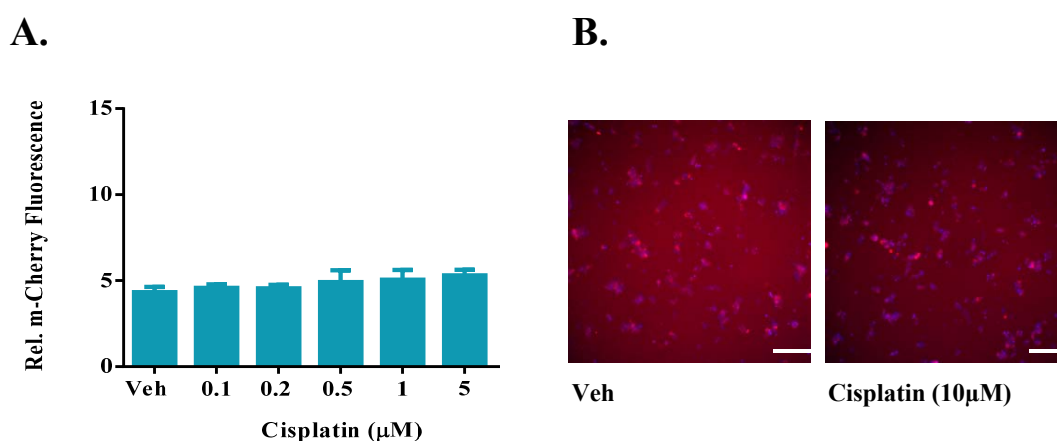
Figure 5.16

HEK-HSE cells stably transfected with a mCherry HSE reporter were seeded at 2.5 x 10^4 cells in 6mm diameter culture wells in DMEM phenol-free media. The cells were allowed to settle for ≥ 3 hours then treated with cisplatin (0.1, 0.2, 0.5, 1 and 5μM) or DMSO ("Veh") for 24 hours. At 24 hours, Hoechst dye (10μg/ml) was added to the wells and the cells incubated at 37°C for 15 minutes. The levels of mCherry were collected using an Arrayscan VTI High Content Screening instrument. The percentage threshold of mCherry was measured against the DMSO vehicle control. At 24 hours, the chemotherapeutic, cisplatin, did not increase HSF1 activity in the HEK-HSE cells relative to the DMSO vehicle control. **(B.)** Depiction of mCherry levels in DMSO vehicle control and cisplatin treated cells from the Arrayscan VTI High Content Screening instrument. Scale bar - 100μm. All data is represented as the mean ± SEM of four independent experiments. Statistical Analysis was performed by ANOVA, Dunnett's post *hoc* test.

Cisplatin Increases the Protein Levels of HSP72 and Transcription Factors

A.   **B.**
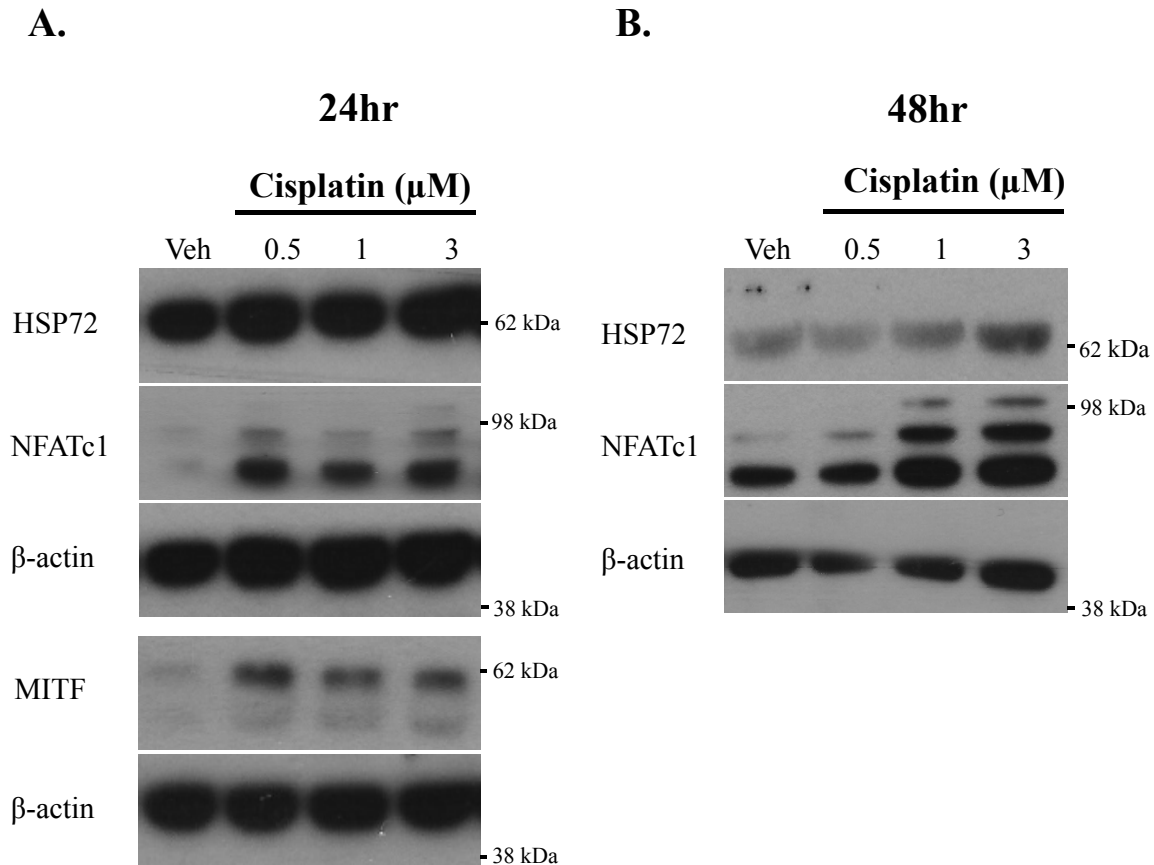
Figure 5.17

RAW264.7 cells were seeded at 2 x10^5 in 35mm diameter culture wells and were treated the following day with cisplatin (0. 5, 1 and 3 μM) or DMSO ("Veh") for 24 and 48 hours. The cells were lysed and HSP72, NFATc1 and MITF protein levels determined by immunoblot analysis. Cisplatin treatment increased the protein levels of HSP72 at both 24 and 48 hours. Cisplatin treatment increased protein levels of osteoclast transcription factor NFATc1 at 24 and 48 hours. In addition, MITF protein levels were also increased by cisplatin treatment for 24 hours. Western blots were performed 2 to 3 times with independent lysates.

marrow cells were also treated with the same concentrations of cisplatin as the RAW264.7 cells for 6 days. Similar to the RAW264.7 cells, cisplatin treatment significantly increased osteoclast formation from bone marrow cultures in a dose-dependent manner (Figure 3.18 B.).

5.2.16 The Effect of HSF1 Inhibition upon Cisplatin Enhancement of Osteoclastogenesis

To ascertain the role of HSF1 in the cisplatin mediated increase in osteoclast formation, HSF1 was inhibited using KNK437 and osteoclast assays performed using primary bone marrow cells. The RANKL and M-CSF stimulated cell cultures were treated with cisplatin (1μM) in the presence or absence of KNK437 (10μM). Cisplatin treatment significantly increases osteoclast formation in bone marrow progenitor cells (Figure 3.19) and addition of KNK437 abolished this increase in osteoclast formation (Figure 3.19). Similarly, initial experiments showed inhibition of HSF1 in RAW264.7 cells decreased the cisplatin-mediated increase in osteoclast numbers (Appendix Figure B12).

5.2.17 The Effect of Ethanol upon HSP72 Expression in RAW264.7 Cells

Ethanol is not a chemotherapeutic agent however, it is well known to cause a classic oxidative stress in cells (Ambade and Mandrekar, 2012; Pignataro *et al.*, 2007). In addition to causing oxidative stress, ethanol has also been shown to affect HSF1 activity and interestingly the cell responses to alcohol often intersect with molecules in the HSR pathway (Pignataro *et al.*, 2007). Consistent with these reports, Chai *et al.* showed that ethanol causes a HSF1 mediated cell stress response by increasing HSP70 protein expression in RAW264.7 cells at 24 hours (Chai *et al.*, 2014).

Based on this data, the same line of enquiry was followed for ethanol as for the chemotherapeutics. Firstly, the effects ethanol has upon osteoclastogenic factors MITF was determined. Ethanol treatment increased the late acting transcription factor MITF protein expression at both 24 and 48 hours relative to the negative control (Figure 5.20 A-B.). This data shows ethanol increases the protein levels of osteogenic transcription factor, MITF in RAW264.7 cell cultures. Initial studies have also shown ethanol treatment to increase protein levels of NFATc1 (Appendix Figure B11).

Cisplatin Enhances Osteoclast Formation in RAW264.7 and Bone Marrow Cells

A.

B.
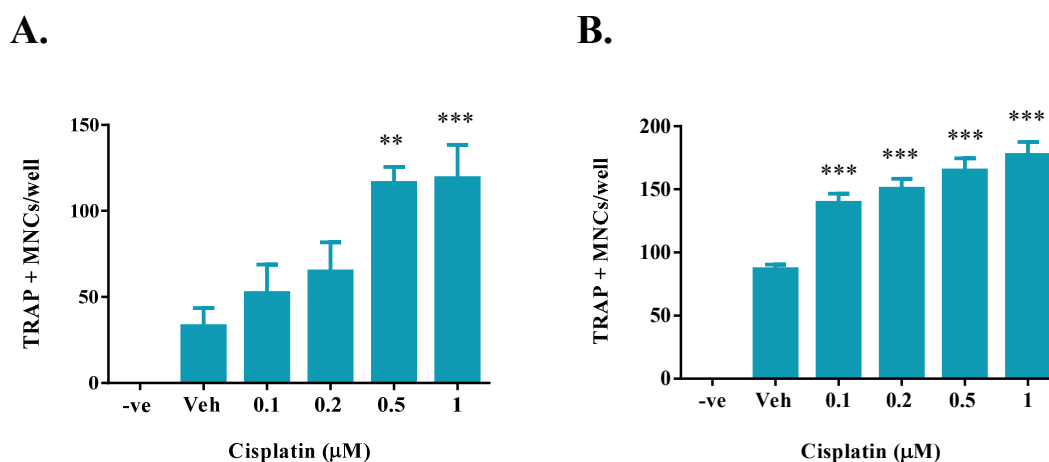
Figure 5.18

(A.) RAW264.7 cells, **(B.)** Bone Marrow Cells. RAW264.7 cells were seeded at 10^4 cells and Bone Marrow cells at 10^5 cells in 6mm diameter wells in the presence of RANKL (20ng/ml) and RANKL (20ng/ml) and M-CSF (30ng/ml), respectively. **(A-B.)** The cultures were treated with cisplatin (0. 1, 0.2, 0.5, and 1μM) or DMSO ("Veh") for 6 days. As a negative control cells were also left untreated "-ve". On day 6 multinucleated and TRAP positive cells were counted as osteoclasts. Cisplatin treatment significantly increased RANKL mediated osteoclast formation relative to the DMSO vehicle control. All data is expressed as the mean ± SEM of **(A.)** three and **(B.)** eight independent experiments. Statistical analysis was performed using ANOVA, Dunnett's post *hoc* test ** $p \leq 0.01$, *** $p \leq 0.001$.

KNK437 Abolishes the Cisplatin Elicited Increase in Osteoclast Formation

Cisplatin (1µM)	-	Veh	-	+	-
RANKL (20ng/ml)	-ve	+	+	+	+
KNK437 (10µM)	-	-	+	-	+
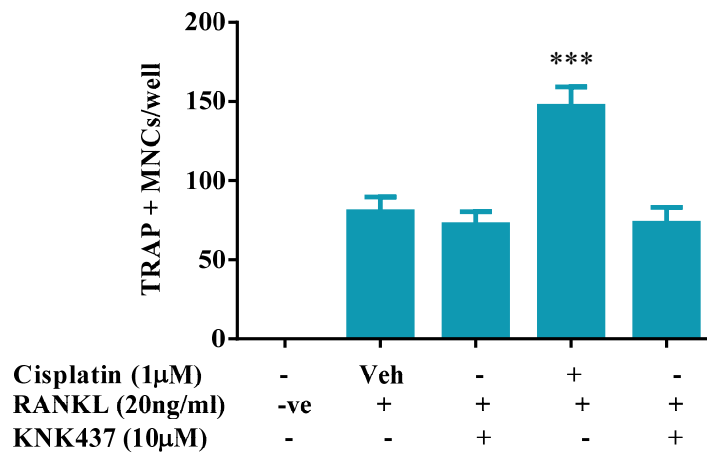
Figure 5.19

Bone Marrow Cells were seeded at 10^5 cells in 6mm diameter wells in the presence of RANKL (20ng/ml) and M-CSF (30ng/ml). The cultures were treated with cisplatin (1µM) in the presence or absence of KNK437 (10µM) for 6 days. The cultures were also treated with DMSO ("Veh") or KNK437 (10µM) alone. The cells were fixed and stained for TRAP. Multinucleated and TRAP positive cells were counted as osteoclasts. As previously shown cisplatin increases osteoclast formation from bone marrow cells. Adding KNK437 to inhibit HSF1 eradicated the cisplatin mediated increase in osteoclast numbers to DMSO vehicle control levels. All data is expressed as mean ± SEM of four independent experiments. Statistical analysis was performed using ANOVA, Dunnett's post *hoc* test *** $p \leq 0.001$.

Ethanol Increases the Protein Levels of MITF

A.   **B.**

24hr   **48hr**
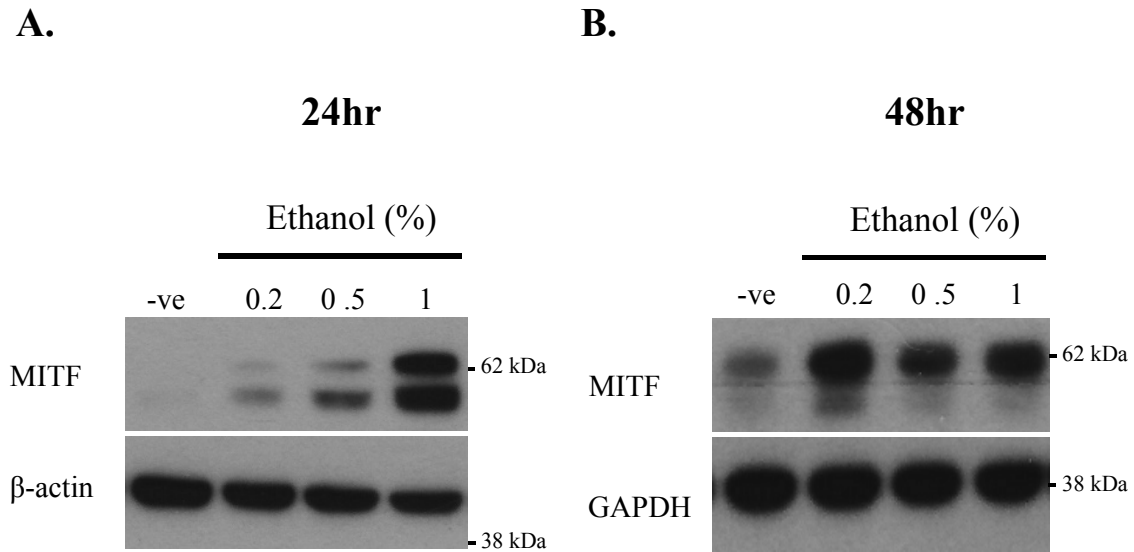
Figure 5.20

RAW264.7 cells were seeded at 2 x10^5 in 35mm diameter culture wells and were treated the following day with ethanol (0.2,0 .5 and 1%) for **(A.)** 24 and **(B.)**. 48 hour. As a negative control the cells were left untreated, "-ve". The cells were lysed and MITF protein levels determined by immunoblotting analysis. Ethanol treatment increased MITF protein levels at both 24 and 48 hours relative to the negative control. Western blots were performed at least 2 to 3 times with independent lysates.

5.2.18 The Effect of Ethanol upon Osteoclast Formation

The effects of ethanol treatment upon osteoclast formation were then studied using both RAW264.7 and bone marrow cells. RAW264.7 cells were seeded at 10^4 cells in 6 mm diameter wells in the presence of RANKL and were treated with ethanol (0.2, 0.5 and 1%). Ethanol treatment significantly increased osteoclastogenesis in the RANKL stimulated RAW264.7 cell line (Figure 5.21 A.). Similarly, RANKL (20ng/ml) and M-CSF (30ng/ml) stimulated primary bone marrow cells were also treated with ethanol (0.2, 0.5 and 1%) for 6 days. Likewise, ethanol treatment significantly increased osteoclast formation in bone marrow cultures (Figure 5.21 B.).

As earlier described ethanol causes HSF1 activation in RAW264.7 cells (Chai *et al.*, 2014). In addition, key osteoclastogenic transcription factors NFATc1 and MITF protein levels are increased in response to ethanol treatment. Paramount to this is that ethanol increases osteoclast formation in RAW264.7 and bone marrow cells (also shown by (Chai *et al.*, 2014). To determine whether ethanol enhanced osteoclast formation is dependent upon HSF1, osteoclast formation assays were performed in the presence of KNK437. RAW264.7 cells and primary bone marrow cells were treated with ethanol (1%) in the presence or absence of KNK437 (10µM). As previously described ethanol treatment increases osteoclast formation in both RAW264.7 and bone marrow cells; however, addition of KNK437 abolishes the ethanol enhanced osteoclast formation back to DMSO vehicle control levels (Appendix Figure B13).

Ethanol Enhances Osteoclast Formation in RAW264.7 and Bone Marrow Cells

A.

B.
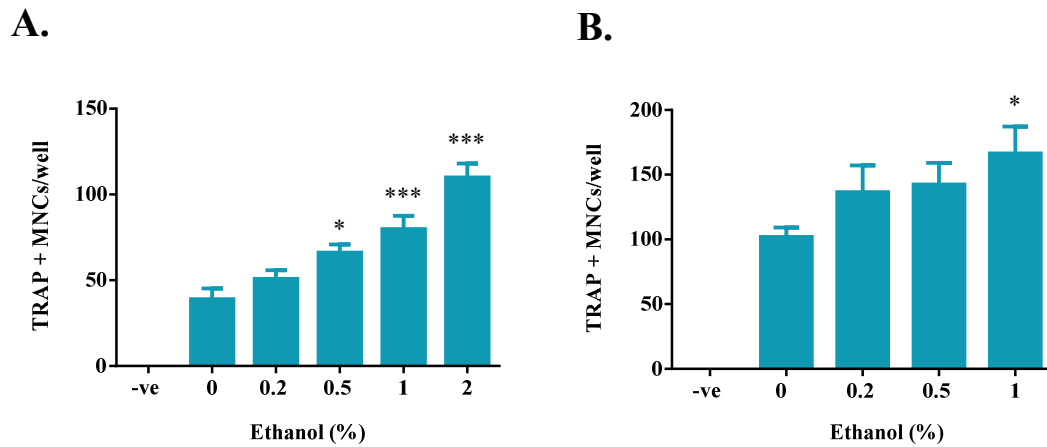
Figure 5.21

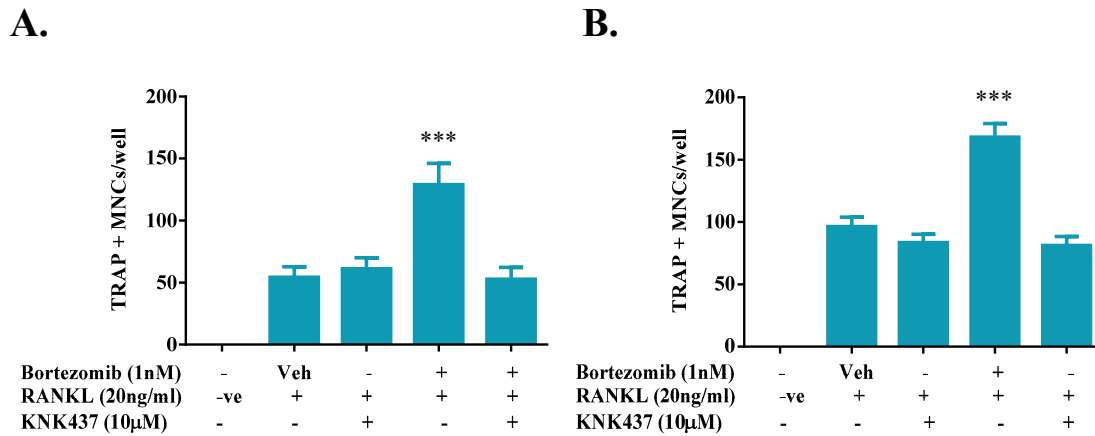**(A.)** RAW264.7 cells, **(B.)** Bone Marrow Cells. (A-B.) RAW264.7 cells were seeded at 10^4 cells and bone marrow cells at 10^5 cells in 6mm diameter wells in the presence of RANKL (20ng/ml) and RANKL (20ng/ml) and M-CSF (30ng/ml), respectively. The cultures were treated with ethanol (0.2, 0.5, and 1%) for 6 days. Multinucleated and TRAP positive cells were counted as osteoclasts. Ethanol treatment significantly increased RANKL mediated osteoclast formation relative to the RANKL (20ng/ml) control in both cultures. All data is expressed as the mean ± SEM of **(A.)** three and **(B.)** four independent experiments. Statistical analysis was performed using ANOVA, Dunnett's post *hoc* test * p ≤ 0.05, *** p ≤0.001.

5.3 Discussion

The experiments described in this chapter were designed to investigate the hypothesis that compounds, which induce cell stress by mechanisms other than direct HSP90 inhibition have the ability to increase osteoclast formation *in vitro* in a manner similar to 17-AAG. The list of stimuli was not exhaustive but focussed on compounds that have been reported to cause some type of stress response in other cells, mainly cytotoxic compounds. Initial experiments were also performed with some other compounds, including thapsigargin (an ER stress inducer and calcium dependent pathway inhibitor), hydrogen peroxide (a classic oxidative stressor) and celastrol (thought to be direct HSF1 inducer). However, initial studies with thapsigargin showed it did not increase osteoclast formation with the concentrations used, and the others displayed strong toxicity at concentrations where HSF1 induction occurs (data not shown). As a result these compounds were not pursued further. High toxicity is also a feature of the HSP90 inhibitor geldanamycin, which made that compound similarly unsuitable for study. Five stimuli were chosen for particular study: doxorubicin, bortezomib, MG132, cisplatin and ethanol. All of these compounds have significant clinical importance and affect bone metabolism *in vivo* although their effect on osteoclast biology are either not known or poorly characterised (Kemp *et al.*, 2011; Rana *et al.*, 2013; Friedlaender *et al.*, 1984; van Leeuwen *et al.*, 2000; Hadji *et al.*, 2009).

There are a number of cell stress pathways including oxidative stress, ER stress, genotoxic stress and metabolic stress but HSF1 is categorized as the critical mediator of cell stress regulating the HSR within the cell (Fulda *et al.*, 2010; Davenport *et al.*, 2007; Cuenda and Rousseau, 2007; Chaudhari *et al.*, 2014; Morimoto, 2002; Christmann and Kaina, 2013). As previously described, HSF1 is activated by cell stress stimuli that induce HSP gene transcription and expression, which requires HSF1 binding to HSEs present within the promoters of HSP coding genes (ÅKerfelt *et al.*, 2007; Morimoto, 2002). This HSE dependency is seen in classic stress inducible chaperones such as HSP72, HSP70B and HSP90 (Åkerfelt *et al.*, 2010; Stephanou and Latchman, 2011). However, active HSF1 also promotes the expression of a range of other target genes, which include RANKL and MITF in osteoblasts and endothelial cells, respectively (Laramie *et al.*, 2008; Roccisana *et al.*, 2004). While HSF1 plays a crucial role in cell responses to heat shock and cytotoxic stresses that cause protein misfolding, the HSR functionally overlaps with other cell response pathways such as ER and metabolic stress, oxidative stress, and genotoxic stress pathways (Gutterman,

2005; Fucikova *et al.*, 2011; Desai *et al.*, 2013; Lee and Hahn, 1988; Beckmann *et al.*, 1992; Vabulas *et al.*, 2010; Martindale and Holbrook, 2002). It is notable that p38 and JNK MAP kinase pathways, are also activated by many types of cellular stress, but how these factors functionally interact with HSF1 is unclear (Kim *et al.*, 1997; Obata *et al.*, 2000; Raingeaud *et al.*, 1995; Rafiee *et al.*, 2006).

N-Terminal HSP90 inhibitors cause a HSF1 stress response by causing HSF1 to displace from HSP90 and its subsequent activation (Zou *et al.*, 1998; Taylor *et al.*, 2007; Kamal *et al.*, 2004). However, chemotherapeutics that are not HSP90 inhibitors cause cytotoxic stress to the cell and hence can cause strong HSF1 activation, possibly through HSP90 client protein misfolding (Bracci *et al.*, 2014). The effect of four chemotherapeutics, including doxorubicin and the proteasome inhibitors MG132 and bortezomib upon HSE-dependent activity was studied in HEK-HSE cells. Treatment with these chemotherapeutics significantly increased HSF1 transcriptional activity at 24 hours, which is consistent with previous reports that both MG132 and bortezomib activate HSF1 (Fucikova *et al.*, 2011; Holmberg *et al.*, 2000; Du *et al.*, 2009; Kim *et al.*, 1999). MG132 treatment has been shown to increase HSF1 nuclear localization in HeLa cells causes the formation of HSF1 nuclear stress bodies, and it is notable that HSF1 inhibition increases MG132 toxicity (Du *et al.*, 2009; Holmberg *et al.*, 2000). This suggests that induction of an HSR blunts to some degree the cancer toxicity shown by this drug. In addition, MG132 has also been shown to cause HSF1 trimerization (Guo and Peng, 2013). Moreover, MG132 and another 26S proteasome inhibitor, lactacystin, induce HSF1 hyper-phosphorylation and increase HSF1 DNA binding activity in the apparent absence of heat shock, i.e., HSP induction (Kim *et al.*, 1999; Guo and Peng, 2013). It is proposed that this action of MG132 occurs by a HSF-targeting kinase whose expression is increased upon MG132 treatment although the kinases casein kinase II, p38, protein kinase C, myosin light chain kinase, calmodulin protein kinase, PI-3K and DNA-PK are not involved in this process (Kim *et al.*, 1999). A simpler explanation, however, is that MG132 inhibition of the proteasome stops the degradation of proteins, which are misfolded, and thereby triggers the UPR response and activation of HSP90 and HSF1. The data presented in this chapter is consistent with these findings, with HSF1 transcriptional activity being increased with MG132 treatment. In addition, MG132-induced HSF1 activity was decreased by the use of the HSF1 inhibitor KNK437. MG132 treatment also up-regulated HSP72 protein in RAW264.7 cells, a clear indication of HSF1 activation and a subsequent heat-shock response.

It should also be noted that MG132 has also been implicated in a number of other cell stress pathways including oxidative stress and MAP kinase pathways that include p38, JNK and ERK (Yong Hwan Han and Woo Hyun Park, 2010). MG132, although a proteasome inhibitor, is thought to cause cell apoptosis mainly through the production of ROS (Yong Hwan Han and Woo Hyun Park, 2010; Han *et al.*, 2010). MG132 has been shown to increase ROS production and decrease GSH levels in A549 lung cells and As4.1 juxtaglomerular cells (Yong Hwan Han and Woo Hyun Park, 2010; Han *et al.*, 2010). Mild changes in the oxidative-redox equilibrium are known to activate the stress MAP kinases JNK and p38, suggesting that MG132 effects upon ROS and GSH levels may additionally activate the p38 pathway (Yong Hwan Han and Woo Hyun Park, 2010). Thus, p38 may have a role in MG132 pro-osteoclastogenic effects, possibly by affecting MITF pools. It is interesting to note GSH/GSSH levels have been shown to regulate osteoclastogenesis, which is discussed in more detail later (Huh *et al.*, 2005; Romagnoli *et al.*, 2013; Iitsuka *et al.*, 2012).

Bortezomib, another proteasome inhibitor that is used clinically to treat multiple myeloma patients, also increases HSF1 transcriptional activity in HEK-HSE cells at 24 hours. Furthermore, initial experiments have shown HSF1 inhibition decreases the bortezomib-mediated increase in HSF1 transcriptional activity. In addition, bortezomib increased inducible HSP72 protein levels in RAW264.7 cells. Similarly, Kao *et al*. 2013 found bortezomib increased HSE response element activity and also HSF1 protein expression in the TOV112D ovarian cancer cell line (Kao *et al.*, 2013). Similar responses have been noted in various other cell types also (Selimovic *et al.*, 2013; Kao *et al.*, 2013). Induction of such HSF1 dependent responses is probably a consequence of several actions of bortezomib proteasomal inhibition including: cell cycle initiation of apoptosis pathways, the induction of ER stress (UPR) and also the deregulation of NFκB activity (Selimovic *et al.*, 2013). It should be noted, however, that such responses may differ greatly between cells types. Bortezomib has also been shown to trigger the phosphorylation of IRE1α, ASK1, JNK and p38 and enhance the DNA binding activity of transcription factors: Activator protein-1 (AP-1), Activating transcription factor 2 (ATF-2), E26 avian leukemia oncogene 1, 5' domain (Ets-1), and HSF1 (Selimovic *et al.*, 2013). These molecules participate in cell stress signalling cascades including ER stress (UPR), p38 stress signalling and the HSR. ER stress (UPR) has previously been shown to increase osteoclast formation with ER stress inducers thapsigargin and tunicamycin increasing osteoclast markers including TRAP (Wang *et al.*,

2011b; Yip *et al.*, 2005). This data suggests ER stress may have a role in osteoclastogenesis. Thapsigargin, effects on osteoclast differentiation are currently unclear, however, ER stress induced autophagy has been implicated in positively regulating osteoclastogenesis (Wang *et al.*, 2011a). Autophagy is a cytoprotective process in which cells break down proteins and organelles promoting cell survival in stressful conditions (Hocking *et al.*, 2012; Wirawan *et al.*, 2012). ER stress induced autophagy is thought to occur through the MCPIP protein, which is involved in oxidative stress, ER stress (UPR) and autophagy (Wang *et al.*, 2011b). Inhibition of ER stress abolished autophagy and correspondingly decreased expression of osteoclast markers (Wang *et al.*, 2011b). Recently MAP kinases and HSR have also been implicated in ER-stress-induced autophagy (Selimovic *et al.*, 2013). ROS generated by bortezomib effect upon the mitochondria cause the phosphorylation of the ASK1 protein, which is important in ER stress processes (UPR) (Selimovic *et al.*, 2013). This protein phosphorylates both JNK and p38. and inhibition studies of ASK1 and JNK showed that bortezomib induction of HSP72 was abrogated (Selimovic *et al.*, 2013). It is interesting to note HSP90 inhibitors geldanamycin, 17-AAG and NVP-AUY922 have all been shown to induce or enhance autophagic processes (Qing *et al.*, 2006; Mori *et al.*, 2015b; Rusmini *et al.*, 2011; Hsueh *et al.*, 2013).

Doxorubicin and cisplatin, two of the most commonly used cancer therapeutics, act to cause cell apoptosis through DNA intercalation and cross-linking, respectively (Nussbaumer *et al.*, 2011; Basu and Krishnamurthy, 2010). DNA intercalating and cross-linking both result in genotoxic stress and activation of a number of stress pathways (Nussbaumer *et al.*, 2011; Basu and Krishnamurthy, 2010). Anthracyclines, such as doxorubicin, have been shown to cause oxidative stress through mitochondrial dysfunction and the resulting increase in ROS production (Ewer and Lippman, 2005). Interestingly, anthracyclines have also been shown to increase the expression of HSPs in human prostate, ovarian and acute lymphoblastic leukemic cells, and neuroblastoma cells (Fucikova *et al.*, 2011; Zanini *et al.*, 2007). This data supports the hypothesis that stress mechanisms other than genotoxic stress may be involved in doxorubicin mediated cytotoxicity. In HEK-HSE cells, doxorubicin significantly increased HSF1 transcriptional activity whilst initial studies have shown HSF1 inhibition with KNK437 decreased it. Moreover, RAW264.7 cells treated with doxorubicin had increased levels of HSP72 at 24 and 48 hour time points, which is further evidence of the activation of HSF1 by this compound. Interestingly, cisplatin has also been shown to induce HSP72 transcription in response to ROS, which are generated by cisplatin inhibition of RNA transcription (Ohtsuboa

et al., 2000; Huber, 1992). The second generation platinum coordination complex carboplatin has also recently been shown to activate HSF1 and increase expression of Autophagy Related 7 (ATG7) protein, an important protein in autophagy processes such as membrane fusion (Desai *et al.*, 2013). However, the actions of cisplatin in the current study were not as consistent as seen with the other stressors presented here with cisplatin not affecting HSF1 activity despite high concentrations (up to 5μM) being used. Despite cisplatin treatment not affecting HSF1 activity assays in HEK-HSE cells, it did increase HSP72 protein levels at both 24 and 48 hours in RAW264.7 cells. The reasons for this apparent discrepancy are unclear. It may be that HSP72 protein is increased by cisplatin treatment through post-translational modifications of HSF1. However, treatment with cisplatin, as well as doxorubicin, both causes an increase in osteoclast formation in a dose-dependent manner in RAW264.7 cell and bone marrow cells. Inhibition of HSF1 with KNK437 abolished both these therapeutics' effects upon osteoclast formation in primary bone marrow cells. This data shows that a HSR (however, incomplete in the case of cisplatin) is sufficient to affect cells similarly to the HSP90 inhibitors.

Ethanol is not a chemotherapeutic, however, does cause a classic oxidative stress in the cell (Albano, 2006). Ethanol exposure has previously been shown to cause the translocation of HSF1 to the nucleus, the formation of stress granules and the transcription of HSPs including HSP72 and HSP90 (Pignataro *et al.*, 2007; Morimoto, 1998). The similarities between heat shock and ethanol exposure were examined in the neuron specific gene Gabra4,which is activated by alcohol and contains alcohol response elements (AREs) (Pignataro *et al.*, 2007). Surprisingly, the effect of heat shock mimicked the effects of ethanol upon Gabra4 expression (Pignataro *et al.*, 2007). Electrophoretic mobility shift assay (EMSA) experiments showed that HSF1 can bind to ARE sequences suggesting that both ethanol and HSF1 can mediate their effects through this sequence (Pignataro *et al.*, 2007). Further, many alcohol-responsive genes (ARGs) contain alcohol response element (ARE)-like sequences and some of these genes have been shown to be activated by heat shock (Pignataro *et al.*, 2007). These results suggest that ethanol can activate pathways in which some molecules are involved in the heat shock response and ARE-like sequences may be involved in this process (Pignataro *et al.*, 2007). Chai *et al.* (2014) also showed ethanol to increase HS70 protein expression in the RAW264.7 cell line.

The studies in Chapters 3 and 4 have shown that HSP90 inhibitor effects upon osteoclast formation occur through HSF1 and are associated with increased MITF levels. Furthermore, MITF induction by 17-AAG was shown to be HSF1 dependent (Chai *et al.*, 2014). These observations were consistent with observations here that ethanol, MG132, bortezomib, cisplatin, and doxorubicin all increased RANKL driven osteoclast differentiation in both RAW264.7 cells and bone marrow cell cultures. Thus, chemotherapeutics and compounds that do not inhibit HSP90 have pro-osteoclastogenic effects. Significantly, all these compounds were shown to activate HSF1 and inhibition of HSF1, through KNK437, eradicated the chemotherapeutics' enhancement of osteoclast formation. The data suggests that these chemotherapeutics, like 17-AAG and NVP-AUY922, are dependent upon HSF1 for their enhancement of osteoclast formation, and that stress stimuli that activate HSF1 have an important role in enhancing osteoclast formation. As noted earlier, the promoter region of the *Mitf* gene has been reported to contain HSE motifs that are sensitive to heat shock, which might mediate the effects of these stressors on osteoclast formation (Laramie *et al.*, 2008). However, this is yet to be demonstrated properly with attempts to show binding of HSF1 to *Mitf* promoter sequences by our group chromatin immunoprecipitation being unsuccessful to date (data not shown). However, the role of stress activated molecules in osteoclast formation is not limited to HSF1 mediated stress alone, as ROS, pro-inflammatory cytokines, and p38 either increase or are essential for osteoclastogenesis (Li *et al.*, 2002; Kim *et al.*, 2009; Bezerra *et al.*, 2005; Kim *et al.*, 2006; Ha *et al.*, 2004; Lee *et al.*, 2005). These compounds studied have been implicated to also activate these molecules, and, as such, further investigations should be made of the effects of these compounds upon these molecules in relation to osteoclastogenesis. It may be that crosstalk between pathways cause the activation of HSF1, p38 and other molecules or processes, which are important in osteoclastogenesis.

The effects of these chemotherapeutics upon important osteoclastogenic transcription factors including NFATc1 and MITF were thus examined to explore the mechanism of action of these compounds. Interestingly, all the chemotherapeutics increased NFATc1 protein expression to some degree. Initial studies with ethanol treatment also increased NFATc1 protein levels at both 24 and 48 hours. This is in contrast to the actions of the N-terminal HSP90 inhibitor 17-AAG, which did not increase NFAT transcriptional activity nor NFATc1 protein levels but rather led to a slight decrease in activity and protein levels. Rather 17-AAG only affected the late acting osteoclastogenic transcription factor MITF. Like 17-AAG, chemotherapeutics, MG132, doxorubicin, cisplatin, and bortezomib all increased MITF

protein levels. Ethanol treatment also increased MITF protein expression. This data suggests that these chemotherapeutics are increasing osteoclast formation, at least in part, through the activation of these molecules. The fact that HSF1 is required for the enhancement of osteoclast formation suggests that HSF1 may act upon these osteoclastogenic factors to increase osteoclast formation. For example, the compounds may increase MITF in a HSF1 dependent manner, like 17-AAG, or, alternatively, the increased protein levels of NFATc1 might feed into MITF protein expression. However, as described previously, these chemotherapeutics cause a myriad of stress pathways and signalling molecules to be activated, which may affect osteoclast formation through other mechanisms. Nevertheless, the association of HSR and increased osteoclast formation is striking. This has clear pathophysiological implications, and is suggestive of HSF1 roles in osteoclast formation even though it may not be a direct action through MITF.

Interestingly, BMM generated from mice exposed to ethanol over a three week period have been previously shown to have significantly increased mRNA levels of RANK, c-FOS, c-JUN, TRAP and CTSK but M-CSF and c-FMS mRNA levels are not affected (Iitsuka *et al.*, 2012). Ethanol treatment also increased the mRNA and protein levels of PU.1 and its associated transcription factor MITF (Iitsuka *et al.*, 2012). In the same report, ethanol was shown to increase osteoclast formation of bone marrow-derived macrophage/monocyte precursor cells *in vitro* and *in vivo* with higher numbers of osteoclasts being present in the proximal tibia (Iitsuka *et al.*, 2012). Similar to 17-AAG, ethanol treatment did not affect the osteoclast precursor cells that respond to M-CSF but rather affected the progenitor cells through RANKL signalling. The increase in osteoclastogenesis was associated with the activation of ERK through ROS production and increased levels of the RANK receptor (Iitsuka *et al.*, 2012). The increased RANK levels were shown to be mediated through ethanol's induction of PU.1 and MITF expression (Iitsuka *et al.*, 2012). Interestingly, increased lipid peroxidation (and associated lower GSH levels), which has been found to increase osteoclast differentiation was also reported in these mice. (Iitsuka *et al.*, 2012; Sanbe *et al.*, 2009). This data suggests stress pathways work cooperatively to affect osteoclastogenesis. From the data presented in this chapter, ethanol treatment was shown to similarly increase protein levels of MITF and also of NFATc1. The effect of ethanol upon these osteoclast transcription factors may directly enhance osteoclastogenesis. Alternatively, there might be a number of mechanisms that are occurring in concert with one another to cause the increase in osteoclast formation including increased RANK expression. This data

provides some explanation for the effects of ethanol administration to lower bone mass in mice (Mercer *et al.*, 2012; Zhang *et al.*, 2002a). Similarly, alcoholism is known to induce osteopenia, although the consequences of alcohol-related liver damage on bone, complicate any interpretation of ethanol effects on bone (Alvisa-Negrín *et al.*, 2009). Further work looking into the possible effect of HSF1 induction of MITF and NFATc1 and the effect of the induction of these transcription factors upon RANK expression should be followed up for the compounds studied in this chapter.

Bone loss observed in pathological conditions such as osteoporosis and inflammatory diseases as a result of increased osteoclast numbers (Kim *et al.*, 2006; Boyle *et al.*, 2003). In these conditions often the inflammatory cytokine TNF-α strongly synergizes with RANKL and large amounts of ROS are produced (Kim *et al.*, 2006). Evidence for the role of ROS in increasing osteoclast formation is steadily building. RANKL or RANKL/TNF-α driven osteoclast formation can be inhibited by the antioxidant α-lipoic acid (α-LA) *in vitro* (Kim *et al.*, 2006). Also this antioxidant can supress *in vivo* RANKL driven or RANKL/TNF driven bone loss in a calvarial remodeling model (Kim *et al.*, 2006). Lifestyle choices, which are risk factors for osteoporosis, such as smoking, hypertension and diabetes mellitus are also associated with increased oxidative stress and increased free radicals levels (Sheweita and Khoshhal, 2007). This suggests that ROS generated from these chemotherapeutics may act to increase osteoclast differentiation. These reports implicate a wide range of stress stimuli to be involved in the enhancement of osteoclast differentiation.

Chemotherapeutics generally have an adverse effect on the bone marrow as a whole. However, the effects of the studied chemotherapeutics enhancing osteoclast formation in the clinical setting are not known, i.e., any effects that these chemotherapeutics are having on osteoclast formation *in vivo* may be masked by the more general deleterious effects upon bone. Cisplatin has been shown to decrease: mineralized bone volume, the percentage of woven bone volume and the percent of osteoclast-covered bone (Ehrhart *et al.*, 2002). Despite these reductions cisplatin treatment did not affect total bone mineral density (Ehrhart *et al.*, 2002). The authors of this work suggested that cisplatin treatment may result in the uncoupling of bone formation due to either increased osteoclast activity or a delayed response by the osteoblasts to lay down new bone matrix. (Ehrhart *et al.*, 2002). Doxorubicin also negatively affects the bone marrow in a similar manner (Shusterman and Meadows, 2000; van Leeuwen *et al.*, 2000; Hadji *et al.*, 2009; Friedlaender *et al.*, 1984). Recently,

doxorubicin has been shown to increase osteoclast differentiation (Rana *et al.*, 2013). In a 4T1 breast cancer model in which tumour cells naturally metastasise to bone from mammary fat pads, doxorubicin increased osteolytic lesions eight fold, relative to untreated tumour-bearing mice (Rana *et al.*, 2013). Furthermore, trabecular bone volume was decreased by 50% (Rana *et al.*, 2013). Interestingly, the authors presented data that doxorubicin actions upon bone loss are mediated through both TGF-β and oxidative stress (ROS) (Rana *et al.*, 2013). However, this data was not conclusive as their blockade can inhibit osteoclast formation in general (Rana *et al.*, 2013). It may be possible that doxorubicin ability to increase TGF-β acts upon NFATc1; whilst ROS may increase p38 and HSF1 activation and expression, which can affect MITF levels. The antimetabolite methotrexate has also been shown to decrease trabecular bone volume (Friedlaender *et al.*, 1984). Although these compounds have complex actions on bone, due to their osteolytic actions it is essential to study the effect that these chemotherapeutics are having *in vivo* upon osteoclast formation in the presence of cancer that has metastasized to bone. As previously described in Chapter 1.9.4, the HSP90 inhibitor, 17-AAG, increased tumour growth in the hind limbs of mice by increasing osteoclast formation and the proposed augmentation of the vicious cycle (Price *et al.*, 2005; Yano *et al.*, 2006). 17-AAG increase of osteoclast formation and resorptive activity would have released a milieu of bone matrix factors, which promoted tumour growth and metastatic bone disease (Price *et al.*, 2005). Therefore the effects that these chemotherapeutics, at dosages, which would be used to treat tumours, have upon osteoclast formation, upon the vicious cycle of tumour growth and bone resorption, needs to be assessed. It may be that the administration of such drugs to patients with cancers that have metastasized to bone may increase their growth there.

In summary, five compounds of clinical importance chosen for their known or putative abilities to induce HSF1 dependent cell stress in some cell lines were studied for their abilities to affect osteoclast differentiation. These compounds were chemically unrelated and varied markedly in their actions on cells. However, all increased osteoclast formation and induced cell stress responses that included HSP72 induction. Similarly, the increased osteoclast formation observed with these treatments were reduced by co-treatment with HSF1 inhibitor KNK437. This data suggests that, like HSP90 inhibitors, these compounds enhanced osteoclastogenesis in an HSF1 dependent manner. Furthermore, all of the compounds increased the protein levels of MITF in RAW264.7 cells, which again is similar to the actions of HSP90 inhibitors. One difference between the action of these compounds and that of

HSP90 inhibitors is that they did increase NFATc1 protein levels, which itself may lead to MITF induction (Lu *et al.*, 2014). Thus, a number of stressors have been demonstrated to display cell stress dependent effects on osteoclast progenitors, which is potentially highly osteolytic. The results are not conclusive in regarding whether all the stressors act directly to regulate MITF as they may act indirectly via some NFATc1 regulation. However, given the critical role of the MITF transcription factor in osteoclast formation their actions on MITF levels are consistent with a strongly pro-osteoclastogenic action. These stressors have complex effects on bone cells *in vivo* but it seems highly plausible that they may exert osteolytic actions in bone.

Chapter 6
The Effect of 17-AAG Treatment on the RAW264.7 Transcriptome

Chapter 6 The Effect of 17-AAG Treatment on the RAW264.7 Transcriptome

6.1 Introduction

The data presented in Chapters 3 and 4 have suggested that HSP90 N-terminal domain inhibitors influence osteoclast progenitor differentiation through their effects on cell stress and HSF1 activation. However, there may be responses to these compounds that are either not HSF1 dependent or involve HSF1-regulated genes, which are not classically associated with cell stress responses that influence osteoclast formation and function. To investigate these possibilities, the influences of 17-AAG treatment upon osteoclast progenitor mRNA expression were investigated in an unbiased manner by generating an RNA-seq profile of 17-AAG treated RAW264.7 cells. RNA-seq, a relatively new deep sequencing technology, is used for whole transcriptome analysis, including not just mRNA but also non-coding RNA sequences (Wang *et al.*, 2009; Trapnell *et al.*, 2012; Trapnell *et al.*, 2009). RNA-seq analysis involves RNA being converted to a cDNA library of fragments that are then amplified in a high throughput manner resulting in the formation of short sequences, which are attached to adaptors present on the fragment ends (Wang *et al.*, 2009). The sequencing reads are then aligned to a reference transcriptome or they may be assembled into a genome – scale transcription map if no reference map is available (Wang *et al.*, 2009; Trapnell *et al.*, 2012). Each RNA-seq reading of a transcript gives a direct measure of the level of expression for each RNA transcript (Wang *et al.*, 2009; Trapnell *et al.*, 2009).

The approach taken therefore was to take RNA extracted from RAW264.7 cells treated for 24 hours with or without 17-AAG (500nM). After a few preporatory steps (Chapter 2.16) libraries were prepared and RNA-seq performed (17 million reads per sample) by the Gandel Trust Sequencing Laboratory, Hudson Insititue of Medical Research, Clayton.

6.2 Results

Informatics analysis on the data files generated by the Gandel Trust Sequencing Laboratory was initially performed by Dr Ross Chapman (Centre for Innate Immunity and Infectious Diseases, Hudson Institute of Medical Research) who created BAM files from the RNA-seq analysis. Subsequent informatics analysis on the data files was kindly performed by Dr Gholamreza Haffari and Milena Mitic (Dept of Information Technology, Monash University). Because RNA-seq identifies alternative transcription and splicing, an algorithm, which is not restricted by this or by prior gene annotations was required (Trapnell *et al.*, 2010). The open-source Cufflinks software, which assembles aligned RNA-seq reads into a set of transcripts provides such algorithms and was used to analyse the RNA-seq reads - (Trapnell *et al.*, 2010; Center for Computational Biology) (Dr Gholamreza Haffari and Milena Mitic, Monash University). Two approaches were used to analyse the RNA-seq reads. Initial analysis (Approach 1) was performed by putting the original sorted BAM files (Ross Chapman, Hudson Institute of Medical Research) through Cufflinks and Cuffmerge software to assemble the RNA-seq files and the reference genome annotation into one transcriptome annotation list with relative gene abundancies (Trapnell *et al.*, 2012). Following this, Cuffdiff software analysis was used to compare gene expression between the conditions in the merged transcriptome annotation list and tabulate differential gene expression (Figure 6.1) (Trapnell *et al.*, 2012). Initial analyses from Approach 1 revealed that the RAW264.7 transcriptome data was noisy and many of the transcript results from this comparison had an unmeasurable (NO TEST) outcome i.e., not enough alignments for testing. Therefore, a second approach called the 'Tuxedo Protocol' was performed by aggregating the reads made of the different RNA isolates (Figure 6.1 Approach 2) (Trapnell *et al.*, 2012). The Tuxedo protocol uses both Cufflink and complementary Tophat software to map to provide a transcriptional annotation list (Trapnell *et al.*, 2012; Center for Computational Biology). The Tophat software is a high level aligner, which uses Bowtie algorithms to align the RNA-seq reads to the genome (Trapnell *et al.*, 2012; Center for Computational Biology). Thus for Approach 2, the BAM files were converted back to fastq files, and new mapping of the two condition, 17-AAG vs no treatment "-ve" was done through Tophat software. This was done in order to use the same reference genome files throughout the process. After realigning the RNA-seq reads through Tophat software, Cufflinks and Cubmerge software produced transcriptome annotation files, determined gene abundancies and produced a merged file as previously described. This transcriptome annotation list was then analysed by Cuffdiff software

Schematic of Software used to Analyse RNA-seq Reads
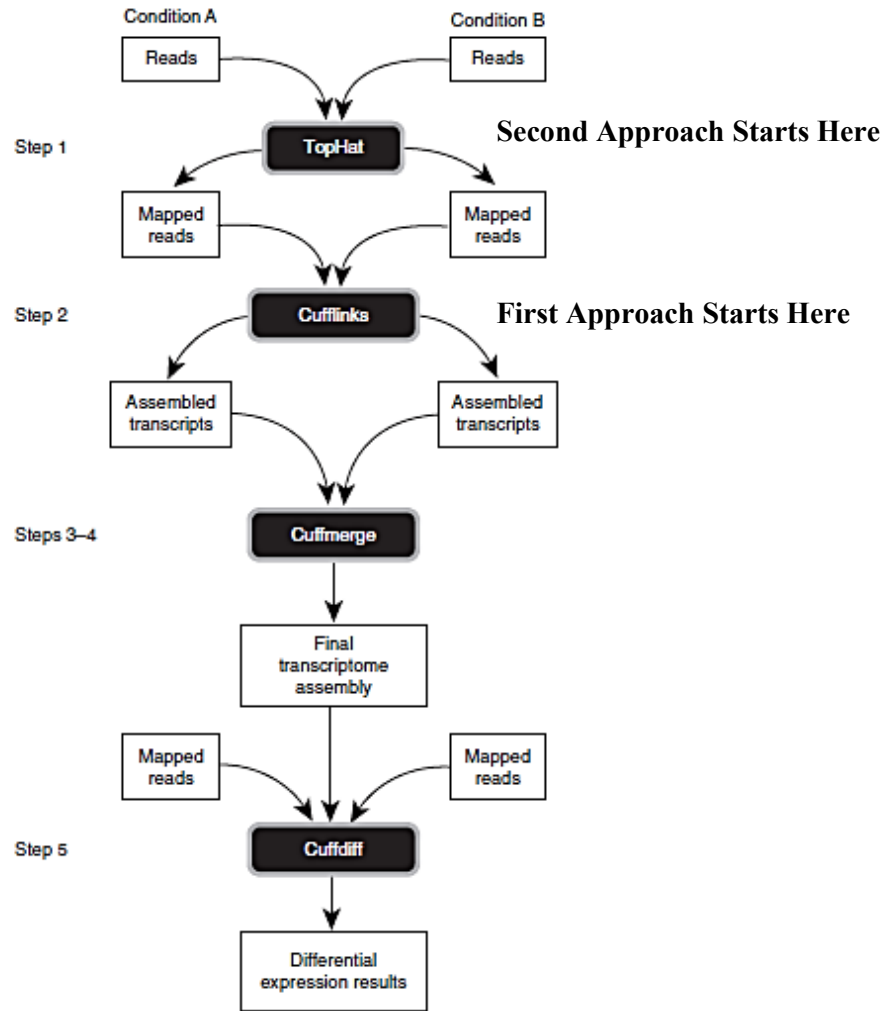
Figure 6.1

The RNA-seq data was first analysed by 'approach 1' where the BAM files previously generated from the RNA-seq experiments (by Ross Chapman) were put through Cufflinks, Cuffmerge and Cuffdiff software to compare the RNA-seq reads. However, due to the transcriptome data being noisy, a second approach ('approach 2') to analyse the data was performed. In approach 2 the original BAM files were converted back to fastq files and the reads made of RNA isolate aggregated. New mapping was done by Tophat software. The aligned reads then underwent analysis by Cufflinks, Cuffmerge and Cuffdiff software as previously. Cuffdif software identified a number of tested genes were differentially expressed when treated with 17-AAG. Approximately 500 genes showed a significance of $p \leq 0.05$ relative to the untreated control, "-ve". Figure sourced from (Trapnell *et al.*, 2012).

(Figure 6.1, Approach 2) (Trapnell *et al.*, 2012). Using this approach, 'Approach 2', the number of NOTEST results was thus reduced to half, and a number of genes important to osteoclast formation were identified as possibly regulated by 17-AAG. Of those that were tested, a number of genes were differentially expressed with about 500 genes showing a significance of $p \leq 0.05$ relative to the untreated negative control, "-ve". However, the comparison software labelled most comparisons as 'not significant', which was unusual given the very small p values. The Tophat mapping software discarded a number of reads, which may account for the software identifying lack of significance in much of the data (personal communication). Table 6.1 details the top 130 differentially expressed genes as identified by the RNA-seq analysis**.** Note at the end of the table are genes which were not differentially expressed but due to their putative or know on role in osteoclastogenesis were included.

6.2.1 RNA-seq Analysis Reads

Many genes that are involved in osteoclast formation were identified to be regulated by 17-AAG including *Dc-stamp*, *Atp6v0d2, Acp5 (TRAP), Adam8*, urokinase activator of plasminogen (*uPA*) and carbonic anhydrase II (*Car 2*) (Table 6.2) (Kudo *et al.*, 2002; Crasto *et al.*, 2013; Väänänen and Zhao, 2002; Syggelos *et al.*, 2013; Everts *et al.*, 2008). In addition, a number of genes, which are also putatively involved in osteoclast formation, were found to be regulated by 17-AAG treatment including *Ccl9* and *Cd74* (Lean *et al.*, 2002; Gu *et al.*, 2015). 17-AAG ability to induce HSP was corroborated with 17-AAG treatment inducing the expression of a number of *HSP* genes including *Hspa13* (HSP70 family member), *Hsp90ab1, Hspb7 (Hsp2*7), as well as an important autophagy-associated HSP cognate protein *Hspa8 (HSP73/Hsc70)* (Figure 6.2). Consistent with the notion that cross-talk occurs between different stress response pathways, 17-AAG treatment also induced the expression of a number of molecules that are induced by a heat shock response, oxidative stress, genotoxic stress (DNA damage) and mitotic stress (Figure 6.2) (York *et al.*, 2007; Thornley *et al.*, 2014; Kameda *et al.*, 2013; Clarkson and Wood, 2005; Tan *et al.*, 2014; Su *et al.*, 2013; Toivola *et al.*, 2010; Pérez de Castro and Malumbres, 2012). Some of these genes include Sialic acid binding Ig-like lectin 1(*Siglec1*), Excision repair cross complementation group 2 *(Ercc2)*, Nuclear receptor subfamily 1, group D, member 2 (*Nrld2*), Nesting, intermediate filament (*Nes*) and TPX2, microtubule-associated (*Tpx2*) (York *et al.*, 2007; Thornley *et al.*, 2014; Kameda *et al.*, 2013; Clarkson and Wood, 2005; Tan *et al.*, 2014; Su *et al.*, 2013; Toivola *et al.*, 2010; Pérez de Castro and Malumbres, 2012). Interestingly, a number of 17-AAG upregulated genes, which are involved or have a likely involvement in

osteoclast function have also been reported to be activated by stress including, *Ccl9*, *Car 2* and *uPA/P*lau (Figure 6.2) (Sharma *et al.*, 2013; Luparello *et al.*, 2003; Lean *et al.*, 2002; Ravindran *et al.*, 2010; Erdelyi *et al.*, 2009; Edwards and Weivoda, 2012).

Table 6.1 Table of Annotations of Genes Identified to be Regulated by 17-AAG

■ Genes of high interest

■ Genes of lesser interest

Gene	Description	Osteoclast involvement	Value 1	Value 2	log$_2$(fold change)	p value	Q value	Sig
Hist1h4m	Histone cluster 1, H4m (Hist1h4m). Histone protein, nuclear protein involved in DNA organisation (U.S. National Library of Medicine, 2009)	Not reported	276.66	120.558	-1.19839	**5.00E-05**	0.041973	**Yes**
Slc39a2	Solute carrier family 39 (zinc transporter), member 2 (Slc39a2). Possible involvement in osteoclast biology (Hadley *et al.*, 2010).	**Possible**	9.67387	21.7805	1.17087	**5.00E-05**	0.041973	**Yes**
Dc-stamp	Dendrocyte expressed seven transmembrane protein (Dc-stamp). Osteoclast fusion and differentiation membrane protein, which has an essential role in Osteoclast biology (Vignery, 2005).	**Yes**	8.58076	25.9317	1.59554	**5.00E-05**	0.041973	**Yes**
Racgap1	Rac GTPase-activating protein 1 (Racgap1). The human gene is involved in haematopoietic differentiation (Tcherkezian and Lamarche-Vane, 2007).	Not reported	36.2821	16.0352	-1.17801	**5.00E-05**	0.041973	**Yes**
Spink5	Serine peptidase inhibitor, Kazal type 1 (Spink5) Protease inhibitor (also called LEKTI) is an immune system modulator (Lee *et al.*, 2010a).	Not reported	2.4817	6.8697	1.46892	**5.00E-05**	0.041973	**Yes**

Siglec1	Sialic acid binding Ig-like lectin 1, sialoadhesin, adhesion factor. Possible regulation of osteoclast differentiation (Kameda *et al.*, 2013). This factor is stress induced in macrophages (Thornley *et al.*, 2014; York *et al.*, 2007).	Not reported	3.36172	7.57848	1.17271	**5.00E-05**	0.041973	**Yes**
Cxcl2	Chemokine (C-X-C motif) ligand 2 (Cxcl2). Potential involvement in osteoclast differentiation (Ha *et al.*, 2010).	**Possible**	3.36828	11.917	1.82294	**5.00E-05**	0.041973	**Yes**
Clec4n	C-type lectin domain family 4, member n (Clec4n), Lectin protein activated by LPS treatment in RAW264.7 (Ban *et al.*, 2011).	**Not reported**	17.0436	37.4298	1.13496	**5.00E-05**	0.041973	**Yes**
Itgax	Integrin alpha-X (Itgax). Adhesion receptor expressed by osteoclasts so it may have a potential involvement in osteoclast biology (Nesbitt *et al.*, 1993).	Possible	4.76307	11.2414	1.23886	**5.00E-05**	0.041973	**Yes**
Rprl3	Ribonuclease P RNA-like 3 (Rpr13) (U.S. National Library of Medicine, 2009).	Not reported	1558.06	3486.66	1.16209	**5.00E-05**	0.041973	**Yes**
Tmem202	Transmembrane protein 202 (Tmem202), Unknown function (U.S. National Library of Medicine, 2009).	Not reported	2.19243	8.3726	1.93314	**5.00E-05**	0.041973	**Yes**
Il1rn	Interleukin 1 receptor antagonist (Il1rn). Antagonist of IL1-α is a critical inflammatory factor (U.S. National Library of Medicine, 2009).	Not reported	43.6477	97.8534	1.16472	**0.0001**	0.071954	**No**
Chpf2	Chondroitin polymerizing factor 2 (Chpf2). Its function is unknown (U.S. National Library of Medicine, 2009).	Not reported	160.655	23.0467	-2.80133	**0.0001**	0.071954	**No**
Prc1	Protein regulator of cytokinesis 1 (Prc1). It is involved in cytokine production (U.S. National Library of	Not reported	16.019	6.99636	-1.1951	**0.00015**	0.100735	**No**

Gene	Description							
	Medicine, 2009).							
F10	Coagulation factor X (F10). This gene encodes the vitamin K-dependent coagulation factor X , which is involved in the blood coagulation cascade (U.S. National Library of Medicine, 2009).	Not reported	12.2169	25.8706	1.08243	**0.00015**	0.100735	**No**
Prr11	Proline rich 11 (Prr11) is a cell cycle progression gene (Ji *et al.*, 2013).	Not reported	8.74297	4.02733	-1.1183	**0.00025**	0.143907	**No**
Capsl	Calcyphosine-like (Capsl). Currently its function is unknown (U.S. National Library of Medicine, 2009).	Not reported	0	0.403369	Inf	**0.00025**	0.143907	**No**
Kif2c	Kinesin family member 2C (Kif2c). The human gene encodes a protein , which functions as a microtubule-dependent molecular motor that promotes mitotic chromosome segregation (U.S. National Library of Medicine, 2009).	Not reported	6.02456	2.57523	-1.22616	**0.00025**	0.143907	**No**
Ercc2	Excision repair cross complementation group 2 (Ercc2) Functions as a DNA repair enzyme , which is activated to respond to DNA damage (Clarkson and Wood, 2005).	Not reported	41.5408	8.45721	-2.29627	**0.0003**	0.151103	**No**
Saa3	Serum amyloid A 3 (Saa3) (U.S. National Library of Medicine, 2009).	Not reported	40.8802	87.2404	1.09359	**0.0003**	0.151102	**No**
Kif18b	Kinesin family member 18B (Kif18b). Human Gene encodes a protein, which has microtubule functions in mitotic cells (Stout *et al.*, 2011).	Not reported	2.9781	1.1884	-1.32537	**0.00035**	0.153292	**No**
Nr1d2	Nuclear receptor subfamily 1, group D, member 2 (Nrld2) Rev-erbA-beta transcription factor, involved in energy homeostasis. Reports of being regulated by	Not reported	10.8736	5.41098	-1.00687	**0.0004**	0.157398	**No**

	stress in hepatic cells (Tan *et al.*, 2014).							
Car2	Carbonic anhydrase II, Critical function in osteoclast biology notably in the formation of acid (Edwards and Weivoda, 2012).Possibility that Car 2 may be stress sensitive in some cells (Sharma *et al.*, 2013).	**Yes**	6.68936	14.909	1.15624	**0.0004**	0.157398	**No**
Aif1	Allograft inflammatory factor 1 (Aif1), Functions as an Inflammatory factor (U.S. National Library of Medicine, 2009).	Not reported	4.34051	11.4751	1.40257	**0.00045**	0.157398	**No**
Ttk	Ttk protein kinase (U.S. National Library of Medicine, 2009).	Not reported	4.5684	1.96927	-1.21403	**0.00045**	0.157398	**No**
Tacc3	Transforming, acidic coiled-coil containing protein 3 (Tacc3). Intracellular protein, which may influence early osteoblast maturation (Bargo *et al.*, 2010).	**Possible**	13.615	6.53861	-1.05814	**0.00055**	0.170475	**No**
Ect2	Ect2 oncogene (Ect2). Functions to regulate the cell cycle and cell division. Has been shown to be upregulated by DNA damage (genotoxic stress) (Srougi and Burridge, 2011).	Not reported	10.3088	5.28714	-0.96332	**0.00065**	0.192582	**No**
Kif4	Kinesin family member 4 (Kif4). Is a microtubule motor protein, which functions to transport membranous organelles (U.S. National Library of Medicine, 2009).	Not reported	5.39806	2.61701	-1.04452	**0.00065**	0.192582	**No**
Marcksl1	MARCKS-like 1 (Marcksl1). Human coding protein functions as a cytoskeleton protein (U.S. National Library of Medicine, 2009)	Not reported	3.21471	8.17633	1.34676	**0.00075**	0.204193	**No**
Aspm	Asp (abnormal spindle)-like, microcephaly associated (Aspm). In Drosophila, this gene is essential for normal	Not reported	3.73721	1.86556	-1.00235	**0.0008**	0.212663	**No**

	mitotic spindle function. (U.S. National Library of Medicine, 2009).							
Dio2	Deiodinase, iodothyronine, type II protein. Human coding protein activates the Thyroid hormone (Curcio-Morelli *et al.*, 2003).	Not reported	3.24228	1.53739	-1.07652	**0.00085**	0.212663	**No**
Cep55	Centrosomal protein 55 (Cep55). Mitosis and cytokinesis functions in humans (Fabbro *et al.*).	Not reported	9.42929	4.5179	-1.0615	**0.00085**	0.212663	**No**
Mcm10	Minichromosome Maintenance Complex Component 10 (Mcm10) protein. Mitosis functions (Homesley *et al.*, 2000).	Not reported	3.93906	1.80475	-1.12605	**0.00085**	0.212663	**No**
Fbxo5	F-Box Protein 5 (Fbxo5). Functions as a mitotic protein (U.S. National Library of Medicine, 2009).	Not reported	7.66325	3.23056	-1.24617	**0.00095**	0.212663	**No**
Fam64a	Family With Sequence Similarity 64, Member A (Fam64a). Mitotic protein. Human protein can also influences leukemic fusion protein CALM/AF10 (Archangelo *et al.*, 2013).	Not reported	11.7652	5.34923	-1.13712	**0.00095**	0.212663	**No**
Asf1b	Anti-Silencing Function 1B Histone Chaperone. Functions as a Histone chaperone (U.S. National Library of Medicine, 2009).	Not reported	16.4917	7.83898	-1.073	**0.00095**	0.212663	**No**
Mcm7	Minichromosome maintenance deficient 7. Human coding protein functions in DNA replication (U.S. National Library of Medicine, 2009).	Not reported	13.5239	6.86522	-0.97813	**0.001**	0.218989	**No**
Kif11	Kinesin Family Member 11 (Kif11). Functions in Mitosis(U.S. National Library of Medicine, 2009).	Not reported	9.00294	4.78241	-0.91266	**0.00115**	0.246479	**No**
Ephx1	Epoxide hydrolase enzyme.(U.S. National Library of Medicine, 2009).	Not reported	10.8595	20.7223	0.932229	**0.0012**	0.246698	**No**

Gene	Description							
Mmp14	Matrix metalloprotein-14 (Mmp14). Likely involvment in osteoclast biology and has been shown to shed RANKL (Rodríguez *et al.*, 2010; Sato *et al.*, 1997).	**Likely**	1.0585	2.90574	1.45689	**0.0012**	0.246698	No
Uhrf1	Ubiquitin-Like With PHD And Ring Finger Domains 1 (Uhrf1). It functions as an epigenetic regulator (Ying *et al.*, 2015).	Not reported	5.65482	2.66953	-1.0829	**0.0012**	0.246698	No
Fgr	Feline Gardner-Rasheed Sarcoma Viral Oncogene Homolog. Tyrosine kinase (*Fgr*). Coding protein is involved in immune responses (Futosi *et al.*, 2013; U.S. National Library of Medicine, 2009). FGR is expressed in osteoclasts and its expression is RANKL inducible (Lowell *et al.*, 1996; Cappellen *et al.*, 2002).	**Possible**	1.65823	3.68084	1.15039	**0.0012**	0.246698	No
uPA	Urokinase-type plasminogen activator. This factor breaks down extracellular matrix and is involved in osteoclast function (Everts *et al.*, 2008) This factor is also HSF1 activated (Luparello *et al.*, 2003).	**Yes**	53.6952	95.475	0.830329	**0.00125**	0.254381	No
Mastl	Microtubule associated serine/threonine kinase-like. Human coding protein functions as a microtubule protein (U.S. National Library of Medicine, 2009).	Not reported	3.3375	1.56333	-1.09414	**0.0013**	0.261911	No
Scarna3a	Small Cajal body-specific RNA 3A (Scarna3a). Currently its function is unknown (U.S. National Library of Medicine, 2009).	Not reported	33399	14128.3	-1.24122	**0.00135**	0.269292	No
Birc5	Baculoviral IAP repeat-containing 5 (Birc5) (also known as survivin). Member of the Inhibitor of Apopotosis family (IAP). HSF1 regulates surviving levels. In addition survivin has been reported to be	**Possible**	26.9118	13.0187	-1.04766	**0.0014**	0.27121	No

	activated by M-CSF during osteoclastogenesis (Bradley *et al.*, 2008; Meng *et al.*, 2010; U.S. National Library of Medicine, 2009).							
Hmmr	Hyaluronan mediated motility receptor (Hmmr). The human coded protein has motility functions(U.S. National Library of Medicine, 2009).	Not reported	13.9582	7.54448	-0.88762	**0.0014**	0.27121	**No**
Zfp951	Zinc finger protein 951 (Zfp951) (U.S. National Library of Medicine, 2009).	Not reported	1.00998	2.44662	1.27647	**0.0014**	0.27121	**No**
Ndc80	NDC80 kinetochore complex component (Ndc80). Human coding protein functions as a kinetochore protein (U.S. National Library of Medicine, 2009).	Not reported	7.92474	3.73893	-1.08374	**0.0015**	0.285099	No
Hbegf	Heparin-binding EGF-like growth factor (Hbegf)	Not reported	0.221588	1.71008	2.94812	**0.0015**	0.285099	No
Hmgb2	High mobility group box 2 (Hmgb2). The human coding protein functions as a DNA binding protein. May be stress induced (U.S. National Library of Medicine, 2009; Tang *et al.*, 2011).	Not reported	28.6943	15.5388	-0.88489	**0.00155**	0.289147	No
Depdc1a	(Dishevelled, EGL-10, Pleckstrin) domain contained protein 1A (Depdc1a) is a Myeloma marker (Kassambara *et al.*, 2013).	Not reported	5.04761	2.194	-1.20204	**0.0016**	0.293047	No
Clspn	Claspin (Clspn). Human coding protein regulates cell cycle checkpoints and is needed for S phase during mitosis (U.S. National Library of Medicine, 2009).	Not reported	1.69198	0.732224	-1.20835	**0.0016**	0.293047	No
Ccl9	CCL-9, MIP1gamma Chemokine. Involved in osteoclast function. *Ccl9* is the major chemokine expressed by osteoclasts (Lean *et al.*, 2002) .This Chemokine has been shown to be both RANKL and	**Yes**	66.5021	116.598	0.810072	**0.0017**	0.297825	No

	stress induced (Ravindran *et al.*, 2010; Lean *et al.*, 2002; Erdelyi *et al.*, 2009).							
Scimp	SLP adaptor and CSK interacting membrane protein (Scimp). The human coding protein serves as a regulator of antigen presentation (Draber *et al.*, 2011).	Not reported	0.747318	2.92853	1.97038	**0.00175**	0.301344	No
Ccnf	Cyclin F (Ccnf). Human protein functions in cell cycle control(D'Angiolella *et al.*, 2010; U.S. National Library of Medicine, 2009).	Not reported	8.11228	4.07525	-0.99322	**0.00175**	0.301344	No
Pilra	Paired immunoglobulin-like type 2 receptor alpha (PILRalpha) (U.S. National Library of Medicine, 2009)	Not reported	0.783919	2.17976	1.47539	**0.0019**	0.318994	No
Kif18a	Kinesin-like protein 8a (Kifl8a) (U.S. National Library of Medicine, 2009)	Not reported	4.68125	2.28433	-1.03513	**0.00195**	0.324683	No
H2-Q7	Histocompatibility 2, Q region locus 7 (H2-Q7) Unknown – histone (U.S. National Library of Medicine, 2009).	Not reported	13.3374	6.25916	-1.09144	**0.002**	0.327594	No
Kif15	Kinesin family member 15b (Kif15)(U.S. National Library of Medicine, 2009).	Not reported	4.13263	2.08666	-0.98586	**0.002**	0.327593	No
Kif20b	Kinesin family member 20b (Kif20b)(U.S. National Library of Medicine, 2009).	Not reported	5.06031	2.69063	-0.91128	**0.0021**	0.33847	No
Aim1l	Absent in melanoma 1-like protein (Aim11) (U.S. National Library of Medicine, 2009)	Not reported	1.14371	3.30075	1.52908	**0.0021**	0.33847	No
Nes	Nesting, intermediate filament, May be induced by oxidative and mechanical stress (Su *et al.*, 2013; Toivola *et al.*, 2010).	Not reported	0.058782	0.383724	2.70663	**0.00215**	0.343778	No
Kif14	kinesin family member 14 (Kif14), Human coding protein binds microtubules (U.S. National Library of	Not reported	1.56437	0.754838	-1.05134	**0.0022**	0.346277	No

	Medicine, 2009).							
Haus4	HAUS augmin-like complex, subunit 4 (Haus4) Unknown function of coding protein in mice (U.S. National Library of Medicine, 2009).	Not reported	5.04074	2.14995	-1.22933	**0.0022**	0.346277	**No**
Dtl	Denticleless homolog (Drosophila) (Dtl) Unknown function (U.S. National Library of Medicine, 2009).	Not reported	3.99094	1.98975	-1.00414	**0.0023**	0.351046	**No**
Ncaph	Non-SMC condensin I complex, subunit H (Ncaph). Human coding protein is a chromosomal protein (U.S. National Library of Medicine, 2009) .	Not reported	6.29693	3.22315	-0.96618	**0.0023**	0.351046	**No**
Shcbp1	Cell spindle protein.	Not reported	10.3599	5.19221	-0.99659	**0.0023**	0.351046	**No**
Atp6v0d2	vATPase v0d2 isoform. Critical in Osteoclast biology. Functions to acidify the Howeship's Lacunae and is involved in osteoclast fusion (Wu *et al.*, 2009). This molecule is regulated by MITF (Feng *et al.*, 2009).	**Yes**	48.1166	84.2218	0.807659	**0.0024**	0.363555	**No**
Anln	Anillin, actin binding protein. Human coding protein has a role in cell growth, migration and mitosis(U.S. National Library of Medicine, 2009).	Not reported	13.919	7.75151	-0.84451	**0.00265**	0.398429	**No**
Cfb	Complement factor b (Cfb). Protein is a complement factor (Pekna *et al.*, 1998).	Not reported	0.412122	1.32765	1.68773	**0.0027**	0.40148	**No**
Pttg1	Pituitary tumour-transforming 1. Coding protein regulates Cell cycle progression (Wang *et al.*, 2001; U.S. National Library of Medicine, 2009).	Not reported	33.6379	16.8257	-0.99942	**0.00275**	0.40148	**No**
Bub1b	Budding uninhibited by benzimidazoles 1 homolog, beta (S. cerevisiae) (Bub1b) Mitotic checkpoint, cell cycle division protein (Kyuragi *et al.*, 2015; U.S. National Library of Medicine, 2009).	Not reported	20.1368	11.4024	-0.8205	**0.00275**	0.40148	**No**

Cenpi	Centromere protein I (Cenpi). Coding protein is consitutively associated with centromeres (U.S. National Library of Medicine, 2009).	Not reported	6.88829	3.50523	-0.97464	**0.00275**	0.40148	**No**
Snord61	Small nucleolar RNA, C/D box 61 RNA (Snord61). Small nucleolar RNA, non coding (Hüttenhofer *et al.*, 2001; U.S. National Library of Medicine, 2009).	Not reported	254762	144760	-0.81549	**0.00285**	0.413086	**No**
Alyref	Aly/REF export factor (also called (THOC4). The Human protein codes a molecular chaperone (U.S. National Library of Medicine, 2009).	Not reported	114.744	66.7939	-0.78064	**0.0029**	0.417331	**No**
Plekhg3	Pleckstrin homology domain containing, family G (with RhoGef domain) member 3 (Plekhg3). Unknown function of coding protein (U.S. National Library of Medicine, 2009).	Not reported	3.05451	1.55827	-0.971	**0.00305**	0.423782	**No**
Rrm1	Ribonucleoside-diphosphate reductase enzyme (Rrm1) (Caras and Martin, 1988).	Not reported	21.6538	12.5379	-0.78833	**0.00305**	0.423782	**No**
Cenpn	Centromere protein N (Cenpn). The human coding protein has a role in kinetochore assembly during mitosis (U.S. National Library of Medicine, 2009).	Not reported	7.15561	3.31472	-1.11019	**0.0031**	0.427779	**No**
Knstrn	Kinetochore-localized astrin/SPAG5 binding (Knstrn). Currently its function is unknown (U.S. National Library of Medicine, 2009).	Not reported	10.8108	5.88127	-0.87827	**0.00325**	0.445427	**No**
H1f0	H1 histone family, member 0. Histone nuclear protein (U.S. National Library of Medicine, 2009).	Not reported	94.7192	55.937	-0.75985	**0.0033**	0.449224	**No**
Irg1	Immunoresponsive gene 1 (Irg1). Human coding protein promotes endotoxin tolerance (U.S. National Library of Medicine, 2009).	Not reported	3.99601	7.8008	0.965061	**0.00335**	0.450657	**No**

Scarna3b	Small Cajal body-specific RNA 3B (Scarna3b). Currently its function is unknown.	Not reported	38.6123	17.8844	-1.11036	**0.0034**	0.450657	**No**
Arhgef39	Rho guanine nucleotide exchange factor (GEF) 39.Currently its function is unknown (U.S. National Library of Medicine, 2009).	Not reported	4.40382	1.78658	-1.30156	**0.0034**	0.450657	**No**
Kntc1	Kinetochore associated 1 (Kntc1) Human coding protein functions in the cell cycle (U.S. National Library of Medicine, 2009)	Not reported	4.92218	2.68598	-0.87385	**0.0034**	0.450657	**No**
Gsta3	Glutathione S-transferase A3. Expression has been shown to be increased upon oxidative stress (U.S. National Library of Medicine, 2009; Ilic *et al.*, 2010).	Not reported	1.79629	4.39432	1.29062	**0.0035**	0.460879	**No**
Gins1	DNA replication complex GINS protein can be activated by DNA replication stress (Flach *et al.*, 2014; U.S. National Library of Medicine, 2009).	Not reported	9.11597	4.00591	-1.18627	**0.0037**	0.484051	**No**
Ercc6l	Excision repair cross-complementing rodent repair deficiency complementation group 6 like (Ercc61). Ercc61 belongs to the SNF-2 family member and is a nuclear protein, (Yin *et al.*, 2011; U.S. National Library of Medicine, 2009).	Not reported	2.85356	1.39947	-1.02789	**0.00375**	0.487427	**No**
Cenpf	Centromere protein F. Coding protein regulates cell cycle G2/M checkpoint (Evans *et al.*, 2007; U.S. National Library of Medicine, 2009).	Not reported	3.90096	2.20367	-0.82392	**0.0038**	0.488033	**No**
Mcm5	Minichromosome maintenance deficient 5, cell division cycle 46 (S. cerevisiae) (Mcm5). In humans the coding protein acts as a DNA replication licensing factor (Stoeber *et al.*, 2001; U.S. National Library of	Not reported	13.3929	7.59948	-0.8175	**0.00385**	0.488033	**No**

	Medicine, 2009).							
Fam212b	Family with sequence similarity 212, member B (Fam212b). Currently its coding protein's function is unknown (U.S. National Library of Medicine, 2009).	Not reported	0.40134	1.01778	1.34254	**0.0039**	0.488033	**No**
Stil	Scl/Tal1 interrupting locus (Stil). Coding protein functions as a centrosomal protein (U.S. National Library of Medicine, 2009; Castiel *et al.*, 2011).	Not reported	1.37432	0.638611	-1.10571	**0.00405**	0.503675	**No**
Ptma	Prothymosin alpha (Ttma). Coding protein functions as a chromatin remodelling protein and is a component of a linker histone chaperone (George and Brown, 2010; U.S. National Library of Medicine, 2009). Human coding protein is overexpressed in a number of cancers (Ioannou *et al.*, 2012).	Not reported	652.27	383.778	-0.7652	**0.0041**	0.506765	**No**
Hist1h2bb	Histone cluster 1, H2bb (Hist1h2bb). Coding protein is a histone nuclear protein (U.S. National Library of Medicine, 2009).	Not reported	66.122	33.8181	-0.96733	**0.0043**	0.52188	**No**
Sgol1	Shugoshin-like 1 (Sgol1). Human coding protein is important in mitosis (U.S. National Library of Medicine, 2009).	Not reported	2.97414	1.41707	-1.06956	**0.0043**	0.52188	**No**
Tcam1	Testicular cell adhesion molecule 1(Tcam1) . Currently the coding protein function is unknown (U.S. National Library of Medicine, 2009).	Not reported	0.318689	1.06022	1.73414	**0.00435**	0.524787	**No**
Nek2	NIMA (never in mitosis gene a)-related expressed kinase 2. Protein codes a serine/threonine-protein kinase whose role is to mitotic processes including spindle formation. (Hayward and Fry, 2006; Marina	Not reported	11.7779	6.56236	-0.8438	**0.00445**	0.530498	**No**

	and Saavedra, 2014). It is also overexpressed in cancer (Marina and Saavedra, 2014).							
Ckap2l	Cytoskeleton associated protein 2-like (Ckap2l). Mouse coding protein function is unclear (U.S. National Library of Medicine, 2009).	Not reported	2.51514	1.17676	-1.09582	**0.0046**	0.545154	**No**
Hist1h3i	Histone cluster 1, H3i (Histlh3i). Coding protein functions as a histone nuclear protein (U.S. National Library of Medicine, 2009).	Not reported	88.7055	44.2755	-1.00252	**0.00475**	0.54999	**No**
Sepp1	Selenoprotein P, plasma, 1 (Sepp1). Coding protein acts as a heparin binding antioxidant (U.S. National Library of Medicine, 2009)	Not reported	5.84278	10.765	0.881614	**0.00475**	0.54999	**No**
Sf3b3	Splicing factor 3b subunit b (Sf3b3). Human coding protein functions as a splicing factor and has a role in transcriptional modifications (U.S. National Library of Medicine, 2009).	Not reported	323.702	101.03	-1.67988	**0.00475**	0.54999	**No**
Abcd4	ATP-binding cassette, sub-family D (ALD), member 4 (Abcd4). Coding protein functions as a protein transporter (U.S. National Library of Medicine, 2009).	Not reported	13.8445	24.103	0.799894	**0.00485**	0.55836	**No**
Nod1	Nucleotide-binding oligomerization domain-containing protein 1 (Nod1). Human coding protein is an intracellular receptor, which initiates an inflammatory response (U.S. National Library of Medicine, 2009).	Not reported	0.517577	1.25987	1.28343	**0.00495**	0.566634	**No**
Acp5	Acid phosphatase 5, tartrate resistant (Acp5). Tartrate resistant alkaline phosphatase (TRAP) enzyme. Protein is essential for osteoclast function (Boyle *et al.*, 2003).	**Yes**	8.72943	16.2722	0.898453	**0.00545**	0.620345	**No**

Pygl	Liver glycogen phosphorylase (Pygl). Coding protein functions as an enzyme, which has a role in degrading glycogen chains to free glucose (McInerney *et al.*, 2002).	Not reported	3.15899	6.00894	0.927646	**0.00565**	0.632392	**No**
Nckap1	Nck-associated protein 1. Function of coding protein is not clear (U.S. National Library of Medicine, 2009).	Not reported	2.14727	4.14177	0.94774	**0.00565**	0.632392	**No**
Spc25	SPC25, NDC80 kinetochore complex component, homolog (S. cerevisiae) Kinetochore NDC80 protein complex (cytokeratins), which functions in mitotic spindle checkpoint and microtubule kinetochore attachment (U.S. National Library of Medicine, 2009).	Not reported	16.9001	9.27835	-0.86509	**0.0057**	0.634464	**No**
Igf2bp2	Insulin-like growth factor 2 mRNA-binding protein 2. Human coding protein is a member of the IGF-II mRNA-binding protein (IMP) family and functions to regulate IGF2 translation (U.S. National Library of Medicine, 2009).	Not reported	3.87249	7.04451	0.863237	**0.00595**	0.656967	**No**
Hspa8	Heat shock protein 8. The coding protein is a HSP70 (HSP73 or HSC70) family member. Hspa8 is not stress inducible but has a similar function as HSP70 i.e. facilitating correct protein folding (Zhang *et al.*, 2014a; U.S. National Library of Medicine, 2009). This protein is also important in many signal pathways (Giebel *et al.*, 1988; U.S. National Library of Medicine, 2009).		952.692	1872.13	0.974596	**0.0061**	0.664306	**No**
Gen1	Gen homolog 1, endonuclease (Gen1). Coding protein is an endonuclease (U.S. National Library of Medicine, 2009).	Not reported	1.89814	0.859467	-1.14307	**0.00625**	0.676983	**No**

Fancd2	Fanconi anemia complementation group, D2. Coding protein belongs to Fanconi anemia complementation group (FANC), which includes other protein i.e. FANCD1 (also called BRCA2). Fancd2 is involved in the DNA damage response and repair system along with BRAC1 and BRAC2 (tumour suppressor genes)(U.S. National Library of Medicine, 2009).	Not reported	3.39305	1.81862	-0.89974	**0.00635**	0.680497	**No**
Chaf1a	Chromatin assembly factor 1 subunit A (Chaf1a). Human protein is a histone associated protein, which may be regulated by oxidative stress (U.S. National Library of Medicine, 2009; Hybertson *et al.*, 2011)	Not reported	2.06586	0.982085	-1.07282	**0.0067**	0.705656	**No**
Efcab11	EF-hand calcium binding domain 11. Coding protein has currently unknown function (U.S. National Library of Medicine, 2009).	Not reported	2.98799	1.26907	-1.2354	**0.00675**	0.705656	**No**
Hmgn5	High-mobility group nucleosome binding domain 5 (Hmgn5). Human coding protein function as a nucleosome binding factor and transcriptional activating protein (U.S. National Library of Medicine, 2009).	Not reported	3.76366	1.80635	-1.05906	**0.00685**	0.705656	**No**
Tpx2	TPX2, microtubule-associated protein homolog (Tpx2). Nuclear protein involved in cell proliferation. Role in oncogene-induced mitotic stress (Pérez de Castro and Malumbres, 2012; U.S. National Library of Medicine, 2009).	Not reported	13.8634	8.31168	-0.73807	**0.0069**	0.705656	**No**
Scgb2b23-ps	Secretoglobin, family 2B, member 23, pseudogene (Scgb2b23-ps) (U.S. National Library of Medicine,	Not reported	0	0.444387	Inf	**0.0069**	0.705656	**No**

2009).

Gene	Description							
Spdl1	Spindle apparatus coiled-coil protein 1. Currently its function is unknown (U.S. National Library of Medicine, 2009).	Not reported	17.5706	10.3516	-0.76331	**0.0073**	0.742793	**No**
Mmp19	Matrix metalloprotein-19 (Mmp19). Potential role in osteoclast biology as other Mmp family members including Mmp9 have a role in ECM degradation (Delaissé *et al.*, 2003; Ben-david *et al.*, 2012; Hou *et al.*, 2004).	**Possible**	4.78073	9.142	0.935278	**0.0075**	0.759234	**No**
Cd74	CD74 antigen (invariant polypeptide of major histocompatibility complex, class II antigen-associated). Coding protein is a receptor for MIF. Potential role in Osteoclast function (Gu *et al.*, 2015; Mun *et al.*, 2013).	**Possible**	198.656	275.752	0.473101	**1.80888**	0.0628	**No**
Mif	Macrophage migration inhibitory factor (*Mif*). Likely involvement in osteoclast function although poorly defined (Gu *et al.*, 2015).	**Likely**	996.706	1276.67	0.357148	**2.71427**	0.17125	**No**
Tnf	Tumour necrosis factor, inflammatory agent (*Tnf*). Coding protein has important effects upon osteoclast biology (Azuma *et al.*, 2000; Fuller *et al.*, 2002; Horowitz and Lorenzo, 2002).	**Yes**	7.26639	12.6831	0.803592	**2.45236**	0.01285	**No**
Il-1a	Interleukin 1 alpha (IL-1α). Coding protein is an inflammatory agent, which has important effects on osteoclasts (Kim *et al.*, 2009; Horowitz and Lorenzo, 2002; Lee *et al.*, 2010b).	**Yes**	1.82619	3.36815	0.883114	**2.23224**	0.0252	**No**

Due to the difficulties in progressing with gene expression analysis with this approach, mRNA levels of the putatively regulated genes highlighted by the RNA-seq analysis were examined further by quantitative qRT-PCR analysis using the RNA that was used in the RNA-seq experiment. Note that principle component analysis (PCA) showed the replicates of one set of RNA did not cluster with the replicates from the other two independent experiments for both the untreated and 17-AAG treated samples (data not shown). Therefore only the replicates in two of the three RNA sets were compared and analysed between the untreated, "-ve" and 17-AAG treatment group. The RNA from the two independent experiments whose replicates clustered as shown by PCA analysis was used for validation. For this study, the mRNAs of genes implicated in osteoclast biology were prioritised and selected from the list (Table 6.1). Target genes to examine included: DC-STAMP, which is involved in osteoclast fusion; the pro-osteoclastogenic and inflammatory cytokine IL-1α; chemokine *Ccl9*, which is abundantly expressed on osteoclasts; Chemokine (C-X-C motif) ligand 2 (Cxcl2), which has been shown to enhance osteoclastogenesis; uPA, which is involved in ECM degradation; MIF receptor *Cd74* that has been reported to have a putative role in osteoclast biology; and MITF target gene ATP6V0d2 (Table 6.2) (Kudo *et al.*, 2002; Tani-Ishii *et al.*, 1999; Edwards and Weivoda, 2012; Lean *et al.*, 2002; Vignery, 2005; Wu *et al.*, 2009; Gu *et al.*, 2015; Ha *et al.*, 2010; Everts *et al.*, 2008). In particular, *Dc-stamp* was identified to be highly regulated by 17-AAG in the RNA-seq analysis. However, due to PCR primer issues with both *Cxcl2* and *Dc-stamp* (i.e., primer pairs that give reliable results by quantitative qRT-PCR in RAW264.7 cell RNA could not be identified), validation of the effects of 17-AAG upon their transcript levels could not be studied. Since *Dc-stamp* cooperates with another protein, *Oc-stamp* in osteoclast fusion, preliminary analysis of 17-AAG effects upon this osteoclast fusion molecule was performed (Appendix Figure B12) (Miyamoto *et al.*, 2012). Despite *Oc-stamp* not being identified in the RNA-seq analysis to be differentially regulated by 17-AAG treatment, initial qRT-PCR analysis shows 17-AAG treatment significantly increases *Oc-stamp* mRNA levels (Appendix Figure B15).

qRT-PCR analysis of cDNA derived from RNA-seq RNA showed that cultures treated with 17-AAG had higher *Il-1α* mRNA expression relative to the control n=2 (Table 6.2). Similarly, validation by qRT-PCR showed that 17-AAG treatment increased *Atp6v0d*2 mRNA expression (n=2) (Table 6.2). Note that ATP6V0d2 is name of the transcript variant that gives rise to v-ATPase V0d2 (a subunit variant of the osteoclastic proton pump), which was shown to be regulated by 17-AAG studied in Chapter 3. qRT-PCR analysis showed that

17-AAG treated cultures had higher levels also of carbonic anhydrase II (*Car 2*), which like v-ATPase V0d2 has an important role in acidification of Howship's lacuna by converting carbon dioxide and water to bicarbonate ions and carbonic acid (n=2) (Table 6.2) (Nakamura, 2007). Likewise, initial qRT-PCR validation using RNA-seq RNA showed cultures treated with 17-AAG had increased *Car2* mRNA expression relative to the control (n=2) (Table 6.2). Similarly, qRT-PCR data showed 17-AAG treatment increases MIF receptor, *Cd74*, plasminogen activator *uPA* and chemokine *Ccl9* mRNA (n=2) (Table 6.2).

RNA-seq Analysis of Target Genes and Initial qRT-PCR Validation

Gene (mouse)	Description	RNA-seq Analysis						qRT-PCR		
		Fold change Value 1	Fold change Value 2	log2(fold_change)	p value	Q value	Sig	Fold Change	SEM	n
Il-1α	Interleukin 1 alpha. Inflammatory cytokine Involvement in osteoclast biology(Kim *et al.*, 2009; Horowitz and Lorenzo, 2002; Lee *et al.*, 2010b).	1.83	3.37	0.88	**2.2322**	0.03	No	**4.12**	0.54	2
Atp6v0d2	vATPase v0d2 isoform. Critical in osteoclast fusion and proton pumping (Wu *et al.*, 2009). Regulated by MITF (Feng *et al.*, 2009).	48.12	84.22	0.81	**0.0024**	0.36	No	**2.76**	0.56	2
Car2	Carbonic anhydrase II. Critical in osteoclast function notably in the formation of acid (Edwards and Weivoda, 2012). Stress sensitive in some cells (Sharma *et al.*, 2013).	6.69	14.91	1.16	**0.0004**	0.16	No	**2.84**	1.34	2
Ccl9	MIP1gamma Chemokine *Ccl9* is expressed abundantly by osteoclasts (Lean *et al.*, 2002). RANKL induced, stress induced (Lean *et al.*, 2002; Ravindran *et al.*, 2010; Erdelyi *et al.*, 2009).	66.50	116.60	0.81	**0.0017**	0.30	No	**4.25**	0.50	2
Upa	urokinase-type plasminogen activator. Breaks down extracellular matrix. uPA is involved in osteoclast function(Everts *et al.*, 2008). UPA has been shown to be activated by HSF1 (Luparello *et al.*, 2003).	53.70	95.48	0.83	**0.0013**	0.25	No	**1.93**	0.27	2
Cd74	MIF receptor. Potential role in Osteoclast Biology(Gu *et al.*, 2015).	198.66	275.75	0.47	**1.8088**	0.06	No	**3.60**	0.80	2

Table 6.2

Genes selected from RNA-seq analysis to follow up including *IL-1α, Atp6v0d2, Car2, Ccl9, Upa and Cd74.* RNA-seq analysis for the selected gene including the fold changes, p values and significance as determine by the Cuffdif software is shown is shown for the selected gene in the RNA-seq Analysis section of the table. Follow up qRT-PCR validation using the RNA from the RNA-seq experiment was done. The Ct Fold change between no treatment negative control "-ve" and 17-AAG treatment of two pooled independent experiments is expressed in the qRT-PCR fold change column.

6.2.2 qRT-PCR Validation

Subsequent qRT-PCR validations were performed in freshly isolated RNA from RAW264.7 cells treated in the same manner as the RNA-seq preparation. In addition, a 48 hour time point was included. Target genes were the same as those examined with the RNA-seq RNA. RAW264.7 cells treated with 17-AAG (500nM) for 24 and 48 hours increased *Il-1α* expression. At 24 hours 17-AAG treatment significantly increased *Il-1α* expression relative to the DMSO vehicle control (Figure 6.2 A.). Likewise, at 48 hours 17-AAG treatment also significantly increased *Il-1α* levels (Figure 6.2 B.). 17-AAG treatment also significantly increased the mRNA expression of *Atp6v0d2* at both 24 and 48 hours (Figure 6.3 A-B.). 17-AAG treatment did not increase *Ccl9* mRNA expression at 24 hours, but after 48 hours *Ccl9* mRNA expression was increased relative to the DMSO vehicle control (Figure 6.4 A-B.). Similarly, *uPA* and *Cd74* expression levels were not affected by 17-AAG treatment at 24 hours; however, *Cd74* expression was increased by 17-AAG treatment at 48 hours (Figure 6.5 and Figure 6.6 A-B.). 17-AAG effects upon enzyme *Car 2* and osteoclast fusion molecule *Oc-stamp* were also performed (Appendix Figures B14 and B15).

17-AAG Treatment Increases *Il-1α* mRNA Expression in RAW264.7 Cells

A.

B.
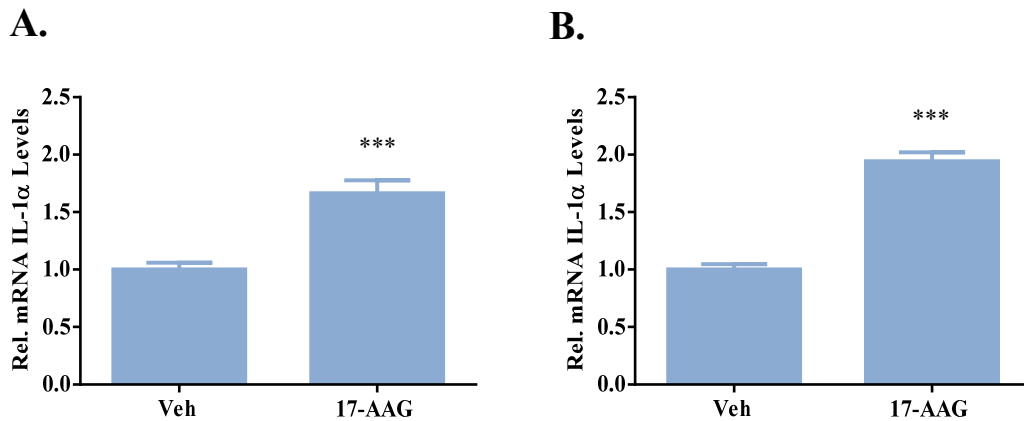
Figure 6.2

(A-B.) RAW264.7 cells were seeded at 10^4 cells in 35mm diameter wells. The following day the cells were treated with 17-AAG (500nM) or a DMSO vehicle control "veh" for 24 or 48 hours. RNA was Extracted, DNase treated and cDNA prepared and employed in qRT-PCR. **(A.)** 17-AAG increased *Il-1α* mRNA expression at **(A.)** 24 hours and at **(B.)** 48 hours. Data was normalised to HRPT mRNA and is shown relative to DMSO vehicle control. All data are expressed as mean ± SEM of **(A.)** three **(B.)** four independent experiments. Statistical analysis was performed using a Student's two tailed unpaired t-test *** $p \leq 0.001$.

17-AAG Treatment Increases V-*Atp6v0d2* mRNA Expression in RAW264.7 Cells

A.

B.
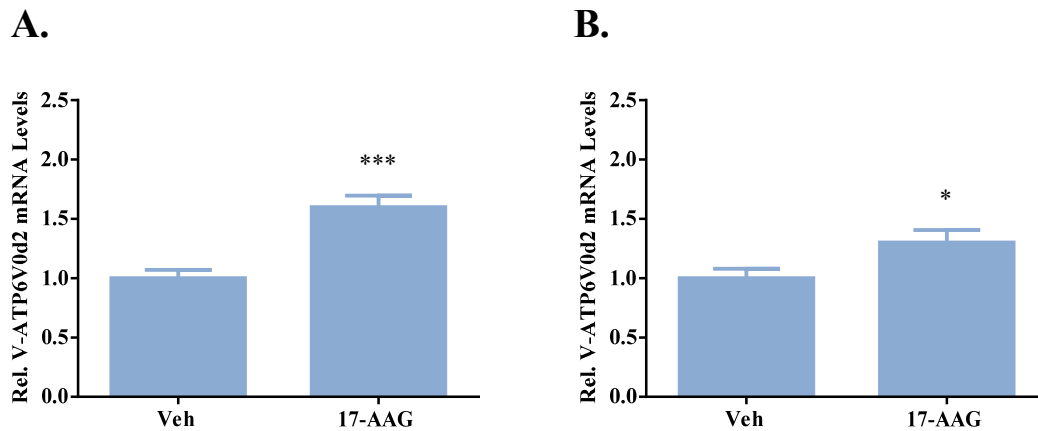
Figure 6.3

(A-B.) RAW264.7 cells were seeded at 10^4 cells in 35mm diameter wells. The following day the cells were treated with 17-AAG (500nM) or a DMSO vehicle control "Veh" for 24 or 48 hours. RNA was Extracted, DNase treated and cDNA prepared and analysed by qRT-PCR. **(A.)** 17-AAG treatment significantly increased *Atp6v0d2* mRNA levels at 24 hours. **(B.)** Likewise at 48 hours, 17-AAG treatment significantly increased *Atp6v0d2* mRNA levels. Data was normalised to HRPT mRNA, and is shown relative to DMSO vehicle control. All data are expressed as mean ± SEM of **(A.)** three **(B.)** four independent experiments. Statistical analysis was performed using a Student's two tailed unpaired t-test * $p \leq 0.05$, *** $p \leq 0.001$.

The Effect of 17-AAG Treatment upon *Ccl9* mRNA Expression in RAW264.7 Cells

A.

B.
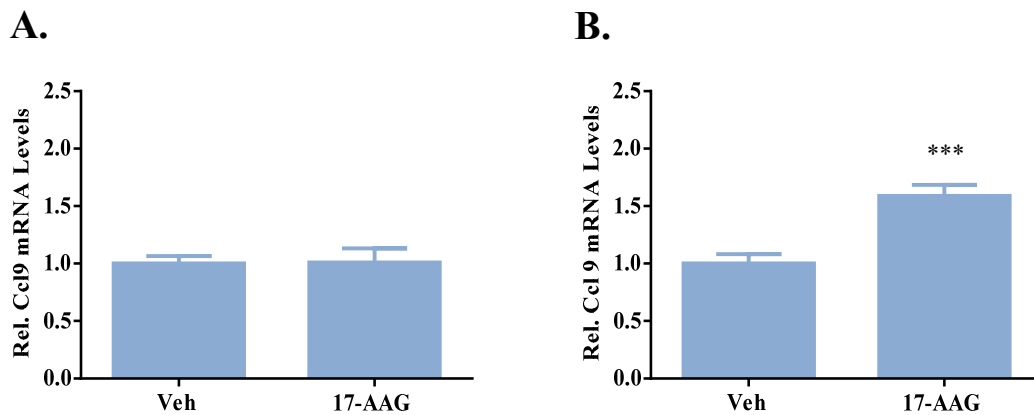
Figure 6.4

(A-B.) RAW264.7 cells were seeded at 10^4 cells in 35mm diameter wells. The following day the cells were treated with 17-AAG (500nM) or a DMSO vehicle control "Veh" for 24 or 48 hours. RNA was Extracted, DNase treated and cDNA prepared and analysed by qRT-PCR. **(A.)** 17-AAG treatment did not affect *Ccl9* expression at 24 hours; however, at **(B.)** 48 hours 17-AAG treatment significantly increased *Ccl9* expression levels. Data was normalised to HRPT mRNA and is shown relative to DMSO vehicle control. All data expressed as mean ± SEM of three independent experiments. Statistical analysis was performed using a Student's two tailed unpaired t-test *** $p \leq 0.001$.

The Effect of 17-AAG Treatment upon *uPA* mRNA Expression in RAW264.7 Cells
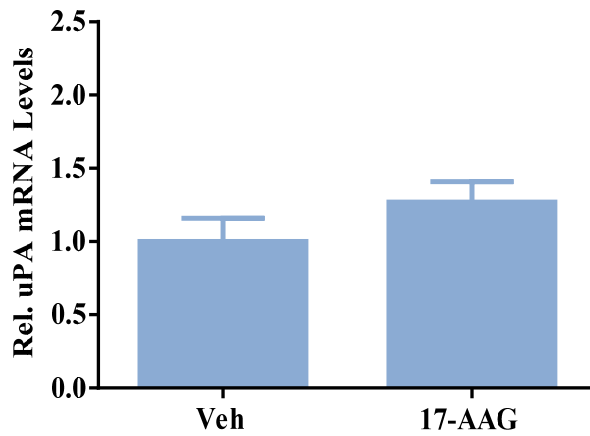
Figure 6.5

RAW264.7 cells were seeded at 10^4 cells in 35mm diameter wells. The following day the cells were treated with 17-AAG (500nM) or a vehicle DMSO control "Veh" for 24 hours. RNA was extracted, DNase treated and cDNA prepared, and cDNA prepared and analysed by qRT-PCR. 17-AAG treatment did not affect *uPA* expression at 24 hours. Data was normalised to HRPT mRNA and is shown relative to DMSO vehicle control. All data expressed as mean ± SEM of 3 independent experiments. Statistical analysis was performed using a Student's two tailed unpaired t-test.

The Effect of 17-AAG Treatment upon *Cd74* mRNA Expression in RAW264.7 Cells

A.

B.
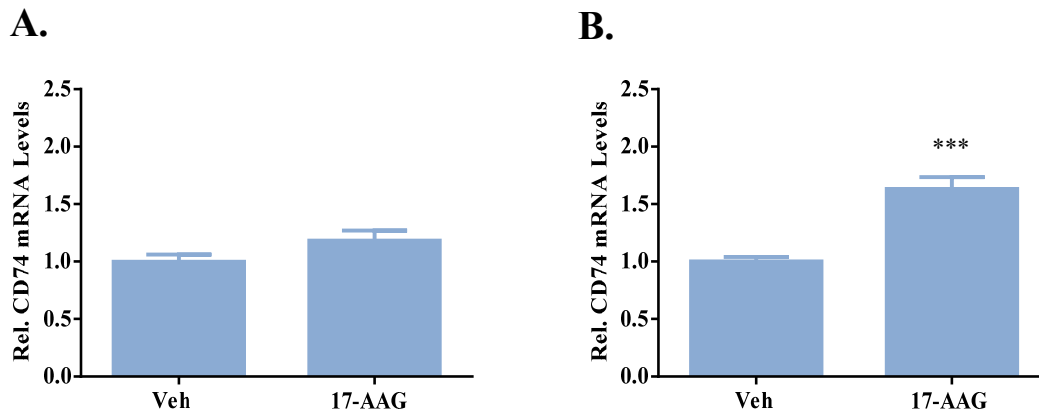
Figure 6.6

(A-B.) RAW264.7 cells were seeded at 10^4 cells in 35mm diameter wells. The following day the cells were treated with 17-AAG (500nM) or a DMSO vehicle control "Veh" for **(A.)** 24 or **(B.)** 48 hours. RNA was Extracted, DNase treated and cDNA prepared and analysed by qRT-PCR. **(A.)** At 24 hours 17-AAG did not affect Cd74 expression. **(B.)** After 48 hours of 17-AAG treatment however, Cd74 expression levels were significantly increased. Data was normalised to HRPT mRNA and is shown relative to DMSO vehicle control. All data is expressed as mean ± SEM of 3 experiments. Statistical analysis was performed using a Student's two tailed unpaired t-test *** $p \leq 0.001$.

6.3 Discussion

RNA-seq identified a number of transcripts whose levels were regulated by 17-AAG treatment in RAW264.7 cells. Amongst these were molecules having a known role and a putative role in osteoclast biology (Kudo *et al.*, 2002; Tani-Ishii *et al.*, 1999; Edwards and Weivoda, 2012; Everts *et al.;* Lean *et al.*, 2002; Vignery, 2005; Wu *et al.*, 2009; Gu *et al.*, 2015; Ha *et al.*, 2010). Interestingly, some of these genes have been reported to be regulated by stress responses (Sharma *et al.*, 2013; Luparello *et al.*, 2003; Lean *et al.*, 2002; Ravindran *et al.*, 2010; Erdelyi *et al.*, 2009; Edwards and Weivoda, 2012). 17-AAG treatment also regulated a number of genes, which are induced by stress whose encoded proteins have various functions (York *et al.*, 2007; Thornley *et al.*, 2014; Kameda *et al.*, 2013; Clarkson and Wood, 2005; Tan *et al.*, 2014; Su *et al.*, 2013; Toivola *et al.*, 2010; Pérez de Castro and Malumbres, 2012). For the purpose of this chapter genes were prioritised according to their role in osteoclast biology and included *Il-1α*, v-ATP6 V0d2, *Ccl9*, *uPa*, *Cd74, Oc-stamp and Car 2*.

IL-1α is an isoform of IL-1, an inflammatory cytokine, which is a known stimulator of osteoclastogenesis (Boyle *et al.*, 2003; Tani-Ishii *et al.*, 1999; Jules *et al.*, 2012). IL-1 principally mediates its effects on osteoclastogenesis by increasing RANKL expression on osteoblasts, but also can act directly upon osteoclast progenitors to augment RANKL signalling (Kudo *et al.*, 2002; Lee *et al.*, 2002b; Jules *et al.*, 2012). In the presence of RANKL, IL-1 has been shown to increase NFATc1 expression and can increase the expression of Car2, TRAP, MMP9 and CTSK (Jules *et al.*, 2012). The IL-1α isoform of IL-1 has been shown to be particularly important in increasing osteoclast differentiation (Kudo *et al.*, 2003; Tani-Ishii *et al.*, 1999). Adding anti- IL-1α antibodies to a co-culture of C57BL/6N mouse bone marrow and MC3T3-G2/PA6 cells decreased osteoclast numbers by 25% and the ratio of mononuclear to multinuclear to was 90:10 relative to control 60:40 (Tani-Ishii *et al.*, 1999). The reduction in the numbers of fused osteoclasts resulted in less resorption and thus decreased pit sizes (Tani-Ishii *et al.*, 1999). Likewise, *Il-1α* knockout mice have significantly higher bone mineral density and significantly fewer osteoclasts present upon their femur trabecular bone (Lee *et al.*, 2010b). These observations, in sum, suggest that the IL-1α isoform of IL-1 may play a role in 17-AAG induced osteolysis. Possible regulation in RAW264.7 cells was studied by qRT-PCR and the data showed 17-AAG treatment did indeed enhance *Il-1α* mRNA expression dramatically at both 24 and 48 hours (Figure 6.4).

17-AAG ability to increase *Il-1*α gene expression might also contribute to 17-AAG mediated increase in osteoclast differentiation from progenitor cells including its effects on cellular mediators such as MITF. In the context of metastatic bone disease, this factor may participate in 17-AAG osteolytic effects that increase metastatic bone tumour growth in xenograft mouse models.

The MITF target gene *Atp6v0d2*, the name of the transcript for v-ATPase V0d2 proton pump isoform studied in Chapter 3 was also identified by the RNA-seq analysis as a potential target of 17-AAG (Feng *et al.*, 2009). 17-AAG regulation ofATP6v0d2 mRNA is consistent with our results that showed 17-AAG increases *Atp6v0d2* transcriptional activity in RAW264.7 cells. The v-ATPase pump plays an essential role in osteoclast bone resorption by pumping hydrogen into Howship's lacuna and osteoclasts have a high expression of v-ATPase a3 and v-ATPase d2 subunit isoforms (Crasto *et al.*, 2013; Väänänen and Zhao, 2002; Yang *et al.*, 2012; Matsumoto *et al.*, 2014). Mice that lack the v-ATPaseV0d2 (and a3) subunit have impaired bone resorption and increased bone mass (Lee *et al.*, 2006; Crasto *et al.*, 2013). The role of ATP6v0d2 in bone resorption is not strictly relevant here as the cells were not cultured on bone; however, a second striking property of this protein is its participation in osteoclast fusion (Lee *et al.*, 2006). Osteoclasts derived from mice lacking the v-ATPase V0d2 subunit are predominantly mononuclear with a concomitant decrease in bone resorption (Lee *et al.*, 2006). qRT-PCR validation of the RNA-seq analysis confirmed 17-AAG treatment significantly increased the mRNA levels of v-ATPaseV0d2 expression at both 24 and 48 hours. Increased expression of this molecule is consistent with all the prior observations of 17-AAG driving increased differentiation and osteoclast size, as previously noted in Chapter 3.2.2. Another factor similarly implicated in osteoclast fusion was *Dc-stamp*, which showed some indication of upregulation in the RNA-seq data. *Dc-stamp*, as well as *Cxcl2*, upregulation, however, could not be confirmed by qRT-PCR due to technical problems with primer design that could not be resolved. Despite this, initial qRT-PCR experiments suggest 17-AAG increases expression of the fusion molecule *Oc-stamp* (Appendix Figure B15). This molecule has been shown to act in concert with *Dc-stamp* to mediate osteoclast fusion (Miyamoto *et al.*, 2012). Another gene identified by the RNA-seq to be regulated by 17-AAG is *Car2*. This enzyme is essential for osteoclast function as it generates hydrogen ions to acidify Howship's lacunae allowing for the mobilization of inorganic bone matrix (Billecocq *et al.*, 1990; Laitala-Leinonen *et al.*, 1999; Lehenkari *et al.*, 1998; Laitala and Vaananen,

1993). Initial analysis suggests 17-AAG treatment also increases *Car 2* mRNA levels at both 24 and 48 hours (Appendix Figure B14).

17-AAG treatment was also found to regulate chemokine (C-C motif) ligand 9 (*Ccl9*), which is also known as macrophage inflammatory protein δ or MIP-1δ (Maurer and von Stebut, 2004). CCL9 belongs to the MIP-1 family of C-C chemokines whose members include CClL3/MIP-1α, CCl4/MIP-1β, *C*CL9/MIP-1δ and CCL15/MIP-1γ (Maurer and von Stebut, 2004). MIP-1 proteins including CCL9 have a role in many inflammatory processes both physiological and pathological (Maurer and von Stebut, 2004). The CCL9 family member is reported to be the main chemokine expressed by mouse osteoclasts and has been shown to be important in the process of osteoclastogenesis and also mature osteoclast function (Yang *et al.*, 2006; Lean *et al.*, 2002). *Ccl9* gene expression is induced by RANKL treatment in the middle stages of osteoclastogenesis and increases the differentiation and survival of mouse osteoclasts (Yang *et al.*, 2006; Okamatsu *et al.*, 2004). Furthermore, inhibiting CCL9 with an anti-CCL9 antibody suppresses osteoclast formation *in vitro* and *in vivo* (Yang *et al.*, 2006). CCL9 also regulates mature osteoclast activity by stimulating cytoplasmic motility and polarization, which are required for osteoclast activation prior to resorption (Lean *et al.*, 2002). qRT-PCR analysis of mRNA from RAW264.7 cell cultures showed 17-AAG treatment significantly increased *Ccl9* expression at 48 hours. As previously shown, 17-AAG treatment does not affect osteoclast survival rates (Chapter 3.2.2). However, 17-AAG effects upon CCL9 might play a role, as other chemokines are suspected to, in chemotaxis of osteoclast precursors possibly allowing them to identify each other prior to fusion.

Another RNA-seq target gene identified was plasminogen activator, urokinase (*Plau*), which is also called urokinase Plasminogen Activator (*uPA*) (Figure 6.2 and 6.3) (Furlan *et al.*, 2007). uPA binds its membrane bound co-factor uPA receptor (*uPA*R) and converts the inactive precursor plasminogen to the active serine protease plasmin (Furlan *et al.*, 2007; Lu *et al.*, 2011; Syggelos *et al.*, 2013). In the context of bone, active plasmin can also degrade the bone collagen matrix as well as numerous other extracellular matrix proteins (Syggelos *et al.*, 2013; Lu *et al.*, 2011). uPa further regulates bone matrix degradation through its activation of certain precursor MMPs including MMP-3, MMP-9, MMP-12, and MMP-13 (Furlan *et al.*, 2007; Syggelos *et al.*, 2013). Kubota *et al.* found that uPA expression was increased during RANKL-mediated RAW264.7 osteoclast differentiation (Kubota *et al.*, 2003). In addition, mice that lack the uPA receptor (uPAR) have increased osteoblasts with a

concomitant increase in bone mass (Furlan *et al.*, 2007). These mice also have decreased osteoclast numbers and the active osteoclasts have defective actin rings (Furlan *et al.*, 2007). In contrast however, Daci *et al*. showed osteoclast numbers were not reduced in a $1,25(OH)_2D_3$ -stimulated co-culture of osteoblasts and bone marrow cells from *uPA^{-/-}* mice (Daci *et al.*, 1999). Initial qRT-PCR validation showed 17-AAG treatment doesn't affect *uPA* expression levels at 24 hours (Figure 6.5). However, after 48 hours of 17-AAG treatment, 17-AAG significantly increased *uPA* mRNA levels (Figure 6.5).

The transmembrane protein *Cd74* was shown not to be differentially regulated by 17-AAG in the RNA-seq analyses; however, initial qRT-PCR suggested some regulation. CD74 actions as a receptor for macrophage migration inhibitory factor (MIF) has suggested it may have a role in osteoclast biology (Gu *et al.*, 2015). A recent report showed bone marrow cells from *Cd74^{-/-}* mice exhibited decreased RANKL-mediated osteoclastogenesis (Gu *et al.*, 2015). In contrast Mun *et al*. 2013 showed RANKL stimulated osteoclast differentiation was increased when using bone marrow cells from *Cd74^{-/-}* mice (Mun *et al.*, 2013). 17-AAG treatment did not affect *Cd74* expression at 24 hours; however, after 48 hours of treatment *Cd74* expression levels were increased (Figure 6.6).

This data shows that in RAW264.7 cells 17-AAG impacts mRNA levels of a number of molecules previously shown to be important in osteoclast differentiation and activity. In pathological diseases including rheumatoid arthritis, osteolytic metastasis or myeloma the induction of these genes would act to increase disease progression through osteoclast formation and their interactions with the microenvironment i.e., vicious cycle observed in cancer invasion of bone. Further follow up work including qRT-PCR analysis on primary bone marrow cells and protein work should be addressed. To determine the role of HSF1 in these genes regulation, qRT-PCR and protein studies can be done using primary bone marrow cells from HSF1 null mice and also through HSF1 pharmacological inhibition. Based on these results, further over-expression or inhibitory studies to assess what role these genes are in osteoclast differentiation and activity in response to 17-AAG would be a useful future direction.

Chapter 7

Summary and Conclusions

7.1 Summary and Conclusions

The work studied in this thesis focussed on the effects of cell-stressing compounds, including HSP90 inhibitors, clinically used chemotherapeutics and ethanol upon osteoclast differentiation. 17-AAG and the more recently developed HSP90 inhibitors, CCT018159 and NVP-AUY922, were shown in this thesis to increase osteoclastogenesis. This work has shown a role for HSF1-dependent cell stress and a previously unsuspected regulatory role for MITF in osteoclast differentiation. Further investigation revealed similar effects of certain chemotherapeutic factors and of ethanol on osteoclast formation, and a similar involvement of cell stress and MITF. Osteoclast formation *in vitro* and *in vivo* is generally controlled by calcitropic hormones including PTH, Vit D_3 and calcitonin (Onal *et al.*, 2012; Bouillon and Suda, 2014; Suda *et al.*, 1999). However, these studies have uncovered a new class of stimuli-stress inducing compounds that may be of particular importance in pathological and iatrogenic bone loss.

Osteoclastogenesis occurs through the stimulation of osteoclast precursor cells to survive by M-CSF signals and to differentiate by RANKL stimulation (Boyle *et al.*, 2003; Feng, 2005). RANK signalling causes the activation of downstream signalling pathways inducing the expression of osteoclast transcription genes and the activation of signalling molecules, which are necessary for the differentiation and activation of osteoclasts (Feng, 2005; Boyle *et al.*, 2003). Amongst these transcription factors and signalling molecules are NFκB, NFATc1, c-FOS (a subunit of AP-1), MITF, and p38 (Asagiri and Takayanagi, 2007; Mansky *et al.*, 2002a; Gohda *et al.*, 2005; Yamashita *et al.*, 2007; Boyle *et al.*, 2003; Raggatt and Partridge, 2010). Mice that lack these molecules are osteopetrotic and have greatly increased bone mass (Asagiri and Takayanagi, 2007; Mansky *et al.*, 2002a; Gohda *et al.*, 2005; Yamashita *et al.*, 2007; Del Fattore *et al.*, 2008). In contrast, osteoclast-stimulating factors such as RANKL raise the activation of these factors and over-expression of NFκB, NFATc1 and MITF all increase osteoclast differentiation and resorptive activity (Yamashita *et al.*, 2007; Meadows *et al.*, 2007; Takayanagi *et al.*, 2002). Therefore, the regulation of these important molecules is inherent to the osteoclast activity and also indirectly through coupling signals to osteoblast bone formation (Boyle *et al.*, 2003).

Most skeletal diseases are the result of increased osteoclast activity where it is hypothesized that the balance between bone resorption and bone formation is skewed in the direction of

bone resorption (Boyle *et al.*, 2003; Hienz *et al.*, 2014). Prior work to this thesis showed that 17-AAG treatment caused tumour growth and bone loss in metastatic bone disease in MDA-MB-231 innoculated mice (Price *et al.*, 2005). The 17-AAG mediated increase in tumour growth in the bone was contrary to 17-AAG anti-cancer effects in soft tumours (Price *et al.*, 2005; Solit *et al.*, 2003; Solit *et al.*, 2002; Kelland *et al.*, 1999). This was hypothesized to occur through the vicious cycle which occurs in osteolytic metastasis (Price *et al.*, 2005). Further work showed 17-AAG treatment decreased bone volume in tumour naïve mice through its actions to increase osteoclast formation (Price *et al.*, 2005). Similarly, Yano *et al.* found 17-AAG treatment to also increase tumour growth and bone loss through 17-AAG actions to increase osteoclast formation (Yano *et al.*, 2008). This data suggested the drug had pro-osteolytic activity. One of the aims of this thesis was to confirm 17-AAG pro-osteoclastogenic effects upon osteoclast progenitors. In addition, the effect upon osteoclast differentiation was studied of more recently developed HSP90 inhibitors, CCT018159 and NVP-AUY922, the latter of which is currently undergoing phase I and II clinical trials (Cheung *et al.*, 2005; Eccles *et al.*, 2008; Sharp *et al.*, 2007a; National Institute of Health, 2014). As previously published by our group, 17-AAG treatment significantly increased the differentiation of osteoclast progenitors into mature osteoclasts in a dose-dependent manner in both the RAW264.7 cells and in primary bone marrow cells. Not only did 17-AAG treatment increase the number of TRAP and CTR positive cells, but the osteoclasts formed were larger than RANKL stimulated. This suggested 17-AAG also affects osteoclast fusion and therefore activity. The finding that 17-AAG increases osteoclast formation is consistent with studies by Yano *et al.*, where 17-AAG was shown to increase osteoclast differentiation from primary bone marrow cells (Yano *et al.*, 2008). Like 17-AAG, the more recently developed CCT018159 and NVP-AUY922 exerted pro-osteoclastogenic effects upon osteoclast progenitors increasing osteoclast formation (Table 7.1, CCT018159 not shown).

Although the effects of NVP-AUY922 and CCT018159 on bone and tumours in tumour naïve and laden mice were not studied, these compounds have the potential to increase tumour growth through their pro-osteolytic actions. Therefore this data impresses the requirement for future studies to investigate this possibility. This data shows N-terminal HSP90 inhibitors increases osteoclast formation and suggests that the increase in osteoclastogenesis is a common effect amongst N-terminal HSP90 inhibitors. This research provides novel data on the effect of HSP90 drugs, which were in or are currently going

Sumary Table of Thesis Findings

■ Cell Stress markers
■ Osteoclastogenic responses

Chemotherapeutics	HEK-HSE Cells HSF1 Transcriptional Activity	Bone Marrow Cells HSP72 Protein	RAW264.7 Cells HSP72 Protein	Phospho p38 Protein	NFATc1 Protein	MITF Protein	Osteoclast Differentiation	Bone Marrow Cells
17-AAG	↑	↑	↑	↑	↓	↑	↑	↑
NVP-AUY922	↑	↑	↑	↑	Not Tested	↑	↑	↑
Cisplatin	No Effect	Not Tested	↑	Not Tested	↑	↑	↑	↑
Doxorubicin	↑	Not Tested	↑	Not Tested	↑	↑	↑	↑
Bortezomib	↑	Not Tested	↑	Not Tested	↑	↑	↑	↑
MG132	↑	Not Tested	↑	Not Tested	↑	↑	↑	↑

Table 7.1

This table provides a summary of the treatment effects of experimental and clinically used chemotherapeutics upon cell stress markers, osteoclast transcription factors and osteoclast differentiation in HEK-HSE cells and RAW264.7 cells.

through clinical trials upon bone metabolism that has not previously been assessed. This work should impress the need to understand and screen the effects of HSP90 inhibitors upon bone as they may cause secondary problems i.e., tumour growth in metastatic disease in the case of 17-AAG.

17-AAG acts to inhibit HSP90 by binding to the N-terminal ATPase pocket, which inhibits its cycling between ATP and ADP- bound confirmations (Goetz *et al.*, 2003; Koga *et al.*, 2009; Patel *et al.*, 2011). This causes HSP90 to be in an open confirmation and bound to ADP with co-chaperones, which targets HSP90 oncogenic client proteins for proteasomal degradation (Patel *et al.*, 2011; Koga *et al.*, 2009). In addition, 17-AAG inhibits HSP90 cytoprotective role in the cell against environmental, genetic and protein instability(Neckers and Workman, 2012). Through these actions 17-AAG mediates the anti-cancer effects seen in soft tumour models. Why 17-AAG increases osteoclast formation through HSP90 inhibition brought forth many questions to the mechanism by which it acts. One of the aims of this thesis was to study the mechanism whereby 17-AAG acts to increase osteoclastogenesis. How does HSP90 inhibition cause an increase in osteoclast formation? Osteoclastogenesis is a tightly regulated process involving a number of signalling pathways downstream of RANK activation (Feng, 2005; Boyle *et al.*, 2003; Raggatt and Partridge, 2010). Within these pathways are the key osteoclast transcription factors (including NFκB, AP-1, NFATc1 and MITF) whose expression and activities are induced by RANKL to drive the differentiation of progenitor haemopoietic cells into mature cells (Raggatt and Partridge, 2010). Therefore, the effects of HSP90 inhibition through 17-AAG upon these transcription factors were assessed. 17-AAG treatment did not affect NFκB or c-FOS. Interestingly, 17-AAG decreased the transcriptional activity and protein levels of NFATc1, which is considered the major regulator of osteoclastogenesis and is highly regulated by RANKL (Sharma *et al.*, 2007; Takayanagi, 2007a). The fact that 17-AAG treatment had a negative effect upon NFATc1 was surprising and shows that 17-AAG is not acting to increase osteoclast formation through NFATc1. As unexpected as 17-AAG negative effects upon NFATc1 were, it is consistent with a previous report that NFATc1 is HSP90 client protein and is therefore degraded when 17-AAG is bound to HSP90 (Ruffenach *et al.*, 2015). Further supporting this finding was the data showing 17-AAG acts to increase osteoclast differentiation in the latter half of the osteoclast formation pathway. In contrast, TGF-β acts to increase osteoclastogenesis in the earlier part of the process possibly through its actions upon NFATc1. This data indicates TGF-β and 17-AAG act by different mechanisms. This data also suggests that NFATc1

regulation during osteoclast formation is not quite the limiting factor in osteoclast formation that it is generally considered to be in the literature. Rather this data suggests that there is another point of control during osteoclastogenesis.

Through work presented in this thesis MITF was identified as likely to be a novel point of control in osteoclastogenesis. Unlike 17-AAG effects upon other osteoclast transcription factors, 17-AAG treatment increased the protein expression of MITF in a time and dose-dependent manner (Table 7.1). The MITF transcription factor is essential for osteoclast differentiation with mi/mi mice having low numbers of osteoclasts and the limited osteoclast numbers present having defective ruffled borders and resorptive activity (Hershey and Fisher, 2004; Luchin *et al.*, 2000; Steingrimsson *et al.*, 2002; Motyckova *et al.*, 2001; Sharma *et al.*, 2007). MITF drives osteoclast differentiation by causing (in concert with NFATc1 and other transcription factors) the expression of osteoclastogenic genes (Boyle *et al.*, 2003). In contrast to other osteoclastic transcription factors MITF activation occurs late in the osteoclast signalling/transcription factor cascade, i.e., in a manner dependent on the earlier induced factors (Boyle *et al.*, 2003). Supporting this, studies have suggested MITF activation is probably downstream of NFATc1 although NFAT binding sites in MITF promoters have not been reported (Bronisz *et al.*, 2006; Hershey and Fisher, 2004; Lu *et al.*, 2014). The finding 17-AAG treatment increases MITF protein expression is consistent with 17-AAG acting late in the osteoclastogenesis pathway to increase osteoclast formation. Interestingly, the MITF isoforms A and in particular E have been previously identified to be important for osteoclast formation (Lu *et al.*, 2010a). Lu *et al.* found RANKL stimulation to increase MITF-E protein levels, and also identified MITF isoform E to be a more potent osteoclastogenic factor than isoform A (Lu *et al.*, 2010a). More recently the same group also identified MITF-E to be regulated by NFATc1 (Lu *et al.*, 2014). Overexpression of NFATc1 was able to increase MITF-E protein levels in the absence of RANKL (Lu *et al.*, 2014). TGF-β has also been shown to increase RANKL-induced MITF-E expression and osteoclastogenesis (Asai *et al.*, 2014). This may occur through TGF-β stimulation of NFATc1, which may then feed into MITF, as described by the study above (Asai *et al.*, 2014; Lu *et al.*, 2014). As mentioned above MITF drives the expression of osteoclast genes including, *Apc5* (TRAP), *Ctsk*, *Clcn7*, *E-cadherin* and the *Atp6v0d2* (Lu *et al.*, 2010a; Feng *et al.*, 2009). Work in this thesis showed 17-AAG treatment increased the transcriptional activity of MITF target gene Atp6v0d2. Using a luciferase reporter construct containing the promoter region of the MITF target gene-Atp6v0d2, 17-AAG treatment increased the

transcriptional activity Atp6v0d2 in a dose-dependent manner although it was uncertain if this is dependent upon MITF induction. However, mutating the MITF binding regions in this construct abolished the 17-AAG mediated increase in Atp6v0d2 transcriptional activity, confirming MITF role in its induction. The more recently developed HSP90 inhibitor NVP-AUY922 was also found to increase MITF protein expression (Table 7.1). This data suggests HSP90 inhibitors increase osteoclast differentiation through their ability to increase MITF expression although other transcription factors might also play a role in NVP-AUY922 actions.

There are several ways in which 17-AAG inhibition of HSP90 might increase osteoclast formation. HSP90 inhibition results in the proteasomal degradation of many HSP90 client proteins, raising the possibility of the degradation of some intracellular osteoclast inhibitors, perhaps one that reduces MITF levels (Pratt *et al.*, 2010). Such osteoclast differentiation inhibitors include MAFB and IRF8; however, these are factors that affect NFATc1 and would be expected to raise NFATc1 mRNA levels. Studies by lab members have not so far found 17-AAG to affect any of these inhibitors, but others may exist that remain unidentified. Similarly other endogenous osteoclast inhibitors, NFκBp100 and RBP-J, respectively, may be degraded. However, a critical point to note is that degradation of these inhibitors greatly enhances NFATc1 levels, which is not observed with 17-AAG treatment (Zhao *et al.*, 2012; Yao *et al.*, 2009). Collectively, this data suggests that these endogenous osteoclast inhibitors are unlikely to mediate 17-AAG actions on osteoclast formation in these cultures (Zhao *et al.*, 2012; Yao *et al.*, 2009).

A well characterised feature of 17-AAG is its ability to indirectly activate HSF1 by its binding to HSP90 (Goetz *et al.*, 2003). 17-AAG binds to the same N-terminal region as HSF1, therefore displacing it, which allows for its activation. This activation of HSF1 results in a HSR and increased expression of HSPs such as HSP72. HSF1 activation and HSP72 expression was observed in these studies in HSP90 inhibitor-treated RAW264.7 and primary cells. For this reason, the hypothesis that 17-AAG (and other N terminal HSP90 inhibitors) increases osteoclast formation through HSF1 was studied. To study the role of HSF1 in 17-AAG mediated osteoclast formation, three approaches were used: pharmacological inhibition, using bone marrow cells from mice lacking HSF1, and silencing HSF1. All three approaches gave a similar outcome. The effects of 17-AAG and NVP-AUY922 were first examined and

confirmed to cause increased HSF1 transcriptional activity and increased expression of the stress induced HSP72. Pharmacologically inhibiting HSF1 by KNK437 inhibited the 17-AAG mediated increase in osteoclast formation. Similarly NVP-AUY922 enhanced osteoclast numbers were reduced to DMSO vehicle control levels with KNK437 treatment. Silencing HSF1 with siRNA methods ablated the 17-AAG mediated increase in osteoclast formation at submaximal and maximal RANKL concentrations. Moreover, bone marrow cells isolated from HSF1$^{-/-}$ mice did not exhibit increased osteoclast formation upon 17-AAG treatment. Together this data, the latter two of which was done in collaboration with Dr Ryan Chai shows the novel finding that the 17-AAG induced increase in osteoclast formation is dependent upon HSF1. To some extent NVP-AUY922 pro-osteoclastogenic were also shown to be dependent upon HSF1. However, it does not prove that the actions are directly mediated by HSF1 alone. Further studies examining the role of HSF1 in NVP-AUY922 mediated increase in osteoclast formation will need to be addressed using the additional approaches of HSF1 silencing and knockdown as used for 17-AAG. In addition, further studies looking at NVP-AUY922 mediated increase in osteoclastogenesis using some method that increases HSF1 levels without induction of cell stress should be performed. This would involve transduction by viral or other vectors to overexpress HSF1, which has been attempted by colleague Dr Ryan Chai when studying 17-AAG (Chai *et al.*, 2014). This data indicated that HSF1 overexpression itself did not increase osteoclast formation but that response of cells to stressors such as 17AAG was higher. This might indicate that the actions of HSF1 require a co-factor or co-factors that are also induced. Other 17AAG-induced factors and hence possible co-factors were identified through RNA-seq analysis of the RAW264.7 transcriptome. These 17-AAG regulated molecules included Atp6v0d2, IL-1α, Ccl9, and *Cd74*. However, in reference to the transduction method of Dr Chai, it has some technical drawbacks, such as cell line drift and selection bias, so that improved methods are needed to make this work more conclusive. Adding to these findings, Chai *et al.* also showed that other N-terminal HSP90 inhibitors including radicicol and the more water soluble 17-AAG derivative 17-DMAG activate HSF1 and increase osteoclast formation (Chai *et al.*, 2014). In contrast HSP90 inhibitors novobiocin and courmamycin, which bind to the C-terminal and thus do not cause HSF1 to be displaced nor cause a detectable HSR, do not affect osteoclast differentiation (Chai *et al.*, 2014). This supports the notion, suggested by work presented in this thesis, that HSP90 inhibitors, which bind to the HSP90 N terminal are dependent on HSF1 activation for their effects on osteoclast formation.

It is important to note here that MITF, so far, appears to be the only osteoclast-associated transcription factor to be regulated by 17-AAG. Surprisingly, the 17-AAG mediated increase in MITF protein levels is dependent upon HSF1 i.e., in bone marrow cells from HSF1$^{-/-}$ mice, 17-AAG did not induce MITF expression (Chai *et al.*, 2014). . This suggests 17-AAG and NVP-AUY922 indirect activation of HSF1 might lead to its binding to the MITF promoter, thereby increasing its expression. The increased expression of MITF may then lead to an increase in osteoclast formation. To further elucidate this, in the future ChIP experiments could be performed to determine firstly if HSF1 binds to MITF and secondly if 17-AAG and also NVP-AUY922 treatment increases the association of the two molecules. MITF is possibly the only factor to be influenced by a HSR, with no others having been so reported. Supporting this notion, Laramie *et al.* 2008 found that MITF mRNA levels in endothelial cells are regulated by heat shock (Laramie *et al.*, 2008). Furthermore, they also demonstrated that HSE elements to which HSF1 might bind are present in promoter sequences upstream of the coding region (Laramie *et al.*, 2008). This HSE motif was not in a standard triplicate form (HSF1 typically binds as a trimer to triplet HSE sequences, nTTCnnGAAnnTTCn, in HSP70 promoters), but as a dimer (Laramie *et al.*, 2008). This may indicate a requirement for a more complex transcriptional factor complex (Laramie *et al.*, 2008). In addition, the SPl1/PU.1 gene, which codes for the myeloid transcription factor PU.1 has been shown to have multiple HSE-like sequences. PU.1 and MITF associate in bone marrow progenitors to regulate a large number of osteoclast genes and mice lacking either of these genes, lack osteoclasts (Sharma *et al.*, 2007). However, to date, our laboratory has not found HSR regulation of PU.1 in RAW264.7 cells in response to 17-AAG (Boudesco *et al.*, 2015). It may be that MITF is affected in general by cell stress. Supporting this, MITF has also been shown to be regulated by oxidative stress (Liu *et al.*, 2008). Liu *et al.* showed the melanocyte isoform of MITF, MITF-M, is able to regulate cellular responses to ROS treatment (Liu *et al.*, 2008). In response to H_2O_2 treatment, MITF-M has been shown to be phosphorylated and induce the expression of target gene apurinic/apyrimidinic endonuclease (APE-1/Ref-1) in Sk-Mel-28 and c83-2C melanoma cell lines respectively (Liu *et al.*, 2008). It is important to note though that the MITF-M isoform is not found in osteoclast progenitors. In addition, MITF-M drives the expression of PGC1α overexpression in a number of human melanomas and derived cell lines (Gabriel *et al.*, 2014). Interestingly, these cells have higher mitochondrial function and therefore increased ROS (Gabriel *et al.*, 2014). Moreover, MITF has been shown to be activated by lysosomal stressors and activate the glycoprotein non-metastatic melanoma protein B (Gpnmb), whose expression has been found to correlate with body weight

(Vazquez *et al.*, 2013). This data suggests that the transcription factor MITF is sensitive to cellular stress in a number of cell types. It is important to note RANKL, which belongs to the TNF cytokine family, has also been shown to contain a HSE motif in its promoter region (Roccisana *et al.*, 2004). This suggests that RANKL and therefore osteoclastogenesis might also be regulated by cell stress. This hypothesis is supported by the fact that many skeletal diseases including rheumatoid arthritis, osteolytic bone metastasis cause the bone niche to be stressed and these diseases have increased osteoclast formation and bone destruction. Moreover the TNF cytokines to which RANKL belongs are involved in inflammation and apoptosis further suggesting RANKL and osteoclastogenesis is regulated by stress(Hehlgans and Pfeffer, 2005).

In addition to 17-AAG and NVP-AUY922 activating a HSR, both these compounds also activated the stress MAP kinase p38 robustly (Table 7.1). This MAP Kinase is responsive to a wide variety of stresses and is essential for osteoclast formation (Zarubin and Han, 2005; Wagner and Nebreda, 2009; Matsumoto *et al.*, 2000). Within the cell many recent reports suggests that stress pathways engage in crosstalk with one another and interestingly some studies have shown regulation between p38 and HSF1(Patel, 2009). HSF1 inhibition, by KNK437, ablates p38 MAP kinase levels in NaCl treated medullary cells (Patel, 2009). To determine whether 17-AAG and NVP-AUY922 mediated HSF1 activation is regulated by p38, HSF1 was inhibited and p38 activation assessed. HSF1 inhibition did not decrease 17-AAG or NVP-AUY922 activation of p38. Rather it seemed that inhibition of HSF1 slightly increased p38 activation. This may result because p38 has to cope with an additional stress load due to HSF1 being incapacitated. In addition, HSP90 inhibition through 17-AAG and NVP-AUY922 would activate the UPR, and the inhibition of HSF1 would not allow for HSP expression to be increased as a coping mechanism to the UPR. Thus, the inhibition of HSF1 would increase the stress load to the cell and potentially increase the activation of other stress molecules. Inversely, p38 inhibition has also been shown to decrease HSP70 levels in medullary cells (Patel, 2009). In addition, human esophageal microvascular endothelial cells have been shown to respond to acidic pH stress by p38 MAPK-regulated induction of HSP70 and HSP27 (Rafiee *et al.*, 2006). Further studies assessing p38 role in 17-AAG and NVP-AUY922 induction of HSP72 are thus needed. It is interesting to note that the stress sensitive MITF is also regulated by p38 during osteoclastogenesis (Mansky *et al.*, 2002a). Upon RANKL stimulation,p38 phosphorylates MITF on Ser307 in progenitor cells causing the induction of osteoclastogenic genes including TRAP (Mansky *et al.*, 2002b). Work in this

thesis showed inhibiting p38 decreased both 17-AAG and NVP-AUY922 induction of MITF. This data suggests that p38 might contribute to the 17-AAG and NVP-AU922 mediated induction of MITF; however, p38 inhibition alone decreased MITF. Both HSF1 and p38 activation from 17-AAG and NVP-AUY922 might act dually to increase MITF protein levels translating to increased osteoclastogenesis. This data further implicates MITF sensitivity to stress and that its induction through stress increases osteoclastogenesis.

There are a number of cell stress pathways within the cell. The fact that 17-AAG activates the HSR and the stress molecule p38 (Table 7.1) led to the hypothesis that other compounds that activate stress pathways may influence osteoclastogenesis. Compounds that caused oxidative stress, ER stress, UPR, and genotoxic stress were found to activate HSF1 transcriptional activity and causing the induction of stress inducible HSP72. The data presented here shows the novel finding that these compounds, which vary in their targets and mechanism mode, activate a HSR in RAW264.7 cells (Table 7.1). This data suggests further that there is a crosstalk between stress pathways. MG132 and Bortezomib are both proteasome inhibitors, which cause a UPR response. Due to the cells no longer being able to degrade misfolded proteins, the cells undergo proteotoxic stress, which would suggest the activation of HSF1. Interestingly in a number of other cell types both MG132 and Bortezomib have been reported to activate HSF1 and increase HSP gene transcription (Du *et al.*, 2009; Holmberg *et al.*, 2000; Kim *et al.*, 1999). Similarly, Kao *et al.* 2013 found bortezomib increased HSE-dependent response element activity, and also HSF1 protein expression in the TOV112D ovarian cancer cell line (Kao *et al.*, 2013). The genotoxic stress-inducing compounds doxorubicin and second generation platinum coordination, carboplatin, have also been reported to activate HSF1. Anthracyclines including doxorubicin increase the expression of HSPs in human prostate, ovarian and acute lymphoblastic leukemic cells, and neuroblastoma cells (Fucikova *et al.*, 2011; Zanini *et al.*, 2007). Another stress response, oxidative stress, which occurs in response to ROS generation, has been shown to activate HSF1. Ethanol exposure, which causes ROS generation and oxidative stress has been shown to cause the translocation of HSF1 to the nucleus, the formation of stress granules and the transcription of HSPs including HSP70 and HSP90 (Morimoto, 1998; Pignataro *et al.*, 2007). Pignataro *et al.* showed that the response to alcohol and heat shock have a similar profile. HSF1 was shown to be able to bind to alcohol response elements (ARE) sequences and ARE like sequences, which are present in many alcohol-responsive genes (Pignataro *et al.*, 2007). Many of these genes have been shown to be activated by heat shock suggesting alcohol can activate

molecules that are involved in the HSR (Pignataro *et al.*, 2007). Interestingly, these HSF1 activating chemotherapeutics and ethanol were shown to increase osteoclast formation to variable degrees in RAW264.7 cells. This data shows the novel finding that anti-cancer agents and ethanol, which cause different stress responses in the cell can also activate HSF1 and increase osteoclast formation (Table 7.1). Inhibition of HSF1, by KNK437, ablated the increased osteoclast formation caused by these compounds. This data shows compounds that cause genotoxic stress, ER stress (UPR), and oxidative stress can increase osteoclast formation at least partly through HSF1. This adds to the earlier data that the HSR increases osteoclast formation and suggests that many kinds of stress can regulate osteoclast formation with HSF1 potentially acting as a hub protein. Interestingly, the UPR, which occurs due to the accumulation of incorrectly folded proteins in the ER lumen, has been shown to have a role in osteoclastogenesis (Ron and Walter, 2007; Liu and Kaufman, 2003; Oslowski and Urano, 2011). The ER inhibitors thapsigargin and tunicamycin have been shown to increase osteoclast differention genes Acp5 (coding for TRAP) and Ctsk (cathepsin K) (Wang *et al.*, 2011b). ROS has also been shown to be important in osteoclast formation in several ways, including increased RANKL expression in osteoblasts (Bai *et al.*, 2005). At a physiological level, a biochemical link between increased oxidative stress and reduced bone density has also been identified in patient samples. (Basu *et al.*, 2001). Coenzyme Q10, selenium and curcumin, which are powerful antioxidants have been shown to markedly inhibit the formation of TRAP and multinucleated cells in both BMM and RAW264.7 cells (Moon *et al.*, 2012a). Treatment with these antioxidants decreased NFATc1, TRAP and OSCAR expression (Moon *et al.*, 2012a). These antioxidants were shown to scavenge intracellular ROS generation within osteoclast progenitors during RANKL stimulated osteoclastogenesis (Moon *et al.*, 2012a). Similarly, peroxiredoxin (PRX)-like 2 activated in M-CSF stimulated monocytes (PAMM), which functions as redox regulatory protein also regulates osteoclastogenesis (Xu *et al.*, 2010). PAMM, which acts to increases the GSH/GSSH ratio, is decreased upon M-CSF and RANKL co-stimulation (Xu *et al.*, 2010). Overexpression of PAMM has been shown to decrease NFκB and c-Jun expression with a resultant decrease in osteoclast numbers (Xu *et al.*, 2010). Moreover, it is interesting to note that RANKL stimulation in RAW264.7 cells decreases the GSH/GSSG ratio reflecting an increase in ROS expression (Xu *et al.*, 2010). This suggests that oxidative stress plays a significant role in osteoclastogenesis. Although not examined in this thesis another stress-related pathway that is implicated in osteoclast formation is autophagy, a pathways originally observed as a response to nutrient deprivation (Levonen *et al.*, 2014; Hocking *et al.*, 2012). Haemopoietic

stem cells, precursor cells to osteoclasts, which lack the autophagy-related gene Atg7$^{-/-}$ fail to differentiate into osteoclasts (Hocking *et al.*, 2012). Recently Desai *et al.* 2013 showed that HSF1 is involved in chemotherapeutic agent-induced cytoprotective autophagy, which occurs in a HSR independent manner through the upregulation of ATG7 (Desai *et al.*, 2013). Interestingly, HSP90 N-terminal inhibitors including geldanamycin, 17-AAG and NVP-AUY922 have all been implicated in causing autophagy (Hsueh *et al.*, 2013; Riedel *et al.*, 2010; Karkoulis *et al.*, 2013; Mori *et al.*, 2015b).

The cancer therapeutics studied in this thesis have been implicated in activating a range of stress pathways in addition to the stress pathway they target. Bortezomib, which causes a UPR has been shown to activate signalling molecules, including p38, and enhance the DNA binding activity of transcription factors AP-1, Ets-1 and HSF1 (Selimovic *et al.*, 2013). These molecules are involved in a number of stress pathways including the stress MAP kinases, HSR and in ER-stress-induced autophagy. In addition, the UPR inducing MG132 has been implicated in oxidative stress and the MAP kinase pathways by decreasing GSH levels and causing p38 activation (Yong Hwan Han and Woo Hyun Park, 2010). Anthracyclines, such as doxorubicin, have been shown to cause mitochondrial dysfunction resulting in oxidative stress through increased ROS production (Gouspillou *et al.*, 2015). These molecules and stress pathways have been implicated in osteoclast formation (Moon *et al.*, 2012a). This suggests that crosstalk between these pathways may cooperate to increase osteoclastogenesis through a stress dependent mechanism. It is important to note however, that not all of the anti-cancer agents are known to cause bone loss. For example, bortezomib greatly increases osteoblast activity *in vivo* (Bai *et al.*, 2005). As a future study the effect of cell stress upon osteoblast differentiation and function would be important to consider. Some chemotherapeutic compounds damage bone, but are thought to do so through the generalised damage they cause to bone and bone marrow cells (Wang *et al.*, 2006). Nevertheless, this data points to the possibility of osteoclast-accelerated bone loss contributing to the damage they cause.

Unlike the HSP90 inhibitors, these anti-cancer agents (MG132, Bortezomib, cisplatin and doxorubicin) and ethanol were also shown to increase NFATc1 protein expression in addition to MITF protein expression (Table 7.1). This data suggests their mechanism of action to increase osteoclastogenesis may have very significant differences to that of HSP90 inhibitors. Alternatively, it may reflect the fact that they induce a number of pathways, which all feed

into increased MITF levels. Due to the suggested stress sensitivity of MITF, further work using bone marrow progenitor cells from HSF1^{-/-} mice and pharmacological inhibition of HSF1 can be used to detect HSF1 role in MITF induction by these compounds. In addition, the effect of multiple stressors, which activate alternative stress pathways including oxidative stress, ER stress (UPR) and genotoxic stress (DDR) upon MITF activation in context of osteoclast formation, should be addressed. Moreover, the effect of the cancer therapeutics and ethanol upon other osteoclast transcription factors and signalling molecules including c-FOS and p38 should be studied. Further studies regarding this NFATc1 induction by the compounds should also be addressed.

7.1.1 Clinical importance

The chemotherapeutics studied in this thesis have complex effects on bone cells *in vivo* but the experimental results suggest they may exert osteolytic actions in bone. If so, this would result in a significantly negative clinical impact upon individuals already suffering from pathological bone diseases. As mentioned earlier cisplatin, doxorubicin and ethanol have all been shown to cause clinical bone loss, consistant with the results reported here (Rana *et al.*, 2013; Ehrhart *et al.*, 2002; Iitsuka *et al.*, 2012; Alvisa-Negrín *et al.*, 2009). Chemotherapy-induced bone loss and the resulting SRE has already been identified as a major problem for patients (Guise, 2006; Lipton *et al.*, 2009a). For young and adolescent patients, chemotherapy-induced bone loss inhibits bone growth, causes low bone volume, osteonecrosis and fractures (Fan *et al.*, 2011; Fan *et al.*, 2012). Middle to later aged patients in whom bone growth has stopped do not appear to have this predisposition. However, remodelling processes would be affected due to the uncoupled rates of bone formation and loss that is present in osteolytic bone pathologies (Fan *et al.*, 2011; Feng and McDonald, 2011; Boyle *et al.*, 2003). These patients would be more likely to have fractures due to decreased bone integrity (Coleman, 2006; Mundy, 2002). Methotrexate, a treatment commonly given to young and adolescent patients with acute lymphoblastic leukaemia, is also used to treat patients with rheumatoid arthritis and has been shown to cause SRE (Fan *et al.*, 2011; Cronstein, 2005). Folinic acid, which acts as an antidote to methotrextate treament, decreases growth plate and metaphseal damage thus being a possible treatment option for skeletal growth in young patients (Fan *et al.*, 2011). Methotrexate increases osteoclast formation in a manner at least partly dependent on HSF1 *in vitro* (Chai *et al.*, 2014). Consistent with these notions, antioxidants (which counteract ROS actions) along with exercise, vitamin D and bisphosphonate treatment is recommend for chemotherapy induced

bone loss (Fan *et al.*, 2011; Mundy, 2002; Simos *et al.*, 2013; Israeli, 2008). In the context of metastastatic bone disease these experimental and clinically used chemotherapeutics might increase tumour progression through osteolysis. As earlier described, 17-AAG treatment was shown to increase tumour growth in the bone in a MD-MB-231 mouse model and this promotion of tumour growth was hypothesized to depend on its osteolytic effects *in vivo* (Price *et al.*, 2005). As with 17-AAG, it is conceivable that cisplatin doxorubcin and bortezomib treatment may act similarly to increase bone metastastic disease through the augmentation of the vicious cycle. Increased bone metastatic disease would cause the secondary complication of further bone loss and SRE as described above. Despite being a secondary complication to metastasis, SRE cause most of the patient burden including pain, spincal cord compression and mortality as treatment is refractory (Weilbaecher *et al.*, 2011; Simos *et al.*, 2013; Mundy, 2002). Increased osteolysis would also cause increased fracture incidence (Mundy, 2002; Coleman, 2006). Therefore, the effect of these chemotherapeutics upon metastatic bone disease needs to be carefully studied. A number of chemotherapeutic agents also negatively affect affect bone formation, although the reason for this is usually unclear but it is typically seen in the context of widespread damage to bone marrow (Wang *et al.*, 2006). Though the chemotherapeutics methotrexate, doxorubicin and cisplatin have been shown to decrease bone formation rates by their actions upon osteoblasts (Morcuende *et al.*, 2004; Friedlaender *et al.*, 1984; Stine *et al.*, 2014). However, bortezomib has been shown to increase osteoblast differentiation suggesting bortezomib has complex effects on the bone microenvironment and can increases both osteolysis and bone formation (Bai *et al.*, 2005). In addition to the tested chemotherapeutics, ethanol consumption has been shown to decrease bone volume (Alvisa-Negrín *et al.*, 2009; Turner *et al.*, 1987). The work in this thesis also suggests a possible wider clinical relevance of cell stress dependent enhancement of osteoclast differentiation since cell stress may occur in response to many pathological stimuli including inflmmatin and infection (Muralidharan and Mandrekar, 2013; Morimoto, 1993; Åkerfelt *et al.*, 2010; Fulda *et al.*, 2010; Richter *et al.*, 2010). Thus cell stress may underlie at least part of the bone loss seen in other bone pathologies including the inflammatory rheumatoid arthritis and infectious peri-dontal and peri-implant diseases. Thus HSF1-dependent cell stress might excerbate osteoclast activity thus contributing to the disease activity in patients with these pathologies.

In summary, cancer therapeutics act to cause cytotoxicity through very different mechanisms and induce a number of stress pathways in the cell including ER stress (UPR), oxidative stress, and genotoxic stress. Interestingly, a number of these stress pathways have been implicated in regulating osteoclastogenesis including oxidative stress and ER stress. Our data shows the novel findings of these anti-cancer agents. These chemotherapeutics, including those going through clinical trials and those using clinically, were shown to increase osteoclastogenesis in part through HSF1 activation and the HSR. Therefore, a number of stressors have been demonstrated to display cell stress dependent effects on osteoclast progenitors, which is potentially highly osteolytic. This data suggests that cellular stress regulates osteoclastogenesis. Consistent with this RANKL has a HSE element present within its promoter further suggesting osteoclastogenesis is regulated by stress (Roccisana *et al.*, 2004) Another transcription factor, which has been reported to have a HSE and is suggested to be stress sensitive is MITF (Ruffenach *et al.*, 2015). These compounds caused increased MITF expression in osteoclast progenitor cells. The results are not conclusive in regard to whether all the stressors act directly to regulate MITF as they may act indirectly via some NFATc1 regulation. However, given the critical role of this transcription factor in osteoclast formation, their actions on MITF levels are consistent with a strongly pro-osteoclastogenic action. These stressors have complex effects on bone cells *in vivo,* but it seems highly likely that they may exert osteolytic actions in bone. In the context of metastatic bone disease, these drugs, like 17-AAG, may act to increase tumour progression through osteolysis and the vicious cycle model. Bone metastasis also results in SRE, which have negative impacts upon an individual's health. Most often once having metastasized, the tumours are refractory to treatment. Thus, any increase in osteolysis would further disease progression and be detrimental to the patient. For these reasons, it is important that developing and clinically used anti-cancer therapeutics should be screened for effects on bone metabolism. This work further suggests that stress stimuli and stress pathways, which are often activated in pathological bone diseases including rheumatoid arthritis, contribute to the often disordered differentiation of osteoclasts and their activity.
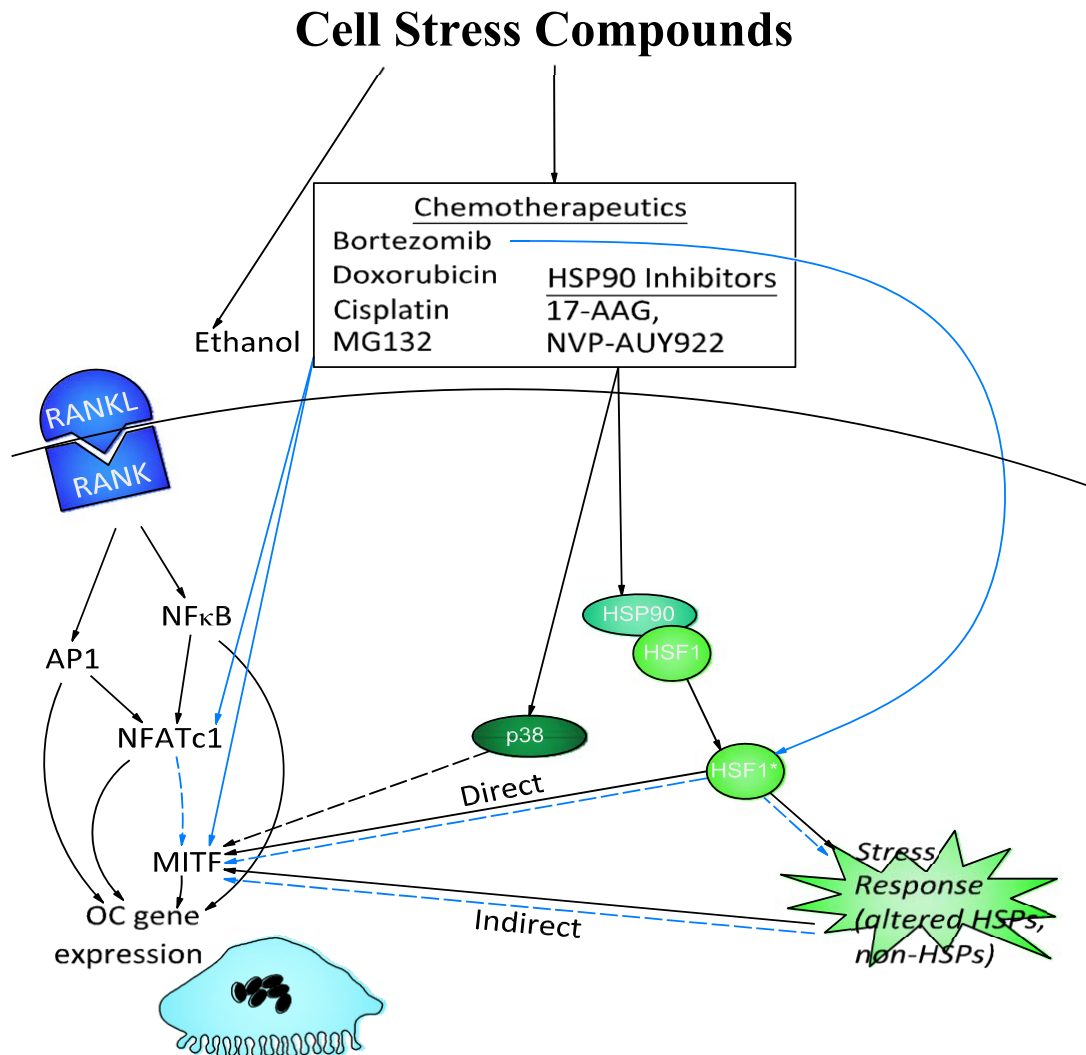
Figure 7.1 Proposed Model of Cell Stressor Action upon Osteoclastogenesis
Cell stressors, chemotherapeutics (17-AAG, NVP-AUY922, bortezomib, cisplatin, MG132, and doxorubicin) and ethanol increase osteoclastogenesis by targeting key transcription factors in the RANK signalling pathway. The increase in osteoclastogenesis by these compounds is dependent upon HSF-1 activation and the heat shock response. The N-terminal HSP90 inhibitors act to increase osteoclast differentiation by increasing the expression of late acting transcription factor MITF in a HSF-1 dependent manner. These inhibitors also activate the p38 MAP kinase stress pathway which may also feed into MITF activation. MG132 and clinically used chemotherapeutics cisplatin, doxorubicin and bortezomib do not inhibit HSP90 but cause cytotoxicity in a range of mechanisms including proteasome inhibition (ER stress). These compounds and ethanol increase MITF expression also; however, unlike N-terminal HSP90 inhibitors, they increase NFATc1 protein levels. MITF expression may be increased through increased expression of NFATc1 or alternatively through HSF-1 like the HSP90 inhibitors. Full lines show demonstrated results. Dotted lines represent possible mechanisms. Image adapted from Chai *et al.* (2014).

Bibliography

ABE, M., HIURA, K., WILDE, J., MORIYAMA, K., HASHIMOTO, T., OZAKI, S., WAKATSUKI, S., KOSAKA, M., KIDO, S., INOUE, D. & MATSUMOTO, T. 2002. Role for macrophage inflammatory protein (MIP)-1alpha and MIP-1beta in the development of osteolytic lesions in multiple myeloma. *Blood,* 100**,** 2195-202.

ABE, M., HIURA, K., WILDE, J., SHIOYASONO, A., MORIYAMA, K., HASHIMOTO, T., KIDO, S., OSHIMA, T., SHIBATA, H., OZAKI, S., INOUE, D. & MATSUMOTO, T. 2004. Osteoclasts enhance myeloma cell growth and survival via cell-cell contact: a vicious cycle between bone destruction and myeloma expansion. *Blood,* 104**,** 2484-91.

ADAMS, J. 2002. Development of the Proteasome Inhibitor PS-341. *The Oncologist,* 7**,** 9-16.

ADAMS, J. 2003. The proteasome: structure, function, and role in the cell. *Cancer Treatment Reviews,* 29, Supplement 1**,** 3-9.

ADAMS, J. 2004. The development of proteasome inhibitors as anticancer drugs. *Cancer Cell,* 5**,** 417-421.

AESCHLIMANN, D. & EVANS, B. A. J. 2004. The vital osteoclast: how is it regulated? *Cell Death Differ,* 11**,** S5-S7.

AGASHE, V. R. & HARTL, F. U. 2000. Roles of molecular chaperones in cytoplasmic protein folding. *Seminars in Cell & Developmental Biology,* 11**,** 15-25.

AHN, S.-G., LIU, P. C. C., KLYACHKO, K., MORIMOTO, R. I. & THIELE, D. J. 2001. The loop domain of heat shock transcription factor 1 dictates DNA-binding specificity and responses to heat stress. *Genes & Development,* 15**,** 2134-2145.

AIHW, A. I. O. H. A. W. N. B. C. C. 2006. Australian Institute of Health and Welfare & National Breast Cancer Centre 2006. Breast cancer in Australia: an overview, Cancer series no. 34.

AKAGAWA, K. S., TAKASUKA, N., NOZAKI, Y., KOMURO, I., AZUMA, M., UEDA, M., NAITO, M. & TAKAHASHI, K. 1996. Generation of CD1+RelB+ dendritic cells and tartrate-resistant acid phosphatase-positive osteoclast-like multinucleated giant cells from human monocytes. *Blood,* 88**,** 4029-4039.

AKAMA, K. T., ALBANESE, C., PESTELL, R. G. & VAN ELDIK, L. J. 1998. Amyloid β-peptide stimulates nitric oxide production in astrocytes through an NFκB-dependent mechanism. *Proceedings of the National Academy of Sciences of the United States of America,* 95**,** 5795-5800.

ÅKERFELT, M., MORIMOTO, R. I. & SISTONEN, L. 2010. Heat shock factors: integrators of cell stress, development and lifespan. *Nature Reviews. Molecular Cell Biology,* 11**,** 545-555.

ÅKERFELT, M., TROUILLET, D., MEZGER, V. & SISTONEN, L. E. A. 2007. Heat Shock Factors at a Crossroad between Stress and Development. *Annals of the New York Academy of Sciences,* 1113**,** 15-27.

AL-DUJAILI, S. A., LAU, E., AL-DUJAILI, H., TSANG, K., GUENTHER, A. & YOU, L. 2011. Apoptotic osteocytes regulate osteoclast precursor recruitment and differentiation in vitro. *Journal of Cellular Biochemistry,* 112**,** 2412-2423.

ALBANO, E. 2006. Alcohol, oxidative stress and free radical damage. *Proc Nutr Soc,* 65**,** 278-90.

ALBERTS, B., JOHNSON, A., LEWIS, J., RAFF, M., ROBERTS, K. & WALTER, P. 2002. *Molecular Biology of the Cell, Fourth Edition*, Garland Science.

ALVISA-NEGRÍN, J., GONZÁLEZ-REIMERS, E., SANTOLARIA-FERNÁNDEZ, F., GARCÍA-VALDECASAS-CAMPELO, E., VALLS, M. R. A., PELAZAS-

GONZÁLEZ, R., DURÁN-CASTELLÓN, M. C. & DE LOS ÁNGELES GÓMEZ-RODRÍGUEZ, M. 2009. Osteopenia in Alcoholics: Effect of Alcohol Abstinence. *Alcohol and Alcoholism,* 44**,** 468-475.

AMBADE, A. & MANDREKAR, P. 2012. Oxidative Stress and Inflammation: Essential Partners in Alcoholic Liver Disease. *International Journal of Hepatology,* 2012.

AMERICAN CANCER SOCIETY. 2007. *American Cancer Society,* [Online]. American Cancer Society. Available: www.cancer.org [Accessed November 2014].

ANCKAR, J. & SISTONEN, L. 2011. Regulation of HSF1 Function in the Heat Stress Response: Implications in Aging and Disease. *Annual Review of Biochemistry,* 80**,** 1089-1115.

ANDERSEN, T. L., SONDERGAARD, T. E., SKORZYNSKA, K. E., DAGNAES-HANSEN, F., PLESNER, T. L., HAUGE, E. M., PLESNER, T. & DELAISSE, J.-M. 2009. A Physical Mechanism for Coupling Bone Resorption and Formation in Adult Human Bone. *The American Journal of Pathology,* 174**,** 239-247.

ANDERSON, D. M., MARASKOVSKY, E., BILLINGSLEY, W. L., DOUGALL, W. C., TOMETSKO, M. E., ROUX, E. R., TEEPE, M. C., DUBOSE, R. F., COSMAN, D. & GALIBERT, L. 1997. A homologue of the TNF receptor and its ligand enhance T-cell growth and dendritic-cell function. *Nature,* 390**,** 175-179.

ARCHANGELO, L. F., GREIF, P. A., MAUCUER, A., MANCEAU, V., KONERU, N., BIGARELLA, C. L., NIEMANN, F., DOS SANTOS, M. T., KOBARG, J., BOHLANDER, S. K. & SAAD, S. T. O. 2013. The CATS (FAM64A) protein is a substrate of the Kinase Interacting Stathmin (KIS). *Biochimica et Biophysica Acta (BBA) - Molecular Cell Research,* 1833**,** 1269-1279.

ARLANDER, S. J. H., EAPEN, A. K., VROMAN, B. T., MCDONALD, R. J., TOFT, D. O. & KARNITZ, L. M. 2003. Hsp90 Inhibition Depletes Chk1 and Sensitizes Tumor Cells to Replication Stress. *Journal of Biological Chemistry,* 278**,** 52572-52577.

ARMSTRONG, A. P., MILLER, R. E., JONES, J. C., ZHANG, J., KELLER, E. T. & DOUGALL, W. C. 2008. RANKL acts directly on RANK-expressing prostate tumor cells and mediates migration and expression of tumor metastasis genes. *The Prostate,* 68**,** 92-104.

ARNHEITER, H. 2010. The discovery of the microphthalmia locus and its gene, Mitf. *Pigment Cell & Melanoma Research,* 23**,** 729-735.

ASAGIRI, M., SATO, K., USAMI, T., OCHI, S., NISHINA, H., YOSHIDA, H., MORITA, I., WAGNER, E. F., MAK, T. W., SERFLING, E. & TAKAYANAGI, H. 2005. Autoamplification of NFATc1 expression determines its essential role in bone homeostasis. *The Journal of Experimental Medicine,* 202**,** 1261-1269.

ASAGIRI, M. & TAKAYANAGI, H. 2007. The molecular understanding of osteoclast differentiation. *Bone,* 40**,** 251-264.

ASAI, K., FUNABA, M. & MURAKAMI, M. 2014. Enhancement of RANKL-induced MITF-E expression and osteoclastogenesis by TGF-β. *Cell Biochemistry and Function,* 32**,** 401-409.

ASH, P., LOUTIT, J. F. & TOWNSEND, K. M. S. 1980. Osteoclasts derived from haematopoietic stem cells. *Nature,* 283**,** 669-670.

ATHANASOU, N. A. 1996. Current Concepts Review - Cellular Biology of Bone-Resorbing Cells. *J Bone Joint Surg Am,* 78**,** 1096-1112.

ATHANASOU, N. A. & QUINN, J. 1990. Immunophenotypic differences between osteoclasts and macrophage polykaryons: immunohistological distinction and implications for osteoclast ontogeny and function. *Journal of Clinical Pathology,* 43**,** 997-1003.

ATHANASOU, N. A. & SABOKBAR, A. 1999. Human osteoclast ontogeny and pathological bone resorption. *Histol Histopathol,* 14**,** 635-47.

ATKINS, G. J. & FINDLAY, D. M. 2012. Osteocyte regulation of bone mineral: a little give and take. *Osteoporosis International,* 23**,** 2067-2079.

ATKINS, G. J., HAYNES, D. R., GRAVES, S. E., EVDOKIOU, A., HAY, S., BOURALEXIS, S. & FINDLAY, D. M. 2000. Expression of Osteoclast Differentiation Signals by Stromal Elements of Giant Cell Tumors. *Journal of Bone and Mineral Research,* 15**,** 640-649.

AXMANN, R., BOHM, C., KRONKE, G., ZWERINA, J., SMOLEN, J. & SCHETT, G. 2009. Inhibition of interleukin-6 receptor directly blocks osteoclast formation in vitro and in vivo. *Arthritis Rheum,* 60**,** 2747-56.

AZUMA, Y., KAJI, K., KATOGI, R., TAKESHITA, S. & KUDO, A. 2000. Tumor Necrosis Factor-α Induces Differentiation of and Bone Resorption by Osteoclasts. *Journal of Biological Chemistry,* 275**,** 4858-4864.

BAGATELL, R., PAINE-MURRIETA, G. D., TAYLOR, C. W., PULCINI, E. J., AKINAGA, S., BENJAMIN, I. J. & WHITESELL, L. 2000. Induction of a Heat Shock Factor 1-dependent Stress Response Alters the Cytotoxic Activity of Hsp90-binding Agents. *Clinical Cancer Research,* 6**,** 3312-3318.

BAI, X.-C., LU, D., LIU, A.-L., ZHANG, Z.-M., LI, X.-M., ZOU, Z.-P., ZENG, W.-S., CHENG, B.-L. & LUO, S.-Q. 2005. Reactive Oxygen Species Stimulates Receptor Activator of NF-κB Ligand Expression in Osteoblast. *Journal of Biological Chemistry,* 280**,** 17497-17506.

BALTASAR SANCHEZ, A. & GONZALEZ SISTAL, A. 2014. A Quantitative Method for the Characterization of Lytic Metastases of the Bone from Radiographic Images. *The Scientific World Journal,* 2014**,** 5.

BAN, J. Y., KIM, B. S., KIM, S. C., KIM, D. H. & CHUNG, J.-H. 2011. Microarray Analysis of Gene Expression Profiles in Response to Treatment with Melatonin in Lipopolysaccharide Activated RAW 264.7 Cells. *The Korean Journal of Physiology & Pharmacology : Official Journal of the Korean Physiological Society and the Korean Society of Pharmacology,* 15**,** 23-29.

BANDYOPADHYAY-GHOS, S. 2008. Bone as a Collagen-hydroxyapatite Composite and its Repair. *Trends Biomater. Artif. Organs, ,* 22**,** 116-124.

BANERJI, U., O'DONNELL, A., SCURR, M., PACEY, S., STAPLETON, S., ASAD, Y., SIMMONS, L., MALONEY, A., RAYNAUD, F., CAMPBELL, M., WALTON, M., LAKHANI, S., KAYE, S., WORKMAN, P. & JUDSON, I. 2005a. Phase I pharmacokinetic and pharmacodynamic study of 17-allylamino, 17-demethoxygeldanamycin in patients with advanced malignancies. *J Clin Oncol,* 23**,** 4152-61.

BANERJI, U., O'DONNELL, A., SCURR, M., PACEY, S., STAPLETON, S., ASAD, Y., SIMMONS, L., MALONEY, A., RAYNAUD, F., CAMPBELL, M., WALTON, M., LAKHANI, S., KAYE, S., WORKMAN, P. & JUDSON, I. 2005b. Phase I Pharmacokinetic and Pharmacodynamic Study of 17-Allylamino, 17-Demethoxygeldanamycin in Patients With Advanced Malignancies. *Journal of Clinical Oncology,* 23**,** 4152-4161.

BARANČíK, M., BOHÁČOVÁ, V., KVAČKAJOVÁ, J., HUDECOVÁ, S., KRIŽANOVÁ, O. G. & BREIER, A. 2001. SB203580, a specific inhibitor of p38-MAPK pathway, is a new reversal agent of P-glycoprotein-mediated multidrug resistance. *European Journal of Pharmaceutical Sciences,* 14**,** 29-36.

BARGO, S., RAAFAT, A., MCCURDY, D., AMIRJAZIL, I., SHU, Y., TRAICOFF, J., PLANT, J., VONDERHAAR, B. K. & CALLAHAN, R. 2010. Transforming acidic

coiled-coil protein-3 (Tacc3) acts as a negative regulator of Notch signaling through binding to CDC10 /Ankyrin repeats. *Biochemical and biophysical research communications,* 400**,** 606-612.

BARON, R., FERRARI, S. & RUSSELL, R. G. G. 2011. Denosumab and bisphosphonates: Different mechanisms of action and effects. *Bone,* 48**,** 677-692.

BARON, R. & HORNE, W. 2005. Regulation of Osteoclast Activity. *In:* BRONNER, F., FARACH-CARSON, M. & RUBIN, J. (eds.) *Bone Resorption.* Springer London.

BARON, R. & KNEISSEL, M. 2013. WNT signaling in bone homeostasis and disease: from human mutations to treatments. *Nat Med,* 19**,** 179-192.

BARON, R., NEFF, L., TRAN VAN, P., NEFUSSI, J. R. & VIGNERY, A. 1986. Kinetic and cytochemical identification of osteoclast precursors and their differentiation into multinucleated osteoclasts. *Am J Pathol,* 122**,** 363-78.

BARTKOVA, J., HOREJSI, Z., KOED, K., KRAMER, A., TORT, F., ZIEGER, K., GULDBERG, P., SEHESTED, M., NESLAND, J. M., LUKAS, C., ORNTOFT, T., LUKAS, J. & BARTEK, J. 2005. DNA damage response as a candidate anti-cancer barrier in early human tumorigenesis. *Nature,* 434**,** 864-870.

BASELGA, J. 2001. Phase I and II clinical trials of trastuzumab. *Ann Oncol,* 12 Suppl 1**,** S49-55.

BASU, A. & KRISHNAMURTHY, S. 2010. Cellular Responses to Cisplatin-Induced DNA Damage. *Journal of Nucleic Acids,* 2010**,** 16.

BASU, S., MICHAËLSSON, K., OLOFSSON, H., JOHANSSON, S. & MELHUS, H. 2001. Association between Oxidative Stress and Bone Mineral Density. *Biochemical and Biophysical Research Communications,* 288**,** 275-279.

BATTAGLINO, R., FU, J., SPATE, U., ERSOY, U., JOE, M., SEDAGHAT, L. & STASHENKO, P. 2004. Serotonin regulates osteoclast differentiation through its transporter. *J Bone Miner Res,* 19**,** 1420-31.

BAUER, K., BROWN, M., CRESS, R., PARISE, C. & CAGGIANO, V. 2007. Descriptive analysis of estrogen receptor (ER)-negative, progesterone receptor (PR)-negative, and HER2-negative invasive breast cancer, the so-called triple-negative phenotype: a population-based study from the California Cancer Registry. *Cancer,* 109**,** 1721 - 1728.

BECK, F. X., GRUNBEIN, R., LUGMAYR, K. & NEUHOFER, W. 2000. Heat shock proteins and the cellular response to osmotic stress. *Cell Physiol Biochem,* 10**,** 303-6.

BECKMANN, R. P., LOVETT, M. & WELCH, W. J. 1992. Examining the function and regulation of hsp 70 in cells subjected to metabolic stress. *J Cell Biol,* 117**,** 1137-50.

BÉLANGER, L. 1969. Osteocytic osteolysis. *Calcified Tissue Research,* 4**,** 1-12.

BEN-DAVID, D., LIVNE, E. & REZNICK, A. Z. 2012. The involvement of oxidants and NF-[kappa]B in cytokine-induced MMP-9 synthesis by bone marrow-derived osteoprogenitor cells. *Inflammation Research,* 61**,** 673-88.

BENBROOK, D. M. & LONG, A. 2012. Integration of autophagy, proteasomal degradation, unfolded protein response and apoptosis. *Exp Oncol,* 34**,** 286-97.

BERENSON, J. R. 2005. Recommendations for Zoledronic Acid Treatment of Patients with Bone Metastases. *The Oncologist,* 10**,** 52-62.

BERNARDS, R. & WEINBERG, R. A. 2002. Metastasis genes: A progression puzzle. *Nature,* 418**,** 823-823.

BEZERRA, M. C., CARVALHO, J. F., PROKOPOWITSCH, A. S. & PEREIRA, R. M. R. 2005. RANK, RANKL and osteoprotegerin in arthritic bone loss. *Brazilian Journal of Medical and Biological Research,* 38**,** 161-170.

BHANDARY, B., MARAHATTA, A., KIM, H.-R. & CHAE, H.-J. 2013. An Involvement of Oxidative Stress in Endoplasmic Reticulum Stress and Its Associated Diseases. *International Journal of Molecular Sciences,* 14**,** 434-456.

BHINGE, K., GUPTA, V., HOSAIN, S., SATYANARAYANAJOIS, S. D., MEYER, S. A., BLAYLOCK, B., ZHANG, Q.-J. & LIU, Y.-Y. 2012. The opposite effects of Doxorubicin on bone marrow stem cells versus breast cancer stem cells depend on glucosylceramide synthase. *The international journal of biochemistry & cell biology,* 44**,** 1770-1778.

BILLECOCQ, A., EMANUEL, J. R., LEVENSON, R. & BARON, R. 1990. 1 alpha,25-dihydroxyvitamin D3 regulates the expression of carbonic anhydrase II in nonerythroid avian bone marrow cells. *Proc Natl Acad Sci U S A,* 87**,** 6470-4.

BIRBEN, E., SAHINER, U. M., SACKESEN, C., ERZURUM, S. & KALAYCI, O. 2012. Oxidative stress and antioxidant defense. *World Allergy Organ J,* 5**,** 9-19.

BIRKENKAMP, K. U., TUYT, L. M. L., LUMMEN, C., WIERENGA, A. T. J., KRUIJER, W. & VELLENGA, E. 2000. The p38 MAP kinase inhibitor SB203580 enhances nuclear factor-kappa B transcriptional activity by a non-specific effect upon the ERK pathway. *British Journal of Pharmacology,* 131**,** 99-107.

BOCK, O. & FELSENBERG, D. 2008. Bisphosphonates in the management of postmenopausal osteoporosis – optimizing efficacy in clinical practice. *Clinical Interventions in Aging,* 3**,** 279-297.

BODY, J.-J., FACON, T., COLEMAN, R. E., LIPTON, A., GEURS, F., FAN, M., HOLLOWAY, D., PETERSON, M. C. & BEKKER, P. J. 2006. A study of the biological receptor activator of nuclear factor-kappaB ligand inhibitor, denosumab, in patients with multiple myeloma or bone metastases from breast cancer. *Clinical Cancer Research,* 12**,** 1221-1228.

BOHONOWYCH, J. E., GOPAL, U. & ISAACS, J. S. 2010. Hsp90 as a Gatekeeper of Tumor Angiogenesis: Clinical Promise and Potential Pitfalls. *Journal of Oncology,* 2010**,** 412985.

BONEWALD, L. F. & JOHNSON, M. L. 2008. Osteocytes, Mechanosensing and Wnt Signaling. *Bone,* 42**,** 606-615.

BORN, E. J., HARTMAN, S. V. & HOLSTEIN, S. A. 2013. Targeting HSP90 and monoclonal protein trafficking modulates the unfolded protein response, chaperone regulation and apoptosis in myeloma cells. *Blood Cancer Journal,* 3**,** e167.

BOSKEY, A. L. & COLEMAN, R. 2010. Aging and Bone. *Journal of Dental Research,* 89**,** 1333-1348.

BOUDESCO, C., RATTIER, T., GARRIDO, C. & JEGO, G. 2015. Do not stress, just differentiate: role of stress proteins in hematopoiesis. *Cell Death Dis,* 6**,** e1628.

BOUILLON, R. & SUDA, T. 2014. Vitamin D: calcium and bone homeostasis during evolution. *BoneKEy Rep,* 3.

BOULON, S., WESTMAN, B. J., HUTTEN, S., BOISVERT, F.-M. & LAMOND, A. I. 2010. The Nucleolus under Stress. *Molecular Cell,* 40**,** 216-227.

BOYCE, B. F. 2003. Bad bones, grey hair, one mutation. *Nat Med,* 9**,** 395-396.

BOYCE, B. F. 2013. Advances in the Regulation of Osteoclasts and Osteoclast Functions. *Journal of Dental Research,* 92**,** 860-867.

BOYCE, B. F. & XING, L. 2007. Biology of RANK, RANKL, and osteoprotegerin. *Arthritis Research & Therapy,* 9**,** S1-S1.

BOYCE, B. F., XING, L., JILKA, R. L., BELLIDO, T., WEINSTEIN, R. S., PARFITT, A. M. & MANOLAGAS, S. C. 2002. Chapter 10 - Apoptosis in Bone Cells. *In:* RODAN, J. P. B. G. R. A. (ed.) *Principles of Bone Biology (Second Edition).* San Diego: Academic Press.

BOYCE, B. F., YAO, Z. & XING, L. 2010. Functions of NF-κB in Bone. *Annals of the New York Academy of Sciences,* 1192**,** 367-375.

BOYCE, B. F. A. X., L. 2002. *Principles of Bone Biology.*

BOYLE, W. J., SIMONET, W. S. & LACEY, D. L. 2003. Osteoclast differentiation and activation. *Nature,* 423**,** 337-42.

BRACCI, L., SCHIAVONI, G., SISTIGU, A. & BELARDELLI, F. 2014. Immune-based mechanisms of cytotoxic chemotherapy: implications for the design of novel and rationale-based combined treatments against cancer. *Cell Death Differ,* 21**,** 15-25.

BRADHAM, C. & MCCLAY, D. R. 2006. p38 MAPK in Development and Cancer. *Cell Cycle,* 5**,** 824-828.

BRADLEY, E. W., RUAN, M. M. & OURSLER, M. J. 2008. PAK1 IS A NOVEL MEK-INDEPENDENT RAF TARGET CONTROLLING EXPRESSION OF THE IAP SURVIVIN IN M-CSF-MEDIATED OSTEOCLAST SURVIVAL. *Journal of cellular physiology,* 217**,** 752-758.

BRANA, M. F., CACHO, M., GRADILLAS, A., DE PASCUAL-TERESA, B. & RAMOS, A. 2001a. Intercalators as anticancer drugs. *Curr Pharm Des,* 7**,** 1745-80.

BRANA, M. F., CACHO, M., GRADILLAS, A., PASCUAL-TERESA, B. & RAMOS, A. 2001b. Intercalators as Anticancer Drugs. *Current Pharmaceutical Design,* 7**,** 1745-1780.

BRANCHO, D., TANAKA, N., JAESCHKE, A., VENTURA, J.-J., KELKAR, N., TANAKA, Y., KYUUMA, M., TAKESHITA, T., FLAVELL, R. A. & DAVIS, R. J. 2003. Mechanism of p38 MAP kinase activation in vivo. *Genes & Development,* 17**,** 1969-1978.

BRANDI, M. L. 2009. Microarchitecture, the key to bone quality. *Rheumatology,* 48**,** iv3-iv8.

BRONISZ, A., SHARMA, S. M., HU, R., GODLEWSKI, J., TZIVION, G., MANSKY, K. C. & OSTROWSKI, M. C. 2006. Microphthalmia-associated Transcription Factor Interactions with 14-3-3 Modulate Differentiation of Committed Myeloid Precursors. *Molecular Biology of the Cell,* 17**,** 3897-3906.

BROUGH, P. A., AHERNE, W., BARRIL, X., BORGOGNONI, J., BOXALL, K., CANSFIELD, J. E., CHEUNG, K.-M. J., COLLINS, I., DAVIES, N. G. M., DRYSDALE, M. J., DYMOCK, B., ECCLES, S. A., FINCH, H., FINK, A., HAYES, A., HOWES, R., HUBBARD, R. E., JAMES, K., JORDAN, A. M., LOCKIE, A., MARTINS, V., MASSEY, A., MATTHEWS, T. P., MCDONALD, E., NORTHFIELD, C. J., PEARL, L. H., PRODROMOU, C., RAY, S., RAYNAUD, F. I., ROUGHLEY, S. D., SHARP, S. Y., SURGENOR, A., WALMSLEY, D. L., WEBB, P., WOOD, M., WORKMAN, P. & WRIGHT, L. 2007. 4,5-Diarylisoxazole Hsp90 Chaperone Inhibitors: Potential Therapeutic Agents for the Treatment of Cancer. *Journal of Medicinal Chemistry,* 51**,** 196-218.

BUCCI, C., THOMSEN, P., NICOZIANI, P., MCCARTHY, J. & VAN DEURS, B. 2000. Rab7: A Key to Lysosome Biogenesis. *Molecular Biology of the Cell,* 11**,** 467-480.

BUCHAN, J. R., YOON, J.-H. & PARKER, R. 2011. Stress-specific composition, assembly and kinetics of stress granules in Saccharomyces cerevisiae. *Journal of Cell Science,* 124**,** 228-239.

BURGER, A. M., FIEBIG, H. H., STINSON, S. F. & SAUSVILLE, E. A. 2004. 17-(Allylamino)-17-demethoxygeldanamycin activity in human melanoma models. *Anticancer Drugs,* 15**,** 377-87.

BUSA, R., GEREMIA, R. & SETTE, C. 2010. Genotoxic stress causes the accumulation of the splicing regulator Sam68 in nuclear foci of transcriptionally active chromatin. *Nucleic Acids Res,* 38**,** 3005-18.

CALDERWOOD, S. K. 2010. Heat shock proteins in breast cancer progression--a suitable case for treatment? *Int J Hyperthermia,* 26**,** 681-5.

CALDERWOOD, S. K. 2013. Molecular Cochaperones: Tumor Growth and Cancer Treatment. *Scientifica,* 2013**,** 13.

CALDERWOOD, S. K., KHALEQUE, M. A., SAWYER, D. B. & CIOCCA, D. R. 2006. Heat shock proteins in cancer: chaperones of tumorigenesis. *Trends in Biochemical Sciences,* 31**,** 164-172.

CAPPELLEN, D., LUONG-NGUYEN, N.-H., BONGIOVANNI, S., GRENET, O., WANKE, C. & ŠUŠA, M. 2002. Transcriptional Program of Mouse Osteoclast Differentiation Governed by the Macrophage Colony-stimulating Factor and the Ligand for the Receptor Activator of NFκB. *Journal of Biological Chemistry,* 277**,** 21971-21982.

CARAS, I. W. & MARTIN, D. W. 1988. Molecular cloning of the cDNA for a mutant mouse ribonucleotide reductase M1 that produces a dominant mutator phenotype in mammalian cells. *Molecular and Cellular Biology,* 8**,** 2698-2704.

CARGNELLO, M. & ROUX, P. P. 2011. Activation and Function of the MAPKs and Their Substrates, the MAPK-Activated Protein Kinases. *Microbiology and Molecular Biology Reviews : MMBR,* 75**,** 50-83.

CASIMIRO, S., GUISE, T. A. & CHIRGWIN, J. 2009. The critical role of the bone microenvironment in cancer metastases. *Molecular and Cellular Endocrinology,* 310**,** 71-81.

CASIMIRO, S., MOHAMMAD, K. S., PIRES, R., TATO-COSTA, J., ALHO, I., TEIXEIRA, R., CARVALHO, A., RIBEIRO, S., LIPTON, A., GUISE, T. A. & COSTA, L. 2013. RANKL/RANK/MMP-1 Molecular Triad Contributes to the Metastatic Phenotype of Breast and Prostate Cancer Cells <italic>In Vitro</italic>. *PLoS ONE,* 8**,** e63153.

CASTIEL, A., DANIELI, M. M., DAVID, A., MOSHKOVITZ, S., APLAN, P. D., KIRSCH, I. R., BRANDEIS, M., KRÄMER, A. & IZRAELI, S. 2011. The Stil protein regulates centrosome integrity and mitosis through suppression of Chfr. *Journal of Cell Science,* 124**,** 532-539.

CENTER FOR COMPUTATIONAL BIOLOGY, J. H. U. *Center for Computational Biology, Software* [Online]. Johns Hopkins University,. Available: https://ccb.jhu.edu/software.shtml 2015].

CEPEDA, V., FUERTES, M. A., CASTILLA, J., ALONSO, C., QUEVEDO, C. & PEREZ, J. M. 2007. Biochemical mechanisms of cisplatin cytotoxicity. *Anticancer Agents Med Chem,* 7**,** 3-18.

CERVANTES-GOMEZ, F., NIMMANAPALLI, R. & GANDHI, V. 2009. Transcription Inhibition of Heat Shock Proteins: A Strategy for Combination of 17-allylamino-17-demethoxygeldanamycin and Actinomycin D. *Cancer research,* 69**,** 3947-3954.

CHAI, R. C., KOUSPOU, M. M., LANG, B. J., NGUYEN, C. H., VAN DER KRAAN, A. G. J., VIEUSSEUX, J. L., LIM, R. C., GILLESPIE, M. T., BENJAMIN, I. J., QUINN, J. M. W. & PRICE, J. T. 2014. Molecular Stress Inducing Compounds Increase Osteoclast Formation in a Heat Shock Factor 1 Dependent Manner. *Journal of Biological Chemistry*.

CHAMBERS, T. J. 2000. Regulation of the differentiation and function of osteoclasts. *The Journal of Pathology,* 192**,** 4-13.

CHAMBERS, T. J., REVELL, P. A., FULLER, K. & ATHANASOU, N. A. 1984. Resorption of bone by isolated rabbit osteoclasts. *Journal of Cell Science,* 66**,** 383-399.

CHANG, L. & KARIN, M. 2001. Mammalian MAP kinase signalling cascades. *Nature,* 410**,** 37-40.

CHAUDHARI, N., TALWAR, P., PARIMISETTY, A., LEFEBVRE D'HELLENCOURT, C. & RAVANAN, P. 2014. A Molecular Web: Endoplasmic Reticulum Stress, Inflammation and Oxidative Stress. *Frontiers in Cellular Neuroscience,* 8.

CHELI, Y., OHANNA, M., BALLOTTI, R. & BERTOLOTTO, C. 2010. Fifteen-year quest for microphthalmia-associated transcription factor target genes. *Pigment Cell & Melanoma Research,* 23**,** 27-40.

CHEN, C., ZHOU, J. & JI, C. 2010a. Quercetin: A potential drug to reverse multidrug resistance. *Life Sciences,* 87**,** 333-338.

CHEN, D. & DOU, Q. P. 2010. The ubiquitin-proteasome system as a prospective molecular target for cancer treatment and prevention. *Curr Protein Pept Sci,* 11**,** 459-70.

CHEN, D., FREZZA, M., SCHMITT, S., KANWAR, J. & DOU, Q. P. 2011. Bortezomib as the first proteasome inhibitor anticancer drug: current status and future perspectives. *Curr Cancer Drug Targets,* 11**,** 239-53.

CHEN, Q., JONES, T. W., BROWN, P. C. & STEVENS, J. L. 1990. The mechanism of cysteine conjugate cytotoxicity in renal epithelial cells. Covalent binding leads to thiol depletion and lipid peroxidation. *Journal of Biological Chemistry,* 265**,** 21603-11.

CHEN, Q. & STEVENS, J. L. 1991. Inhibition of iodoacetamide and t-butylhydroperoxide toxicity in LLC-PK1 cells by antioxidants: a role for lipid peroxidation in alkylation induced cytotoxicity. *Arch Biochem Biophys,* 284**,** 422-30.

CHEN, Y.-C., SOSNOSKI, D. & MASTRO, A. 2010b. Breast cancer metastasis to the bone: mechanisms of bone loss. *Breast Cancer Research,* 12**,** 215.

CHEN, Y., CHEN, J., LOO, A., JAEGER, S., BAGDASARIAN, L., YU, J., CHUNG, F., KORN, J., RUDDY, D., GUO, R., MCLAUGHLIN, M. E., FENG, F., ZHU, P., STEGMEIER, F., PAGLIARINI, R., PORTER, D. & ZHOU, W. 2013. Targeting HSF1 sensitizes cancer cells to HSP90 inhibition. *Oncotarget,* 4**,** 816-829.

CHENG, Q., CHANG, J. T., GERADTS, J., NECKERS, L. M., HAYSTEAD, T., SPECTOR, N. L. & LYERLY, H. K. 2012. Amplification and high-level expression of heat shock protein 90 marks aggressive phenotypes of human epidermal growth factor receptor 2 negative breast cancer. *Breast Cancer Research : BCR,* 14**,** R62-R62.

CHEUNG, K.-M. J., MATTHEWS, T. P., JAMES, K., ROWLANDS, M. G., BOXALL, K. J., SHARP, S. Y., MALONEY, A., ROE, S. M., PRODROMOU, C., PEARL, L. H., AHERNE, G. W., MCDONALD, E. & WORKMAN, P. 2005. The identification, synthesis, protein crystal structure and in vitro biochemical evaluation of a new 3,4-diarylpyrazole class of Hsp90 inhibitors. *Bioorganic & Medicinal Chemistry Letters,* 15**,** 3338-3343.

CHIOSIS, G. 2006a. Discovery and development of purine-scaffold Hsp90 inhibitors. *Curr Top Med Chem,* 6**,** 1183-91.

CHIOSIS, G. 2006b. Targeting chaperones in transformed systems – a focus on Hsp90 and cancer. *Expert Opinion on Therapeutic Targets,* 10**,** 37-50.

CHRISTMANN, M. & KAINA, B. 2013. Transcriptional regulation of human DNA repair genes following genotoxic stress: trigger mechanisms, inducible responses and genotoxic adaptation. *Nucleic Acids Res,* 41**,** 8403-20.

CICCIA, A. & ELLEDGE, S. J. 2010. The DNA Damage Response: Making It Safe to Play with Knives. *Molecular Cell,* 40**,** 179-204.

CIOCCA, D. R. & CALDERWOOD, S. K. 2005. Heat shock proteins in cancer: diagnostic, prognostic, predictive, and treatment implications. *Cell Stress & Chaperones,* 10**,** 86-103.

CLARKE, B. 2008. Normal Bone Anatomy and Physiology. *Clinical Journal of the American Society of Nephrology,* 3**,** S131-S139.

CLARKSON, S. G. & WOOD, R. D. 2005. Polymorphisms in the human XPD (ERCC2) gene, DNA repair capacity and cancer susceptibility: An appraisal. *DNA Repair,* 4**,** 1068-1074.

CLOVER, J., DODDS, R. A. & GOWEN, M. 1992. Integrin subunit expression by human osteoblasts and osteoclasts in situ and in culture. *Journal of Cell Science,* 103**,** 267-271.

COLEMAN, R. E. 2006. Clinical Features of Metastatic Bone Disease and Risk of Skeletal Morbidity. *Clinical Cancer Research,* 12**,** 6243s-6249s.

COLLIN-OSDOBY, P. 2004. Regulation of Vascular Calcification by Osteoclast Regulatory Factors RANKL and Osteoprotegerin. *Circulation Research,* 95**,** 1046-1057.

COLLIN-OSDOBY, P. & OSDOBY, P. 2012. RANKL-Mediated Osteoclast Formation from Murine RAW 264.7 cells. *In:* HELFRICH, M. H. & RALSTON, S. H. (eds.) *Bone Research Protocols.* Humana Press.

COLLIN-OSDOBY, P., YU, X., ZHENG, H. & OSDOBY, P. 2003. RANKL-mediated osteoclast formation from murine RAW 264.7 cells. *Methods in molecular medicine,* 80**,** 153-166.

CONTI, M. 2007. Chemistry and Pharmacology of Anticancer Drugs. By David E. Thurston. *ChemMedChem,* 2**,** 1370-1370.

CRAIG, E. A. & SCHLESINGER, M. J. 1985. The Heat Shock Respons. *Critical Reviews in Biochemistry and Molecular Biology,* 18**,** 239-280.

CRASTO, G. J., KARTNER, N., YAO, Y., LI, K., BULLOCK, L., DATTI, A. & MANOLSON, M. F. 2013. Luteolin inhibition of V-ATPase a3–d2 interaction decreases osteoclast resorptive activity. *Journal of Cellular Biochemistry,* 114**,** 929-941.

CROCKETT, J. C., ROGERS, M. J., COXON, F. P., HOCKING, L. J. & HELFRICH, M. H. 2011. Bone remodelling at a glance. *Journal of Cell Science,* 124**,** 991-998.

CRONSTEIN, B. N. 2005. Low-Dose Methotrexate: A Mainstay in the Treatment of Rheumatoid Arthritis. *Pharmacological Reviews,* 57**,** 163-172.

CROTTI, T. N., DHARMAPATNI, A. A., ALIAS, E., ZANNETTINO, A. C. W., SMITH, M. D. & HAYNES, D. R. 2012. The immunoreceptor tyrosine-based activation motif (ITAM) -related factors are increased in synovial tissue and vasculature of rheumatoid arthritic joints. *Arthritis Research & Therapy,* 14**,** R245-R245.

CROTTI, T. N., SHARMA, S. M., FLEMING, J. D., FLANNERY, M. R., OSTROWSKI, M. C., GOLDRING, S. R. & MCHUGH, K. P. 2008. PU.1 and NFATc1 mediate osteoclastic induction of the mouse β3 integrin promoter. *Journal of Cellular Physiology,* 215**,** 636-644.

CUENDA, A. & ROUSSEAU, S. 2007. p38 MAP-Kinases pathway regulation, function and role in human diseases. *Biochimica et Biophysica Acta (BBA) - Molecular Cell Research,* 1773**,** 1358-1375.

CUETARA, B. L. V., CROTTI, T. N., O'DONOGHUE, A. J. & MCHUGH, K. P. 2006. CLONING AND CHARACTERIZATION OF OSTEOCLAST PRECURSORS FROM THE RAW264.7 CELL LINE. *In Vitro Cellular & Developmental Biology,* 42**,** 182-8.

CURCIO-MORELLI, C., ZAVACKI, A. M., CHRISTOFOLLETE, M., GEREBEN, B., DE FREITAS, B. C. G., HARNEY, J. W., LI, Z., WU, G. & BIANCO, A. C. 2003. Deubiquitination of type 2 iodothyronine deiodinase by von Hippel–Lindau protein–interacting deubiquitinating enzymes regulates thyroid hormone activation. *Journal of Clinical Investigation,* 112**,** 189-196.

CZUPALLA, C., MANSUKOSKI, H., RIEDL, T., THIEL, D., KRAUSE, E. & HOFLACK, B. 2006. Proteomic analysis of lysosomal acid hydrolases secreted by osteoclasts: implications for lytic enzyme transport and bone metabolism. *Mol Cell Proteomics,* 5**,** 134-43.

D'ANTONIO, C., PASSARO, A., GORI, B., DEL SIGNORE, E., MIGLIORINO, M. R., RICCIARDI, S., FULVI, A. & DE MARINIS, F. 2014. Bone and brain metastasis in lung cancer: recent advances in therapeutic strategies. *Ther Adv Med Oncol,* 6**,** 101-14.

D'ANGIOLELLA, V., DONATO, V., VIJAYAKUMAR, S., SARAF, A., FLORENS, L., WASHBURN, M. P., DYNLACHT, B. & PAGANO, M. 2010. SCF(Cyclin F) controls centrosome homeostasis and mitotic fidelity via CP110 degradation. *Nature,* 466**,** 138-142.

DACI, E., UDAGAWA, N., MARTIN, T. J., BOUILLON, R. & CARMELIET, G. 1999. The Role of the Plasminogen System in Bone Resorption In Vitro. *Journal of Bone and Mineral Research,* 14**,** 946-952.

DAI, C., WHITESELL, L., ROGERS, A. B. & LINDQUIST, S. 2007. Heat Shock Factor 1 Is a Powerful Multifaceted Modifier of Carcinogenesis. *Cell,* 130**,** 1005-1018.

DAI, S., TANG, Z., CAO, J., ZHOU, W., LI, H., SAMPSON, S. & DAI, C. 2014. Suppression of the HSF1-mediated proteotoxic stress response by the metabolic stress sensor AMPK. *The EMBO Journal***,** n/a-n/a.

DALLAS, S. L., PRIDEAUX, M. & BONEWALD, L. F. 2013. The Osteocyte: An Endocrine Cell and More. *Endocrine reviews*.

DALLAS, S. L., ROSSER, J. L., MUNDY, G. R. & BONEWALD, L. F. 2002. Proteolysis of Latent Transforming Growth Factor-β (TGF-β)-binding Protein-1 by Osteoclasts: A CELLULAR MECHANISM FOR RELEASE OF TGF-β FROM BONE MATRIX. *Journal of Biological Chemistry,* 277**,** 21352-21360.

DARLING, J. M., GOLDRING, S. R., HARADA, Y., HANDEL, M. L., GLOWACKI, J. & GRAVALLESE, E. M. 1997. Multinucleated cells in pigmented villonodular synovitis and giant cell tumor of tendon sheath express features of osteoclasts. *The American Journal of Pathology,* 150**,** 1383-1393.

DATTA, R., IMAMURA, K., GOLDMAN, S. J., DIANOUX, A. C., KUFE, D. W. & SHERMAN, M. L. 1992. Functional expression of the macrophage colony-stimulating factor receptor in human THP-1 monocytic leukemia cells. *Blood,* 79**,** 904-12.

DAVENPORT, E. L., MOORE, H. E., DUNLOP, A. S., SHARP, S. Y., WORKMAN, P., MORGAN, G. J. & DAVIES, F. E. 2007. *Heat shock protein inhibition is associated with activation of the unfolded protein response pathway in myeloma plasma cells*.

DAVID, W., STEVEN, P. G. & WILLIAM, D. J. 1999. Heat shock proteins: A review of the molecular chaperones. *Journal of vascular surgery : official publication, the Society for Vascular Surgery [and] International Society for Cardiovascular Surgery, North American Chapter,* 29**,** 748-751.

DE BILLY, E., POWERS, M. V., SMITH, J. R. & WORKMAN, P. 2009. Drugging the heat shock factor 1 pathway: Exploitation of the critical cancer cell dependence on the guardian of the proteome. *Cell Cycle,* 8**,** 3806-3808.

DEL FATTORE, A., CAPPARIELLO, A. & TETI, A. 2008. Genetics, pathogenesis and complications of osteopetrosis. *Bone,* 42**,** 19-29.

DELAISSÉ, J.-M., ANDERSEN, T. L., ENGSIG, M. T., HENRIKSEN, K., TROEN, T. & BLAVIER, L. 2003. Matrix metalloproteinases (MMP) and cathepsin K contribute differently to osteoclastic activities. *Microscopy Research and Technique,* 61**,** 504-513.

DEN, R. B. & LU, B. 2012. Heat shock protein 90 inhibition: rationale and clinical potential. *Therapeutic Advances in Medical Oncology,* 4**,** 211-218.

DESAI, S., LIU, Z., YAO, J., PATEL, N., CHEN, J., WU, Y., AHN, E. E.-Y., FODSTAD, O. & TAN, M. 2013. Heat Shock Factor 1 (HSF1) Controls Chemoresistance and Autophagy through Transcriptional Regulation of Autophagy-related Protein 7 (ATG7). *The Journal of Biological Chemistry,* 288**,** 9165-9176.

DILLER, K. R. 2006. STRESS PROTEIN EXPRESSION KINETICS. *Annual Review of Biomedical Engineering,* 8**,** 403-424.

DONATI, Y. R., SLOSMAN, D. O. & POLLA, B. S. 1990. Oxidative injury and the heat shock response. *Biochem Pharmacol,* 40**,** 2571-7.

DONNELLY, A. & BLAGG, B. 2008. Novobiocin and Additional Inhibitors of the Hsp90 C-Terminal Nucleotide- binding Pocket. *Current Medicinal Chemistry,* 15**,** 2702-2717.

DOUBROVIN, M., CHE, J. T., SERGANOVA, I., MOROZ, E., SOLIT, D. B., AGEYEVA, L., KOCHETKOVA, T., PILLARSETTI, N., FINN, R., ROSEN, N. & BLASBERG, R. G. 2012. Monitoring the induction of heat shock factor 1/heat shock protein 70 expression following 17-allylamino-demethoxygeldanamycin treatment by positron emission tomography and optical reporter gene imaging. *Mol Imaging,* 11**,** 67-76.

DOUGALL, W. C. 2010. Mechanistic Role of RANKL in Cancer-induced Bone Diseases and Development of a Targeted Therapy to Inhibit this Pathway. *In:* DOMINIQUE, H. (ed.) *Bone Cancer.* San Diego: Academic Press.

DOUGALL, W. C., GLACCUM, M., CHARRIER, K., ROHRBACH, K., BRASEL, K., DE SMEDT, T., DARO, E., SMITH, J., TOMETSKO, M. E., MALISZEWSKI, C. R., ARMSTRONG, A., SHEN, V., BAIN, S., COSMAN, D., ANDERSON, D., MORRISSEY, P. J., PESCHON, J. J. & SCHUH, J. 1999. RANK is essential for osteoclast and lymph node development. *Genes & Development,* 13**,** 2412-2424.

DOUGALL, W. C., HOLEN, I. & GONZALEZ SUAREZ, E. 2014. Targeting RANKL in metastasis. *BoneKEy Rep,* 3.

DOWNEY, P. & SIEGEL, M. 2006. Bone Biology and the Clinical Implications for Osteoporosis. *Physical Therapy,* 86**,** 77-91.

DOYLE, K. M., KENNEDY, D., GORMAN, A. M., GUPTA, S., HEALY, S. J. M. & SAMALI, A. 2011. Unfolded proteins and endoplasmic reticulum stress in neurodegenerative disorders. *Journal of Cellular and Molecular Medicine,* 15**,** 2025-2039.

DRABER, P., VONKOVA, I., STEPANEK, O., HRDINKA, M., KUCOVA, M., SKOPCOVA, T., OTAHAL, P., ANGELISOVA, P., HOREJSI, V., YEUNG, M., WEISS, A. & BRDICKA, T. 2011. SCIMP, a Transmembrane Adaptor Protein Involved in Major Histocompatibility Complex Class II Signaling. *Molecular and Cellular Biology,* 31**,** 4550-4562.

DRAKE, M. T., CLARKE, B. L. & KHOSLA, S. 2008. Bisphosphonates: Mechanism of Action and Role in Clinical Practice. *Mayo Clinic proceedings. Mayo Clinic,* 83**,** 1032-1045.

DRYSDALE, M., BROUGH, P., MASSEY, A., JENSEN, M. & SCHOEPFER, J. 2006. Targeting Hsp90 for the treatment of cancer. *Curr Opin Drug Discov Devel,* 9**,** 483 - 495.

DRYSDALE, M. J. & BROUGH, P. A. 2008. Medicinal Chemistry of Hsp90 Inhibitors. *Current Topics in Medicinal Chemistry,* 8**,** 859-868.

DU, Z.-X., ZHANG, H.-Y., MENG, X., GAO, Y.-Y., ZOU, R.-L., LIU, B.-Q., GUAN, Y. & WANG, H.-Q. 2009. Proteasome inhibitor MG132 induces BAG3 expression through activation of heat shock factor 1. *Journal of Cellular Physiology,* 218**,** 631-637.

DUBOIS, E. A., RISSMANN, R. & COHEN, A. F. 2011. Denosumab. *British Journal of Clinical Pharmacology,* 71**,** 804-806.

ECCLES, S. A., MASSEY, A., RAYNAUD, F. I., SHARP, S. Y., BOX, G., VALENTI, M., PATTERSON, L., DE HAVEN BRANDON, A., GOWAN, S., BOXALL, F., AHERNE, W., ROWLANDS, M., HAYES, A., MARTINS, V., URBAN, F., BOXALL, K., PRODROMOU, C., PEARL, L., JAMES, K., MATTHEWS, T. P., CHEUNG, K.-M., KALUSA, A., JONES, K., MCDONALD, E., BARRIL, X., BROUGH, P. A., CANSFIELD, J. E., DYMOCK, B., DRYSDALE, M. J., FINCH, H., HOWES, R., HUBBARD, R. E., SURGENOR, A., WEBB, P., WOOD, M., WRIGHT, L. & WORKMAN, P. 2008. NVP-AUY922: A Novel Heat Shock Protein 90 Inhibitor Active against Xenograft Tumor Growth, Angiogenesis, and Metastasis. *Cancer Research,* 68**,** 2850-2860.

EDWARDS, J. R. & WEIVODA, M. M. 2012. Osteoclasts: malefactors of disease and targets for treatment. *Discov Med,* 13**,** 201-10.

EGORIN, M. J., ROSEN, D. M., WOLFF, J. H., CALLERY, P. S., MUSSER, S. M. & EISEMAN, J. L. 1998. Metabolism of 17-(allylamino)-17-demethoxygeldanamycin (NSC 330507) by murine and human hepatic preparations. *Cancer Res,* 58**,** 2385-96.

EGORIN, M. J., ZUHOWSKI, E. G., ROSEN, D. M., SENTZ, D. L., COVEY, J. M. & EISEMAN, J. L. 2001. Plasma pharmacokinetics and tissue distribution of 17-(allylamino)-17-demethoxygeldanamycin (NSC 330507) in CD2F1 mice1. *Cancer Chemother Pharmacol,* 47**,** 291-302.

EHRHART, N., EURELL, J. A. C., TOMMASINI, M., CONSTABLE, P. D., JOHNSON, A. L. & FERETTI, A. 2002. Effect of cisplatin on bone transport osteogenesis in dogs. *American Journal of Veterinary Research,* 63**,** 703-711.

ENGDAHL, C., LINDHOLM, C., STUBELIUS, A., OHLSSON, C., CARLSTEN, H. & LAGERQUIST, M. K. 2013. Periarticular Bone Loss in Antigen-Induced Arthritis. *Arthritis & Rheumatism,* 65**,** 2857-2865.

ERDELYI, I., LEVENKOVA, N., LIN, E. Y., PINTO, J. T., LIPKIN, M., QUIMBY, F. W. & HOLT, P. R. 2009. Western-Style Diets Induce Oxidative Stress and Dysregulate Immune Responses in the Colon in a Mouse Model of Sporadic Colon Cancer. *The Journal of Nutrition,* 139**,** 2072-2078.

ERIKSSON, M. 2005. *AP-1 TRANSCRIPTION FACTOR IN CELL DIFFERENTIATION AND SURVIVAL.* University of Helsinki, Finland.

EVANS, H. J., EDWARDS, L. & GOODWIN, R. L. 2007. Conserved C-Terminal domains of mCenp-F (LEK1) regulate subcellular localization and mitotic checkpoint delay. *Experimental cell research,* 313**,** 2427-2437.

EVERTS, V., DACI, E., TIGCHELAAR-GUTTER, W., HOEBEN, K. A., TORREKENS, S., CARMELIET, G. & BEERTSEN, W. 2008. Plasminogen activators are involved in the degradation of bone by osteoclasts. *Bone,* 43**,** 915-920.

EWER, M. S. & LIPPMAN, S. M. 2005. Type II Chemotherapy-Related Cardiac Dysfunction: Time to Recognize a New Entity. *Journal of Clinical Oncology,* 23**,** 2900-2902.

FABBRO, M., ZHOU, B.-B., TAKAHASHI, M., SARCEVIC, B., LAL, P., GRAHAM, M. E., GABRIELLI, B. G., ROBINSON, P. J., NIGG, E. A., ONO, Y. & KHANNA, K. K. Cdk1/Erk2- and Plk1-Dependent Phosphorylation of a Centrosome Protein, Cep55, Is Required for Its Recruitment to Midbody and Cytokinesis. *Developmental Cell,* 9**,** 477-488.

FAN, C.-M., FOSTER, B. K., HUI, S. K. & XIAN, C. J. 2012. Prevention of Bone Growth Defects, Increased Bone Resorption and Marrow Adiposity with Folinic Acid in Rats Receiving Long-Term Methotrexate. *PLoS ONE,* 7**,** e46915.

FAN, C., FOSTER, B. K., WALLACE, W. H. & XIAN, C. J. 2011. Pathobiology and prevention of cancer chemotherapy-induced bone growth arrest, bone loss, and osteonecrosis. *Curr Mol Med,* 11**,** 140-51.

FELIX, R., CECCHINI, M. G. & FLEISCH, H. 1990. Macrophage colony stimulating factor restores in vivo bone resorption in the op/op osteopetrotic mouse. *Endocrinology,* 127**,** 2592-4.

FENG, H., CHENG, T., STEER, J. H., JOYCE, D. A., PAVLOS, N. J., LEONG, C., KULAR, J., LIU, J., FENG, X., ZHENG, M. H. & XU, J. 2009. Myocyte Enhancer Factor 2 and Microphthalmia-associated Transcription Factor Cooperate with NFATc1 to Transactivate the V-ATPase d2 Promoter during RANKL-induced Osteoclastogenesis. *Journal of Biological Chemistry,* 284**,** 14667-14676.

FENG, X. 2005. RANKing intracellular signaling in osteoclasts. *IUBMB Life,* 57**,** 389-95.

FENG, X. & MCDONALD, J. M. 2011. Disorders of Bone Remodeling. *Annual review of pathology,* 6**,** 121-145.

FENG, Z., ZENG, S., WANG, Y., ZHENG, Z. & CHEN, Z. 2013. Bisphosphonates for the Prevention and Treatment of Osteoporosis in Patients with Rheumatic Diseases: A Systematic Review and Meta-Analysis. *PLoS ONE,* 8**,** e80890.

FILVAROFF, E., ERLEBACHER, A., YE, J., GITELMAN, S. E., LOTZ, J., HEILLMAN, M. & DERYNCK, R. 1999. Inhibition of TGF-beta receptor signaling in osteoblasts leads to decreased bone remodeling and increased trabecular bone mass. *Development,* 126**,** 4267-79.

FLACH, J., BAKKER, S. T., MOHRIN, M., CONROY, P. C., PIETRAS, E. M., REYNAUD, D., ALVAREZ, S., DIOLAITI, M. E., UGARTE, F., FORSBERG, E. C., LE BEAU, M. M., STOHR, B. A., MENDEZ, J., MORRISON, C. G. & PASSEGUE, E. 2014. Replication stress is a potent driver of functional decline in ageing haematopoietic stem cells. *Nature,* 512**,** 198-202.

FOX, S. W., EVANS, K. E. & LOVIBOND, A. C. 2008. Transforming growth factor-β enables NFATc1 expression during osteoclastogenesis. *Biochemical and Biophysical Research Communications,* 366**,** 123-128.

FRANZ-ODENDAAL, T. A., HALL, B. K. & WITTEN, P. E. 2006. Buried alive: How osteoblasts become osteocytes. *Developmental Dynamics,* 235**,** 176-190.

FRANZOSO, G., CARLSON, L., XING, L., POLJAK, L., SHORES, E. W., BROWN, K. D., LEONARDI, A., TRAN, T., BOYCE, B. F. & SIEBENLIST, U. 1997. Requirement for NF-κB in osteoclast and B-cell development. *Genes & Development,* 11**,** 3482-3496.

FREEMAN, M. L., BORRELLI, M. J., SYED, K., SENISTERRA, G., STAFFORD, D. M. & LEPOCK, J. R. 1995. Characterization of a signal generated by oxidation of protein thiols that activates the heat shock transcription factor. *Journal of Cellular Physiology,* 164**,** 356-366.

FRIEDLAENDER, G. E., TROSS, R. B., DOGANIS, A. C., KIRKWOOD, J. M. & BARON, R. 1984. Effects of chemotherapeutic agents on bone. I. Short-term methotrexate and doxorubicin (adriamycin) treatment in a rat model. *The Journal of Bone & Joint Surgery,* 66**,** 602-607.

FUCIKOVA, J., KRALIKOVA, P., FIALOVA, A., BRTNICKY, T., ROB, L., BARTUNKOVA, J. & ŠPÍŠEK, R. 2011. Human Tumor Cells Killed by Anthracyclines Induce a Tumor-Specific Immune Response. *Cancer Research,* 71**,** 4821-4833.

FUKUYO, Y., HUNT, C. R. & HORIKOSHI, N. 2010. Geldanamycin and its anti-cancer activities. *Cancer Letters,* 290**,** 24-35.

FULDA, S., GORMAN, A. M., HORI, O. & SAMALI, A. 2010. Cellular Stress Responses: Cell Survival and Cell Death. *International Journal of Cell Biology,* 2010.

FULLER, K., MURPHY, C., KIRSTEIN, B., FOX, S. W. & CHAMBERS, T. J. 2002. TNFα Potently Activates Osteoclasts, through a Direct Action Independent of and Strongly Synergistic with RANKL. *Endocrinology,* 143**,** 1108-1118.

FURLAN, F., GALBIATI, C., JORGENSEN, N. R., JENSEN, J.-E. B., MRAK, E., RUBINACCI, A., TALOTTA, F., VERDE, P. & BLASI, F. 2007. Urokinase Plasminogen Activator Receptor Affects Bone Homeostasis by Regulating Osteoblast and Osteoclast Function. *Journal of Bone and Mineral Research,* 22**,** 1387-1396.

FUTOSI, K., FODOR, S. & MÓCSAI, A. 2013. Neutrophil cell surface receptors and their intracellular signal transduction pathways(). *International Immunopharmacology,* 17**,** 638-650.

GABAI, V. L. & SHERMAN, M. Y. 2002. Molecular Biology of Thermoregulation: Invited Review: Interplay between molecular chaperones and signaling pathways in survival of heat shock. *J Appl Physiol,* 92**,** 1743-1748.

GABRIEL, T. L., TOL, M. J., OTTENHOF, R., VAN ROOMEN, C., ATEN, J., CLAESSEN, N., HOOIBRINK, B., DE WEIJER, B., SERLIE, M. J., ARGMANN, C., VAN ELSENBURG, L., AERTS, J. M. F. G. & VAN EIJK, M. 2014. Lysosomal Stress in Obese Adipose Tissue Macrophages Contributes to MITF-Dependent Gpnmb Induction. *Diabetes,* 63**,** 3310-3323.

GANDHAPUDI, S. K., MURAPA, P., THRELKELD, Z. D., WARD, M., SARGE, K. D., SNOW, C. & WOODWARD, J. G. 2013. Heat Shock Transcription Factor 1 Is Activated as a Consequence of Lymphocyte Activation and Regulates a Major Proteostasis Network in T Cells Critical for Cell Division During Stress. *The Journal of Immunology,* 191**,** 4068-4079.

GAO, Y., GRASSI, F., RYAN, M. R., TERAUCHI, M., PAGE, K., YANG, X., WEITZMANN, M. N. & PACIFICI, R. 2007. IFN-γ stimulates osteoclast formation and bone loss in vivo via antigen-driven T cell activation. *The Journal of Clinical Investigation,* 117**,** 122-132.

GARRINGTON, T. P. & JOHNSON, G. L. 1999. Organization and regulation of mitogen-activated protein kinase signaling pathways. *Curr Opin Cell Biol,* 11**,** 211-8.

GASPAR, N., SHARP, S. Y., ECCLES, S. A., GOWAN, S., POPOV, S., JONES, C., PEARSON, A., VASSAL, G. & WORKMAN, P. 2010. Mechanistic Evaluation of the Novel HSP90 Inhibitor NVP-AUY922 in Adult and Pediatric Glioblastoma. *Molecular Cancer Therapeutics,* 9**,** 1219-1233.

GE, B., GRAM, H., DI PADOVA, F., HUANG, B., NEW, L., ULEVITCH, R. J., LUO, Y. & HAN, J. 2002. MAPKK-independent activation of p38alpha mediated by TAB1-dependent autophosphorylation of p38alpha. *Science,* 295**,** 1291-4.

GE, J., NORMANT, E., PORTER, J. R., ALI, J. A., DEMBSKI, M. S., GAO, Y., GEORGES, A. T., GRENIER, L., PAK, R. H., PATTERSON, J., SYDOR, J. R., TIBBITTS, T. T., TONG, J. K., ADAMS, J. & PALOMBELLA, V. J. 2006. Design, synthesis, and biological evaluation of hydroquinone derivatives of 17-amino-17-demethoxygeldanamycin as potent, water-soluble inhibitors of Hsp90. *J Med Chem,* 49**,** 4606-15.

GENIN, E., REBOUD-RAVAUX, M. & VIDAL, J. 2010. Proteasome inhibitors: recent advances and new perspectives in medicinal chemistry. *Current Topics in Medicinal Chemistry,* 10**,** 232-256.

GEORGE, E. M. & BROWN, D. T. 2010. Prothymosin α is a component of a linker histone chaperone. *FEBS letters,* 584**,** 2833-2836.

GEORGE, P., BALI, P., ANNAVARAPU, S., SCUTO, A., FISKUS, W., GUO, F., SIGUA, C., SONDARVA, G., MOSCINSKI, L., ATADJA, P. & BHALLA, K. 2005. *Combination of the histone deacetylase inhibitor LBH589 and the hsp90 inhibitor 17-AAG is highly active against human CML-BC cells and AML cells with activating mutation of FLT-3.*

GHOSAL, G. & CHEN, J. 2013. DNA damage tolerance: a double-edged sword guarding the genome. *Translational Cancer Research,* 2**,** 107-129.

GIEBEL, L. B., DWORNICZAK, B. P. & BAUTZ, E. K. F. 1988. Developmental regulation of a constitutively expressed mouse mRNA encoding a 72-kDa heat shock-like protein. *Developmental Biology,* 125**,** 200-207.

GILBERT, S. F. 2000. *Osteogenesis: The Development of Bones,* MA, Sunderland (MA): Sinauer Associates; 2000.

GOETZ, M. P., TOFT, D., REID, J., AMES, M., STENSGARD, B., SAFGREN, S., ADJEI, A. A., SLOAN, J., ATHERTON, P., VASILE, V., SALAZAAR, S., ADJEI, A., CROGHAN, G. & ERLICHMAN, C. 2005. Phase I trial of 17-allylamino-17-demethoxygeldanamycin in patients with advanced cancer. *J Clin Oncol,* 23**,** 1078-87.

GOETZ, M. P., TOFT, D. O., AMES, M. M. & ERLICHMAN, C. 2003. The Hsp90 chaperone complex as a novel target for cancer therapy. *Annals of Oncology,* 14**,** 1169-1176.

GOHDA, J., AKIYAMA, T., KOGA, T., TAKAYANAGI, H., TANAKA, S. & INOUE, J. I. 2005. *RANK-mediated amplification of TRAF6 signaling leads to NFATc1 induction during osteoclastogenesis.*

GOLDBERG, A. L. 2003. Protein degradation and protection against misfolded or damaged proteins. *Nature,* 426**,** 895-899.

GOLDRING, S. R. 2003. Pathogenesis of bone and cartilage destruction in rheumatoid arthritis. *Rheumatology (Oxford),* 42 Suppl 2**,** ii11-6.

GONG, X., LUO, T., DENG, P., LIU, Z., XIU, J., SHI, H. & JIANG, Y. 2012. Stress-induced interaction between p38 MAPK and HSP70. *Biochemical and Biophysical Research Communications,* 425**,** 357-362.

GORDON, S. & TAYLOR, P. R. 2005. Monocyte and macrophage heterogeneity. *Nat Rev Immunol,* 5**,** 953-964.

GOUSPILLOU, G., SCHEEDE-BERGDAHL, C., SPENDIFF, S., VUDA, M., MEEHAN, B., MLYNARSKI, H., ARCHER-LAHLOU, E., SGARIOTO, N., PURVES-SMITH, F. M., KONOKHOVA, Y., RAK, J., CHEVALIER, S., TAIVASSALO, T., HEPPLE, R. T. & JAGOE, R. T. 2015. Anthracycline-containing chemotherapy causes long-term impairment of mitochondrial respiration and increased reactive oxygen species release in skeletal muscle. *Scientific Reports,* 5**,** 8717.

GRANGER, B. L., GREEN, S. A., GABEL, C. A., HOWE, C. L., MELLMAN, I. & HELENIUS, A. 1990. Characterization and cloning of lgp110, a lysosomal membrane glycoprotein from mouse and rat cells. *Journal of Biological Chemistry,* 265**,** 12036-12043.

GRASSET, M.-F., GOBERT-GOSSE, S., MOUCHIROUD, G. & BOURETTE, R. P. 2010. Macrophage differentiation of myeloid progenitor cells in response to M-CSF is regulated by the dual-specificity phosphatase DUSP5. *Journal of Leukocyte Biology,* 87**,** 127-135.

GRIGORIADIS, A., WANG, Z., CECCHINI, M., HOFSTETTER, W., FELIX, R., FLEISCH, H. & WAGNER, E. 1994. c-Fos: a key regulator of osteoclast-macrophage lineage determination and bone remodeling. *Science,* 266**,** 443-448.

GRIMAUD, E., SOUBIGOU, L., COUILLAUD, S., COIPEAU, P., MOREAU, A., PASSUTI, N., GOUIN, F., REDINI, F. & HEYMANN, D. 2003. Receptor Activator

of Nuclear Factor κB Ligand (RANKL)/Osteoprotegerin (OPG) Ratio Is Increased in Severe Osteolysis. *The American Journal of Pathology,* 163**,** 2021-2031.

GROB, G. N. 2011. From Aging to Pathology: The Case of Osteoporosis. *Journal of the History of Medicine and Allied Sciences,* 66**,** 1-39.

GU, R., SANTOS, L. L., NGO, D., FAN, H., SINGH, P. P., FINGERLE-ROWSON, G., BUCALA, R., XU, J., QUINN, J. M. W. & MORAND, E. F. 2015. Macrophage migration inhibitory factor is essential for osteoclastogenic mechanisms in vitro and in vivo mouse model of arthritis. *Cytokine,* 72**,** 135-145.

GUISE, T. A. 1997. Parathyroid hormone-related protein and bone metastases. *Cancer,* 80**,** 1572-80.

GUISE, T. A. 2006. Bone Loss and Fracture Risk Associated with Cancer Therapy. *The Oncologist,* 11**,** 1121-1131.

GUISE, T. A. 2009. Breaking down bone: new insight into site-specific mechanisms of breast cancer osteolysis mediated by metalloproteinases. *Genes & Development,* 23**,** 2117-2123.

GUISE, T. A. 2013. Breast cancer bone metastases: it's all about the neighborhood. *Cell,* 154**,** 957-9.

GUISE, T. A., MOHAMMAD, K. S., CLINES, G., STEBBINS, E. G., WONG, D. H., HIGGINS, L. S., VESSELLA, R., COREY, E., PADALECKI, S., SUVA, L. & CHIRGWIN, J. M. 2006. Basic Mechanisms Responsible for Osteolytic and Osteoblastic Bone Metastases. *Clinical Cancer Research,* 12**,** 6213s-6216s.

GUISE, T. A., YIN, J. J., TAYLOR, S. D., KUMAGAI, Y., DALLAS, M., BOYCE, B. F., YONEDA, T. & MUNDY, G. R. 1996. Evidence for a causal role of parathyroid hormone-related protein in the pathogenesis of human breast cancer-mediated osteolysis. *J Clin Invest,* 98**,** 1544-9.

GUO, F., ROCHA, K., BALI, P., PRANPAT, M., FISKUS, W., BOYAPALLE, S., KUMARASWAMY, S., BALASIS, M., GREEDY, B., ARMITAGE, E. S. M., LAWRENCE, N. & BHALLA, K. 2005a. Abrogation of Heat Shock Protein 70 Induction as a Strategy to Increase Antileukemia Activity of Heat Shock Protein 90 Inhibitor 17-Allylamino-Demethoxy Geldanamycin. *Cancer Research,* 65**,** 10536-10544.

GUO, N. & PENG, Z. 2013. MG132, a proteasome inhibitor, induces apoptosis in tumor cells. *Asia-Pacific Journal of Clinical Oncology,* 9**,** 6-11.

GUO, W., REIGAN, P., SIEGEL, D., ZIRROLLI, J., GUSTAFSON, D. & ROSS, D. 2005b. Formation of 17-allylamino-demethoxygeldanamycin (17-AAG) hydroquinone by NAD(P)H:quinone oxidoreductase 1: role of 17-AAG hydroquinone in heat shock protein 90 inhibition. *Cancer Res,* 65**,** 10006-15.

GUO, Y.-L., CHAKRABORTY, S., RAJAN, S. S., WANG, R. & HUANG, F. 2010. Effects of Oxidative Stress on Mouse Embryonic Stem Cell Proliferation, Apoptosis, Senescence, and Self-Renewal. *Stem Cells and Development,* 19**,** 1321-1331.

GUPTA, G. P. & MASSAGUÉ, J. 2006. Cancer Metastasis: Building a Framework. *Cell,* 127**,** 679-695.

GUPTA, S., DEEPTI, A., DEEGAN, S., LISBONA, F., HETZ, C. & SAMALI, A. 2010. HSP72 Protects Cells from ER Stress-induced Apoptosis via Enhancement of IRE1α-XBP1 Signaling through a Physical Interaction. *PLoS Biology,* 8**,** e1000410.

GUTTERMAN, D. D. 2005. Mitochondria and Reactive Oxygen Species: An Evolution in Function. *Circulation Research,* 97**,** 302-304.

HA, H., BOK KWAK, H., WOONG LEE, S., MI JIN, H., KIM, H.-M., KIM, H.-H. & HEE LEE, Z. 2004. Reactive oxygen species mediate RANK signaling in osteoclasts. *Experimental Cell Research,* 301**,** 119-127.

HA, J., CHOI, H. S., LEE, Y., KWON, H. J., SONG, Y. W. & KIM, H. H. 2010. CXC chemokine ligand 2 induced by receptor activator of NF-kappa B ligand enhances osteoclastogenesis. *J Immunol,* 184**,** 4717-24.

HADJI, P., ZILLER, M., MASKOW, C., ALBERT, U. & KALDER, M. 2009. The influence of chemotherapy on bone mineral density, quantitative ultrasonometry and bone turnover in pre-menopausal women with breast cancer. *Eur J Cancer,* 45**,** 3205-12.

HADLEY, K. B., NEWMAN, S. M. & HUNT, J. R. 2010. Dietary zinc reduces osteoclast resorption activities and increases markers of osteoblast differentiation, matrix maturation, and mineralization in the long bones of growing rats. *Journal of Nutritional Biochemistry,* 21**,** 297-303.

HAHN, W. C. & WEINBERG, R. A. 2002. Modelling the molecular circuitry of cancer. *Nat Rev Cancer,* 2**,** 331-341.

HAKEDA, Y. & KUMEGAWA, M. 1991. Osteoclasts in bone metabolism. *Kaibogaku Zasshi,* 66**,** 215-225.

HALLEEN, J. M., RAISANEN, S., SALO, J. J., REDDY, S. V., ROODMAN, G. D., HENTUNEN, T. A., LEHENKARI, P. P., KAIJA, H., VIHKO, P. & VAANANEN, H. K. 1999. Intracellular fragmentation of bone resorption products by reactive oxygen species generated by osteoclastic tartrate-resistant acid phosphatase. *J Biol Chem,* 274**,** 22907-10.

HAN, Y. H., KIM, S. Z., KIM, S. H. & PARK, W. H. 2010. Treatment with p38 inhibitor intensifies the death of MG132-treated As4.1 juxtaglomerular cells via the enhancement of GSH depletion. *Drug and Chemical Toxicology,* 33**,** 367-376.

HANAHAN, D. & WEINBERG, ROBERT A. 2011. Hallmarks of Cancer: The Next Generation. *Cell,* 144**,** 646-674.

HARADA, S. & RODAN, G. A. 2003. Control of osteoblast function and regulation of bone mass. *Nature,* 423**,** 349-55.

HATTERSLEY, G. & CHAMBERS, T. J. 1989. Generation of Osteoclastic Function in Mouse Bone Marrow Cultures: Multinuclearity and Tartrate- Resistant Acid Phosphatase Are Unreliable Markers for Osteoclastic Differentiation. *Endocrinology,* 124**,** 1689-1696.

HATTERSLEY, G., OWENS, J., FLANAGAN, A. M. & CHAMBERS, T. J. 1991. Macrophage colony stimulating factor (M-CSF) is essential for osteoclast formation in vitro. *Biochemical and Biophysical Research Communications,* 177**,** 526-531.

HAYNES, D. R., CROTTI, T. N., POTTER, A. E., LORIC, M., ATKINS, G. J., HOWIE, D. W. & FINDLAY, D. M. 2001. The osteoclastogenic molecules RANKL and RANK are associated with periprosthetic osteolysis. *Journal of Bone & Joint Surgery, British Volume,* 83-B**,** 902-911.

HAYWARD, D. G. & FRY, A. M. 2006. Nek2 kinase in chromosome instability and cancer. *Cancer Letters,* 237**,** 155-166.

HEHLGANS, T. & PFEFFER, K. 2005. The intriguing biology of the tumour necrosis factor/tumour necrosis factor receptor superfamily: players, rules and the games. *Immunology,* 115**,** 1-20.

HELD, P. 2015. *An Introduction to Reactive Oxygen Species Measurement of ROS in Cells* [Online]. BioTek Instruments, Inc.

HENDRICK, J. P. & HARTL, F. 1993. Molecular Chaperone Functions of Heat-Shock Proteins. *Annual Review of Biochemistry,* 62**,** 349-384.

HENRY, D. H., COSTA, L., GOLDWASSER, F., HIRSH, V., HUNGRIA, V., PRAUSOVA, J., SCAGLIOTTI, G. V., SLEEBOOM, H., SPENCER, A., VADHAN-RAJ, S., VON MOOS, R., WILLENBACHER, W., WOLL, P. J., WANG, J., JIANG, Q., JUN, S., DANSEY, R. & YEH, H. 2011. Randomized, Double-Blind Study of

Denosumab Versus Zoledronic Acid in the Treatment of Bone Metastases in Patients With Advanced Cancer (Excluding Breast and Prostate Cancer) or Multiple Myeloma. *Journal of Clinical Oncology,* 29**,** 1125-1132.

HERSHEY, C. L. & FISHER, D. E. 2004. Mitf and Tfe3: members of a b-HLH-ZIP transcription factor family essential for osteoclast development and function. *Bone,* 34**,** 689-696.

HERSHEY, C. L. & FISHER, D. E. 2005. Genomic analysis of the Microphthalmia locus and identification of the MITF-J/Mitf-J isoform. *Gene,* 347**,** 73-82.

HIENZ, S. A., PALIWAL, S. & IVANOVSKI, S. 2014. Mechanisms of Bone Resorption in Periodontitis. *Journal of Immunology Research.*

HOCKING, L. J., WHITEHOUSE, C. & HELFRICH, M. H. 2012. Autophagy: A new player in skeletal maintenance? *Journal of Bone and Mineral Research,* 27**,** 1439-1447.

HOFBAUER, L., RACHNER, T. & SINGH, S. 2008. Fatal attraction: why breast cancer cells home to bone. *Breast Cancer Research,* 10**,** 101.

HOFBAUER, L. C., KHOSLA, S., DUNSTAN, C. R., LACEY, D. L., BOYLE, W. J. & RIGGS, B. L. 2000. The roles of osteoprotegerin and osteoprotegerin ligand in the paracrine regulation of bone resorption. *J Bone Miner Res,* 15**,** 2-12.

HOGAN, P. G., CHEN, L., NARDONE, J. & RAO, A. 2003. Transcriptional regulation by calcium, calcineurin, and NFAT. *Genes & Development,* 17**,** 2205-2232.

HOLEN, I. & COLEMAN, R. 2010. Anti-tumour activity of bisphosphonates in preclinical models of breast cancer. *Breast Cancer Research,* 12**,** 214.

HOLMBERG, C. I., ILLMAN, S. A., KALLIO, M., MIKHAILOV, A. & SISTONEN, L. 2000. Formation of nuclear HSF1 granules varies depending on stress stimuli. *Cell Stress Chaperones,* 5**,** 219-28.

HOMESLEY, L., LEI, M., KAWASAKI, Y., SAWYER, S., CHRISTENSEN, T. & TYE, B. K. 2000. Mcm10 and the MCM2–7 complex interact to initiate DNA synthesis and to release replication factors from origins. *Genes & Development,* 14**,** 913-926.

HOROWITZ, M. C. & LORENZO, J. A. 2002. Chapter 53 - Local Regulators of Bone: IL-1, TNF, Lymphotoxin, Interferon-γ, IL-8, IL-10, IL-4, the LIF/IL-6 Family, and Additional Cytokines. *In:* RODAN, J. P. B. G. R. A. (ed.) *Principles of Bone Biology (Second Edition).* San Diego: Academic Press.

HOTOKEZAKA, H., SAKAI, E., KANAOKA, K., SAITO, K., MATSUO, K.-I., KITAURA, H., YOSHIDA, N. & NAKAYAMA, K. 2002. U0126 and PD98059, Specific Inhibitors of MEK, Accelerate Differentiation of RAW264.7 Cells into Osteoclast-like Cells. *Journal of Biological Chemistry,* 277**,** 47366-47372.

HOU, P., TROEN, T., OVEJERO, M. C., KIRKEGAARD, T., ANDERSEN, T. L., BYRJALSEN, I., FERRERAS, M., SATO, T., SHAPIRO, S. D., FOGED, N. T. & DELAISSÉ, J.-M. 2004. Matrix metalloproteinase-12 (MMP-12) in osteoclasts: new lesson on the involvement of MMPs in bone resorption. *Bone,* 34**,** 37-47.

HSUEH, Y.-S., YEN, C.-C., SHIH, N.-Y., CHIANG, N.-J., LI, C.-F. & CHEN, L.-T. 2013. Autophagy is involved in endogenous and NVP-AUY922-induced KIT degradation in gastrointestinal stromal tumors. *Autophagy,* 9**,** 220-233.

HU, M., LU, H. & GAGEL, R. 2010. Cancer Therapies and Bone Health. *Current Rheumatology Reports,* 12**,** 177-185.

HUANG, H., CHANG, E.-J., RYU, J., LEE, Z. H., LEE, Y. & KIM, H.-H. 2006. Induction of c-Fos and NFATc1 during RANKL-stimulated osteoclast differentiation is mediated by the p38 signaling pathway. *Biochemical and Biophysical Research Communications,* 351**,** 99-105.

HUBER, S. A. 1992. Heat-shock protein induction in adriamycin and picornavirus-infected cardiocytes. *Laboratory investigation; a journal of technical methods and pathology,* 67**,** 218-224.

HUH, Y. J., KIM, J. M., KIM, H., SONG, H., SO, H., LEE, S. Y., KWON, S. B., KIM, H. J., KIM, H. H., LEE, S. H., CHOI, Y., CHUNG, S. C., JEONG, D. W. & MIN, B. M. 2005. Regulation of osteoclast differentiation by the redox-dependent modulation of nuclear import of transcription factors. *Cell Death Differ,* 13**,** 1138-1146.

HUME, D. A., ROSS, I. L., HIMES, S. R., SASMONO, R. T., WELLS, C. A. & RAVASI, T. 2002. The mononuclear phagocyte system revisited. *Journal of Leukocyte Biology,* 72**,** 621-627.

HUNG, J.-J., CHENG, T.-J., LAI, Y.-K. & CHANG, M. D.-T. 1998. Differential Activation of p38 Mitogen-activated Protein Kinase and Extracellular Signal-regulated Protein Kinases Confers Cadmium-induced HSP70 Expression in 9L Rat Brain Tumor Cells. *Journal of Biological Chemistry,* 273**,** 31924-31931.

HÜTTENHOFER, A., KIEFMANN, M., MEIER-EWERT, S., O'BRIEN, J., LEHRACH, H., BACHELLERIE, J.-P. & BROSIUS, J. 2001. RNomics: an experimental approach that identifies 201 candidates for novel, small, non-messenger RNAs in mouse. *The EMBO Journal,* 20**,** 2943-2953.

HYBERTSON, B. M., GAO, B., BOSE, S. K. & MCCORD, J. M. 2011. Oxidative stress in health and disease: The therapeutic potential of Nrf2 activation. *Molecular Aspects of Medicine,* 32**,** 234-246.

IITSUKA, N., HIE, M., NAKANISHI, A. & TSUKAMOTO, I. 2012. Ethanol increases osteoclastogenesis associated with the increased expression of RANK, PU.1 and MITF in vitro and in vivo. *Int J Mol Med,* 30**,** 165-72.

IKEDA, K. & TAKESHITA, S. 2014. Factors and Mechanisms Involved in the Coupling from Bone Resorption to Formation: How Osteoclasts Talk to Osteoblasts. *Journal of Bone Metabolism,* 21**,** 163-167.

ILIC, Z., CRAWFORD, D., EGNER, P. A. & SELL, S. 2010. Glutathione-S-transferase A3 knockout mice are sensitive to acute cytotoxic and genotoxic effects of aflatoxin B1. *Toxicology and applied pharmacology,* 242**,** 241.

IOANNOU, K., SAMARA, P., LIVANIOU, E., DERHOVANESSIAN, E. & TSITSILONIS, O. 2012. Prothymosin alpha: a ubiquitous polypeptide with potential use in cancer diagnosis and therapy. *Cancer Immunology, Immunotherapy,* 61**,** 599-614.

IOTSOVA, V., CAAMANO, J., LOY, J., YANG, Y., LEWIN, A. & BRAVO, R. 1997. Osteopetrosis in mice lacking NF-[kappa]B1 and NF-[kappa]B2. *Nat Med,* 3**,** 1285-1289.

IPENBERG, I., GUTTMANN-RAVIV, N., KHOURY, H. P., KUPERSHMIT, I. & AYOUB, N. 2013. Heat Shock Protein 90 (Hsp90) Selectively Regulates the Stability of KDM4B/JMJD2B Histone Demethylase. *Journal of Biological Chemistry,* 288**,** 14681-14687.

IQBAL, J., SUN, L. & ZAIDI, M. 2009. Coupling bone degradation to formation. *Nat Med,* 15**,** 729-731.

ISAACS, J. S., XU, W. & NECKERS, L. 2003. Heat shock protein 90 as a molecular target for cancer therapeutics. *Cancer Cell,* 3**,** 213-217.

ISRAELI, R. S. 2008. Managing Bone Loss and Bone Metastases in Prostate Cancer Patients: A Focus on Bisphosphonate Therapy. *Reviews in Urology,* 10**,** 99-110.

ITZSTEIN, C., COXON, F. P. & ROGERS, M. J. 2011. The regulation of osteoclast function and bone resorption by small GTPases. *Small GTPases,* 2**,** 117-130.

JACKSON, S. P. & BARTEK, J. 2009. The DNA-damage response in human biology and disease. *Nature,* 461**,** 1071-1078.

JAEGER, A. M., MAKLEY, L. N., GESTWICKI, J. E. & THIELE, D. J. 2014. Genomic Heat Shock Element Sequences Drive Cooperative Human Heat Shock Factor 1 DNA Binding and Selectivity. *Journal of Biological Chemistry,* 289**,** 30459-69.

JAKOB, U., LILIE, H., MEYER, I. & BUCHNER, J. 1995. Transient Interaction of Hsp90 with Early Unfolding Intermediates of Citrate Synthase: IMPLICATIONS FOR HEAT SHOCK IN VIVO. *Journal of Biological Chemistry,* 270**,** 7288-7294.

JAMES, D. E., NESTOR, B. J., SCULCO, T. P., IVASHKIV, L. B., ROSS, F. P., GOLDRING, S. R. & PURDUE, P. E. 2010. The Relative Timing of Exposure to Phagocytosable Particulates and to Osteoclastogenic Cytokines Is Critically Important in the Determination of Myeloid Cell Fate. *Journal of immunology (Baltimore, Md. : 1950),* 185**,** 1265-1273.

JANSEN, I. D. C., VERMEER, J. A. F., BLOEMEN, V., STAP, J. & EVERTS, V. 2012. Osteoclast Fusion and Fission. *Calcified Tissue International,* 90**,** 515-522.

JAVELAUD, D., MOHAMMAD, K. S., MCKENNA, C. R., FOURNIER, P., LUCIANI, F., NIEWOLNA, M., ANDRÉ, J., DELMAS, V., LARUE, L., GUISE, T. A. & MAUVIEL, A. 2007. Stable Overexpression of Smad7 in Human Melanoma Cells Impairs Bone Metastasis. *Cancer Research,* 67**,** 2317-2324.

JEGO, G., HAZOUMÉ, A., SEIGNEURIC, R. & GARRIDO, C. 2013. Targeting heat shock proteins in cancer. *Cancer Letters,* 332**,** 275 - 285

JENSEN, M., SCHOEPFER, J., RADIMERSKI, T., MASSEY, A., GUY, C., BRUEGGEN, J., QUADT, C., BUCKLER, A., COZENS, R., DRYSDALE, M., GARCIA-ECHEVERRIA, C. & CHENE, P. 2008. NVP-AUY922: a small molecule HSP90 inhibitor with potent antitumor activity in preclinical breast cancer models. *Breast Cancer Research,* 10**,** R33.

JHAVERI, K., TALDONE, T., MODI, S. & CHIOSIS, G. 2012. Advances in the clinical development of heat shock protein 90 (Hsp90) inhibitors in cancers. *Biochimica et Biophysica Acta (BBA) - Molecular Cell Research,* 1823**,** 742-755.

JI, Y., XIE, M., LAN, H., ZHANG, Y., LONG, Y., WENG, H., LI, D., CAI, W., ZHU, H., NIU, Y., YANG, Z., ZHANG, C., SONG, F. & BU, Y. 2013. PRR11 is a novel gene implicated in cell cycle progression and lung cancer. *The International Journal of Biochemistry & Cell Biology,* 45**,** 645-656.

JIANG, Y., CHEN, C., LI, Z., GUO, W., GEGNER, J. A., LIN, S. & HAN, J. 1996. Characterization of the structure and function of a new mitogen-activated protein kinase (p38beta). *J Biol Chem,* 271**,** 17920-6.

JILKA, R. L. 2003. Biology of the basic multicellular unit and the pathophysiology of osteoporosis. *Medical and Pediatric Oncology,* 41**,** 182-185.

JIMENEZ-ANDRADE, J. M., MANTYH, W. G., BLOOM, A. P., FERNG, A. S., GEFFRE, C. P. & MANTYH, P. W. 2010. Bone cancer pain. *Ann N Y Acad Sci,* 1198**,** 173-81.

JIMI, E., AOKI, K., SAITO, H., D'ACQUISTO, F., MAY, M. J., NAKAMURA, I., SUDO, T., KOJIMA, T., OKAMOTO, F., FUKUSHIMA, H., OKABE, K., OHYA, K. & GHOSH, S. 2004. Selective inhibition of NF-[kappa]B blocks osteoclastogenesis and prevents inflammatory bone destruction in vivo. *Nat Med,* 10**,** 617-624.

JIN, X., EROGLU, B., MOSKOPHIDIS, D. & MIVECHI, N. F. 2011. Targeted Deletion of Hsf1, 2, and 4 Genes in Mice. *Methods in molecular biology (Clifton, N.J.),* 787**,** 1-20.

JULES, J., ZHANG, P., ASHLEY, J. W., WEI, S., SHI, Z., LIU, J., MICHALEK, S. M. & FENG, X. 2012. Molecular basis of requirement of receptor activator of nuclear factor kappaB signaling for interleukin 1-mediated osteoclastogenesis. *J Biol Chem,* 287**,** 15728-38.

JUNTTILA, M. R., LI, S.-P. & WESTERMARCK, J. 2008. Phosphatase-mediated crosstalk between MAPK signaling pathways in the regulation of cell survival. *The FASEB Journal,* 22**,** 954-965.

KAJARABILLE, N., DIAZ-CASTRO, J., HIJANO, S., LÓPEZ-FRÍAS, M., LÓPEZ-ALIAGA, I. & OCHOA, J. J. 2013. A New Insight to Bone Turnover: Role of -3 Polyunsaturated Fatty Acids. *The Scientific World Journal,* 2013**,** 16.

KAJIYA, H., ITO, M., OHSHIMA, H., KENMOTSU, S.-I., RIES, W. L., BENJAMIN, I. J. & REDDY, S. V. 2006. RANK ligand expression in heat shock factor-2 deficient mouse bone marrow stromal/preosteoblast cells. *Journal of Cellular Biochemistry,* 97**,** 1362-1369.

KAMAL, A., BOEHM, M. F. & BURROWS, F. J. 2004. Therapeutic and diagnostic implications of Hsp90 activation. *Trends in Molecular Medicine,* 10**,** 283-290.

KAMAL, A., THAO, L., SENSINTAFFAR, J., ZHANG, L., BOEHM, M., FRITZ, L. & BURROWS, F. 2003. A high-affinity conformation of Hsp90 confers tumour selectivity on Hsp90 inhibitors. *Nature,* 425**,** 407 - 410.

KAMEDA, Y., TAKAHATA, M., KOMATSU, M., MIKUNI, S., HATAKEYAMA, S., SHIMIZU, T., ANGATA, T., KINJO, M., MINAMI, A. & IWASAKI, N. 2013. Siglec-15 Regulates Osteoclast Differentiation by Modulating RANKL-Induced Phosphatidylinositol 3-Kinase/Akt and Erk Pathways in Association With Signaling Adaptor DAP12. *Journal of Bone and Mineral Research,* 28**,** 2463-2475.

KANEHISA, J., YAMANAKA, T., DOI, S., TURKSEN, K., HEERSCHE, J. N. M., AUBIN, J. E. & TAKEUCHI, H. 1990. A band of F-actin containing podosomes is involved in bone resorption by osteoclasts. *Bone,* 11**,** 287-293.

KANG, Y., HE, W., TULLEY, S., GUPTA, G. P., SERGANOVA, I., CHEN, C.-R., MANOVA-TODOROVA, K., BLASBERG, R., GERALD, W. L. & MASSAGUÉ, J. 2005. Breast cancer bone metastasis mediated by the Smad tumor suppressor pathway. *Proceedings of the National Academy of Sciences of the United States of America,* 102**,** 13909-13914.

KANG, Y., SIEGEL, P. M., SHU, W., DROBNJAK, M., KAKONEN, S. M., CORDÓN-CARDO, C., GUISE, T. A. & MASSAGUÉ, J. 2003. A multigenic program mediating breast cancer metastasis to bone. *Cancer Cell,* 3**,** 537-549.

KANSARA, M., TENG, M. W., SMYTH, M. J. & THOMAS, D. M. 2014. Translational biology of osteosarcoma. *Nat Rev Cancer,* 14**,** 722-35.

KAO, C., CHAO, A., TSAI, C. L., LIN, C. Y., CHUANG, W. C., CHEN, H. W., YEN, T. C., WANG, T. H., LAI, C. H. & WANG, H. S. 2013. Phosphorylation of signal transducer and activator of transcription 1 reduces bortezomib-mediated apoptosis in cancer cells. *Cell Death Dis,* 4**,** e512.

KARKOULIS, P., STRAVOPODIS, D., KONSTANTAKOU, E. & VOUTSINAS, G. 2013. Targeted inhibition of heat shock protein 90 disrupts multiple oncogenic signaling pathways, thus inducing cell cycle arrest and programmed cell death in human urinary bladder cancer cell lines. *Cancer Cell International,* 13**,** 11.

KASSAMBARA, A., SCHOENHALS, M., MOREAUX, J., VEYRUNE, J.-L., RÈME, T., GOLDSCHMIDT, H., HOSE, D. & KLEIN, B. 2013. Inhibition of DEPDC1A, a Bad Prognostic Marker in Multiple Myeloma, Delays Growth and Induces Mature Plasma Cell Markers in Malignant Plasma Cells. *PLoS ONE,* 8**,** e62752.

KATAGIRI, T. & TAKAHASHI, N. 2002. Regulatory mechanisms of osteoblast and osteoclast differentiation. *Oral Diseases,* 8**,** 147-159.

KAUFMAN, R. J., SCHEUNER, D., SCHRODER, M., SHEN, X., LEE, K., LIU, C. Y. & ARNOLD, S. M. 2002. The unfolded protein response in nutrient sensing and differentiation. *Nat Rev Mol Cell Biol,* 3**,** 411-421.

KELLAND, L. 2007. The resurgence of platinum-based cancer chemotherapy. *Nat Rev Cancer,* 7**,** 573-584.

KELLAND, L. R., SHARP, S. Y., ROGERS, P. M., MYERS, T. G. & WORKMAN, P. 1999. DT-Diaphorase expression and tumor cell sensitivity to 17-allylamino, 17-demethoxygeldanamycin, an inhibitor of heat shock protein 90. *J Natl Cancer Inst,* 91**,** 1940-9.

KEMP, K., MORSE, R., SANDERS, K., HOWS, J. & DONALDSON, C. 2011. Alkylating chemotherapeutic agents cyclophosphamide and melphalan cause functional injury to human bone marrow-derived mesenchymal stem cells. *Annals of Hematology,* 90**,** 777-789.

KERSCHNITZKI, M., KOLLMANNSBERGER, P., BURGHAMMER, M., DUDA, G. N., WEINKAMER, R., WAGERMAIER, W. & FRATZL, P. 2013. Architecture of the osteocyte network correlates with bone material quality. *Journal of Bone and Mineral Research,* 28**,** 1837-1845.

KHOSLA, S. 2001. Minireview: The OPG/RANKL/RANK System. *Endocrinology,* 142**,** 5050-5055.

KIKUTA, J., WADA, Y., KOWADA, T., WANG, Z., SUN-WADA, G.-H., NISHIYAMA, I., MIZUKAMI, S., MAIYA, N., YASUDA, H., KUMANOGOH, A., KIKUCHI, K., GERMAIN, R. N. & ISHII, M. 2013. Dynamic visualization of RANKL and Th17-mediated osteoclast function. *The Journal of Clinical Investigation,* 123**,** 866-873.

KIM, D., KIM, S.-H. & LI, G. C. 1999. Proteasome Inhibitors MG132 and Lactacystin Hyperphosphorylate HSF1 and Induce hsp70 and hsp27 Expression. *Biochemical and Biophysical Research Communications,* 254**,** 264-268.

KIM, H. J., CHANG, E.-J., KIM, H.-M., LEE, S. B., KIM, H.-D., SU KIM, G. & KIM, H.-H. 2006. Antioxidant α-lipoic acid inhibits osteoclast differentiation by reducing nuclear factor-κB DNA binding and prevents in vivo bone resorption induced by receptor activator of nuclear factor-κB ligand and tumor necrosis factor-α. *Free Radical Biology and Medicine,* 40**,** 1483-1493.

KIM, I., XU, W. & REED, J. C. 2008a. Cell death and endoplasmic reticulum stress: disease relevance and therapeutic opportunities. *Nat Rev Drug Discov,* 7**,** 1013-30.

KIM, J., NUEDA, A., MENG, Y.-H., DYNAN, W. S. & MIVECHI, N. F. 1997. Analysis of the phosphorylation of human heat shock transcription factor-1 by MAP kinase family members. *Journal of Cellular Biochemistry,* 67**,** 43-54.

KIM, J. H., JIN, H. M., KIM, K., SONG, I., YOUN, B. U., MATSUO, K. & KIM, N. 2009. The mechanism of osteoclast differentiation induced by IL-1. *J Immunol,* 183**,** 1862-70.

KIM, J. H. & KIM, N. 2014. Regulation of NFATc1 in Osteoclast Differentiation. *Journal of Bone Metabolism,* 21**,** 233-241.

KIM, K., LEE, S.-H., HA KIM, J., CHOI, Y. & KIM, N. 2008b. NFATc1 Induces Osteoclast Fusion Via Up-Regulation of Atp6v0d2 and the Dendritic Cell-Specific Transmembrane Protein (DC-STAMP). *Molecular Endocrinology,* 22**,** 176-185.

KIM, M. S., DAY, C. J. & MORRISON, N. A. 2005a. MCP-1 Is Induced by Receptor Activator of Nuclear Factor-κB Ligand, Promotes Human Osteoclast Fusion, and Rescues Granulocyte Macrophage Colony-stimulating Factor Suppression of Osteoclast Formation. *Journal of Biological Chemistry,* 280**,** 16163-16169.

KIM, N., KADONO, Y., TAKAMI, M., LEE, J., LEE, S.-H., OKADA, F., KIM, J. H., KOBAYASHI, T., ODGREN, P. R., NAKANO, H., YEH, W.-C., LEE, S.-K., LORENZO, J. A. & CHOI, Y. 2005b. Osteoclast differentiation independent of the TRANCE–RANK–TRAF6 axis. *The Journal of Experimental Medicine,* 202**,** 589-595.

KIM, S. W., PAJEVIC, P. D., SELIG, M., BARRY, K. J., YANG, J.-Y., SHIN, C. S., BAEK, W.-Y., KIM, J.-E. & KRONENBERG, H. M. 2012. Intermittent PTH Administration Converts Quiescent Lining Cells to Active Osteoblasts. *Journal of bone and mineral research : the official journal of the American Society for Bone and Mineral Research,* 27**,** 2075-2084.

KIM, Y., SATO, K., ASAGIRI, M., MORITA, I., SOMA, K. & TAKAYANAGI, H. 2005c. Contribution of nuclear factor of activated T cells c1 to the transcriptional control of immunoreceptor osteoclast-associated receptor but not triggering receptor expressed by myeloid cells-2 during osteoclastogenesis. *J Biol Chem,* 280**,** 32905-13.

KINGSLEY, L., FOURNIER, P., CHIRGWIN, J. & GUISE, T. 2007. Molecular Biology of Bone Metastasis. *Molecular Cancer Therapeutics,* 6**,** 2609-2617.

KLAUNIG, J. E., KAMENDULIS, L. M. & HOCEVAR, B. A. 2010. Oxidative Stress and Oxidative Damage in Carcinogenesis. *Toxicologic Pathology,* 38**,** 96-109.

KODAMA, H., NOSE, M., NIIDA, S. & YAMASAKI, A. 1991a. Essential role of macrophage colony-stimulating factor in the osteoclast differentiation supported by stromal cells. *J Exp Med,* 173**,** 1291-4.

KODAMA, H., YAMASAKI, A., NOSE, M., NIIDA, S., OHGAME, Y., ABE, M., KUMEGAWA, M. & SUDA, T. 1991b. Congenital osteoclast deficiency in osteopetrotic (op/op) mice is cured by injections of macrophage colony-stimulating factor. *J Exp Med,* 173**,** 269-72.

KOGA, F., KIHARA, K. & NECKERS, L. 2009. Inhibition of Cancer Invasion and Metastasis by Targeting the Molecular Chaperone Heat-shock Protein 90. *Anticancer Research,* 29**,** 797-807.

KOGA, F., TSUTSUMI, S. & NECKERS, L. M. 2007. Low Dose Geldanamycin Inhibits Hepatocyte Growth Factor- and Hypoxia-Stimulated Invasion of Cancer Cells. *Cell Cycle,* 6**,** 1393-1402.

KOHARA, H., KITAURA, H., FUJIMURA, Y., YOSHIMATSU, M., MORITA, Y., EGUCHI, T., MASUYAMA, R. & YOSHIDA, N. 2011. IFN-γ directly inhibits TNF-α-induced osteoclastogenesis in vitro and in vivo and induces apoptosis mediated by Fas/Fas ligand interactions. *Immunology Letters,* 137**,** 53-61.

KOISHI, M., YOKOTA, S. I., MAE, T., NISHIMURA, Y., KANAMORI, S., HORII, N., SHIBUYA, K., SASAI, K. & HIRAOKA, M. 2001. The Effects of KNK437, a Novel Inhibitor of Heat Shock Protein Synthesis, on the Acquisition of Thermotolerance in a Murine Transplantable Tumor in Vivo. *Clinical Cancer Research,* 7**,** 215-219.

KOPESKY, P., TIEDEMANN, K., ALKEKHIA, D., ZECHNER, C., MILLARD, B., SCHOEBERL, B. & KOMAROVA, S. V. 2014. Autocrine signaling is a key regulatory element during osteoclastogenesis. *Biology Open*.

KOSTOVA, I. 2006. Platinum complexes as anticancer agents. *Recent Pat Anticancer Drug Discov,* 1**,** 1-22.

KOUL, H. K., PAL, M. & KOUL, S. 2013. Role of p38 MAP Kinase Signal Transduction in Solid Tumors. *Genes & Cancer,* 4**,** 342-359.

KREGEL, K. C. 2002. Invited Review: Heat shock proteins: modifying factors in physiological stress responses and acquired thermotolerance. *Journal of Applied Physiology,* 92**,** 2177-2186.

KRISHNAN, V., VOGLER, E. A., SOSNOSKI, D. M. & MASTRO, A. M. 2014. In Vitro Mimics of Bone Remodeling and the Vicious Cycle of Cancer in Bone. *Journal of Cellular Physiology,* 229**,** 453-462.

KROEMER, G. & POUYSSEGUR, J. 2008. Tumor Cell Metabolism: Cancer's Achilles' Heel. *Cancer Cell,* 13**,** 472-482.

KRUUV, J., GLOFCHESKI, D., CHENG, K. H., CAMPBELL, S. D., AL-QYSI, H. M., NOLAN, W. T. & LEPOCK, J. R. 1983. Factors influencing survival and growth of mammalian cells exposed to hypothermia. I. Effects of temperature and membrane lipid perturbers. *J Cell Physiol,* 115**,** 179-85.

KRYLOV, D., KASAI, K., ECHLIN, D. R., TAPAROWSKY, E. J., ARNHEITER, H. & VINSON, C. 1997. A general method to design dominant negatives to B-HLHZip proteins that abolish DNA binding. *Proc Natl Acad Sci U S A,* 94**,** 12274-9.

KUBOTA, K., WAKABAYASHI, K. & MATSUOKA, T. 2003. Proteome analysis of secreted proteins during osteoclast differentiation using two different methods: Two-dimensional electrophoresis and isotope-coded affinity tags analysis with two-dimensional chromatography. *PROTEOMICS,* 3**,** 616-626.

KUDO, O., FUJIKAWA, Y., ITONAGA, I., SABOKBAR, A., TORISU, T. & ATHANASOU, N. A. 2002. Proinflammatory cytokine (TNFα/IL-1α) induction of human osteoclast formation. *The Journal of Pathology,* 198**,** 220-227.

KUDO, O., SABOKBAR, A., POCOCK, A., ITONAGA, I., FUJIKAWA, Y. & ATHANASOU, N. A. 2003. Interleukin-6 and interleukin-11 support human osteoclast formation by a RANKL-independent mechanism. *Bone,* 32**,** 1-7.

KUHL, N. M. & RENSING, L. 2000. Heat shock effects on cell cycle progression. *Cell Mol Life Sci,* 57**,** 450-63.

KUIPER, R. P., SCHEPENS, M., THIJSSEN, J., SCHOENMAKERS, E. F. P. M. & VAN KESSEL, A. G. 2004. Regulation of the MiTF/TFE bHLH-LZ transcription factors through restricted spatial expression and alternative splicing of functional domains. *Nucleic Acids Research,* 32**,** 2315-2322.

KUMAR, B., KOUL, S., KHANDRIKA, L., MEACHAM, R. B. & KOUL, H. K. 2008. Oxidative Stress Is Inherent in Prostate Cancer Cells and Is Required for Aggressive Phenotype. *Cancer Research,* 68**,** 1777-1785.

KURODA, Y. & MATSUO, K. 2012. Molecular mechanisms of triggering, amplifying and targeting RANK signaling in osteoclasts. *World Journal of Orthopedics,* 3**,** 167-174.

KYURAGI, R., MATSUMOTO, T., HARADA, Y., SAITO, S., ONIMARU, M., NAKATSU, Y., TSUZUKI, T., NOMURA, M., YONEMITSU, Y. & MAEHARA, Y. 2015. BubR1 Insufficiency Inhibits Neointimal Hyperplasia Through Impaired Vascular Smooth Muscle Cell Proliferation in Mice. *Arteriosclerosis, Thrombosis, and Vascular Biology,* 35**,** 341-347.

LACEY, D. L., TIMMS, E., TAN, H. L., KELLEY, M. J., DUNSTAN, C. R., BURGESS, T., ELLIOTT, R., COLOMBERO, A., ELLIOTT, G., SCULLY, S., HSU, H., SULLIVAN, J., HAWKINS, N., DAVY, E., CAPPARELLI, C., ELI, A., QIAN, Y. X., KAUFMAN, S., SAROSI, I., SHALHOUB, V., SENALDI, G., GUO, J., DELANEY, J. & BOYLE, W. J. 1998. Osteoprotegerin Ligand Is a Cytokine that Regulates Osteoclast Differentiation and Activation. *Cell,* 93**,** 165-176.

LAITALA-LEINONEN, T., LOWIK, C., PAPAPOULOS, S. & VAANANEN, H. K. 1999. Inhibition of intravacuolar acidification by antisense RNA decreases osteoclast differentiation and bone resorption in vitro. *J Cell Sci,* 112 (Pt 21)**,** 3657-66.

LAITALA, T. & VÄÄNÄNEN, H. K. 1994. Inhibition of bone resorption in vitro by antisense RNA and DNA molecules targeted against carbonic anhydrase II or two subunits of vacuolar H(+)-ATPase. *Journal of Clinical Investigation,* 93**,** 2311-2318.

LAITALA, T. & VAANANEN, K. 1993. Proton channel part of vacuolar H(+)-ATPase and carbonic anhydrase II expression is stimulated in resorbing osteoclasts. *J Bone Miner Res,* 8**,** 119-26.

LANG, B. J., NGUYEN, L., NGUYEN, H. C., VIEUSSEUX, J. L., CHAI, R. C., CHRISTOPHI, C., FIFIS, T., KOUSPOU, M. M. & PRICE, J. T. 2012. Heat stress

induces epithelial plasticity and cell migration independent of heat shock factor 1. *Cell Stress Chaperones,* 17**,** 765-78.

LARAMIE, J. M., CHUNG, T. P., BROWNSTEIN, B., STORMO, G. D. & COBB, J. P. 2008. Transcriptional profiles of human epithelial cells in response to heat: computational evidence for novel heat shock proteins. *Shock,* 29**,** 623-30.

LATCHMAN, D. S. 2001. Heat shock proteins and cardiac protection. *Cardiovascular Research,* 51**,** 637-646.

LAWSON, S. K., DOBRIKOVA, E. Y., SHVEYGERT, M. & GROMEIER, M. 2013. p38α Mitogen-Activated Protein Kinase Depletion and Repression of Signal Transduction to Translation Machinery by miR-124 and -128 in Neurons. *Molecular and Cellular Biology,* 33**,** 127-135.

LAYH-SCHMITT, G., YANG, E. Y., KWON, G. & COLBERT, R. A. 2013. HLA-B27 Alters the Response to TNFα and Promotes Osteoclastogenesis in Bone Marrow Monocytes from HLA-B27 Transgenic Rats. *Arthritis and rheumatism,* 65**,** 10.1002/art.38001.

LEAN, J. M., MURPHY, C., FULLER, K. & CHAMBERS, T. J. 2002. CCL9/MIP-1gamma and its receptor CCR1 are the major chemokine ligand/receptor species expressed by osteoclasts. *J Cell Biochem,* 87**,** 386-93.

LEBRUN, J.-J. 2012. The Dual Role of TGF in Human Cancer: From Tumor Suppression to Cancer Metastasis. *ISRN Molecular Biology,* 2012**,** 28.

LECKER, S. H., GOLDBERG, A. L. & MITCH, W. E. 2006. Protein Degradation by the Ubiquitin–Proteasome Pathway in Normal and Disease States. *Journal of the American Society of Nephrology,* 17**,** 1807-1819.

LEE, K. J. & HAHN, G. M. 1988. Abnormal proteins as the trigger for the induction of stress responses: heat, diamide, and sodium arsenite. *J Cell Physiol,* 136**,** 411-20.

LEE, N. K., CHOI, Y. G., BAIK, J. Y., HAN, S. Y., JEONG, D.-W., BAE, Y. S., KIM, N. & LEE, S. Y. 2005. A crucial role for reactive oxygen species in RANKL-induced osteoclast differentiation. *Blood,* 106**,** 852-859.

LEE, S.-H., RHO, J., JEONG, D., SUL, J.-Y., KIM, T., KIM, N., KANG, J.-S., MIYAMOTO, T., SUDA, T., LEE, S.-K., PIGNOLO, R. J., KOCZON-JAREMKO, B., LORENZO, J. & CHOI, Y. 2006. v-ATPase V0 subunit d2-deficient mice exhibit impaired osteoclast fusion and increased bone formation. *Nat Med,* 12**,** 1403-1409.

LEE, S. E., JEONG, S. K. & LEE, S. H. 2010a. Protease and Protease-Activated Receptor-2 Signaling in the Pathogenesis of Atopic Dermatitis. *Yonsei Medical Journal,* 51**,** 808-822.

LEE, S. E., WOO, K. M., KIM, S. Y., KIM, H. M., KWACK, K., LEE, Z. H. & KIM, H. H. 2002a. The phosphatidylinositol 3-Kinase, p38, and extracellular signal-regulated kinase pathways are involved in osteoclast differentiation. *Bone,* 30**,** 71-77.

LEE, S. K., GOLDRING, S. R. & LORENZO, J. A. 1995. Expression of the calcitonin receptor in bone marrow cell cultures and in bone: a specific marker of the differentiated osteoclast that is regulated by calcitonin. *Endocrinology,* 136**,** 4572-81.

LEE, S. K., KALINOWSKI, J., JASTRZEBSKI, S. & LORENZO, J. A. 2002b. 1,25(OH)2 vitamin D3-stimulated osteoclast formation in spleen-osteoblast cocultures is mediated in part by enhanced IL-1 alpha and receptor activator of NF-kappa B ligand production in osteoblasts. *J Immunol,* 169**,** 2374-80.

LEE, Y.-M., FUJIKADO, N., MANAKA, H., YASUDA, H. & IWAKURA, Y. 2010b. IL-1 plays an important role in the bone metabolism under physiological conditions. *International Immunology,* 22**,** 805-816.

LEE, Z. H. & KIM, H.-H. 2003. Signal transduction by receptor activator of nuclear factor kappa B in osteoclasts. *Biochemical and Biophysical Research Communications,* 305**,** 211-214.

LEHENKARI, P., HENTUNEN, T. A., LAITALA-LEINONEN, T., TUUKKANEN, J. & VÄÄNÄNEN, H. K. 1998. Carbonic Anhydrase II Plays a Major Role in Osteoclast Differentiation and Bone Resorption by Effecting the Steady State Intracellular pH and Ca2+. *Experimental Cell Research,* 242**,** 128-137.

LEVONEN, A. L., HILL, B. G., KANSANEN, E., ZHANG, J. & DARLEY-USMAR, V. M. 2014. Redox regulation of antioxidants, autophagy, and the response to stress: implications for electrophile therapeutics. *Free Radic Biol Med,* 71**,** 196-207.

LEVY, C., KHALED, M. & FISHER, D. E. 2006. MITF: master regulator of melanocyte development and melanoma oncogene. *Trends in Molecular Medicine,* 12**,** 406-414.

LI, B., WONG, M. & PAVLAKIS, N. 2014. Treatment and Prevention of Bone Metastases from Breast Cancer: A Comprehensive Review of Evidence for Clinical Practice. *Journal of Clinical Medicine,* 3**,** 1-24.

LI, J. & BUCHNER, J. 2013a. Structure, function and regulation of the hsp90 machinery. *Biomed J,* 36**,** 106-17.

LI, J. & BUCHNER, J. 2013b. *Structure, Function and Regulation of the Hsp90 Machinery.*

LI, J., SAROSI, I., YAN, X.-Q., MORONY, S., CAPPARELLI, C., TAN, H.-L., MCCABE, S., ELLIOTT, R., SCULLY, S., VAN, G., KAUFMAN, S., JUAN, S.-C., SUN, Y., TARPLEY, J., MARTIN, L., CHRISTENSEN, K., MCCABE, J., KOSTENUIK, P., HSU, H., FLETCHER, F., DUNSTAN, C. R., LACEY, D. L. & BOYLE, W. J. 2000. RANK is the intrinsic hematopoietic cell surface receptor that controls osteoclastogenesis and regulation of bone mass and calcium metabolism. *Proceedings of the National Academy of Sciences of the United States of America,* 97**,** 1566-1571.

LI, X., UDAGAWA, N., ITOH, K., SUDA, K., MURASE, Y., NISHIHARA, T., SUDA, T. & TAKAHASHI, N. 2002. p38 MAPK-Mediated Signals Are Required for Inducing Osteoclast Differentiation But Not for Osteoclast Function. *Endocrinology,* 143**,** 3105-3113.

LI, X., ZHANG, K. & LI, Z. 2011. Unfolded protein response in cancer: the physician's perspective. *J Hematol Oncol,* 4**,** 8.

LI, Y., ZHANG, D., XU, J., SHI, J., JIANG, L., YAO, N. & YE, W. 2012. Discovery and development of natural heat shock protein 90 inhibitors in cancer treatment. *Acta Pharmaceutica Sinica B,* 2**,** 238-245.

LI, Z., KONG, K. & QI, W. 2006. Osteoclast and its roles in calcium metabolism and bone development and remodeling. *Biochemical and Biophysical Research Communications,* 343**,** 345-350.

LILA, P., NYKANEN, P. & SISTONEN, L. 2001. Roles of the heat shock transcription factors in regulation of the heat shock response and beyond. *The FASEB Journal,* 15**,** 1118-1131.

LIN, H., LEE, E., HESTIR, K., LEO, C., HUANG, M., BOSCH, E., HALENBECK, R., WU, G., ZHOU, A., BEHRENS, D., HOLLENBAUGH, D., LINNEMANN, T., QIN, M., WONG, J., CHU, K., DOBERSTEIN, S. K. & WILLIAMS, L. T. 2008. Discovery of a cytokine and its receptor by functional screening of the extracellular proteome. *Science,* 320**,** 807-11.

LINDQUIST, S. 1986. The Heat-Shock Response. *Annual Review of Biochemistry,* 55**,** 1151-1191.

LIPTON, A. 2004. Pathophysiology of bone metastases: how this knowledge may lead to therapeutic intervention. *J Support Oncol,* 2**,** 205-13; discussion 213-4, 216-7, 219-20.

LIPTON, A., FIZAZI, K., STOPECK, A. T., HENRY, D. H., BROWN, J. E., YARDLEY, D. A., RICHARDSON, G. E., SIENA, S., MAROTO, P., CLEMENS, M., BILYNSKYY, B., CHARU, V., BEUZEBOC, P., RADER, M., VINIEGRA, M., SAAD, F., KE, C., BRAUN, A. & JUN, S. Superiority of denosumab to zoledronic acid for prevention of skeletal-related events: A combined analysis of 3 pivotal, randomised, phase 3 trials. *European Journal of Cancer,* 48**,** 3082-3092.

LIPTON, A., UZZO, R., AMATO, R. J., ELLIS, G. K., HAKIMIAN, B., ROODMAN, G. D. & SMITH, M. R. 2009a. The science and practice of bone health in oncology: managing bone loss and metastasis in patients with solid tumors. *J Natl Compr Canc Netw,* 7 Suppl 7**,** S1-29; quiz S30.

LIPTON, A., UZZO, R., AMATO, R. J., ELLIS, G. K., HAKIMIAN, B., ROODMAN, G. D. & SMITH, M. R. 2009b. The Science and Practice of Bone Health in Oncology: Managing Bone Loss and Metastasis in Patients With Solid Tumors. *Journal of the National Comprehensive Cancer Network : JNCCN,* 7**,** S1-S30.

LIU, C. Y. & KAUFMAN, R. J. 2003. The unfolded protein response. *J Cell Sci,* 116**,** 1861-2.

LIU, F., FU, Y. & MEYSKENS, F. L., JR. 2008. MiTF Regulates Cellular Response to Reactive Oxygen Species through Transcriptional Regulation of APE-1/Ref-1. *J Invest Dermatol,* 129**,** 422-431.

LIU, H., ZHAO, S., ZHANG, Y., WU, J., PENG, H., FAN, J. & LIAO, J. 2011. Reactive oxygen species-mediated endoplasmic reticulum stress and mitochondrial dysfunction contribute to polydatin-induced apoptosis in human nasopharyngeal carcinoma CNE cells. *Journal of Cellular Biochemistry,* 112**,** 3695-3703.

LIU, P. C. C. & THIELE, D. J. 1999. Modulation of Human Heat Shock Factor Trimerization by the Linker Domain. *Journal of Biological Chemistry,* 274**,** 17219-17225.

LIU, Y., SHI, Z., SILVEIRA, A., LIU, J., SAWADOGO, M., YANG, H. & FENG, X. 2003. Involvement of Upstream Stimulatory Factors 1 and 2 in RANKL-induced Transcription of Tartrate-resistant Acid Phosphatase Gene during Osteoclast Differentiation. *Journal of Biological Chemistry,* 278**,** 20603-20611.

LOMAGA, M. A., YEH, W.-C., SAROSI, I., DUNCAN, G. S., FURLONGER, C., HO, A., MORONY, S., CAPPARELLI, C., VAN, G., KAUFMAN, S., VAN DER HEIDEN, A., ITIE, A., WAKEHAM, A., KHOO, W., SASAKI, T., CAO, Z., PENNINGER, J. M., PAIGE, C. J., LACEY, D. L., DUNSTAN, C. R., BOYLE, W. J., GOEDDEL, D. V. & MAK, T. W. 1999. TRAF6 deficiency results in osteopetrosis and defective interleukin-1, CD40, and LPS signaling. *Genes & Development,* 13**,** 1015-1024.

LOUTIT, J. F. & NISBET, N. W. 1982. The Origin of Osteoclasts. *Immunobiology,* 161**,** 193-203.

LOWELL, C. A., NIWA, M., SORIANO, P. & VARMUS, H. E. 1996. Deficiency of the Hck and Src tyrosine kinases results in extreme levels of extramedullary hematopoiesis. *Blood,* 87**,** 1780-92.

LU, P., TAKAI, K., WEAVER, V. M. & WERB, Z. 2011. Extracellular Matrix Degradation and Remodeling in Development and Disease. *Cold Spring Harbor Perspectives in Biology,* 3.

LU, S.-Y., LI, M. & LIN, Y.-L. 2010a. Mitf Induction by RANKL Is Critical for Osteoclastogenesis. *Mol. Biol. Cell,* 21**,** 1763-1771.

LU, S.-Y., LI, M. & LIN, Y.-L. 2014. Mitf regulates osteoclastogenesis by modulating NFATc1 activity. *Experimental Cell Research,* 328**,** 32-43.

LU, S.-Y., WAN, H.-C., LI, M. & LIN, Y.-L. 2010b. Subcellular localization of Mitf in monocytic cells. *Histochemistry and Cell Biology,* 133**,** 651-658.

LUCHIN, A., PURDOM, G., MURPHY, K., CLARK, M.-Y., ANGEL, N., CASSADY, A. I., HUME, D. A. & OSTROWSKI, M. C. 2000. The Microphthalmia Transcription Factor Regulates Expression of the Tartrate-Resistant Acid Phosphatase Gene During Terminal Differentiation of Osteoclasts. *Journal of Bone and Mineral Research,* 15**,** 451-460.

LUCHT, U. 1972. Cytoplasmic vacuoles and bodies of the osteoclast. *Zeitschrift für Zellforschung und Mikroskopische Anatomie,* 135**,** 229-244.

LUO, J., SOLIMINI, N. L. & ELLEDGE, S. J. 2009. Principles of Cancer Therapy: Oncogene and Non-oncogene Addiction. *Cell,* 136**,** 823-837.

LUPARELLO, C., SIRCHIA, R. & PUPELLO, D. 2003. PTHrP [67-86] regulates the expression of stress proteins in breast cancer cells inducing modifications in urokinase-plasminogen activator and MMP-1 expression. *Journal of Cell Science,* 116**,** 2421-2430.

MACKIE, E. J. 2003. Osteoblasts: novel roles in orchestration of skeletal architecture. *The International Journal of Biochemistry & Cell Biology,* 35**,** 1301-1305.

MACLAUCHLAN, S., SKOKOS, E. A., MEZNARICH, N., ZHU, D. H., RAOOF, S., SHIPLEY, J. M., SENIOR, R. M., BORNSTEIN, P. & KYRIAKIDES, T. R. 2009. Macrophage fusion, giant cell formation, and the foreign body response require matrix metalloproteinase 9. *Journal of Leukocyte Biology,* 85**,** 617-626.

MALONEY, A. & WORKMAN, P. 2002. HSP90 as a new therapeutic target for cancer therapy: the story unfolds. *Expert Opinion on Biological Therapy,* 2**,** 3-24.

MANCINI, M. & TOKER, A. 2009. NFAT proteins: emerging roles in cancer progression. *Nat Rev Cancer,* 9**,** 810-820.

MANOLAGAS, S. C. 2000. Birth and death of bone cells: basic regulatory mechanisms and implications for the pathogenesis and treatment of osteoporosis. *Endocr Rev,* 21**,** 115-37.

MANSKY, K. C., SANKAR, U., HAN, J. & OSTROWSKI, M. C. 2002a. Microphthalmia Transcription Factor Is a Target of the p38 MAPK Pathway in Response to Receptor Activator of NF-κB Ligand Signaling. *Journal of Biological Chemistry,* 277**,** 11077-11083.

MANSKY, K. C., SULZBACHER, S., PURDOM, G., NELSEN, L., HUME, D. A., REHLI, M. & OSTROWSKI, M. C. 2002b. The microphthalmia transcription factor and the related helix-loop-helix zipper factors TFE-3 and TFE-C collaborate to activate the tartrate-resistant acid phosphatase promoter. *Journal of Leukocyte Biology,* 71**,** 304-310.

MANWELL, L. A. & HEIKKILA, J. J. 2007. Examination of KNK437- and quercetin-mediated inhibition of heat shock-induced heat shock protein gene expression in Xenopus laevis cultured cells. *Comparative Biochemistry and Physiology - Part A: Molecular & Integrative Physiology,* 148**,** 521-530.

MARCU, M. G., DOYLE, M., BERTOLOTTI, A., RON, D., HENDERSHOT, L. & NECKERS, L. 2002. Heat Shock Protein 90 Modulates the Unfolded Protein Response by Stabilizing IRE1α. *Molecular and Cellular Biology,* 22**,** 8506-8513.

MARIEB, E. 2004. *In:* MURRAY, M. A. (ed.) *Human Anatomy and Physiology.* 6 ed. San Francisco, CA: Pearson Benjamin Cummings.

MARINA, M. & SAAVEDRA, H. I. 2014. Nek2 and Plk4: prognostic markers, drivers of breast tumorigenesis and drug resistance. *Frontiers in bioscience (Landmark edition),* 19**,** 352-365.

MARKS, S. C. 1983. The origin of osteoclasts. *Journal of Oral Pathology & Medicine,* 12**,** 226-256.

MARKS, S. C., JR. 1982. Morphological evidence of reduced bone resorption in osteopetrotic (op) mice. *Am J Anat,* 163**,** 157-67.

MARTIN, T. J., KONG WAH, N. & NICHOLSON, G. C. 1988. 1 Cell biology of bone. *Baillière's Clinical Endocrinology and Metabolism,* 2**,** 1-29.

MARTINDALE, J. L. & HOLBROOK, N. J. 2002. Cellular response to oxidative stress: Signaling for suicide and survival*. *Journal of Cellular Physiology,* 192**,** 1-15.

MATES, J. M., SEGURA, J. A., MARTIN-RUFIAN, M., CAMPOS-SANDOVAL, J. A., ALONSO, F. J. & MARQUEZ, J. 2013. Glutaminase isoenzymes as key regulators in metabolic and oxidative stress against cancer. *Curr Mol Med,* 13**,** 514-34.

MATSUMOTO, M., KOGAWA, M., WADA, S., TAKAYANAGI, H., TSUJIMOTO, M., KATAYAMA, S., HISATAKE, K. & NOGI, Y. 2004. Essential Role of p38 Mitogen-activated Protein Kinase in Cathepsin K Gene Expression during Osteoclastogenesis through Association of NFATc1 and PU.1. *Journal of Biological Chemistry,* 279**,** 45969-45979.

MATSUMOTO, M., SUDO, T., SAITO, T., OSADA, H. & TSUJIMOTO, M. 2000. Involvement of p38 Mitogen-activated Protein Kinase Signaling Pathway in Osteoclastogenesis Mediated by Receptor Activator of NF-κB Ligand (RANKL). *Journal of Biological Chemistry,* 275**,** 31155-31161.

MATSUMOTO, N., DAIDO, S., SUN-WADA, G.-H., WADA, Y., FUTAI, M. & NAKANISHI-MATSUI, M. 2014. Diversity of proton pumps in osteoclasts: V-ATPase with a3 and d2 isoforms is a major form in osteoclasts. *Biochimica et Biophysica Acta (BBA) - Bioenergetics,* 1837**,** 744-749.

MATSUO, K., GALSON, D. L., ZHAO, C., PENG, L., LAPLACE, C., WANG, K. Z. Q., BACHLER, M. A., AMANO, H., ABURATANI, H., ISHIKAWA, H. & WAGNER, E. F. 2004. Nuclear Factor of Activated T-cells (NFAT) Rescues Osteoclastogenesis in Precursors Lacking c-Fos. *Journal of Biological Chemistry,* 279**,** 26475-26480.

MATSUO, K. & RAY, N. 2004. Osteoclasts, mononuclear phagocytes, and c-Fos: new insight into osteoimmunology. *The Keio Journal of Medicine,* 53**,** 78-84.

MATSUZAKI, K., UDAGAWA, N., TAKAHASHI, N., YAMAGUCHI, K., YASUDA, H., SHIMA, N., MORINAGA, T., TOYAMA, Y., YABE, Y., HIGASHIO, K. & SUDA, T. 1998. Osteoclast Differentiation Factor (ODF) Induces Osteoclast-like Cell Formation in Human Peripheral Blood Mononuclear Cell Cultures. *Biochemical and Biophysical Research Communications,* 246**,** 199-204.

MATTERN, M. R., WU, J. & NICHOLSON, B. 2012. Ubiquitin-based anticancer therapy: Carpet bombing with proteasome inhibitors vs surgical strikes with E1, E2, E3, or DUB inhibitors. *Biochimica et Biophysica Acta (BBA) - Molecular Cell Research,* 1823**,** 2014-2021.

MAURER, M. & VON STEBUT, E. 2004. Macrophage inflammatory protein-1. *The International Journal of Biochemistry & Cell Biology,* 36**,** 1882-1886.

MAYER, M. P. & BUKAU, B. 2005. Hsp70 chaperones: Cellular functions and molecular mechanism. *Cellular and Molecular Life Sciences,* 62**,** 670-684.

MCDONOUGH, H. & PATTERSON, C. 2003. CHIP: a link between the chaperone and proteasome systems. *Cell Stress & Chaperones,* 8**,** 303-308.

MCHUGH, K. P., HODIVALA-DILKE, K., ZHENG, M.-H., NAMBA, N., LAM, J., NOVACK, D., FENG, X., ROSS, F. P., HYNES, R. O. & TEITELBAUM, S. L. 2000. Mice lacking β3 integrins are osteosclerotic because of dysfunctional osteoclasts. *Journal of Clinical Investigation,* 105**,** 433-440.

MCHUGH, K. P., SHEN, Z., CROTTI, T. N., FLANNERY, M. R., O'SULLIVAN, R. P., PURDUE, P. E. & GOLDRING, S. R. 2010. The role of cell–substrate interaction in

regulating osteoclast activation: potential implications in targeting bone loss in rheumatoid arthritis. *Annals of the Rheumatic Diseases,* 69**,** i83-i85.

MCINERNEY, M., SERRANO RODRIGUEZ, G., PAWLINA, W., HURT, C. B., FLETCHER, B. S., LAIPIS, P. J. & FROST, S. C. 2002. Glycogen phosphorylase is activated in response to glucose deprivation but is not responsible for enhanced glucose transport activity in 3T3-L1 adipocytes. *Biochimica et Biophysica Acta (BBA) - General Subjects,* 1570**,** 53-62.

MCMILLAN, D. R., XIAO, X., SHAO, L., GRAVES, K. & BENJAMIN, I. J. 1998. Targeted Disruption of Heat Shock Transcription Factor 1 Abolishes Thermotolerance and Protection against Heat-inducible Apoptosis. *Journal of Biological Chemistry,* 273**,** 7523-7528.

MEADOWS, N. A., SHARMA, S. M., FAULKNER, G. J., OSTROWSKI, M. C., HUME, D. A. & CASSADY, A. I. 2007. The Expression of Clcn7 and Ostm1 in Osteoclasts Is Coregulated by Microphthalmia Transcription Factor. *Journal of Biological Chemistry,* 282**,** 1891-1904.

MELLING, C. W. J., THORP, D. B., MILNE, K. J. & NOBLE, E. G. 2009. Myocardial Hsp70 phosphorylation and PKC-mediated cardioprotection following exercise. *Cell Stress & Chaperones,* 14**,** 141-150.

MELLIS, D. J., ITZSTEIN, C., HELFRICH, M. H. & CROCKETT, J. C. 2011. The skeleton: a multi-functional complex organ. The role of key signalling pathways in osteoclast differentiation and in bone resorption. *Journal of Endocrinology,* 211**,** 131-143.

MENG, L., GABAI, V. L. & SHERMAN, M. Y. 2010. Heat-shock transcription factor HSF1 has a critical role in human epidermal growth factor receptor-2-induced cellular transformation and tumorigenesis. *Oncogene,* 29**,** 5204-5213.

MERCER, K. E., WYNNE, R. A., LAZARENKO, O. P., LUMPKIN, C. K., HOGUE, W. R., SUVA, L. J., CHEN, J.-R., MASON, A. Z., BADGER, T. M. & RONIS, M. J. J. 2012. Vitamin D Supplementation Protects against Bone Loss Associated with Chronic Alcohol Administration in Female Mice. *Journal of Pharmacology and Experimental Therapeutics,* 343**,** 401-412.

MILLSON, S. H., TRUMAN, A. W., KING, V., PRODROMOU, C., PEARL, L. H. & PIPER, P. W. 2005. A Two-Hybrid Screen of the Yeast Proteome for Hsp90 Interactors Uncovers a Novel Hsp90 Chaperone Requirement in the Activity of a Stress-Activated Mitogen-Activated Protein Kinase, Slt2p (Mpk1p). *Eukaryotic Cell,* 4**,** 849-860.

MINAMI, M., NAKAMURA, M., EMORI, Y. & MINAMI, Y. 2001. Both the N- and C-terminal chaperone sites of Hsp90 participate in protein refolding. *Eur J Biochem,* 268**,** 2520-4.

MIYAMOTO, H., SUZUKI, T., MIYAUCHI, Y., IWASAKI, R., KOBAYASHI, T., SATO, Y., MIYAMOTO, K., HOSHI, H., HASHIMOTO, K., YOSHIDA, S., HAO, W., MORI, T., KANAGAWA, H., KATSUYAMA, E., FUJIE, A., MORIOKA, H., MATSUMOTO, M., CHIBA, K., TAKEYA, M., TOYAMA, Y. & MIYAMOTO, T. 2012. Osteoclast stimulatory transmembrane protein and dendritic cell–specific transmembrane protein cooperatively modulate cell–cell fusion to form osteoclasts and foreign body giant cells. *Journal of Bone and Mineral Research,* 27**,** 1289-1297.

MIYAMOTO, T. 2011. Regulators of Osteoclast Differentiation and Cell-Cell Fusion. *The Keio Journal of Medicine,* 60**,** 101-105.

MIYAZAKI, T., TOKIMURA, F. & TANAKA, S. 2014. A review of denosumab for the treatment of osteoporosis. *Patient preference and adherence,* 8**,** 463-471.

MIZUKAMI, J., TAKAESU, G., AKATSUKA, H., SAKURAI, H., NINOMIYA-TSUJI, J., MATSUMOTO, K. & SAKURAI, N. 2002. Receptor Activator of NF-κB Ligand

(RANKL) Activates TAK1 Mitogen-Activated Protein Kinase Kinase Kinase through a Signaling Complex Containing RANK, TAB2, and TRAF6. *Molecular and Cellular Biology,* 22**,** 992-1000.

MKELE, G. 2010. Rational selection of Cancer Therapeutics. *SA Pharmaceutical Journal***,** 32-34.

MODI, S., STOPECK, A., LINDEN, H., SOLIT, D., CHANDARLAPATY, S., ROSEN, N., D'ANDREA, G., DICKLER, M., MOYNAHAN, M. E., SUGARMAN, S., MA, W., PATIL, S., NORTON, L., HANNAH, A. L. & HUDIS, C. 2011. HSP90 Inhibition Is Effective in Breast Cancer: A Phase II Trial of Tanespimycin (17-AAG) Plus Trastuzumab in Patients with HER2-Positive Metastatic Breast Cancer Progressing on Trastuzumab. *Clinical Cancer Research,* 17**,** 5132-5139.

MOON, H.-J., KO, W.-K., HAN, S. W., KIM, D.-S., HWANG, Y.-S., PARK, H.-K. & KWON, I. K. 2012a. Antioxidants, like coenzyme Q10, selenite, and curcumin, inhibited osteoclast differentiation by suppressing reactive oxygen species generation. *Biochemical and Biophysical Research Communications,* 418**,** 247-253.

MOON, J. B., KIM, J. H., KIM, K., YOUN, B. U., KO, A., LEE, S. Y. & KIM, N. 2012b. Akt Induces Osteoclast Differentiation through Regulating the GSK3β/NFATc1 Signaling Cascade. *The Journal of Immunology,* 188**,** 163-169.

MORCUENDE, J. A., GOMEZ, P., STACK, J., OJI, G., MARTIN, J., FREDERICKS, D. C. & BUCKWALTER, J. A. 2004. Effect of Chemotherapy on Segmental Bone Healing Enhanced by rhBMP-2. *The Iowa Orthopaedic Journal,* 24**,** 36-42.

MORI, G., AMELIO, P., FACCIO, R. & BRUNETTI, G. 2015a. Bone-Immune Cell Crosstalk: Bone Diseases. *Journal of Immunology Research,* 2015**,** 11.

MORI, M., HITORA, T., NAKAMURA, O., YAMAGAMI, Y., HORIE, R., NISHIMURA, H. & YAMAMOTO, T. 2015b. Hsp90 inhibitor induces autophagy and apoptosis in osteosarcoma cells. *International Journal of Oncology,* 46**,** 47-54.

MORIMOTO, R. 2002. Heat-Shock Response. *Encyclopedia of Molecular Biology.* John Wiley & Sons, Inc.

MORIMOTO, R. I. 1993. Cells in stress: transcriptional activation of heat shock genes. *Science,* 259**,** 1409-10.

MORIMOTO, R. I. 1998. Regulation of the heat shock transcriptional response: cross talk between a family of heat shock factors, molecular chaperones, and negative regulators. *Genes & Development,* 12**,** 3788-3796.

MORIMOTO, R. I. 2008. Proteotoxic stress and inducible chaperone networks in neurodegenerative disease and aging. *Genes & Development,* 22**,** 1427-1438.

MORRISON, S. J. & SCADDEN, D. T. 2014. The bone marrow niche for haematopoietic stem cells. *Nature,* 505**,** 327-334.

MOSSER, D. D. & MORIMOTO, R. I. 2004. Molecular chaperones and the stress of oncogenesis. *Oncogene,* 23**,** 2907-2918.

MOTYCKOVA, G., WEILBAECHER, K. N., HORSTMANN, M., RIEMAN, D. J., FISHER, D. Z. & FISHER, D. E. 2001. Linking osteopetrosis and pycnodysostosis: Regulation of cathepsin K expression by the microphthalmia transcription factor family. *Proceedings of the National Academy of Sciences,* 98**,** 5798-5803.

MULLER, P., RUCKOVA, E., HALADA, P., COATES, P. J., HRSTKA, R., LANE, D. P. & VOJTESEK, B. 2013. C-terminal phosphorylation of Hsp70 and Hsp90 regulates alternate binding to co-chaperones CHIP and HOP to determine cellular protein folding/degradation balances. *Oncogene,* 32**,** 3101-3110.

MUN, S. H., WON, H. Y., HERNANDEZ, P., AGUILA, H. L. & LEE, S.-K. 2013. Deletion of CD74, a putative MIF receptor, in mice enhances osteoclastogenesis and decreases

bone mass. *Journal of bone and mineral research : the official journal of the American Society for Bone and Mineral Research,* 28**,** 948-959.

MUNDY, G. R. 1991. Mechanisms of osteolytic bone destruction. *Bone,* 12**,** S1-S6.

MUNDY, G. R. 1997. Mechanisms of bone metastasis. *Cancer,* 80**,** 1546-56.

MUNDY, G. R. 2002. Metastasis: Metastasis to bone: causes, consequences and therapeutic opportunities. *Nat Rev Cancer,* 2**,** 584-593.

MUNDY, G. R. 2007. Osteoporosis and Inflammation. *Nutrition Reviews,* 65**,** S147-S151.

MUNDY, G. R. & GUISE, T. A. 1997. Hypercalcemia of malignancy. *Am J Med,* 103**,** 134-45.

MURALIDHARAN, S. & MANDREKAR, P. 2013. Cellular stress response and innate immune signaling: integrating pathways in host defense and inflammation. *Journal of Leukocyte Biology,* 94**,** 1167-1184.

MURATA, S., CHIBA, T. & TANAKA, K. 2003. CHIP: a quality-control E3 ligase collaborating with molecular chaperones. *The International Journal of Biochemistry & Cell Biology,* 35**,** 572-578.

MURESAN, M. M., OLIVIER, P., LECLÈRE, J., SIRVEAUX, F., BRUNAUD, L., KLEIN, M., ZARNEGAR, R. & WERYHA, G. 2008. Bone metastases from differentiated thyroid carcinoma. *Endocrine-Related Cancer,* 15**,** 37-49.

MURPHY, MICHAEL P. 2009. How mitochondria produce reactive oxygen species. *Biochemical Journal,* 417**,** 1-13.

NAHAS, N., MOLSKI, T. F., FERNANDEZ, G. A. & SHA'AFI, R. I. 1996. Tyrosine phosphorylation and activation of a new mitogen-activated protein (MAP)-kinase cascade in human neutrophils stimulated with various agonists. *Biochemical Journal,* 318**,** 247-253.

NAKAJIMA, S., KATO, H., TAKAHASHI, S., JOHNO, H. & KITAMURA, M. 2011. Inhibition of NF-κB by MG132 through ER stress-mediated induction of LAP and LIP. *FEBS Letters,* 585**,** 2249-2254.

NAKAMOTO, H. & VÍGH, L. 2007. The small heat shock proteins and their clients. *Cellular and Molecular Life Sciences,* 64**,** 294-306.

NAKAMURA, H. 2007. Morphology, Function, and Differentiation of Bone Cells. *Journal of Hard Tissue Biology,* 16**,** 15-22.

NAKAMURA, H., HIRATA, A., TSUJI, T. & YAMAMOTO, T. 2003. Role of Osteoclast Extracellular Signal-Regulated Kinase (ERK) in Cell Survival and Maintenance of Cell Polarity. *Journal of Bone and Mineral Research,* 18**,** 1198-1205.

NAKASHIMA, T., HAYASHI, M., FUKUNAGA, T., KURATA, K., OH-HORA, M., FENG, J. Q., BONEWALD, L. F., KODAMA, T., WUTZ, A., WAGNER, E. F., PENNINGER, J. M. & TAKAYANAGI, H. 2011. Evidence for osteocyte regulation of bone homeostasis through RANKL expression. *Nat Med,* 17**,** 1231-1234.

NAKAYAMA, A., NGUYEN, M.-T. T., CHEN, C. C., OPDECAMP, K., HODGKINSON, C. A. & ARNHEITER, H. 1998. Mutations in microphthalmia, the mouse homolog of the human deafness gene MITF, affect neuroepithelial and neural crest-derived melanocytes differently. *Mechanisms of Development,* 70**,** 155-166.

NAKKA, V., PRAKASH-BABU, P. & VEMUGANTI, R. 2014. Crosstalk Between Endoplasmic Reticulum Stress, Oxidative Stress, and Autophagy: Potential Therapeutic Targets for Acute CNS Injuries. *Molecular Neurobiology***,** 1-13.

NATIONAL INSTITUTE OF HEALTH. 2014. *Clinicaltrials.gov: a service of the US National Institute of Health (NIH)* [Online]. Available: http://clinicaltrials.gov.

NECKERS, L. 2002. Hsp90 inhibitors as novel cancer chemotherapeutic agents. *Trends in Molecular Medicine,* 8**,** S55-S61.

NECKERS, L. & WORKMAN, P. 2012. Hsp90 Molecular Chaperone Inhibitors: Are We There Yet? *Clinical Cancer Research,* 18**,** 64-76.

NEEF, D. W., JAEGER, A. M. & THIELE, D. J. 2013. Genetic Selection for Constitutively Trimerized Human HSF1 Mutants Identifies a Role for Coiled-Coil Motifs in DNA Binding. *G3: Genes|Genomes|Genetics,* 3**,** 1315-1324.

NEGISHI-KOGA, T. & TAKAYANAGI, H. 2009. Ca2+-NFATc1 signaling is an essential axis of osteoclast differentiation. *Immunological Reviews,* 231**,** 241-256.

NEIDHARDT, F. C., VANBOGELEN, R. A. & VAUGHN, V. 1984. The genetics and regulation of heat-shock proteins. *Annu Rev Genet,* 18**,** 295-329.

NESBITT, S., NESBIT, A., HELFRICH, M. & HORTON, M. 1993. Biochemical characterization of human osteoclast integrins. Osteoclasts express alpha v beta 3, alpha 2 beta 1, and alpha v beta 1 integrins. *Journal of Biological Chemistry,* 268**,** 16737-16745.

NESBITT, S. A. & HORTON, M. A. 1997. Trafficking of Matrix Collagens Through Bone-Resorbing Osteoclasts. *Science,* 276**,** 266-269.

NEUEDER, A., ACHILLI, F., MOUSSAOUI, S. & BATES, G. P. 2014. Novel Isoforms of Heat Shock Transcription Factor 1, HSF1γα and HSF1γβ, Regulate Chaperone Protein Gene Transcription. *Journal of Biological Chemistry*.

NEVE, A., CORRADO, A. & CANTATORE, F. P. 2011. Osteoblast physiology in normal and pathological conditions. *Cell and Tissue Research,* 343**,** 289-302.

NGUYEN, C. H., LANG, B. J., CHAI, R. C., VIEUSSEUX, J. L., KOUSPOU, M. M. & PRICE, J. T. 2013. Heat-shock factor 1 both positively and negatively affects cellular clonogenic growth depending on p53 status. *Biochem J,* 452**,** 321-9.

NICHOLSON, G. C., MOSELEY, J. M., SEXTON, P. M., MENDELSOHN, F. A. & MARTIN, T. J. 1986. Abundant calcitonin receptors in isolated rat osteoclasts. Biochemical and autoradiographic characterization. *Journal of Clinical Investigation,* 78**,** 355-360.

NISHIKAWA, K., NAKASHIMA, T., HAYASHI, M., FUKUNAGA, T., KATO, S., KODAMA, T., TAKAHASHI, S., CALAME, K. & TAKAYANAGI, H. 2010. Blimp1-mediated repression of negative regulators is required for osteoclast differentiation. *Proceedings of the National Academy of Sciences of the United States of America,* 107**,** 3117-3122.

NOBLE, B. S. 2008. The osteocyte lineage. *Archives of Biochemistry and Biophysics,* 473**,** 106-111.

NOONAN, E. J., PLACE, R. F., RASOULPOUR, R. J., GIARDINA, C. & HIGHTOWER, L. E. 2007. Cell number-dependent regulation of Hsp70B′ expression: Evidence of an extracellular regulator. *Journal of Cellular Physiology,* 210**,** 201-211.

NOORI, S. 2012. An Overview of Oxidative Stress and Antioxidant Defensive System. *Open Access Scientific Reports,* 1.

NOVACK, D. V., YIN, L., HAGEN-STAPLETON, A., SCHREIBER, R. D., GOEDDEL, D. V., ROSS, F. P. & TEITELBAUM, S. L. 2003. The IκB Function of NF-κB2 p100 Controls Stimulated Osteoclastogenesis. *The Journal of Experimental Medicine,* 198**,** 771-781.

NOVER, L. & SCHARF, K. D. 1997. Heat stress proteins and transcription factors. *Cell Mol Life Sci,* 53**,** 80-103.

NUSSBAUMER, S., BONNABRY, P., VEUTHEY, J.-L. & FLEURY-SOUVERAIN, S. 2011. Analysis of anticancer drugs: A review. *Talanta,* 85**,** 2265-2289.

O'BRIEN, C., A. 2010. Control of RANKL gene expression. *Bone,* 46**,** 911-919.

OBATA, T., BROWN, G. E. & YAFFE, M. B. 2000. MAP kinase pathways activated by stress: the p38 MAPK pathway. *Crit Care Med,* 28**,** N67-77.

ODGREN, P. R., KIM, N., MACKAY, C. A., MASON-SAVAS, A., CHOI, Y. & MARKS, J. S. C. 2003. The Role of RANKL (TRANCE/TNFSF11), a Tumor Necrosis Factor Family Member, in Skeletal Development: Effects of Gene Knockout and Transgenic Rescue. *Connective Tissue Research,* 44**,** 264-271.

OFFICE OF THE SURGEON GENERAL (US) 2004. *2 The Basics of Bone in Health and Diseasel,* Rockville (MD), Office of the Surgeon General (US).

OHNISHI, K., TAKAHASHI, A., YOKOTA, S. & OHNISHI, T. 2004. Effects of a heat shock protein inhibitor KNK437 on heat sensitivity and heat tolerance in human squamous cell carcinoma cell lines differing in p53 status. *International Journal of Radiation Biology,* 80**,** 607-614.

OHNO, K., ISHIHATA, K., TANAKA-AZUMA, Y. & YAMADA, T. 2008. A genotoxicity test system based on p53R2 gene expression in human cells: assessment of its reactivity to various classes of genotoxic chemicals. *Mutat Res,* 656**,** 27-35.

OHTSUBOA, T., KANOB, E., UEDAC, K., MATSUMOTOB, H., SAITOA, T., HAYASHIB, S., HATASHITAB, M., JINB, Z.-H. & SAITOA, H. 2000. Enhancement of heat-induced heat shock protein (hsp)72 accumulation by doxorubicin (Dox) in vitro. *Cancer Letters,* 159**,** 49-55.

OKAMATSU, Y., KIM, D., BATTAGLINO, R., SASAKI, H., SPÄTE, U. & STASHENKO, P. 2004. MIP-1γ Promotes Receptor Activator of NF-κB Ligand-Induced Osteoclast Formation and Survival. *The Journal of Immunology,* 173**,** 2084-2090.

ONAL, M., GALLI, C., FU, Q., XIONG, J., WEINSTEIN, R. S., MANOLAGAS, S. C. & O'BRIEN, C. A. 2012. The RANKL Distal Control Region Is Required for the Increase in RANKL Expression, But Not the Bone Loss, Associated with Hyperparathyroidism or Lactation in Adult Mice. *Molecular Endocrinology,* 26**,** 341-348.

ORTIZ, A. & LIN, S. H. 2012. Osteolytic and osteoblastic bone metastases: two extremes of the same spectrum? *Recent Results Cancer Res,* 192**,** 225-33.

OSLOWSKI, C. M. & URANO, F. 2011. Measuring ER stress and the unfolded protein response using mammalian tissue culture system. *Methods in enzymology,* 490**,** 71-92.

OZGUR, A. & TUTAR, Y. 2014. Heat Shock Protein 90 Inhibitors in Oncology. *Current Proteomics,* 11**,** 2-16.

PACEY, S., BANERJI, U., JUDSON, I. & WORKMAN, P. 2006. Hsp90 inhibitors in the clinic. *Handb Exp Pharmacol***,** 331-58.

PACIFICI, R., BROWN, C., PUSCHECK, E., FRIEDRICH, E., SLATOPOLSKY, E., MAGGIO, D., MCCRACKEN, R. & AVIOLI, L. V. 1991. Effect of surgical menopause and estrogen replacement on cytokine release from human blood mononuclear cells. *Proceedings of the National Academy of Sciences,* 88**,** 5134-5138.

PAJEVIC, P. D. 2009. Regulation of bone resorption and mineral homeostasis by osteocytes. *IBMS BoneKEy,* 6**,** 63-70.

PALAFOX, M., FERRER, I., PELLEGRINI, P., VILA, S., HERNANDEZ-ORTEGA, S., URRUTICOECHEA, A., CLIMENT, F., SOLER, M. T., MUÑOZ, P., VIÑALS, F., TOMETSKO, M., BRANSTETTER, D., DOUGALL, W. C. & GONZÁLEZ-SUÁREZ, E. 2012. RANK Induces Epithelial–Mesenchymal Transition and Stemness in Human Mammary Epithelial Cells and Promotes Tumorigenesis and Metastasis. *Cancer Research,* 72**,** 2879-2888.

PALMQVIST, P., PERSSON, E., CONAWAY, H. H. & LERNER, U. H. 2002. IL-6, leukemia inhibitory factor, and oncostatin M stimulate bone resorption and regulate the expression of receptor activator of NF-kappa B ligand, osteoprotegerin, and receptor activator of NF-kappa B in mouse calvariae. *J Immunol,* 169**,** 3353-62.

PALOKANGAS, H., MULARI, M. & VAANANEN, H. K. 1997. Endocytic pathway from the basal plasma membrane to the ruffled border membrane in bone-resorbing osteoclasts. *J Cell Sci,* 110 (Pt 15)**,** 1767-80.

PAN, M. G., XIONG, Y. & CHEN, F. 2013. NFAT Gene Family in Inflammation and Cancer. *Current molecular medicine,* 13**,** 543-554.

PARK, H. R., MIN, S. K., CHO, H. D., KIM, D. H., SHIN, H. S. & PARK, Y. E. 2003. Expression of Osteoprotegerin and RANK Ligand in Breast Cancer Bone Metastasis. *J Korean Med Sci,* 18**,** 541-546.

PARK, J. & LIU, A. Y. C. 2001. JNK phosphorylates the HSF1 transcriptional activation domain: Role of JNK in the regulation of the heat shock response. *J Cell Biochem,* 82**,** 326-338.

PARKER, W. B. 2009. Enzymology of Purine and Pyrimidine Antimetabolites Used in the Treatment of Cancer. *Chemical reviews,* 109**,** 2880-2893.

PATEL, H. J., MODI, S., CHIOSIS, G. & TALDONE, T. 2011. Advances in the discovery and development of heat-shock protein 90 inhibitors for cancer treatment. *Expert Opinion on Drug Discovery,* 6**,** 559-587.

PATEL, P. 2009. *Role of p38MAPK, heat shock proteins, HSP27 and HSP70 in osmotic stress in renal vs. blood cells: A comparative study.* Thesis, University of the Sciences in Philadephia.

PAVLOS, N. J., XU, J., RIEDEL, D., YEOH, J. S. G., TEITELBAUM, S. L., PAPADIMITRIOU, J. M., JAHN, R., ROSS, F. P. & ZHENG, M. H. 2005. Rab3D Regulates a Novel Vesicular Trafficking Pathway That Is Required for Osteoclastic Bone Resorption. *Molecular and Cellular Biology,* 25**,** 5253-5269.

PEKNA, HIETALA, LANDIN, NILSSON, LAGERBERG, BETSHOLTZ & PEKNY 1998. Mice Deficient for the Complement Factor B Develop and Reproduce Normally. *Scandinavian Journal of Immunology,* 47**,** 375-380.

PENG, X., PENTASSUGLIA, L. & SAWYER, D. B. 2010. Emerging anti-cancer therapeutic targets and the cardiovascular system: Is there cause for concern? *Circulation research,* 106**,** 1022-1034.

PEREZ, C., CAMPAYO, L., NAVARRO, P., GARCIA-BERMEJO, L. & ALLER, P. 1994. The action of the DNA intercalating agents 4'-(9-acridinylamino) methanesulphon-m-anisidide and 1,4-bis(butylamino) benzo[g]phthalazine in U-937 human promonocytic cells: relationship between cell cycle and differentiation. *Biochem Pharmacol,* 48**,** 75-82.

PÉREZ DE CASTRO, I. & MALUMBRES, M. 2012. Mitotic Stress and Chromosomal Instability in Cancer: The Case for TPX2. *Genes & Cancer,* 3**,** 721-730.

PETTIT, A. R., JI, H., VON STECHOW, D., MULLER, R., GOLDRING, S. R., CHOI, Y., BENOIST, C. & GRAVALLESE, E. M. 2001. TRANCE/RANKL knockout mice are protected from bone erosion in a serum transfer model of arthritis. *Am J Pathol,* 159**,** 1689-99.

PHONG, M. S., VAN HORN, R. D., LI, S., TUCKER-KELLOGG, G., SURANA, U. & YE, X. S. 2010. p38 Mitogen-Activated Protein Kinase Promotes Cell Survival in Response to DNA Damage but Is Not Required for the G2 DNA Damage Checkpoint in Human Cancer Cells. *Molecular and Cellular Biology,* 30**,** 3816-3826.

PIERCE, A. M., LINDSKOG, S. & HAMMARSTRÖM, L. 1991. Osteoclasts: Structure and function. *Electron Microscopy Reviews,* 4**,** 1-45.

PIGNATARO, L., MILLER, A. N., MA, L., MIDHA, S., PROTIVA, P., HERRERA, D. G. & HARRISON, N. L. 2007. Alcohol Regulates Gene Expression in Neurons via Activation of Heat Shock Factor 1. *The Journal of Neuroscience,* 27**,** 12957-12966.

PIKOR, L., THU, K., VUCIC, E. & LAM, W. 2013. The detection and implication of genome instability in cancer. *Cancer and Metastasis Reviews,* 32**,** 341-352.

PIPERDI, B., LING, Y.-H., LIEBES, L., MUGGIA, F. & PEREZ-SOLER, R. 2011. Bortezomib: Understanding the Mechanism of Action. *Molecular Cancer Therapeutics,* 10**,** 2029-2030.

PIRKKALA, L., NYKANEN, P. & SISTONEN, L. 2001. Roles of the heat shock transcription factors in regulation of the heat shock response and beyond. *The FASEB Journal,* 15**,** 1118-1131.

PITTAS, A. G., ADLER, M., FAZZARI, M., TICKOO, S., ROSAI, J., LARSON, S. M. & ROBBINS, R. J. 2000. Bone metastases from thyroid carcinoma: clinical characteristics and prognostic variables in one hundred forty-six patients. *Thyroid,* 10**,** 261-8.

POGENBERG, V., ÖGMUNDSDÓTTIR, M., BERGSTEINSDÓTTIR, K., SCHEPSKY, A., PHUNG, B., DEINEKO, V., MILEWSKI, M., STEINGRÍMSSON, E. & WILMANNS, M. 2012. Restricted leucine zipper dimerization and specificity of DNA recognition of the melanocyte master regulator MITF. *Genes & Development,* 26**,** 2647-2658.

POLASCIK, T. J. & MOURAVIEV, V. 2008. Zoledronic acid in the management of metastatic bone disease. *Therapeutics and Clinical Risk Management,* 4**,** 261-268.

POLJSAK, B., #X160, UPUT, D., #X161, AN & MILISAV, I. 2013. Achieving the Balance between ROS and Antioxidants: When to Use the Synthetic Antioxidants. *Oxidative Medicine and Cellular Longevity,* 2013**,** 11.

PONTANO, L. L., AGGARWAL, P., BARBASH, O., BROWN, E. J., BASSING, C. H. & DIEHL, J. A. 2008. Genotoxic Stress-Induced Cyclin D1 Phosphorylation and Proteolysis Are Required for Genomic Stability. *Molecular and Cellular Biology,* 28**,** 7245-7258.

PORTER, J. R., FRITZ, C. C. & DEPEW, K. M. 2010. Discovery and development of Hsp90 inhibitors: a promising pathway for cancer therapy. *Current Opinion in Chemical Biology,* 14**,** 412-420.

POWERS, M. V. & WORKMAN, P. 2007. Inhibitors of the heat shock response: Biology and pharmacology. *FEBS Letters,* 581**,** 3758-3769.

PRATT, W. B., MORISHIMA, Y., PENG, H.-M. & OSAWA, Y. 2010. Proposal for a role of the Hsp90/Hsp70-based chaperone machinery in making triage decisions when proteins undergo oxidative and toxic damage. *Experimental Biology and Medicine,* 235**,** 278-289.

PRICE, J. T., QUINN, J. M. W., SIMS, N. A., VIEUSSEUX, J., WALDECK, K., DOCHERTY, S. E., MYERS, D., NAKAMURA, A., WALTHAM, M. C., GILLESPIE, M. T. & THOMPSON, E. W. 2005. The Heat Shock Protein 90 Inhibitor, 17-Allylamino-17-demethoxygeldanamycin, Enhances Osteoclast Formation and Potentiates Bone Metastasis of a Human Breast Cancer Cell Line. *Cancer Research,* 65**,** 4929-4938.

QI, B., CONG, Q., LI, P., MA, G., GUO, X., YEH, J., XIE, M., SCHNEIDER, M. D., LIU, H. & LI, B. 2014. Ablation of Tak1 in osteoclast progenitor leads to defects in skeletal growth and bone remodeling in mice. *Sci. Rep.,* 4.

QIN, A., CHENG, T. S., PAVLOS, N. J., LIN, Z., DAI, K. R. & ZHENG, M. H. 2012. V-ATPases in osteoclasts: Structure, function and potential inhibitors of bone resorption. *The International Journal of Biochemistry & Cell Biology,* 44**,** 1422-1435.

QING, G., YAN, P. & XIAO, G. 2006. Hsp90 inhibition results in autophagy-mediated proteasome-independent degradation of I[kappa]B kinase (IKK). *Cell Res,* 16**,** 895-901.

QUAN, J., JOHNSON, N., ZHOU, G., PARSONS, P., BOYLE, G. & GAO, J. 2012. Potential molecular targets for inhibiting bone invasion by oral squamous cell carcinoma: a review of mechanisms. *Cancer and Metastasis Reviews,* 31**,** 209-219.

QUINN, J. M. W., ELLIOTT, J., GILLESPIE, M. T. & MARTIN, T. J. 1998. A Combination of Osteoclast Differentiation Factor and Macrophage-Colony Stimulating Factor Is Sufficient for both Human and Mouse Osteoclast Formation in Vitro. *Endocrinology,* 139**,** 4424-4427.

QUINN, J. M. W., FUJIKAWA, Y., MCGEE, J. O. D. & ATHANASOU, N. A. 1997. Rodent osteoblast-like cells support osteoclastic differentiation of human cord blood monocytes in the presence of M-CSF and 1,25 dihydroxyvitamin D3. *The International Journal of Biochemistry & Cell Biology,* 29**,** 173-179.

QUINN, J. M. W., ITOH, K., UDAGAWA, N., HÄUSLER, K., YASUDA, H., SHIMA, N., MIZUNO, A., HIGASHIO, K., TAKAHASHI, N., SUDA, T., MARTIN, T. J. & GILLESPIE, M. T. 2001. Transforming Growth Factor β Affects Osteoclast Differentiation via Direct and Indirect Actions. *Journal of Bone and Mineral Research,* 16**,** 1787-1794.

QUINN, J. M. W., MORFIS, M., LAM, M. H. C., ELLIOTT, J., KARTSOGIANNIS, V., WILLIAMS, E. D., GILLESPIE, M. T., MARTIN, T. J. & SEXTON, P. M. 1999. Calcitonin receptor antibodies in the identification of osteoclasts. *Bone,* 25**,** 1-8.

RAFIEE, P., THERIOT, M. E., NELSON, V. M., HEIDEMANN, J., KANAA, Y., HOROWITZ, S. A., ROGACZEWSKI, A., JOHNSON, C. P., ALI, I., SHAKER, R. & BINION, D. G. 2006. Human esophageal microvascular endothelial cells respond to acidic pH stress by PI3K/AKT and p38 MAPK-regulated induction of Hsp70 and Hsp27. *American Journal of Physiology - Cell Physiology,* 291**,** C931-C945.

RAFIQUE, S. 2010. Transition metal complexes as potential therapeutic agents. *Biotechnology and Molecular Biology Reviews,* 5**,** 38-45.

RAGGATT, L. J. & PARTRIDGE, N. C. 2010. Cellular and molecular mechanisms of bone remodeling. *J Biol Chem,* 285**,** 25103-8.

RAHIM, F., HAJIZAMANI, S., MORTAZ, E., AHMADZADEH, A., SHAHJAHANI, M., SHAHRABI, S. & SAKI, N. 2014. Molecular Regulation of Bone Marrow Metastasis in Prostate and Breast Cancer. *Bone Marrow Research,* 2014**,** 12.

RAINGEAUD, J., GUPTA, S., ROGERS, J. S., DICKENS, M., HAN, J., ULEVITCH, R. J. & DAVIS, R. J. 1995. Pro-inflammatory Cytokines and Environmental Stress Cause p38 Mitogen-activated Protein Kinase Activation by Dual Phosphorylation on Tyrosine and Threonine. *Journal of Biological Chemistry,* 270**,** 7420-7426.

RALHAN, R. & KAUR, J. 2007. Alkylating agents and cancer therapy. *Expert Opinion on Therapeutic Patents,* 17**,** 1061-1075.

RALPH, P. & NAKOINZ, I. 1977. Antibody-Dependent Killing of Erythrocyte and Tumor Targets by Macrophage-Related Cell Lines: Enhancement by PPD and LPS. *The Journal of Immunology,* 119**,** 950-954.

RAMASWAMY, B. & SHAPIRO, C. L. 2003. Bisphosphonates in the prevention and treatment of bone metastases. *Oncology (Williston Park),* 17**,** 1261-70; discussion 1270-2, 1277-8, 1280.

RAMSEY, D. M., KITSON, R. R. A., LEVIN, J. I., MOODY, C. J. & MCALPINE, A. R. 2014. Recent Advances in Macrocyclic HSP90 Ihibitors. *In:* LEVIN, J. I. (ed.) *Macrocycles in Drug Discovery.* Royal Society of Chemistry.

RANA, T., CHAKRABARTI, A., FREEMAN, M. & BISWAS, S. 2013. Doxorubicin-Mediated Bone Loss in Breast Cancer Bone Metastases Is Driven by an Interplay between Oxidative Stress and Induction of TGFβ. *PLoS ONE,* 8**,** e78043.

RASCHKE, W., BAIRD, S., RALPH, P. & NAKOINZ, I. 1978. Functional macrophage cell lines transformed by Abelson leukemia virus. *Cell,* 15**,** 261 - 267.

RAVINDRAN, C., CHENG, Y.-C. & LIANG, S.-M. 2010. CpG-ODNs induces up-regulated expression of chemokine CCL9 in mouse macrophages and microglia. *Cellular Immunology,* 260**,** 113-118.

REUTER, S., GUPTA, S. C., CHATURVEDI, M. M. & AGGARWAL, B. B. 2010. Oxidative stress, inflammation, and cancer: How are they linked? *Free radical biology & medicine,* 49**,** 1603-1616.

RICHARDSON, P. G., MITSIADES, C. S., LAUBACH, J. P., LONIAL, S., CHANAN-KHAN, A. A. & ANDERSON, K. C. 2011. Inhibition of heat shock protein 90 (HSP90) as a therapeutic strategy for the treatment of myeloma and other cancers. *Br J Haematol,* 152**,** 367-79.

RICHTER, K., HASLBECK, M. & BUCHNER, J. 2010. The Heat Shock Response: Life on the Verge of Death. *Molecular Cell,* 40**,** 253-266.

RIEDEL, M., GOLDBAUM, O., SCHWARZ, L., SCHMITT, S. & RICHTER-LANDSBERG, C. 2010. 17-AAG Induces Cytoplasmic α-Synuclein Aggregate Clearance by Induction of Autophagy. *PLoS ONE,* 5**,** e8753.

RIZZOLI, R., YASOTHAN, U. & KIRKPATRICK, P. 2010. Denosumab. *Nat Rev Drug Discov,* 9**,** 591-592.

ROBINSON, M. J. & COBB, M. H. 1997. Mitogen-activated protein kinase pathways. *Curr Opin Cell Biol,* 9**,** 180-6.

ROBSON, H. 1999. Bone growth mechanisms and the effects of cytotoxic drugs. *Archives of Disease in Childhood,* 81**,** 360-364.

ROCCISANA, J. L., KAWANABE, N., KAJIYA, H., KOIDE, M., ROODMAN, G. D. & REDDY, S. V. 2004. Functional role for heat shock factors in the transcriptional regulation of human RANK ligand gene expression in stromal/osteoblast cells. *J Biol Chem,* 279**,** 10500-7.

RODRIGUES, L. M., CHUNG, Y.-L., AL SAFFAR, N. M. S., SHARP, S. Y., JACKSON, L. E., BANERJI, U., STUBBS, M., LEACH, M. O., GRIFFITHS, J. R. & WORKMAN, P. 2012. Effects of HSP90 inhibitor 17-allylamino-17-demethoxygeldanamycin (17-AAG) on NEU/HER2 overexpressing mammary tumours in MMTV-NEU-NT mice monitored by Magnetic Resonance Spectroscopy. *BMC Research Notes,* 5**,** 250-250.

RODRÍGUEZ, D., MORRISON, C. J. & OVERALL, C. M. 2010. Matrix metalloproteinases: What do they not do? New substrates and biological roles identified by murine models and proteomics. *Biochimica et Biophysica Acta (BBA) - Molecular Cell Research,* 1803**,** 39-54.

ROMAGNOLI, C., MARCUCCI, G., FAVILLI, F., ZONEFRATI, R., MAVILIA, C., GALLI, G., TANINI, A., IANTOMASI, T., BRANDI, M. L. & VINCENZINI, M. T. 2013. Role of GSH/GSSG redox couple in osteogenic activity and osteoclastogenic markers of human osteoblast-like SaOS-2 cells. *FEBS Journal,* 280**,** 867-879.

RON, D. & WALTER, P. 2007. Signal integration in the endoplasmic reticulum unfolded protein response. *Nat Rev Mol Cell Biol,* 8**,** 519-529.

ROODMAN, G. D. 1991. Osteoclast Differentiation. *Critical Reviews in Oral Biology & Medicine,* 2**,** 389-409.

ROODMAN, G. D. 2004. Mechanisms of Bone Metastasis. *New England Journal of Medicine,* 350**,** 1655-1664.

ROODMAN, G. D. & DOUGALL, W. C. 2008. RANK ligand as a therapeutic target for bone metastases and multiple myeloma. *Cancer Treatment Reviews,* 34**,** 92-101.

ROSENBERG, A. E. & ROTH, S. I. 2012. Bone. *In:* MILLS, S. (ed.) *Histology for Pathologists.* Lippincott Williams & Wilkins.

ROSS, F. P. 2006. M-CSF, c-Fms, and Signaling in Osteoclasts and their Precursors. *Annals of the New York Academy of Sciences,* 1068**,** 110-116.

ROSS, F. P. & TEITELBAUM, S. L. 2003. Genetic regulation of osteoclast development and function. *Nature Reviews Genetics,* 4**,** 638+.

ROUSSEL, M., FACON, T., MOREAU, P., HAROUSSEAU, J.-L. & ATTAL, M. 2011. Firstline Treatment and Maintenance in Newly Diagnosed Multiple Myeloma Patients. *In:* MOEHLER, T. & GOLDSCHMIDT, H. (eds.) *Multiple Myeloma.* Springer Berlin Heidelberg.

RUCCI, N. 2008. Molecular biology of bone remodelling. *Clinical Cases in Mineral and Bone Metabolism,* 5**,** 49-56.

RUFFENACH, G., LE GUEN, M., CHABOT, S., BREUILS-BONNET, S., TREMBLAY, E., PROVENCHER, S. & BONNET, S. 2015. The Chaperone Protein Hsp90 is Upregulated in Human Pulmonary Hypertension. *The FASEB Journal,* 29.

RUOSLAHTI, E. 1996. RGD AND OTHER RECOGNITION SEQUENCES FOR INTEGRINS. *Annual Review of Cell and Developmental Biology,* 12**,** 697-715.

RUSMINI, P., SIMONINI, F., CRIPPA, V., BOLZONI, E., ONESTO, E., CAGNIN, M., SAU, D., FERRI, N. & POLETTI, A. 2011. 17-AAG increases autophagic removal of mutant androgen receptor in spinal and bulbar muscular atrophy. *Neurobiology of Disease,* 41**,** 83-95.

SAHI, C., KNOX, J. J., CLEMONS, M., JOSHUA, A. M. & BROOM, R. 2010. Renal cell carcinoma bone metastases: clinical advances. *Therapeutic Advances in Medical Oncology,* 2**,** 75-83.

SALO, J., LEHENKARI, P., MULARI, M., METSIKKO, K. & VAANANEN, H. K. 1997. Removal of osteoclast bone resorption products by transcytosis. *Science,* 276**,** 270-3.

SANBE, T., TOMOFUJI, T., EKUNI, D., AZUMA, T., IRIE, K., TAMAKI, N., YAMAMOTO, T. & MORITA, M. 2009. Vitamin C intake inhibits serum lipid peroxidation and osteoclast differentiation on alveolar bone in rats fed on a high-cholesterol diet. *Archives of Oral Biology,* 54**,** 235-240.

SANDERSON, S., VALENTI, M., GOWAN, S., PATTERSON, L., AHMAD, Z., WORKMAN, P. & ECCLES, S. A. 2006. Benzoquinone ansamycin heat shock protein 90 inhibitors modulate multiple functions required for tumor angiogenesis. *Molecular Cancer Therapeutics,* 5**,** 522-532.

SATO, T., DEL CARMEN OVEJERO, M., HOU, P., HEEGAARD, A. M., KUMEGAWA, M., FOGED, N. T. & DELAISSE, J. M. 1997. Identification of the membrane-type matrix metalloproteinase MT1-MMP in osteoclasts. *Journal of Cell Science,* 110**,** 589-596.

SAUVAGEOT, C. M.-E., WEATHERBEE, J. L., KESARI, S., WINTERS, S. E., BARNES, J., DELLAGATTA, J., RAMAKRISHNA, N. R., STILES, C. D., KUNG, A. L.-J., KIERAN, M. W. & WEN, P. Y. C. 2009. Efficacy of the HSP90 inhibitor 17-AAG in human glioma cell lines and tumorigenic glioma stem cells. *Neuro-Oncology,* 11**,** 109-121.

SAWYERS, C. 2004. Targeted cancer therapy. *Nature,* 432**,** 294-297.

SCHETT, G. & REDLICH, K. 2009. Osteoclasts and Osteoblasts. *In:* MARC, C. H., MD, MPH, ALAN, J. S., FRCP, JOSEF, S. S., MICHAEL, E. W. & MICHAEL, H. W. (eds.) *Rheumatoid Arthritis.* Philadelphia: Mosby.

SCHEVEN, B. A. A., VISSER, J. W. M. & NIJWEIDE, P. J. 1986. In vitro osteoclast generation from different bone marrow fractions, including a highly enriched haematopoietic stem cell population. *Nature,* 321**,** 79-81.

SCHLESINGER, P. H., BLAIR, H. C., TEITELBAUM, S. L. & EDWARDS, J. C. 1997. Characterization of the Osteoclast Ruffled Border Chloride Channel and Its Role in Bone Resorption. *Journal of Biological Chemistry,* 272**,** 18636-18643.

SCHULTE, T. W. & NECKERS, L. M. 1998. The benzoquinone ansamycin 17-allylamino-17-demethoxygeldanamycin binds to HSP90 and shares important biologic activities with geldanamycin. *Cancer Chemotherapy and Pharmacology,* 42**,** 273-279.

SEETHALA, R. R., GOLDBLUM, J. R., HICKS, D. G., LEHMAN, M., KHURANA, J. S., PASHA, T. L. & ZHANG, P. J. 2004. Immunohistochemical evaluation of microphthalmia-associated transcription factor expression in giant cell lesions. *Mod Pathol,* 17**,** 1491-1496.

SELIMOVIC, D., PORZIG, B. B. O. W., EL-KHATTOUTI, A., BADURA, H. E., AHMAD, M., GHANJATI, F., SANTOURLIDIS, S., HAIKEL, Y. & HASSAN, M. 2013. Bortezomib/proteasome inhibitor triggers both apoptosis and autophagy-dependent pathways in melanoma cells. *Cellular Signalling,* 25**,** 308-318.

SERFLING, E., AVOTS, A., KLEIN-HESSLING, S., RUDOLF, R., VAETH, M. & BERBERICH-SIEBELT, F. 2012. NFATc1/alphaA: The other Face of NFAT Factors in Lymphocytes. *Cell Commun Signal,* 10**,** 16.

SGOBBA, M., FORESTIERO, R., DEGLIESPOSTI, G. & RASTELLI, G. 2010. Exploring the Binding Site of C-Terminal Hsp90 Inhibitors. *Journal of Chemical Information and Modeling,* 50**,** 1522-1528.

SHACKELFORD, R. E., KAUFMANN, W. K. & PAULES, R. S. 1999. Cell cycle control, checkpoint mechanisms, and genotoxic stress. *Environmental Health Perspectives,* 107**,** 5-24.

SHARMA, P., JHA, A. B., DUBEY, R. S. & PESSARAKLI, M. 2012. Reactive Oxygen Species, Oxidative Damage, and Antioxidative Defense Mechanism in Plants under Stressful Conditions. *Journal of Botany,* 2012**,** 26.

SHARMA, S., ZINGDE, S. & GOKHALE, S. 2013. Identification of Human Erythrocyte Cytosolic Proteins Associated with Plasma Membrane During Thermal Stress. *The Journal of Membrane Biology,* 246**,** 591-607.

SHARMA, S. M., BRONISZ, A., HU, R., PATEL, K., MANSKY, K. C., SIF, S. & OSTROWSKI, M. C. 2007. MITF and PU.1 Recruit p38 MAPK and NFATc1 to Target Genes during Osteoclast Differentiation. *Journal of Biological Chemistry,* 282**,** 15921-15929.

SHARP, S. Y., BOXALL, K., ROWLANDS, M., PRODROMOU, C., ROE, S. M., MALONEY, A., POWERS, M., CLARKE, P. A., BOX, G., SANDERSON, S., PATTERSON, L., MATTHEWS, T. P., CHEUNG, K.-M. J., BALL, K., HAYES, A., RAYNAUD, F., MARAIS, R., PEARL, L., ECCLES, S., AHERNE, W., MCDONALD, E. & WORKMAN, P. 2007a. In vitro Biological Characterization of a Novel, Synthetic Diaryl Pyrazole Resorcinol Class of Heat Shock Protein 90 Inhibitors. *Cancer Research,* 67**,** 2206-2216.

SHARP, S. Y., PRODROMOU, C., BOXALL, K., POWERS, M. V., HOLMES, J. L., BOX, G., MATTHEWS, T. P., CHEUNG, K.-M. J., KALUSA, A., JAMES, K., HAYES, A., HARDCASTLE, A., DYMOCK, B., BROUGH, P. A., BARRIL, X., CANSFIELD, J. E., WRIGHT, L., SURGENOR, A., FOLOPPE, N., HUBBARD, R. E., AHERNE, W., PEARL, L., JONES, K., MCDONALD, E., RAYNAUD, F., ECCLES, S., DRYSDALE, M. & WORKMAN, P. 2007b. Inhibition of the heat shock protein 90 molecular chaperone in vitro and in vivo by novel, synthetic, potent resorcinylic pyrazole/isoxazole amide analogues. *Molecular Cancer Therapeutics,* 6**,** 1198-1211.

SHEN, C.-L., YEH, J. K., CAO, J. & WANG, J.-S. 2009. Green Tea and Bone metabolism. *Nutrition research (New York, N.Y.),* 29**,** 437-456.

SHEWEITA, S. A. & KHOSHHAL, K. I. 2007. Calcium metabolism and oxidative stress in bone fractures: role of antioxidants. *Curr Drug Metab,* 8**,** 519-25.

SHIBATA, H., ABE, M., HIURA, K., WILDE, J., MORIYAMA, K., SANO, T., KITAZOE, K.-I., HASHIMOTO, T., OZAKI, S., WAKATSUKI, S., KIDO, S., INOUE, D. & MATSUMOTO, T. 2005. Malignant B-Lymphoid Cells with Bone Lesions Express Receptor Activator of Nuclear Factor-κB Ligand and Vascular Endothelial Growth Factor to Enhance Osteoclastogenesis. *Clinical Cancer Research,* 11**,** 6109-6115.

SHU, S. T., MARTIN, C. K., THUDI, N. K., DIRKSEN, W. P. & ROSOL, T. J. 2010. Osteolytic bone resorption in adult T-cell leukemia/lymphoma. *Leukemia & lymphoma,* 51**,** 702-714.

SHUSTERMAN, S. & MEADOWS, A. T. 2000. Long term survivors of childhood leukemia. *Current Opinion in Hematology,* 7**,** 217-222.

SIDDIK, Z. H. 2005. Mechanisms of Action of Cancer Chemotherapeutic Agents: DNA-Interactive Alkylating Agents and Antitumour Platinum-Based Drugs. *The Cancer Handbook.* John Wiley & Sons, Ltd.

SIMONET, W. S., LACEY, D. L., DUNSTAN, C. R., KELLEY, M., CHANG, M. S., LÜTHY, R., NGUYEN, H. Q., WOODEN, S., BENNETT, L., BOONE, T., SHIMAMOTO, G., DEROSE, M., ELLIOTT, R., COLOMBERO, A., TAN, H. L., TRAIL, G., SULLIVAN, J., DAVY, E., BUCAY, N., RENSHAW-GEGG, L., HUGHES, T. M., HILL, D., PATTISON, W., CAMPBELL, P., SANDER, S., VAN, G., TARPLEY, J., DERBY, P., LEE, R. & BOYLE, W. J. 1997. Osteoprotegerin: A Novel Secreted Protein Involved in the Regulation of Bone Density. *Cell,* 89**,** 309-319.

SIMOS, D., ADDISON, C., KUCHUK, I., HUTTON, B., MAZZARELLO, S. & CLEMONS, M. 2013. Bone-Targeted Agents for the Management of Breast Cancer Patients with Bone Metastases. *Journal of Clinical Medicine,* 2**,** 67-88.

SIMS, N. A. & MARTIN, T. J. 2014. Coupling the activities of bone formation and resorption: a multitude of signals within the basic multicellular unit. *BoneKEy Rep,* 3.

SINGH, P. P., VAN DER KRAAN, A. G. J., XU, J., GILLESPIE, M. T. & QUINN, J. M. W. 2012. Membrane-bound receptor activator of NFκB ligand (RANKL) activity displayed by osteoblasts is differentially regulated by osteolytic factors. *Biochemical and Biophysical Research Communications,* 422**,** 48-53.

SMITH, L., CORNELIUS, V., PLUMMER, C., LEVITT, G., VERRILL, M., CANNEY, P. & JONES, A. 2010. Cardiotoxicity of anthracycline agents for the treatment of cancer: Systematic review and meta-analysis of randomised controlled trials. *BMC Cancer,* 10**,** 337.

SMITH, M. R., SAAD, F., COLEMAN, R., SHORE, N., FIZAZI, K., TOMBAL, B., MILLER, K., SIEBER, P., KARSH, L., DAMIÃO, R., TAMMELA, T. L., EGERDIE, B., VAN POPPEL, H., CHIN, J., MOROTE, J., GÓMEZ-VEIGA, F., BORKOWSKI, T., YE, Z., KUPIC, A., DANSEY, R. & GOESSL, C. Denosumab and bone-metastasis-free survival in men with castration-resistant prostate cancer: results of a phase 3, randomised, placebo-controlled trial. *The Lancet,* 379**,** 39-46.

SOBACCHI, C., FRATTINI, A., GUERRINI, M. M., ABINUN, M., PANGRAZIO, A., SUSANI, L., BREDIUS, R., MANCINI, G., CANT, A., BISHOP, N., GRABOWSKI, P., DEL FATTORE, A., MESSINA, C., ERRIGO, G., COXON, F. P., SCOTT, D. I., TETI, A., ROGERS, M. J., VEZZONI, P., VILLA, A. & HELFRICH, M. H. 2007. Osteoclast-poor human osteopetrosis due to mutations in the gene encoding RANKL. *Nat Genet,* 39**,** 960-962.

SOBACCHI, C., SCHULZ, A., COXON, F. P., VILLA, A. & HELFRICH, M. H. 2013. Osteopetrosis: genetics, treatment and new insights into osteoclast function. *Nature Reviews Endocrinology,* 9**,** 522+.

SOLIMINI, N. L., LUO, J. & ELLEDGE, S. J. 2007. Non-Oncogene Addiction and the Stress Phenotype of Cancer Cells. *Cell,* 130**,** 986-988.

SOLIT, D., BASSO, A., OLSHEN, A., SCHER, H. & ROSEN, N. 2003. Inhibition of heat shock protein 90 function down-regulates Akt kinase and sensitizes tumors to Taxol. *Cancer Res,* 63**,** 2139 - 2144.

SOLIT, D. B., ZHENG, F. F., DROBNJAK, M., MÜNSTER, P. N., HIGGINS, B., VERBEL, D., HELLER, G., TONG, W., CORDON-CARDO, C., AGUS, D. B., SCHER, H. I. & ROSEN, N. 2002. 17-Allylamino-17-demethoxygeldanamycin Induces the Degradation of Androgen Receptor and HER-2/neu and Inhibits the Growth of Prostate Cancer Xenografts. *Clinical Cancer Research,* 8**,** 986-993.

SONG, I., KIM, J. H., KIM, K., JIN, H. M., YOUN, B. U. & KIM, N. 2009. Regulatory mechanism of NFATc1 in RANKL-induced osteoclast activation. *FEBS Letters,* 583**,** 2435-2440.

SOYSA, N. S. & ALLES, N. 2009. NF-κB functions in osteoclasts. *Biochemical and Biophysical Research Communications,* 378**,** 1-5.

SOYSA, N. S., ALLES, N., AOKI, K. & OHYA, K. 2012. Osteoclast formation and differentiation: an overview. *J Med Dent Sci,* 59**,** 65-74.

SROUGI, M. C. & BURRIDGE, K. 2011. The Nuclear Guanine Nucleotide Exchange Factors Ect2 and Net1 Regulate RhoB-Mediated Cell Death after DNA Damage. *PLoS ONE,* 6**,** e17108.

STADTMAN, E. R. 2004. Role of oxidant species in aging. *Curr Med Chem,* 11**,** 1105-12.

STANLEY, E. R. & GUILBERT, L. J. 1981. Methods for the purification, assay, characterization and target cell binding of a colony stimulating factor (CSF-1). *Journal of Immunological Methods,* 42**,** 253-284.

STARK, Z. & SAVARIRAYAN, R. 2009. Osteopetrosis. *Orphanet Journal of Rare Diseases,* 4**,** 5.

STEER, J. H., KROEGER, K. M., ABRAHAM, L. J. & JOYCE, D. A. 2000. Glucocorticoids Suppress Tumor Necrosis Factor-α Expression by Human Monocytic THP-1 Cells by Suppressing Transactivation through Adjacent NF-κB and c-Jun-Activating Transcription Factor-2 Binding Sites in the Promoter. *Journal of Biological Chemistry,* 275**,** 18432-18440.

STEGER, G. G. & BARTSCH, R. 2011. Denosumab for the treatment of bone metastases in breast cancer: evidence and opinion. *Therapeutic Advances in Medical Oncology,* 3**,** 233-243.

STEINGRÍMSSON, E., COPELAND, N. G. & JENKINS, N. A. 2004. MELANOCYTES AND THE MICROPHTHALMIA TRANSCRIPTION FACTOR NETWORK. *Annual Review of Genetics,* 38**,** 365-411.

STEINGRIMSSON, E., MOORE, K. J., LAMOREUX, M. L., FERRE-D'AMARE, A. R., BURLEY, S. K., ZIMRING, D. C., SKOW, L. C., HODGKINSON, C. A., ARNHEITER, H., COPELAND, N. G. & ET AL. 1994. Molecular basis of mouse microphthalmia (mi) mutations helps explain their developmental and phenotypic consequences. *Nat Genet,* 8**,** 256-63.

STEINGRIMSSON, E., TESSAROLLO, L., PATHAK, B., HOU, L., ARNHEITER, H., COPELAND, N. G. & JENKINS, N. A. 2002. Mitf and Tfe3, two members of the Mitf-Tfe family of bHLH-Zip transcription factors, have important but functionally redundant roles in osteoclast development. *Proc Natl Acad Sci U S A,* 99**,** 4477-82.

STEINMAN, R. M. & COHN, Z. A. 1972. The interaction of soluble horseradish peroxidase with mouse peritoneal macrophages in vitro. *J Cell Biol,* 55**,** 186-204.

STENBECK, G. 2002. Formation and function of the ruffled border in osteoclasts. *Seminars in Cell & Developmental Biology,* 13**,** 285-292.

STENBECK, G. & HORTON, M. A. 2004. Endocytic trafficking in actively resorbing osteoclasts. *J Cell Sci,* 117**,** 827-36.

STEPHANOU, A. & LATCHMAN, D. S. 2011. Transcriptional Modulation of Heat-Shock Protein Gene Expression. *Biochemistry Research International,* 2011.

STERLING, J. A., EDWARDS, J. R., MARTIN, T. J. & MUNDY, G. R. 2011. Advances in the biology of bone metastasis: How the skeleton affects tumor behavior. *Bone,* 48**,** 6-15.

STINE, K. C., WAHL, E. C., LIU, L., SKINNER, R. A., SCHILDEN, J. V., BUNN, R. C., MONTGOMERY, C. O., SUVA, L. J., ARONSON, J., BECTON, D. L., NICHOLAS, R. W., SWEARINGEN, C. J. & LUMPKIN, C. K. 2014. Cisplatin Inhibits Bone Healing During Distraction Osteogenesis. *Journal of orthopaedic research : official publication of the Orthopaedic Research Society,* 32**,** 464-470.

STOEBER, K., TLSTY, T. D., HAPPERFIELD, L., THOMAS, G. A., ROMANOV, S., BOBROW, L., WILLIAMS, E. D. & WILLIAMS, G. H. 2001. DNA replication licensing and human cell proliferation. *Journal of Cell Science,* 114**,** 2027-2041.

STOPECK, A. T., LIPTON, A., BODY, J.-J., STEGER, G. G., TONKIN, K., DE BOER, R. H., LICHINITSER, M., FUJIWARA, Y., YARDLEY, D. A., VINIEGRA, M., FAN, M., JIANG, Q., DANSEY, R., JUN, S. & BRAUN, A. 2010. Denosumab Compared With Zoledronic Acid for the Treatment of Bone Metastases in Patients With Advanced Breast Cancer: A Randomized, Double-Blind Study. *Journal of Clinical Oncology,* 28**,** 5132-5139.

STOUT, J. R., YOUNT, A. L., POWERS, J. A., LEBLANC, C., EMS-MCCLUNG, S. C. & WALCZAK, C. E. 2011. Kif18B interacts with EB1 and controls astral microtubule length during mitosis. *Molecular Biology of the Cell,* 22**,** 3070-3080.

STURGE, J., CALEY, M. P. & WAXMAN, J. 2011. Bone metastasis in prostate cancer: emerging therapeutic strategies. *Nat Rev Clin Oncol,* 8**,** 357-368.

SU, P.-H., CHEN, C.-C., CHANG, Y.-F., WONG, Z.-R., CHANG, K.-W., HUANG, B.-M. & YANG, H.-Y. 2013. Identification and Cytoprotective Function of a Novel Nestin Isoform, Nes-S, in Dorsal Root Ganglia Neurons. *The Journal of Biological Chemistry,* 288**,** 8391-8404.

SUBBARAO SREEDHAR, A., KALMÁR, É., CSERMELY, P. & SHEN, Y.-F. 2004. Hsp90 isoforms: functions, expression and clinical importance. *FEBS Letters,* 562**,** 11-15.

SUDA, T., NAKAMURA, I., JIMI, E. & TAKAHASHI, N. 1997. Regulation of Osteoclast Function. *Journal of Bone and Mineral Research,* 12**,** 869-879.

SUDA, T., TAKAHASHI, N., UDAGAWA, N., JIMI, E., GILLESPIE, M. T. & MARTIN, T. J. 1999. Modulation of Osteoclast Differentiation and Function by the New Members of the Tumor Necrosis Factor Receptor and Ligand Families. *Endocrine Reviews,* 20**,** 345-357.

SUDO, T., KAWAI, K., MATSUZAKI, H. & OSADA, H. 2005. p38 mitogen-activated protein kinase plays a key role in regulating MAPKAPK2 expression. *Biochemical and Biophysical Research Communications,* 337**,** 415-421.

SUN, S.-C. 2012. The noncanonical NF-κB pathway. *Immunological Reviews,* 246**,** 125-140.

SUTTON, J. S. & WEISS, L. 1966. TRANSFORMATION OF MONOCYTES IN TISSUE CULTURE INTO MACROPHAGES, EPITHELIOID CELLS, AND

MULTINUCLEATED GIANT CELLS : An Electron Microscope Study. *The Journal of Cell Biology,* 28**,** 303-332.

SYGGELOS, S. A., ALETRAS, A. J., SMIRLAKI, I. & SKANDALIS, S. S. 2013. Extracellular Matrix Degradation and Tissue Remodeling in Periprosthetic Loosening and Osteolysis: Focus on Matrix Metalloproteinases, Their Endogenous Tissue Inhibitors, and the Proteasome. *BioMed Research International,* 2013**,** 18.

SZALAY, M. S., KOVÁCS, I. A., KORCSMÁROS, T., BÖDE, C. & CSERMELY, P. 2007. Stress-induced rearrangements of cellular networks: Consequences for protection and drug design. *FEBS Letters,* 581**,** 3675-3680.

TACHIBANA, M. 2001. Cochlear Melanocytes and MITF Signaling. *J Investig Dermatol Symp Proc,* 6**,** 95-98.

TAIPALE, M., JAROSZ, D. F. & LINDQUIST, S. 2010. HSP90 at the hub of protein homeostasis: emerging mechanistic insights. *Nat Rev Mol Cell Biol,* 11**,** 515-28.

TAKAHASHI, N., AKATSU, T., UDAGAWA, N., SASAKI, T., YAMAGUCHI, A., MOSELEY, J. M., MARTIN, T. J. & SUDA, T. 1988a. OSTEOBLASTIC CELLS ARE INVOLVED IN OSTEOCLAST FORMATION. *Endocrinology,* 123**,** 2600-2602.

TAKAHASHI, N., EJIRI, S., YANAGISAWA, S. & OZAWA, H. 2007. Regulation of osteoclast polarization. *Odontology,* 95**,** 1-9.

TAKAHASHI, N., UDAGAWA, N., AKATSU, T., TANAKA, H., ISOGAI, Y. & SUDA, T. 1991. Deficiency of osteoclasts in osteopetrotic mice is due to a defect in the local microenvironment provided by osteoblastic cells. *Endocrinology,* 128**,** 1792-6.

TAKAHASHI, N., UDAGAWA, N. & SUDA, T. 1999. A New Member of Tumor Necrosis Factor Ligand Family, ODF/OPGL/TRANCE/RANKL, Regulates Osteoclast Differentiation and Function. *Biochemical and Biophysical Research Communications,* 256**,** 449-455.

TAKAHASHI, N., YAMANA, H., YOSHIKI, S., ROODMAN, G. D., MUNDY, G. R., JONES, S. J., BOYDE, A. & SUDA, T. 1988b. Osteoclast-Like Cell Formation and its Regulation by Osteotropic Hormones in Mouse Bone Marrow Cultures. *Endocrinology,* 122**,** 1373-1382.

TAKALO, M., SALMINEN, A., SOININEN, H., HILTUNEN, M. & HAAPASALO, A. 2013. Protein aggregation and degradation mechanisms in neurodegenerative diseases. *American Journal of Neurodegenerative Disease,* 2**,** 1-14.

TAKAYANAGI, H. 2007a. Osteoimmunology: shared mechanisms and crosstalk between the immune and bone systems. *Nature Reviews Immunology,* 7**,** 292+.

TAKAYANAGI, H. 2007b. The Role of NFAT in Osteoclast Formation. *Annals of the New York Academy of Sciences,* 1116**,** 227-237.

TAKAYANAGI, H. 2008a. Receptor Activator of NF-[kappa]B (RANK) Signaling. *In:* JOHN, P. B., LAWRENCE, G. R. & MARTIN, T. J. (eds.) *Principles of Bone Biology (Third Edition).* San Diego: Academic Press.

TAKAYANAGI, H. 2008b. Regulation of osteoclastogenesis and osteoimmunology. *Bone,* 42**,** S40-S40.

TAKAYANAGI, H., KIM, S., KOGA, T., NISHINA, H., ISSHIKI, M., YOSHIDA, H., SAIURA, A., ISOBE, M., YOKOCHI, T., INOUE, J.-I., WAGNER, E. F., MAK, T. W., KODAMA, T. & TANIGUCHI, T. 2002. Induction and Activation of the Transcription Factor NFATc1 (NFAT2) Integrate RANKL Signaling in Terminal Differentiation of Osteoclasts. *Developmental Cell,* 3**,** 889-901.

TALDONE, T., GOZMAN, A., MAHARAJ, R. & CHIOSIS, G. 2008. Targeting Hsp90: small-molecule inhibitors and their clinical development. *Current Opinion in Pharmacology,* 8**,** 370-374.

TALDONE, T., ZATORSKA, D., PATEL, P. D., ZONG, H., RODINA, A., AHN, J. H., MOULICK, K., GUZMAN, M. L. & CHIOSIS, G. 2011. Design, Synthesis and Evaluation of Small Molecule Hsp90 Probes. *Bioorganic & medicinal chemistry,* 19**,** 2603-2614.

TAN, H.-L., MORAN, N. E., CICHON, M. J., RIEDL, K. M., SCHWARTZ, S. J., ERDMAN, J. W., PEARL, D. K., THOMAS-AHNER, J. M. & CLINTON, S. K. 2014. β-Carotene-9′,10′-Oxygenase Status Modulates the Impact of Dietary Tomato and Lycopene on Hepatic Nuclear Receptor–, Stress-, and Metabolism-Related Gene Expression in Mice. *The Journal of Nutrition,* 144**,** 431-439.

TANG, D., KANG, R., ZEH, H. J. & LOTZE, M. T. 2011. High-Mobility Group Box 1, Oxidative Stress, and Disease. *Antioxidants & Redox Signaling,* 14**,** 1315-1335.

TANG, Y., WU, X., LEI, W., PANG, L., WAN, C., SHI, Z., ZHAO, L., NAGY, T. R., PENG, X., HU, J., FENG, X., VAN HUL, W., WAN, M. & CAO, X. 2009. TGF-[beta]1-induced migration of bone mesenchymal stem cells couples bone resorption with formation. *Nat Med,* 15**,** 757-765.

TANI-ISHII, N., TSUNODA, A., TERANAKA, T. & UMEMOTO, T. 1999. Autocrine regulation of osteoclast formation and bone resorption by IL-1 alpha and TNF alpha. *J Dent Res,* 78**,** 1617-23.

TAYLOR, D. M., TRADEWELL, M. L., MINOTTI, S. & DURHAM, H. D. 2007. Characterizing the role of Hsp90 in production of heat shock proteins in motor neurons reveals a suppressive effect of wild-type Hsf1. *Cell Stress & Chaperones,* 12**,** 151-162.

TCHERKEZIAN, J. & LAMARCHE-VANE, N. 2007. Current knowledge of the large RhoGAP family of proteins. *Biology of the Cell,* 99**,** 67-86.

TEITELBAUM, S. L. 2000. Bone Resorption by Osteoclasts. *Science,* 289**,** 1504.

TEITELBAUM, S. L. 2007. Osteoclasts: What Do They Do and How Do They Do It? *Am J Pathol,* 170**,** 427-435.

TEITELBAUM, S. L., TONDRAVI, M. M. & ROSS, F. P. 1997. Osteoclasts, macrophages, and the molecular mechanisms of bone resorption. *J Leukoc Biol,* 61**,** 381-8.

TETI, A. & ZALLONE, A. 2008. Do osteocytes contribute to bone mineral homeostasis? Osteocytic osteolysis revisited. *Bone,* 44**,** 11-16.

THEODORAKI, M. A. & CAPLAN, A. J. 2012. Quality control and fate determination of Hsp90 client proteins. *Biochimica et Biophysica Acta (BBA) - Molecular Cell Research,* 1823**,** 683-688.

THOMAS, R. J., GUISE, T. A., YIN, J. J., ELLIOTT, J., HORWOOD, N. J., MARTIN, T. J. & GILLESPIE, M. T. 1999. Breast Cancer Cells Interact with Osteoblasts to Support Osteoclast Formation. *Endocrinology,* 140**,** 4451-4458.

THORNLEY, T. B., FANG, Z., BALASUBRAMANIAN, S., LAROCCA, R. A., GONG, W., GUPTA, S., CSIZMADIA, E., DEGAUQUE, N., KIM, B. S., KOULMANDA, M., KUCHROO, V. K. & STROM, T. B. 2014. Fragile TIM-4–expressing tissue resident macrophages are migratory and immunoregulatory. *The Journal of Clinical Investigation,* 124**,** 3443-3454.

TODD, D. J., LEE, A.-H. & GLIMCHER, L. H. 2008. The endoplasmic reticulum stress response in immunity and autoimmunity. *Nat Rev Immunol,* 8**,** 663-674.

TOIVOLA, D. M., STRNAD, P., HABTEZION, A. & OMARY, M. B. 2010. Intermediate filaments take the heat as stress proteins. *Trends in cell biology,* 20**,** 79-91.

TORTORA, G. J. A. G., S. R. 2000. *Principles of Anatomy and Physiology,* New York, John Wiley and Sons, INC.

TOUYZ, R. M. 2004. Reactive oxygen species and angiotensin II signaling in vascular cells: implications in cardiovascular disease. *Brazilian Journal of Medical and Biological Research,* 37**,** 1263-1273.

TRACHOOTHAM, D., LU, W., OGASAWARA, M. A., VALLE, N. R.-D. & HUANG, P. 2008. Redox Regulation of Cell Survival. *Antioxidants & Redox Signaling,* 10**,** 1343-1374.

TRAPNELL, C., PACHTER, L. & SALZBERG, S. L. 2009. TopHat: discovering splice junctions with RNA-Seq. *Bioinformatics,* 25**,** 1105-1111.

TRAPNELL, C., ROBERTS, A., GOFF, L., PERTEA, G., KIM, D., KELLEY, D. R., PIMENTEL, H., SALZBERG, S. L., RINN, J. L. & PACHTER, L. 2012. Differential gene and transcript expression analysis of RNA-seq experiments with TopHat and Cufflinks. *Nat. Protocols,* 7**,** 562-578.

TRAPNELL, C., WILLIAMS, B. A., PERTEA, G., MORTAZAVI, A., KWAN, G., VAN BAREN, M. J., SALZBERG, S. L., WOLD, B. J. & PACHTER, L. 2010. Transcript assembly and quantification by RNA-Seq reveals unannotated transcripts and isoform switching during cell differentiation. *Nat Biotech,* 28**,** 511-515.

TRAVERS, J., SHARP, S. & WORKMAN, P. 2012. HSP90 inhibition: two-pronged exploitation of cancer dependencies. *Drug Discovery Today,* 17**,** 242-252.

TREPEL, J., MOLLAPOUR, M., GIACCONE, G. & NECKERS, L. 2010. Targeting the dynamic HSP90 complex in cancer. *Nat Rev Cancer,* 10**,** 537-549.

TRINKLEIN, N. D., MURRAY, J. I., HARTMAN, S. J., BOTSTEIN, D. & MYERS, R. M. 2004. The Role of Heat Shock Transcription Factor 1 in the Genome-wide Regulation of the Mammalian Heat Shock Response. *Molecular Biology of the Cell,* 15**,** 1254-1261.

TSUTSUMI, S. & NECKERS, L. 2007. Extracellular heat shock protein 90: A role for a molecular chaperone in cell motility and cancer metastasis. *Cancer Science,* 98**,** 1536-1539.

TUMBER, A., MORGAN, H. M., MEIKLE, M. C. & HILL, P. A. 2001. Human breast-cancer cells stimulate the fusion, migration and resorptive activity of osteoclasts in bone explants. *International Journal of Cancer,* 91**,** 650-653.

TURJANSKI, A. G., VAQUE, J. P. & GUTKIND, J. S. 2007. MAP kinases and the control of nuclear events. *Oncogene,* 26**,** 3240-3253.

TURNER, R. T., GREENE, V. S. & BELL, N. H. 1987. Demonstration that ethanol inhibits bone matrix synthesis and mineralization in the rat. *Journal of Bone and Mineral Research,* 2**,** 61-66.

U.S. NATIONAL LIBRARY OF MEDICINE. 2009. *Gene; National Center for Biotechnology Information; National Library of Medicine,* [Online]. U.S. National Library of Medicine,. [Accessed June 2015].

UDAGAWA, N., TAKAHASHI, N., AKATSU, T., TANAKA, H., SASAKI, T., NISHIHARA, T., KOGA, T., MARTIN, T. J. & SUDA, T. 1990. Origin of osteoclasts: mature monocytes and macrophages are capable of differentiating into osteoclasts under a suitable microenvironment prepared by bone marrow-derived stromal cells. *Proceedings of the National Academy of Sciences,* 87**,** 7260-7264.

UEHARA, Y. 2003. Natural product origins of Hsp90 inhibitors. *Curr Cancer Drug Targets,* 3**,** 325-30.

URBAN, M. J., DOBROWSKY, R. T. & BLAGG, B. S. J. 2012. Heat shock response and insulin-associated neurodegeneration. *Trends in Pharmacological Sciences,* 33**,** 129-137.

VAANANEN, H. K. & HORTON, M. 1995. The osteoclast clear zone is a specialized cell-extracellular matrix adhesion structure. *J Cell Sci,* 108 (Pt 8)**,** 2729-32.

VAANANEN, H. K. & LAITALA-LEINONEN, T. 2008. Osteoclast lineage and function. *Arch Biochem Biophys,* 473**,** 132-8.

VAANANEN, H. K., ZHAO, H., MULARI, M. & HALLEEN, J. M. 2000. The cell biology of osteoclast function. *Journal of Cell Science,* 113**,** 377-381.

VÄÄNÄNEN, K. & ZHAO, H. 2002. Chapter 8 - Osteoclast Function: Biology and Mechanisms. *In:* RODAN, J. P. B. G. R. A. (ed.) *Principles of Bone Biology (Second Edition).* San Diego: Academic Press.

VABULAS, R. M., RAYCHAUDHURI, S., HAYER-HARTL, M. & HARTL, F. U. 2010. Protein Folding in the Cytoplasm and the Heat Shock Response. *Cold Spring Harbor Perspectives in Biology,* 2.

VALKO, M., RHODES, C. J., MONCOL, J., IZAKOVIC, M. & MAZUR, M. 2006. Free radicals, metals and antioxidants in oxidative stress-induced cancer. *Chemico-Biological Interactions,* 160**,** 1-40.

VAN DER KRAAN, A. G., CHAI, R. C., SINGH, P. P., LANG, B. J., XU, J., GILLESPIE, M. T., PRICE, J. T. & QUINN, J. M. 2013. HSP90 inhibitors enhance differentiation and MITF (microphthalmia transcription factor) activity in osteoclast progenitors. *Biochem J,* 451**,** 235-44.

VAN LEEUWEN, B. L., KAMPS, W. A., HARTEL, R. M., VETH, R. P. H., SLUITER, W. J. & HOEKSTRA, H. J. 2000. Effect of single chemotherapeutic agents on the growing skeleton of the rat. *Annals of Oncology,* 11**,** 1121-1126.

VAN RIJTHOVEN, A. W., DIJKMANS, B. A., GOEI THE, H. S., HERMANS, J., MONTNOR-BECKERS, Z. L., JACOBS, P. C. & CATS, A. 1986. Cyclosporin treatment for rheumatoid arthritis: a placebo controlled, double blind, multicentre study. *Annals of the Rheumatic Diseases,* 45**,** 726-731.

VANNEMAN, M. & DRANOFF, G. 2012. Combining immunotherapy and targeted therapies in cancer treatment. *Nat Rev Cancer,* 12**,** 237-251.

VAZQUEZ, F., LIM, J.-H., CHIM, H., BHALLA, K., GIRNUN, G., PIERCE, K., CLISH, CLARY B., GRANTER, SCOTT R., WIDLUND, HANS R., SPIEGELMAN, BRUCE M. & PUIGSERVER, P. 2013. PGC1α Expression Defines a Subset of Human Melanoma Tumors with Increased Mitochondrial Capacity and Resistance to Oxidative Stress. *Cancer Cell,* 23**,** 287-301.

VERGHESE, J., ABRAMS, J., WANG, Y. & MORANO, K. A. 2012. Biology of the Heat Shock Response and Protein Chaperones: Budding Yeast (Saccharomyces cerevisiae) as a Model System. *Microbiology and Molecular Biology Reviews : MMBR,* 76**,** 115-158.

VIGNERY, A. 2005. Macrophage fusion: the making of osteoclasts and giant cells. *The Journal of Experimental Medicine,* 202**,** 337-340.

VISENTIN, L., DODDS, R. A., VALENTE, M., MISIANO, P., BRADBEER, J. N., ONETA, S., LIANG, X., GOWEN, M. & FARINA, C. 2000. A selective inhibitor of the osteoclastic V-H(+)-ATPase prevents bone loss in both thyroparathyroidectomized and ovariectomized rats. *Journal of Clinical Investigation,* 106**,** 309-318.

VOELLMY, R. 2004. On mechanisms that control heat shock transcription factor activity in metazoan cells. *Cell Stress Chaperones,* 9**,** 122-33.

VOGELSTEIN, B. & KINZLER, K. W. 1993. The multistep nature of cancer. *Trends in Genetics,* 9**,** 138-141.

VOLLOCH, V., GABAI, V. L., RITS, S., FORCE, T. & SHERMAN, M. Y. 2000. HSP72 can protect cells from heat-induced apoptosis by accelerating the inactivation of stress kinase JNK. *Cell Stress & Chaperones,* 5**,** 139-147.

VOLLOCH, V. & SHERMAN, M. 1999. Oncogenic potential of Hsp72. *Oncogene,* 18**,** 3648-3651.

WADA, S., MARTIN, T. J. & FINDLAY, D. M. 1995. Homologous regulation of the calcitonin receptor in mouse osteoclast-like cells and human breast cancer T47D cells. *Endocrinology,* 136**,** 2611-21.

WADA, T., NAKASHIMA, T., HIROSHI, N. & PENNINGER, J. M. 2006. RANKL–RANK signaling in osteoclastogenesis and bone disease. *Trends in Molecular Medicine,* 12**,** 17-25.

WAGNER, E. F. & NEBREDA, A. R. 2009. Signal integration by JNK and p38 MAPK pathways in cancer development. *Nat Rev Cancer,* 9**,** 537-549.

WALKER, D. G. 1975a. Bone resorption restored in osteopetrotic mice by transplants of normal bone marrow and spleen cells. *Sience* 190**,** 784-785.

WALKER, D. G. 1975b. Control of bone resorption by hematopoietic tissue. The induction and reversal of congenital osteopetrosis in mice through use of bone marrow and splenic transplants. *The Journal of Experimental Medicine,* 142**,** 651-663.

WALSBY, E., PEARCE, L., BURNETT, A. K., FEGAN, C. & PEPPER, C. 2012. The Hsp90 inhibitor NVP-AUY922-AG inhibits NF-κB signaling, overcomes microenvironmental cytoprotection and is highly synergistic with fludarabine in primary CLL cells. *Oncotarget,* 3**,** 525-534.

WALSH, M. C. & CHOI, Y. 2014. Biology of the RANKL–RANK–OPG System in Immunity, Bone, and Beyond. *Frontiers in Immunology,* 5**,** 511.

WAN, P., HU, Y. & HE, L. 2011. Regulation of melanocyte pivotal transcription factor MITF by some other transcription factors. *Molecular and Cellular Biochemistry,* 354**,** 241-246.

WANG, C., STEER, J. H., JOYCE, D. A., YIP, K. H. M., ZHENG, M. H. & XU, J. 2003a. 12-O-tetradecanoylphorbol-13-acetate (TPA) Inhibits Osteoclastogenesis by Suppressing RANKL-Induced NF-κB Activation. *Journal of Bone and Mineral Research,* 18**,** 2159-2168.

WANG, J., CUI, S., ZHANG, X., WU, Y. & TANG, H. 2013. High Expression of Heat Shock Protein 90 Is Associated with Tumor Aggressiveness and Poor Prognosis in Patients with Advanced Gastric Cancer. *PLoS ONE,* 8**,** e62876.

WANG, K., NIU, J., KIM, H. & KOLATTUKUDY, P. E. 2011a. Osteoclast precursor differentiation by MCPIP via oxidative stress, endoplasmic reticulum stress, and autophagy. *Journal of Molecular Cell Biology,* 3**,** 360-368.

WANG, K., NIU, J., KIM, H. & KOLATTUKUDY, P. E. 2011b. Osteoclast precursor differentiation by MCPIP via oxidative stress, endoplasmic reticulum stress, and autophagy. *J Mol Cell Biol,* 3**,** 360-8.

WANG, L., SCHUMANN, U., LIU, Y., PROKOPCHUK, O. & STEINACKER, J. M. 2012. Heat shock protein 70 (Hsp70) inhibits oxidative phosphorylation and compensates ATP balance through enhanced glycolytic activity. *Journal of Applied Physiology,* 113**,** 1669-1676.

WANG, S., DILLER, K. R. & AGGARWAL, S. J. 2003b. Kinetics study of endogenous heat shock protein 70 expression. *J Biomech Eng,* 125**,** 794-7.

WANG, Y., LIU, Y., MALEK, SAMI N., ZHENG, P. & LIU, Y. 2011c. Targeting HIF1± Eliminates Cancer Stem Cells in Hematological Malignancies. *Cell stem cell,* 8**,** 399-411.

WANG, Y. & MCALPINE, S. R. 2015. N-terminal and C-terminal modulation of Hsp90 produce dissimilar phenotypes. *Chemical Communications,* 28**,** 1410-3.

WANG, Y., PROBIN, V. & ZHOU, D. 2006. Cancer therapy-induced residual bone marrow injury-Mechanisms of induction and implication for therapy. *Current cancer therapy reviews,* 2**,** 271-279.

WANG, Z.-Q., OVITT, C., GRIGORIADIS, A. E., MOHLE-STEINLEIN, U., RUTHER, U. & WAGNER, E. F. 1992. Bone and haematopoietic defects in mice lacking c-fos. *Nature,* 360**,** 741-745.

WANG, Z., GERSTEIN, M. & SNYDER, M. 2009. RNA-Seq: a revolutionary tool for transcriptomics. *Nature reviews. Genetics,* 10**,** 57-63.

WANG, Z., YU, R. & MELMED, S. 2001. Mice Lacking Pituitary Tumor Transforming Gene Show Testicular and Splenic Hypoplasia, Thymic Hyperplasia, Thrombocytopenia, Aberrant Cell Cycle Progression, and Premature Centromere Division. *Molecular Endocrinology,* 15**,** 1870-1879.

WASKIEWICZ, A. J. & COOPER, J. A. 1995. Mitogen and stress response pathways: MAP kinase cascades and phosphatase regulation in mammals and yeast. *Curr Opin Cell Biol,* 7**,** 798-805.

WATANABE, M., SUZUKI, K. & KODAMA, S. 2001. Molecular and Cellular Factors Determining Cell Susceptibility to Heat Shock. *In:* KOSAKA, M., SUGAHARA, T., SCHMIDT, K. & SIMON, E. (eds.) *Thermotherapy for Neoplasia, Inflammation, and Pain.* Springer Japan.

WEBER, G. F. 2007. *Molecular Mechanisms of Cancer*, Springer.

WEILBAECHER, K. N., MCCAULEY, L. K. & GUISE, T. A. 2011. Cancer to bone: a fatal attraction. *Nature Reviews Cancer,* 11**,** 411-425.

WEILBAECHER, K. N., MOTYCKOVA, G., HUBER, W. E., TAKEMOTO, C. M., HEMESATH, T. J., XU, Y., HERSHEY, C. L., DOWLAND, N. R., WELLS, A. G. & FISHER, D. E. 2001. Linkage of M-CSF Signaling to Mitf, TFE3, and the Osteoclast Defect in Mitfmi/mi Mice. *Molecular Cell,* 8**,** 749-758.

WEITZMANN, M. N. 2013. The Role of Inflammatory Cytokines, the RANKL/OPG Axis, and the Immunoskeletal Interface in Physiological Bone Turnover and Osteoporosis. *Scientifica,* 2013**,** 29.

WELCH, W. J. & SUHAN, J. P. 1985. Morphological study of the mammalian stress response: characterization of changes in cytoplasmic organelles, cytoskeleton, and nucleoli, and appearance of intranuclear actin filaments in rat fibroblasts after heat-shock treatment. *The Journal of Cell Biology,* 101**,** 1198-1211.

WENTE, M. N., EIBL, G., REBER, H. A., FRIESS, H., BUCHLER, M. W. & HINES, O. J. 2005. The proteasome inhibitor MG132 induces apoptosis in human pancreatic cancer cells. *Oncol Rep,* 14**,** 1635-8.

WHITESELL, L. & LINDQUIST, S. 2005. HSP90 and the chaperoning of cancer. *Nat Rev Cancer,* 5**,** 761 - 772.

WHITESELL, L. & LINDQUIST, S. 2009. Inhibiting the transcription factor HSF1 as an anticancer strategy. *Expert Opinion on Therapeutic Targets,* 13**,** 469-478.

WHITESELL, L., MIMNAUGH, E. G., DE COSTA, B., MYERS, C. E. & NECKERS, L. M. 1994. Inhibition of heat shock protein HSP90-pp60v-src heteroprotein complex formation by benzoquinone ansamycins: essential role for stress proteins in oncogenic transformation. *Proceedings of the National Academy of Sciences,* 91**,** 8324-8328.

WIKTOR-JEDRZEJCZAK, W. W., AHMED, A., SZCZYLIK, C. & SKELLY, R. R. 1982. Hematological characterization of congenital osteopetrosis in op/op mouse. Possible mechanism for abnormal macrophage differentiation. *The Journal of Experimental Medicine,* 156**,** 1516-1527.

WINKLHOFER, K. F., REINTJES, A., HOENER, M. C., VOELLMY, R. & TATZELT, J. 2001. Geldanamycin Restores a Defective Heat Shock Responsein Vivo. *Journal of Biological Chemistry,* 276**,** 45160-45167.

WINSLOW, M. M., PAN, M., STARBUCK, M., GALLO, E. M., DENG, L., KARSENTY, G. & CRABTREE, G. R. 2006. Calcineurin/NFAT Signaling in Osteoblasts Regulates Bone Mass. *Developmental Cell,* 10**,** 771-782.

WIRAWAN, E., BERGHE, T. V., LIPPENS, S., AGOSTINIS, P. & VANDENABEELE, P. 2012. Autophagy: for better or for worse. *Cell Res,* 22**,** 43-61.

WONDRAK, G. 2015. Melanomagenic Gene Alterations Viewed from a Redox Perspective: Molecular Mechanisms and Therapeutic Opportunities. *In:* WONDRAK, G. T. (ed.) *Stress Response Pathways in Cancer.* Springer Netherlands.

WONG, B. R., RHO, J., ARRON, J., ROBINSON, E., ORLINICK, J., CHAO, M., KALACHIKOV, S., CAYANI, E., BARTLETT, F. S., FRANKEL, W. N., LEE, S. Y. & CHOI, Y. 1997. TRANCE Is a Novel Ligand of the Tumor Necrosis Factor Receptor Family That Activates c-Jun N-terminal Kinase in T Cells. *Journal of Biological Chemistry,* 272**,** 25190-25194.

WORKMAN, P. 2004a. Altered states: selectively drugging the Hsp90 cancer chaperone. *Trends in Molecular Medicine,* 10**,** 47-51.

WORKMAN, P. 2004b. Combinatorial attack on multistep oncogenesis by inhibiting the Hsp90 molecular chaperone. *Cancer Letters,* 206**,** 149-157.

WORKMAN, P., BURROWS, F., NECKERS, L. E. N. & ROSEN, N. 2007. Drugging the Cancer Chaperone HSP90. *Annals of the New York Academy of Sciences,* 1113**,** 202-216.

WORKMAN, P. & COLLINS, I. 2010. Probing the Probes: Fitness Factors For Small Molecule Tools. *Chemistry & Biology,* 17**,** 561-577.

WU, C. 1995. Heat Shock Transcription Factors: Structure and Regulation. *Annual Review of Cell and Developmental Biology,* 11**,** 441-469.

WU, H., XU, G. & LI, Y.-P. 2009. Atp6v0d2 Is an Essential Component of the Osteoclast-Specific Proton Pump That Mediates Extracellular Acidification in Bone Resorption. *Journal of Bone and Mineral Research,* 24**,** 871-885.

WU, Y., HUMPHREY, M. B. & NAKAMURA, M. C. 2008. Osteoclasts—the innate immune cells of the bone. *Autoimmunity,* 41**,** 183-194.

XIAO, L., LU, X. & RUDEN, D. M. 2006. Effectiveness of hsp90 inhibitors as anti-cancer drugs. *Mini Rev Med Chem,* 6**,** 1137-43.

XIAO, X., ZUO, X., DAVIS, A. A., MCMILLAN, D. R., CURRY, B. B., RICHARDSON, J. A. & BENJAMIN, I. J. 1999. *HSF1 is required for extra‐embryonic development, postnatal growth and protection during inflammatory responses in mice.*

XING, L., XIU, Y. & BOYCE, B. F. 2012. Osteoclast fusion and regulation by RANKL-dependent and independent factors. *World Journal of Orthopedics,* 3**,** 212-222.

XIONG, M. P., YÁÑEZ, J. A., KWON, G. S., DAVIES, N. M. & FORREST, M. L. 2009. A Cremophor-Free Formulation for Tanespimycin (17-AAG) using PEO-b-PDLLA Micelles: Characterization and Pharmacokinetics in Rats. *Journal of pharmaceutical sciences,* 98**,** 1577-1586.

XU, L., CHEN, S. & BERGAN, R. C. 2006. MAPKAPK2 and HSP27 are downstream effectors of p38 MAP kinase-mediated matrix metalloproteinase type 2 activation and cell invasion in human prostate cancer. *Oncogene,* 25**,** 2987-2998.

XU, W. & NECKERS, L. 2007. Targeting the Molecular Chaperone Heat Shock Protein 90 Provides a Multifaceted Effect on Diverse Cell Signaling Pathways of Cancer Cells. *Clinical Cancer Research,* 13**,** 1625-1629.

XU, Y., MORSE, L. R., DA SILVA, R. A., ODGREN, P. R., SASAKI, H., STASHENKO, P. & BATTAGLINO, R. A. 2010. PAMM: a redox regulatory protein that modulates osteoclast differentiation. *Antioxid Redox Signal,* 13**,** 27-37.

YADAV, R. K., CHAE, S.-W., KIM, H.-R. & CHAE, H. J. 2014. Endoplasmic Reticulum Stress and Cancer. *Journal of Cancer Prevention,* 19**,** 75-88.

YAGI, M., MIYAMOTO, T., SAWATANI, Y., IWAMOTO, K., HOSOGANE, N., FUJITA, N., MORITA, K., NINOMIYA, K., SUZUKI, T., MIYAMOTO, K., OIKE, Y., TAKEYA, M., TOYAMA, Y. & SUDA, T. 2005. DC-STAMP is essential for cell–cell fusion in osteoclasts and foreign body giant cells. *The Journal of Experimental Medicine,* 202**,** 345-351.

YAMADA, H., NAKAJIMA, T., DOMON, H., HONDA, T. & YAMAZAKI, K. 2015. Endoplasmic reticulum stress response and bone loss in experimental periodontitis in mice. *J Periodontal Res,* 50**,** 500-8.

YAMADA, S.-I., ONO, T., MIZUNO, A. & NEMOTO, T. K. 2003. A hydrophobic segment within the C-terminal domain is essential for both client-binding and dimer formation of the HSP90-family molecular chaperone. *European Journal of Biochemistry,* 270**,** 146-154.

YAMASAKI, N., TSUBOI, H., HIRAO, M., NAMPEI, A., YOSHIKAWA, H. & HASHIMOTO, J. 2009. High oxygen tension prolongs the survival of osteoclast precursors via macrophage colony-stimulating factor. *Bone,* 44**,** 71-79.

YAMASHITA, T., YAO, Z., LI, F., ZHANG, Q., BADELL, I. R., SCHWARZ, E. M., TAKESHITA, S., WAGNER, E. F., NODA, M., MATSUO, K., XING, L. & BOYCE, B. F. 2007. NF-kappaB p50 and p52 regulate receptor activator of NF-kappaB ligand (RANKL) and tumor necrosis factor-induced osteoclast precursor differentiation by activating c-Fos and NFATc1. *J Biol Chem,* 282**,** 18245-53.

YANG, D.-Q., FENG, S., CHEN, W., ZHAO, H., PAULSON, C. & LI, Y.-P. 2012. V-ATPase subunit ATP6AP1 (Ac45) regulates osteoclast differentiation, extracellular acidification, lysosomal trafficking, and protease exocytosis in osteoclast-mediated bone resorption. *Journal of bone and mineral research : the official journal of the American Society for Bone and Mineral Research,* 27**,** 1695-1707.

YANG, J., YU, Y., HAMRICK, H. E. & DUERKSEN-HUGHES, P. J. 2003. ATM, ATR and DNA-PK: initiators of the cellular genotoxic stress responses. *Carcinogenesis,* 24**,** 1571-1580.

YANG, M., MAILHOT, G., MACKAY, C. A., MASON-SAVAS, A., AUBIN, J. & ODGREN, P. R. 2006. Chemokine and chemokine receptor expression during colony stimulating factor-1–induced osteoclast differentiation in the toothless osteopetrotic rat: a key role for CCL9 (MIP-1γ) in osteoclastogenesis in vivo and in vitro. *Blood,* 107**,** 2262-2270.

YANO, A., TSUTSUMI, S., SOGA, S., LEE, M.-J., TREPEL, J., OSADA, H. & NECKERS, L. 2008. Inhibition of Hsp90 activates osteoclast c-Src signaling and promotes growth of prostate carcinoma cells in bone. *Proceedings of the National Academy of Sciences,* 105**,** 15541-15546.

YANO, M., NAKAMUTA, S., WU, X., OKUMURA, Y. & KIDO, H. 2006. A Novel Function of 14-3-3 Protein: 14-3-3ζ Is a Heat-Shock–related Molecular Chaperone That Dissolves Thermal-aggregated Proteins. *Molecular Biology of the Cell,* 17**,** 4769-4779.

YAO, Z., XING, L. & BOYCE, B. F. 2009. NF-κB p100 limits TNF-induced bone resorption in mice by a TRAF3-dependent mechanism. *The Journal of Clinical Investigation,* 119**,** 3024-3034.

YARILINA, A., XU, K., CHEN, J. & IVASHKIV, L. B. 2011. TNF activates calcium–nuclear factor of activated T cells (NFAT)c1 signaling pathways in human macrophages. *Proceedings of the National Academy of Sciences of the United States of America,* 108**,** 1573-1578.

YASUDA, H., SHIMA, N., NAKAGAWA, N., MOCHIZUKI, S.-I., YANO, K., FUJISE, N., SATO, Y., GOTO, M., YAMAGUCHI, K., KURIYAMA, M., KANNO, T., MURAKAMI, A., TSUDA, E., MORINAGA, T. & HIGASHIO, K. 1998a. Identity of Osteoclastogenesis Inhibitory Factor (OCIF) and Osteoprotegerin (OPG): A Mechanism by which OPG/OCIF Inhibits Osteoclastogenesis in Vitro. *Endocrinology,* 139**,** 1329-1337.

YASUDA, H., SHIMA, N., NAKAGAWA, N., YAMAGUCHI, K., KINOSAKI, M., MOCHIZUKI, S.-I., TOMOYASU, A., YANO, K., GOTO, M., MURAKAMI, A., TSUDA, E., MORINAGA, T., HIGASHIO, K., UDAGAWA, N., TAKAHASHI, N. & SUDA, T. 1998b. Osteoclast differentiation factor is a ligand for osteoprotegerin/osteoclastogenesis-inhibitory factor and is identical to TRANCE/RANKL. *Proceedings of the National Academy of Sciences,* 95**,** 3597-3602.

YEON, J. T., CHOI, S. W., PARK, K. I., CHOI, M. K., KIM, J. J., YOUN, B. S., LEE, M. S. & OH, J. 2012. Glutaredoxin2 isoform b (Glrx2b) promotes RANKL-induced osteoclastogenesis through activation of the p38-MAPK signaling pathway. *BMB Rep,* 45**,** 171-6.

YIN, J. J., POLLOCK, C. B. & KELLY, K. 2005. Mechanisms of cancer metastasis to the bone. *Cell Res,* 15**,** 57-62.

YIN, J. J., SELANDER, K., CHIRGWIN, J. M., DALLAS, M., GRUBBS, B. G., WIESER, R., MASSAGUÉ, J., MUNDY, G. R. & GUISE, T. A. 1999. TGF-β signaling blockade inhibits PTHrP secretion by breast cancer cells and bone metastases development. *The Journal of Clinical Investigation,* 103**,** 197-206.

YIN, Y., TANG, L., ZHANG, J., TANG, B. & LI, Z. 2011. Molecular Cloning and Gene Expression Analysis of Ercc6l in Sika Deer (Cervus nippon hortulorum). *PLoS ONE,* 6**,** e20929.

YING, L., LIN, J., QIU, F., CAO, M., CHEN, H., LIU, Z. & HUANG, Y. 2015. Epigenetic repression of regulator of G-protein signaling 2 by ubiquitin-like with PHD and ring-finger domain 1 promotes bladder cancer progression. *FEBS Journal,* 282**,** 174-182.

YIP, K. H., ZHENG, M. H., STEER, J. H., GIARDINA, T. M., HAN, R., LO, S. Z., BAKKER, A. J., CASSADY, A. I., JOYCE, D. A. & XU, J. 2005. Thapsigargin Modulates Osteoclastogenesis Through the Regulation of RANKL-Induced Signaling Pathways and Reactive Oxygen Species Production. *Journal of Bone and Mineral Research,* 20**,** 1462-1471.

YOKOTA, S.-I., KITAHARA, M. & NAGATA, K. 2000. Benzylidene Lactam Compound, KNK437, a Novel Inhibitor of Acquisition of Thermotolerance and Heat Shock Protein Induction in Human Colon Carcinoma Cells. *Cancer Research,* 60**,** 2942-2948.

YONG HWAN HAN & WOO HYUN PARK 2010. MG132 as a proteasome inhibitor induces cell growth inhibition and cell death in A549 lung cancer cells via influencing reactive oxygen species and GSH level. *Human & Experimental Toxicology,* 29**,** 607-614.

YORK, M. R., NAGAI, T., MANGINI, A. J., LEMAIRE, R., VAN SEVENTER, J. M. & LAFYATIS, R. 2007. A macrophage marker, siglec-1, is increased on circulating monocytes in patients with systemic sclerosis and induced by type i interferons and toll-like receptor agonists. *Arthritis & Rheumatism,* 56**,** 1010-1020.

YOSHIDA, H., HAYASHI, S., KUNISADA, T., OGAWA, M., NISHIKAWA, S., OKAMURA, H., SUDO, T., SHULTZ, L. D. & NISHIKAWA, S. 1990. The murine mutation osteopetrosis is in the coding region of the macrophage colony stimulating factor gene. *Nature,* 345**,** 442-4.

YOUNG, J. C., MOAREFI, I. & HARTL, F. U. 2001. Hsp90: a specialized but essential protein-folding tool. *J Cell Biol,* 154**,** 267-73.

YU, M., QI, X., MORENO, J. L., FARBER, D. L. & KEEGAN, A. D. 2011. NF-kappaB signaling participates in both RANKL- and IL-4-induced macrophage fusion: receptor cross-talk leads to alterations in NF-kappaB pathways. *J Immunol,* 187**,** 1797-806.

YUAN, B. Z., CHAPMAN, J. A. & REYNOLDS, S. H. 2008. Proteasome Inhibitor MG132 Induces Apoptosis and Inhibits Invasion of Human Malignant Pleural Mesothelioma Cells. *Transl Oncol,* 1**,** 129-40.

ZAIDI, M., PAZIANAS, M., SHANKAR, V. S., BAX, B. E., BAX, C. M., BEVIS, P. J., STEVENS, C., HUANG, C. L., BLAKE, D. R., MOONGA, B. S. & ET AL. 1993. Osteoclast function and its control. *Exp Physiol,* 78**,** 721-39.

ZANINI, C., GIRIBALDI, G., MANDILI, G., CARTA, F., CRESCENZIO, N., BISARO, B., DORIA, A., FOGLIA, L., DI MONTEZEMOLO, L. C., TIMEUS, F. & TURRINI, F. 2007. Inhibition of heat shock proteins (HSP) expression by quercetin and differential doxorubicin sensitization in neuroblastoma and Ewing's sarcoma cell lines. *Journal of Neurochemistry,* 103**,** 1344-1354.

ZARUBIN, T. & HAN, J. 2005. Activation and signaling of the p38 MAP kinase pathway. *Cell Res,* 15**,** 11-8.

ZAWAWI, M. S. F., DHARMAPATNI, A. A. S. S. K., CANTLEY, M. D., MCHUGH, K. P., HAYNES, D. R. & CROTTI, T. N. 2012. Regulation of ITAM adaptor molecules and their receptors by inhibition of calcineurin-NFAT signalling during late stage osteoclast differentiation. *Biochemical and Biophysical Research Communications,* 427**,** 404-409.

ZHANG, J., DAI, J., LIN, D. L., HABIB, P., SMITH, P., MURTHA, J., FU, Z., YAO, Z., QI, Y. & KELLER, E. T. 2002a. Osteoprotegerin abrogates chronic alcohol ingestion-induced bone loss in mice. *J Bone Miner Res,* 17**,** 1256-63.

ZHANG, J., DAI, J., QI, Y., LIN, D.-L., SMITH, P., STRAYHORN, C., MIZOKAMI, A., FU, Z., WESTMAN, J. & KELLER, E. T. 2001. Osteoprotegerin inhibits prostate cancer–induced osteoclastogenesis and prevents prostate tumor growth in the bone. *The Journal of Clinical Investigation,* 107**,** 1235-1244.

ZHANG, P., LEU, J. I. J., MURPHY, M. E., GEORGE, D. L. & MARMORSTEIN, R. 2014a. Crystal Structure of the Stress-Inducible Human Heat Shock Protein 70 Substrate-Binding Domain in Complex with Peptide Substrate. *PLoS ONE,* 9**,** e103518.

ZHANG, T. 2011. *A NOVEL HSP90 INHIBITOR TO DISRUPT HSP90/p50CDC37 COMPLEX FOR PANCREATIC CANCER THERAPY* Dissertion, The University of Michigan.

ZHANG, Y., AHN, Y.-H., BENJAMIN, I. J., HONDA, T., HICKS, R. J., CALABRESE, V., COLE, P. A. & DINKOVA-KOSTOVA, A. T. 2011. HSF1-Dependent Upregulation of Hsp70 by Sulfhydryl-Reactive Inducers of the KEAP1/NRF2/ARE Pathway. *Chemistry & biology,* 18**,** 1355-1361.

ZHANG, Y., DAYALAN NAIDU, S., SAMARASINGHE, K., VAN HECKE, G. C., PHEELY, A., BORONINA, T. N., COLE, R. N., BENJAMIN, I. J., COLE, P. A., AHN, Y. H. & DINKOVA-KOSTOVA, A. T. 2014b. Sulphoxythiocarbamates modify cysteine residues in HSP90 causing degradation of client proteins and inhibition of cancer cell proliferation. *Br J Cancer,* 110**,** 71-82.

ZHANG, Y., HUANG, L., ZHANG, J., MOSKOPHIDIS, D. & MIVECHI, N. F. 2002b. Targeted disruption of hsf1 leads to lack of thermotolerance and defines tissue-specific regulation for stress-inducible Hsp molecular chaperones. *J Cell Biochem,* 86**,** 376-93.

ZHAO, B., GRIMES, S. N., LI, S., HU, X. & IVASHKIV, L. B. 2012. TNF-induced osteoclastogenesis and inflammatory bone resorption are inhibited by transcription factor RBP-J. *The Journal of Experimental Medicine,* 209**,** 319-334.

ZHAO, H., LAITALA-LEINONEN, T., PARIKKA, V. & VÄÄNÄNEN, H. K. 2001. Downregulation of Small GTPase Rab7 Impairs Osteoclast Polarization and Bone Resorption. *Journal of Biological Chemistry,* 276**,** 39295-39302.

ZHAO, Q., WANG, X., LIU, Y., HE, A. & JIA, R. 2010. NFATc1: Functions in osteoclasts. *The International Journal of Biochemistry & Cell Biology,* 42**,** 576-579.

ZOU, J., GUO, Y., GUETTOUCHE, T., SMITH, D. F. & VOELLMY, R. 1998. Repression of Heat Shock Transcription Factor HSF1 Activation by HSP90 (HSP90 Complex) that Forms a Stress-Sensitive Complex with HSF1. *Cell,* 94**,** 471-480.

ZOU, W., KITAURA, H., REEVE, J., LONG, F., TYBULEWICZ, V. L. J., SHATTIL, S. J., GINSBERG, M. H., ROSS, F. P. & TEITELBAUM, S. L. 2007. Syk, c-Src, the αvβ3 integrin, and ITAM immunoreceptors, in concert, regulate osteoclastic bone resorption. *The Journal of Cell Biology,* 176**,** 877-888.

ZUBRIENĖ, A., GUTKOWSKA, M., MATULIENĖ, J., CHALECKIS, R., MICHAILOVIENĖ, V., VORONCOVA, A., VENCLOVAS, Č., ZYLICZ, A., ZYLICZ, M. & MATULIS, D. 2010. Thermodynamics of radicicol binding to human Hsp90 alpha and beta isoforms. *Biophysical Chemistry,* 152**,** 153-163.

ZUEHLKE, A. & JOHNSON, J. L. 2010. Hsp90 and co-chaperones twist the functions of diverse client proteins. *Biopolymers,* 93**,** 211-217.

Appendix A: Solution and Buffer Recipes

Appendix A: Solution and Buffer Recipes

SOB Medium (per Litre)
20g of Tryptone
5g of yeast extract
0.5 NaCl
Deionised H_2O to 1L
Autoclaved
Add 10ml of filter-sterilized $MgCl_2$ (1M) and 10ml of filter sterilized $MgSO_4$ (1 M) prior to use

SOC Medium (per 100ml)
1ml of filter-sterilized glucose (2 M)
SOB medium (autoclaved) to a final volume of 100ml*
* This medium is required to be prepared immediately before use

LB Broth (per 400ml)

Tryptone (OXOID L42)	4 g
Yeast extract (OXOID L21)	2 g
Sodium Chloride	4 g
MQ water to 400mls	
Autoclave	

LB-Agar (per 400ml)

Tryptone (OXOID L42)	4 g
Yeast extract (OXOID L21)	2 g
Sodium Chloride	4 g
Agar (OXOID)	6 g
MQ water to 400mls	
Autoclave	

1M $MgSO_4$

$MgSO_4$	123.2 g
dH_2O	500ml
Autoclave	

1M $MgCl_2$

$MgCl_2$	101.7g
dH_2O	500ml
Autoclave	

2M Glucose

Glucose	18g
Autoclaved dH$_2$O	50ml

*Filter sterilize

Acetic Acid

Glacial acetic acid	100ml
dH$_2$O	900ml

EDTA 100mM pH8

EDTA	37.22g
Autoclaved H$_2$O	1 litre

*Adjust pH to 8.

Radioimmunoprecipitation assay (RIPA) buffer

50 mMol/L Tris-HCl (pH 7.4)
1% NP40
0.25% Na deoxycholate
150 mMol/L NaCl
dH$_2$O   250ml

*Before use EDTA free Complete Protease Inhibitors (Halt (Thermo Fisher Scientific, Rockford, IL, USA) and Phosphatase inhibitors were added (Sigma-Aldrich, Castle Hill, NSW, AUS)

10 X TBS (per Litre)

0.5M TRIS	60.57g
1.5M NaCl	87.66g

Dilute in 800ml of dH$_2$O, pH to 7.4. Top up with dH$_2$O to 1 Litre

1 X TBS/1%Tween

dH$_2$O	900 ml
10 x TBS	100ml
Tween-20	1ml

25 X Transfer Buffer

25mM TRIS-HCl	30.3g
192mM Glycine	144g
Deionised H$_2$O to 1L	

1 X Transfer Buffer (per 500ml)

25 x Novex transfer buffer	40ml
dH$_2$O	360ml
Methanol	100ml

TRAP histochemical stain buffer

Sodium acetate (2.05 g) and potassium sodium tartrate (5.65 g) was dissolved in 400 ml dH$_2$O.The pH was adjusted to 5.0 with glacial acetic acid and diluted to a final volume of 500 ml with dH$_2$O resulting in a final solution containing sodium acetate (50 mM) and potassium sodium tartrate (40 mM). The solution was stored at 4°C for up to 3 months.

4 % Formaldehyde

10 ml formaldehyde (BDH) (40 %) was diluted in 90 ml dH$_2$O and stored at room temperature in a light-proof bottle.

Methanol: Acetone solution

Equal volumes of Methanol and Acetone were combined and mixed thoroughly.

Crystal Violet Stain

Add 2ml of EtoH (100%) to 98ml autoclaved H$_2$O.Add crystal violet (1 g). Filter the solution.

Appendix B Additional Figures

Appendix B Additional Figures
The Effect of HSP90 Inhibitors upon RAW264.7 Cell Growth
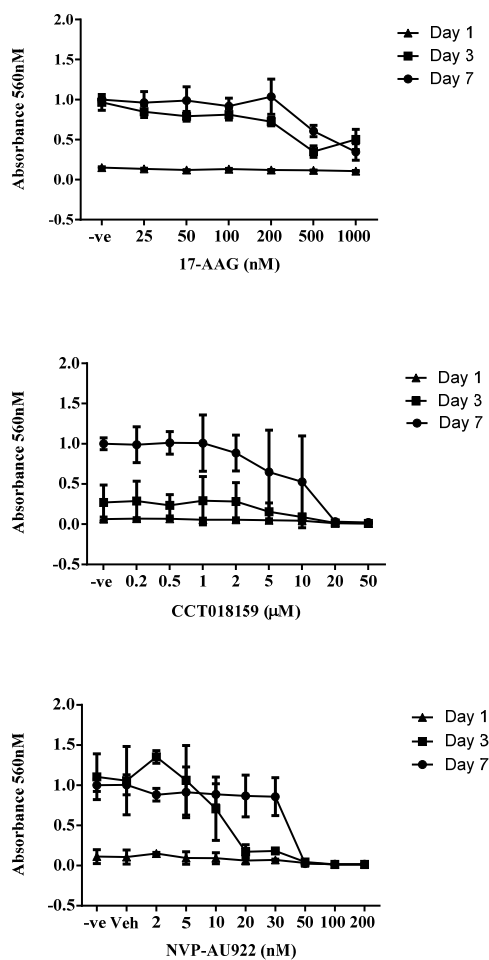
Appendix Figure B1

RAW264.7 cells were seeded at 10^4 in 6mm wells and were allowed to adhere overnight. The cells were treated with HSP90 inhibitors: 17-AAG (0.02, 0.05, 0.1, 0.2, 0.5, 1μM), CCT08159 (0.2, 0.5, 1, 2, 5, 10, 20 and 50μM) and NVP-AUY922 (2, 5, 10, 20, 30, 50, 100, 200nM) and were incubated (37°C and 5%CO_2) for 1, 3, and 7 days. At these time points the cells were washed in PBS (1x), fixed in formaldehyde (4%) and washed again in PBS (1x). The cells were stained with 3-4 drops of crystal violet and were incubated at room temperature for 10 minutes. The stain was washed out and the cells air-dried overnight. The crystal violet stained cells were eluted in 10% acetic acid (200μl) and shaken for 15 minutes at room temperature. The absorbance (560nM) was read on an EnVision plate reader.

# The Effect of HSF1 Inhibitor, KNK437, upon RAW264.7 Cell Growth
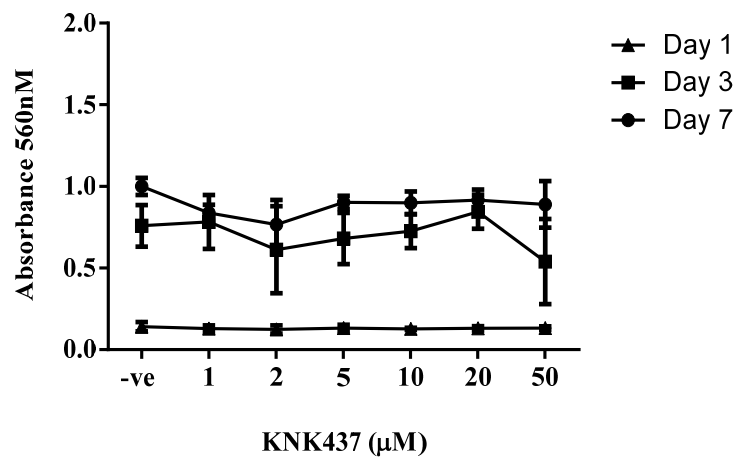
Appendix Figure B2

RAW264.7 cells were seeded at 10^4 in 6mm diameter wells, and allowed to adhere overnight. The RAW264.7 cells were treated with KNK437 (1, 2, 5, 10 and 20 μM) and were incubated (37°C and 5% CO_2) for 1, 3, and 7 days. At these time points the cells were washed in PBS (1x), fixed in 4% for 5 minutes at room temperature and washed again in PBS (1x). The cells were: stained with 3-4 drops of crystal violet, incubated at room temperature for 10 minutes, washed to remove excess stain and air-dried overnight. The crystal violet stained cells were eluted in 10% acetic acid (200μl) and were shaken for 15 minutes at room temperature. The absorbance (560nM) was read on an EnVision plate reader.

The Effect of Chemotherapeutics upon RAW264.7 Cell Growth
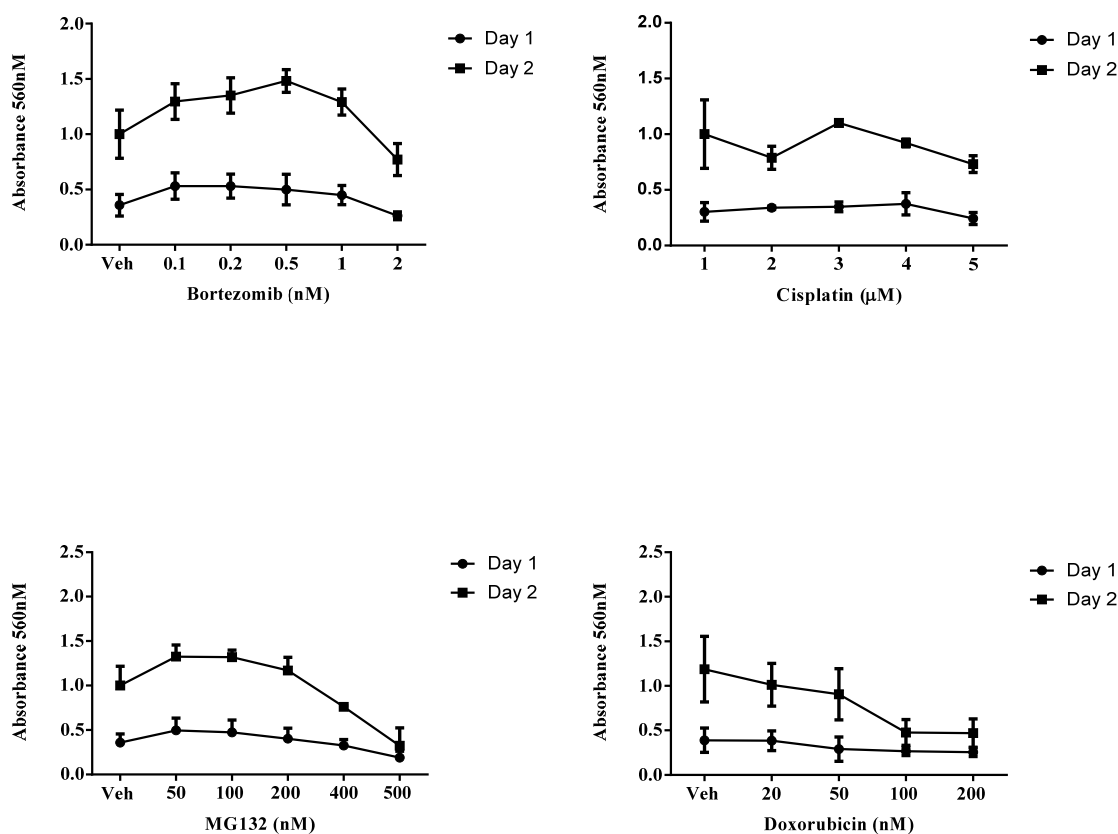
Appendix Figure B3

RAW264.7 cells were seeded at 10^4 in 6mm diameter wells. The cells were treated with chemotherapeutics: bortezomib (0.1, 0.2, 0.5, 1 and 2nM), cisplatin (1, 2, 3, 4 and 5μM), MG132 (50, 100, 200, 400 and 500nM) and doxorubicin (20, 50, 100 and 200nM) and were incubated (37°C and 5%CO_2) for 1 or 2 days. At these time points the cells were washed in PBS (1x), fixed in formaldehyde (4%) and washed again in PBS (1x). The cells were stained with 3-4 drops of crystal violet and were incubated at room temperature for 10 minutes. The stain was washed out and the cells air-dried overnight. The crystal violet stained cells were eluted in 10% acetic acid (200μl) and shaken for 15 minutes at room temperature. The absorbance (560nM) was read on an EnVision plate reader.

The Effect of Chemotherapeutics upon HEK-HSE Cell Growth
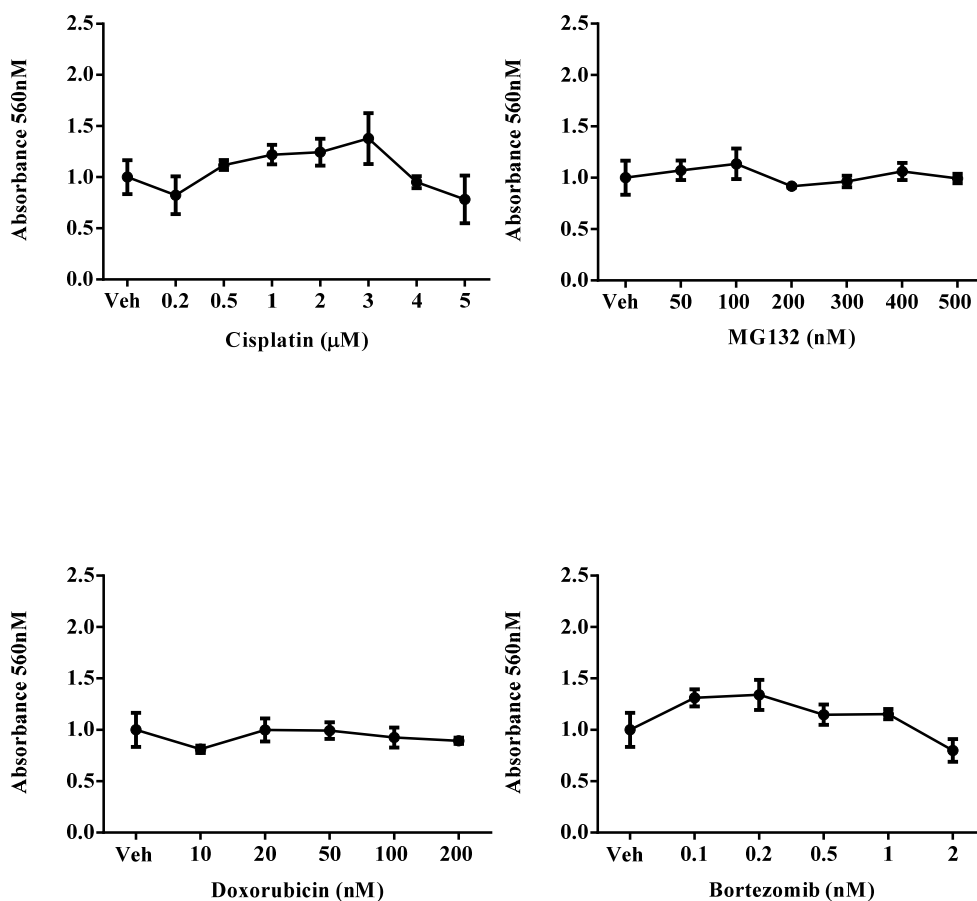
Appendix Figure B4

HEK-HSE cells (2.5×10^4) were seeded and allowed to adhere for ≥ 3 hours. The cells were treated with chemotherapeutics: cisplatin (0.2, 0.5, 1, 2, 3, 4 and 5μM), MG132 (50, 100, 200, 300, 400 and 500nM), doxorubicin (10, 20, 50, 100 and 200nM) and bortezomib (0.1, 0.2, 0.5, 1 and 2 nM) and were incubated (37°C and $5\%CO_2$) for 24 hours. At this time point the cells were washed in PBS (1x), fixed in formaldehyde (4%) and washed again in PBS (1x). The cells were stained with 3-4 drops of crystal violet and were incubated at room temperature for 10 minutes. The stain was washed out and the cells air-dried overnight. The crystal violet stained cells were eluted in 10% acetic acid (200μl) and shaken for 15 minutes at room temperature. The absorbance (560nM) was read on an EnVision plate reader.

The Effect of KNK437 upon Osteoclast Formation

A.

B.
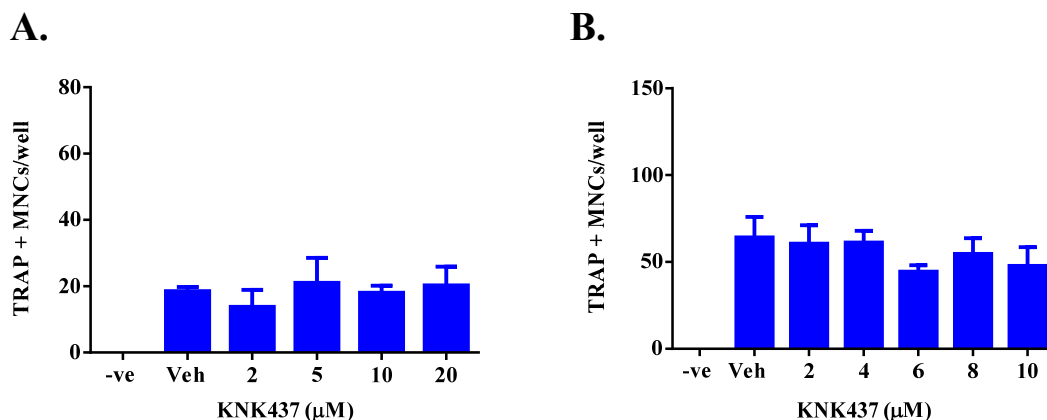
Appendix Figure B5

(A.) RAW264.7 cells, **(B.)** Bone Marrow Cells. RAW264.7 cells were seeded at 10^4 cells and bone marrow cells at 10^5 cells in 6mm diameter wells in the presence of RANKL (20ng/ml) and RANKL (20ng/ml) and M-CSF (30ng/ml), respectively. RAW264.7 cells and bone marrow cells were treated with KNK437 (2, 5, 10 and 20μM) and KNK437 (2, 4, 6, 8 and 10μM) respectively. The cultures were also treated with DMSO ("Veh"). As a negative control the cells were not treated with RANKL, as denoted by "-ve". On day 6, the cells were fixed and stained for TRAP. Multinucleated and TRAP positive cells were counted as osteoclasts. **(A.)** Data is expressed as mean ± SD of one independent experiment with 4 replicates per treatment. **(B.)** Data is expressed as mean ± SEM of two independent experiments.

KNK437 Abolishes the Doxorubicin Elicited HSE-dependent Activity in HSE-HEK Cells

17-AAG (200nM)	-	Veh	-	+	+
RANKL (20ng/ml)	-ve	+	+	+	+
KNK437(10μM)	-	-	+	-	+
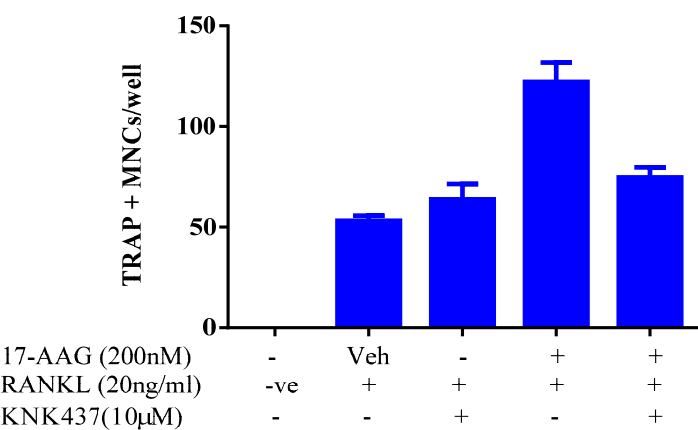
Appendix Figure B6

RAW264.7 cells were seeded at 10^4 cells in 6mm diameter wells in the presence of RANKL (20ng/ml). The cultures were treated with 17-AAG (200nM)) in the presence or absence of KNK437 (10μM) for 6 days. The cultures were also treated with DMSO ("Veh") or KNK437 (10μM) alone. As a negative control the cells were not treated with RANKL, as denoted by "-ve". On day 6, multinucleated and TRAP positive cells were counted as osteoclasts. 17-AAG treatment increased osteoclast formation as previously observed; however, the addition of KNK437 reduces osteoclast numbers similar to that in the DMSO vehicle control. All data is expressed as mean ± SD of one independent experiment with 4 replicates per treatments (as per all osteoclast assays performed).

KNK437 Abolishes the Doxorubicin Elicited HSF1 Transcriptional Activity in HSE-HEK Cells

Doxorubicin (5nM)	Veh	-	+	+
KNK437 (10μM)	-	+	-	+
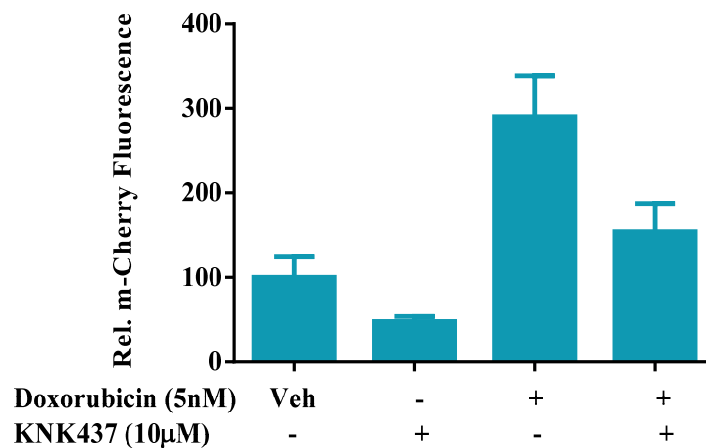
Appendix Figure B7

HEK-HSE cell were seeded at 2.5 x 10^4 cells in 6mm diameter wells in DMEM phenol-free media and were left to adhere for $\geq$ 3 hours. The cells were then treated with doxorubicin (5nM) in the presence or absence of KNK437 (10μM). The cells were also treated with KNK437 (10μM) alone. At 24 hours Hoechst dye (10μg/ml) was added to the wells and the cells incubated (37°C, 5% CO_2 for 15 minutes). The levels of mCherry were collected using an Arrayscan VTI High Content Screening instrument. Individual cells were identified by Hoechst nuclear stain and the percentage threshold of mCherry was measured relative to the DSMO vehicle control, "Veh". After 24 hours of treatment, doxorubicin treatment increased HSF1 transcriptional activity; however, the addition of KNK437 ablated this increase. KNK437 treatment alone also reduced HSF1 transcriptional activity. All data is expressed as the mean ± SEM of two independent experiments.

KNK437 Ablates the Bortezomib Mediated Increase in HSF1 Transcriptional Activity in HSE-HEK Cells

| Bortezomib (50nM) | Veh | - | + | + |
| KNK437 (10μM) | - | + | - | + |
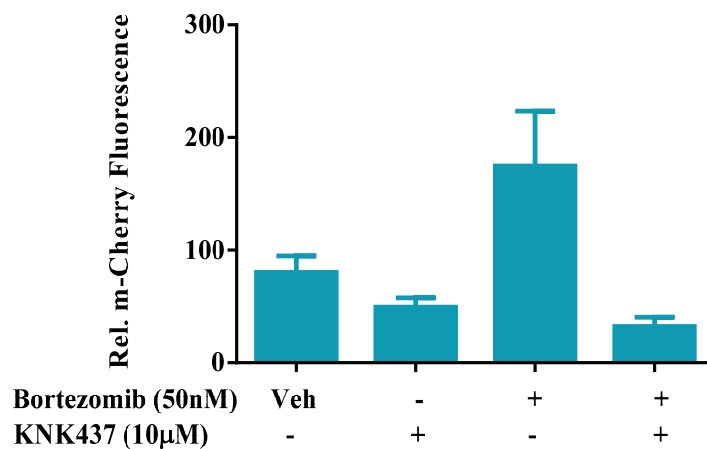
Appendix Figure B8

HEK-HSE cell were seeded at 2.5 x 10^4 cells in 6mm diameter wells in DMEM phenol-free media. The cells were allowed to settle for ≥ 3 hours then treated with bortezomib (50nM) in the presence or absence of KNK437 (10μM). Cells were also treated with KNK437 (10μM) alone. At 24 hours, Hoechst dye (10μg/ml) was added to the wells and the cells incubated (37 °C, 5% CO_2 for 15 minutes). The levels of mCherry were collected using an Arrayscan VTI High Content Screening instrument. Individual cells were identified by Hoechst nuclear stain and the percentage threshold of mCherry was measured against a DMSO vehicle control, "Veh". Bortezomib increased HSF1 activity as previously shown; however, KNK437 decreases the bortezomib mediated increase in HSF1 activity. Also KNK437 treatment alone reduces basal HSE transcriptional activity. All data is expressed as mean ± SEM of 2 independent experiments.

Bortezomib Treatment Increases RANKL Mediated-RAW264.7 Cell Osteoclast Formation

A.

B.

Veh   Bortezomib (1000pM)
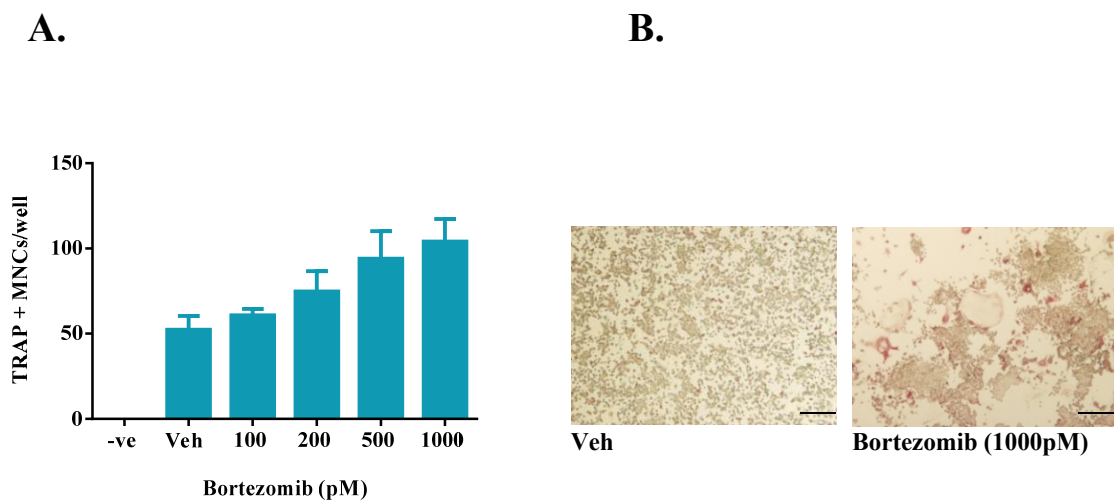
Appendix Figure B9

(A-B.) RAW264.7 cells were seeded at 10^4 cells in 6mm diameter wells and stimulated with RANKL (20ng/ml). The cells were treated with bortezomib (100, 200, 500 and 1000pM) or DMSO ("Veh") for 6 days. As a negative control the cells were not treated with RANKL denoted by "-ve". On day 6, multinucleated and TRAP positive cells were counted as osteoclasts. Bortezomib treatment increases osteoclast formation in a dose dependent manner relative to the DMSO vehicle control. **(B.)** Image of RAW264.7 cells treated with Veh or bortezomib (1000pM). Representative graph of two independent experiments. Scale bar - 50μM.

Cisplatin increases MITF Protein Expression in RAW264.7 Cells at 48 hours

48hr

Cisplatin (μM)

| Veh | 0.5 | 1 |

MITF — 62kDa

β-actin — 38kDa
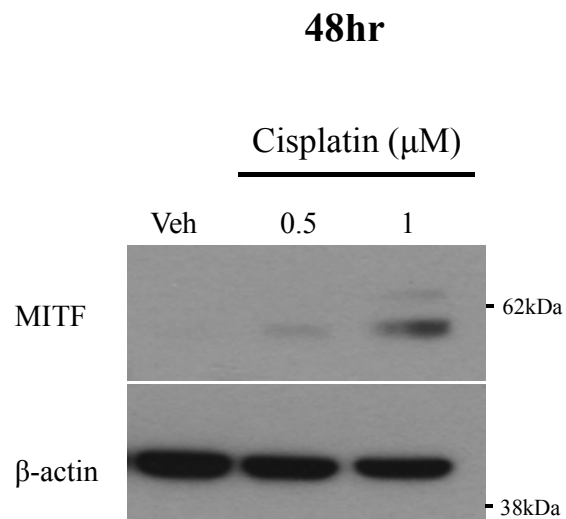
Appendix Figure B10

RAW264.7 cells were seeded at 2 x10^5 in 35mm diameter culture wells and were treated the following day with cisplatin (0.5, 1 and 3 μM) or a DMSO vehicle control, "Veh", for 48 hours. The cells were lysed and MITF protein levels determined by immunoblotting analysis. Cisplatin treatment increased MITF protein levels at 48 hours relative to the DMSO vehicle control.

Ethanol Increases NFATc1 Protein Expression

A.

24hr

B.

48hr
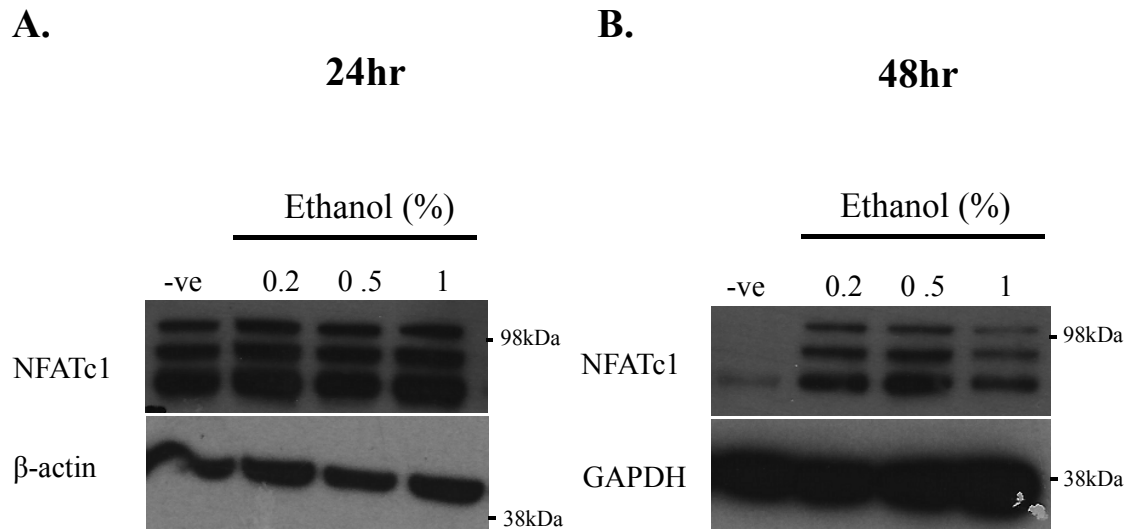
Appendix Figure B11

RAW264.7 cells were seeded at 2 x10^5 in 35mm diameter culture wells and were treated the following day with ethanol (0.2,0 .5 and 1%) for **(A.)** 24 and **(B.)**. 48 hour. As a negative control the cells were left untreated, "-ve". The cells were lysed and NFATc1 protein levels determined by immunoblotting analysis. Ethanol treatment increased NFATc1 protein levels at both 24 and 48 hours relative to the negative control.

KNK437 Ablates the Chemotherapeutic-Mediated Increase in RAW264.7 Cell Osteoclast Formation

A.

Doxorubicin (5nM)	-ve	Veh	-	+	+
RANKL (20ng/ml)	-	+	+	+	+
KNK437 (10μM)	-	-	+	-	+

B.

MG132 (100nM)	-ve	Veh	-	+	+
RANKL (20ng/ml)	-	+	+	+	+
KNK437 (10μM)	-	-	+	-	+

C.

Cisplatin (1μM)	-ve	Veh	-	+	+
RANKL (20ng/ml)	-	+	+	+	+
KNK437 (10μM)	-	-	+	-	+
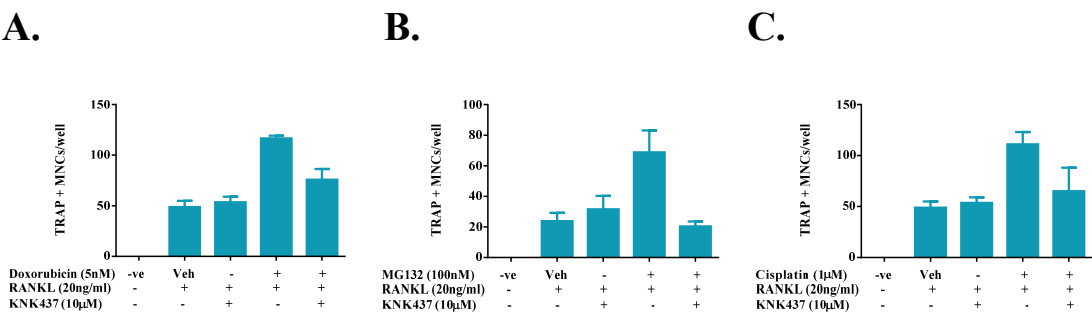
Appendix Figure B12

(A-C.) RAW264.7 cells were seeded at 10^4 cells in 6mm diameter wells in the presence of RANKL (20ng/ml). The cultures were treated with **(A.)** doxorubicin (5nM), **(B.)** MG132 (100nM) and **(C.)** cisplatin (1μM) in the presence or absence of KNK437 (10μM) for 6 days. **(A-C.)**The cultures were also treated with DMSO ("Veh") or KNK437 (10μM) alone. As a negative control the cells were not treated with RANKL, as denoted by "-ve". On day 6 the cells were fixed and stained for TRAP. Multinucleated and TRAP positive cells were counted as osteoclasts. Doxorubicin, MG132 and cisplatin treatment all increase osteoclast formation as previously observed; however, the addition of KNK437 reduces osteoclast numbers similar to that in the DMSO vehicle control. All data is expressed as mean ± SD of one independent experiment with 4 replicates per treatments (as per all osteoclast assays performed).

KNK437 Treatment Abrogates the Ethanol Mediated Increase in Osteoclast Formation

A.

B.
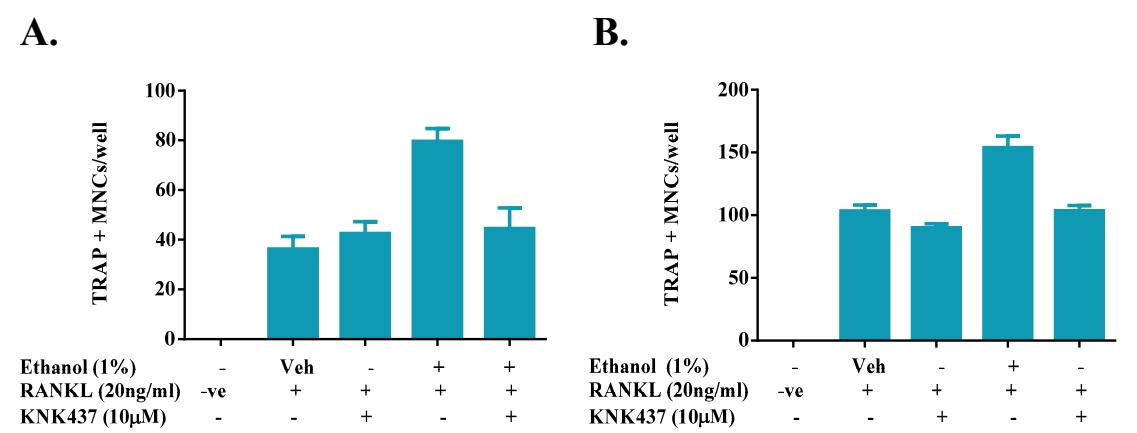
Appendix Figure B13

(A.) RAW264.7 cells, **(B.)** Bone Marrow Cells. **(A-B.)** RAW264.7 cells were seeded at 10^4 cells and bone marrow cells at 10^5 cells in 6mm diameter wells in the presence of RANKL (20ng/ml) and RANKL (20ng/ml) and M-CSF (30ng/ml), respectively. The cultures were treated with Ethanol (1%) in the presence or absence of KNK437 (10μM) for 6 days. The cultures were also treated with DMSO ("Veh") or KNK437 (10μM) alone. As a negative control the cells were not treated with RANKL, as denoted by "-ve". On day 6, multinucleated and TRAP positive cells were counted as osteoclasts. Ethanol increases osteoclast formation in both cultures; however, the addition of KNK437 decreases osteoclast numbers similar to that in the DSMO vehicle control. All data is expressed as mean ± SEM of two independent experiments for both **(A-B.)**.

The Effect of 17-AAG Treatment upon Carbonic Anhydrase II (CAR2) mRNA Expression

A.

B.
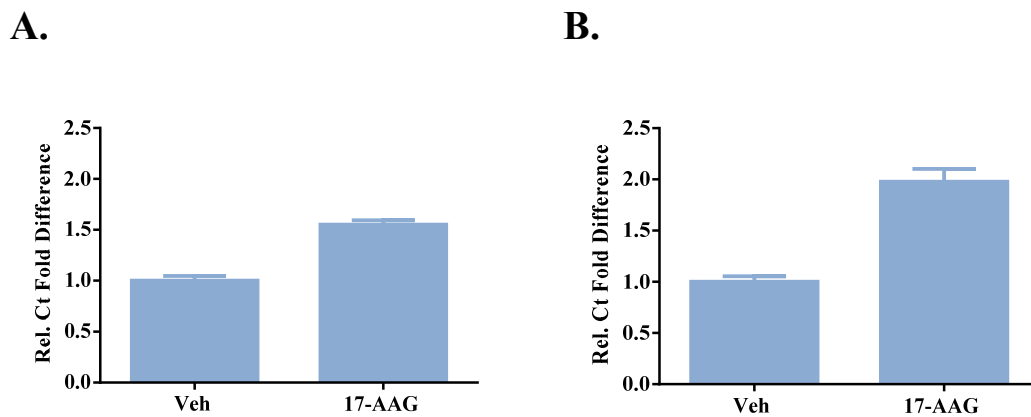
Appendix Figure B14

RAW264.7 cells were seeded at 10^4 cells in 35mm diameter wells. The following day the cells were treated with 17-AAG (500nM) or a DMSO vehicle control for 24 or 48 hours. RNA was extracted, DNase treated and cDNA prepared and used in qRT-PCR. Data was normalised to HRPT mRNA and is shown relative to DMSO vehicle control. 17-AAG increased CAR 2 mRNA expression at **(A.)** 24 hours and at **(B.)** 48 hours. All data are expressed as mean ± SEM of two independent experiments for both **(A-B.)**.

The Effect of 17-AAG Treatment upon OC-STAMP mRNA Expression

A.

B.
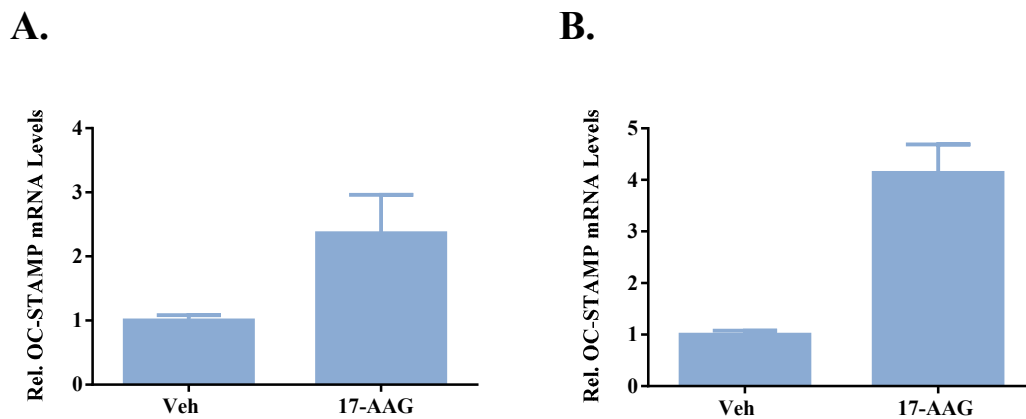
Appendix Figure B15

RAW264.7 cells were seeded at 10^4 cells in 35mm diameter wells. The following day the cells were treated with 17-AAG (500nM) or a DMSO vehicle control for 24 hours. RNA was extracted, DNase treated and cDNA prepared and used in qRT-PCR. Data was normalised to HRPT mRNA and is shown relative to DMSO vehicle control. 17-AAG increased OC-STAMP mRNA expression at **(A.)** 24 hours and **(B.)** 48 hours. Data is expressed as mean ± SD of one independent experiment.

Appendix C

Journal Articles Arising from this Work

HSP90 inhibitors enhance differentiation and MITF (microphthalmia transcription factor) activity in osteoclast progenitors

A. Gabrielle J. van der Kraan*†, Ryan C. C. Chai†, Preetinder P. Singh*, Benjamin J. Lang†, Jiake Xu‡, Matthew T. Gillespie*†, John T. Price†[1] and Julian M. W. Quinn*†[1,2]

*Prince Henry's Institute, Monash Medical Centre, Clayton, VIC 3168, Australia, †Department of Biochemistry and Molecular Biology, School of Biomedical Sciences, Monash University, Clayton, VIC 3800, Australia, and ‡School of Pathology and Laboratory Medicine, University of Western Australia, Crawley, WA 6009, Australia

The HSP90 (heat-shock protein 90) inhibitor 17-AAG (17-allylamino-demethoxygeldanamycin) increases osteoclast formation both *in vitro* and *in vivo*, an action that can enhance cancer invasion and growth in the bone microenvironment. The cellular mechanisms through which 17-AAG exerts this action are not understood. Thus we sought to clarify the actions of 17-AAG on osteoclasts and determine whether other HSP90 inhibitors had similar properties. We determined that 17-AAG and the structurally unrelated HSP90 inhibitors CCT018159 and NVP-AUY922 dose-dependently increased RANKL [receptor activator of NF-κB (nuclear factor κB) ligand]-stimulated osteoclastogenesis in mouse bone marrow and pre-osteoclastic RAW264.7 cell cultures. Moreover, 17-AAG also enhanced RANKL- and TNF (tumour necrosis factor)-elicited osteoclastogenesis, but did not affect RANKL-induced osteoclast survival, suggesting that only differentiation mechanisms are targeted. 17-AAG affected the later stages of progenitor maturation (after 3 days of incubation), whereas the osteoclast formation enhancer TGFβ (transforming growth factor β) acted prior to this, suggesting different mechanisms of action. In studies of RANKL-elicited intracellular signalling, 17-AAG treatment did not increase c-Fos or NFAT (nuclear factor of activated T-cells) c1 protein levels nor did 17-AAG increase activity in luciferase-based NF-κB- and NFAT-response assays. In contrast, 17-AAG treatment (and RANKL treatment) increased both MITF (microphthalmia-associated transcription factor) protein levels and MITF-dependent vATPase-d2 (V-type proton ATPase subunit d2) gene promoter activity. These results indicate that HSP90 inhibitors enhance osteoclast differentiation in an NFATc1-independent manner that involves elevated MITF levels and activity.

Key words: 17-allylamino-demethoxygeldanamycin (17-AAG), bone, cell signal, heat-shock protein 90 (HSP90), osteoclast, osteolysis.

INTRODUCTION

The osteoclast is a multinucleated macrophage-related cell that has a central role in bone metabolism through its ability to directly resorb bone [1]. In bone remodelling and repair, bone resorbed by osteoclasts is replaced by new bone formed by mesenchymally derived osteoblasts [2], the balance between these two cellular actions maintains bone mass, structure and mechanical qualities. However, this balance can be perturbed by pathological stimuli that increase osteoclast numbers to cause a net loss of bone. This is commonly seen in inflammation and with the invasion of the bone by metastasizing cancer cells, notably breast cancer cells, that cause hypercalcaemia and pathological fractures at the affected sites [2–5]; such osteolysis releases bone matrix-associated factors that considerably enhance tumour growth within the bone. The mechanisms that underlie pathological bone loss are not well understood, but are of major clinical interest.

Osteoclast formation from macrophage lineage progenitors is a major point of control in bone resorption and is normally driven by RANKL {RANK [receptor activator of NF-κB (nuclear factor κB)] ligand} and M-CSF (macrophage colony-stimulating factor), the latter a macrophage proliferation and survival factor

[1,6]. RANKL, a member of the TNF (tumour necrosis factor) family, binds its cognate receptor RANK on progenitor cells to elicit signals essential for osteoclastic gene expression [7,8]. RANKL and its receptor are essential for osteoclast formation *in vivo* and mice lacking RANK or RANKL are devoid of osteoclasts [9], although in some circumstances TNF has a low capacity to elicit osteoclast formation [10,11]. Osteoclast formation is normally regulated by RANKL expression levels in osteoblasts and osteocytes, which is in turn regulated by osteolytic hormones [12]. However, a few local factors can directly act on osteoclast progenitors to enhance RANKL-dependent osteoclastogenesis, notably TGFβ (transforming growth factor β) [13,14].

HSP (heat-shock protein) 90 is a ubiquitously expressed ATPase-dependent molecular chaperone that mediates the conformational maturation and stability of its client proteins [15], including many that participate in cell signalling pathways. These include numerous protein kinases, steroid receptors and transcription factors, some critical for cancer cell growth, survival and progression [16]. Owing to the importance of HSP90 to cancer cells, HSP90 has emerged as a significant therapeutic target in cancer. As a result, a number of HSP90

inhibitors have been generated, primarily targeting the N-terminal ATPase domain of the molecule. Most of these agents can be grouped according to their structural similarity to the compounds GM (geldanamycin) and RD (radicicol) [17]. These include, respectively, the benzoquinone ansamycin 17-AAG (17-allyl-17-demethoxygeldanamycin) and the resorcinol isoxazole derivative NVP-AUY922.

Although 17-AAG potently inhibits soft tissue tumour growth in numerous models [18,19] and HSP90 inhibition can perturb the signalling molecules involved in osteoclast formation [20–22], we found that 17-AAG can still strongly enhance RANKL-driven osteoclast formation *in vitro* and *in vivo*, causing significant bone loss [23]. This was consistent with our observation that 17-AAG, surprisingly, increased breast cancer bone metastasis, but not soft tissue tumour growth or invasion in xenograft mouse models [23]. Yano et al. [24] subsequently made similar findings in a prostate cancer xenograft model which further confirmed the importance of osteoclasts in the deleterious effect of 17-AAG on bone. Although the latter study suggested a mediating action for Src kinase, the lack of a fundamental role for Src in osteoclast differentiation suggests other mechanisms exist. The strong enhancement of RANKL-dependent osteoclast formation by 17-AAG raises the possibility that 17-AAG actions are mediated by intracellular signals and/or transcription factors which are induced by RANKL. These include NF-κB, NFATc1 (nuclear factor of activated T-cells, cytoplasmic 1), AP-1 (activator protein 1; a c-Fos/c-Jun dimer) and MITF (microphthalmia-associated transcription factor); when these factors are blocked or absent osteoclast formation does not occur [1]. NFATc1 in particular is considered a critical regulator of osteoclastogenesis as its forced overexpression causes RANKL-independent osteoclast formation [25]. Many osteoclast inhibitory factors can reduce NFATc1 levels, whereas other factors, such as TGFβ, can enhance them [25,26]. Activated NFATc1 forms complexes that can include transcription factors PU.1, AP-1, NF-κB and MITF [3,25] and these drive the expression of numerous osteoclast-associated genes.

In the present study we sought to identify critical mechanisms of action of 17-AAG by examining the kinetics of its influence on osteoclast formation and its effects on RANKL-elicited cell signals. Moreover, we also investigated whether other structurally unrelated HSP90 inhibitors with emerging therapeutic potential, namely CCT018159 and NVP-AUY922, similarly influence osteoclast formation. The results of the present study confirm that the those HSP90 inhibitors do indeed potently increase osteoclast formation. Additionally, our extended analysis of 17-AAG demonstrates surprisingly that although no effects on NFATc1, c-Fos or NF-κB were observed, 17-AAG significantly enhances MITF levels and activity. This influence on MITF may thus constitute a novel NFATc1-independent mechanism driving bone loss associated with HSP90 inhibitor treatment, and so may potentially contribute to other types of pathological osteolysis.

MATERIALS AND METHODS

Reagents

17-AAG was purchased from LC Labs, CCT018159 was from Cayman Chemical and NVP-AUY922 purchased from Biovision. L-cell conditioned medium (an impure source of secreted murine M-CSF) was prepared as described in Yeung et al. [27]. For TRAP (tartrate-resistant acid phosphatase) staining, fast Red Violet LB Salt F-1625, naphthol AS-MX phosphate and dimethylformamide were purchased from Sigma–Aldrich. Recombinant soluble murine RANKL was purchased from Oriental Yeast Company,

and human M-CSF and TGFβ (TGFβ1 isoform) from R&D Systems.

Antibodies and Animals

Purified anti-CTR (calcitonin receptor) antibody was produced in-house following the method of Tikellis et al. [28]. Mouse monoclonal anti-MITF antibody (C5; ab12039) was purchased from Abcam, and anti-NFATc1 (7A6; sc-7294) and anti-MITF (N15; sc-10999) antibodies were purchased from Santa Cruz Biotechnology. Anti-β-actin clone AC-15 which was used as a loading control for immunoblotting was purchased from Sigma–Aldrich. HRP (horseradish peroxidase)-conjugated anti-(mouse IgG) and anti-(goat IgG) secondary antibodies for immunohistochemistry and immunoblotting were obtained from Pierce and Thermo Scientific respectively. Alexa Fluor™ 680 goat anti-rabbit (A21076) and Alexa Fluor™ 750 goat anti-mouse (A21037) antibodies were obtained from Life Technologies. C57BL/6 mice were obtained from Monash Animal Services (Monash University, Clayton, Australia) and maintained at the Monash Medical Centre Animal Facility (Clayton, Australia) according to procedures approved by Monash Medical Centre Animal Ethics Committee B, authorization MMCB-2011/19. Bone marrow cells for culture were immediately isolated from humanely killed mice by flushing the bone marrow cavity of long bones with PBS.

Cell cultures

Primary bone marrow macrophage cultures were maintained in L-cell conditioned medium to induce macrophage proliferation as described previously [29]. RAW264.7 cells (A.T.C.C.) and primary bone marrow cells undergoing osteoclast differentiation were cultured in MEM (α-minimal essential medium; Life Technologies) supplemented with 10 % FBS (fetal bovine serum; CSL Biosciences) and containing 0.005 % penicillin (10 000 units/ml)/streptomycin (10 000 units/ml) (Life Technologies), L-glutamine (29.95 mg/ml; Life Technologies) and Hepes (Sigma–Aldrich). Cells were maintained in a 37 °C incubator in a humidified atmosphere containing 5 % CO_2.

Assays of osteoclast progenitor differentiation, proliferation and activity

Assays for osteoclast formation were performed as described previously [23,29] with all experiments being performed in quadruplicate wells for each independent experiment. Briefly, RAW264.7 cells (10^4 cells/well) or mouse bone marrow cells (10^5 cells/well) were cultured in 6-mm diameter tissue culture wells containing 0.2 ml of medium (MEM/FBS) with the mouse bone marrow cells being supplemented with 30 ng/ml M-CSF. To induce osteoclast differentiation, the indicated concentrations of RANKL or TNF were added to the cells and replaced after day 3 of culture. On day 6 of incubation, cells were fixed in 4 % buffered formalin for 10 min then washed in methanol/acetone (1:1 ratio), air-dried and histochemically stained for TRAP [30]; TRAP$^+$ cells with >2 nuclei by light microscopy were counted as MNCs (multinucleated cells) or osteoclasts. Some osteoclast-forming cultures were performed on glass coverslips to allow immunohistochemical detection of CTR. On day 6 these cultures were washed, acetone-fixed, dried and immunoperoxidase-stained with 5 μg/ml purified anti-CTR antibody and haematoxylin counterstained as described previously [30]; as an immunostaining control the anti-CTR

antibody was neutralized via incubation with 100 μg/ml antigen (CTR peptide) prior to use [30]. For osteoclast survival assays, osteoclasts were first generated by stimulation of bone marrow cells (5×10^6 cells) in 10-cm diameter tissue culture dishes for 6 days with 100 ng/ml RANKL and 30 ng/ml M-CSF. Cells were then dispersed using non-enzymic cell dispersion buffer (catalogue number C5914, Sigma), rinsed in PBS, resuspended in MEM/10 % FBS and plated at 10^5 cells/well in 6-mm culture wells. Cells were cultured for 24 h with survival factor (RANKL) in conjunction with other treatments. Cells were then fixed and histochemically stained for TRAP and the osteoclast numbers counted; results are expressed relative to the positive control cultures stimulated by 100 ng/ml RANKL alone. For cell proliferation assays RAW264.7 cells were seeded at 10^4 cells per 6-mm diameter culture well and treated with HSP90 inhibitors. Cells were fixed in 4 % formaldehyde and Crystal Violet stained after 1, 3 and 7 days of incubation then dried and eluted before the absorbance at 560 nm was measured on a Wallac EnVision multilabel plate reader (PerkinElmer).

Immunoblot analysis

Immunoblot analysis was performed as described previously [23]. Briefly, cell lysates were generated using modified RIPA buffer [50 mmol/l Tris/HCl (pH 7.4), 1 % Nonidet P40, 0.25 % sodium deoxycholate and 150 mmol/l NaCl] containing protease and phosphatase inhibitors. Protein concentrations were determined by the BCA (bicinchoninic acid) protein assay as per manufacturer's protocol (Pierce). Cell lysates were run on 4–12 % Bis-Tris gradient SDS/PAGE with Mes SDS running buffer (Life Technologies) under reducing conditions and transferred on to PVDF membranes (Roche). Membranes were blocked for 1 h with 3 % dried skimmed milk (Diploma, Fonterra Food services) in PBST (PBS and 0.1 % Tween 20) and incubated overnight at 4°C with the appropriate primary antibodies. Immunoblot visualization was achieved by incubation with appropriate HRP-conjugated secondary antibodies and the use of an ECL (enhanced chemiluminescence) detection system according to the manufacturer's instructions (Pierce).

Luciferase reporter assays

RAW264.7 cells that had been stably transfected with a construct expressing firefly luciferase driven by a promoter containing either an NF-κB- or an NFAT-response element-containing promoter were used in luciferase reporter assays as described previously [31]. Briefly, reporter cells were seeded at 4×10^4 cells/6-mm diameter culture well in MEM/FBS and incubated overnight. Treatments were performed in triplicate over 24 h, PBS rinsed then lysed with Passive Lysis buffer (Promega) for 24 h at 4°C. Lysates were transferred to a white flat bottomed 96-well microplate (Corning) and signal was measured using firefly luciferase substrate (Promega) as per manufacturer's instructions using a EnVision multilabel plate reader. Transient transfection of RAW264.7 cells (6×10^4 cells/well) with the vATPase-d2 (V-type proton ATPase subunit d2) promoter [32] and the M(M1–3)vATPase-d2 promoter (containing mutations in the three MITF-binding sites rendering them non-functional [32]) was carried out using Lipofectamine™ LTX Plus reagent (Life Technologies) according to the manufacturer's instructions. The vATPase-d2 promoter–luciferase construct (0.2 μg/well) was co-transfected with pRL *Renilla* luciferase construct (0.1 μg/well; Promega) and after 24 h, cells were rinsed and stimuli applied (in 200 μl of MEM/FBS) for a further 24 h, after which time cells were lysed as above and levels of luciferase determined using luciferase

substrate and Stop and Glo® reagent (Promega) according to the manufacturer's instructions, and light emission was measured using the EnVision plate reader.

Statistical analysis

Data were analysed using Graphpad Prism 5 software, and statistical significance determined using Student's unpaired *t* test for pair-wise comparisons and ANOVA/Dunnett's post-hoc test (as indicated) for multiple comparisons.

RESULTS

Characterization of the effects of 17-AAG on osteoclast formation *in vitro*

To characterize the effects of 17-AAG upon osteoclast formation, we employed both M-CSF-stimulated mouse bone marrow cells and the macrophage/pre-osteoclast cell line RAW264.7. Cultures treated with 100 ng/ml RANKL for 6 days, as described previously [23,31], resulted in formation of numerous TRAP$^+$ mononuclear cells and TRAP$^+$ MNCs, the latter counted as osteoclasts; omission of RANKL resulted only in numerous TRAP$^-$ mononuclear cells. In M-CSF-stimulated bone marrow cell cultures, 20 ng/ml RANKL (a submaximal concentration in this assay) yielded approximately 40 TRAP$^+$ MNCs per culture well (Figures 1A–1C). 17-AAG dose-dependently increased TRAP$^+$ MNC numbers over 25–100 nM, the latter concentration increasing formation over 3-fold (Figure 1A). MNCs in these cultures also expressed CTR, confirming their osteoclast identity [30] (Figure 1D). At concentrations of 200 nM and above, high cell toxicity with reduced cell survival was observed; similar toxicity was seen in M-CSF-dependent bone marrow-derived macrophages (results not shown). RANKL concentrations were also titrated in the presence of 100 nM 17-AAG or vehicle control (Figure 1B), which showed that 17-AAG did not increase osteoclast formation in the absence of RANKL or in the presence of 5 or 10 ng/ml RANKL, but enhancement of TRAP$^+$ MNC formation was seen with 20, 50 and 100 ng/ml RANKL treatments (Figure 1B). The 50 and 100 ng/ml RANKL treatments resulted in very large MNCs being formed, and in those treated with 17-AAG MNCs with a high number of nuclei were noted. This increased cell fusion was not necessarily reflected in a concomitant increase in total MNC numbers, presumably since fusion between existing MNCs may actually serve to decrease the overall numbers. 17-AAG also enhanced TRAP$^+$ MNC formation in RAW264.7 cells treated with 20 ng/ml RANKL, although these cells tolerated up to 200 nM 17-AAG (Figure 1E).

Since TNF can also weakly drive osteoclast formation *in vitro* we investigated whether 17-AAG could also influence its action. In M-CSF-treated bone marrow cells, TNF caused formation of very low numbers of TRAP$^+$ MNCs compared with RANKL (less than 3 TRAP$^+$ MNCs per well), but this was greatly enhanced by 17-AAG treatment (Figure 1F), indicating that 17-AAG enhances osteoclastogenic stimuli, not merely RANK signals. 17-AAG also increased TRAP$^+$ cell formation in TNF-treated RAW264.7 cells (results not shown).

To determine whether 17-AAG influences other actions of RANKL, we examined the effect of 17-AAG on the osteoclast pro-survival effects of RANKL. In dispersed osteoclast-rich cultures generated from bone marrow cells there was no cell survival observed in the absence of any RANKL treatment after 24 h of incubation (Figure 1G), whereas 100 ng/ml RANKL stimulus (in the absence of M-CSF) resulted in large numbers of TRAP$^+$
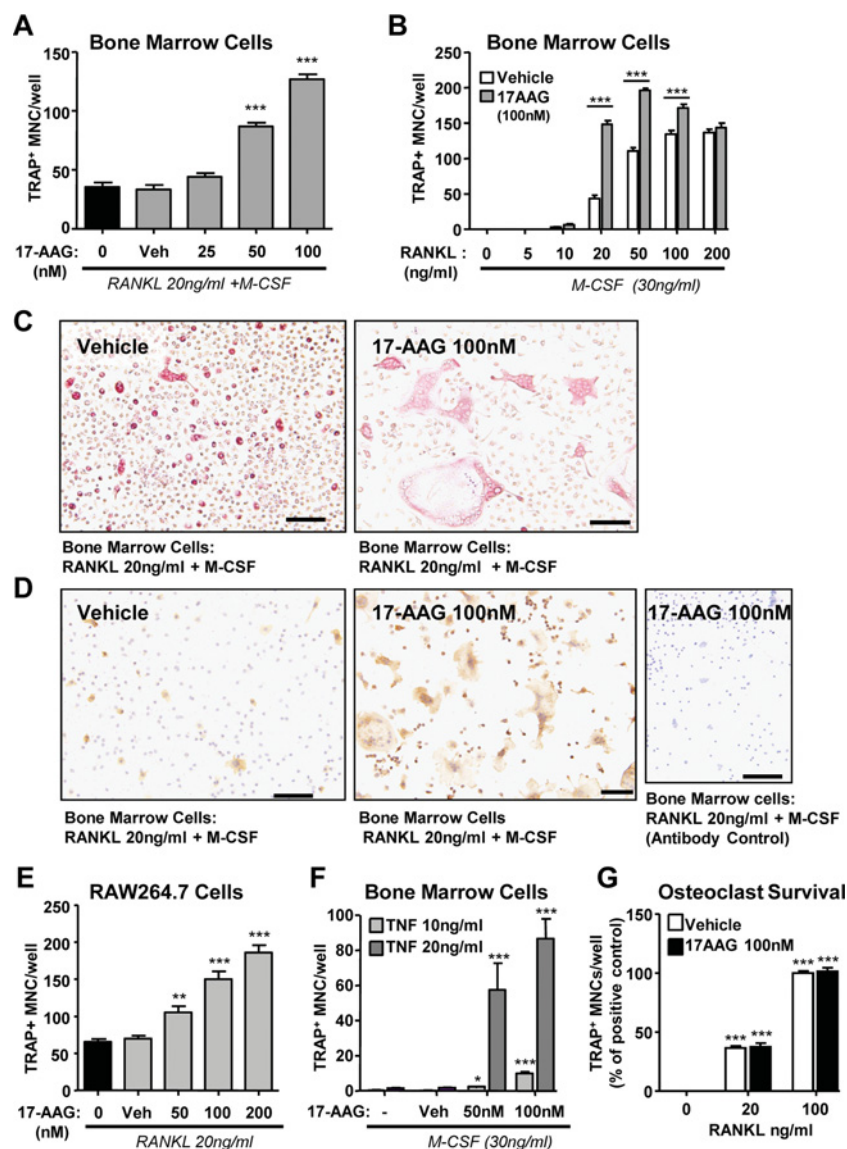
Figure 1   17-AAG strongly increases RANKL- and TNF-dependent TRAP$^+$ MNC formation *in vitro*

(**A**) Dose response of 17-AAG in bone marrow cell populations treated with 20 ng/ml RANKL (submaximal concentration) and 30 ng/ml M-CSF ($n = 5$). (**B**) Titration of RANKL concentration in 17-AAG- and vehicle-treated bone marrow cultures ($n = 3$). (**C**) Images of TRAP$^+$ MNCs formed in 17-AAG- and RANKL-treated bone marrow cells. (**D**) Similar cultures were immunoperoxidase-stained by an anti-CTR antibody (antibody control was the anti-CTR antibody neutralized by prior incubation with the CTR peptide) and haematoxylin-counterstained. Scale bar $= 100\ \mu$m. (**E**) 17-AAG dose dependently increases TRAP$^+$ MNC formation in 20 ng/ml RANKL-stimulated RAW264.7 cells ($n = 3$). (**F**) 17-AAG also greatly enhances TRAP$^+$ MNC formation in TNF-treated bone marrow cells ($n = 4$). (**G**) 17-AAG does not affect RANKL actions as a survival factor for osteoclasts ($n = 5$). Results are means $\pm$ S.E.M. for the indicated number of pooled replicate experiments. Veh, DMSO vehicle control. *$P < 0.05$, **$P < 0.01$ and ***$P < 0.001$ relative to untreated controls using ANOVA/Dunnett's post-hoc test.

MNCs surviving after 24 h; 20 ng/ml RANKL resulted in lower survival levels than 100 ng/ml. Co-treatment of the cells with 17-AAG (100 nM) was found to have no effect on the osteoclast survival effects of RANKL at any of these concentrations (Figure 1G).

Enhancement of osteoclast formation by CCT018159, NVP-AUY922 and TGFβ

As CCT018159 and NVP-AUY922 strongly inhibit HSP90 by binding to the N-terminal ATPase domain of the molecule, yet are structurally distinct from 17-AAG, we studied their influence on osteoclast formation. NVP-AUY922 treatment up to a 10 nM concentration dose-dependently increased TRAP$^+$

MNC formation in both bone marrow and RAW264.7 cell cultures (Figures 2A and 2B), beyond which cell toxicity was observed. Similarly, increased osteoclast formation was observed with CCT018159 treatment (Figures 2C–2E). As with 17-AAG, increased osteoclast numbers with CCT018159 treatment were seen in cultures maximally stimulated with RANKL (100 ng/ml; Figures 1B and 2F).

TGFβ strongly enhances RANKL (and TNF) stimulation of osteoclast formation [14] in a manner that resembles 17-AAG. Since we previously found that TGFβ acts in the earlier phases of osteoclast formation we investigated the time course of 17-AAG action on bone marrow cell–osteoclast differentiation. A time-course analysis of RANKL plus M-CSF-stimulated bone marrow cultures showed that TRAP$^+$ MNCs were not evident
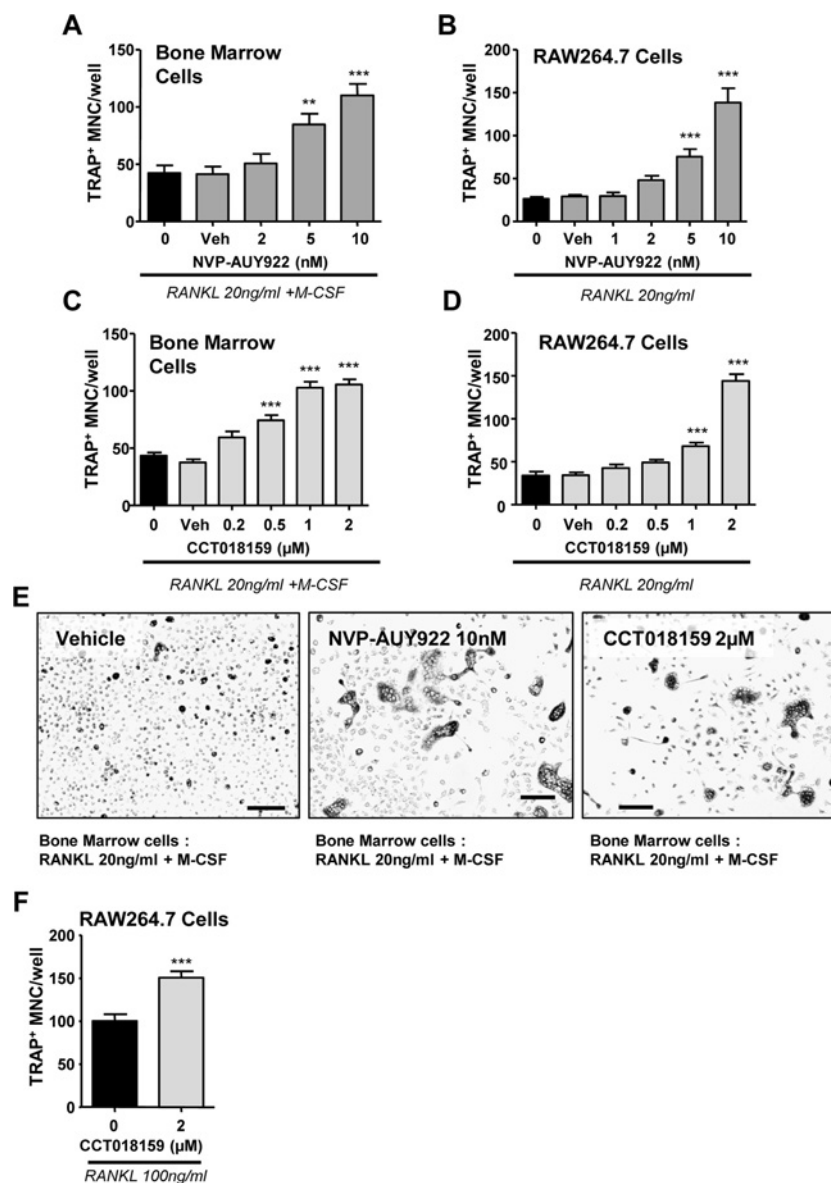
Figure 2   Enhancement of TRAP$^+$ MNC formation *in vitro* by second generation (resorcinol-containing) HSP90 inhibitors

Dose response of NVP-AUY922 in bone marrow cell populations treated with 20 ng/ml RANKL (submaximal concentration) and 30 ng/ml M-CSF ($n = 5$) (**A**) and RAW264.7 cells stimulated with 20 ng/ml RANKL ($n = 3$) (**B**). Dose response of CCT018159 in bone marrow cell populations treated with 20 ng/ml RANKL and 30 ng/ml M-CSF ($n = 5$) (**C**) and RAW264.7 cells stimulated with 20 ng/ml RANKL ($n = 5$) (**D**). (**E**) Images of TRAP histochemically stained cells in NYP-AUY922 and CCT018159 enhanced osteoclast formation in RANKL- and M-CSF-stimulated bone marrow cell cultures. Scale bar $= 100$ μm. (**F**) CCT018159 enhanced TRAP$^+$ cell formation in RAW264.7 cells stimulated with 100 ng/ml RANKL ($n = 3$). Results are means $\pm$ S.E.M. of the indicated number of pooled replicate experiments. $**P < 0.01$ and $***P < 0.001$ relative to the untreated controls using ANOVA/Dunnett's post-hoc test.

until day 4 of the incubation period (Figure 3A), indicating that the early commitment phase of osteoclast formation lasts for at least 3 days in this culture system. TGFβ enhanced TRAP$^+$ MNC formation when added during days 0–3, but not days 3–6 of these cultures (Figure 3B). In contrast, 17-AAG actions were significant only when added at day 3. This suggests that 17-AAG probably exerts its actions on osteoclast formation through a mechanism significantly different to that of TGFβ.

17-AAG does not stimulate levels of key osteoclast transcription factors NF-κB, NFATc1 and the AP-1 subunit c-Fos

To investigate potential mechanisms of 17-AAG in osteoclast formation, we investigated its actions on transcription factors

known to be elicited by RANKL, namely NF-κB, c-Fos and NFATc1 using immunoblotting and transcriptional luciferase reporter assays that employed RAW264.7 cells. In RAW264.7 cells stably transfected with an NF-κB–luciferase reporter construct [31] 17-AAG did not affect NF-κB signals either directly or with co-stimulation by 100 ng/ml RANKL (Figure 4A). Immunoblot analysis also demonstrated that RANKL treatment increased the levels of NFATc1 in a time- and dose-dependent manner, whereas 17-AAG had no effect (Figures 4B and 4C). As with NFATc1, a strong increase in c-Fos levels by RANKL was observed, but no effect of 17-AAG was seen (Figures 4B and 4C). Consistent with the lack of effect of 17-AAG on NFATc1 protein levels, a luciferase-based activity assay indicated a similar lack of effect on NFATc1 activity (Figure 4D).
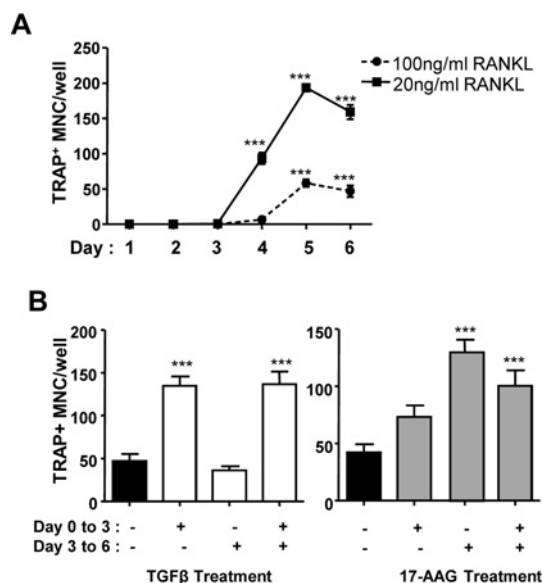
Figure 3   Time-course evaluation of TRAP$^+$ MNC formation shows that 17-AAG and TGFβ influence different phases of osteoclast commitment

(**A**) Formation of TRAP$^+$ MNCs in response to RANKL and M-CSF (30 ng/ml) stimulus of bone marrow cells over 6 days of culture. (**B**) TGFβ acts during the earlier phase, whereas 17-AAG principally acts within the later phase of osteoclast formation of bone marrow cells treated with RANKL and M-CSF. Results are means $\pm$ S.E.M. for three replicate pooled experiments. ***$P < 0.001$ relative to day 0 controls (**A**) or untreated controls (**B**) using ANOVA/Dunnett's post-hoc test.

This assay employed RAW264.7 cells stably transfected with an NFAT-dependent luciferase reporter construct (with promoter-binding sites for NFATc1) and both RANKL and TGFβ treatments strongly induced the luciferase signal as described previously [31], whereas 17-AAG did not (Figure 4D). 17-AAG also did not enhance RANKL-induced activity in this assay. These data suggest that NF-κB, NFATc1 and c-Fos, although regulated by numerous factors that influence osteoclast formation, are not the probable mediators of 17-AAG action in osteoclast formation.

17-AAG enhances MITF protein levels and the promoter activity of the MITF target vATPase-d2

MITF is an essential osteoclast transcription factor whose activation has been shown to be dependent on NF-κB, AP-1 and NFATc1 and thus its effects are probably exerted relatively late within the RANKL-dependent transcription factor cascade. In concordance with Lu et al. [8], we found that RANKL treatment of RAW264.7 cells increased MITF protein expression levels (Figures 5A and 5B); note that a number of MITF isoforms have been described although all bands detected by immunoblotting appeared to be raised by RANKL treatment. We also found that 17-AAG increased MITF levels in RAW264.7 cells in a dose- and time-dependent manner (Figures 5A and 5B) with very strong enhancement of MITF protein levels at 48 h. This suggests that MITF could be a mediator of the actions of 17-AAG upon osteoclast formation. To further investigate the action of 17-AAG on MITF, we employed a luciferase reporter construct containing the promoter region of a MITF target gene, vATPase-d2 (Figure 5C). In RAW264.7 cells transiently transfected with this construct RANKL treatment significantly increased the activity of this promoter as reported previously (Figure 5D)

[32]. Moreover, like RANKL, 17-AAG caused a dose-dependent increase in the activity of the reporter construct (Figure 5E). This indicates activation of the MITF target gene vATPase-d2 by both RANKL and 17-AAG. As a further control, we employed a similar construct [M(M1–3)vATPase-d2] containing mutations in all three MITF-binding sites (Figure 5C) which render the construct unresponsive to MITF, as described previously [32]. 17-AAG failed to induce a response in RAW264.7 cells transfected with this mutant construct (Figure 5F, left-hand panel). As a method control, the latter experiments were carried out alongside the same RAW264.7 cells transfected with the wild-type vATPase-d2 construct which did respond to 17-AAG (Figure 5F, right-hand panel) as before. In conclusion, these results point to an action of 17-AAG in osteoclast formation via its ability to regulate MITF protein expression levels and its activity.

DISCUSSION

We and others have previously identified that benzoquinone ansamycin HSP90 inhibitors, such as 17-AAG and herbimycin, enhance osteoclast formation *in vitro* and *in vivo* [23,24]. These were surprising observations given that HSP90 is an important molecular chaperone that maintains the activity and stability of many important cell signalling proteins [18,19]. To clarify this action of 17-AAG we first investigated whether enhancing osteoclast formation is a unique feature of the GM class of HSP90 inhibitors to which it belongs. High-throughput biochemical screening originally identified CCT08159 as a high-affinity resorcinol-containing HSP90 ATPase inhibitor that reduced HCT116 human colon cell proliferation [18,33–35] and further structure-based rational drug-based design identified NVP-AUY922. The latter is currently undergoing Phase II clinical trials in HER2$^+$ (human epidermal growth factor receptor 2) ERα^+ (oestrogen receptor α) locally advanced or metastatic breast cancer [19]. CCT018159 and NVP-AUY922 have better pharmacokinetic profiles than 17-AAG and are more likely to provide clinical benefit [36]; we found both HSP90 inhibitors (compounds structurally dissimilar from those of the GM class) also greatly increased osteoclast numbers *in vitro*. This suggests that pro-osteoclastic effects are not limited to GM-based HSP90 inhibitors. This may also suggest that such compounds, like 17-AAG, might also provoke bone loss *in vivo*. Nevertheless, they are anti-cancer compounds with some promise [15,18], and if bone loss emerges as a clinical problem it is likely to be overcome by the appropriate use of anti-osteolytic therapies such as bisphosphonates. However, this issue may be more acute in cancers that metastasize to bone, such as breast carcinomas, where osteolysis mediated by osteoclasts is provoked by the invading cancer cells and results in the release of factors from the bone matrix that potently stimulate tumour growth [37]. Consistent with this, a low calcium diet in mice increases bone resorption that in turn increases tumour invasion and growth in bone [38]. In addition, bone metastasis establishment not only results in focal bone damage and other serious complications, but can also result in tumours more refractory to treatment [39]. For these reasons it seems desirable that potential anti-cancer therapeutics such as these should be screened for effects on bone metabolism.

The results of the present study have provided new and surprising insights into the effects of HSP90 inhibitors upon osteoclast progenitors, namely that 17-AAG does not influence their levels of c-Fos (an AP-1 subunit), NF-κB or NFATc1, but does increase the levels of MITF. These are transcription factors critical for osteoclast formation and induced by RANKL, and NFATc1 in particular is regarded as a highly regulated and critical
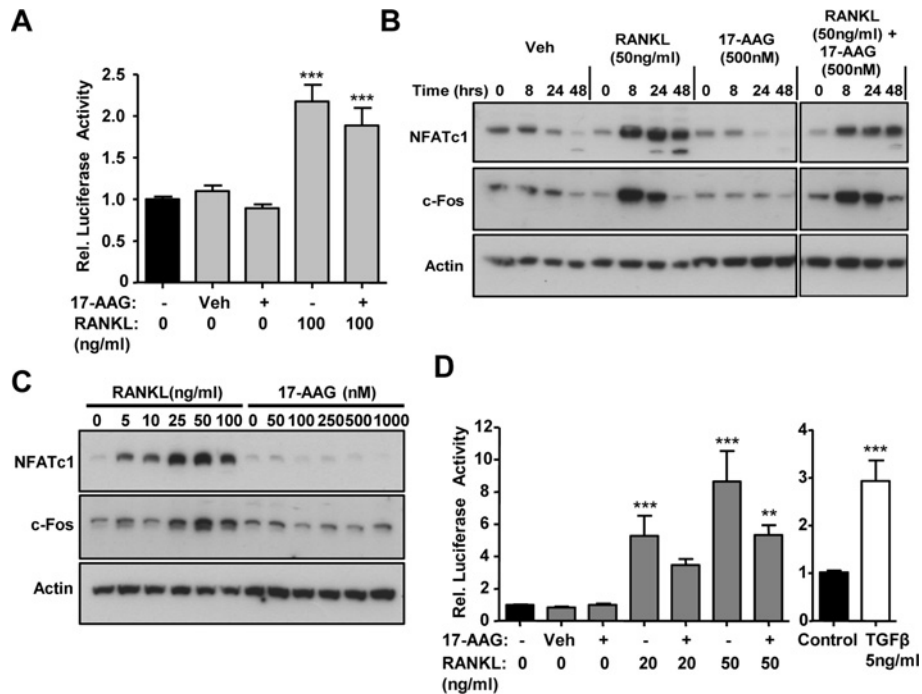
Figure 4   Unlike RANKL, 17-AAG does not induce NF-κB, c-Fos or NFATc1 levels or activity in RAW264.7 cells

(**A**) Induction of signal in NF-κB RAW reporter cells by RANKL, but not by 17-AAG (500 nM) after a 24 h treatment period ($n = 5$). (**B**) Time-course analysis of RANKL (50 ng/ml), 17-AAG (500 nM) and a combination treatment of both demonstrated that RANKL increased both NFATc1 and c-Fos levels, whereas 17-AAG had no effect. The combination treatment showed little difference to that of RANKL treatment alone. All lanes pictured were derived from the same gel. (**C**) NFATc1 and c-Fos protein levels were increased by a 24 h treatment of RANKL in a dose-dependent manner, whereas levels of these proteins in the RAW264.7 cells were not increased by 17-AAG treatment. (**D**) Signal induction in the NFAT RAW reporter cell line (at 24 h) shows induction by RANKL (left-hand panel) and TGFβ (right-hand panel), but not by 17-AAG (left-hand panel) in these RAW264.7-derived cells ($n = 4$). Results are means $\pm$ S.E.M. for the indicated number of pooled replicate experiments. **$P < 0.01$ and ***$P < 0.001$ relative to untreated control using ANOVA/Dunnett's post-hoc test for multiple comparisons and Student's t test for two-way comparison. Veh', DMSO vehicle control.

determinant of osteoclast formation [1]. There are thus several ways in which 17-AAG might increase osteoclast formation. HSP90 inhibition results in the proteosomal degradation of many HSP90 client proteins [40], raising the possibility of the degradation of some intracellular osteoclast inhibitor, perhaps one that reduces MITF levels. It is notable that removal of RANKL- and TNF-inducible endogenous osteoclast inhibitors [NF-κBp100 and RBP-Jκ (recombination signal-binding protein 1 for Jκ) respectively] has been proposed by Zhao et al. [41] and Yao et al. [11] to explain increased osteoclast formation in their models. These factors, however, also result in greatly enhanced NFATc1 levels, which we do not observe with 17-AAG treatment. A more likely possibility is suggested by the observations that many HSP90 inhibitors cause a dissociation of the HSP90 complex with HSF1 (heat-shock factor 1) leading to HSF1 activation and the initiation of an HSF1-mediated cell stress response [42] characterized by increased levels of HSPs such as HSP70. This raises the possibility that the increased MITF levels observed upon 17-AAG treatment may be cell-stress-dependent. Indeed, MITF levels have been shown to be induced in epithelial cells upon heat shock and consistent with this the MITF gene promoter is known to contain a number of HSF1-binding motifs [43]. 17-AAG activation of HSF1 may thus explain increased MITF levels and, through that, osteoclast formation. Consistent with this we have identified HSF1-dependent actions enhancing osteoclast formation in RAW264.7 cells (R.C.C. Chai, A.G. van der Kraan, B.J. Lang, M.M. Kouspou, M.T. Gillespie, J.M.W. Quinn and J.T. Price, unpublished work) which might point to HSF1/MITF mediation of 17-AAG action on osteoclasts, although further work is required to clarify this. A third possible explanation

for pro-osteoclastic effects of 17-AAG is via MAPK (mitogen-activated protein kinase) signalling proteins. HSP90 inhibition can lead to increased p38 activation [44] and p38 activity is critical in osteoclast differentiation [1]. It should be noted, however, that the effect of 17-AAG on MAPK proteins varies between cell types [21] and has not yet been examined in osteoclast progenitors. In addition, since p38 inhibition completely blocks osteoclast formation its role in this process is not easy to determine.

Further characterization of the 17-AAG pro-osteoclastic action (confirmed by detection of CTR expression in the MNCs) showed that this action clearly required a minimal RANKL stimulus of the osteoclast progenitors; in the present study this was a >10 ng/ml RANKL stimulus, a level that barely elicits detectable TRAP$^+$ cell formation (Figure 1B). 17-AAG also caused supramaximal increases in RANKL-stimulated osteoclast formation. These data are consistent with an action of 17-AAG to enhance differentiation mechanisms somewhere downstream of RANK binding, i.e. it did not simply raise the general sensitivity of cells to RANKL. The lack of effects of 17-AAG on RANKL-dependent osteoclast survival also suggests this conclusion, as does the huge effect of 17-AAG on osteoclast formation driven by TNF (Figures 1F and 1G). TNF does not bind the RANKL receptor (RANK), but acts via the TNFR (TNF receptor) p55 and p75 receptors to elicit the activation of NF-κB and a number of downstream mediators, the same as RANKL treatment does. The results of the present study also raise the possibility that HSP90 inhibitors may enhance TNF-driven osteolysis, although the influence of TNF, especially *in vivo*, is complex. High TNF levels are associated with osteolysis *in vivo*, often in the context of chronic inflammation, but
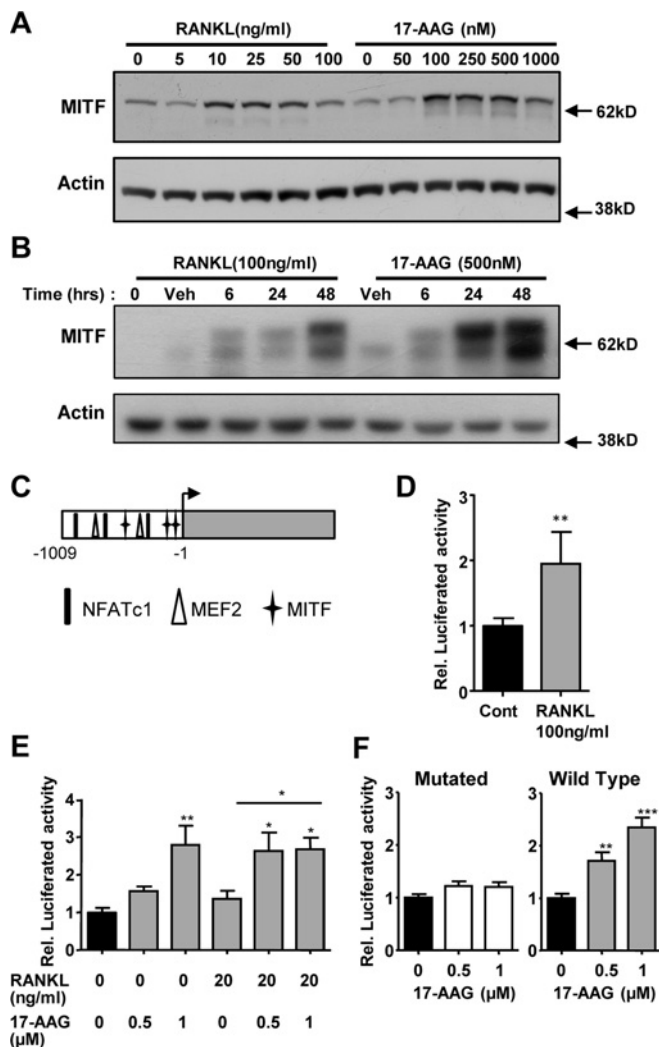
Figure 5   17-AAG increases MITF levels in RAW264.7 cells independently of RANKL

(**A**) Immunoblot demonstrating the dose response of MITF protein levels to increasing concentrations of RANKL and 17-AAG. (**B**) Immunoblot analysis of a time course of MITF protein levels in response to RANKL and 17-AAG treatment over a 48 h period. Veh, vehicle control. (**C**) Diagram of the 1 kb vATPase-d2 construct showing transcription factor-binding domains as indicated and the luciferase-encoding region (grey). (**D**) RANKL treatment response of the 1 kb vATPase-d2 reporter construct transiently transfected into the RAW264.7 cell construct. $**P < 0.01$ relative to the untreated control using Student's t test ($n = 5$). Cont, no treatment control. (**E**) Transiently transfected RAW264.7 cells with the 1 kb vATPase-d2 reporter construct demonstrated that 17-AAG and RANKL plus 17-AAG treatments increased reporter activity, whereas a combination treatment generated an additive affect. (**F**) 17-AAG did not induce luciferase activity in RAW264.7 cells transfected with the M(M1–3)vATPase-d2 construct containing mutated MITF-binding sites (left-hand panel 'Mutated') in experiments conducted in parallel with studies conducted with 1 kb vATPase-d2 constructs (right-hand panel, 'Wild Type'). (**E** and **F**) $*P < 0.05$, $**P < 0.01$ and $***P < 0.001$ relative to the control using ANOVA/Bonferroni's post-hoc test ($n = 5$).

TNF also induces RANKL protein expression in osteoblasts and suppresses bone formation. *In vitro* TNF-dependent osteoclast formation is well attested, but is not observed in RANK-null mice *in vivo*, suggesting that TNF-driven osteoclast formation *in vivo* is totally RANKL dependent. This lack of direct action of TNF was explained by two studies that identified osteoclast-suppressive intracellular pathways involving NF-κBp100 and RBP-Jκ (see above) which are induced by TNF [11,41]; disabling

these mechanisms by genetic manipulation resulted in direct TNF-driven osteoclast formation in RANK-null mice *in vivo*. Although mechanistically interesting it is not yet clear if these molecules play a role in TNF-induced bone loss in human disease or inflammatory models of wild-type mice, so it is currently unclear whether the effect of 17-AAG on bone might include TNF-mediated actions.

Since TGFβ is one of the few exogenous factors that can enhance osteoclast formation by direct action on progenitors, we compared its influence to that of 17-AAG. TGFβ can prime osteoclast progenitors to respond to RANKL [45]. As observed previously [26,46] we found that, like RANKL, TGFβ enhanced NFATc1 levels, consistent with the effects of TGFβ being mainly evident in the earlier period of the bone marrow culture period (Figure 3). In contrast, 17-AAG exerted its influence later than this, suggesting that the mechanism of actions of TGFβ and 17-AAG differ substantially.

The lack of effects of 17-AAG on NFATc1 levels played a major role in our decision to focus on MITF as a possible mediating transcription factor. It should be noted that we examined the total cellular levels of NFATc1 (i.e. in unfractionated cell lysates) since this typically reflects the levels of NFATc1 in the nucleus and is a widely adopted approach. As a transcription factor, NFATc1 requires nuclear translocation to act, indeed NFATc1 binds to the promoter of its own gene further accelerating its own transcription and production [46]. However, to date, the nuclear transport of NFATc1 has not been determined to be a point of control in osteoclast differentiation. To definitively identify any effects of 17-AAG on NFATc1 activity we used an NFAT-luciferase reporter assay in RAW264.7 cells. Consistent with our findings of a lack of an effect of 17-AAG upon NFATc1 protein levels, 17-AAG (unlike TGFβ) had no effect on NFATc1 activity. However, MITF activation is downstream of NFATc1 and occurs later in the osteoclast signalling/transcription factor cascade. MITF is a widely expressed basic helix–loop–leucine zipper transcription factor required for the latter stages of osteoclastogenesis [3,47]. MITF binds to a conserved 7 bp motif, TCANGTG, in the promoter region of target genes, which include vATPase-d2 subunit, TRAP [Acp5 (acid phosphatase 5, tartrate resistant)], Ctsk (cathepsin K) and E-cadherin [3,32,48]. MITF participates in the transcription factor complexes needed for osteoclast gene expression, complexes which include NFATc1, PU.1, NF-κB and AP-1. Mice that express mutant alleles of the MITF gene, *mi*, have few and defective osteoclasts [48] and mice null for MITF display osteopetrosis and lack osteoclasts. The MITF gene transcript is alternatively spliced and exists in at least 8 isoforms, and when isoforms A and E are overexpressed osteoclast formation is enhanced [8]. MITF protein levels induction may thus plausibly explain, at least in part, the actions of 17-AAG in osteoclast formation. Given that 17-AAG does not enhance NFATc1 and other important upstream targets of RANKL, MITF levels might be rate limiting for osteoclast formation. Although the importance of MITF in osteoclasts has been long recognized, it is not generally considered as a point of regulation, although Kim et al. [49] have suggested that IL-1 (interleukin 1) regulation of MITF activity might enhance osteoclast formation when IL-1 is added late in the osteoclast maturation period. This latter observation seems similar to our observations with 17-AAG (Figure 3).

Thus, in summary, HSP90 inhibitors have a powerful stimulatory effect on osteoclast formation *in vitro* which is consistent with previously observed osteolytic actions of 17-AAG in mice [23,24]. 17-AAG, even in the absence of RANKL, increases the levels of MITF in osteoclast progenitors, an essential transcription factor in osteoclast formation. This may underlie the osteoclastic effects of HSP90 inhibitors. If that is the case it seems

likely that osteolysis provoked by 17-AAG reflects an increase in the sensitivity of osteoclast progenitors to the effects of RANKL present in the bone microenvironment.

REFERENCES

1 Nakashima, T. and Takayanagi, H. (2011) New regulation mechanisms of osteoclast differentiation. Ann. N.Y. Acad. Sci. **1240**, E13–E18

2 Iqbal, J., Sun, L. and Zaidi, M. (2009) Coupling bone degradation to formation. Nat. Med. **15**, 729–731

3 Sharma, S. M., Bronisz, A., Hu, R., Patel, K., Mansky, K. C., Sif, S. and Ostrowski, M. C. (2007) MITF and PU.1 recruit p38 MAPK and NFATc1 to target genes during osteoclast differentiation. J. Biol. Chem. **282**, 15921–15929

4 Boyle, W. J., Simonet, W. S. and Lacey, D. L. (2003) Osteoclast differentiation and activation. Nature **423**, 337–342

5 Guise, T. (2010) Examining the metastatic niche: targeting the microenvironment. Semin. Oncol. **37**, S2–S14

6 Katagiri, T. and Takahashi, N. (2002) Regulatory mechanisms of osteoblast and osteoclast differentiation. Oral Dis. **8**, 147–159

7 O'Brien, C. A. (2010) Control of *RANKL* gene expression. Bone **46**, 911–919

8 Lu, S.-Y., Li, M. and Lin, Y.-L. (2010) Mitf induction by RANKL is critical for osteoclastogenesis. Mol. Biol. Cell **21**, 1763–1771

9 Dougall, W. C., Glaccum, M., Charrier, K., Rohrbach, K., Brasel, K., De Smedt, T., Daro, E., Smith, J., Tometsko, M. E., Maliszewski, C. R. et al. (1999) RANK is essential for osteoclast and lymph node development. Genes Dev. **13**, 2412–2424

10 Kobayashi, K., Takahashi, N., Jimi, E., Udagawa, N., Takami, M., Kotake, S., Nakagawa, N., Kinosaki, M., Yamaguchi, K., Shima, N. et al. (2000) Tumor necrosis factor alpha stimulates osteoclast differentiation by a mechanism independent of the ODF/RANKL–RANK interaction. J. Exp. Med. **191**, 275–286

11 Yao, Z., Xing, L. and Boyce, B. F. (2009) NF-κB p100 limits TNF-induced bone resorption in mice by a TRAF3-dependent mechanism. J. Clin. Invest. **119**, 3024–3034

12 Horwood, N. J., Elliott, J., Martin, T. J. and Gillespie, M. T. (1998) Osteotropic agents regulate the expression of osteoclast differentiation factor and osteoprotegerin in osteoblastic stromal cells. Endocrinology **139**, 4743–4746

13 Sells Galvin, R. J., Gatlin, C. L., Horn, J. W. and Fuson, T. R. (1999) TGF-β enhances osteoclast differentiation in hematopoietic cell cultures stimulated with RANKL and M-CSF. Biochem. Biophys. Res. Commun. **265**, 233–239

14 Quinn, J. M. W., Itoh, K., Udagawa, N., Häusler, K., Yasuda, H., Shima, N., Mizuno, A., Higashio, K., Takahashi, N., Suda, T. et al. (2001) Transforming growth factor β affects osteoclast differentiation via direct and indirect actions. J. Bone Miner. Res. **16**, 1787–1794

15 Porter, J. R., Fritz, C. C. and Depew, K. M. (2010) Discovery and development of Hsp90 inhibitors: a promising pathway for cancer therapy. Curr. Opin. Chem. Biol. **14**, 412–420

16 Whitesell, L. and Lindquist, S. L. (2005) HSP90 and the chaperoning of cancer. Nat. Rev. Cancer **5**, 761–772

17 Jhaveri, K., Taldone, T., Modi, S. and Chiosis, G. (2012) Advances in the clinical development of heat shock protein (Hsp90) inhibitors in cancers. Biochim. Biophys. Acta **1823**, 742–755

18 Travers, J., Sharp, S. and Workman, P. (2012) HSP90 inhibition: two-pronged exploitation of cancer dependencies. Drug Discovery Today **17**, 242–252

19 Eccles, S. A., Massey, A., Raynaud, F. I., Sharp, S. Y., Box, G., Valenti, M., Patterson, L., de Haven Brandon, A., Gowan, S., Boxall, F. et al. (2008) NVP-AUY922: a novel heat shock protein 90 inhibitor active against xenograft tumor growth, angiogenesis, and metastasis. Cancer Res. **68**, 2850–2860

20 Yun, T. J., Harning, E. K., Giza, K., Rabah, D., Li, P., Arndt, J. W., Luchetti, D., Biamonte, M. A., Shi, J., Lundgren, K. et al. (2011) EC144, a synthetic inhibitor of heat shock protein 90, blocks innate and adaptive immune responses in models of inflammation and autoimmunity. J. Immunol. **186**, 563–575

21 Poulaki, V., Iliaki, E., Mitsiades, N., Mitsiades, C. S., Paulus, Y. N., Bula, D. V., Gragoudas, E. S. and Miller, J. W. (2007) Inhibition of Hsp90 attenuates inflammation in endotoxin-induced uveitis. FASEB J. **21**, 2113–2123

22 Chen, G., Cao, P. and Goeddel, D. V. (2002) TNF-induced recruitment and activation of the IKK complex require Cdc37 and Hsp90. Mol. Cell **9**, 401–410

23 Price, J. T., Quinn, J. M. W., Sims, N. A., Vieusseux, J., Waldeck, K., Docherty, S. E., Myers, D., Nakamura, A., Waltham, M. C., Gillespie, M. T. and Thompson, E. W. (2005) The heat shock protein 90 inhibitor, 17-allylamino-17-demethoxygeldanamycin, enhances osteoclast formation and potentiates bone metastasis of a human breast cancer cell line. Cancer Res. **65**, 4929–4938

24 Yano, A., Tsutsumi, S., Soga, S., Lee, M. J., Trepel, J., Osada, H. and Neckers, L. (2008) Inhibition of Hsp90 activates osteoclast c-Src signaling and promotes growth of prostate carcinoma cells in bone. Proc. Natl. Acad. Sci. U.S.A. **105**, 15541–15546

25 Song, I., Kim, J. H., Kim, K., Jin, H. M., Youn, B. U. and Kim, N. (2009) Regulatory mechanism of NFATc1 in RANKL-induced osteoclast activation. FEBS Lett. **583**, 2435–2440

26 Fox, S. W., Evans, K. E. and Lovibond, A. C. (2008) Transforming growth factor-β enables NFATc1 expression during osteoclastogenesis. Biochem. Biophys. Res. Commun. **366**, 123–128

27 Yeung, Y. G., Jubinsky, P. T., Sengupta, A., Yeung, D. C. and Stanley, E. R. (1987) Purification of the colony-stimulating factor 1 receptor and demonstration of its tyrosine kinase activity. Proc. Natl. Acad. Sci. U.S.A. **84**, 1268–1271

28 Tikellis, C., Xuereb, L., Casley, D., Brasier, G., Cooper, M. E. and Wookey, P. J. (2003) Calcitonin receptor isoforms expressed in the developing rat kidney. Kidney Int. **63**, 416–426

29 Quinn, J. M., Whitty, G. A., Byrne, R. J., Gillespie, M. T. and Hamilton, J. A. (2002) The generation of highly enriched osteoclast-lineage cell populations. Bone **30**, 164–170

30 Quinn, J. M., Morfis, M., Lam, M. H., Elliott, J., Kartsogiannis, V., Williams, E. D., Gillespie, M. T., Martin, T. J. and Sexton, P. M. (1999) Calcitonin receptor antibodies in the identification of osteoclasts. Bone **25**, 1–8

31 Singh, P. P., van der Kraan, A. G., Xu, J., Gillespie, M. T. and Quinn, J. M. (2012) Membrane-bound receptor activator of NF-κB ligand (RANKL) activity displayed by osteoblasts is differentially regulated by osteolytic factors. Biochem. Biophys. Res. Commun. **422**, 48–53

32 Feng, H., Cheng, T., Steer, J. H., Joyce, D. A., Pavlos, N. J., Leong, C., Kular, J., Liu, J., Feng, X., Zheng, M. H. and Xu, J. (2009) Myocyte enhancer factor 2 and microphthalmia-associated transcription factor cooperate with NFATc1 to transactivate the V-ATPase d2 promoter during RANKL-induced osteoclastogenesis. J. Biol. Chem. **284**, 14667–14676

33 Taldone, T., Sun, W. and Chiosis, G. (2009) Discovery and development of heat shock protein 90 inhibitors. Bioorg. Med. Chem. **17**, 2225–2235

34 Taldone, T., Gozman, A., Maharaj, R. and Chiosis, G. (2008) Targeting Hsp90: small-molecule inhibitors and their clinical development. Curr. Opin. Pharmacol. **8**, 370–374

35 Smith, N. F., Hayes, A., James, K., Nutley, B. P., McDonald, E., Henley, A., Dymock, B., Drysdale, M. J., Raynaud, F. I. and Workman, P. (2006) Preclinical pharmacokinetics and metabolism of a novel diaryl pyrazole resorcinol series of heat shock protein 90 inhibitors. Mol. Cancer Ther. **5**, 1628–1637

36 Sharp, S. Y., Prodromou, C., Boxall, K., Powers, M. V., Holmes, J. L., Box, G., Matthews, T. P., Cheung, K.-M. J., Kalusa, A., James, K. et al. (2007) Inhibition of the heat shock protein 90 molecular chaperone *in vitro* and *in vivo* by novel, synthetic, potent resorcinylic pyrazole/isoxazole amide analogues. Mol. Cancer Ther. **6**, 1198–1211

37 Sterling, J. A., Edwards, J. R., Martin, T. J. and Mundy, G. R. (2011) Advances in the biology of bone metastasis: how the skeleton affects tumor behavior. Bone **48**, 6–15

38 Zheng, Y., Zhou, H., Modzelewski, J. R., Kalak, R., Blair, J. M., Seibel, M. J. and Dunstan, C. R. (2007) Accelerated bone resorption, due to dietary calcium deficiency, promotes breast cancer tumor growth in bone. Cancer Res. **67**, 9542–9548

39 Mundy, G. R. (1997) Mechanisms of bone metastasis. Cancer **80**, 1546–1556

40 Pratt, W. B., Morishima, Y., Peng, H. M. and Osawa, Y. (2010) Proposal for a role of the Hsp90/Hsp70-based chaperone machinery in making triage decisions when proteins undergo oxidative and toxic damage. Exp. Biol. Med. **235**, 278–289

41 Zhao, B., Grimes, S. N., Li, S., Hu, X. and Ivashkiv, L. B. (2012) TNF-induced osteoclastogenesis and inflammatory bone resorption are inhibited by transcription factor RBP-J. J. Exp. Med. **209**, 319–334

42 Neckers, L. and Workman, P. (2012) Hsp90 molecular chaperone inhibitors: are we there yet? Clin. Cancer Res. **18**, 64–76

43 Laramie, J. M., Chung, T. P., Brownstein, B., Stormo, G. D. and Cobb, J. P. (2008) Transcriptional profiles of human epithelial cells in response to heat: computational evidence for novel heat shock proteins. Shock **29**, 623–630

44 Adachi, S., Yasuda, I., Nakashima, M., Yamauchi, T., Yamauchi, J., Natsume, H., Moriwaki, H. and Kozawa, O. (2010) HSP90 inhibitors induce desensitization of EGF receptor via p38 MAPK-mediated phosphorylation at Ser[1046/1047] in human pancreatic cancer cells. Oncol. Rep. **23**, 1709–1714

45 Fuller, K., Lean, J. M., Bayley, K. E., Wani, M. R. and Chambers, T. J. (2000) A role for TGFβ1 in osteoclast differentiation and survival. J. Cell Sci. **113**, 2445–2453

46 Takayanagi, H., Kim, S., Koga, T., Nishina, H., Isshiki, M., Yoshida, H., Saiura, A., Isobe, M., Yokochi, T., Inoue, J.-i. et al. (2002) Induction and activation of the transcription factor NFATc1 (NFAT2) integrate RANKL signaling in terminal differentiation of osteoclasts. Dev. Cell **3**, 889–901

47 Asagiri, M. and Takayanagi, H. (2007) The molecular understanding of osteoclast differentiation. Bone **40**, 251–264

48 Mansky, K. C., Sankar, U., Han, J. and Ostrowski, M. C. (2002) Microphthalmia transcription factor is a target of the p38 MAPK pathway in response to receptor activator of NF-κB ligand signaling. J. Biol. Chem. **277**, 11077–11083

49 Kim, J. H., Jin, H. M., Kim, K., Song, I., Youn, B. U., Matsuo, K. and Kim, N. (2009) The mechanism of osteoclast differentiation induced by IL-1. J. Immunol. **183**, 1862–1870

Membrane-bound receptor activator of NFκB ligand (RANKL) activity displayed by osteoblasts is differentially regulated by osteolytic factors

Preetinder P. Singh [a,*], A. Gabrielle J. van der Kraan [a,b], Jiake Xu [c], Matthew T. Gillespie [a,b], Julian M.W. Quinn [a,b]

[a] Prince Henry's Institute, Clayton, Australia
[b] Department of Biochemistry and Molecular Biology, Monash University, Clayton, Australia
[c] School of Pathology and Laboratory Medicine, The University of Western Australia, Nedlands, Australia

ARTICLE INFO

ABSTRACT

Osteoclast formation is central to bone metabolism, occurring when myelomonocytic progenitors are stimulated by membrane-bound receptor activator of NFκB ligand (RANKL) on osteoblasts. Osteolytic hormones induce osteoblast RANKL expression, and reduce production of RANKL decoy receptor osteoprotegerin (OPG). However, rather than RANKL and OPG mRNA or protein levels, to measure hormonally-induced osteoclastogenic stimuli the net RANKL activity at the osteoblast surface needs to be determined. To estimate this we developed a cell reporter approach employing pre-osteoclast RAW264.7 cells transfected with luciferase reporter constructs controlled by NFκB (NFκB-RAW) or NFATc1 (NFAT-RAW)-binding promoter elements. Strong signals were induced in these cells by recombinant RANKL over 24 h. When NFκB-RAW cells were co-cultured on osteoblastic cells (primary osteoblasts or Kusa O cells) stimulated by osteolytic factors $1,25(OH)_2$ vitamin D_3 ($1,25(OH)_2D_3$) and prostaglandin E_2 (PGE_2), a strong dose dependent signal in NFκB-RAW cells was induced. These signals were completely blocked by soluble recombinant RANKL receptor, RANK.Fc. This osteoblastic RANKL activity was sustained for 3 days in Kusa O cells; with $1,25(OH)_2D_3$ withdrawal, RANKL-induced signal was still detectable 24 h later. However, conditioned medium from stimulated osteoblasts induced no signal. TGFβ treatment inhibited osteoclast formation supported by $1,25(OH)_2D_3$-treated Kusa O cells, and likewise blocked RANKL-dependent signals in NFAT-RAW co-cultured with these cells. These data indicate net RANKL stimulus at the osteoblast surface is increased by $1,25(OH)_2D_3$ and PGE_2, and suppressed by TGFβ, in line with their effects on RANKL mRNA levels. These results demonstrate the utility of this simple co-culture-based reporter assay for osteoblast RANKL activity.

1. Introduction

RANKL, a TNF-related protein, is a key factor regulating bone metabolism through its role in stimulating the formation and activation of bone resorbing osteoclasts [1]. The high bone mass and osteoclast deficiency in mice lacking RANKL or its receptor RANK [1–3] demonstrates the fundamental role of these molecules in bone metabolism. There is also ample clinical evidence that inhibiting RANKL actions significantly suppresses bone resorption both clinically and in mouse models [4,5]. The major source of RANKL at the bone surface is the bone forming cells, osteoblasts, as well as osteoblast-related osteocytes and bone lining cells. These cells produce both RANKL [6] and its secreted decoy receptor osteoprotegerin (OPG) in a highly regulated manner. Thus osteolytic factors

like IL-6 family cytokines, PTH and dihydroxyvitamin D_3 ($1,25(OH)_3D_3$), drive osteoclast formation from hematopoietic cells by increasing RANKL production in osteoblasts [1,6] and reducing their production of OPG (illustrated in Fig. 1A). Activated T cells and myeloma cells also produce RANKL either in a secreted or shed soluble form [7,8]. Osteoblasts appear to produce only membrane-associated RANKL as, at least *in vitro*, contact between osteoclast progenitors and osteoblasts is required for osteoclast formation. However, soluble RANKL production by osteocytes has been suggested by recent work [9].

From the foregoing it is clear that measurement of RANKL in osteoblasts and stromal cells is of great interest. This is commonly studied by quantifying RANKL and OPG mRNA levels [6]. Estimating relative RANKL protein levels in osteoblast cell membrane extracts can be achieved by Western blotting but low sensitivity can be a problem and may also detect the significant amounts of RANKL bound to intracellular membranes [10,11]. Another concern is that it is not the RANKL levels *per se* that drive osteoclast formation but

* Corresponding author. Address: Prince Henry's Institute, Monash Medical Centre, 246 Clayton Road, Clayton, Victoria 3168, Australia. ███████
███████

the net RANKL stimulus produced, i.e., net of OPG inhibitory effects [12]. The magnitude of this net RANKL stimulus can be inferred by studying osteoclast formation in co-cultures of bone marrow progenitors (or other hematopoietic population) with osteoblasts treated with stimuli of interest. However, such osteoclast formation is only observed after several days and involves complex differentiation pathway dynamics.

With these considerations we developed a simple, robust and rapid method to estimate functional RANKL stimulus in live osteoblastic cells by incubating osteoblasts with RANK$^+$ reporter cells derived from RAW264.7 cells. These cells efficiently form osteoclasts in response to RANKL, i.e., respond similarly to osteoclast precursors. RAW264.7 cells were stably transfected with vectors containing luciferase-expressing constructs under the control of promoters sensitive to NFκB and the NFATc1 transcription factors, both of which are critical for RANKL-dependent osteoclast formation [13,14]. Stimuli that induce signals in these reporter cells were confirmed as RANKL when their effects were ablated by soluble RANK.Fc, a truncated chimeric form of RANK which binds RANKL alone [3]. We used these methods to study two significant questions about RANKL induction – namely whether mRNA levels of RANKL stimulus reflects the net functional RANKL stimulus, and whether the induced RANKL stimulus is sustained or transient. The latter is particularly important in considering RANKL stimulation by relatively unstable local hormones like prostaglandins.

2. Materials and methods

2.1. Cells and reagents

Tissue culture medium used in all cultures was minimal essential medium-alpha (MEM) (Gibco BRL, Gaithersburg, MD) supplemented with fetal bovine serum 10% (CSL Biosciences, Parkville, Australia) and penicillin 50 U/mL; streptomycin 50 μg/mL and 2 mM L-glutamine (Gibco BRL).

C57BL/6J mice were obtained from Monash Animal Services, Clayton, Australia and were maintained at Monash Medical Centre Animal facility, Clayton, Australia with procedures approved by the institute ethics committee. Osteoblasts were prepared from newborn mouse calvariae by sequential digestion with 0.1% collagenase plus 0.2% dispase (Godo Shusei, Tokyo, Japan) and cultured for 3–4 days to confluence prior to use. Mouse bone marrow was obtained from adult (6–12 week old) male C57black6/J mice. Kusa O cells were cultured as previously described [15]. Rabbit anti-mouse/rat calcitonin receptor antibody was produced in house as per Tikellis et al. [16].

2.2. Cytokines and hormones

Recombinant GST-RANKL$^{158–316}$ (RANKL) was obtained from the Oriental Yeast Co. Ltd. (Itabashi City, Tokyo, Japan). Other recombinant proteins were obtained from R&D Systems (Minneapolis, MN). 1,25(OH)$_2$D$_3$ was obtained from Wako Pure Chemical Co. (Osaka, Japan) and Prostaglandin E$_2$ (PGE$_2$) was obtained from Sigma Chemical Co. (Castle Hill, Australia). Other reagents were analytical grade obtained from Sigma unless noted.

2.3. Construction of stable reporter cell lines

NFκB-RAWs were generated as previously described [17]. Briefly, RAW264.7 cells were stably transfected with a G418-selectable vector containing a 3kB-Luc-SV40 luciferase reporter with a promoter containing NFκB binding sites (κB). Similarly, NFAT-RAWs were generated by stable transfection of RAW264.7 cells with a GL4.30 [luc2P/NFAT-RE/Hygro] (Promega, South Syd-

ney, Australia) reporter construct with the luciferase production under the control of an NFAT-response element.

2.4. Luciferase reporter cell-based assays

NFκB-RAW and NFAT-RAW cells were routinely maintained in MEM/10%FBS. After trypsinisation 4×10^4 cells were seeded per well in tissue culture 96-wells (0.34 ml TPP grade, Thermo Fisher Scientific, Scoresby, Australia) and treatments were added as described. After incubation at 37 °C for 24 h, cells were rinsed in sterile PBS, lysed by the addition of 40 μl of passive lysis buffer (Promega) followed by an overnight incubation at 4 °C. Lysates were transferred to white 96 well plates (Thermo Fisher) for analysis with luciferase substrate (Promega) using an Envision (model 2103) multi-label plate reader (Perkin Elmer, Waltham, MA).

For luciferase reporter cell co-cultures with osteoblastic cells, the latter (Kusa O, primary osteoblasts and UMR106.01 cells) were seeded 2×10^4 cells/well in standard 96 well plates. Cytokine and hormone treatments were added to the cells at this point (unless otherwise noted) and incubated for 24 h. Reporter NFκB-RAW and NFAT-RAW cells (4×10^4 cells/well) were then added to these osteoblastic assays and the protocol followed the sequence mentioned as above.

2.5. Osteoclast formation assays

Kusa O cells were seeded in 10 mm diameter culture wells (2×10^4/well) in MEM/FBS, and mouse bone marrow cells (10^5 cells/well) added. 1,25(OH)$_2$D$_3$ (10 nM) stimulation was added to the co-cultures, which were incubated at 37 °C for 3 days, then medium and mediators were replenished. After 7 days incubation cells were histochemically stained for TRAP as previously [18]. Some cell preparations were cultured on 6 mm diameter glass coverslips (Thermo Fisher), which were fixed in cold (−20 °C) acetone and immuno-stained with anti-calcitonin receptor (CTR) antibody (5 μg/ml) as previously [19].

2.6. Analysis of mRNA expression

Kusa O cells were cultured in six well plates with or without hormonal stimulation (MEM with 2%FBS). RNA was isolated using TRIZOL (Invitrogen) and treated with DNase (Ambion, Austin, TX) according to the manufacturer's instructions. cDNA was prepared from 5 μg RNA Superscript III Double-Stranded cDNA Synthesis Kit (Invitrogen). Real-Time PCR analysis (Stratagene Mx3000P, Agilent, Santa Clara, CA) was performed using SYBR Green mix (Invitrogen) according to manufacturer's instructions. Data were normalised to hypoxanthine-guanine phosphoribosyl transferase (HPRT)-1 and represented as fold induction over untreated time-point control. The oligonucleotide primer sequences (Sigma Genosys, Castle Hills, Australia) were as follows: RANKL (Gene Accession Number NM_011613), forward primer: 5′-TCCAGCTATGATG-GAAGGCT-3′, reverse primer: 5′-GTACCAAGAGGACAGAGTG-3′. HPRT-1 (Gene Accession Number NM_013556), forward primer: 5′-TGATTAGCGATGATGAACCAG-3′, reverse primer: 5′-AGA-GGGCCACAATGTGATG-3′.

2.7. Statistical analysis

Statistical analyses were performed using one way ANOVA with Tukey's post hoc test, using Graphpad Prism 5 software (Graphpad Software, San Diego, CA). In all cases, $P < 0.05$ was considered significant. All values are presented as mean ± standard error. Data in this manuscript was audited in accordance with the NHMRC (Australia) Code for the Responsible Conduct of Research (PHI Data Audit No. 11–29).

3. Results

3.1. Osteoblast RANKL regulation and the characterisation of NFκB-reporter cells

Kusa O is a pre-osteoblastic and pre-adipocytic cell line that supports osteoclast formation and forms mature osteoblasts in long-term culture [15]. RT-PCR analysis confirmed that 10 nM $1,25(OH)_2D_3$ treatment of Kusa O stromal cells enhanced RANKL mRNA (Fig. 1B). Consistent with this, Kusa O cells co-cultured with mouse bone marrow cells in the presence of $1,25(OH)_2D_3$ for 7 days resulted in osteoclast formation, evidenced by large numbers of TRAP$^+$ and CTR$^+$ mononucleated and multinucleated cells (Fig. 1C).

For NFκB-RAW cell characterisation, 4×10^4 cells were cultured per 6 mm diameter well for 24 h in the presence of recombinant RANKL. The cells showed a robust and dose dependent increase in luciferase signal with RANKL concentration that was maximal at 100 ng/ml, and blocked by 300 ng/ml recombinant RANK.Fc protein (Fig. 1D and E). Shorter periods of RANKL exposure similarly induced a signal but this was usually weaker and less robust (data not shown) so in further experiments, only 24 h incubations were used unless otherwise noted. Other NFκB inducing stimuli were also tested on these cells including TNF (20 ng/ml) (Fig. 1E) and LPS (100 ng/ml) (data not shown), which both induced a strong signal, but as expected these signals were not blocked by RANK.Fc. NFAT-RAW cells prepared and cultured similarly also exhibited a similar dose dependent increase to that observed in NFκB-RAW cells in response to RANKL stimulation (data not shown).

3.2. The use of reporter cells to measure membrane-bound RANKL stimulus in osteoblasts

To test the ability of Kusa O cells to make soluble RANKL detectable by the reporter cells, we incubated Kusa O cell cultures (initially 90% confluent) for 3 days in the presence or absence of $1,25(OH)_2D_3$. Conditioned medium (30%) from these cultures was added to NFκB-RAW cells for 24 h but no significant luciferase signal was observed (Fig. 2A) suggesting little or no transfer of activity RANKL. We then tested the response of NFκB-RAW cells in contact with Kusa O cells stimulated with $1,25(OH)_2D_3$ (illustrated in Fig. 2B). We first confirmed recombinant RANKL-induced signal in these cells was not affected by $1,25(OH)_2D_3$ (Fig. 2C). NFκB-RAW cells were then added to Kusa O cells pre-treated with $1,25(OH)_2D_3$ for 24 h, and a strong dose dependent signal was observed after 24 h of co-culture (Fig. 2D). A maximal stimulation was attained with 100nM $1,25(OH)_2D_3$. Signals induced by $1,25(OH)_2D_3$ were completely ablated by 300 ng/ml RANK.Fc (Fig. 2E) and for further studies this concentration of 300 ng/ml RANK.Fc was routinely used. Co-cultures with NFAT-RAW cells showed a similar pattern (data not shown) indicating that both reporter RAW cell types can be used to assess net RANKL stimulus in Kusa O cells. We also found that primary calvarial mouse osteoblasts also induced signals in reporter NFκB-RAW cells, when treated with the commonly used stimuli 10 nM $1,25(OH)_2D_3$ and 10^{-7} M PGE$_2$ (Fig. 2F); again this was ablated by the presence of RANK.Fc. Rat osteoblastic UMR106.01 cells also generated $1,25(OH)_2D_3$-dependent RANKL signals in co-culture (data not shown).
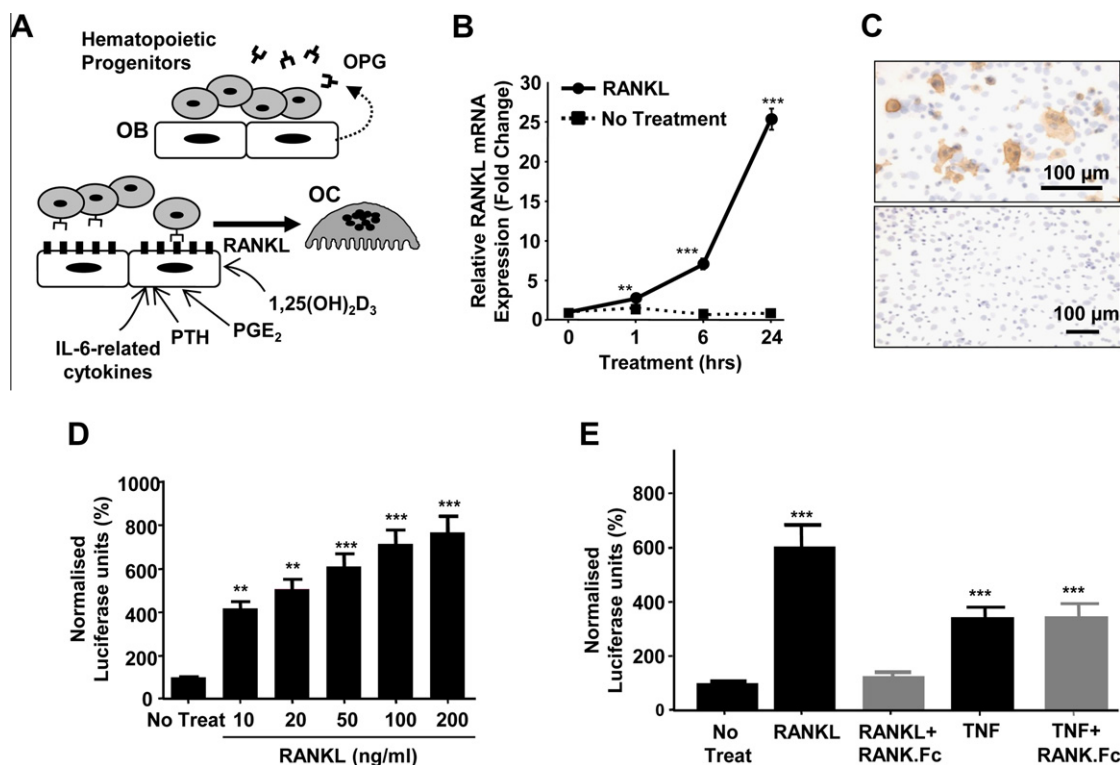

Fig. 1. RANKL production by osteoblastic cells and the characterisation of RANKL-elicited luciferase responses of NFκB-RAW cells. (A) Diagram illustrates osteoclast formation supported by hormonally-stimulated osteoblasts. Osteoblastic cells (OB) and progenitors in unstimulated state produce OPG (shown top). With the stimulation of PTH and osteolytic factors the osteoblasts produce RANKL (and less OPG), driving formation of osteoclasts (OC) (lower diagram). (B) Regulation of mRNA levels of RANKL in Kusa O osteoblastic cells stimulated by $1,25(OH)_2D_3$. (C) Confirmation of osteoclast formation in $1,25(OH)_2D_3$ treated bone marrow cells with Kusa O cells, showing CTR immunostaining (brown colour; top image) and immunostaining control (lower image); black bars = 100 μm. (D) Dose response of signal elicited in NFκB-RAW cells to recombinant RANKL stimulation. (E) Signals elicited in NFκB-RAWs with RANKL (100 ng/ml) but not TNF (20 ng/ml) were blocked by RANK.Fc (300 ng/ml). (For interpretation of the references to color in this figure legend, the reader is referred to the web version of this article.)
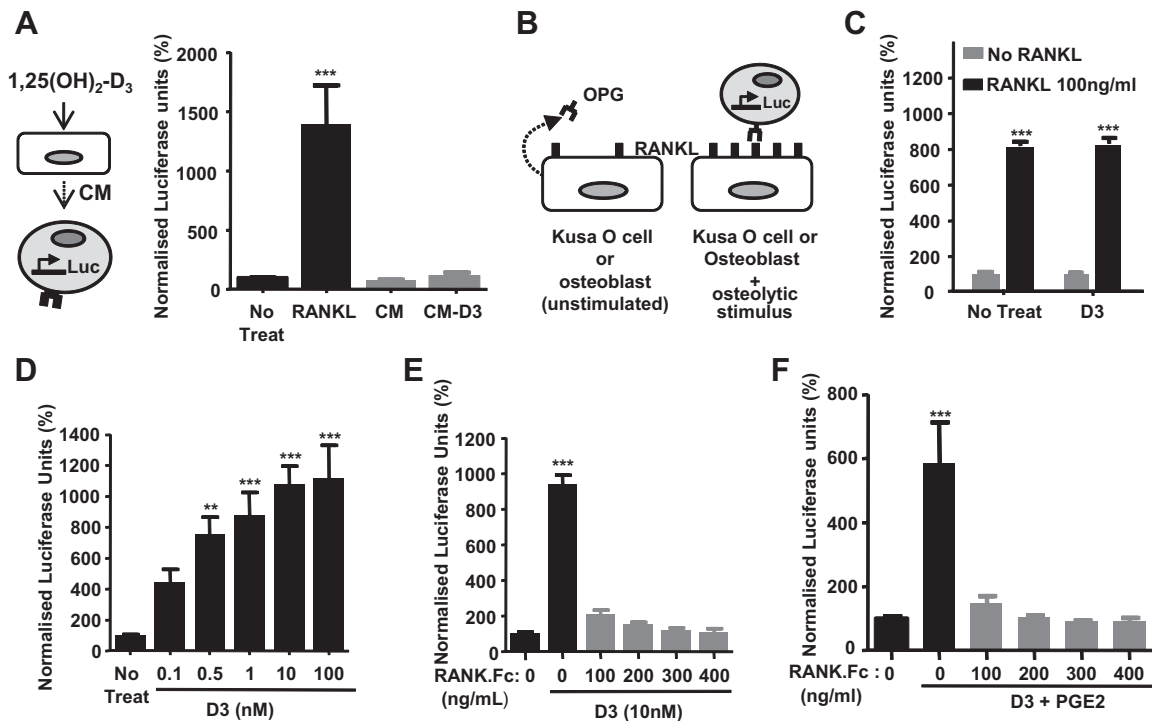
Fig. 2. The use of NFκB-RAW reporter cells to detect expressed RANKL protein in Kusa O and primary osteoblasts. (A) Lack of detectable soluble RANKL activity in 72 h conditioned medium from Kusa O cells (CM) and $1,25(OH)_2D_3$-stimulated Kusa O cell for (CM-D3); RANKL treatment (100 ng/ml) was employed as a positive control. Protocol is illustrated in diagram to the left. (B) Diagram illustrating the transfected reporter cell co-culture method employed in this study. (C) Lack of direct effects of $1,25(OH)_2D_3$ on signal induced in NFκB-RAWs. (D) Dose response of NFκB-RAW reporter cells to $1,25(OH)_2D_3$-stimulated in co-culture with Kusa O cells at 24 h. (E) RANK.Fc blocks elicited signals in NFκB-RAWs in co-culture with $1,25(OH)_2D_3$ stimulated Kusa O cells. (F) RANK.Fc similarly blocks signals induced in NFκB-RAWs by co-culture with primary osteoblasts stimulated by $1,25(OH)_2D_3$ plus PGE_2.

3.3. Persistence of RANKL activity in stimulated Kusa O cells

To determine the stability of the induced RANKL activity in stromal cells and to determine whether the protocol we adopted in Fig. 2 are the best options, we varied the time at which the stimulus (10^{-8} M $1,25(OH)_2D_3$) was added relative to the reporter cells (illustrated in Fig. 3A). 'Day 0' was taken as the time point at which reporter NFκB-RAW cells were added to the Kusa O cells; 'Day −1' is the day prior to NFκB-RAW addition, 'Day −2' 'Day −3' were 2 and 3 days prior. NFκB-RAWs were incubated in these co-cultures for 24 h (i.e., to 'Day +1) and then were lysed for luciferase analysis. We first varied the time course of stimulation in the following manner: no stimulus; $1,25(OH)_2D_3$ stimulus added at Day −1 then removed (washed out) at Day 0; $1,25(OH)_2D_3$ stimulus added at Day 0 only; $1,25(OH)_2D_3$ stimulus added at Day −1, then again at Day 0. In each case there was a full change of medium at Day 0 just prior to reporter cell addition. When $1,25(OH)_2D_3$ stimulation was added at Day −1 then washed out at Day 0 a diminished signal was observed compared to cultures where stimulus continued for a further 24 h (Fig. 3B). Nevertheless, this suggests that RANKL signal persists significantly even when the stimulus is removed. When $1,25(OH)_2D_3$ was added only with the reporter cells (i.e., at Day 0) the signal was detected but as might be expected this was weaker than that achieved by 24 h pre-stimulation. This is consistent with 24 h being required for RANKL protein expression to be maximal.

When $1,25(OH)_2D_3$ stimulus (10^{-8} M) was added at 3 or 2 days prior to reporter cell addition (Day 0), the signal obtained was equivalent to that observed when $1,25(OH)_2D_3$ was added 1 day prior (Fig. 3C). This suggests that either the $1,25(OH)_2D_3$ or the RANKL induction (or both) were stable over this period. We also tested PGE_2 (10 nM) applied in the same way, and indeed a weaker but similarly persistent signal was observed over this period.

3.4. Employing reporter cells to study RANKL suppression – the influence of TGFβ

We previously showed TGFβ treatment suppresses RANKL mRNA levels in primary osteoblasts [20] and reduces osteoclast formation in co-cultures. We first confirmed that in Kusa O cells TGFβ reduced RANKL mRNA levels induced by $1,25(OH)_2D_3$ (Fig. 4A). We then investigated the effects of TGFβ on levels of membrane RANKL activity in Kusa O cells using reporter cell/Kusa O co-cultures. However, first we tested the direct effects of TGFβ on our reporter cells and found TGFβ had a significant negative effect on luciferase signals in NFB-RAW cells (Fig. 4B; left panel). This observation suggested that this reporter cell was unsuitable for investigating TGFβ actions on Kusa O RANKL activity. In contrast, TGFβ (5 ng/ml) did not inhibit luciferase signals in NFAT-RAW cells, indeed enhanced them (Fig. 4B; right panel). Using NFAT-RAW cells co-cultured with $1,25(OH)_2D_3$-treated Kusa O we found that the strong RANKL-activity signal was indeed suppressed by TGFβ (Fig. 4C). TGFβ also blocked osteoclast formation in bone marrow/Kusa O co-cultures (Fig. 4D and E), but this inhibition was rescued by adding recombinant RANKL (200 ng/ml). This indicates that TGFβ inhibition of osteoclast formation is solely due the suppression of RANKL activity in Kusa O cells (Fig. 4D and E).

4. Discussion

This study has demonstrated that a simple co-culture method employing NFκB and NFAT sensitive reporter cells can be used to assess the levels of membrane-associated RANKL in osteoblastic cells. We succeeded in generating stably transfected reporter cells from pre-osteoclast/macrophage RAW264.7 cells (which are generally difficult to transfect) resulting in cells luciferase-responding
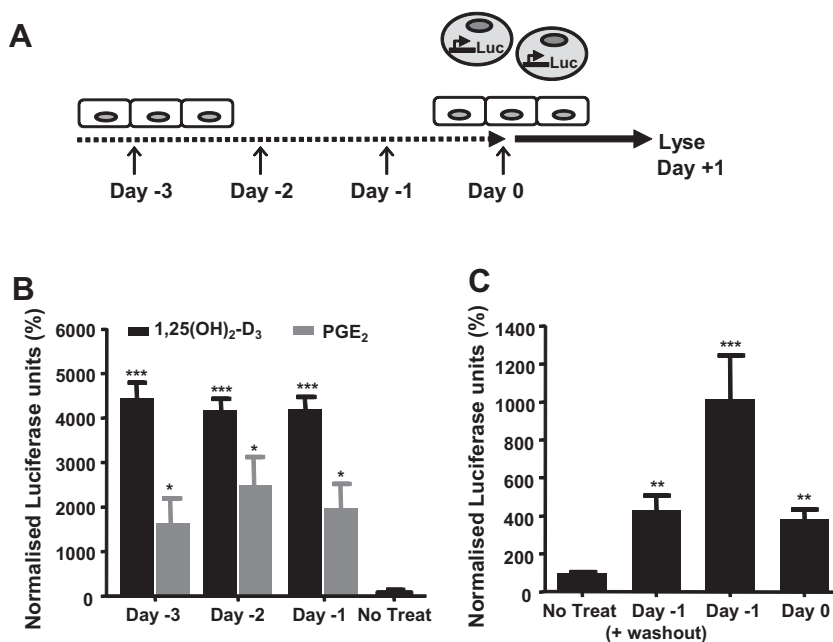
Fig. 3. Time course of signal induction in NFκB-RAWs co–cultured with Kusa O, and persistence of the RANKL induction by 1,25(OH)₂D₃ and PGE₂. (A) Diagram illustrating the stimulation protocol – 'Day 0' was the point when NFκB-RAWs were added to Kusa O cells. Stimuli were added 1, 2 or 3 days prior (i.e., 'Day −1', Day −2' and 'Day −3', respectively) to Day 0. Cells were lysed for analysis 24 h after NFκB-RAWs addition ('Day +1'). (B) Effect of adding 1,25(OH)₂D₃ stimulus on different days, as indicated. "Day −1 + washout" indicates that cells were treated on Day '−1' then the next day (Day 0) medium was replaced with medium without 1,25(OH)₂D₃. (C) Persistence of the signal elicited by adding 1,25(OH)₂D₃ (D3) and PGE₂ over 3, 2 or 1 days prior to reporter cell addition to the cultures.
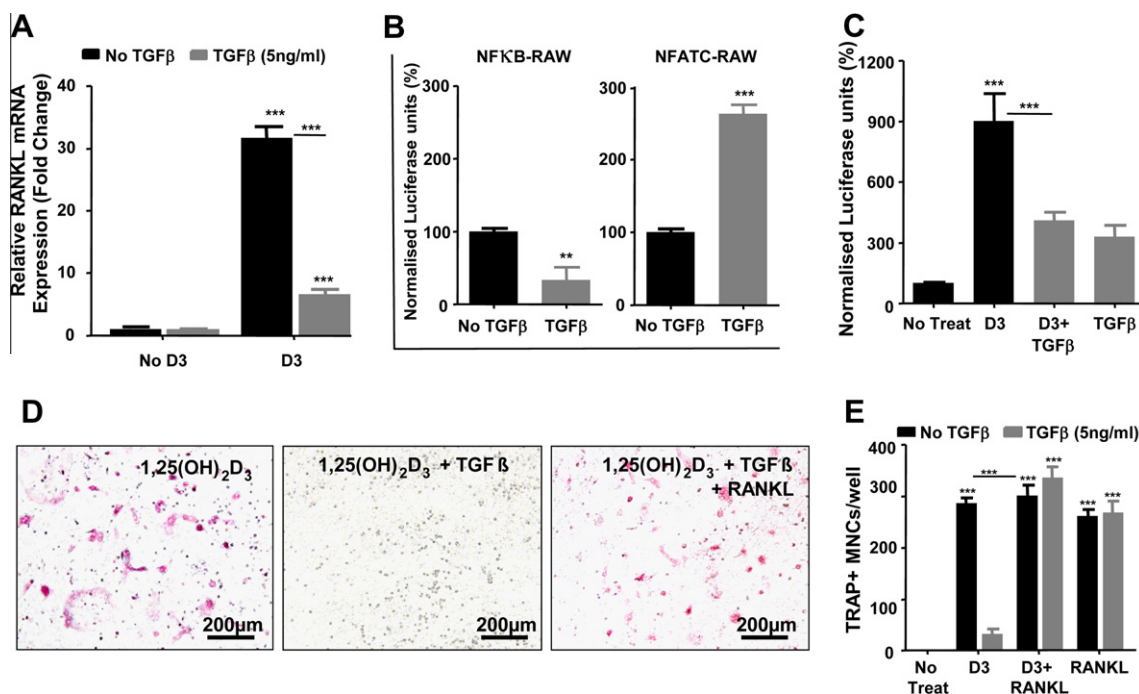

Fig. 4. TGFβ suppression of RANKL levels in Kusa O osteoblastic cells. (A) TGFβ suppressed 1,25(OH)₂D₃-induced RANKL mRNA levels in Kusa O cells at 24 h. (B) NFκB-RAW cells treated with TGFβ showed reduction in signal (left) while NFAT-RAW cells treated with TGFβ showed increased signal (right). (C) NFAT-RAW cells co-cultured with 1,25(OH)₂D₃-treated Kusa O cells showed signal reduction with TGFβ. (D) Images of TRAP⁺ MNC formation in 1,25(OH)₂D₃ treated bone marrow/Kusa O co-cultures. TGFβ inhibition of osteoclast formation was rescued by recombinant RANKL, black bars = 100 μm. (E) Quantitative data from co-cultures illustrated in D.

cells highly responsive to RANKL that were robustly stimulated when incubated in co-cultures with RANKL-expressing osteoblasts. This enabled a consistent and simple assay system for osteoblast RANKL activity, our results showing consistency with osteoblast RANKL mRNA expression levels and RANKL-dependent osteoclast

formation. Our data indicates that relative quantification of functional RANKL signal strength on osteoblast membranes can be attempted in this way, as the results shown in Fig. 2D showed a clear dose response to increasing stimulus. Comparison of the magnitude of the RANKL-induced signals in Fig. 2E (Kusa O) and

Fig. 2F (osteoblasts) suggests that of the two the Kusa O cells provided a greater RANKL stimulus, however a careful estimate of the RANK.Fc concentration needed to ablate the RANKL signal would be needed to confirm this. This is because the linearity of the relationship between RANKL level and luciferase response is unclear, and indeed may be modified by other factors produced by the osteoblastic cells.

Measuring RANKL stimulus using a range of different assays is important to determine what elevates osteoclast formation in pathological tissues [21] and how osteoblastic cells participate in such osteolysis. It is particularly difficult with a membrane-bound protein to determine how much RANKL these cells deliver to osteoclasts, whether increased RANKL levels alone account for elevated osteoclast number. RANKL can be released in soluble form [22] and its detection in the circulation may indicate tissue RANKL levels, however, this may not give a useful indication of RANKL levels in bone, and it is unclear in some studies if detected circulating RANKL is bound to OPG. In our studies we were unable to find any transferable RANKL activity in conditioned medium from stimulated Kusa O (Fig. 2A) which suggests that at least under these conditions osteoblasts produce mainly cell-associated RANKL. Our data also suggests that RANKL activity induced by $1,25(OH)_2D_3$ and PGE_2 is surprisingly persistent long term (Fig. 3B) indicating these factors are stable under culture conditions as RANKL signal drops when the stimulus is removed (Fig. 3C). Alternatively, they may induce other autocrine RANKL-inducing factors from the stromal cells to sustain RANKL levels [23].

As well as investigating RANKL induction in osteoblasts we also sought to clarify paradoxical aspects of TGFβ action on osteoclast generation. TGFβ clearly enhances osteoclast progenitor responses to RANKL (and hence osteoclast numbers [20]) however when RANKL is delivered by osteoblasts TGFβ has inhibitory actions. Consistent with this, TGFβ reduced RANKL mRNA levels, but whether this abolishes RANKL protein production or induces production of some other inhibitor is unclear [20]. As TGFβ itself directly reduced luciferase signals in NFκB-RAW, cells we instead studied this phenomenon using NFAT-RAWs Kusa O co-cultures; these results indicated that RANKL activity induced by $1,25(OH)_2D_3$ was indeed abolished by TGFβ. It was also noted that TGFβ still induced NFAT signals which is significant as many osteoclast inhibitors diminish NFATc1 levels [14]. This data strongly suggests that RANKL activity is simply suppressed by TGFβ treatment, which also explains why simply adding recombinant RANKL was able to restore osteoclast formation in such co-cultures.

In summary, we have developed a reporter co-culture method to estimate the functional membrane-associated RANKL activity induced in osteoblastic cells by osteolytic factors. This demonstrated that RANKL activity is sustained until the osteolytic stimulus is removed, while TGFβ rapidly abolishes induced RANKL activity. This simple approach provides a useful and rapid method to study RANKL activity regulated by hormonal factors.

Acknowledgments

References

[1] H. Yasuda, N. Shima, N. Nakagawa, et al., Osteoclast differentiation factor is a ligand for osteoprotegerin/osteoclastogenesis-inhibitory factor and is identical to TRANCE/RANKL, Proc. Natl. Acad. Sci. USA 95 (1998) 3597–3602.

[2] J. Li, I. Sarosi, X.Q. Yan, et al., RANK is the intrinsic hematopoietic cell surface receptor that controls osteoclastogenesis and regulation of bone mass and calcium metabolism, Proc. Natl. Acad. Sci. USA 97 (2000) 1566–1571.

[3] D.M. Anderson, E. Maraskovsky, W.L. Billingsley, et al., A homologue of the TNF receptor and its ligand enhance T-cell growth and dendritic-cell function, Nature 390 (1997) 175–179.

[4] T.D. Rachner, S. Khosla, L.C. Hofbauer, Osteoporosis: now and the future, Lancet 377 (2011) 1276–1287.

[5] D. Castellano, J.M. Sepulveda, I. Garcia-Escobar, et al., The role of RANK-ligand inhibition in cancer: the story of denosumab, Oncologist 16 (2011) 136–145.

[6] N.J. Horwood, J. Elliott, T.J. Martin, et al., Osteotropic agents regulate the expression of osteoclast differentiation factor and osteoprotegerin in osteoblastic stromal cells, Endocrinology 139 (1998) 4743–4746.

[7] N.J. Horwood, V. Kartsogiannis, J.M. Quinn, et al., Activated T lymphocytes support osteoclast formation in vitro, Biochem. Biophys. Res. Commun. 265 (1999) 144–150.

[8] A.N. Farrugia, G.J. Atkins, L.B. To, et al., Receptor activator of nuclear factor-kappaB ligand expression by human myeloma cells mediates osteoclast formation in vitro and correlates with bone destruction in vivo, Cancer Res. 63 (2003) 5438–5445.

[9] J. Xiong, C.A. O'Brien, Osteocyte RANKL: new insights into the control of bone remodeling, J. Bone Miner. Res. 27 (2012) 499–505.

[10] V. Kartsogiannis, H. Zhou, N.J. Horwood, et al., Localization of RANKL (receptor activator of NF kappa B ligand) mRNA and protein in skeletal and extraskeletal tissues, Bone 25 (1999) 525–534.

[11] S. Aoki, M. Honma, Y. Kariya, et al., Function of OPG as a traffic regulator for RANKL is crucial for controlled osteoclastogenesis, J. Bone Miner. Res. 25 (2010) 1907–1921.

[12] N.L. Fazzalari, J.S. Kuliwaba, G.J. Atkins, et al., The ratio of messenger RNA levels of receptor activator of nuclear factor kappaB ligand to osteoprotegerin correlates with bone remodeling indices in normal human cancellous bone but not in osteoarthritis, J. Bone Miner. Res. 16 (2001) 1015–1027.

[13] B.R. Wong, R. Josien, S.Y. Lee, et al., The TRAF family of signal transducers mediates NF-κB activation by the TRANCE receptor, J. Biol. Chem. 273 (1998) 28355–28359.

[14] H. Takayanagi, The role of NFAT in osteoclast formation, Ann. NY Acad. Sci. 1116 (2007) 227–237.

[15] E.H. Allan, P.W. Ho, A. Umezawa, et al., Differentiation potential of a mouse bone marrow stromal cell line, J. Cell. Biochem. 90 (2003) 158–169.

[16] C. Tikellis, L. Xuereb, D. Casley, et al., Calcitonin receptor isoforms expressed in the developing rat kidney, Kidney Int. 63 (2003) 416–426.

[17] C. Wang, J.H. Steer, D.A. Joyce, et al., 12-O-tetradecanoylphorbol-13-acetate (TPA) inhibits osteoclastogenesis by suppressing RANKL-induced NF-kappaB activation, J. Bone Miner. Res. 18 (2003) 2159–2168.

[18] J.M. Quinn, G.A. Whitty, R.J. Byrne, et al., The generation of highly enriched osteoclast-lineage cell populations, Bone 30 (2002) 164–170.

[19] J.M. Quinn, M. Morfis, M.H. Lam, et al., Calcitonin receptor antibodies in the identification of osteoclasts, Bone 25 (1999) 1–8.

[20] J.M. Quinn, K. Itoh, N. Udagawa, et al., Transforming growth factor beta affects osteoclast differentiation via direct and indirect action, J. Bone Miner. Res. 16 (2001) 1787–1794.

[21] J.M. Quinn, N.J. Horwood, J. Elliott, et al., Fibroblastic stromal cells express receptor activator of NF-kappa B ligand and support osteoclast differentiation, J. Bone Miner. Res. 15 (2000) 1459–1466.

[22] L. Lum, B.R. Wong, R. Josien, et al., Evidence for a role of a TNF-alpha-converting enzyme-like protease in shedding of TRANCE, a TNF family member involved in osteoclastogenesis and dendritic cell survival, J. Biol. Chem. 274 (1999) 13613–13618.

[23] E. Romas, N. Udagawa, H. Zhou, et al., The role of gp130-mediated signals in osteoclast development: regulation of interleukin 11 production by osteoblasts and distribution of its receptor in bone marrow cultures, J. Exp. Med. 183 (1996) 2581–2591.

Molecular Stress-inducing Compounds Increase Osteoclast Formation in a Heat Shock Factor 1 Protein-dependent Manner*

Ryan C. Chai[‡], Michelle M. Kouspou[‡], Benjamin J. Lang[‡], Chau H. Nguyen[‡], A. Gabrielle J. van der Kraan[‡§], Jessica L. Vieusseux[‡], Reece C. Lim[‡], Matthew T. Gillespie[‡§], Ivor J. Benjamin[¶], Julian M. W. Quinn[‡§1], and John T. Price[‡‖1,2]

From the [‡]Department of Biochemistry and Molecular Biology, Monash University, Clayton, Victoria 3800, Australia, [§]Prince Henry's Institute, Clayton, Victoria 3168, Australia, the [¶]Division of Cardiovascular Medicine, Medical College of Wisconsin, Milwaukee, Wisconsin 53226, and the [‖]College of Health and Biomedicine, Victoria University, St. Albans, Melbourne, Victoria 8001, Australia

Background: HSP90 inhibitors increase osteoclast formation and bone loss.
Results: Altered Hsf1 activity impacts the ability of stress-inducing compounds to modulate osteoclast formation.
Conclusion: Hsf1 plays an important role in stress-associated osteoclast formation, potentially via MITF.
Significance: We identified a novel pathway whereby agents inducing stress can enhance osteoclast formation.

Many anticancer therapeutic agents cause bone loss, which increases the risk of fractures that severely reduce quality of life. Thus, in drug development, it is critical to identify and understand such effects. Anticancer therapeutic and HSP90 inhibitor 17-(allylamino)-17-demethoxygeldanamycin (17-AAG) causes bone loss by increasing osteoclast formation, but the mechanism underlying this is not understood. 17-AAG activates heat shock factor 1 (Hsf1), the master transcriptional regulator of heat shock/cell stress responses, which may be involved in this negative action of 17-AAG upon bone. Using mouse bone marrow and RAW264.7 osteoclast differentiation models we found that HSP90 inhibitors that induced a heat shock response also enhanced osteoclast formation, whereas HSP90 inhibitors that did not (including coumermycin A1 and novobiocin) did not affect osteoclast formation. Pharmacological inhibition or shRNAmir knockdown of Hsf1 in RAW264.7 cells as well as the use of Hsf1 null mouse bone marrow cells demonstrated that 17-AAG-enhanced osteoclast formation was Hsf1-dependent. Moreover, ectopic overexpression of Hsf1 enhanced 17-AAG effects upon osteoclast formation. Consistent with these findings, protein levels of the essential osteoclast transcription factor microphthalmia-associated transcription factor were increased by 17-AAG in an Hsf1-dependent manner. In addition to HSP90 inhibitors, we also identified that other agents that induced cellular stress, such as ethanol, doxorubicin, and methotrexate, also directly increased osteoclast formation, potentially in an Hsf1-dependent manner. These results, therefore, indicate that cellular stress can enhance osteoclast differentiation via Hsf1-dependent mechanisms and may significantly contribute to pathological and therapeutic related bone loss.

Maintaining bone mass and quality is critical for sustained health and quality of life by preventing fracture (1). For this reason, bone undergoes continual remodeling throughout adult life to optimize bone quality and structural integrity. This remodeling process involves cycles of bone resorption and formation, mediated by osteoclasts and osteoblasts, respectively (2, 3). Many factors can negatively impact bone health, including a poor diet, gonadal hormonal insufficiency, pathological insult, as well as a range of therapeutic agents (4–7) that often compound the loss of bone mass seen with aging. Factors that are deleterious to bone generally cause a net increase in the formation of the specialized bone-resorbing cell, the osteoclast, causing sustained bone loss that can result in low bone mass, *i.e.* osteopenia or osteoporosis (8, 9), that is not compensated for by increased bone formation. Such bone loss is associated with decreased bone strength and, thus, an increased fracture risk, particularly in the spine, hip, and wrist, with any resulting fractures ultimately leading to a severely diminished quality of life and increased rate of mortality, particularly in elderly patients (10). Localized rapid bone loss may also cause pain and hypercalcemia (4).

It is increasingly recognized that chemotherapeutic agents have a major negative impact upon bone by increasing bone loss and fracture risk more rapidly and severely than seen in normal age-related bone loss (4, 6). Although both hormonal and non-hormonal cancer therapies promote bone loss by inducing hypogonadism, chemotherapeutics can also directly impact osteoclasts (as well as the bone-forming osteoblasts) to cause loss of bone mass and structural integrity, although the mechanisms that underlie this have still to be fully elucidated (4, 11–13). Because of the effectiveness of a number of cancer treatments providing improved survival rates, especially in older patients who may already have low bone mass, it is of

increasing importance to determine the effect of therapeutics on bone turnover and bone loss. Moreover, it is important to identify the mechanisms by which anticancer agents may result in bone loss so that preventative measures, such as administration of antiosteolytic treatments, may be designed effectively.

The process of osteoclast formation is fundamental to the resorption of bone during both physiological and pathophysiological bone resorption. Osteoclasts are multinucleated, hematopoietically derived cells (3) that are highly active and relatively short-lived. Thus, their formation is a highly regulated point of control for bone resorption and is dependent upon the action of RANKL,[3] a TNF-related molecule whose production is locally regulated by many osteotropic hormones. RANKL typically acts in concert with M-CSF, a survival and proliferation factor for osteoclast progenitors and macrophages. RANKL, through interaction with its cognate receptor RANK, activates a cascade of critical transcription factors in osteoclast progenitors, notably involving NFκB, AP-1 (cFos/cJun dimer), NFATc1, and MITF. These factors, in turn, activate osteoclastic gene expression and induce cell fusion, resulting in mature, functional, multinucleated osteoclasts (14, 15).

Heat shock protein 90 (HSP90) is a molecular chaperone that is required for the stability and functionality of a diverse range of proteins (16). In particular, its action is critical for the stability and activity of mutated and overexpressed oncogenic proteins that enhance the survival, growth, and invasive potential of cancer cells (16, 17). Consistent with this, HSP90 is highly expressed in many tumor types and has been associated with poor patient outcomes (16–18). Thus, HSP90 has emerged as a major cancer therapeutic target and, as such, a number of HSP90 inhibitors have been developed, many of which have undergone or are currently in clinical trials (19).

We have found previously that the geldanamycin-derived HSP90 inhibitor and anticancer agent 17-AAG increases bone loss in mouse models through the direct stimulation of osteoclast formation (20). Furthermore, although 17-AAG proved to be effective in reducing the tumor burden at extraosseous sites, it actually increased the tumor burden within the bone and caused elevated bone loss even in the absence of tumor cells (20). Increased tumor growth in bone probably reflects the well characterized effects of the release of tumor growth factors from the bone matrix and is, therefore, secondary to the bone destruction caused by the pro-osteoclastic effects of 17-AAG. Consistent with our findings, Yano *et al.* (21) demonstrated that 17-AAG treatment enhanced prostate tumor growth in the bones of mice, which could be abrogated by the administration of inhibitors of osteoclast formation and function. In addition to 17-AAG, we have demonstrated that other structurally unrelated HSP90 inhibitors also enhance osteoclast formation (20, 22). To date, the mechanism by which HSP90 inhibitors stimulate osteoclast formation has not been clearly defined,

although Src kinase and the elevated expression of the essential osteoclast transcription factor microphthalmia-associated transcription factor (MITF) may play roles (21, 22). However, HSP90 inhibition itself seems unlikely to be directly critical in 17-AAG actions on osteoclasts because many of the RANKL signaling pathways required for osteoclast formation (*e.g.* NFκB activation) are at least partly HSP90-dependent.

An alternative possibility is that the ability of 17-AAG to activate the transcription factor heat shock factor 1 (Hsf1) may play a central role in its effects on osteoclasts. Hsf1 is a critical regulator of stress responses in mammalian cells and is essential for the response to a broad range of stress stimuli, including the regulation of heat shock proteins (HSPs) (23–25). Fundamental to this response is the fact that Hsf1 associates with HSP90 under normal conditions, maintaining Hsf1 in an inactive monomeric state (26, 27). However, upon 17-AAG binding to the N-terminal ATPase domain of HSP90 or upon cellular stress, Hsf1 dissociates from the HSP90 complex, forming homotrimeric complexes, undergoes phosphorylation and SUMOylation (28), and binds to heat shock element sites within the promoters of target genes (28, 29). This results in a characteristic pattern of gene expression that is observed during stress (*e.g.* elevated levels of HSP70 and other HSPs), aiding cell survival. Thus, we examined whether the Hsf1-mediated stress response induced by HSP90 inhibition is responsible for enhancing osteoclast formation.

In this study, we report that the effects of 17-AAG upon osteoclast formation are indeed Hsf1-dependent and that, consistent with this, other Hsf1-inducing stressors have similar effects. Moreover, within the context of the stress response, we found that Hsf1 plays a major role in enhancing the levels of the critical osteoclast formation factor MITF. Our results implicate, for the first time, the role of Hsf1 in osteoclast formation and the influence of stress-induced MITF expression, which points to a direct effect of cell stress and MITF in inducing bone loss that may be important in many diseases that affect bone.

EXPERIMENTAL PROCEDURES

Reagents and Antibodies—The HSP90 inhibitors 17-AAG, 17-DMAG, and radicicol were obtained from LC Labs (Woburn, MA), and coumermycin A1 and novobiocin were obtained from Sigma-Aldrich (Castle Hill, NSW, Australia). KNK437 was a gift from Kaneka Corp. (Takasago, Japan), and quercetin, methotrexate, and doxorubicin were purchased from Merck Millipore (Kilsyth, VIC, Australia). Anti-HSP70 (HSPA1A) antibody (catalog no. ADI-SPA-812) was purchased from Enzo Life Sciences (San Diego, CA). Anti-HSP105/110 (HSPH1) antibody (catalog no. SC-6241) was purchased from Santa Cruz Biotechnology (Dallas, TX). The pan anti-actin antibody (catalog no. MS-1295-P) was purchased from Thermo Fisher Scientific (Scoresby, VIC, Australia), and the anti-Hsf1 antibody (catalog no. 4356) was obtained from Cell Signaling Technology (Danvers, MA). IgG HRP-conjugated secondary antibodies for immunoblotting were purchased from Thermo Fisher Scientific. Recombinant murine soluble RANKL (RANKL[158–316]-GST fusion protein) was obtained from Oriental Yeast Co. (Tokyo, Japan), and human M-CSF and TGFβ (TGFβ1 isoform) were from R&D Systems (Minneapolis, MN). L-cell conditioned medium (a source of secreted murine

---

[3] The abbreviations used are: RANKL, receptor activator of nuclear factor κB ligand; MITF, microphthalmia-associated transcription factor; 17-AAG, 17-(allylamino)-17-demethoxygeldanamycin; 17-DMAG, 17-dimethylaminoethylamino-17-demethoxygeldanamycin; HSP, heat shock protein; TRAP, tartrate-resistant acid phosphatase; MEM, minimal essential medium; BMM, bone marrow macrophage(s); MNC, mononuclear cell; ANOVA, analysis of variance.

M-CSF) was prepared as described by Yeung *et al.* (30). For tartrate resistant acid phosphatase (TRAP) histochemical staining, fast red violet LB salt (F-1625), naphthol AS-MX phosphate, and dimethylformamide were purchased from Sigma-Aldrich.

Animals—C57Black/6 mice were obtained from Monash Animal Services (Monash University, Clayton, VIC, Australia). The mice were maintained at the Monash Medical Centre Animal Facility (Clayton, VIC, Australia) according to procedures approved by the Monash Medical Centre Animal Ethics Committee B (Clayton, VIC, Australia), authorization no. MMCB-2011/19. The C;129-*Hsf1*^{tm1Ijb}/J (stock no. 010543) (31) were purchased from The Jackson Laboratories (Bar Harbor, ME) and maintained in the Animal Resource Laboratories of Monash University (Clayton, VIC, Australia) according to standard husbandry and breeding procedures approved by the Monash Animal Research Platform (MARP) 2 Animal Ethics Committee (Clayton, VIC Australia), authorization no. SOBSB/B/2010/28BC. Mice were maintained on a BALB/cx 129SvEV background, and intercrossed *Hsf1*$^{+/-}$ mice were used to generate *Hsf1*$^{+/+}$, *Hsf1*$^{+/-}$, and *Hsf1*$^{-/-}$ mice. Mouse genotypes were determined by PCR according to the standard protocol for the C;129-*Hsf1*^{tm1Ijb}/J strain provided by The Jackson Laboratory. All mice used in the experiments were age-matched females.

Cell Lines and Culture—RAW264.7 cells were purchased from the ATCC and were maintained in minimal essential medium-α (MEM) (Invitrogen) containing 10% FBS (Thermo Fisher Scientific), penicillin (10000 units/ml), and streptomycin (10000 units/ml) (Invitrogen), and HEPES (Invitrogen). All osteoclast formation assays utilized this medium (MEM/FBS). Primary bone marrow cells for culture were immediately isolated from humanely killed, 6- to 12-week-old mice by flushing the bone marrow cavity of the long bones with PBS in accordance with the MARP Animal Ethics Committee (Monash University, Clayton, VIC, Australia) authorization MARP/2011/048. Primary bone marrow macrophage (BMM) cultures were maintained in L-cell conditioned medium to induce BMM proliferation, as described previously (32) in RPMI 1640 medium (Invitrogen) supplemented with penicillin and streptomycin and 10% heat-inactivated FBS (MEM/HIFBS). All cells were maintained in a 37 °C incubator in a humidified atmosphere containing 5% CO_2.

Hsf1 shRNAmir Knockdown and Hsf1 Ectopic Overexpression—For Hsf1 knockdown, GIPZ lentiviral shRNAmir constructs (V2LMM_226824, V2LMM_82329, V2LMM_82328, V3LMM_415511, and V3LMM_415512) targeted toward mouse *Hsf1* and a GIPZ non-silencing control lentiviral shRNAmir construct (RHS4346) were purchased from Thermo Scientific. The non-silencing control and the targeted mouse GIPZ shRNA constructs were transiently cotransfected with psPAX2 and pMD2.G packaging constructs into HEK293T cells using Lipofectamine LTX according to the instructions of the manufacturer (Invitrogen). The medium was replaced 16 h later, and, after a further 24 h, the lentiviral-conditioned medium was collected and filtered using a 0.45-μm filter. RAW264.7 cells were transduced by the addition of the lentiviral-conditioned medium for a period of 24 h with the addition of 10 mg/ml of Polybrene. Cells were then grown in standard medium, and transduced cells were

selected on the basis of GFP expression using FACS (Flowcore Platform, Monash University) with the selection gates being set to normalize GFP fluorescence intensity between the non-silencing and *Hsf1*-silencing shRNAmir-expressing cells. The most efficient knockdowns were achieved by using the V3LMM_415512 and V2LMM_82329 shRNAmirs, which were used for subsequent experiments and are referred to as mir4 and mir5, respectively.

To ectopically overexpress mouse Hsf1 in RAW264.7 cells, a retroviral expression system was employed. The pBABE-Hsf1-IRES-mCherry retroviral construct was generated by excision of mouse Hsf1 from the Hsf1 construct pcDNA3.1(+) mHsf1 (provided by Richard Voellmy, University of Miami, FL) using HindIII endonuclease refilled by T4 DNA polymerase to generate blunt ends, and this was further digested with EcoRI endonuclease. The resulting product was then ligated with pBABE-puro-IRES-mCherry (33) that had been linearized by BamHI digestion, end-filled with T4 DNA polymerase, and then digested with EcoRI endonuclease. The correct orientation of the mHSF1 insert was confirmed by diagnostic endonuclease digestion. HEK293T cells were cotransfected with pCL-Ampho packaging vector (Imgenex, San Diego, CA) and pBABE-Hsf1-IRES-mCherry using Lipofectamine LTX (Invitrogen). Retroviral-conditioned medium generation, RAW264.7 transduction, and selection of mCherry-expressing transduced cells by FACS were performed according to the lentiviral approaches stated previously.

Osteoclast Progenitor Differentiation and Survival Assays—Osteoclasts were generated by culturing RAW264.7 cells for a 6-day period in 96-well plates at a density of 5×10^3 cells/well in MEM/FBS, 20 ng/ml RANKL and in the presence or absence (vehicle control) of HSP90 inhibitors and other stress-inducing agents, as indicated under "Results." The medium and the agents were replaced at day 3, and on day 6, cells were fixed with 4% formaldehyde and histochemically stained for TRAP as described previously (34). TRAP-positive multinucleated cells (MNCs) containing three or more nuclei per cell, quantified using an inverted light microscope, were counted as osteoclasts. To generate osteoclasts from primary murine cells, bone marrow cells were flushed from bisected long bones of C57black6/J, wild-type (*Hsf1*$^{+/+}$), heterozygous (*Hsf1*$^{+/-}$), or knockout (*Hsf1*$^{-/-}$) C;129-*Hsf1*^{tm1Ijb}/J mice with PBS. Cells were centrifuged and then resuspended in MEM/FBS. Bone marrow cells (10^5 cells/well) were stimulated by 20 ng/ml RANKL and 25 ng/ml M-CSF in the presence or absence of the HSP90 inhibitor 17-AAG for 6 days. Cells were then fixed and stained histochemically for TRAP and osteoclast numbers counted. For BMM preparation for Western blotting, bone marrow cells (10^6 cells/ml) were suspended in RPMI/HIFBS supplemented with 30% L-cell-conditioned medium (30, 32), incubated at 37 °C in a humidified atmosphere containing 5% CO_2 for 3 days, and then, the non-adherent cell fraction was removed. The resulting adherent proliferating cells were then prepared for analysis. These cells were able to form numerous osteoclasts with RANKL/M-CSF treatment, as described previously (32). For cell survival assays RAW264.7 cells were seeded at 5×10^3 cells/well and treated with a range of HSP90 inhibitor concentrations. After a period of 96 h, cells were fixed in 50%

TCA at 4 °C for 1 h, followed by five washes in distilled water. Cells were stained with sulforhodamine B (Sigma-Aldrich), rinsed, and then cell-bound sulforhodamine B was solubilized in 150 μl of 10 mM Tris-HCl (pH 10.5). The absorbance at 550 nm was measured by spectrophotometry using a Multiskan FC absorbance plate reader (Thermo-Lab Systems, MA).

Immunoblot Analysis—Immunoblot analysis was performed as described previously (20, 22, 35). Briefly, cell lysates were generated using modified radioimmune precipitation assay buffer (50 mmol/liter Tris-HCl (pH 7.4), 1% Nonidet P-40, 0.25% sodium deoxycholate, 150 mmol/liter NaCl) containing phosphatase and protease inhibitor mixture (Sigma-Aldrich), sonicated, and then clarified by centrifugation. Protein concentrations were determined using the BCA protein assay according to the instructions of the manufacturer (Thermo Fisher Scientific). Cell lysates were run on 4–12% BisTris gradient SDS-PAGE electrophoresis gels with MES SDS running buffer (Invitrogen) under reducing conditions and transferred to Immobilon-P PVDF membranes (Merck Millipore). Membranes were blocked for 1 h with 3% milk powder (Diploma, Fonterra Food Services, Mount Waverley, Australia) dissolved in PBST (PBS + 0.1% Tween 20). Membranes were then incubated overnight at 4 °C with appropriate primary antibodies. Immunoblot visualization was achieved by incubation with appropriate IgG HRP-conjugated secondary antibodies and an ECL detection system (Supersignal West Pico, Thermo Fisher Scientific) according to the instructions of the manufacturer.

Statistical Analysis—Data were analyzed using Prism 5 software (GraphPad, San Diego, CA), and statistical significance was determined using ANOVA/Dunnett's post hoc test. Quantitative data are presented as mean $\pm$ S.E. of three or more pooled experiments, and significance is represented graphically by *, $p < 0.05$; **, $p < 0.01$; or ***, $p < 0.001$.

RESULTS

HSP90 Inhibitors Enhance Osteoclast Formation in Association with Induction of the Heat Shock Response—To investigate the role of the HSR and, more specifically, Hsf1, in 17-AAG actions on osteoclastogenesis, we first examined the effects of different HSP90 inhibitors on the maturation of murine RAW264.7 cells, a bipotential osteoclast/macrophage progenitor cell line that responds strongly to RANKL treatment by forming osteoclasts. RAW264.7 cells were treated with a submaximal concentration of RANKL (20 ng/ml) that is sufficient to cause low levels of osteoclast formation over 6 days of incubation. Osteoclast formation was completely dependent on RANKL treatment; *i.e.* in cultures where RANKL was omitted, osteoclast formation or mononuclear TRAP$^+$ cells were never seen, as described previously 22. Unlike primary bone marrow cells or BMM, RAW264.7 cells form osteoclasts without M-CSF treatment; *i.e.* they require only RANKL stimulation.

Treatment of RAW264.7 cells with 17-AAG induced a dose-dependent increase in Hsp70 (Hspa1a) protein expression, consistent with induction of the HSR (Fig. 1*A*), and, consistent with previous findings (20, 21), 17-AAG also increased RANKL-stimulated osteoclast formation in a dose-dependent manner (Fig. 1, *B* and *C*). To confirm that this response was not unique to RAW264.7 cells, examination of the effects of 17-AAG in

RANKL- and M-CSF-stimulated primary bone marrow cells derived from C57Black/6 mice was performed. As with that of the RAW264.7 cell line, 17-AAG significantly increased Hsp70 expression (Fig. 1*D*), and this was associated with a marked increase in osteoclast formation (Fig. 1, *E* and *F*). It was noted that the primary bone marrow cultures were more sensitive to 17-AAG with respect to the induction of the HSR and that this correlated with increased osteoclast formation.

In RAW264.7 cells, 17-DMAG, a HSP90 inhibitor that is structurally related to 17-AAG but more potently inhibits HSP90, also enhanced both Hsp70 protein levels (Fig. 2*A*) and RANKL-induced osteoclast formation (Fig. 2*B*) in a dose-dependent manner, although at notably lower concentrations to that of 17-AAG (Fig. 1, *A* and *B*).

To determine the scope of the effect, we examined whether the structurally unrelated HSP90 inhibitor radicicol had similar effects to that of 17-AAG and 17-DMAG. Despite the differing structure of radicicol, it was also found to significantly increase Hsp70 levels (Fig. 2*C*) and significantly increase osteoclast formation (Fig. 1*D*). However, in contrast to these findings, the HSP90 inhibitors coumermycin A1 (Fig. 2*E*) and novobiocin (Fig. 2*G*) did not significantly increase Hsp70 levels, thus failing to induce a robust HSR. Moreover, coumermycin A1 (Fig. 2*F*) and novobiocin (Fig. 2*H*) did not significantly increase osteoclast formation. These two HSP90 inhibitors bind the C-terminal region of HSP90 and, thus, have a different mode of action to that of 17-AAG, 17-DMAG, and radicicol. These results are consistent with the notion that activation of Hsf1 and its ability to induce the HSR induced by N-terminal HSP90 inhibitors enhances RANKL-elicited osteoclast formation.

Pharmacological Inhibition of Hsf1 Reduces 17-AAG Enhancement of RANKL-induced Osteoclast Differentiation—To further investigate whether the HSR was mechanistically important for 17-AAG-enhanced osteoclast formation, we examined whether pharmacological inhibition of the HSR would abrogate the 17-AAG-mediated effect. Quercetin and KNK437 are two compounds that have been shown to inhibit the HSR via impacting Hsf1 functionality (36, 37). Consistent with this, treatment of RAW264.7 cells with KNK437 (Fig. 3*A*) dose-dependently inhibited the induction of Hsp70 protein expression by 17-AAG and significantly abrogated the effects of 17-AAG on RANKL-stimulated osteoclast formation (Fig. 3*B*), indicating a potential influence of Hsf1 on osteoclast formation. Quercetin was also found to inhibit Hsp70 induction by 17-AAG (Fig. 3*C*) and also significantly reduced the effects of 17-AAG upon osteoclast formation (Fig. 3*D*). Of the two compounds, KNK437 was more potent at inhibiting Hsp70 induction and, consistent with this, was more effective at blocking 17-AAG effects upon osteoclast formation (Fig. 3*B*). Interestingly, the enhancement of osteoclast differentiation by TGFβ, a cytokine known to stimulate NFATc1 expression (unlike 17-AAG (22)) and augment RANKL signals (38, 39), was not affected by KNK437-mediated inhibition of Hsf1 (Fig. 3*E*). Thus, this demonstrated a specificity of action of KNK437 upon stress-mediated osteoclast formation and, more importantly, that of Hsf1 in 17-AAG-enhanced osteoclast differentiation.
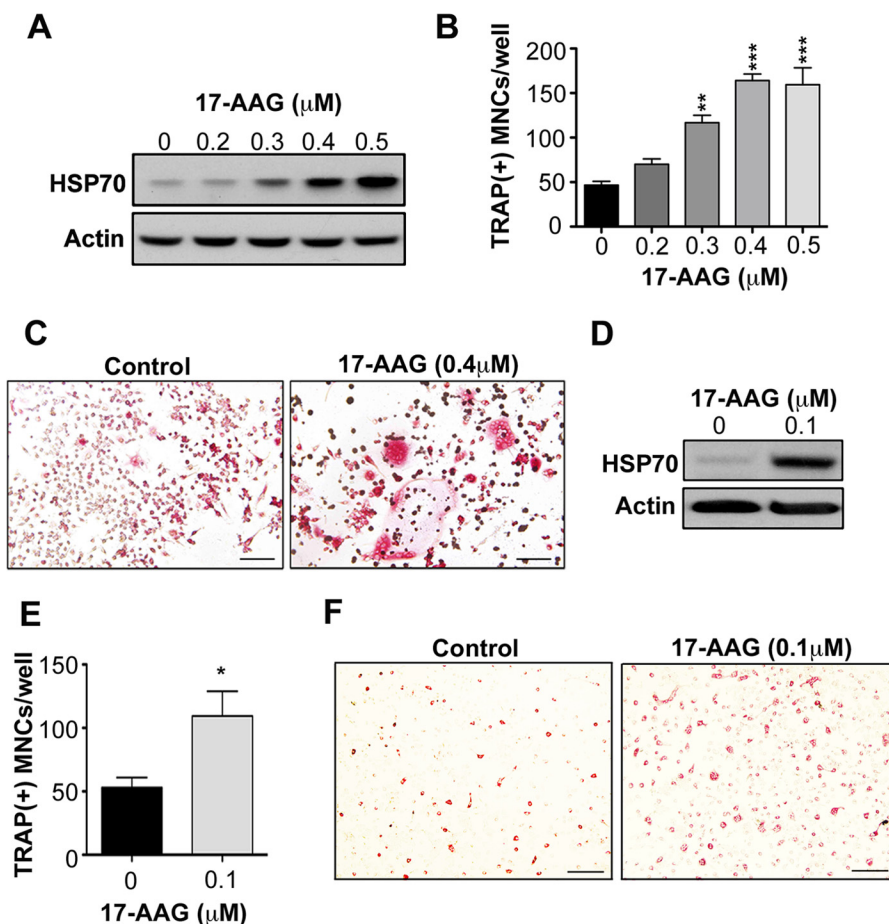
FIGURE 1. **17-AAG enhances RANKL-dependent osteoclastogenesis and induces an HSR.** *A*, murine osteoclast progenitor RAW264.7 cells showed an increase in Hsp70 levels (immunoblot analysis) after treatment with indicated concentrations of 17-AAG for 24 h. *B*, RAW264.7 cells were cultured in 20 ng/ml RANKL and the indicated concentrations of 17-AAG for 6 days, and osteoclasts (TRAP-positive MNCs) were counted. 17-AAG treatment dose-dependently enhanced RANKL-dependent osteoclast formation. *C*, photomicrographs of osteoclasts formed in RANKL-treated RAW264.7 cell cultures showing increased osteoclast formation in 17-AAG-treated (0.4 μM) cells compared with vehicle control (*Veh. Ctl.*). *Red*, TRAP staining. *Scale bars* = 100 μm. *D*, immunoblot analysis of BMMs demonstrated elevated Hsp70 protein levels after treatment with 17-AAG (0.1 μM) after a 24-h treatment period. *E*, as with RAW264.7 cells, mouse bone marrow cells cultured in 20 ng/ml RANKL and M-CSF for 6 days demonstrated a significant increase in TRAP-positive MNCs with 0.1 μM 17-AAG treatment. *F*, photomicrographs of osteoclasts formed in mouse bone marrow cells cultured in 20 ng/ml RANKL and M-CSF for 6 days. Cultures with 17-AAG (0.1 μM) showed an increase in TRAP-positive MNCs when compared with vehicle control. *Red*, TRAP staining. *Scale bars* = 100 μm. *Error bars* represent the mean $\pm$ S.E. of three independent experiments. *, $p < 0.05$; **, $p < 0.01$; ***, $p < 0.001$ relative to RANKL (20 ng/ml)-treated vehicle control using ANOVA/Dunnett's post hoc test.

Hsf1 Knockdown Impairs the Effect of 17-AAG on Osteoclastogenesis—To demonstrate a specific involvement of Hsf1 upon 17-AAG actions in osteoclast formation, we reduced Hsf1 expression by RNA interference methods. We utilized an shRNAmir approach on the basis of the design of the primary microRNA-30 transcript allowing for processing via the endogenous RNAi pathways and allowing for more specific silencing than conventional shRNAi. RAW264.7 cells were transduced using lentiviral constructs that expressed either a non-silencing shRNAmir that had no homology to any known mammalian genes or shRNAmirs with specificity for mouse *Hsf1*. Immunoblot analysis of Hsf1 levels confirmed the efficient knockdown of Hsf1 in RAW264.7 cells using two independent shRNAmirs (Fig. 4*A*). Consistent with the knockdown of Hsf1, the 17-AAG-mediated induction of Hsp70 was abrogated significantly (Fig. 4*A*). In non-silencing shRNAmir control RAW264.7 cells, 17-AAG strongly enhanced osteoclast formation, whereas knockdown of Hsf1 by mir4 or mir5 significantly reduced the effects of 17-AAG upon osteoclast formation (Fig. 4*B*), consis-

tent with the effects of the pharmacological inhibition of Hsf1. Of interest, 17-AAG did not increase the steady-state levels of Hsf1, but, consistent with it being a HSP90 client protein, Hsf1 levels were reduced. To ensure that abrogation of 17-AAG-mediated effects upon osteoclast formation because of Hsf1 knockdown was not merely a result of an increased cell death, we tested the sensitivity of the RAW264.7 cells to 17-AAG-mediated cell death. In standard cell survival assays examining increasing 17-AAG concentrations, no differences were observed between the non-silencing control and Hsf1 knockdown cells (Fig. 4*C*), indicating that any effects on osteoclast formation were not due to alterations in cell survival.

Overexpression of Hsf1 Enhances 17-AAG Effects on RANKL-induced Osteoclast Differentiation—To further investigate the influence of Hsf1 in 17-AAG-enhanced osteoclast differentiation, we examined the effect of overexpressing mouse wild-type Hsf1 in the RAW264.7 cell line. To achieve this, we transduced RAW264.7 cells with retroviral vectors expressing mCherry (control) or wild-type Hsf1 (Hsf1WT). Immunoblot analysis
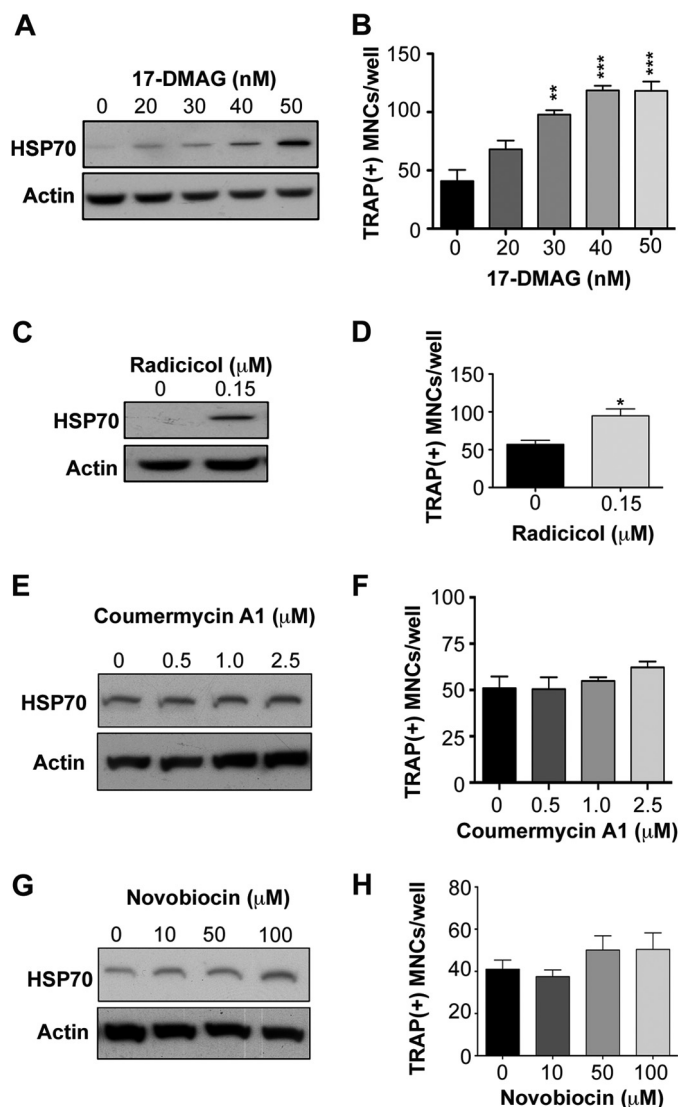
FIGURE 2. **Induction of an HSR by HSP90 inhibitors associates with increased osteoclast formation.** *A*, Hsp70 protein levels in RAW264.7 were dose-dependently increased by 17-DMAG treatment after a 24-h period. *B*, 17-DMAG significantly increased osteoclast formation in RANKL-treated RAW264.7 cells. *C*, the structurally unrelated HSP90 inhibitor radicicol increased Hsp70 levels in RAW264.7 cells after a 24-h treatment period. *D*, radicicol significantly increased osteoclast formation in RAW264.7 cells when compared with vehicle control. The coumermycin A1 (*E* and *F*) and novobiocin (*G* and *H*) HSP90 inhibitors did not induce a heat shock response, indicated by a failure to increase Hsp70 levels in RAW264.7 cells and also failed to increase osteoclast formation. *Error bars* represent the mean ± S.E. of three independent experiments. *, $p < 0.05$; **, $p < 0.01$; ***, $p < 0.001$ relative to RANKL (20 ng/ml)-treated vehicle control using ANOVA/Dunnett's post hoc test.

demonstrated that, although there was a strong overexpression of Hsf1 in the pBABE-Hsf1WT-transduced RAW264.7 cells, Hsf1 was maintained in an inactive state, as demonstrated by the comparative steady-state levels of Hsp70 and Hsp105 between control cells and Hsf1-overexpressing cells (Fig. 5A). However, upon treatment with increasing concentrations of 17-AAG, Hsf1-overexpressing cells demonstrated an augmented response, denoted by increased Hsp70 and Hsp105 expression (Fig. 5A) in comparison with the vector control (pBABE-mCherry)-transduced cells. Consistent with this finding, RAW264.7 cells overexpressing Hsf1 were more sensitive

to the effects of 17-AAG in enhancing osteoclast differentiation (Fig. 5B). Notably, however, Hsf1 overexpression did not alter the osteoclastogenic potential of RAW264.7 cells in the absence of 17-AAG. Therefore, elevated Hsf1 levels appeared to sensitize cells to the actions of 17-AAG rather than directly enhance osteoclast differentiation.

17-AAG-enhanced Osteoclast Formation Is Impaired in Primary Bone Marrow Cells Derived from $Hsf1^{-/-}$ Mice—To extend our findings, we examined the role of Hsf1 in 17-AAG-enhanced osteoclast formation in primary cells using bone marrow cells derived from mice that were wild-type ($Hsf1^{+/+}$), heterozygous ($Hsf1^{+/-}$), and null ($Hsf1^{-/-}$) for Hsf1. Immunoblot analysis showed that the expression level of Hsf1 in BMM derived from $Hsf^{-/-}$ mice was undetectable, whereas its level of expression in $Hsf1^{+/-}$ BMM was observed to be significantly lower than those isolated from wild-type ($Hsf1^{+/+}$) mice (Fig. 6A). Consistent with the steady-state levels of Hsf1 in isolated BMM, the induction of Hsp70 by 17-AAG was absent in the $Hsf1^{-/-}$ BMM and reduced significantly in the $Hsf1^{+/-}$ BMM when compared with $Hsf1^{+/+}$ BMM (Fig. 6A). We then examined osteoclast formation in $Hsf1^{+/+}$, $Hsf1^{+/-}$, and $Hsf1^{-/-}$ bone marrow cells (stimulated with 20 ng/ml RANKL and M-CSF) in the presence of 17-AAG. We found that, in $Hsf^{-/-}$ cell cultures, 17-AAG failed to significantly elevate osteoclast numbers relative to vehicle control cultures, whereas in $Hsf1^{+/+}$ bone marrow cultures, 17-AAG significantly enhanced osteoclast differentiation (Fig. 6, *B* and *C*). Bone marrow cell cultures from $Hsf1^{+/-}$ mice also showed a marked impairment of 17-AAG-enhanced osteoclast formation, consistent with the decreased steady-state and activated levels of Hsf1 in these cells (Figs. 6, *B* and *C*).

17-AAG Treatment Enhances MITF Levels in an Hsf1-dependent Manner—MITF has been shown to be a critical regulator of osteoclast formation and function (40–42), although the regulation of MITF protein expression in osteoclasts is not well characterized. We have shown previously that, although 17-AAG has no enhancing effect upon major RANKL-elicited intracellular signaling components (*e.g.* NFκB, c-fos, and NFATc1), we determined that 17-AAG did potently enhance the cellular protein levels of MITF (22). Therefore, we investigated whether 17-AAG enhanced MITF protein levels in a manner that was mediated via Hsf1. We found that increased MITF protein levels caused by 17-AAG treatment of RAW264.7 cells was reduced significantly by pharmacological inhibition of Hsf1 by KNK437 treatment (Fig. 7A). Similarly, knockdown of Hsf1 by shRNAmir also inhibited the effect of 17-AAG upon MITF protein induction (Fig. 7B). Examination of primary BMM cultures isolated from $Hsf1^{-/-}$ mice demonstrated that MITF protein was low or undetectable by immunoblot analysis, either with or without 17-AAG treatment (Fig. 7C). Conversely, overexpression of Hsf1 in RAW264.7 cells resulted in the elevation of MITF levels when compared with control cells and was increased further with 17-AAG treatment (Fig. 7D). These results indicate that 17-AAG increased RANKL-induced osteoclast differentiation with increased MITF protein levels, which was mediated by the action of Hsf1.
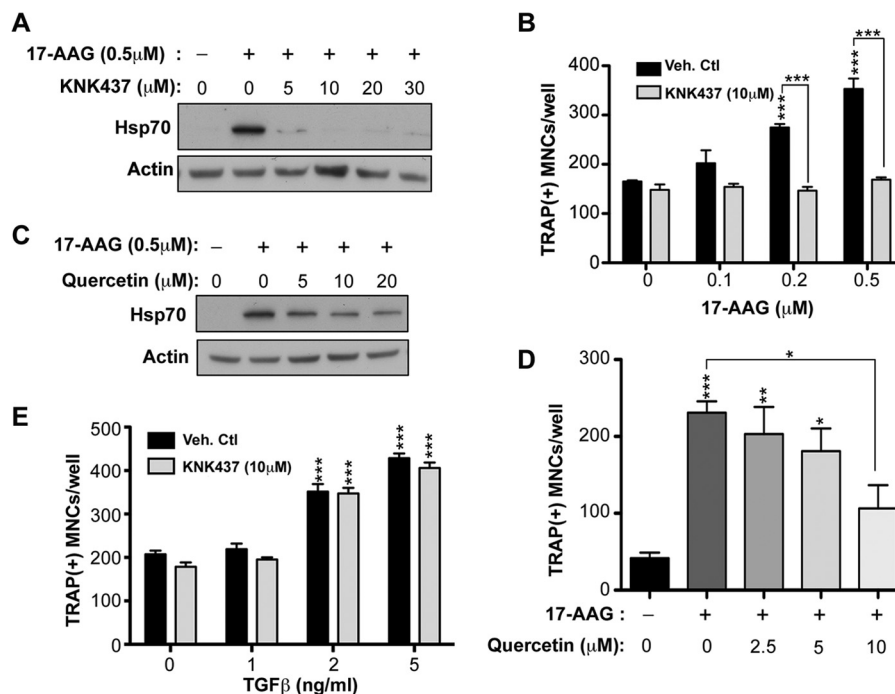
FIGURE 3. **Inhibitors of Hsf1 decrease the effects of 17-AAG, but not TGFβ, on osteoclastogenesis in RANKL-treated RAW264.7 cells.** *A*, immunoblot analysis demonstrated that 24-h cotreatment of RAW264.7 cells with KNK437 ablated 17-AAG-induced Hsp70 protein induction. *B*, KNK437 inhibited 17-AAG-enhanced osteoclast formation in RAW264.7 cells cultured for 6 days in the presence of 20 ng/ml RANKL. *Veh. Ctl.*, vehicle control. Quercetin reduced the effects of 17-AAG treatment on Hsp70 protein expression after 24 h of treatment (*C*) and inhibited the effects of 17-AAG upon enhanced osteoclast numbers in RANKL (20 ng/ml) treated RAW264.7 cells (*D*). *E*, RAW264.7 cells cultured with RANKL showed an increase in osteoclast numbers with TGFβ treatment. However, no effects of KNK437 treatment were observed. *Error bars* represent the mean ± S.E. of four independent experiments. *, $p < 0.05$; **, $p < 0.01$; ***, $p < 0.001$ relative to RANKL-treated (20 ng/ml) vehicle control using ANOVA/Dunnett's post hoc test.

Ethanol and Chemotherapeutic Agents Enhance Osteoclast Differentiation Potentially Mediated by Hsf1—Hsf1 is activated to counteract cellular damage and death caused by proteotoxicity of a wide variety of chemical agents. In addition to HSP90 inhibitors, many cytotoxic chemotherapeutic agents also potently activate Hsf1 and the HSR (43–46). Interestingly, some cytotoxic chemotherapeutic agents are also known to promote osteoclast formation (13). We hypothesized that at least some stress-inducing agents, including some currently used cytotoxic chemotherapeutics, may directly enhance osteoclastogenesis via activation of Hsf1 and the HSR (in a manner similar to that of 17-AAG) if the agent was not too directly toxic to RAW264.7 cells. We examined both ethanol, an oxidative stressor that has been shown previously to enhance osteoclastogenesis and induce the HSR (47, 48), and two cytotoxic chemotherapeutic agents, doxorubicin and methotrexate. Immunoblot analysis demonstrated that ethanol (Fig. 8*A*), doxorubicin (Fig. 8*B*), and methotrexate (Fig. 8*C*) all increased Hsp70 protein expression in a dose-dependent manner, consistent with their activation of Hsf1 and the HSR. Consistent with our previous findings regarding HSP90 inhibitors and the HSR, we observed that these three stressors, ethanol, doxorubicin, and methotrexate, all enhanced RANKL-dependent osteoclast formation in a dose-dependent manner in RAW264.7 cells (Figs. 7, *D–F*). As with 17-AAG, pharmacological inhibition of the HSR and Hsf1 by KNK437 in RAW264.7 cultures treated with ethanol (Fig. 7*G*), doxorubicin (Fig. 7*H*), or methotrexate (Fig. 7*I*) inhibited the pro-osteoclastic effects of the agents, although KN437 did not completely ablate the

effects of methotrexate. In sum, these results demonstrate that, in addition to 17-AAG, other compounds that can induce Hsf1 activation and the HSR are also able to enhance RANKL-induced osteoclastogenesis, potentially through a mechanism that is at least partly Hsf1-dependent.

DISCUSSION

The ability of 17-AAG to cause bone loss and to increase breast and prostate tumor growth and invasion in bone in murine models indicates that this compound has potentially serious negative effects on bone mass (20, 21). Although 17-AAG itself is not likely to be used clinically, functionally similar, second-generation HSP90 inhibitors are currently undergoing clinical trials and may enter the clinic in the future. Thus, it is imperative to elucidate their effects on bone. 17-AAG and other HSP90 inhibitors have profound stimulatory effects on osteoclast formation (20–22, 49), although contributing influences of other cells to the observed bone loss cannot be ruled out (50). In addition, increases in osteoclast numbers and consequent increased bone resorption potentially increase the risk of metastatic tumor growth in bone because of the release of tumor growth factors from the bone matrix (51).

In this study, we demonstrated that 17-AAG and other stressors act in an Hsf1-dependent manner to increase osteoclast formation from their progenitors and that this may involve an increase in the levels of the transcription factor MITF. We investigated Hsf1 involvement in 17-AAG using a number of approaches, including the use of pharmacological inhibition of Hsf1 and HSR by KNK437. This compound is a potent inhibitor
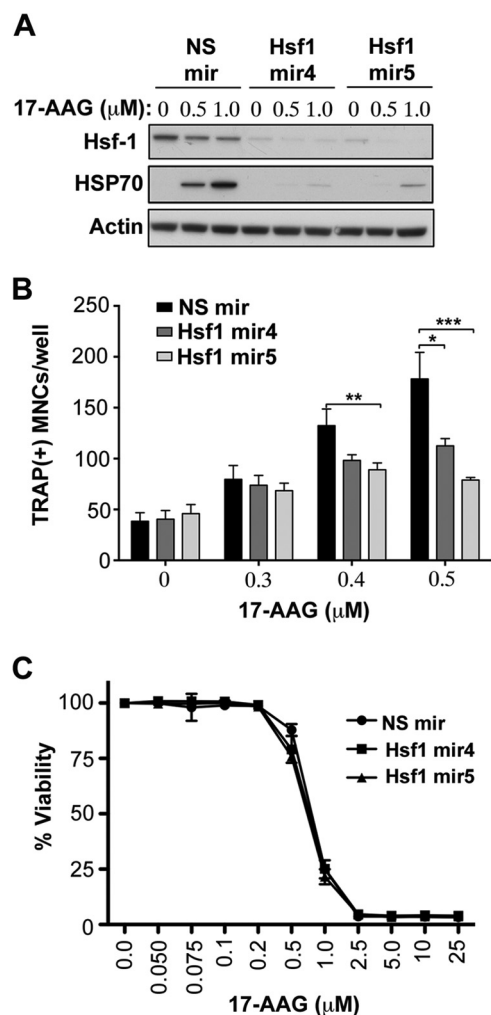
FIGURE 4. **Hsf1 knockdown greatly reduces the effect of 17-AAG upon RANKL-induced osteoclastogenesis.** *A*, lentivirus-transduced RAW264.7 cells with non-silencing (*NS mir*) or *Hsf1*-targeting shRNAmir (*mir4* and *mir5*) constructs were treated with the indicated concentrations of 17-AAG for 24 h. Immunoblot analysis demonstrated decreased Hsf1 protein levels, confirming knockdown. 17-AAG induction of Hsp70 protein was also impaired in the Hsf1 knockdown RAW264.7 cells. *B*, Hsf1 knockdown resulted in a significant reduction of the effects of 17-AAG on osteoclast formation in RAW264.7 cells cultured in 20 ng/ml RANKL. *C*, a dose-response survival assay over 96 h in RAW264.7 cells with indicated concentrations of 17-AAG demonstrated that Hsf1 knockdown had no significant effect upon RAW264.7 cell survival. *Error bars* represent the mean $\pm$ S.E. of three independent experiments. *, $p < 0.05$; **, $p < 0.01$; ***, $p < 0.001$ relative to RANKL-treated (20 ng/ml) vehicle control using ANOVA/Dunnett's post hoc test.

FIGURE 5. **Overexpression of Hsf1 enhances 17-AAG effects on RANKL-induced osteoclastogenesis.** *A*, RAW264.7 cells that had been retrovirus-transduced with pBABE-mCherry control or pBABE-Hsf1WT-mCherry constructs were treated with the indicated concentrations of 17-AAG for 24 h. Immunoblot analysis demonstrated that ectopic expression of Hsf1 increased the levels of Hsp70 and Hsp105 induced by 17-AAG in RAW264.7 cells. *B*, Hsf1 overexpression resulted in a significant increase in TRAP-positive osteoclasts in RAW264.7 cells (cultured in 20 ng/ml RANKL) at increasing concentrations of 17-AAG for 6 days relative to vehicle control. Data are presented as the proportion relative to control (*Rel. %*) $\pm$ S.E. from three independent experiments. *, $p < 0.05$ relative to RANKL-treated (20 ng/ml) vehicle control using ANOVA/Dunnett's post hoc test.

of Hsf1-induced expression of HSPs, such as HSP70, but does not affect the basal levels of their constitutively expressed isoforms (36). It was notable that KNK437 administration at 10 μM completely ablated 17-AAG actions on osteoclast formation but did not decrease it below the control baseline levels induced by 20 ng/ml RANKL alone. This concentration of KNK437 also blocked Hsp70 induction. Quercetin, a widely distributed, naturally occurring flavonoid, also reduces HSP induction and has acceptable toxicity in clinical trials (52, 53). However, it should be noted that quercetin also inhibits c-fos and NFκB actions that play a role in osteoclastogenesis, so its effects cannot be assumed to be via Hsf1 alone (54, 55). Quercetin is not used in any currently approved therapies but has been investigated for anticancer and anti-inflammatory actions, so its clinical use to
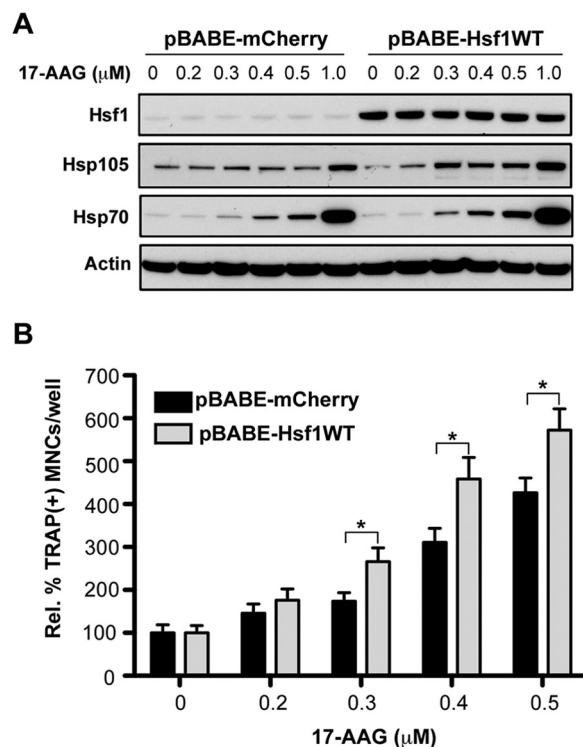
ameliorate pathological bone loss is possible but has not yet been investigated properly.

To more specifically address the role of Hsf1 in 17-AAG osteoclast effects, we targeted *Hsf1* expression by shRNAmirs in RAW264.7 cells. Knockdown of Hsf1 had a similar effect to that of KNK437 in decreasing the effect of 17-AAG on RANKL-induced osteoclast formation as well as inhibiting the induction of HSP70 by 17-AAG. Bone marrow cells from *Hsf1*$^{-/-}$ mice were similarly defective in 17-AAG induction of osteoclast formation. However, the ability of the progenitors to form osteoclasts was not impaired because osteoclast formation in response to RANKL in *Hsf1*$^{-/-}$, *Hsf1*$^{+/-}$, and *Hsf1*$^{+/+}$ were all comparable. Unfortunately, because of fertility problems in these mice (56), we have not been able to undertake a systematic study of the bones or the influence of stressors on their bone parameters. However, with a role for Hsf1 being established, we also sought to identify the sufficiency of Hsf1 induction in mediating 17-AAG actions on osteoclasts. Ectopic overexpression of Hsf1 (28) did not increase osteoclast formation itself but did significantly increase the osteoclastic responsiveness of RAW264.7 cells to 17-AAG. The overexpressed Hsf1 probably remained in an inactive state because we observed no alteration in the steady-state levels of HSP70, indicating that
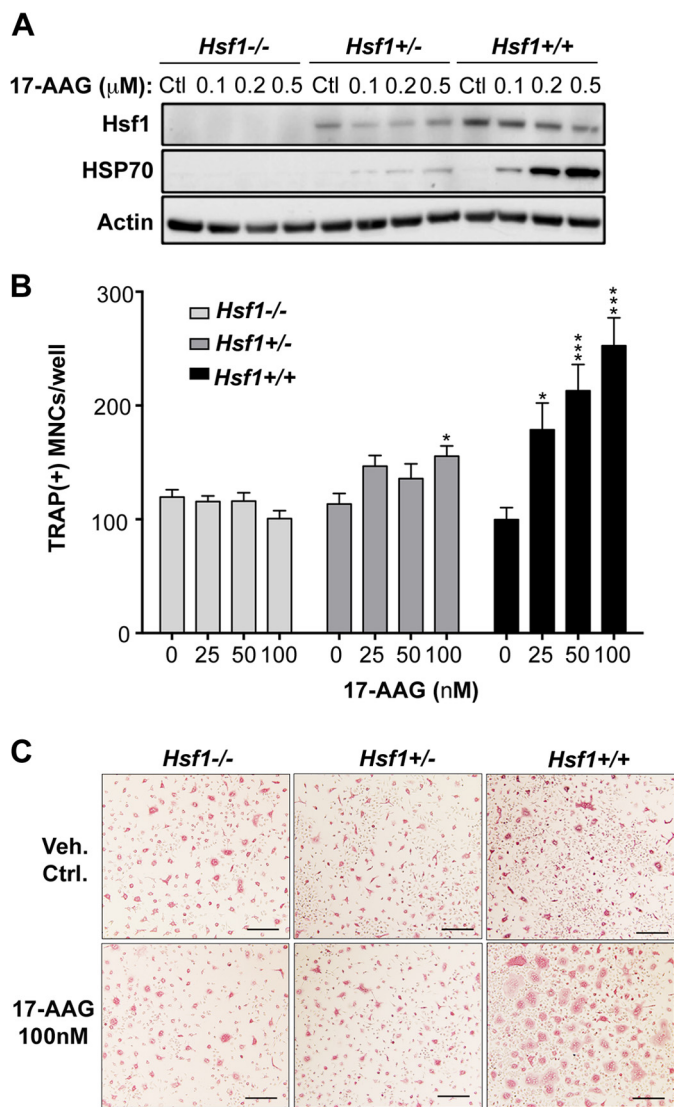
FIGURE 6. **The pro-osteoclastic effects of 17-AAG are impaired in bone marrow cells derived from Hsf1 null mice.** *A*, BMM derived from $Hsf1^{-/-}$, $Hsf1^{+/-}$, and $Hsf1^{+/+}$ mice were treated with the indicated concentrations of 17-AAG for 24 h. Immunoblot analysis showed a complete and partial reduction of Hsf1 protein in $Hsf1^{-/-}$ and $Hsf1^{+/-}$ cells, respectively. Consistent with this, no induction of Hsp70 was observed in $Hsf1^{-/-}$ cells, whereas in $Hsf1^{+/-}$ cells, there was a substantial reduction. *Ctl*, control. *B*, primary bone marrow cells derived from $Hsf1^{-/-}$, $Hsf1^{+/-}$, and $Hsf1^{+/+}$ mice were cultured in 20 ng/ml RANKL, M-CSF, and the indicated concentrations of 17-AAG for 6 days, fixed, and stained histochemically, and then TRAP-positive MNCs were counted. $Hsf1^{-/-}$ cells showed a lack of response to 17-AAG, whereas $Hsf1^{+/-}$ cells demonstrated a marked diminished response to 17-AAG treatment in terms of increased osteoclast formation. *C*, photomicrographs of TRAP-positive (*red*) osteoclast formation in $Hsf1^{-/-}$, $Hsf1^{+/-}$, and $Hsf1^{+/+}$ bone marrow cultures. *Veh. Ctl.*, vehicle control. *Scale bars* $= 200$ μm. *Error bars* represent the mean $\pm$ S.E. of three independent experiments. *, $p < 0.05$; **, $p < 0.01$; ***, $p < 0.001$ relative to RANKL-treated (20 ng/ml) $Hsf1^{+/+}$ control using ANOVA/Dunnett's post hoc test.

Hsf1 expression in itself is insufficient to increase RANKL-induced osteoclast formation but requires activation.

In addition to 17-AAG, we have found other benzoquinone ansamycins, such as herbimycin (20) and 17-DMAG, to also significantly increase RANKL-induced osteoclast formation. However, this action was not limited to this class of compounds because other structurally distinct HSP90 inhibitors, such as radicicol, NVP-AUY922, and CCT018159, also increased oste-

oclast formation (20, 22). Because these compounds all interact with the N-terminal ATPase site of HSP90, causing inhibition, it could be argued that ATPase site binding may be required for their common actions, and although they greatly stimulate the HSR, it may actually be the inhibition of HSP90 that is mechanistically important for enhanced osteoclast formation (28, 57). However, the HSP90 inhibitor novobiocin and its derivative coumermycin A1, known to inhibit HSP90 by binding the C-terminal of HSP90 and inhibiting its autophosphorylation (thus altering both its chaperone activity and client protein interactions), did not enhance RANKL-induced osteoclast formation (58–60). Moreover, we have found no clear correlation between the potency of the HSP90 inhibitors and their ability to induce osteoclast formation. It should also be noted that these compounds had a minimal effect on the induction of HSR, consistent with previous observations that novobiocin causes a dose-dependent decrease in Hsf1 DNA-binding and transcriptional activities (61). Combined, these results suggest that HSP90 inhibition *per se* may not enhance osteoclast formation and is consistent with a role for the involvement of Hsf1 downstream target involvement.

Although Hsf1 itself has not been suggested previously to play a role in osteoclast formation, several types of Hsf1-dependent cellular stressors have been implicated in pathological bone loss. These include chemotherapeutic agents, such as doxorubicin and methotrexate, that have been shown to cause a decrease in trabecular bone volume in a rat model (13, 62). Similarly, ethanol has been associated with the induction of cellular stress and enhances bone loss *in vivo* through the increase of osteoclast numbers (5). These observations provide circumstantial evidence that Hsf1-dependent cell stress induced by stimuli other than HSP90 inhibitors might indeed enhance osteoclastogenesis, although there is no reason to expect their actions to depend on a single mechanism. However, we confirmed here that ethanol, doxorubicin, and methotrexate cause both enhanced osteoclast formation and a cellular stress response that could be ablated by Hsf1 inhibition by KNK437. Thus, our results demonstrate, for the first time, that compounds capable of activating Hsf1-dependent stress pathways can enhance osteoclastogenesis in a manner similar to that of HSP90 inhibitors. It is important to note, however, that compounds that are simply very toxic to cells or that inhibit signaling essential to RANKL responses may not necessarily drive increased osteoclast formation.

Our findings that MITF levels may be involved in the actions of 17-AAG are particularly interesting. MITF is a transcription factor that is critical for osteoclast formation, as evidenced by the *mi/mi* strain of mice that lack MITF and are devoid of osteoclasts (63). In osteoclast progenitors, MITF levels are also enhanced by RANKL, which triggers a signaling cascade by its interaction with RANK, involving rapid induction of NFκB, p38, AP-1 and NFATc1 activity, and leading to increased MITF levels, typically after 24–48 h. The mechanism linking the elevation of MITF levels to the induction by RANKL treatment is currently controversial, but MITF is essential for many (but not all) gene expression that is required by mature osteoclasts, including TRAP (*acp5*), cathepsin K (*ctsk*), and H$^+$ ion pump components (40, 64). This requires cooperation
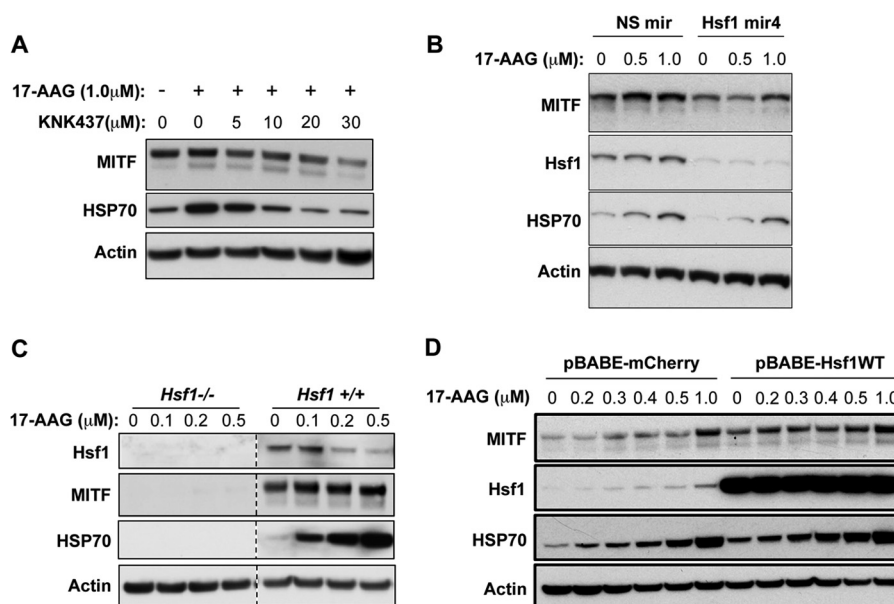
FIGURE 7. **The induction of MITF by 17-AAG osteoclast progenitor cells is dependent upon Hsf1.** *A–D*, protein expression was assessed by immunoblotting of the indicated cell lysates. *A*, Hsf1 inhibition by KNK437 ablated 17-AAG-induced MITF and Hsp70 protein levels after 24 h in RAW264.7 cells. *B*, RAW264.7 cells stably transduced with a lentiviral construct expressing Hsf1 shRNAmir showed a decrease in 17-AAG-induced MITF protein expression after 24 h. *NS*; nonsilencing. *C*, BMM derived from $Hsf1^{-/-}$ and $Hsf1^{+/+}$ mice were treated with M-CSF and the indicated concentrations of 17-AAG for 24 h. $Hsf1^{-/-}$ BMM showed lower MITF protein expression both with and without 17-AAG. *D*, RAW264.7 stably transduced with a retroviral construct expressing Hsf1WT showed an increase in MITF protein expression after 24 h of 17-AAG treatment.
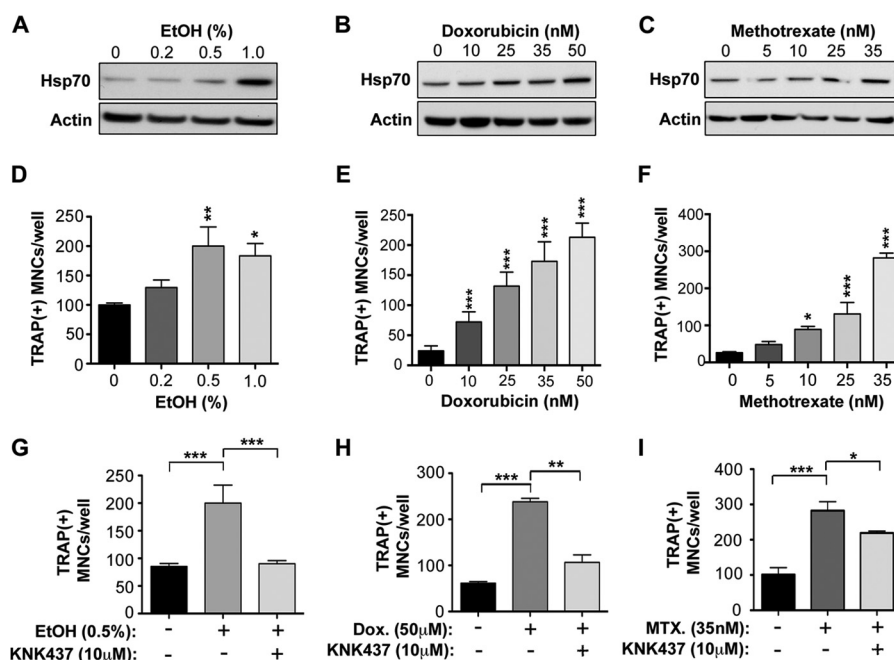

FIGURE 8. **Chemotherapeutic agents and ethanol induce a heat shock response and enhance RANKL-dependent osteoclastogenesis.** Hsp70 protein levels were induced in RAW264.7 cells by EtOH (*A*), doxorubicin (*B*), and methotrexate (*C*) over 24 h, as demonstrated by immunoblot analyses. *D*, RAW264.7 cells treated with RANKL showed a significant increase in osteoclast numbers after 6 days incubation with the indicated concentrations of ethanol. This was also observed when cultures were treated with doxorubicin (*E*) and methotrexate (*F*). *G*, KNK437 treatment inhibited the action of ethanol as well as that of doxorubicin (*Dox.*, *H*) and methotrexate (*MTX*, *I*) on osteoclast formation in RANKL-treated RAW264.7 cells. *Error bars* represent the mean ± S.E. of three independent experiments. *, $p < 0.05$; **, $p < 0.01$; ***, $p < 0.001$ relative to untreated control using ANOVA/Dunnett's post hoc test.

between MITF and the transcription factor PU.1 (the latter is not RANKL-dependent but binds MITF directly) together with AP-1, NFκB, and NFATc1. MITF is a relatively late-activated factor in osteoclast commitment, and it is possible that its induction by 17-AAG results in an increased pool of MITF that may be otherwise rate-limiting. Consistent with

the latter, overexpression of MITF or the MITF-E isoform (the latter isoform is a particular target of RANKL) enhances osteoclast formation and action (65, 66). It should be noted that because MITF ablation abolishes osteoclast formation, its inhibition is not informative in addressing MITF mediation of 17-AAG effects.
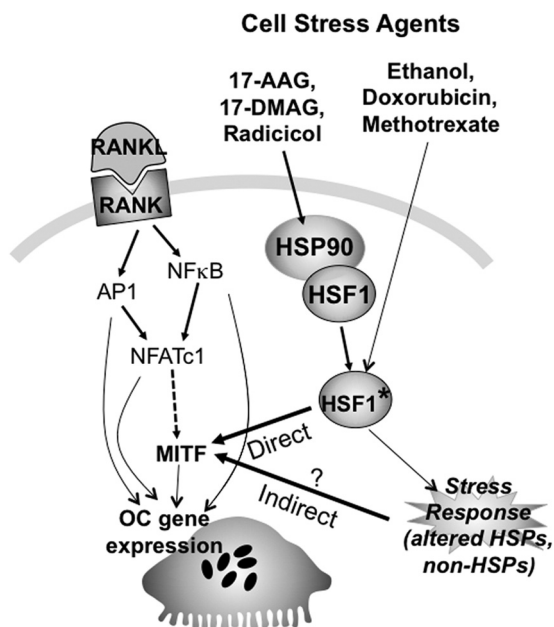
FIGURE 9. **A proposed model of 17-AAG and other cell stress agents upon osteoclast formation.** RANKL binding of RANK induces activation of the NFκB, AP1, and NFATc1 transcription factors. Subsequently, expression of MITF is raised. All four transcription factors are required for osteoclast gene expression. 17-AAG and other HSP90 inhibitors bind to HSP90, inducing a cellular stress response via Hsf1 activation that, in turn, enhances MITF levels either by directly stimulating the *MITF* promoter or indirectly by altering the expression of HSP and/or non-HSP target genes. Other stressor agents (*e.g.* chemotherapeutics) induce a stress response and activate Hsf1, leading to a similar series of events. Elevated MITF levels would, thus, result in an enhanced differentiation response of the osteoclast progenitors to RANKL and greater osteoclast formation. *Hsf1**, activated Hsf1; *OC*, osteoclast.

On the basis of our findings that 17-AAG increases MITF levels and osteoclast formation in a manner sensitive to Hsf1 inhibition, we propose that 17-AAG-induced Hsf1 enhances MITF protein levels and, thereby, amplifies the osteoclastogenic actions of RANKL. This proposed mechanism is summarized in Fig. 9 and incorporates our earlier finding that transcription factors activated early in the RANKL-dependent signaling cascade are not induced by 17-AAG, including NFκB, c-fos (the regulated subunit of AP-1), and NFATc1 (22). The latter findings suggested to us the possibility that a late-acting factor such as MITF would be a more obvious candidate for mediating 17-AAG actions. There is some evidence that MITF can be induced by heat shock elicited by Hsf1 via a direct action on the *MITF* promoter (67). However, for stress-stimulated osteoclast formation, it still has to be determined whether Hsf1 acts directly via *MITF* promoter interaction, by an indirect mechanism such as increased HSP expression that may increase MITF protein stability, or by a combination of both direct and indirect mechanisms. Nevertheless, our findings raise the possibility that any type of cell stress might enhance the levels of this transcription factor, contingent upon other effects the stressor exerts on cells. For example, some recently developed HSP90 inhibitors, such as SNX-2112 and PF-04928473, do not increase osteoclast formation at therapeutically relevant concentrations (49, 68) because, probably, these agents are more potent than 17-AAG at causing degradation of a number of HSP90 clients, such as NFκB, c-fos, NFATc1, and PU.1, which are critical for osteoclast differentiation.

In summary, we have identified a new role for Hsf1 and cell stress in the enhanced formation of osteoclasts that may be highly significant in bone physiology and pathophysiology beyond our focus here on the HSP90 inhibitor 17-AAG. This may result from enhancement of MITF levels, potentially through a direct action of Hsf1 on the *MITF* promoter. 17-AAG actions on osteoclasts may not be solely due to stress or Hsf1 induction, but, nevertheless, inhibition of Hsf1 seems to be a potentially useful approach to reducing osteoclast formation and osteolysis that may be induced by stressor compounds. If stress responses do directly increase the formation of osteoclasts by increasing the responsiveness of osteoclast progenitors to RANKL, we would speculate that other pathological osteolytic stimuli might act, at least in part, by increasing stress via Hsf1 activation and, thus, MITF levels, rather than increasing local net RANKL levels. This raises the possibility that blocking cell stress might reduce excessive pathological osteolysis without necessarily abolishing the bone resorption required for normal bone repair and remodeling.

REFERENCES

1. Karsenty, G., and Ferron, M. (2012) The contribution of bone to whole-organism physiology. *Nature* **481,** 314–320
2. Harada, S., and Rodan, G. A. (2003) Control of osteoblast function and regulation of bone mass. *Nature* **423,** 349–355
3. Boyle, W. J., Simonet, W. S., and Lacey, D. L. (2003) Osteoclast differentiation and activation. *Nature* **423,** 337–342
4. Guise, T. A. (2006) Bone loss and fracture risk associated with cancer therapy. *Oncologist* **11,** 1121–1131
5. Dai, J., Lin, D., Zhang, J., Habib, P., Smith, P., Murtha, J., Fu, Z., Yao, Z., Qi, Y., and Keller, E. T. (2000) Chronic alcohol ingestion induces osteoclastogenesis and bone loss through IL-6 in mice. *J. Clin. Invest.* **106,** 887–895
6. Hadji, P., Ziller, M., Maskow, C., Albert, U., and Kalder, M. (2009) The influence of chemotherapy on bone mineral density, quantitative ultrasonometry and bone turnover in pre-menopausal women with breast cancer. *Eur. J. Cancer* **45,** 3205–3212
7. Mundy, G. R. (2002) Metastasis to bone: causes, consequences and therapeutic opportunities. *Nat. Rev. Cancer* **2,** 584–593
8. Naylor, K., and Eastell, R. (2012) Bone turnover markers: use in osteoporosis. *Nat. Rev. Rheumatol.* **8,** 379–389
9. Pfeilschifter, J., and Diel, I. J. (2000) Osteoporosis due to cancer treatment: pathogenesis and management. *J. Clin. Oncol.* **18,** 1570–1593
10. Nguyen, N. D., Ahlborg, H. G., Center, J. R., Eisman, J. A., and Nguyen, T. V. (2007) Residual lifetime risk of fractures in women and men. *J. Bone Miner. Res.* **22,** 781–788
11. Arikoski, P., Komulainen, J., Riikonen, P., Parviainen, M., Jurvelin, J. S., Voutilainen, R., and Kröger, H. (1999) Impaired development of bone mineral density during chemotherapy: a prospective analysis of 46 children newly diagnosed with cancer. *J. Bone Miner. Res.* **14,** 2002–2009
12. Davies, J. H., Evans, B. A., Jenney, M. E., and Gregory, J. W. (2002) *In vitro* effects of combination chemotherapy on osteoblasts: implications for osteopenia in childhood malignancy. *Bone* **31,** 319–326
13. King, T. J., Georgiou, K. R., Cool, J. C., Scherer, M. A., Ang, E. S., Foster, B. K., Xu, J., and Xian, C. J. (2012) Methotrexate chemotherapy promotes osteoclast formation in the long bone of rats via increased pro-inflammatory cytokines and enhanced NF-κB activation. *Am. J. Pathol.* **181,** 121–129
14. Guise, T. A., Kozlow, W. M., Heras-Herzig, A., Padalecki, S. S., Yin, J. J.,

and Chirgwin, J. M. (2005) Molecular mechanisms of breast cancer metastases to bone. *Clin. Breast Cancer* **5,** S46-S53

15. Asagiri, M., and Takayanagi, H. (2007) The molecular understanding of osteoclast differentiation. *Bone* **40,** 251–264

16. Whitesell, L., and Lindquist, S. L. (2005) HSP90 and the chaperoning of cancer. *Nat. Rev. Cancer* **5,** 761–772

17. Trepel, J., Mollapour, M., Giaccone, G., and Neckers, L. (2010) Targeting the dynamic HSP90 complex in cancer. *Nat. Rev. Cancer* **10,** 537–549

18. Pick, E., Kluger, Y., Giltnane, J. M., Moeder, C., Camp, R. L., Rimm, D. L., and Kluger, H. M. (2007) High HSP90 expression is associated with decreased survival in breast cancer. *Cancer Res.* **67,** 2932–2937

19. Kim, Y. S., Alarcon, S. V., Lee, S., Lee, M.-J., Giaccone, G., Neckers, L., and Trepel, J. B. (2009) Update on Hsp90 inhibitors in clinical trial. *Curr. Top. Med. Chem.* **9,** 1479–1492

20. Price, J. T., Quinn, J. M., Sims, N. A., Vieusseux, J., Waldeck, K., Docherty, S. E., Myers, D., Nakamura, A., Waltham, M. C., Gillespie, M. T., and Thompson, E. W. (2005) The heat shock protein 90 inhibitor, 17-allyl-amino-17-demethoxygeldanamycin, enhances osteoclast formation and potentiates bone metastasis of a human breast cancer cell line. *Cancer Res.* **65,** 4929–4938

21. Yano, A., Tsutsumi, S., Soga, S., Lee, M. J., Trepel, J., Osada, H., and Neckers, L. (2008) Inhibition of Hsp90 activates osteoclast c-Src signaling and promotes growth of prostate carcinoma cells in bone. *Proc. Natl. Acad. Sci. U.S.A.* **105,** 15541–15546

22. van der Kraan, A. G., Chai, R. C., Singh, P. P., Lang, B. J., Xu, J., Gillespie, M. T., Price, J. T., and Quinn, J. M. (2013) HSP90 inhibitors enhance differentiation and MITF (microphthalmia transcription factor) activity in osteoclast progenitors. *Biochem. J.* **451,** 235–244

23. Mosser, D. D., and Morimoto, R. I. (2004) Molecular chaperones and the stress of oncogenesis. *Oncogene* **23,** 2907–2918

24. Calderwood, S. K., Khaleque, M. A., Sawyer, D. B., and Ciocca, D. R. (2006) Heat shock proteins in cancer: chaperones of tumorigenesis. *Trends Biochem. Sci.* **31,** 164–172

25. Anckar, J., and Sistonen, L. (2011) Regulation of HSF1 function in the heat stress response: implications in aging and disease. *Annu. Rev. Biochem.* **80,** 1089–1115

26. Ali, A., Bharadwaj, S., O'Carroll, R., and Ovsenek, N. (1998) HSP90 interacts with and regulates the activity of heat shock factor 1 in *Xenopus* oocytes. *Mol. Cell. Biol.* **18,** 4949–4960

27. Zou, J., Guo, Y., Guettouche, T., Smith, D. F., and Voellmy, R. (1998) Repression of heat shock transcription factor HSF1 activation by HSP90 (HSP90 complex) that forms a stress-sensitive complex with HSF1. *Cell* **94,** 471–480

28. Pirkkala, L., Nykänen, P., and Sistonen, L. (2001) Roles of the heat shock transcription factors in regulation of the heat shock response and beyond. *FASEB J.* **15,** 1118–1131

29. Morimoto, R. I. (1998) Regulation of the heat shock transcriptional response: cross talk between a family of heat shock factors, molecular chaperones, and negative regulators. *Genes Dev.* **12,** 3788–3796

30. Yeung, Y. G., Jubinsky, P. T., Sengupta, A., Yeung, D. C., and Stanley, E. R. (1987) Purification of the colony-stimulating factor 1 receptor and demonstration of its tyrosine kinase activity. *Proc. Natl. Acad. Sci. U.S.A.* **84,** 1268–1271

31. McMillan, D. R., Xiao, X., Shao, L., Graves, K., and Benjamin, I. J. (1998) Targeted disruption of heat shock transcription factor 1 abolishes thermotolerance and protection against heat-inducible apoptosis. *J. Biol. Chem.* **273,** 7523–7528

32. Quinn, J. M., Whitty, G. A., Byrne, R. J., Gillespie, M. T., and Hamilton, J. A. (2002) The generation of highly enriched osteoclast-lineage cell populations. *Bone* **30,** 164–170

33. Nguyen, C. H., Lang, B. J., Chai, R. C., Vieusseux, J. L., Kouspou, M. M., and Price, J. T. (2013) Heat-shock factor 1 both positively and negatively affects cellular clonogenic growth depending on p53 status. *Biochem. J.* **452,** 321–329

34. Quinn, J. M., Morfis, M., Lam, M. H., Elliott, J., Kartsogiannis, V., Williams, E. D., Gillespie, M. T., Martin, T. J., and Sexton, P. M. (1999) Calcitonin receptor antibodies in the identification of osteoclasts. *Bone* **25,** 1–8

35. Lang, B. J., Nguyen, L., Nguyen, H. C., Vieusseux, J. L., Chai, R. C., Chris-

36. Yokota, S., Kitahara, M., and Nagata, K. (2000) Benzylidene lactam compound, KNK437, a novel inhibitor of acquisition of thermotolerance and heat shock protein induction in human colon carcinoma cells. *Cancer Res.* **60,** 2942–2948

37. Nagai, N., Nakai, A., and Nagata, K. (1995) Quercetin suppresses heat shock response by down-regulation of HSF1. *Biochem. Biophys. Res. Commun.* **208,** 1099–1105

38. Fox, S. W., Evans, K. E., and Lovibond, A. C. (2008) Transforming growth factor-β enables NFATc1 expression during osteoclastogenesis. *Biochem. Biophys. Res. Commun.* **366,** 123–128

39. Sells Galvin, R. J., Gatlin, C. L., Horn, J. W., and Fuson, T. R. (1999) TGF-β enhances osteoclast differentiation in hematopoietic cell cultures stimulated with RANKL and M-CSF. *Biochem. Biophys. Res. Commun.* **265,** 233–239

40. Luchin, A., Purdom, G., Murphy, K., Clark, M. Y., Angel, N., Cassady, A. I., Hume, D. A., and Ostrowski, M. C. (2000) The microphthalmia transcription factor regulates expression of the tartrate-resistant acid phosphatase gene during terminal differentiation of osteoclasts. *J. Bone Miner. Res.* **15,** 451–460

41. Motyckova, G., Weilbaecher, K. N., Horstmann, M., Rieman, D. J., Fisher, D. Z., and Fisher, D. E. (2001) Linking osteopetrosis and pycnodysostosis: regulation of cathepsin K expression by the microphthalmia transcription factor family. *Proc. Natl. Acad. Sci. U.S.A.* **98,** 5798–5803

42. Nomura S, Sakuma, T., Higashibata Y, Oboki K, Sato M. (2001) Molecular cause of the severe functional deficiency in osteoclasts by an arginine deletion in the basic domain of Mi transcription factor. *J. Bone Miner. Metab.* **19,** 183–187

43. Richter, K., Haslbeck, M., and Buchner, J. (2010) The heat shock response: life on the verge of death. *Mol. Cell* **40,** 253–266

44. Ciocca, D. R., Fuqua, S. A., Lock-Lim, S., Toft, D. O., Welch, W. J., and McGuire, W. L. (1992) Response of human breast cancer cells to heat shock and chemotherapeutic drugs. *Cancer Res.* **52,** 3648–3654

45. Vargas-Roig, L. M., Gago, F. E., Tello, O., Aznar, J. C., and Ciocca, D. R. (1998) Heat shock protein expression and drug resistance in breast cancer patients treated with induction chemotherapy. *Int. J. Cancer* **79,** 468–475

46. Li, G. C. (1983) Induction of thermotolerance and enhanced heat shock protein synthesis in Chinese hamster fibroblasts by sodium arsenite and by ethanol. *J. Cell Physiol.* **115,** 116–122

47. Iitsuka, N., Hie, M., Nakanishi, A., and Tsukamoto, I. (2012) Ethanol increases osteoclastogenesis associated with the increased expression of RANK, PU. 1 and MITF *in vitro* and *in vivo*. *Int. J. Mol. Med.* **30,** 165–172

48. Mandrekar, P., Catalano, D., Jeliazkova, V., and Kodys, K. (2008) Alcohol exposure regulates heat shock transcription factor binding and heat shock proteins 70 and 90 in monocytes and macrophages: implication for TNF-α regulation. *J. Leukocyte Biol.* **84,** 1335–1345

49. Lamoureux, F., Thomas, C., Yin, M. J., Kuruma, H., Fazli, L., Gleave, M. E., and Zoubeidi, A. (2011) A novel HSP90 inhibitor delays castrate-resistant prostate cancer without altering serum PSA levels and inhibits osteoclastogenesis. *Clin. Cancer Res.* **17,** 2301–2313

50. Roccisana, J. L., Kawanabe, N., Kajiya, H., Koide, M., Roodman, G. D., and Reddy, S. V. (2004) Functional role for heat shock factors in the transcriptional regulation of human RANK ligand gene expression in stromal/osteoblast cells. *J. Biol. Chem.* **279,** 10500–10507

51. Guise, T. (2010) Examining the metastatic niche: targeting the microenvironment. *Semin. Oncol.* **37,** S2–14

52. Zanini, C., Giribaldi, G., Mandili, G., Carta, F., Crescenzio, N., Bisaro, B., Doria, A., Foglia, L., di Montezemolo, L. C., Timeus, F., and Turrini, F. (2007) Inhibition of heat shock proteins (HSP) expression by quercetin and differential doxorubicin sensitization in neuroblastoma and Ewing's sarcoma cell lines. *J. Neurochem.* **103,** 1344–1354

53. Ferry, D. R., Smith, A., Malkhandi, J., Fyfe, D. W., deTakats, P. G., Anderson, D., Baker, J., and Kerr, D. J. (1996) Phase I clinical trial of the flavonoid quercetin: pharmacokinetics and evidence for *in vivo* tyrosine kinase inhibition. *Clin. Cancer Res.* **2,** 659–668

54. Wu, B. Y., and Yu, A. C. (2000) Quercetin inhibits c-fos, heat shock pro-

tein, and glial fibrillary acidic protein expression in injured astrocytes. *J. Neurosci. Res.* **62,** 730–736

55. Rangan, G. K., Wang, Y., Tay, Y. C., and Harris, D. C. (1999) Inhibition of NFκB activation with antioxidants is correlated with reduced cytokine transcription in PTC. *Am. J. Physiol.* **277,** F779–789

56. Xiao, X., Zuo, X., Davis, A. A., McMillan, D. R., Curry, B. B., Richardson, J. A., and Benjamin, I. J. (1999) HSF1 is required for extra-embryonic development, postnatal growth and protection during inflammatory responses in mice. *EMBO J.* **18,** 5943–5952

57. Powers, M. V., and Workman, P. (2007) Inhibitors of the heat shock response: biology and pharmacology. *FEBS Lett.* **581,** 3758–3769

58. Donnelly, A., and Blagg, B. S. (2008) Novobiocin and additional inhibitors of the Hsp90 C-terminal nucleotide-binding pocket. *Curr. Med. Chem.* **15,** 2702–2717

59. Langer, T., Schlatter, H., and Fasold, H. (2002) Evidence that the novobiocin-sensitive ATP-binding site of the heat shock protein 90 (Hsp90) is necessary for its autophosphorylation. *Cell Biol. Int.* **26,** 653–657

60. Radanyi, C., Le Bras, G., Messaoudi, S., Bouclier, C., Peyrat, J. F., Brion, J. D., Marsaud, V., Renoir, J. M., and Alami, M. (2008) Synthesis and biological activity of simplified denoviose-coumarins related to novobiocin as potent inhibitors of heat-shock protein 90 (hsp90). *Bioorg. Med. Chem. Lett.* **18,** 2495–2498

61. Conde, R., Belak, Z. R., Nair, M., O'Carroll, R. F., and Ovsenek, N. (2009) Modulation of Hsf1 activity by novobiocin and geldanamycin. *Biochem. Cell Biol.* **87,** 845–851

62. Friedlaender, G. E., Tross, R. B., Doganis, A. C., Kirkwood, J. M., and Baron, R. (1984) Effects of chemotherapeutic agents on bone: I: short-term methotrexate and doxorubicin (adriamycin) treatment in a rat model. *J. Bone Jt. Surg. Am.* **66,** 602–607

63. Steingrímsson, E., Moore, K. J., Lamoreux, M. L., Ferré-D'Amaré, A. R., Burley, S. K., Zimring, D. C., Skow, L. C., Hodgkinson, C. A., Arnheiter, H., and Copeland, N. G. (1994) Molecular basis of mouse microphthalmia (mi) mutations helps explain their developmental and phenotypic consequences. *Nat. Genet.* **8,** 256–263

64. Sharma, S. M., Bronisz, A., Hu, R., Patel, K., Mansky, K. C., Sif, S., and Ostrowski, M. C. (2007) MITF and PU. 1 recruit p38 MAPK and NFATc1 to target genes during osteoclast differentiation. *J. Biol. Chem.* **282,** 15921–15929

65. Lu, S. Y., Li, M., and Lin, Y. L. (2010) MITF induction by RANKL is critical for osteoclastogenesis. *Mol. Biol. Cell* **21,** 1763–1771

66. Meadows, N. A., Sharma, S. M., Faulkner, G. J., Ostrowski, M. C., Hume, D. A., and Cassady, A. I. (2007) The expression of Clcn7 and Ostm1 in osteoclasts is coregulated by microphthalmia transcription factor. *J. Biol. Chem.* **282,** 1891–1904

67. Laramie, J. M., Chung, T. P., Brownstein, B., Stormo, G. D., and Cobb, J. P. (2008) Transcriptional profiles of human epithelial cells in response to heat: computational evidence for novel heat shock proteins. *Shock* **29,** 623–630

68. Okawa, Y., Hideshima, T., Steed, P., Vallet, S., Hall, S., Huang, K., Rice, J., Barabasz, A., Foley, B., Ikeda, H., Raje, N., Kiziltepe, T., Yasui, H., Enatsu, S., and Anderson, K. C. (2009) SNX-2112, a selective Hsp90 inhibitor, potently inhibits tumor cell growth, angiogenesis, and osteoclastogenesis in multiple myeloma and other hematologic tumors by abrogating signaling via Akt and ERK. *Blood* **113,** 846–855

Cell Biology:

Molecular Stress-inducing Compounds Increase Osteoclast Formation in a Heat Shock Factor 1 Protein-dependent Manner

CELL BIOLOGY

MOLECULAR BASES OF DISEASE

Ryan C. Chai, Michelle M. Kouspou, Benjamin J. Lang, Chau H. Nguyen, A. Gabrielle J. van der Kraan, Jessica L. Vieusseux, Reece C. Lim, Matthew T. Gillespie, Ivor J. Benjamin, Julian M. W. Quinn and John T. Price

Access the most updated version of this article at doi: 10.1074/jbc.M113.530626

Find articles, minireviews, Reflections and Classics on similar topics on the JBC Affinity Sites.

Alerts:
- When this article is cited
- When a correction for this article is posted

Click here to choose from all of JBC's e-mail alerts

This article cites 68 references, 24 of which can be accessed free at
http://www.jbc.org/content/289/19/13602.full.html#ref-list-1